THE UNIVERSITY OF MICHIGAN
INDUSTRY PROGRAM OF THE COLLEGE OF ENGINEERING

ENGINEERING APPROACH TO SURFACE DAMAGE

Lectures given at
THE UNIVERSITY OF MICHIGAN
1958 Summer Conference Course

Edited by
CHARLES LIPSON
Professor, Mechanical Engineering
and
L. V. COLWELL
Professor, Mechanical Engineering

August, 1958
IP - 304

FOREWORD

Each summer the College of Engineering of the University of Michigan presents a number of selected intensive courses treating various engineering areas of either broad or specialized interests. These courses are designed for practicing engineers, educators, and government employees concerned with the subjects at hand.

The lectures summarized in this volume comprise such an intensive course, presented during the week of July 14, 1958, under the sponsorship of the Department of Mechanical Engineering. Various aspects of the Engineering Approach To Surface Damage, including causes and remedies, are treated in these lectures.

Charles Lipson

L. V. Colwell

Ann Arbor, 1958

TABLE OF CONTENTS

LIST OF LECTURERS

	Name	Position	Company
1.	Avery, Howard S.	Research Metallurgist	American Brake Shoe Company
2.	Bisson, E. E.	Assistant Chief, Fluid Systems Division	National Advisory Committee for Aeronautics
3.	Colwell, L. V.	Professor of Mechanical Engineering	University of Michigan
4.	Cram, W. D.	Group Leader, Engineering Power Transmission	United Shoe Machinery Corporation
5.	Davies, Robert	Assistant Head, Mechanical Development Department	General Motors Corporation
6.	Graham, J. D.	Chief Materials Engineer	International Harvester Company
7.	Grover, H. J.	Chief, Applied Mechanics Division, Mechanical Engineering Department	Battelle Memorial Institute
8.	Kelly, B. W.	Staff Research Engineer	Caterpillar Tractor Company
9.	La Belle, J.	Chief Metallurgist	Detroit Diesel Engine Division, General Motors Corporation
10.	La Que, F. L.	Vice-President Development and Research Division	International Nickel Company
11.	Lipson, Charles	Professor of Mechanical Engineering	University of Michigan
12.	McDowell, J. R.	Research Engineer	Westinghouse Electric Company
13.	Norman, T. E.	Metallurgical Engineer	Climax Molybdenum Company
14.	Peterson, M. B.	Physicist, Bearing and Lubrication Center	General Electric Company

LIST OF LECTURERS (CONT'D)

	Name	Position	Company
15.	Rheingans, Wm. J.	Manager, Hydraulic Department	Allis-Chalmers Manufacturing Company
16.	Rote, F. B.	Technical Director	Albion Malleable Iron Company
17.	Rowland, E. S.	Chief Metallurgical Engineer	Timken Roller Bearing Company
18.	Tauschek, M. J.	Chief Engineer, Valve Division	Thompson Products, Inc.

LIST OF PARTICIPANTS

Name	Position	Company and City
Allen, Robert M.	Senior Technologist	United States Steel Corporation Monroeville, Pennsylvania
Barlow, George S., Jr.	Staff Supervisor Metallurgist	Newport News Shipbuilding and Dry Dock Company Newport News, Virginia
Blatter, Al	Engineer	Bendix Aviation Corporation Research Laboratories Division Detroit, Michigan
Breen, Dale H.	Metallurgical Consultant	International Harvester Company Fort Wayne, Indiana
Bruner, James P.	Research Engineer	Armco Steel Corporation Middletown, Ohio
Cutler, James L.	Metallurgical Engineer	Hamilton Standard Windsor Locks, Connecticut
Deagle, Lorenzo	Engineer, Structural Evaluation	General Electric Company Knolls Atomic Power Laboratory Schenectady, New York
Evans, Robert F.	Chief Metallurgist	H.C. Smith Oil Tool Company Compton, California
Garabedian, Charles G.	Project Engineer	Detroit Arsenal Center Line, Michigan
Gibbons, Thomas P.	Project Engineer Mechanical Research Division	Scott Paper Company Chester, Pennsylvania
Halberg, Robert W.	Manager, Mechanical Design	Borg-Warner Research Center Des Plaines, Illinois
Hanink, Dean K.	Chief Metallurgist	Allison Division, General Motors Corporation Indianapolis, Indiana

LIST OF PARTICIPANTS (CONT'D)

	Name	Position	Company and City
13.	Hanzel, Richard W.	Manager, Materials Engineering	Sunbeam Corporation Chicago, Illinois
14.	Hooper, Albert F.	Chemist	Convair San Diego, California
15.	Humphrey, Robert B.	Manager, Mechanical Analysis Laboratory	International Business Mach Poughkeepsie, New York
16.	Kepple, Richard K.	Research Engineer	Research Staff General Motors Corporation Detroit, Michigan
17.	Kingsley, Gerald V.	Director of Research	Bohn Aluminum and Brass Cor Detroit, Michigan
18.	MacPherson, James B.	Mechanical Design Engineer	General Electric Company Erie, Pennsylvania
19.	Matt, Richard J.	Engineering Specialist	Thompson Products, Inc. Cleveland, Ohio
20.	Parr, Ben C.	Engineer	Pontiac Motor Division, GMC Pontiac, Michigan
21.	Parry, Leo S.	Stress Analyst	Massey-Freguson, Inc. Detroit, Michigan
22.	Rodefeld, William A.	Assistant Chief Metallurgist	Perfect Circle Corporation Hagerstown, Indiana
23.	Schwartz, Arthur D.	General Metallurgist	Metallurgy Unit-E & G Branc White Sands, New Mexico
24.	Simon, Carl F.	Supervisor, Mechanical Design	General Electric Company Erie, Pennsylvania
25.	Snow, Walter A.	Engineering Manager Industrial Machinery Dept.	Carrier Corporation Syracuse, New York
26.	Solomon, Alexander	Research Associate	Climax Molybdenum Company Detroit, Michigan

LIST OF PARTICIPANTS (CONT'D)

Name	Position	Company and City
. Timpner, Fred F.	Analytical Engineer	Pontiac Motor Division, GMC Pontiac, Michigan
. Tromel, Frederic C.	Project Engineer	Alco Products, Inc. Schenectady, New York
. Van Camp, Hugh	Development Engineer	Aluminum Company of America Cleveland, Ohio
. Wilde, Richard A.	Chief Metallurgist	Eaton Manufacturing Company Detroit, Michigan

INTRODUCTION

Charles Lipson

Wear may be defined as a deterioration of surface due to use. It occurs in a wide variety of operations and in some industries the annual cost of replacing worn parts represents major expense. Wear is also an important aspect of engineering practice, as in many cases it is the major factor limiting the life and the performance of machine components. It has been said that a 5-ton truck completely worn out weighs five pounds less than when it is new.

Wear can be destructive or normal. However, even when normal, it may be more severe than desirable because of the frequency of parts replacement. No machine member is immune from wear, as wear manifests itself whenever there is load and a motion. Scuffing of pistons in internal combustion engines, pitting in power transmission gears, frettage in press-fitted assemblies, cavitation corrosion in cylinder liners, are all manifestations of wear.

Wear is an extremely complex subject and no general rule holds for all its manifestations. This is because it is affected by a variety of conditions, such as the type and mode of loading, speed, quantity and type of lubricant, temperature, hardness, surface finish, presence of foreign materials and the chemical nature of the environment. Since the conditions are different in each application, so will be the corresponding manifestations of wear.

Furthermore, the wear which occurs in practice is usually a combination of one or more of the elementary forms. For example, small particles resulting from galling may, in turn, cause abrasive wear. Or, in a press-fitted assembly fretting corrosion may be entirely obscured by galling. Thus, it is not always easy in any given application to state which type of wear has taken place.

To this may be added lack of agreement on the nomenclature and lack of good definition of the different manifestations of wear such as scuffing, galling, abrasion and corrosion.

A logical method of classifying wear would involve the nature of the contacting surface as follows:

1. Metal against metal
2. Metal against non-metal
3. Metal against fluid.

These classifications, in turn, would have to be subdivided into lubricated and non-lubricated conditions, sliding or rolling friction, etc. Furthermore, the conditions themselves may change and what was initially metal against metal becomes metal against non-metal, or lubrication initially adequate may fail in further service.

For this reason in actual engineering practice the above classification loses its usefulness. Instead, grouping in terms of commonly understood terms is to be preferred.

Galling, Scuffing, Scoring and Seizing

Although some differences, depending on the severity of action, exist between these forms of wear, from the engineering viewpoint they may be grouped under a single heading. This is probably the most fundamental type of wear and it may be termed an adhesive form of wear. It is caused by a shearing action of micro-welds formed between the surface asperites that actually carry the load between two mating surfaces. This takes place because of the failure of the film which normally separates the two surfaces. Film failure, in turn, is brought about by high temperatures, pressures and sliding velocities.

Abrasion

Abrasive or cutting type of wear takes place whenever hard foreign particles, such as metal grit, metallic oxides, dust and grit from the environment, are present between the rubbing surfaces. These particles first penetrate the metal and then tear off the metallic particles. Depending on severity, abrasive wear may be of the gouging or scratching form. Abrasive wear is one of the most common types encountered in engineering practice and it is probably the highest single cause of wear in many machine applications.

Pitting

Pitting, pitting corrosion, spalling, and case crushing are all the same phenomena, spalling probably being the most common one. It is generally attributed to the cyclical repetition of contact stresses between two mating surfaces, such as a pair of gears or ball and a race, under load. The high stress causes a crack which in turn separates a particle from the main body of the material. The cavity thus formed is a pit which frequently leads to a spalling out of the material. The destructive character of pitting involves a multitude of factors such as: high contact stresses, sliding action accompanying rolling action, possible formation of an elastic wave ahead of the instantaneous area of contact, surface flow and subsurface fatigue. Distinction should be made between incipient pitting, which may be erased by subsequent wearing action, and destructive pitting which leads to fatigue failure.

Frettage

Frettage or frettage corrosion is also known by a variety of other terms such as false brinelling, wear oxidation, friction oxidation, and

chaffing fatigue. It is characterized by minute reciprocating motions between the wearing surfaces which are held together by a normal force, as, for example, in press-fitted assemblies. The damage may vary from only a discoloration of the mating surfaces to the wearing away of a sixteenth of an inch of material. The surface may show the formation of a great deal of corroded material or merely a heavily galled appearance with little oxide. A tentative theory is that the oscillatory motion breaks down any natural protective film carried by the surface, so that the metal adheres and is broken away at each oscillation. The debris may be then converted into an abrasive oxide which causes the severe damage met with in practice. Fretting damage may be found in automobile front wheel bearings (false brinelling), king pins, rocker arms, variable pitch propellers, landing wheels, cam followers in textile machinery and electrical contacts.

Cavitation Erosion

Erosion is a process of surface damage and material removal which is caused by a liquid or gas, without the presence of a second surface. In industrial practice, the most common type of erosion is cavitation erosion (or cavitation corrosion). It occurs in propeller blades, Diesel engine cylinder liners, turbines and pumps. The causes of cavitation erosion are high relative motions between the metal and the liquid. At such motions, the local pressure on the liquid is reduced to the boiling point and small cavities of vapor are formed. When the pressure returns to normal implosion occurs and the cavity collapses. This produces high impact forces on the metal, causing work hardening, fatigue and a formation of cavitation pits. The above is purely a mechanical action, which however frequently exists in the presence of galvanic corrosion.

Galvanic Corrosion

Galvanic corrosion is a complex phenomenon which involves damage to a surface by a flow of current in a liquid, from one metallic surface to another. According to a strict definition the two metals must be different. In a broader sense, these galvanic cells may operate either at the surface of the metal, or between dissimilar metals in electrical contact or between areas of unequal electrolyte concentration. This includes a galvanic action as it is related to corrosion in and around crevices and pitting. When conditions conducive to galvanic corrosion exist in the presence of cavitation (as in Diesel engine cylinder liners) the corrosion can be expected to accelerate the damage because of the removal of the protective film.

COMPATABILITY OF METAL PAIRS

Robert Davies
Assistant Head, Mechanical Development Department
Research Staff, General Motors Corporation

COMPATABILITY OF METAL PAIRS

by

Robert Davies

Two metals usually seize, score, and gall when they slide over each other, even with some boundary lubrication. Thus, it is desirable to know which metal pairs score the least. To select experimentally the best pair from 75 metallic elements requires 5625 experiments. Consequently, it is desirable to have criteria that permit one to predict which pairs of metallic elements slide with minimum scoring.

The following criteria were suggested by Underwood,[2] subsequently improved by Roach, Goodzeit, and Hunnicutt,[3] and then extended by Goodzeit.[4] Two metals can slide on each other with relatively little scoring if both of the following conditions are met:

1. The metals are insoluble in each other -- neither metal dissolves in the other or forms an alloy with it.
2. At least one of the metals is from the B-subgroup of the periodic table -- the elements to the right of the Ni-Pd-Pt column in the periodic table of Figure 1.

The following microscopic picture of the wear process helps to explain why these criteria are necessary and adequate. Figure 2 shows an enlarged view of two metals that are sliding upon each other. The metals are in contact over only the relatively small areas of their high points where there is sufficient scouring to wipe the metals clean of most surface contamination and where sufficient heat is generated to melt one of the metals.[5] The metal-to-metal contact and the heat cause the metals to weld together locally. If the weld is weaker than either metal, then the metals break apart at the weld and there is no metal transferred from one specimen to the other. If the weld is stronger and material is transferred from it to the other resulting in scoring.

If either metal is soluble in the other, or if the two form an alloy, then diffusion occurs at the weld which is thereby hardened and strengthened. Under this condition, the fracture is not at the weld and there is metal transfer with its concomitant scoring.

In order to resist scoring, the two metals must form a weld weaker than either. In case the metals are mutually soluble, the weld is strong. However, a strong weld may occur even when the metals are insoluble. In a true metal, represented by the elements in the left hand column of the periodic table (Figure 1), the bonds that hold the atoms

in the crystal lattice are mobile and the electrons from the outer shell are free to move about inside the crystal. The mobility of "metallic bonding" gives metals their strength and ductility. As one moves toward the right hand side of the periodic table, the bonds become more "covalent" and atoms tend to share electron pairs which are no longer free to move about within the crystal lattice. Covalent crystals are brittle and friable. When two metals are welded together and one tends to covalent bonding, that is, when it is on the right side of the periodic table or in the B-subgroup, then the weld seems to have covalent bonding and is brittle and friable. For such pairs of metals, if no alloy is formed, the weld is weak and fractures before either metal and scoring is minimized.

If the two metals form a chemical compound, the bond in the compound is generally so that the weld is weak and scoring is minimized. At least one metal in an intermetallic compound is almost always from the B-subgroup, and thus the cases of metals that form compounds can be considered as special cases of insoluble metals.

Mr. Goodzeit tested the criteria by holding small square sliders of one metal against a rotating disk of the other metal. The geometry is shown in Figure 3. The square or sliders were 5/8 inch by 5/8 inch and were pressed against the disks with a force that automatically increased to 1200 pounds or until failure occurred. The angle between the slider and disk, which is exaggerated in Figure 3, was 1/2 degree. The disks turned at 5400 revolutions per minute which gave an average sliding velocity of 4640 feet per minute. Kerosene was sprayed on the hub of the disk at a rate of 2.7 cubic centimeters per second to provide some boundary lubrication. Electrical resistance measurements between the slider and the disk indicated that metal-to-metal contact occurred at all loads.

Figure 4 shows the four elements that were used for disk materials. These four were selected in order to obtain the maximum amount of information from the minimum number of tests. The steel alloy SAE 1045 was used in place of pure iron for the disks.

Figure 5 is a photograph of four silver sliders and the disk that they ran against. Aluminum, copper, and silver are all soluble in silver and thus there was considerable metal transfer and scoring in those cases. Silver and iron are insoluble, and silver is a B-subgroup metal, and thus silver ran against steel to the load limit of the machine with little damage or metal transfer.

Figure 6 shows the effect of reversing the roles of the disk and slider metals. When the slider is the softer metal, silver in this case, it is more likely to deform because it is loaded continuously.

The elements that were not used for sliders are shaded in Figure 7. In case an element was rejected for several reasons, only the most convincing reason is indicated. For example, radon was not used because it is gas, it is radio-active, and it is too rare. Only "gas" is indicated

because it is the hardest obstacle to overcome in case radon has to be tested. Some elements were rejected for reasons that were insufficient to reject other elements. For example, the rare earth elements, other than cerium, were not tested spearately because they are so much like cerium and they were tested together as the alloy misch-metal. Figure 8 shows the periodic table arrangement of only the elements that were used for sliders.

The scoring resistance of the sliders are shown in Figures 9 to 12. Tables 1, 2, and 3 give the results that agree with the criteria. Tables 4 and 5 give the results that do not support the criteria. The first three tables have 114 entries and the last two have 9. Thus, the criteria are wrong only 9 times in 123, or about 7% of the time.

Some of the entries in these last tables may not vitiate the criteria. For example, copper and iron may be insoluble in some compositions,[6] and thus copper slider and steel disk may belong in Table 3.

H																	He
Li	Be	B										C	N	O	F	Ne	
Na	Mg	Al										Si	P	S	Cl	A	
K	Ca	Sc		Ti	V	Cr	Mn	Fe	Co	Ni	Cu	Zn	Ga	Ge	As	Se	Br	Kr
Rb	Sr	Y		Zr	Nb	Mo	Tc	Ru	Rh	Pd	Ag	Cd	In	Sn	Sb	Te	I	Xe
Cs	Ba	La	*	Hf	Ta	W	Re	Os	Ir	Pt	Au	Hg	Tl	Pb	Bi	Po	At	Rn
Fr	Ra	Ac	**															

*	Ce	Pr	Nd	Pm	Sm	Eu	Gd	Tb	Dy	Ho	Er	Tm	Yb	Lu
**	Th	Pa	U	Np	Pu	Am	Cm	Bk...						

Figure 1. The Periodic Table.

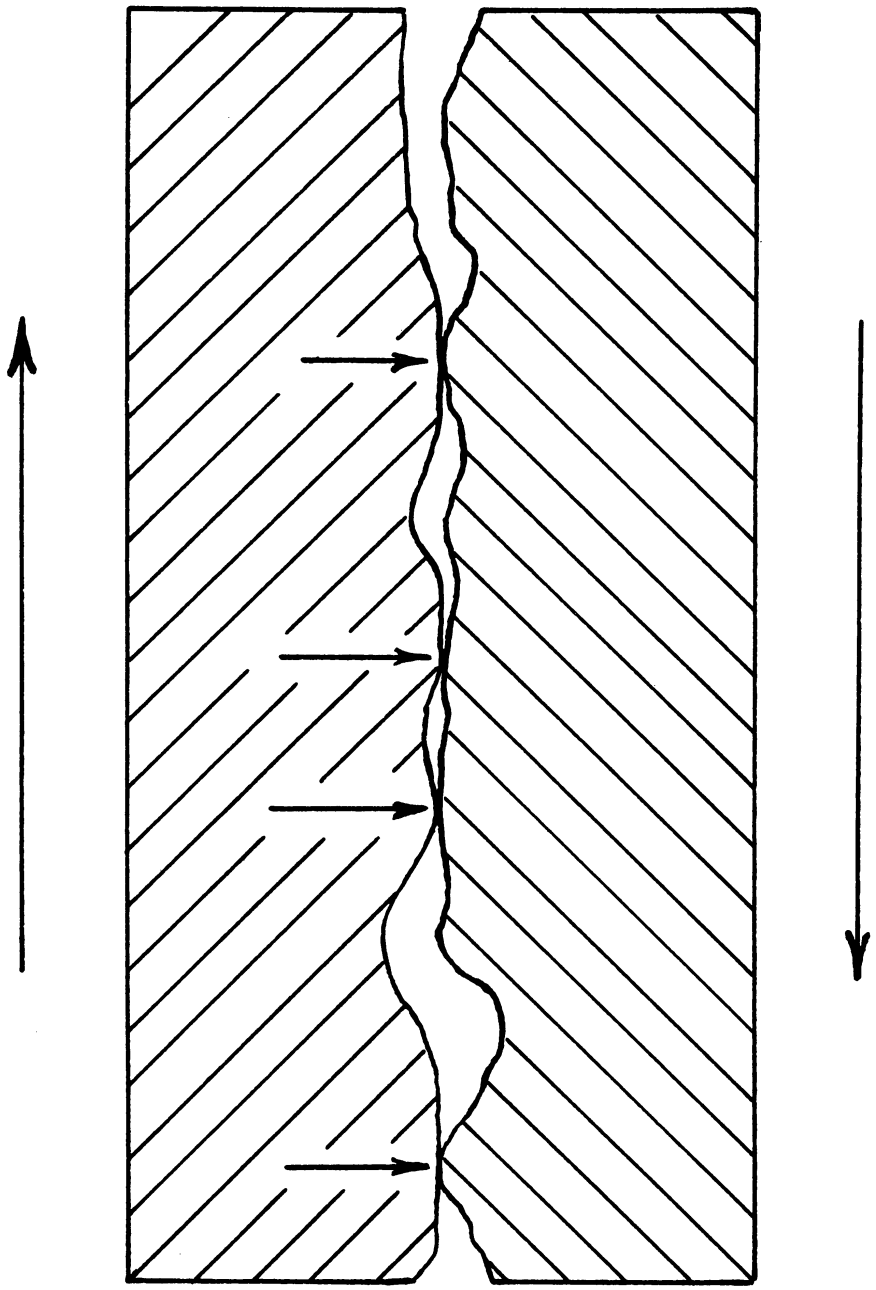

Figure 2. An Enlarged View of Two Solids in Sliding Contact.

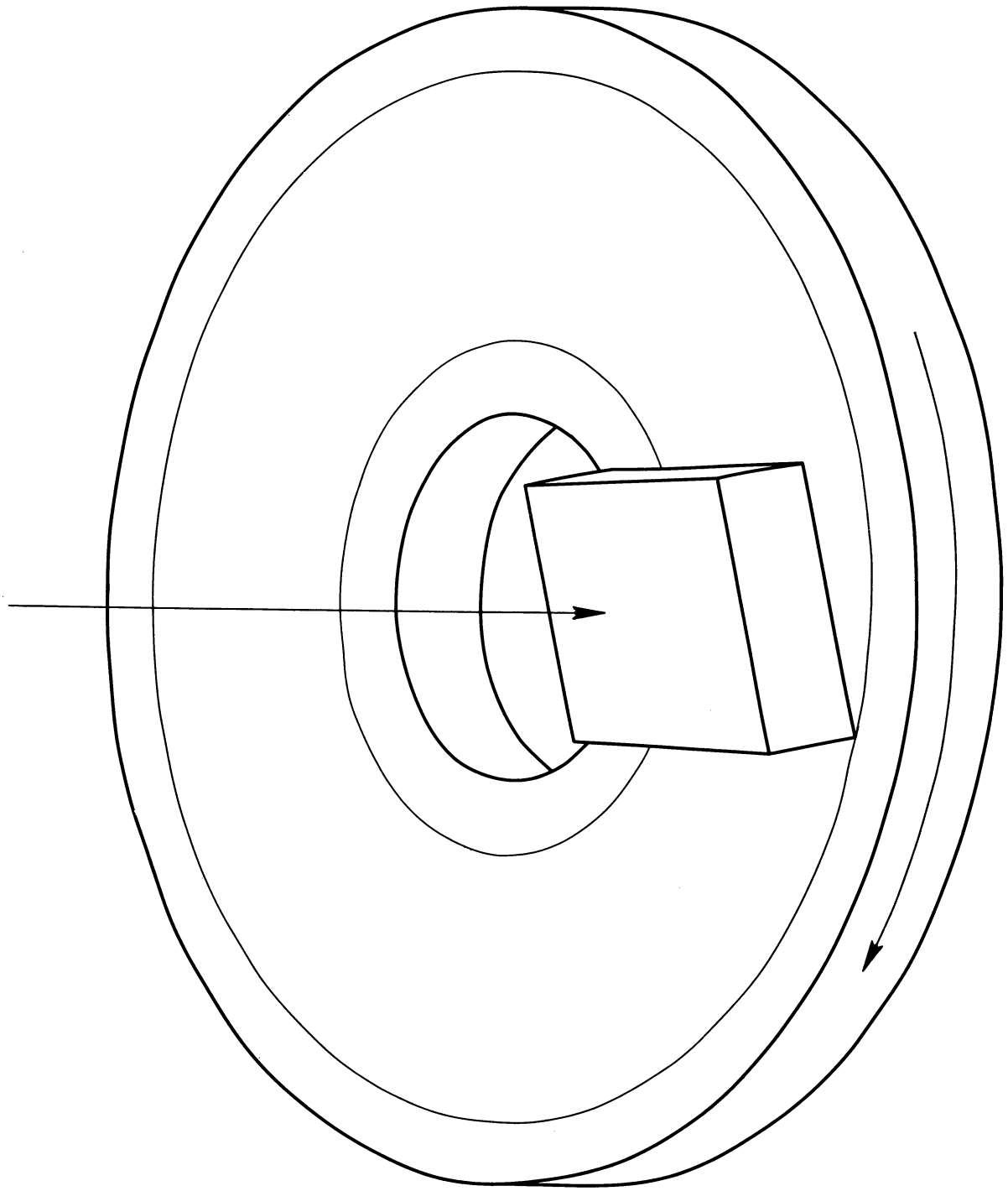

Figure 3. The geometry of the score tests.

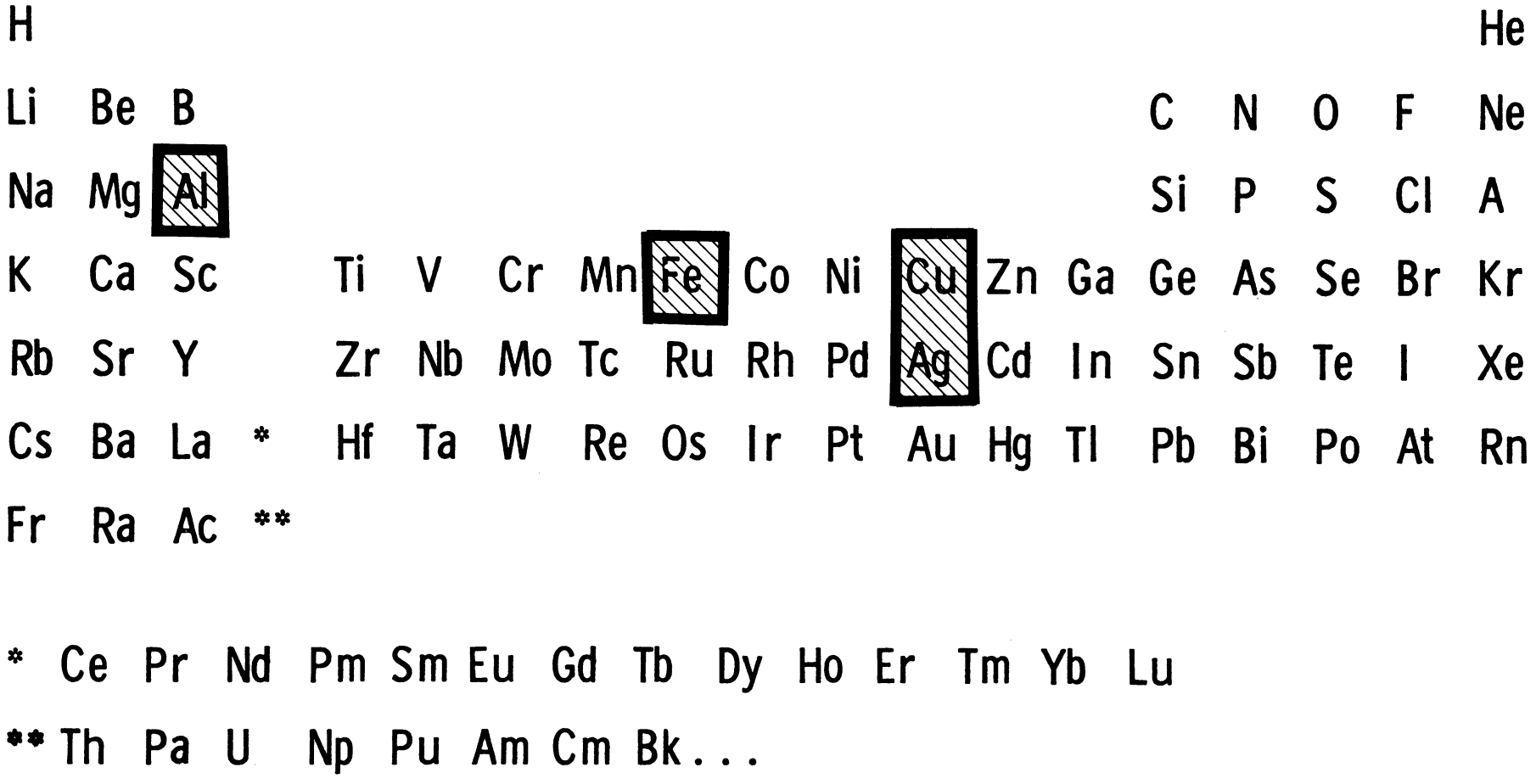

Figure 4. The four materials used for disks.

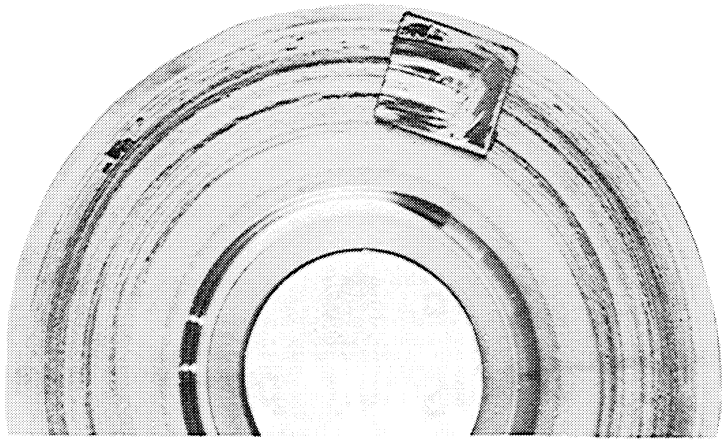

Al DISK

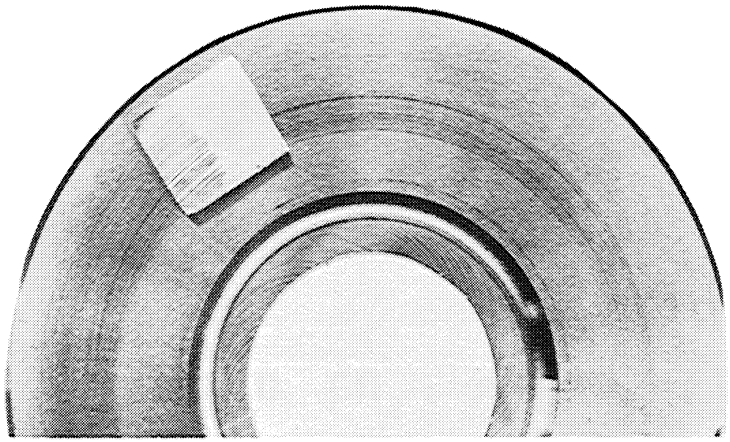

STEEL DISK

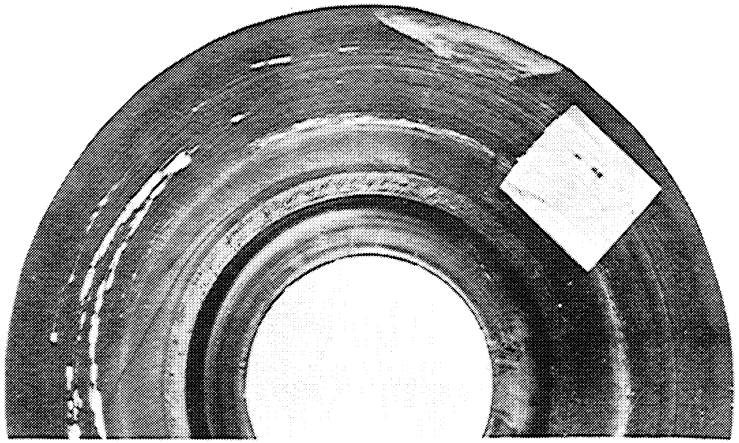

Cu DISK

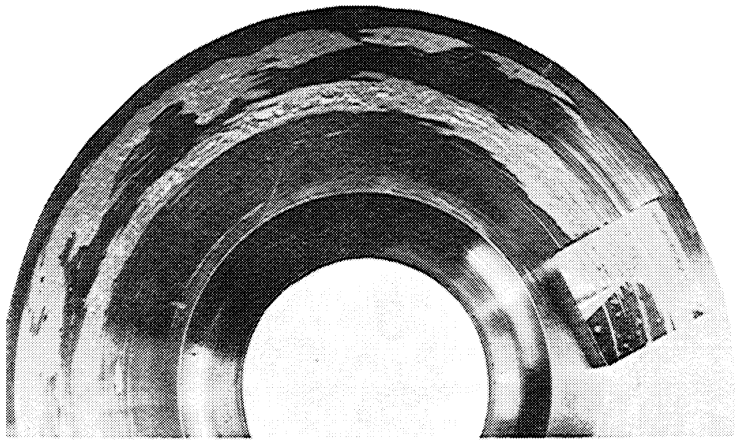

Ag DISK

Figure 5. Silver sliders against each of the four disk materials.

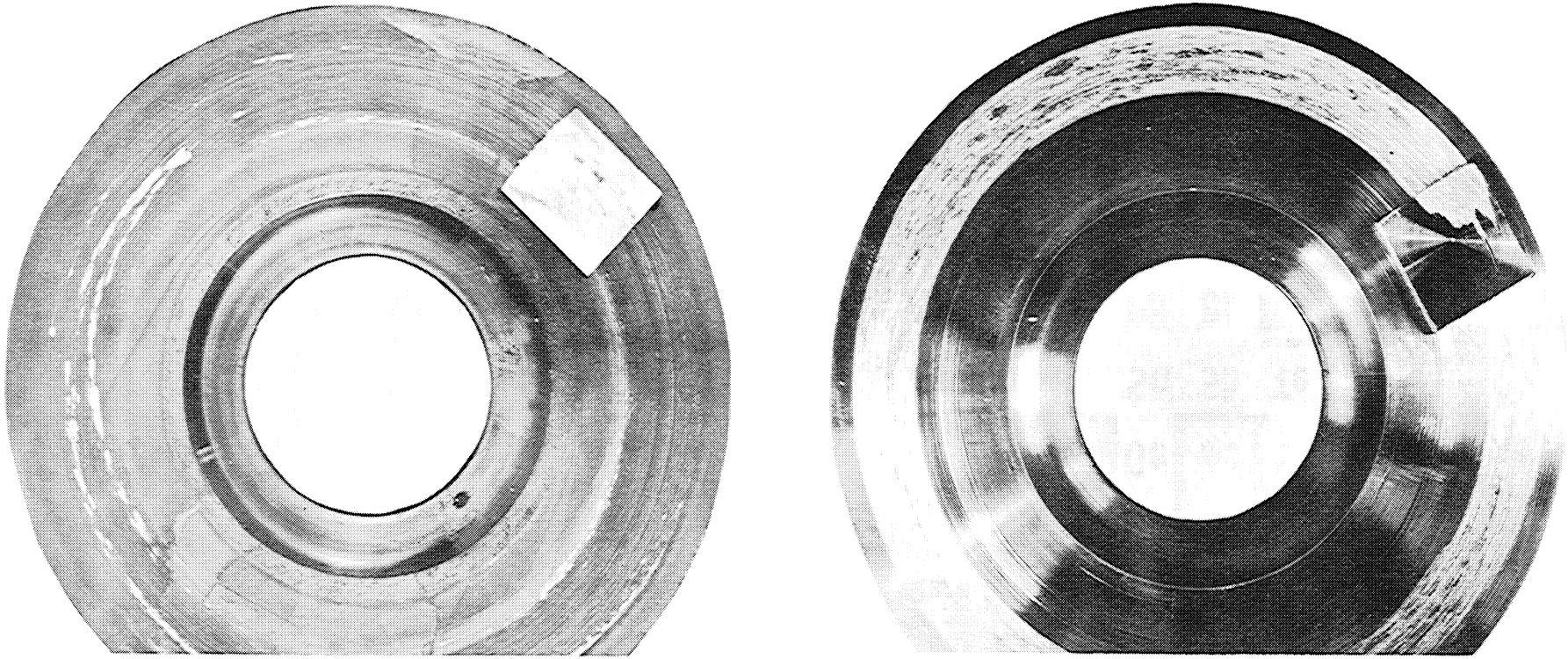

Figure 6. The effect of reversing a pair of metals.

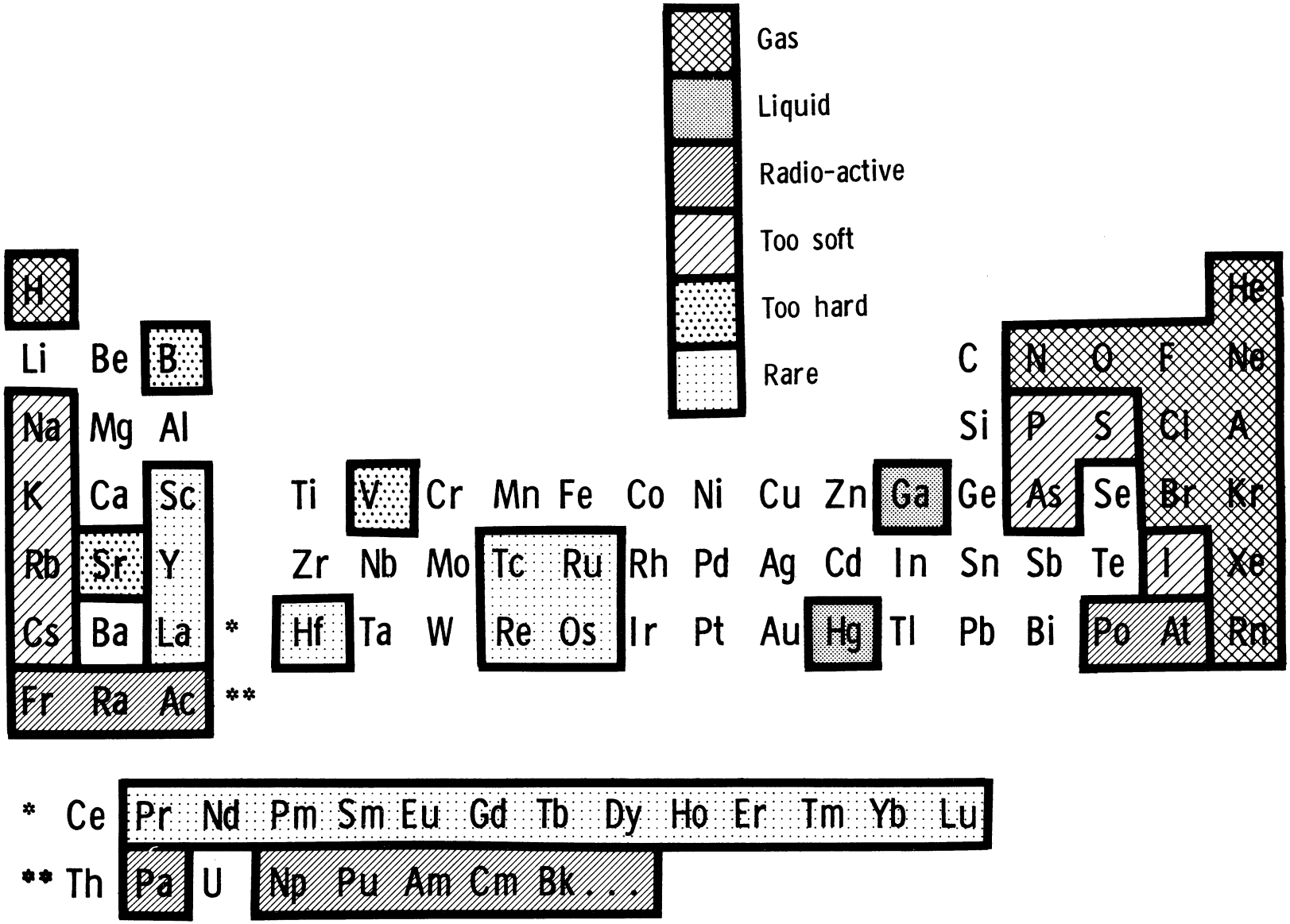

Figure 7. The elements rejected for sliders.

Li	Be													C				
	Mg	Al												Si				
	Ca		Ti		Cr	Mn	Fe	Co	Ni	Cu	Zn			Ge		Se		
			Zr	Nb	Mo			Rh	Pd	Ag	Cd	In		Sn	Sb	Te		
	Ba	*		Ta	W			Ir	Pt	Au		Tl		Pb	Bi			

* Ce

** Th U

Figure 8. The elements used for sliders.

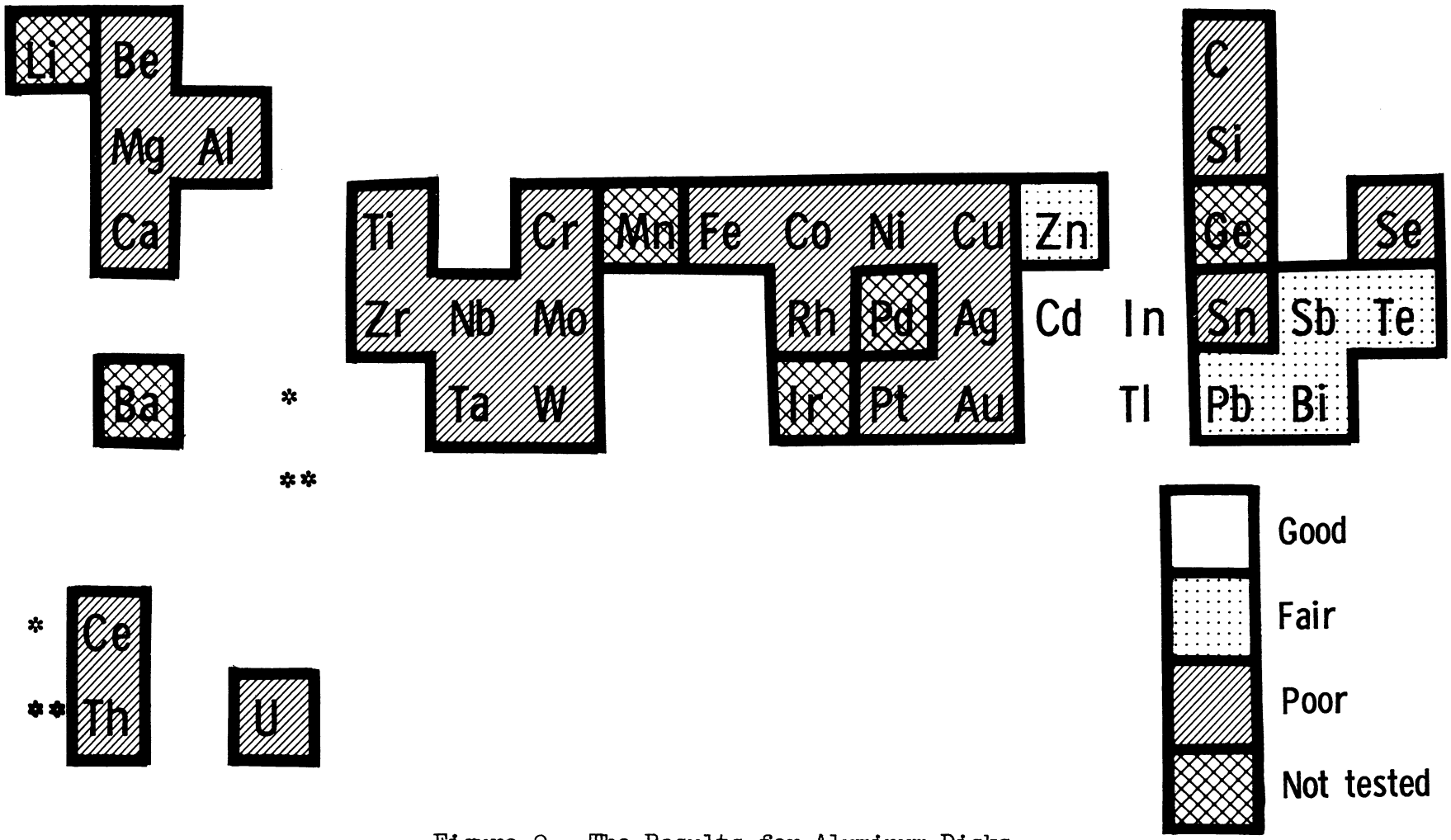

Figure 9. The Results for Aluminum Disks.

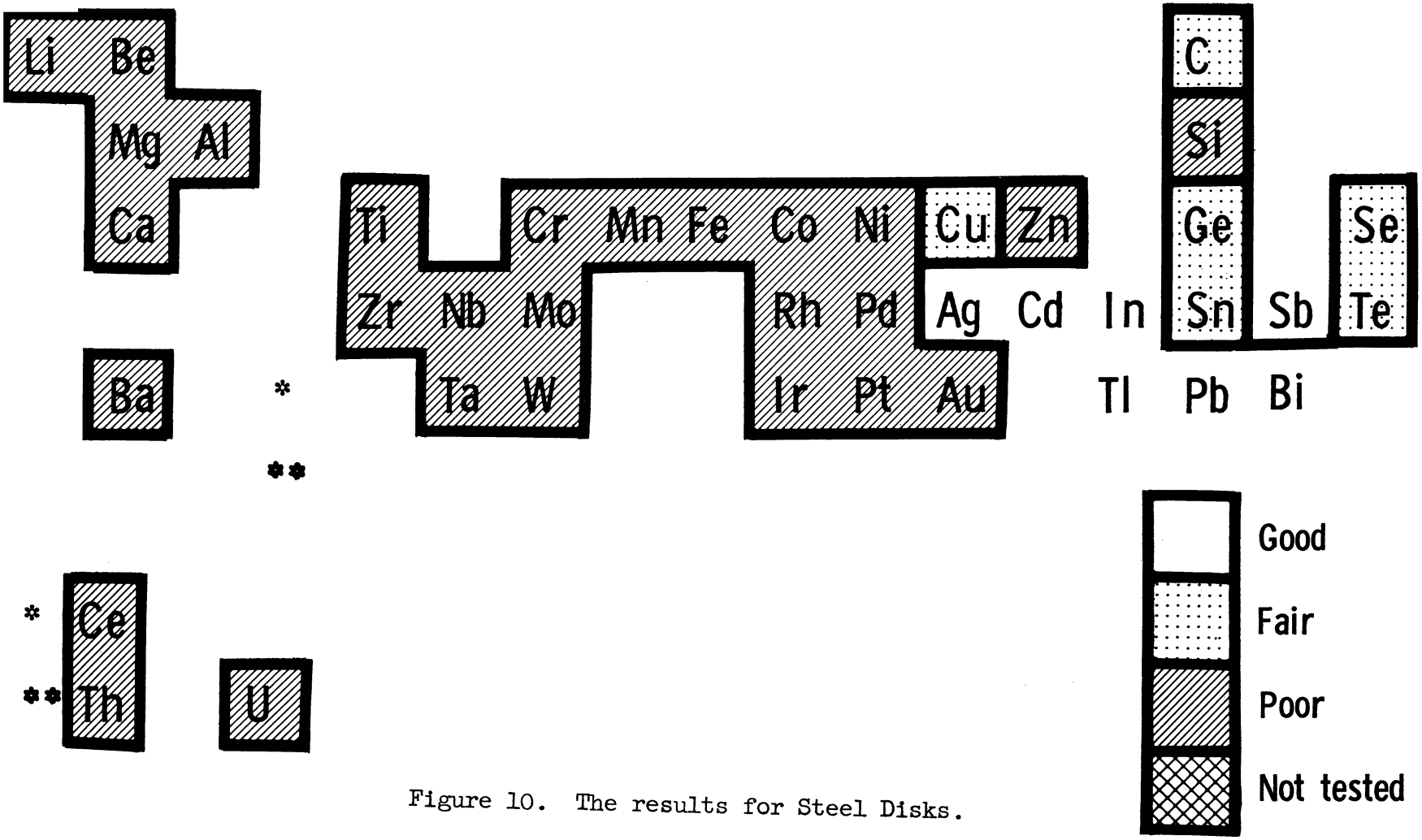

Figure 10. The results for Steel Disks.

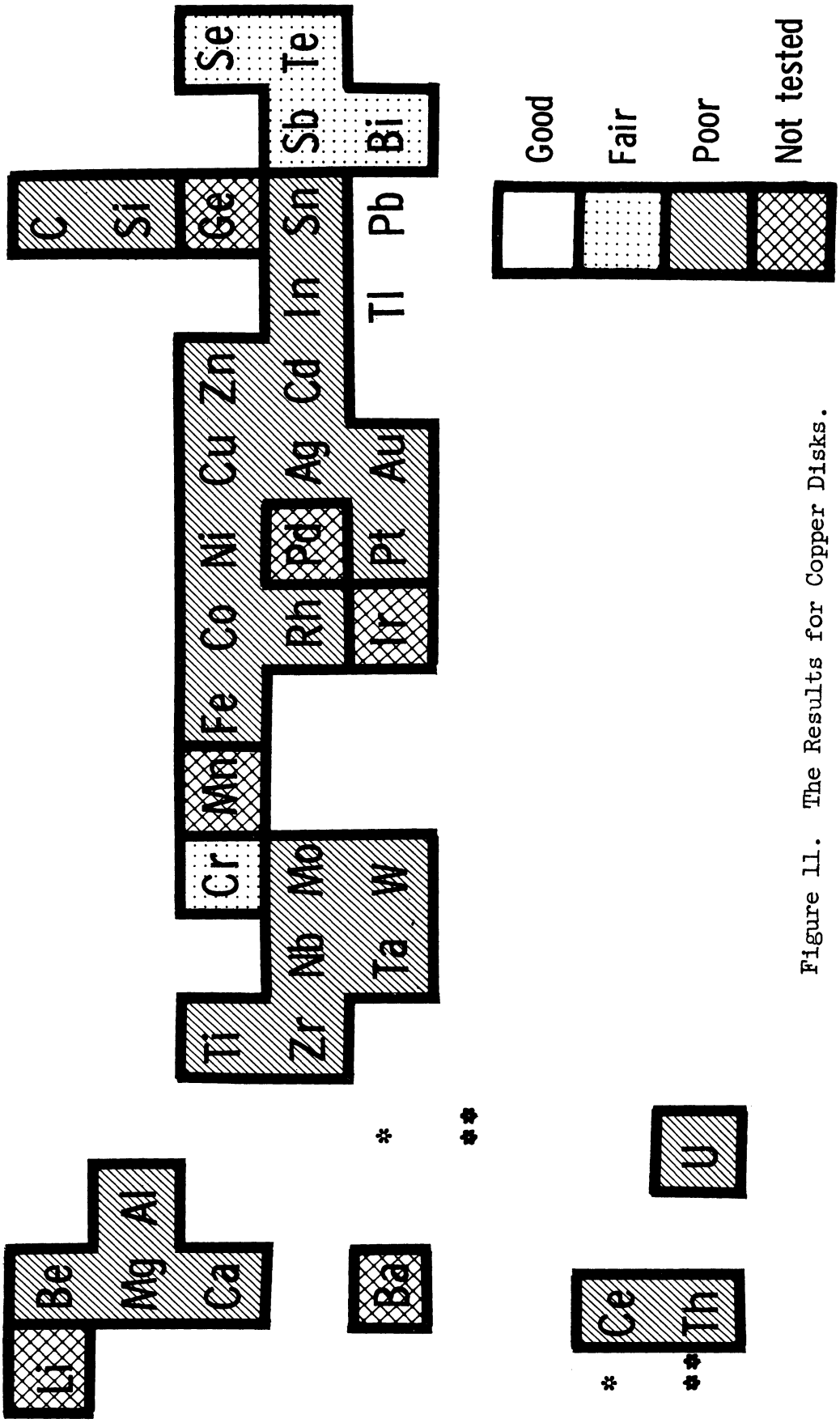

Figure 11. The Results for Copper Disks.

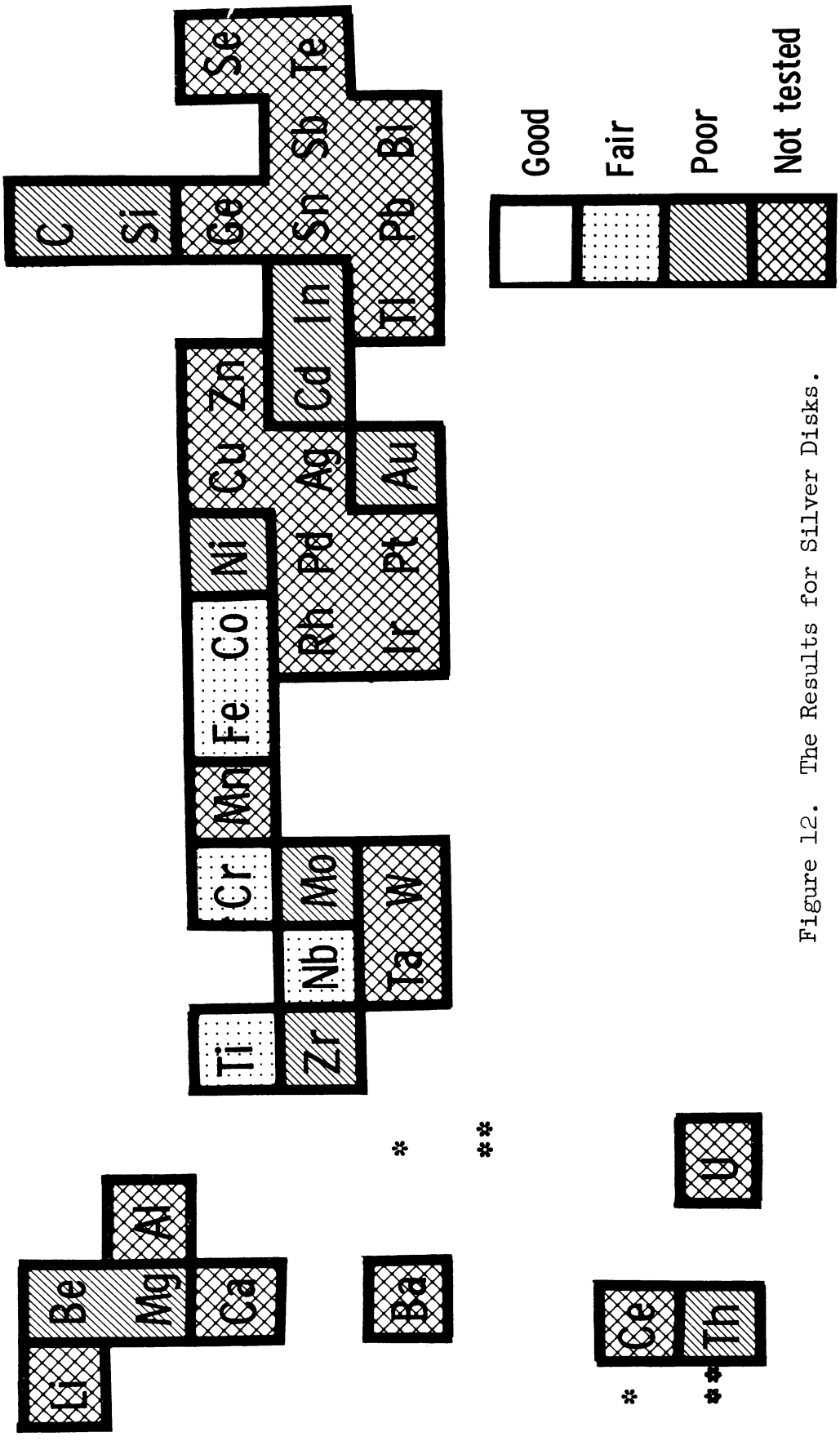

Figure 12. The Results for Silver Disks.

Table 1

Soluble Pairs With Poor Score Resistance

Aluminum Disk	Steel Disk	Copper Disk	Silver Disk	
Be	Be	Be	Be	Beryllium
Mg		Mg	Mg	Magnesium
Al	Al	Al		Aluminum
Si	Si	Si	Si	Silicon
Ca		Ca		Calcium
Ti	Ti	Ti		Titanium
Cr	Cr			Chromium
	Mn			Manganese
Fe	Fe			Iron
Co	Co	Co		Cobalt
Ni	Ni	Ni		Nickel
Cu		Cu		Copper
	Zn	Zn		Zinc
Zr	Zr	Zr	Zr	Zirconium
Nb	Nb	Nb		Niobium
Mo	Mo	Mo		Molybdenum
Rh	Rh	Rh		Rhodium
	Pd			Palladium
Ag		Ag		Silver
		Cd	Cd	Cadium
		In	IN	Indium
Sn		Sn		Tin
Ce	Ce	Ce		Cerium
Ta	Ta	Ta		Tantalum
W	W	W		Tungsten
	Ir			Iridium
Pt	Pt	Pt		Platinum
Au	Au	Au	Au	Gold
Th	Th	Th	Th	Thorium
U	U	U		Uranium

Table 2

Insoluble Pairs, Neither From the B-Subgroup,
With Poor Score Resistance

Steel Disk	
Li	Lithium
Mg	Magnesium
Ca	Calcium
Ba	Barium

Table 3

Insoluble Pairs, One From the B-Subgroup,
With Fair or Good Score Resistance

Aluminum Disk	Steel Disk	Copper Disk	Silver Disk	
	C (fair)			Carbon
			Ti (fair)	Titanium
		Cr (fair)	Cr (fair)	Chromium
			Fe (fair)	Iron
			Co (fair)	Cobalt
		Ge (fair)		Germanium
	Se (fair)	Se (fair)		Selenium
			Nb (fair)	Niobium
	Ag			Silver
Cd	Cd			Cadium
In	In			Indium
	Sn (fair)			Tin
	Sb (fair	Sb		Antimony
Te (fair)	Te (fair)	Te (fair)		Tellurium
Tl	Tl	Tl		Thallium
Pb (Fair)	Pb	Pb		Lead
Bi (fair)	Bi	Bi (fair)		Bismuth

Table 4

Soluble Pairs With Fair or Good Score Resistance

Aluminum Disk	Steel Disk	Copper Disk	
	Cu (fair)		Copper
Zn (fair)			Zinc
		Sb (fair)	Antimony

Table 5

Insoluble Pairs, One From the B-Subgroup, With Poor Score Resistance

Aluminum Disk	Steel Disk	Copper Disk	Silver Disk	
C		C	C	Carbon
			Ni	Nickel
Se				Selenium
			Mo	Molybdenum

REFERENCES

1. Lunn, B., "Some Experiments with Sleeve Bearing Materials," Transactions of the Danish Academy of Technical Sciences, Volume 2, 1952. (This reference is included because of its excellent bibliography.)

2. Underwood, A.F., "Some General Aspects of Rubbing Surfaces," Proceedings of the Special Summer Conference on Friction and Surface Finish, Massachuestts Institute of Technology, 1940.

3. Roach, A.E., Goodzeit, C.L., and Hunnicutt, R.O., "Scoring Characteristics of Thirty-eight Different Elemental Metals on High-speed Contact with Steel, American Society of Mechanical Engineers, paper number 54-A-61, 1954.

4. Goodzeit, C.L., "Compatability of Metals in Bearing Contact," American Society of Mechanical Engineers, paper number 58-MD-9, 1958.

5. Bowden, F.P., and Tabor, D., The Friction and Lubrication of Solids, Clarendon Press, Oxford, England, 1950.

6. Mott, B.W., "Liquid Immiscibility in Metal Systems," The Philosophical Magazine, Volume 2, 1951.

FRICTION, WEAR, AND SURFACE DAMAGE OF METALS AS AFFECTED BY SOLID SURFACE FILMS

Edmond E. Bisson
Assistant Chief, Fluid System Division
National Advisory Committee for Aeronautics

FRICTION, WEAR, AND SURFACE DAMAGE OF METALS AS AFFECTED BY SOLID SURFACE FILMS

by

Edmond E. Bisson

INTRODUCTION

Since this summer course is directed toward the problem of surface damage, it would be well to look at the fundamental aspects of how such surface damage may originate between surfaces in sliding. In the first place, this discussion will be limited to the case of boundary lubrication as contrasted to fluid lubrication. Figure 1 shows these two regions. The curves are curves, for a plain journal bearing, of friction coefficient and film thickness plotted against the well-known parameter ZN/P: Z is viscosity, N is rpm, and P is load. To the right of the dashed vertical line is the region of fluid lubrication; that is, thick, film lubrication, where the surface asperites are completely separated by an oil film of such thickness that no metal-to-metal contact can occur. To the left of the dashed vertical line is the region of boundary or thin film lubrication. As noted in the upper right-hand sketch, the film thickness in boundary lubrication is so small that asperities can, and do, contact through the oil film.

In the case of fluid or thick film lubrication, only the properties of the lubricant are of importance since the asperities do not contact. In the case of boundary or thin film lubrication, the properties of the metals are of primary importance since there is true metal-to-metal contact at the asperities. While the properties of the lubricant under these conditions are of secondary importance, they are not to be neglected since they can strongly influence the type of damage which will occur. The lubricant in this case is serving as a contaminant. This will be discussed in more detail later.

As is well known, the presence of a contaminating film between sliding surfaces can have a marked effect on friction, wear, and surface damage. (A contaminant is defined as any material other than those comprising the sliding surfaces.) Some contaminants are beneficial (lubricants) while others are detrimental (abrasives). Considerable evidence indicates the importance of solid surface films to the friction, wear, and surface failure properties of sliding surfaces.[1-8] Physical and chemical surface changes have been associated with either satisfactory or unsatisfactory operations of metallic sliding surfaces.[2] As an example, "run-in" has long been known to be effective in improving the performance and the load-carrying capacity of surfaces. Among the factors that lead to satisfactory performance are the formation and

maintenance of certain beneficial solid surface films. Some solid film can be formed on sliding surfaces by use of extreme pressure additives in lubricants. Theories for the mechanism of extreme pressure lubrication are discusses in references 3 and 8. Other solid films may be formed naturally, such as by reaction of metallic surfaces under sliding conditions with the ambient atmosphere. Again, other solid films may be preformed and thereafter maintained by proper supply of the lubricating component.

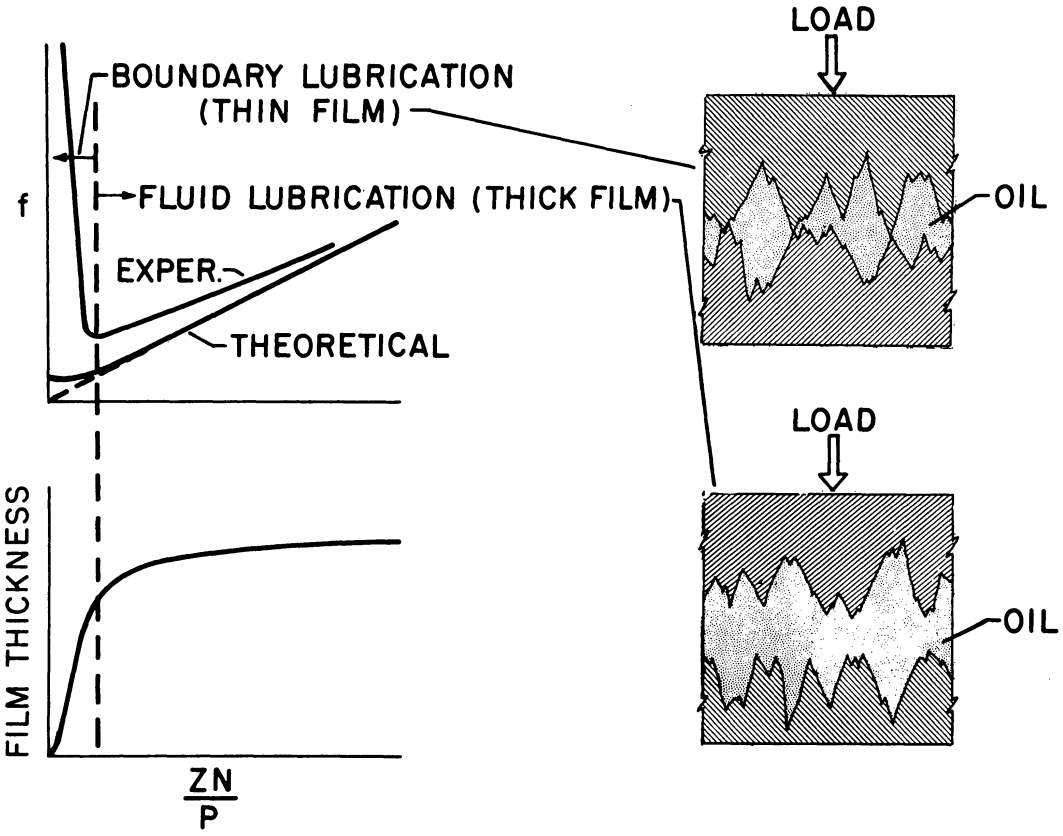

Figure 1. Definition of boundary and fluid lubrication.

The purposes of this paper are:

1. To present the fundamental principles involved in friction and wear.
2. To show the relation of surface films of various types to the friction, wear, and surface damage of sliding metals.

Study of the role of surface films requires consideration of how the film is formed. The film may be:

1. Formed naturally.
2. Preformed
3. Formed by other methods having practical value.

The material covered in this paper is discussed in more detail in reference 9.

THEORY

Analysis of the effects of solid surface films is based on the adhesion theory of friction. This adhesion of friction was advanced by Merchant in the United States,[10] and by Bowden and Tabor in England[8] at about the same time. This theory of friction is based on strong adhesive forces between the contacting asperities. As the load is applied (see upper right-hand sketch of Figure 1), the asperities contact with high stresses at the true contact area. This high stress forces out some of the lubricant and other contaminants. The true area of contact is so small that, following elastic deformation, the stress quickly reaches the yield stress of one of the two materials. Hence, plastic flow occurs and we get a "cleaning" action at the contact area. Because the areas are now somewhat clean, and the stress is relatively high, "cold welding" can occur at the junction. Moving one surface relative to the other now requires shear at this welding junction. Figure 2 presents some of the important concepts of the adhesion theory of friction. This friction theory states that the friction force is equal to the sum of two terms: the first a shear term, the second a ploughing or roughness term. The shear term is that force required to shear at the welded junctions. The ploughing term is that force which results from displacement of the softer of the two metals by an asperity of the hard metal. In many instances the ploughing or roughness term is negligible in comparison to the shear term.

$$\text{FRICTION, } F = S + P = \text{SHEAR} + \text{PLOUGHING} = As + A'p$$

$$\text{CONTACT AREA, } A = \frac{\text{LOAD}}{\text{FLOW PRESSURE}} = \frac{W}{p}$$

$$\text{FRICTION COEFFICIENT, } \mu = \frac{\text{FRICTION}}{\text{LOAD}} = \frac{As}{W} + \frac{A'p}{W} = \frac{s}{p} + \frac{A'p}{W}$$

$$\text{WHEN PLOUGHING TERM IS NEGLIGIBLE,}$$

$$\mu = \frac{s}{p} = \frac{\text{SHEAR STRENGTH}}{\text{FLOW PRESSURE}}$$

Figure 2. Important equations from the adhesion theory of friction.

Each of the two terms comprising the friction force can be represented as the product of an area and a strength--either the shear strength or the flow pressure, Figure 2. The contact area, as is well known, is a function only of load and flow pressure, and is not a function of the apparent area of contact. After the appropriate substitutions are made and the ploughing term is neglegted, the friction coefficient is shown to be equal to the ratio of shear strength to flow pressure.

This last equation shows that, reduction in friction coefficient (and, as will be developed later, reduction in wear) can be obtained if this ratio can be reduced. Reduction of the ratio is obtained with low shear strength or high flow pressure, or both. As is well known, it is extremely unlikely that both low shear strength and high flow pressure can be obtained in any one material. However, by the use of low shear strength films (with thicknesses as small as millionths of an inch) on hard base materials, both desirable conditions may be obtained.(8, page 112) Thus, low shear strength is obtained without appreciable decrease of the yield strength of the combination. The load will, therefore, be supported through the film by the hard base material while shear occurs within the soft thin film. These low shear strength films can be of the following types: oxides, chemical reaction films (chlorides, sulfides, etc.), metals, fluid lubricants, etc.

As an example of the beneficial effect of metallic-plated films, we can consider lead and indium, both of which have very low shear strength. Figure 3 shows some friction results obtained by Bowden and Tabor(8) for lead and indium films on various materials. The solid points are for either solid lead or solid indium. It should be noted that, for equal track widths (which means, in this case, equal shear areas), the friction force is the same whether the films are deposited on metals of various hardnesses or whether the friction force is measured for the solid material. The basic conclusion to be drawn from the results of Figure 3 is that films give low friction, even though the films are relatively thin, when the films are of low shear strength materials.

While there is no direct correlation of friction and wear, it should be noted the adhesion theory of friction shows theoretically that the wear should be considerably reduced if the adhesion between the surfaces can be effectively reduced. The influence of contaminants has, up to this time, been discussed on the basis of reducing shear strength only. However, another important manner in which a contaminant can be beneficial is in its action to reduce the amount of welding by preventing metal-to-metal contact of the "clean" surfaces. It is well know that fluxes must be used to remove contaminants and permit contact of clean surfaces for effective welding. The reverse of this process is, of course, also true. Thus, introduction of a contaminant to prevent contact of clean surfaces should be detrimental to the welding process and should result in less adhesion between the surfaces. This reduced adhesion should, consequently, result in less wear and less metal transfer.

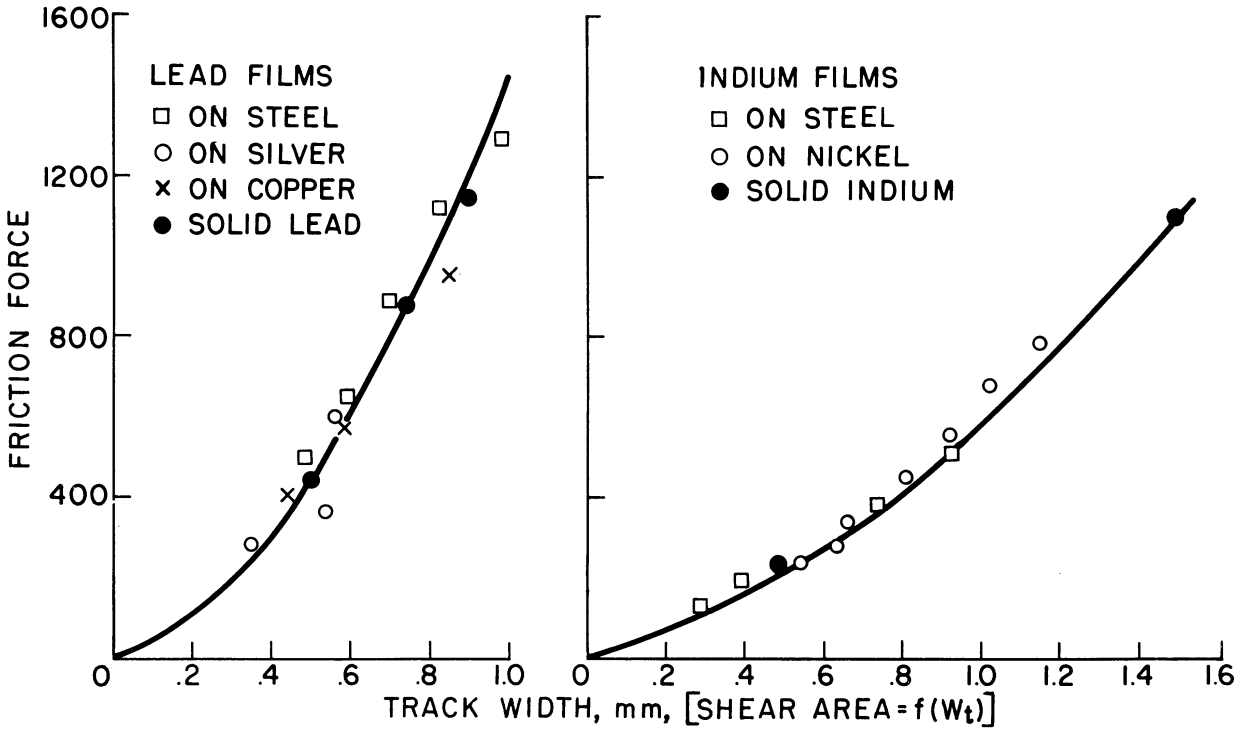

Figure 3. Friction of lead and indium films on various metals.

APPARATUS AND PROCEDURE

Most of the experimental friction and wear studies were conducted with the kinetic friction apparatus shown in Figure 4, or in modifications therof. This apparatus is described in detail in reference 11. The principal elements of the apparatus are the specimens which are an elastically restrained spherical rider and a rotating disk 13 inches in diameter. The rider is loaded by weights applied along its vertical axis. Friction force between the rider and the disk is measured by four strain gages mounted on a beryllium-copper dynamometer ring. A radial-feed mechanism, when operating, causes the rider to traverse a spiral track on the rotating disk; the rider thus slides on virgin surface of the disk. Where solid surface films were investigated, they were usually applied to the disk specimen before testing.

Most of the studies have been made with specimens of steel on steel. Some studies were made with non-ferrous materials such as nickel or copper alloys. The solid films investigated included various oxides, sulfides, and chlorides of iron as well as materials such as molybdenum trioxide. Formation of the various preformed films is described in detail in reference 9. For comparative purposes, a load of 269 g was used in obtaining most of the data presented. This load produces an initial

Hertz surface stress of 126,000 lb/in^2. The friction data presented are typical of data obtained in many runs; for the sake of simplicity, only a typical run is plotted.

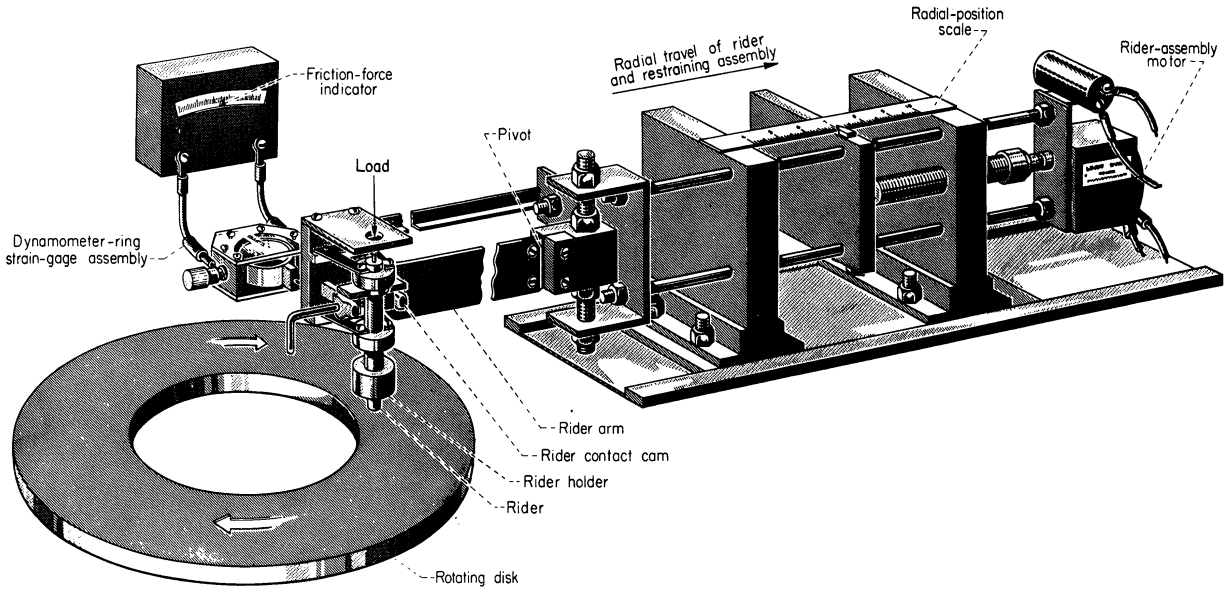

Figure 4. Kinetic-friction apparatus.

RESULTS AND DISCUSSION

Clean Steel on Clean Steel

For steel-on-steel surfaces cleaned by outgassing at 1000° C in vacuum, friction coefficients as high as 3.5 have been measured.[12] These surfaces were considered to be free of ordinary contaminants and most of the oxides. For steel-on-steel surfaces cleaned in air by the method used in experiments of this paper, the maximum friction coefficient of 0.54 were known to have a film of Fe_3O_4 approximately 25 A thick (about 10^{-7} in).[13-14] At the higher sliding velocities, Figure 5 shows that a downward trend of friction coefficient is obtained. For steel-on-steel surfaces lubricated with very thin films of either oleic acid or SAE 10 lubricant, the friction coefficient was approximately 0.10 at minimum sliding velocity, decreasing to 0.06 at 6,600 ft/min, Figure 5.

Surface appearance of the wear area of the ball specimens for both the dry and lubricated runs are shown in Figure 5. The photomicrographs show that surface failure by welding occurred with the dry specimen; no welding is evident for the lubricated specimens but ploughing is apparent. The welding for dry steel was extensive, resulting in appreciable "tearing-out" and metal transfer.

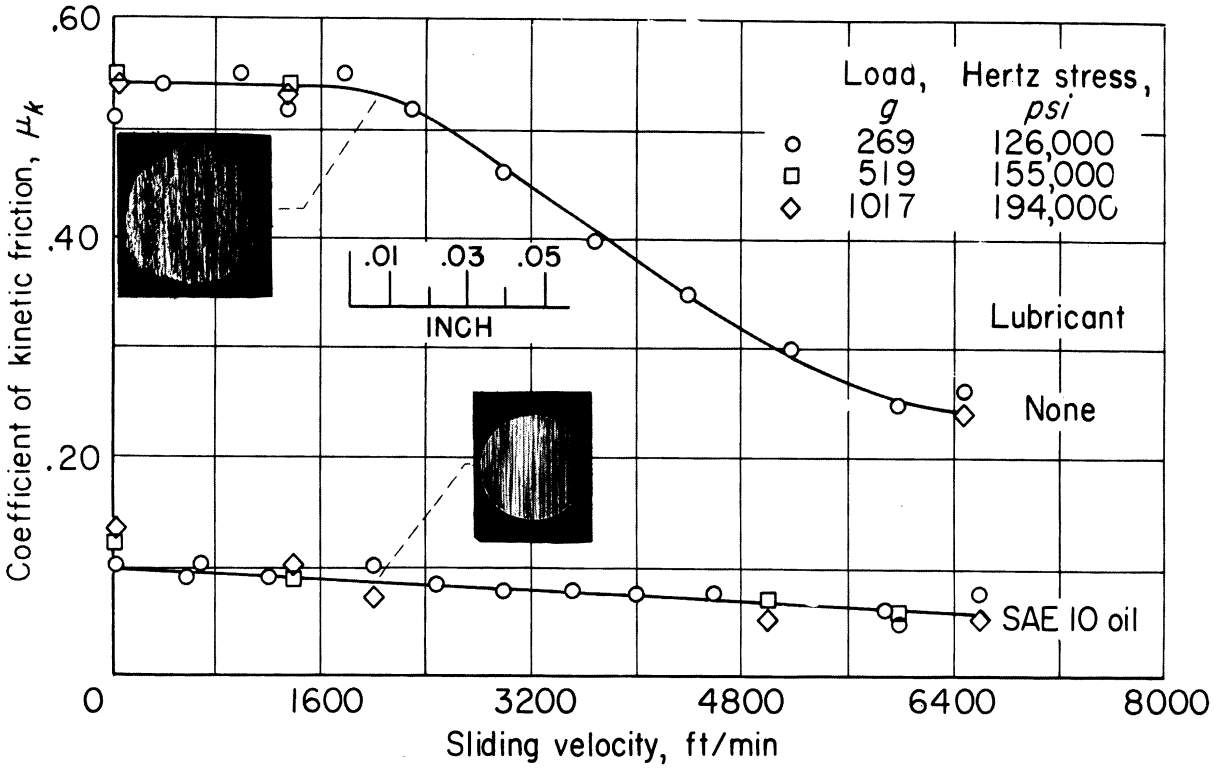

Figure 5. Friction at high sliding velocities of steel. Insets show surfaces of rider specimens after tests.

Naturally Formed Surface Films

Iron oxide films. The downward trend of friction coefficient with increase in sliding velocity for the dry steel specimens of Figure 5 is considered a result of formation of beneficial iron oxide films of appreciable thickness. Formation of oxide films would be accelerated at higher sliding velocities because of higher rate of heat generation at the sliding surfaces resulting from the increased release of frictional energy. In partial confirmation of this concept, when the steel slider was permitted to traverse the same wear track on the disk, Figure 6, FeO was identified (by X-ray diffraction) as the chief constituent in the wear debris; there was a coincident reduction in friction coefficient from 0.38 to 0.24. It is reasonable to assume that the FeO film was being formed at all times; also, that the film thickness was built-up with continued traversals of the same track.

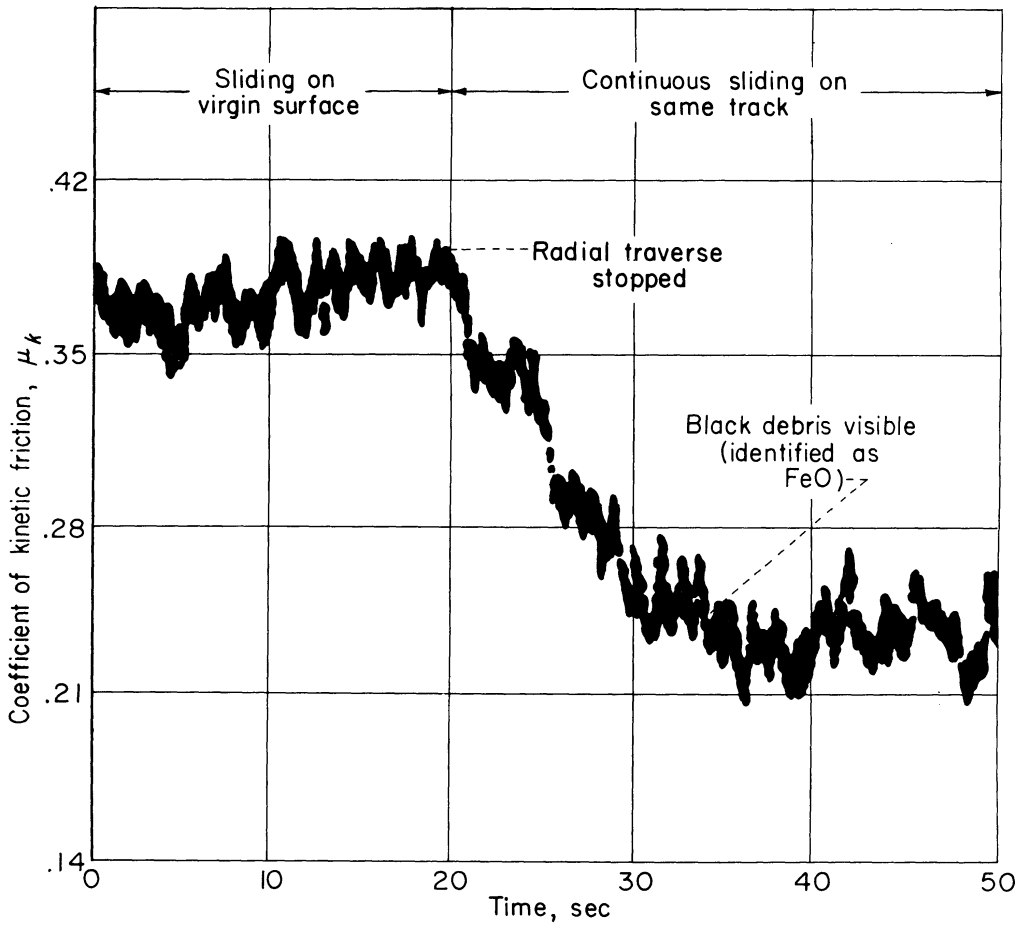

Figure 6. Recording potentiometer trace showing effect of high-velocity sliding over a continuous path (without radial traverse) on coefficient of kinetic friction. Black wear debris (ferrous oxide FeO) was visible at beginning of lower stable friction value. Unlubricated steel; load, 269 grams; sliding velocity, 4000 feet per minute; radius of spherical rider specimen, 1/8 inch.

Since these data show the effect of a naturally formed surface film, it is interesting to study surfaces which are rubbed together under conditions less conducive to formation of naturally formed film. Such a study was made and reported in reference 15.

Data of reference 15 show that prevention of oxide formation by exclusion of oxygen from clean specimens produces a high friction coefficient. Figure 7, from refrence 15, shows that the use of highly purified cetane as a "blanketing" medium produces a friction coefficient greater than 1.0 at high sliding velocities. Similar results on the action of benzene as a "blanketing" medium in metal cutting experiments are reported by Ernst and Merchant;[16] they found that friction coefficient was increased in the presence of benzene and decreased in its absence.

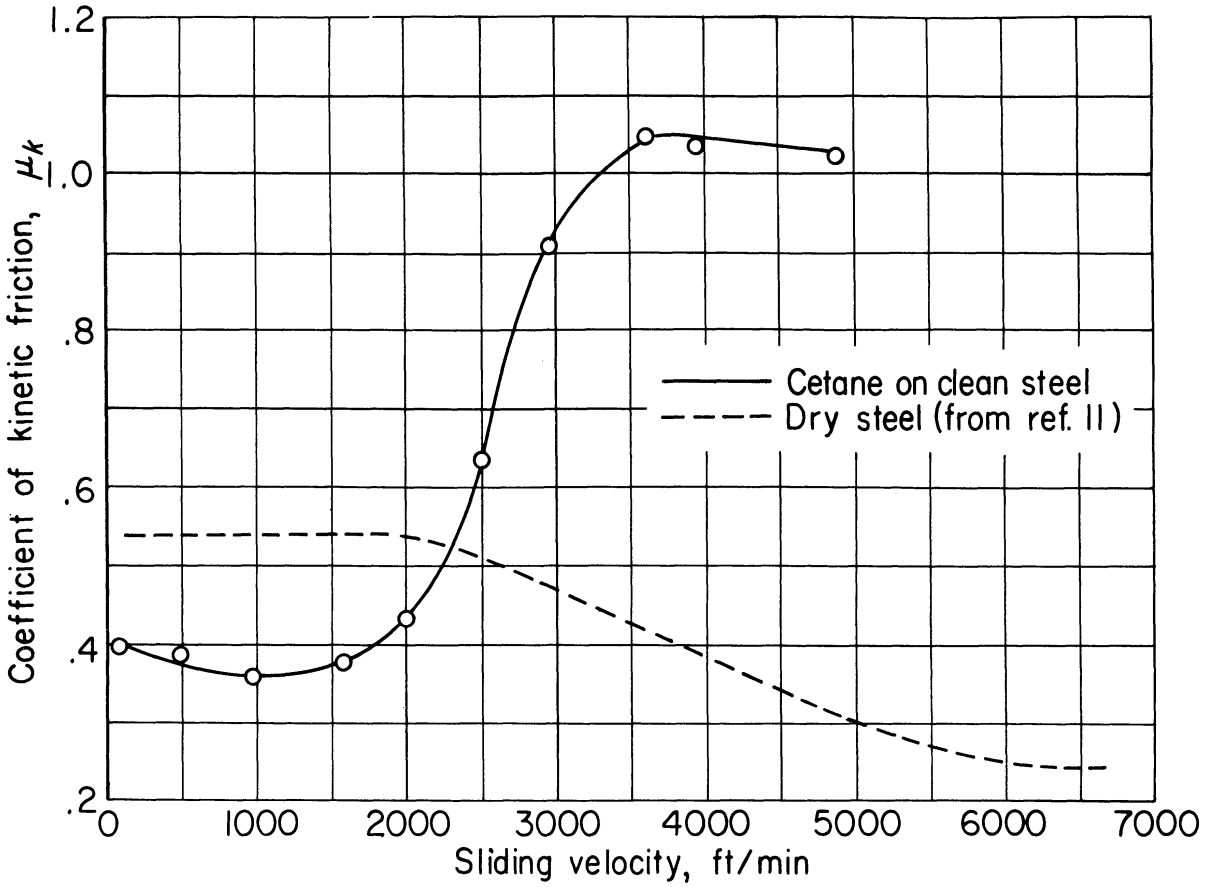

Figure 7. Data showing effect of cetane as blanketing medium (to restrict availability of oxygen to specimen surfaces) on friction of steel against steel. Load, 269 grams; radius of spherical rider specimen, 1/8 inch.

Miscellaneous Films

Figure 8 shows results of wear studies with a number of different materials sliding against SAE 52100 steel. These are plots of wear versus time and the marked differences in wear characteristics are evident. These data are from reference 17. Additional data of this nature are presented in reference 18. Analysis of the wear data, and study of the specimens from references 17 and 18 were made to correlate wear with formation of surface films. The results of these studies showed that, of the various materials, those which resulted in the best performance (from the standpoint of both surface damage and wear) were materials which formed beneficial surface films. The surface films were believed to be either:

1. Derived from within the structure of the various materials (graphitic carbon in the nodular iron and lead in the bronze),

or

2. Formed by oxidation (nickel oxides on the nickel alloys).

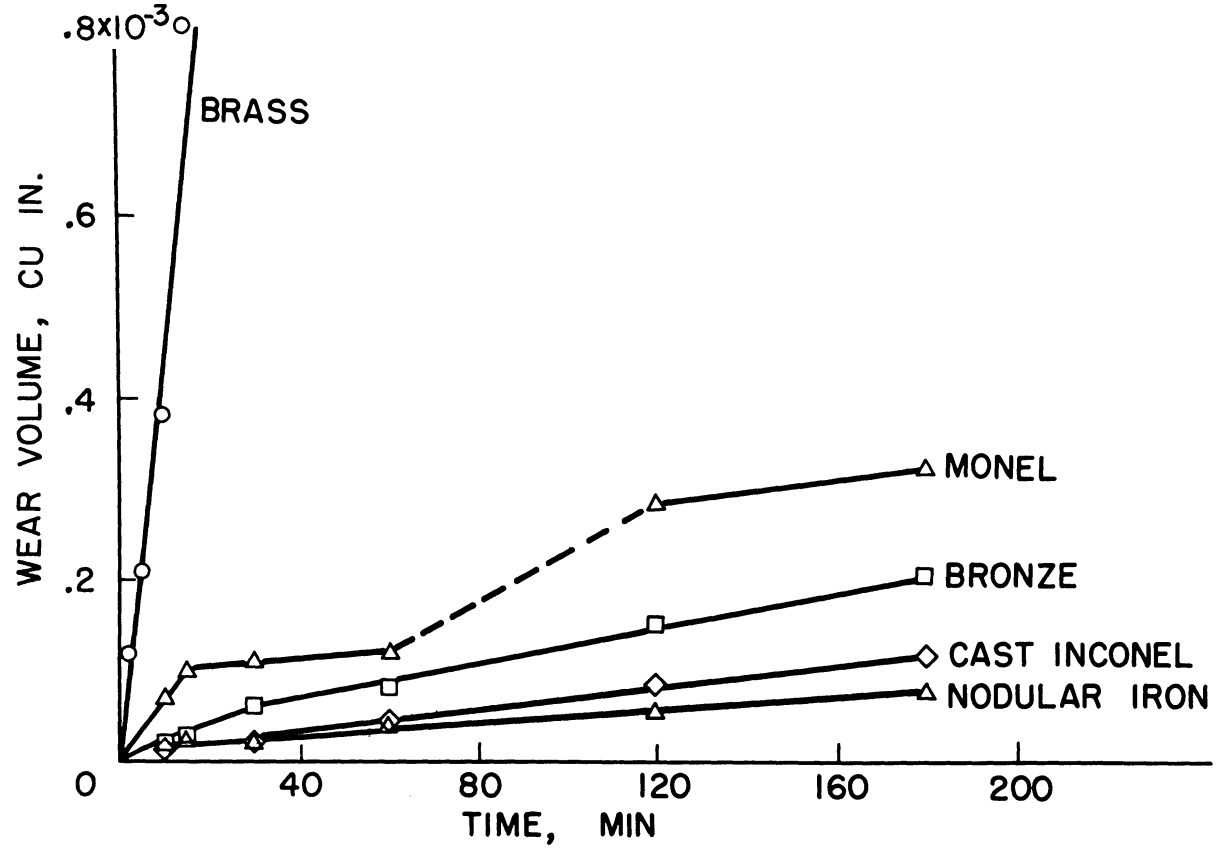

Figure 8. Wear of several cage materials.

Nickel oxide. It was observed[19-20] that good performance (low wear and prevention of surface damage) of nickel alloys was obtained when a surface film of NiO was present. Research by the NACA[21-22] has also shown that, with increase in temperature, wear of Inconel sliding against steel decreases. This result would be expected, since an oxide film could form more readily at the higher temperatures. The reduction in both wear and friction with increase in temperature is shown in Figure 9. The data show that wear at temperatures between 600° and 1000° F is approximately one-twentieth that at 80° F.

The effect of the film on wear was checked with two types of experiment: in the first, specimens with preformed NiO films were tested; in the second, an attempt was made to prevent the natural formation and repair of the oxide film by limiting the availability of oxygen to the specimens. Films were performed by two methods. One film was preformed on a cast Inconel specimen by making a wear run in air at 1000° F; a room-temperature wear run was then made with this same specimen. As indicated in Figure 9(a), the wear rate was approximately one-tenth of that obtained with an untreated specimen. The second method of preforming the film on cast Inconel was by heating it in molten caustic, NaOH.

The specimen was then run at room temperature, and the data, Figure 9(a), show that wear was again approximately one-tenth of that obtained under similar conditions with an untreated specimen of the same material.

The experiment involving oxygen availability was made with cast Inconel at 1000° F in an atmosphere of argon. Although some oxide was undoubtedly formed (because air was present as a contaminant in the argon), wear was higher by a factor of 4. The wear results at 1000° F in both the air and argon atmospheres are shown in bar form, Figure 10(a); also shown in bar graph form are the wear results at 80° F for Inconel specimens with and without the NiO film, Figure 10(b). These results point to the beneficial effect of the nickel oxide film on both wear and prevention of surface damage.

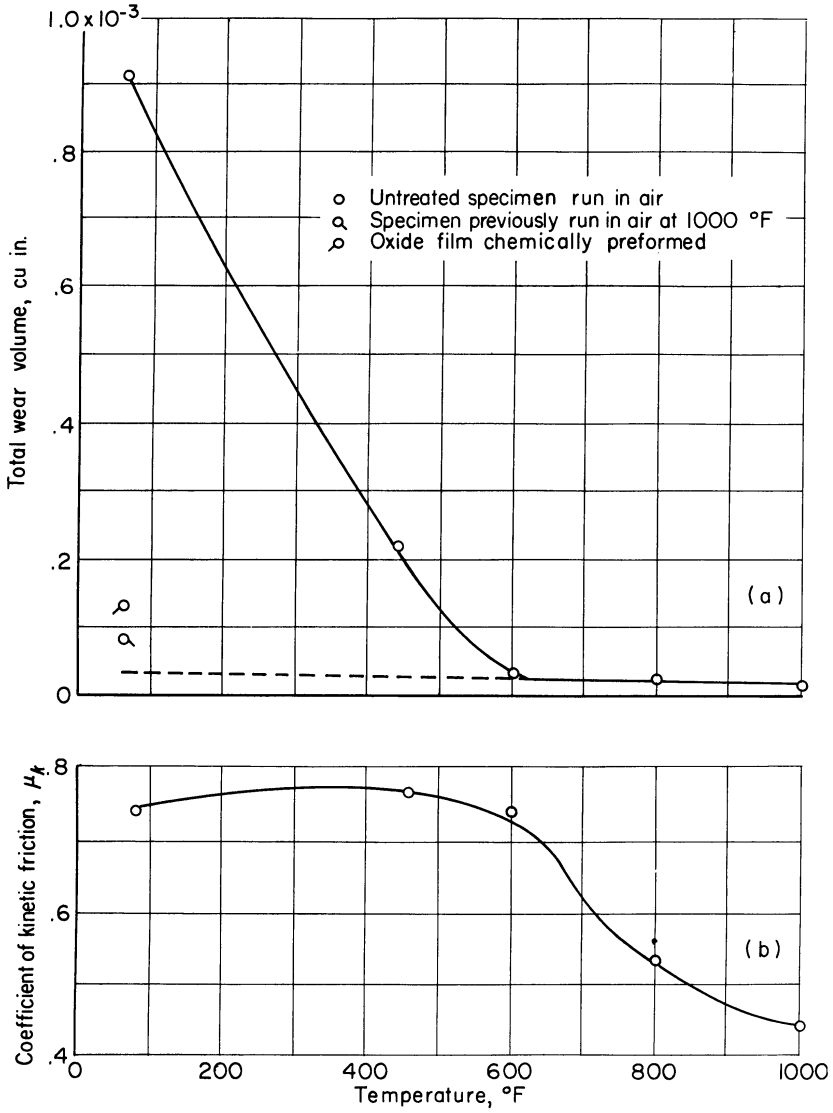

Figure 9. Wear and friction of cast Inconel (rider) sliding against M-10 tool steel (disk) unlubricated. Sliding velocity, 120 feet per minute; load, 1200 grams; radius of spherical rider specimen, 3/16 inch.

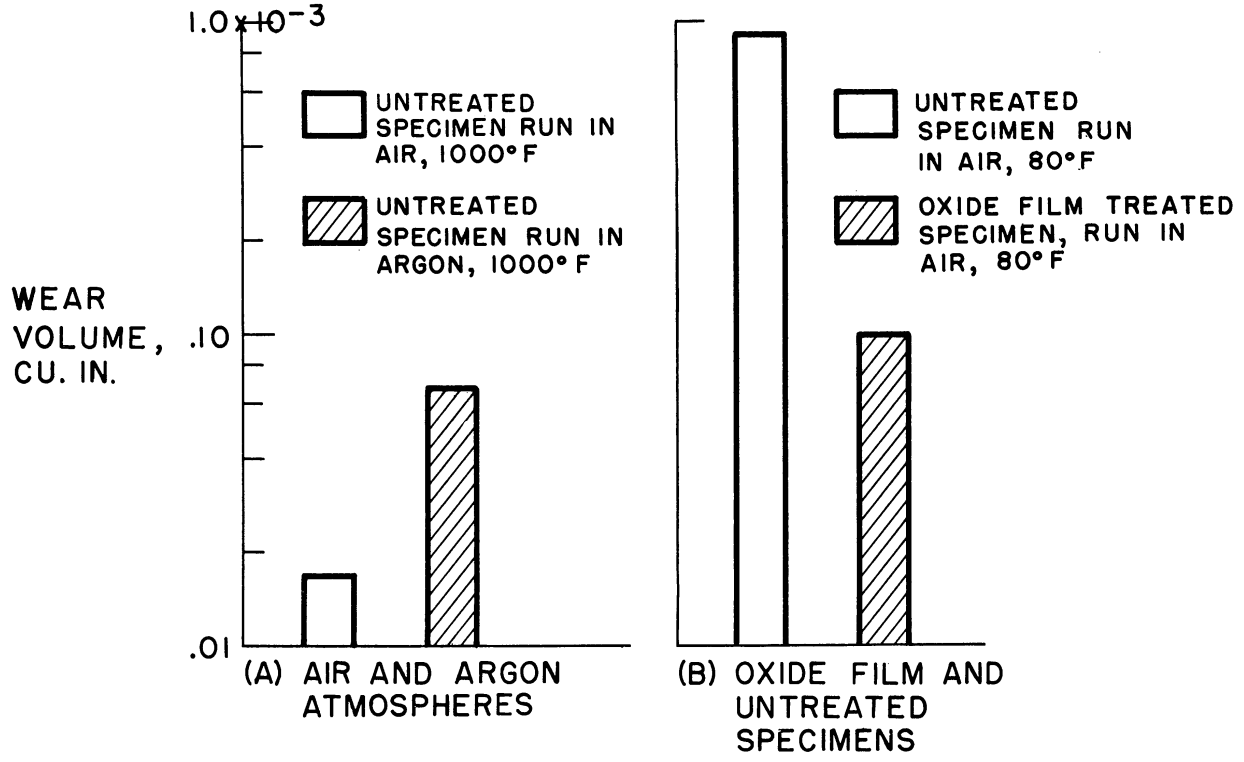

Figure 10. Effect on wear of atmosphere (air or argon) and of surface treatment (oxide treated or untreated).

Preformed Films

Studies were made of a number of preformed solid films of the type formed: 1- naturally (as in the case of oxides), 2- by chemical reaction of surfaces with active additives, or 3- from solid lubricants (such as MoS_2 and graphite) that function as supplemental lubricants.(23)

Iron oxide films. Because of the indicated importance of iron oxides, data were obtained on films 1200 A thick of the specific oxides, Fe_3O_4 and Fe_2O_3. These data, shown in Figure 11, are from reference 24. The friction coefficients, as well as the photomicrographs of the rider surfaces, Figure 11, show that Fe_3O_4 can be quite beneficial in decreasing friction and in preventing surface damage. In comparison, Fe_2O_3 showed high friction, excessive welding, and surface damage.

These data, as well as the data on naturally occurring iron oxide films previously discussed, emphasize the importance of iron oxide films to friction, wear, and surface damage. Effective lubrication under extreme boundary conditions is very often a function also of the nature of the oxide films present.

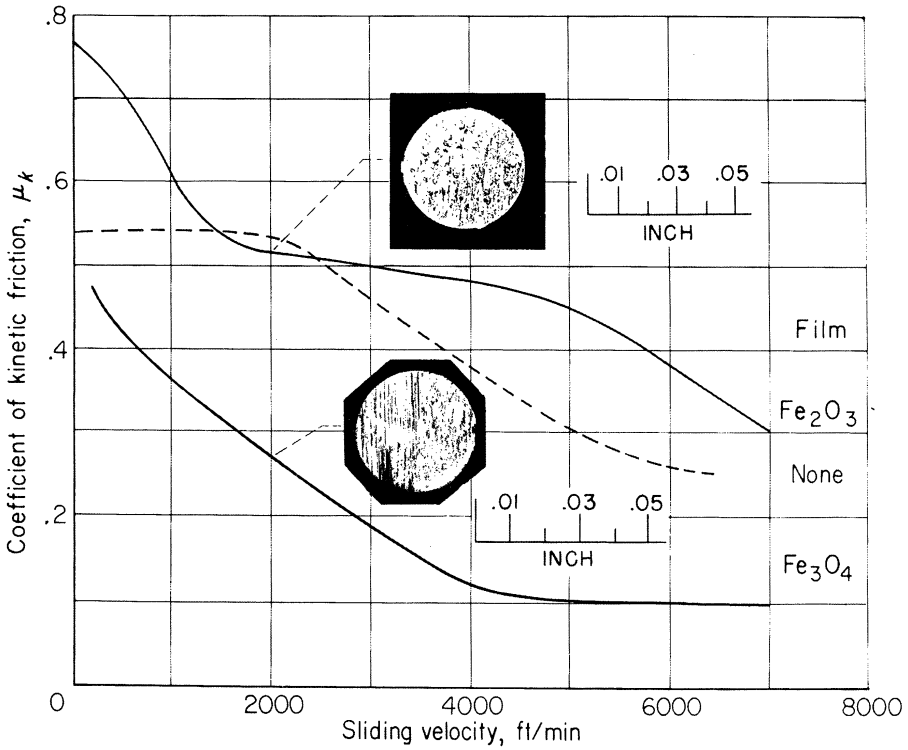

Figure 11. Friction at high sliding velocities of dry unlubricated steel against steel with no film and with preformed films of Fe_3O_4 and Fe_2O_3 approximately 1200 A thick. Radius of spherical specimen, 1/8 inch. Insets show surface of rider specimens after test.

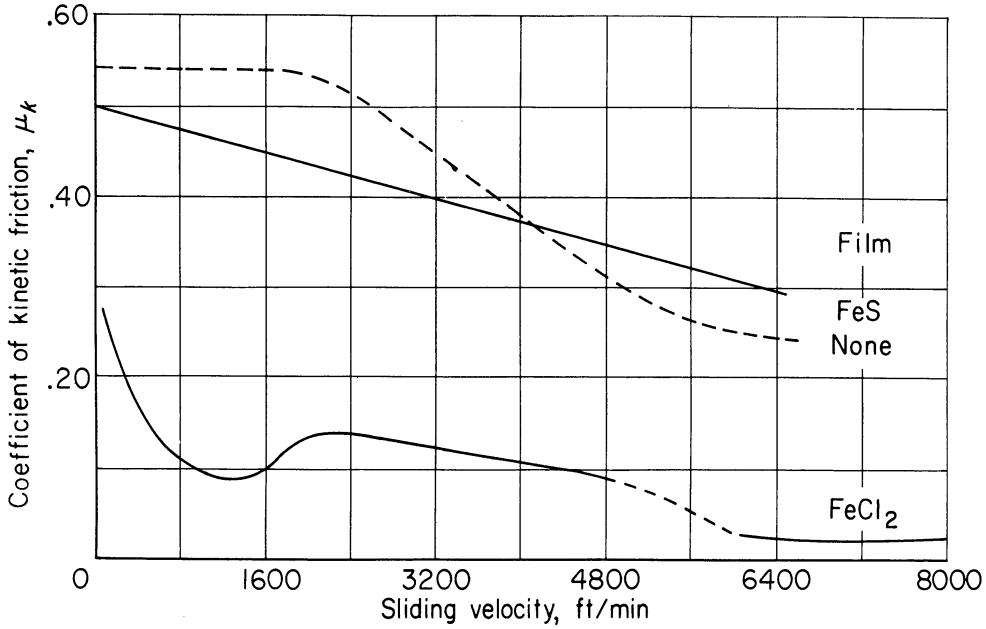

Figure 12. Friction at high sliding velocities of steel against steel with no film and with preformed films of $FeCl_2$ and FeS approximately 1000 A thick. Radius of spherical rider specimen, 1/8 inch.

Chlorides and sulfides. The mechanism of extreme pressure lubricants is considered to be one of chemical reaction between active additives and the metal surfaces. With steel surfaces, iron compounds of chlorine, sulfur, or phosphorus are formed, depending upon the type of additive used. Results of an investigation[24] on preformed chloride and sulfide films approximately 1000 A thick are shown in Figure 12. Visual examination of the surfaces showed that both FeS and $FeCl_2$ are effective in preventing excessive surface damage; $FeCl_2$ is much more effective than FeS, however, in reducing friction, Figure 12.

Solid lubricants. As indicated in reference 25, a "self-repairing" film is the most effective means of maintaining a film at the surface. Other types of film are, however, effective for limited periods of time. In 1947 a review was made of the properties of a number of possible solid lubricants. Based on this review, graphite and MoS_2 were chosen as the most promising solid lubricants of those available at that time. Experimental friction results with preformed films of these two materials are shown in Figure 13. These data are discussed in datail in reference 24. At low speeds, friction is approximately the same; at higher speeds, friction of MoS_2 is lower. Visual observation of the rider specimens indicated that some welding had occurred with the graphite film and none with the MoS_2 film. Occurrence of welding with the graphite film may have been affected by one of two factors: 1- manner of film formation, or 2- humidity. An important difference between the graphite and the MoS_2 film was the manner in which the two films were formed. The graphite film was a rubbed film and may not have adhered well or been completely continuous on the surface. The MoS_2 film was continuous film bonded to the surface by the corn syrup method described in reference 26. The second involves the presence or absence of absorbed water films. At the higher speeds, since the frictional heat generated was greater, it is possible that some desorption of the water films at the surface of the graphite occurred, thus reducing the lubricating effectiveness of the graphite.

The friction of possible solid lubricants with varied crystal structure was determined in order to check lubricating effectiveness and to further understand the basis of their lubricating action. The results of this investigation are reported in detail in reference 27. These experiments were run using three hemispherically tipped riders sliding in a single circumferential path on a flat disk covered with the powered solid lubricant. Friction-time curves were obtained for each solid. Typical friction and wear data are shown in Table 1.

The criterion selected for comparing solid lubricants was that the best solid lubricant was the one that had the lowest coefficient of of friction and the lowest slope on the friction-time curve while giving low wear. Using this criterion, the best solids tested were MoS_2, zinc stearate, graphite, cadium chloride, lead iodide, cobalt chloride and tungsten disulfide; other layer lattice solids that were effective are

mercury iodide and silver sulfate. Not all layer lattice solids were effective lubricants; for example, barium hydroxide, titanium sulfate and sodium sulfate. Effectiveness as a solid lubricant seemed to be associated with the formation of adherent films on both mating specimens. Some low shear-strength solids that do not have a layer lattice were tested and gave initial surface protection. One of the most important results of this investigation was establishing the relative effectiveness of the solid lubricants; they are listed in order of decreasing effectiveness in Table 1. Wide variations in friction coefficients are obtainable with MoS_2 depending on film thickness, humidity, and other variables. This result may be characteristic of many solid lubricants.

TABLE I. - LUBRICATING EFFECTIVENESS OF VARIOUS SOLID LUBRICANTS

[Information from ref. 27. (Listed in order of decreasing effectiveness.) Sliding velocity, 5.7 ft/min; Load, 40 lb; Atmosphere, dry air except for the case of graphite.]

Material	Purity	Coefficient of friction after 30 min. sliding	Slider wear area, sq in.
MoS_2	Possibly slight oxide present	0.05	0.0016
CdI_2	Chemically pure	.06	.0023
$CdCl_2$	Chemically pure	.07	.0019
WS_2	Unknown	.08	.0018
Ag_2SO_4	Chemically pure	.14	Negligible
PbI_2	Chemically pure	.28	.0018
Graphite (run-in moist air)	Purified commercial lubricant small particle size	.11	.0034
$Zn(C_{18}H_{35}O_2)_2$	Chemically pure	.11	.0032
$CoCl_2$	Prepared by dehydration	.10	.0020
HgI_2	Chemically pure	.18	.0021
$CuBr_2$	---	.06	.0021
AgI	Chemically pure	.25	.0033
SAE 60 (for comparison only)	---	.11	.0020

Note: Solids studied that were ineffective lubricants include: $NiCl_2$, $Ca(OH)_2$, $Mo(OH)_2$, TiS_2, I_2, $HgCl_2$, $PbCl_2$, AgCN, CuCl, Na_2SO_4, Fe_3O_4, BN, NiO, Mica, and Talc.

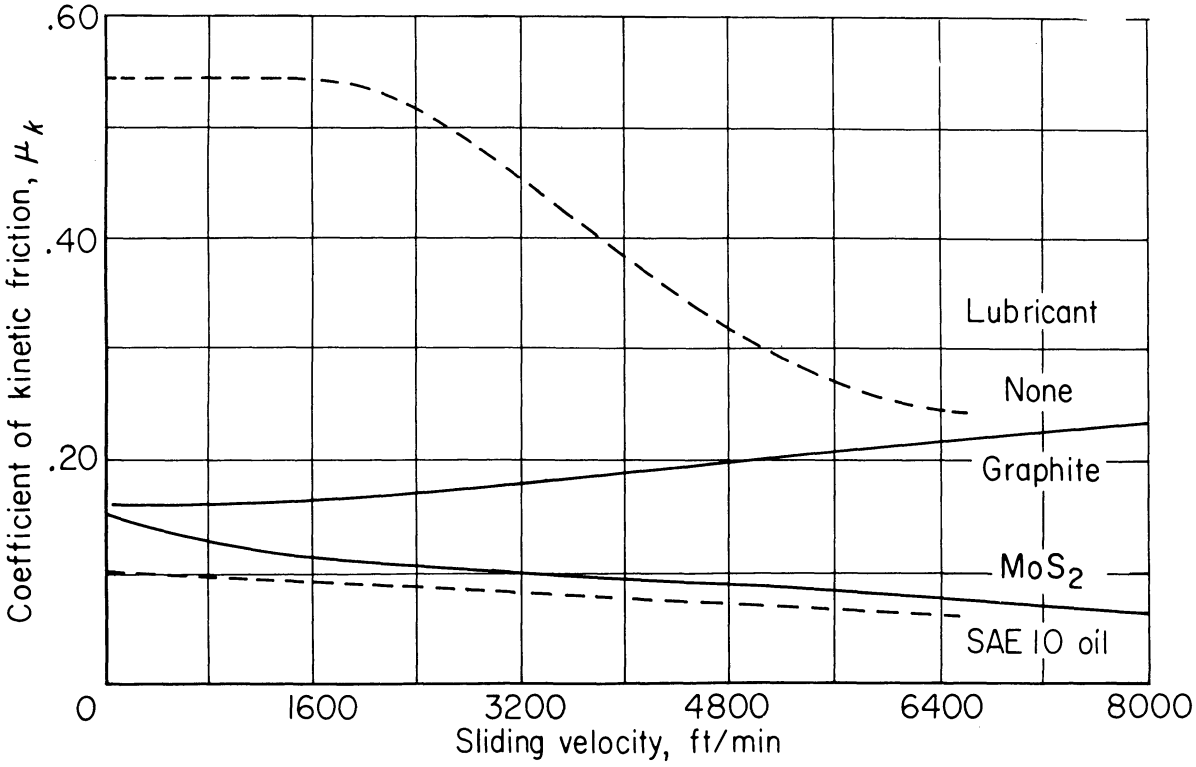

Figure 13. Friction at high sliding velocities of steel against steel with preformed films of MoS_2 and graphite. Radius of spherical rider specimen, 1/8 inch.

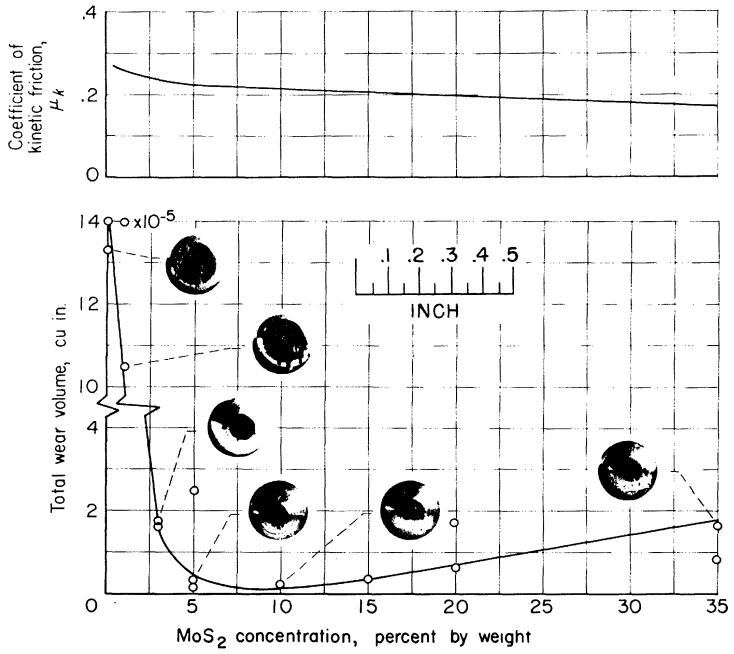

Figure 14. Wear and friction of hot-pressed bearing material containing MoS_2. Rider specimens (on which wear was measured) were composed of 5% copper (by weight), 95-60% silver, and 0-35% MoS_2. Disk specimens were 1020 steel. Sliding velocity, 5000 ft/min; load, 519 grams; time, 60 min; radius of spherical specimen, 3/16 in. Insets show various rider specimens after test.

MoS_2 As a Solid Lubricant

MoS_2 as a minor constituent in powder-metallurgy materials.

An investigation was made[28] to study the lubricating effectiveness of MoS_2 included as a minor constituent in materials made by powder-metallurgy techniques; such bearing materials might be capable of operating successfully even under extreme boundary-lubrication conditions. For these experiments, the rider specimens were powder-metallurgy compacts: copper, 5 per cent (by weight); MoS_2, 0 to 35 per cent, and the remainder silver. Values of friction and wear of these materials are shown in Figure 14.[28] These data show that friction coefficient decreased progressively with increase in concentration of MoS_2. With wear, however, there was a definite optimum in MoS_2 concentration. High wear at low concentrations probably resulted from lack of effective lubrication; high wear at high concentrations probably resulted from lack of physical strength of the material.

In these experiments, welding (as observed visually) was absent for all compacts that contained more than 5 per cent MoS_2. The materials apparently formed an effective lubricating film on the surface by a transfer of solid lubricant from within the structure of the materials. The wear surfaces of the powder-metallurgy compacts, at the various concentrations of MoS_2, are shown after the friction runs (Figure 14).

Oxidation of MoS_2. Since MoS_2 appeared promising in the investigations at room temperature, it was considered as a high-temperature lubricant. An X-ray diffraction investigation of its chemical stability at high temperature was accordingly made.[29] This investigation showed that, in vacuum, there is no change of the MoS_2 at temperatures below 1000°F. In the presence of the oxygen, however, MoS_2 was found to oxidize to molybdenum trioxide, MoO_3, at a very low rate at 750° F; the rate of oxidation increased steadily with increase in temperature as shown in Figure 15.

Since MoO_3 is abrasive, the friction characteristics of both an oxidized film of MoS_2 and a rubbed film of pure MoO_3 were studied. The results are shown in Figure 16.[29] The data show that MoO_3 is a very poor lubricant and its use resulted in high friction and excessive welding. The "oxidized" MoS_2 film, however, showed results remarkably similar to those for the unoxidized MoS_2 film. An explanation of the mechanism of the MoS_2 in the "oxidized" condition must consider the actual surface films in both the oxidized and the unoxidized conditions. Sketches of the two surface films based on a hypothesis that explains the mechanism are shown in Figure 16. While conditions in these experiments were intended to give as near complete oxidation as possible, undoubtedly some fraction of the MoS_2 remains unoxidized. Even though this fraction is extremely small, it acts as an effective solid lubricant at the surface. The film immediately adjacent to the surface, as would be expected, produces the beneficial effect.

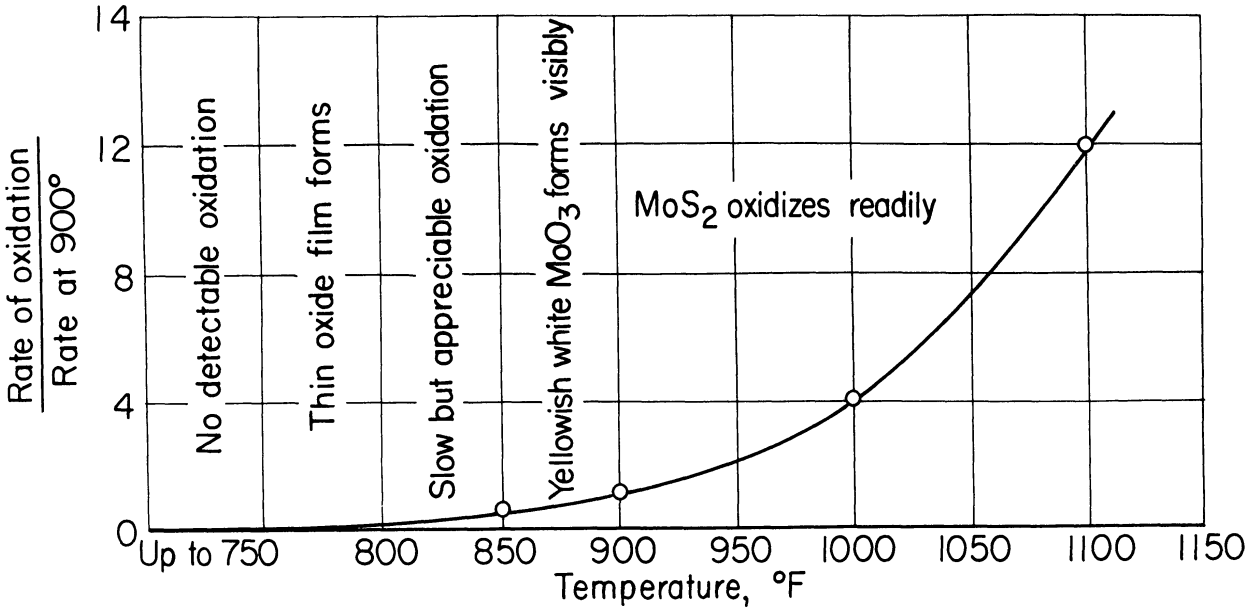

Figure 15. Oxidation characteristics of MoS_2 in air.

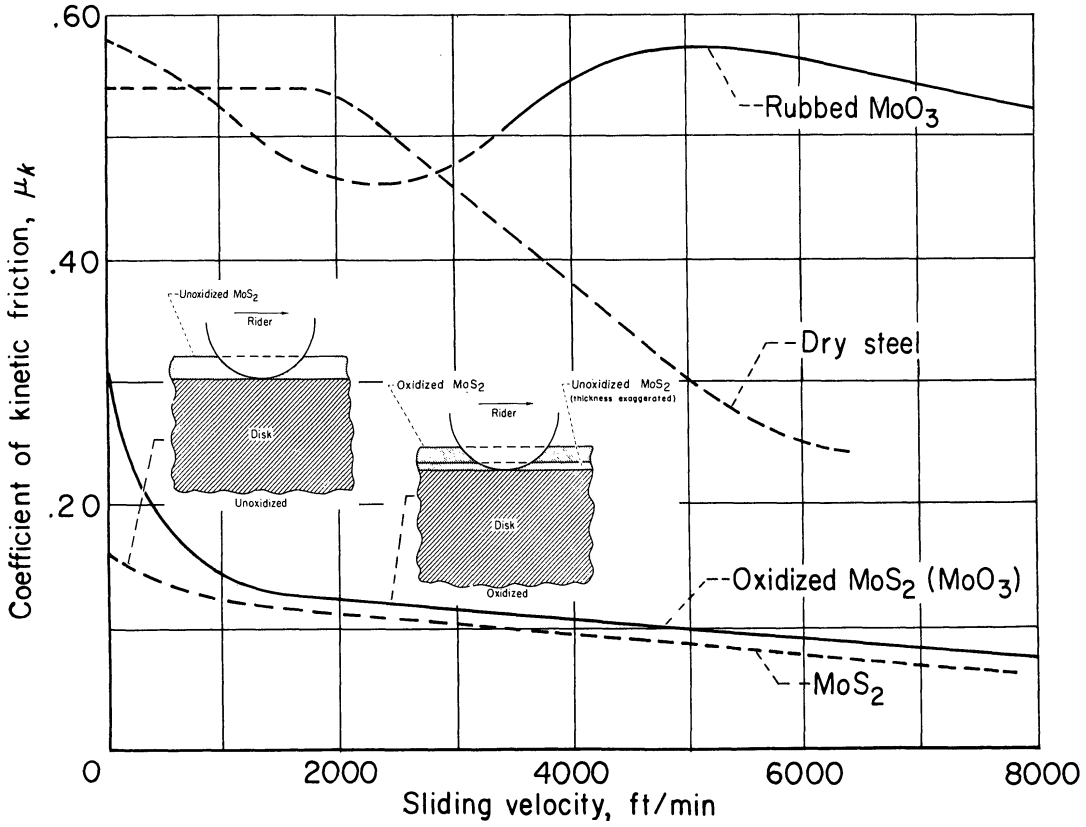

Figure 16. Effect of rubbed MoO_3 and oxidized MoS_2 films on friction of steel against steel at high sliding velocities. Radius of spherical rider specimen, 1/8 inch. Insets show schematic representations of the rider-disk combination with the two types of film.

Studies were made[29] of a film of pure molybdenum trioxide applied to a clean steel disk by an evaporation technique. The MoO_3 was condensed from the vapor state on a disk until a film approximately 0.003 inch thick was present. Friction coefficients obtained with this film (upper curve of Figure 17) were higher than those for clean steel on clean steel at all sliding velocities. Studies were also made[29] of an evaporated MoO_3 film applied to a steel dish on which there was a thin film of mixed iron oxides and carbon; this base film was produced by painting the surface of the hot disk with corn syrup. As discussed in reference 26, the corn syrup reduces Fe_2O_3 to Fe_3O_4 at high temperatures. Friction with the evaporated MoO_3 film applied over the mixed iron oxides and carbon is shown in Figure 17; the data show that the friction coefficient with this film is higher than that for a bonded MoS_2 film, but lower than that with either MoO_3 on clean steel or for clean, dry steel. This result again illustrates the importance of iron oxides to the friction mechanism; the reduction in friction (as compared with either MoO_3 on clean steel or with clean steel) is probably the result of surface protection by the Fe_3O_4 film.

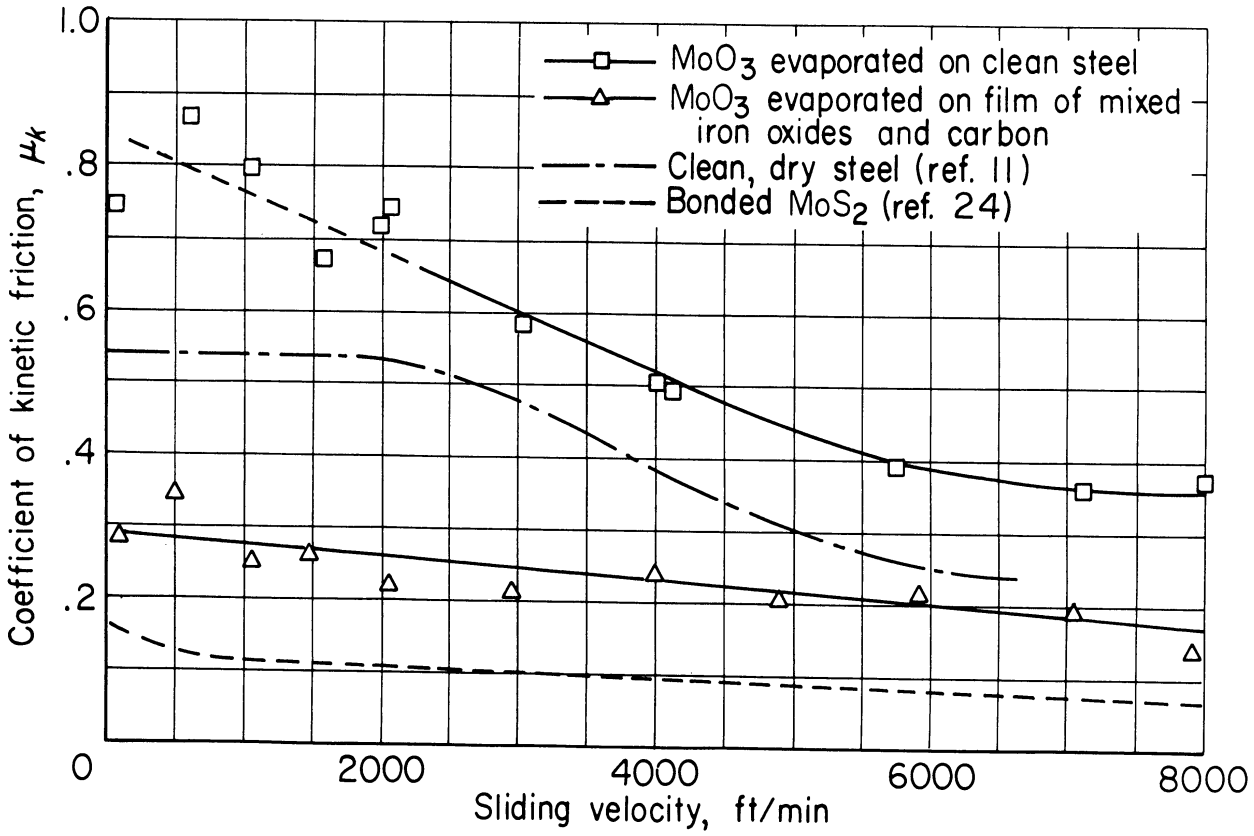

Figure 17. Effect of evaporated MoO_3 films on friction of steel against steel at high sliding velocities. Radius of spherical rider specimen, 1/8 inch.

Figure 18[27] shows the effect on wear of additions of silica to MoS_2. The data show that friction coefficient is affected by only a small amount over the range of 0 to 5 per cent silica addition. Wear, however, is changed considerably by the addition of as little as 0.5 per cent silica. Additions of greater amounts of cilica than 0.5 per cent show a relatively smaller effect. As previously stated, there is no direct correlation between friction and wear. The results shown in Figure 18 vividly illustrate this lack of direct correlation.

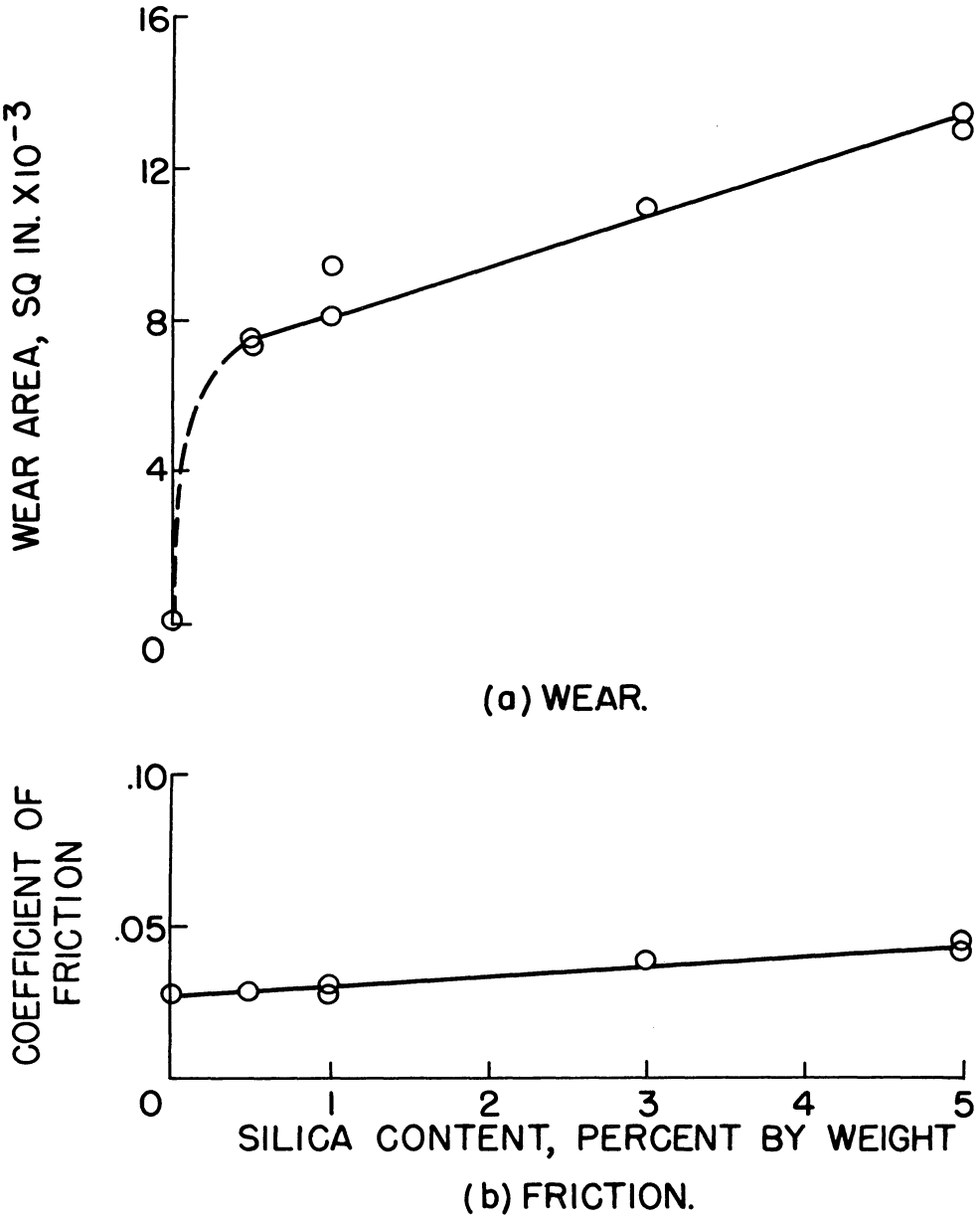

Figure 18. Effect of additions of silica to a highly purified grade of MoS_2 on wear and friction of steel specimens in dry air. Load, 40 pounds; sliding velocity, 5.7 feet per minute; duration, 6 hours.

Other Solids

In a friction study of mixtures of graphite with several metallic oxides and salts, Peterson and Johnson[30] indicated that lead monoxide, PbO, was an effective lubricant at 1000° F. In accordance, an investigation was made of lead monoxide, PbO, and other metal oxides as solid lubricants for temperatures to 1000° F.[31] This investigation showed that PbO was, by far, the most effective of several oxides of heavy metal as a solid lubricant at 1000° F. Friction coefficient was .09 for PbO lubricating a cast Inconel slider on an Inconel-X disk. Higher friction was observed with decreasing temperatures (below 900° F). At room temperature, PbO gives higher friction than would usually be acceptable for a solid lubricant. The variation in friction between the values at 1000° F and at lower temperatures was caused by conversion of PbO to Pb_3O_4 between 700° and 900° F. At temperatures above 1000° F, Pb_3O_4 reverts to PbO. The Pb_3O_4, which is not an effective lubricant by itself, increased friction coefficient in proportion to the amount present in the PbO.[31]

SUMMARY OF RESULTS

Under extreme boundary lubrication conditions where metal-to-metal contact takes place, the adhesion theory of friction predicts that friction and tendency to surface failure (by welding) of rubbing metals can be reduced relatively simply; this reduction can be accomplished by a reduction of the ratio s/p, where s is shear strength of the softer of the two contacting materials, and p is flow (yield) pressure of the softer of the two contacting materials. The most practical means of reducing the ratio s/p is to reduce the value of s. The use of thin low shear strength films on hard base materials results in a reduction of s with negligible reduction of p. Thus, any low shear strength material (for example, certain oxides, sulfides, plated films, liquid lubricants, etc) that acts as an contaminant between sliding surfaces, should be effective in reducing friction and surface failure. The contaminant also acts to reduce welding by its action in reducing contact of clean metal to clean metal. Reduction of surface failure and welding should markedly contribute to lower wear.

Experimental investigation by the NACA produced the following results which are consistent with the views expressed in the preceeding paragraph on the low shear strength contaminating films.

Experiments with iron oxides show that FeO and Fe_3O_4 are generally beneficial, while Fe_2O_3 is harmful. With steel specimens in sliding, exclusion of oxygen by use of a blanketing medium prevented the formation of the beneficial oxides and permitted extensive surface welding. In fact, the results of these and other investigations indicate that, with many metals and particularly ferrous alloys, effective lubrication is very often dependent on the presence of an oxide film which serves to protect the surface.

Wear studies showed that prevention of surface damage and maintenance of low wear could be associated with the formation of naturally occurring surface films on one or both of the sliding specimens; for cast irons, the surface films consisted of graphitic carbon and for various nickel alloys, the film consisted of nickel oxide NiO. In one investigation with cast Inconel sliding against hardened tool steel at temperatures ranging from 80° to 1000° F, a very marked downward trend of wear with increase in temperature was observed. This downward trend is the result of formation of beneficial nickel oxide(s) at the higher temperature. In this investigation, wear at 80° F was reduced by a factor of 10 through pretreatment of the Inconel specimen to form a nickel oxide surface film. In this same investigation, wear at 1000° F was increased by a factor of 10 through pretreatment of the Inconel specimen, wear at 1000° F was increased by a factor of 4 by limiting formation of the oxide film; this was done by limiting the availability of oxygen by displacement of air with argon.

Since MoS_2 appeared promising at low temperatures, an investigation of its high-temperature stability was made. X-ray diffraction studies showed no changes below 1000° F in vacuum. Electron and X-ray diffraction experiments show, however, that, in the presence of air, MoS_2 oxidizes to molybdenum trioxide, MoO_3. The rate of oxidation increases steadily with increase in temperature; it is low below 750° F and becomes high at temperatures above 1050° F. Friction results obtained with rubbed and evaporated MoO_3 films show that MoO_3 is very detrimental; extensive surface damage takes place under these conditions. The presence of a very small amount of unoxidized MoS_2 in an oxidized bonded MoS_2 film will, however, maintain low friction and provide good protection from surface damage.

Of several possible solid lubricants for high-temperature application, lead monoxide, PbO, was by far the most effective at 1000° F. At temperatures below 900° F, however, higher friction was observed because of conversion of PbO to Pb_3O_4. At temperatures above 1000° F, Pb_3O_4 reverts to PbO.

REFERENCES

1. Bowden, F.P., and Tabor, D., "The Lubrication by Thin Metallic Films and the Action of Bearing Metals," Journ. Appl. Phys., Vol. 14, No. 3, March 1943, pp. 141-151.

2. Good, J.N., and Godfrey, Douglas, "Changes Found on Run-In and Scuffed Surfaces of Steel, Chrome Plate, and Cast Iron," NACA TN 1432, 1947.

3. Prutton, C.F., Turnbull, David, and Dloughy, George, "Mechanism of Action of Organic Chlorines and Sulfur Compounds in Extreme-Pressure Lubrication," Jour. Inst. Petroleum, Vol. 32, No. 266, Feb. 1946, pp. 90-118.

4. Hughes, T.P., and Whittingham, G., "The Influence of Surface Films on the Dry and Lubricated Sliding of Metal," Trans. Faraday So., Vol. 38, No 249, Pt. 1, Jan. 1942, pp. 9-27.

5. Webb, Well A, "The Influence of Iron Oxide on Wear of Rubbing Surfaces," Science, Vol. 99, No. 2575, May 5, 1944, pp. 369-371.

6. Campbell, W.E., "Solid Lubricants," Lubrication Eng., Vol. 46, No. 4, August, 1953, pp. 195-200.

7. Tingle, E.D., "The Importance of Surface Oxide Films in the Friction and Lubrication of Metals," Trans. Faraday Soc., Vol. 46, No. 326, Pt. 2, Feb. 1950, pp. 93-102.

8. Bowden, F.P., and Tabor, D., The Friction and Lubrication of Solids, Clarendon Press (Oxford), 1950.

9. Bisson, E.E., Johnson, R.L., Swikert, M., and Godfrey, Douglas, "Friction, Wear, and Surface Damage of Metals as Affected by Solid Surface Films," NACA TN 3444, May 1955.

10. Merchant, M.E., "The Mechanism of Static Friction," Jour. Appl, Phys., Vol. 11, No. 3, Mar. 1940, p. 230.

11. Johnson, Robert L., Swikert, Max A., and Bisson, Edmond E., "Friction at High Sliding Velocities," NACA TN 1442, 1947.

12. Bowden, F.P., and Young, J.D., "Friction of Clean Metals and the Influence of Adsorbed Films," Proc. Roy. Soc. (London), Ser. A. Vol. 208, Sept. 7, 1951, pp. 311-325.

13. Harris, Jay C., "Films and Surface Cleanliness," Metal Finishing, Vol. 44, Nos. 8-9, Aug. and Sept. 1946, pp. 328-333 and pp. 386-388.

14. Nelson, H.R., "The Primary Oxide Film on Iron," Journ. Chem. Phys., Vol. 5, No 4, April. 1937, pp. 252-259.

15. Johnson, Robert L., Swikert, Max A., and Bisson, Edmond E., "Friction at High Sliding Velocities of Surfaces Lubricated with Sulfur as an Additive," NACA TN 1720, 1948.

16. Ernst, Hans, and Merchant, M. Eugene, Chip Formation, Friction and Finish, The Cincinnati Mill Machine Co., Aug. 24, 1940.

17. Johnson, Robert L., Swikert, Max A., and Bisson, Edmond E., "Investigation of Wear and Friction Properties Under Sliding Conditions of Some Materials Suitable for Cages of Rolling-Contact Bearings," NACA Rep. 1062, 1952. (Supercedes NACA TN 2384)

18. Johnson, Robert L., Swikert, Max A., and Bisson, Edmond E., "Effects of Sliding Velocity and Temperature on Wear and Friction of Several Materials," Lubrication Eng, Vol 11, No. 3, May-June, 1955.

19. Johnson, Robert L., Swikert, Max A., and Bisson, Edmond E., "Wear and Sliding Friction Properties of Nickel Alloys Suited for Cage of High-Temperature Rolling-Contact Bearings," Vol. 1--Alloys Retaining Mechanical Properties to 600° F, NACA TN 2758, 1952.

20. Johnson, Robert L., Swikert, Max A., and Bisson, Edmond E., "Wear and Sliding Friction Properties of Nickel Alloys Suited for Cages High-Temperature Rolling-Contact Bearings. Vol 2--Alloys Retaining Mechanical Properties Above 600° F, NACA TN 2759, 1952

21. Johnson, R.L., and Bisson, Edmond E., "Bearings and Lubricants for Aircraft Turbine Engines, NACA - University Conference on Aerodynamics, Construction and Propulsion, Vol. 3--Aircraft Propulsion, Oct. 20-22, 1954.

22. Johnson, R.L., and Bisson, Edmond E., Bearings and Lubricants for Aircraft Turbine Engines," SAE Preprint No. 439; presented at SAE Annual Meeting, Detroit, Michigan, Jan. 10-14, 1955.

23. Bisson, E.E., and Johnson, R.L., "NACA Friction Studies of Lubrication at High Sliding Velocities," Lubrication Eng., Vol. 6, No. 1, Feb. 1950, pp. 16-20.

24. Johnson, R.L., Godfrey, Douglas, and Bisson, Edmond E., "Friction of Solid Films on Steel at High Sliding Velocities," NACA TN 1578, 1948.

25. Bisson, Edmond E.,"The Influence of Solid Surface Films on the Friction and Surface Damage of Steel at High Sliding Velocities," Lubrication Eng., Vol. 9, No. 2, April 1953, pp. 75-77.

26. Godfrey, Douglas, and Bisson, Edmond E., "Bonding of Molybdenum Disulfide to Various Materials to Form a Solid Lubricating Film," Vol. 1--The Bonding Mechanism, NACA TN 2628, 1952.

27. Peterson, M.B., and Johnson, R.L., "Factors Influencing Friction and Wear with Solid Lubricants," Lubrication Eng., Vol. 11, No. 5, Sept.-Oct. 1955.

28. Johnson, R.L., Swikert, Max A., and Bisson, Edmond E., "Friction and Wear of Hot-Pressed Bearing Materials Containing Molybdenum Disulfide," NACA TN 2027, 1950.

29. Godfrey, Douglas, and Nelson, Erva C., "Oxidation Characteristics of Molybdenum Disulfide and Effect of Such Oxidation on Its Role as Solid-Film Lubricant," NACA TN 1882, 1949.

30. Peterson, Marshall B., and Johnson, R.L., "Friction Studies of Graphite and Mixtures of Graphite with Several Metallic Oxides and Salts at Temperatures to 1000° F," NACA TN 3657, 1956.

31. Peterson, Marshall B., and Johnson R.L., "Solid Lubricants for Temperatures to 1000° F," Lubrication Eng., Vol 13, No. 4, April, 1957.

EXPERIMENTAL LOAD-STRESS FACTORS

W. D. Cram
Group Leader, Engineering Power Transmission
United Shoe Machinery Corporation

EXPERIMENTAL LOAD-STRESS FACTORS

By

W. D. Cram

INTRODUCTION

In the design of machine elements subjected to rolling or combined rolling and sliding actions as in gears, cams, rollers, etc., a knowledge of the surface endurance limits of mating materials is of primary importance to machine design engineers.

Due to the increase in load and speed requirements of industrial machines, this knowledge has become as necessary as that of other physical properties of materials such as tensile strength, elastic limit, and flexural fatigue.

Optimum design must therefore consider both the fatigue strength and the resistance to surface fatigue of machine parts to obtain satisfactory working life.

Up to 1931, no test data were available on the surface fatigue of materials. At that time, however, Prof. Earle Buckingham of M.I.T. conceived and designed a relatively simple surface-wear testing machine to determine the experimental load-stress or wear factors of cylinders subjected to rolling and combined rolling and sliding actions. Test cylinders or rolls were chosen, not only to simplify the testing problems, but also becuase the nature of the surface fatigue failures occurring on gear teeth, cams, rollers, ball bearings, etc. is similar to that occurring on mating cylinders. Furthermore, the data obtained from these roll tests could be used in practice in the form of surface load-stress or wear factors to determine the limiting loads for surface wear on gear teeth, cams, rollers, etc.

From 1932 to 1956, surface wear tests were conducted under the supervision of G. J. Talbourdet at the Research Division of the United Shoe Machinery Corporation, Beverly, Massachusetts. Currently, four wear testing machines operate 24 hours a day at the Research Division, and a great deal of data have been accumulated on cast iron, steel, bronze, aluminum, and non-metallic materials.

It is the purpose of this paper to present the experimental load-stress factors for these materials derived by Mr. Talbourdet from accumulated data on roll tests.

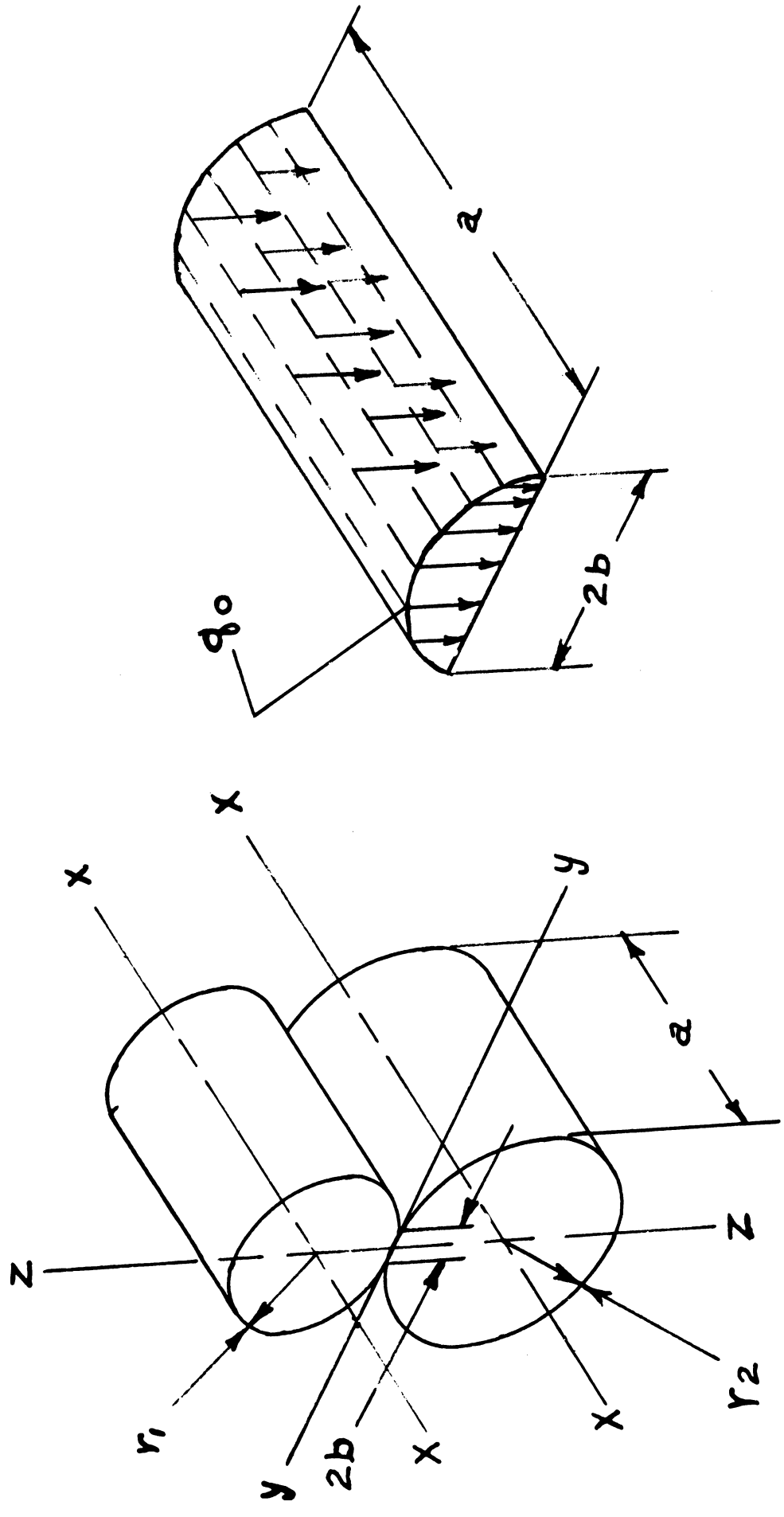

Figure 1. Distribution of pressure at the contact of two cylinders.

Nature of Contact and Stresses in Mating Elastic Cylinders

The first publication on the nature of the contact between compressed cylinders and the magnitude and the type of stresses imposed on and below the surfaces was made by Dr. H. Hertz in 1882. From his theory, which assumes normal pressure and static conditions only, the Hertz equation was derived.

He showed the surface of contact of two cylinders with parallel axes to be a narrow rectangle and the distribution of pressure along the width of this narrow rectangle of contact to follow a semi-ellipse.

From Figure 1:

a = length of contact, in.
$2b$ = width of contact, in.
q = pressure distribution along width of contact, lb./in^2.
p^1 = load per unit length of the surface of contact, lbs.

$$q_o = \frac{2p^1}{\pi b} \tag{1}$$

where q_o is the maximum pressure at the center of the ellipse, or the maximum specific compressive stress in lb/sq. in.

$$b = \sqrt{\frac{4p^1 (k_1 + k_2) R_1 R_2}{R_1 + R_2}} \tag{2}$$

where R_1 = radius of one cylinder, in.
R_2 = radius of mating cylinder, in.

$$k_1 = \frac{1 - \gamma_1^2}{\pi E_1} \quad \text{and} \quad k_2 = \frac{1 - \gamma_2^2}{\pi E_2}$$

E_1 = modulus of elasticity of one cylinder, lb/sq. in.
E_2 = modulus of elasticity of other cylinder, lb/sq.in.
γ = Poisson's ratio; .25 for many engineering materials and .3 for steel

Assuming both cylinders to be of the same material and $\gamma = .3$.

$$\text{then, } b = 1.52 \sqrt{\frac{p1\, R_1 R_2}{E (R_1 + R_2)}} \tag{3}$$

When the radii of the cylinders are the same,
i.e. $R_1 = R_2 = R$

$$\text{them, } b = 1.08 \sqrt{\frac{p^1 R}{E}} \tag{4}$$

For the case of contact of a cylinder with a plane surface

$$b = 1.52 \sqrt{\frac{p^1 R}{E}} \tag{5}$$

To determine the maximum specific compressive stress, substitute in eq. (1) the value of b given in eq. (2)

$$\text{then, } q_o = \sqrt{\frac{.35\, P^1 (1/R_1 + 1/R_2)}{1/E_1 + 1/E_2}} \qquad (6)$$

When the materials of both cylinders are the same

$$q_o = \sqrt{.418 \quad P^1 E\, (1/R_1 + 1/R_2)} \qquad (7)$$

In the case of contact of a cylinder with a plane surface

$$q_o = \sqrt{.418 \quad \frac{P^1 E}{R}} \qquad (8)$$

Knowing q_o and b, the stresses along the z, y, and x axes can be calculated at any point. These stresses are compressive, tensile and shear.

The variation of stress components with the depth below the surface is shown by Timoshenko and reproduced in Figure 2. It indicates that the compressive stress along the "z" axis is maximum on the surface layer and decreases with the depth. The stress along the "y" axis is also maximum on the surface layer and is equal to q_o. It becomes zero when the depth is one and a half times the width of contact or 3b. The stress along the "x" axis is also maximum on the surface layer and is equal to $.6q_o$. It also decreases with the depth. The shear stress is zero on the surface layer along the "z" axis and becomes maximum when the depth is .78b. Its magnitude is $.304q_o$.

Since the test specimens on the surface wear testing machines are cyclinders, it was thought that, although the rolls are subjected to rolling actions and a small amount of friction occurs under the ellipse of contact, the stresses imposed on the rolls due to a normal pressure should follow the Hertz theory.

To verify this assumption, several roll tests were made at the start of this investigation to determine the influence of the radii of the rolls and the elasticity of the mating materials upon the imposed maximum compressive stress. This was done by varying the radii of the rolls and changing the roll materials from cast iron to steel and vice versa. These tests were made under rolling condition only, to minimize the effects of tangential friction loads.

The maximum compressive stress from the test data was found to be in close agreement with the compressive stress calculated from the Hertz equation.

The resume of the Hertz theory for compressed elastic cylinders and its relation to the roll tests has been presented to give a better understanding of the factors involved.

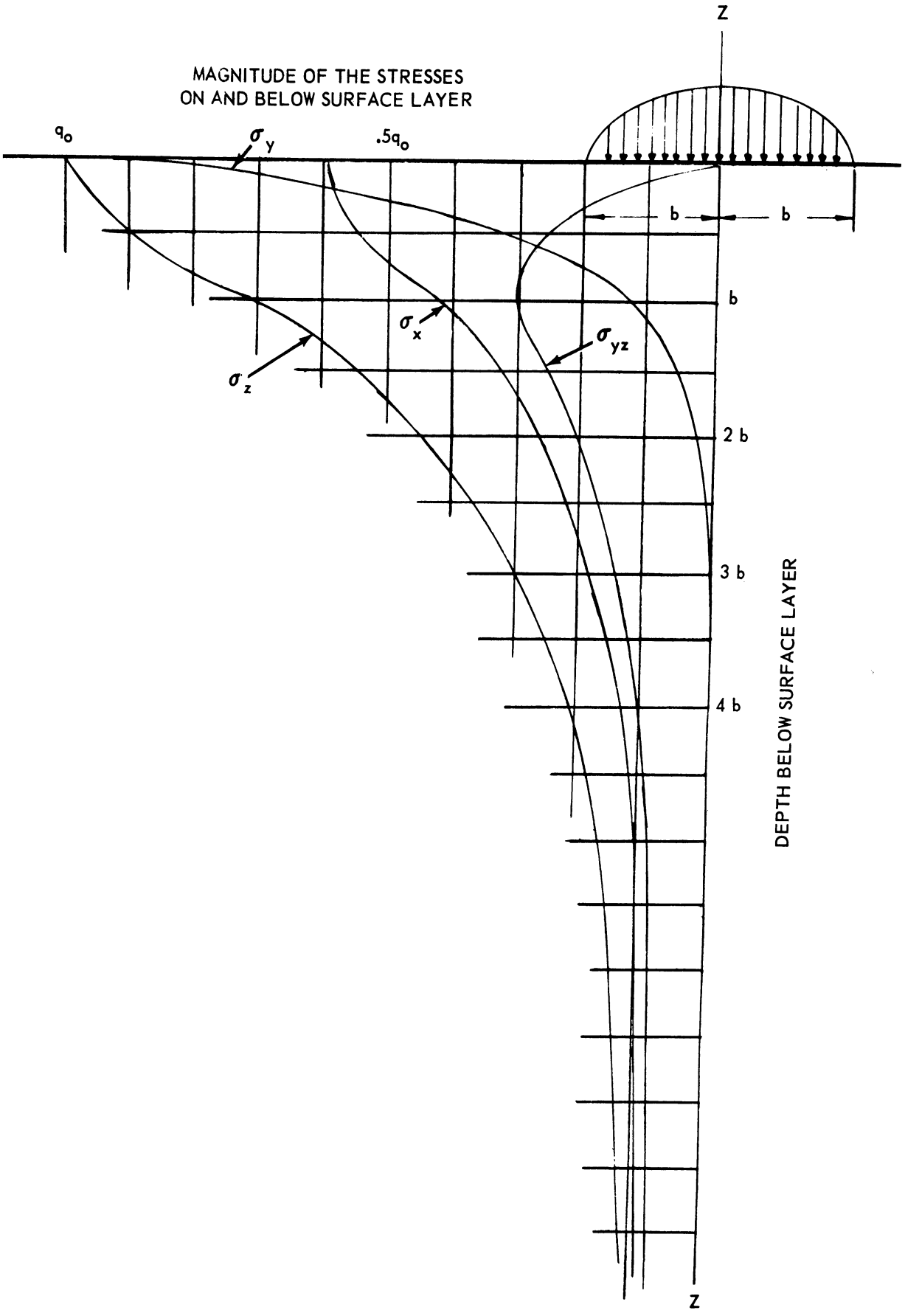

Figure 2. Variation of stress below surface.

When the cylinders are subjected to combined rolling and sliding conditions, the problem is more complex.

Figure 3 illustrates the stress distribution between two celluloid cylinders in contact and subjected to a normal pressure with no applied torque.

Figure 4 shows the stress distribution between these cylinders subjected to the same normal pressure, but with the addition of a tangential force due to an applied torque. The influence of the torque is apparent from an examination of the two figures. It can be seen that when the torque is applied, a shift of the axis of stress and an axial displacement of the contacting surfaces have occurred. Also, these figures demonstrate that the maximum specific compressive stress obtained through the application of the Hertz equation is less than the maximum specific stress set up in the material under the influence of an applied torque.

A publication by J. O. Smith and Chang Ken Liu covers this subject very well. Figures 5 and 6 show the normal and tangential loads on two cylinders and the pressure distribution on the semi-ellipse.

Smith and Chang Ken Liu show that the tangential force Q for a coefficient of friction of 1/3 increases the maximum compressive stress by 39% to 1.39 q_o and the maximum shearing stress by 42% to .43 q_o.

From the photoelastic studies and the findings of the above authors, the load-stress factors for combined rolling and sliding actions should be less than the factors for rolling only. A comparison of the included experimental load-stress factors for cylinders subjected to rolling only and for cylinders subjected to combined rolling and sliding actions substantiates the above findings.

Rolling and Combined Rolling and Sliding Actions

Since the load-stress factors obtained from the roll tests are given for specific conditions such as rolling only and combined rolling and sliding actions, it might be worth while to define these actions.

Rolling only, means that the surface speed of the mating rolls is the same, i.e., when

ω_1 = angular velocity of driving roll, rad/sec.
ω_2 = angular velocity of driven roll, rad/sec.
V_1 = surface speed of driving roll, in/sec.
V_2 = surface speed of driven roll, in/sec.
r_1 = radius of driving roll, in.
r_2 = radius of driven roll, in.
V_s = relative sliding velocity, in/sec.

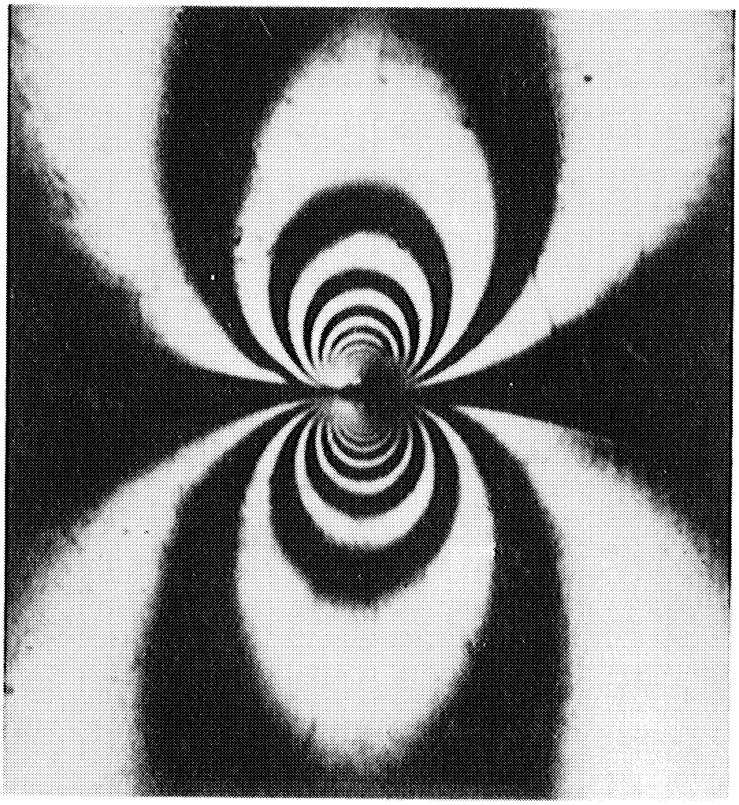

Figure 3. Stress distribution between two cylinders.

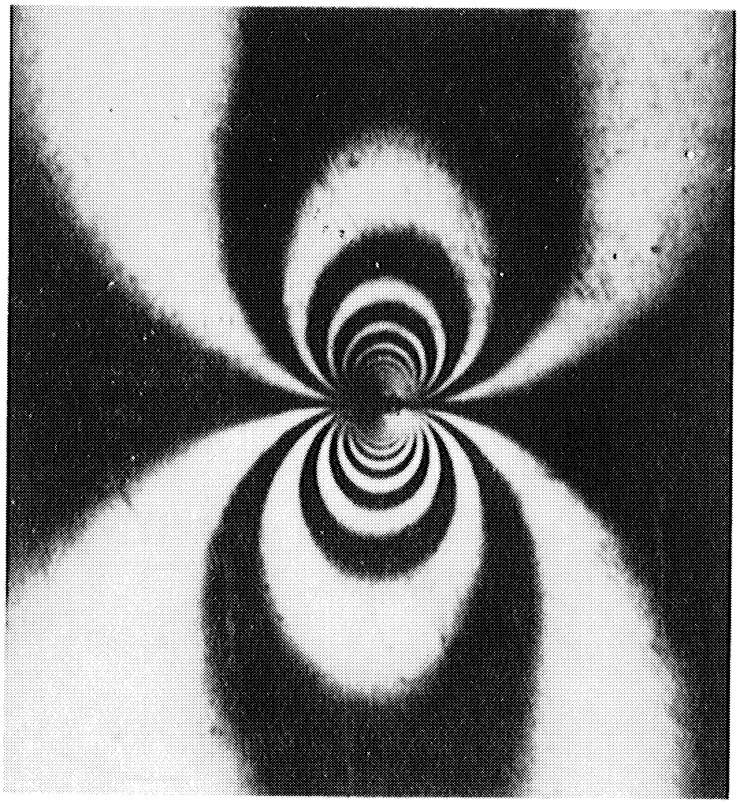

Figure 4. Stress distribution between two cylinders.

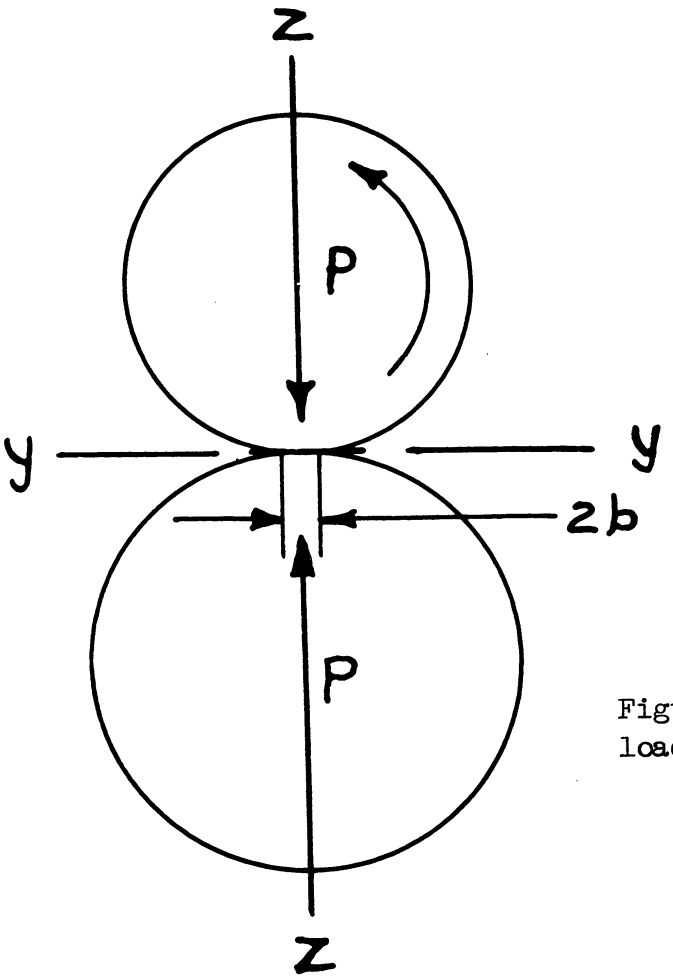

Figure 5. Normal and tangential loads on two cylinders

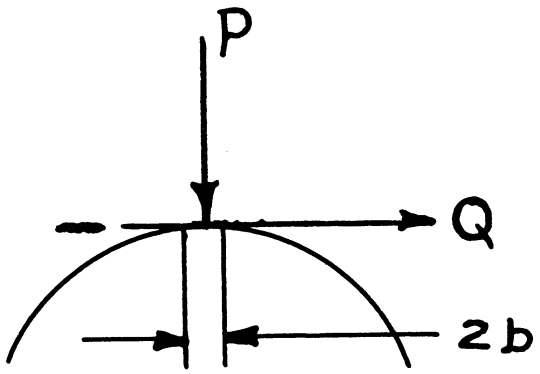

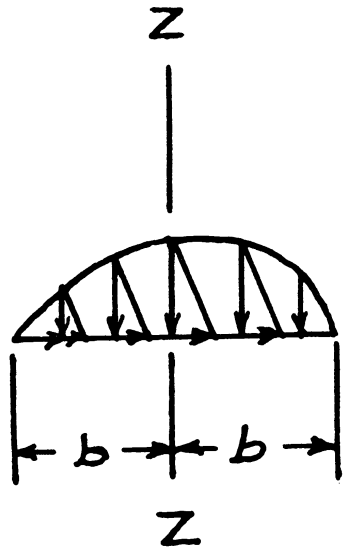

Figure 6. Pressure distribution on the normal ellipse.

then, $V_1 = 2\pi r_1\omega_1$, $V_2 = 2\pi r_2\omega_2$

$$V_s = V_1 - V_2$$

For rolling only $V_1 = V_2$ and $V_s = 0$

$$\therefore \text{per cent sliding} = \frac{V_1 - V_2}{V_1} = 0$$

In this case, the relatively small per cent sliding resulting from the deformation of the loaded surfaces is not considered.

Example: $\omega_1 = 20$; $\omega_2 = 10$; $r_1 = 1"$; $r_2 = 2"$

$\therefore V_1 = 2\pi \times 1 \times 20 = 40\pi$

$V_2 = 2\pi \times 2 \times 10 = 40\pi$

$V_s = V_1 - V_2 = 40\pi - 40\pi = 0$

$$\text{Per cent sliding} = \frac{40\pi - 40\pi}{40\pi} = 0$$

Combined Rolling and Various Per Cent Sliding, means that both mating rolls are subjected to simultaneous rolling and sliding actions. As shown above, the per cent sliding is the ratio of the difference between the surface velocities of the mating rolls and the surface velocity of either roll. That is why the per cent sliding on the driving or on the driven roll is specified.

Example: $\omega_1 = 20$, $\omega_2 = 10$, $r_1 = 2$, $r_2 = 1$,

$\therefore V_1 = 2\pi \times 2 \times 20 = 80\pi$

$V_2 = 2\pi \times 1 \times 10 = 40\pi$

$$\text{Per cent sliding on driver} = \frac{V_1 - V_2}{V_1} = \frac{80\pi - 40\pi}{80\pi} = 50\%$$

$$\text{Per cent sliding on driven} = \frac{V_1 - V_2}{V_2} = \frac{80\pi - 40\pi}{40\pi} = 100\%$$

Sliding velocity $V_s = V_1 - V_2 = 80\pi - 40\pi = 40\pi$ in/sec.

Note that V_1 is in effect the rolling velocity of the driving roll and V_2 the rolling velocity of the driven roll, also that V_s the relative sliding velocity is also the rate of sliding between the contacting rolls.

The per cent sliding is independent of the velocity of the rolls and influences primarily the load-stress factor; i.e., the higher the per cent sliding, the lower the load-stress factor, as shown in Table 2 and the charts in the Appendix. The rate of sliding or sliding velocity varies with the speed of operation and results in higher heat of operation in which the lubrication factor becomes very important as it affects the coefficient of friction and the input torque.

When the contacting surfaces are subjected to rolling only, the coefficient of friction, the input torque and the heat of operation are minimum. Here, the lubrication factor is less critical, the oil film being necessary only to prevent abrasion of the surfaces.

The Testing Machine

The first testing machine conceived and designed by Prof. Buckingham was driven by a small Sprague dynamometer to permit speed variations and to obtaine the torque input and the change in torque during tests.

Since the main purpose is to obtain the load-life characteristics of many engineering materials as rapidly as possible and with a minimum of personal attention, a dynamometer is not used in the present testing machines. They are driven at a constant speed of 1040 rpm approximately. This restricts the investigation with respect to the effects of speed on non-metallic materials, and to the recordings of torque which give a measure of the tangential force of friction on rolls subjected to combined rolling and sliding actions.

The present testing machine, with its covers removed, is shown in Figure 7. The test rolls are mounted on gear driven arbors. One test roll (generally the master or hardened steel roll and denoted as the driving roll throughout the paper), is supported on an arbor mounted on a fixed frame. The other, or driven roll, is supported on a shaft mounted on a pivoted frame. The load is applied by means of a claibrated spring. For rolling and combined rolling and up to 30 per cent sliding on the driving roll, the gear ratio is 1 to 1. For combined rolling and from 50 to 75 per cent sliding on the driving roll, the gear ratio is 23 to 40, from which the speed of the driven test roll is 598 rpm, approximately.

Test roll diameters, per cent sliding, rate of sliding and roll surface velocities, for the various operating conditions are contained in Table 1.

For most tests, the face width of the rolls is 1 in. For tests on heat treated and carburized steels, the face width is reduced to permit high unit loads and minimize shaft deflection.

The test rolls and the supporting bearing are amply lubricated with a straight mineral oil of 280-320 Saybolt Universal Viscosity at 100 F.

To insure uniform loading of the test rolls, a close check is kept on the parallelism of the rolls. With ductile and with nonmetallic materials, a variation of a few tenths of a thousandth of an inch along the width of face is not too critical because of the plastic deformation of the ductile materials and the large elastic deformation of the non-metallic materials. With hardened steel rolls, however, parallelism is important because the surface materials have little plasticity.

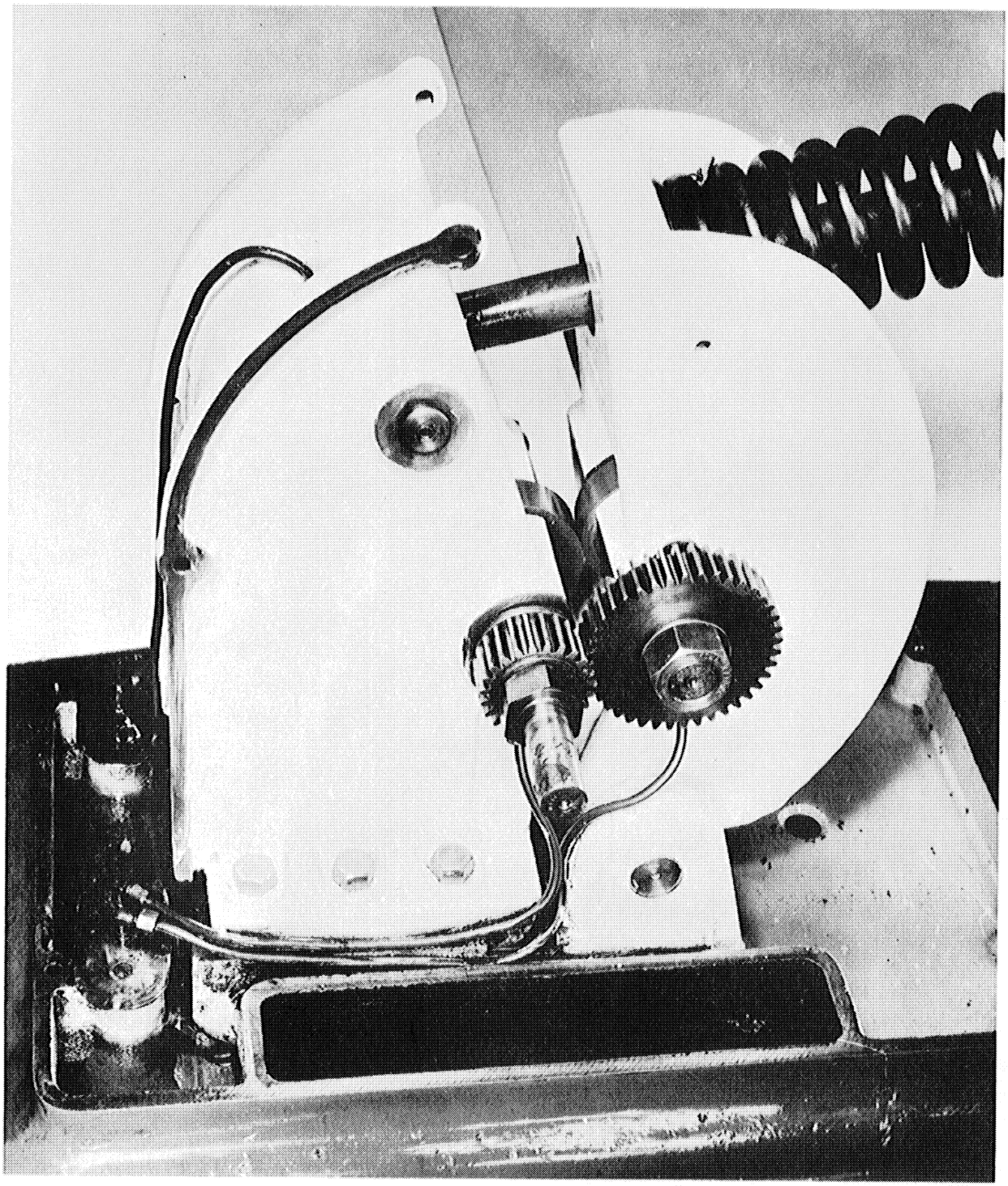

Figure 7. Present testing machine.

Table 1

Test Roll Identification	Test Roll Diameter, in.	Percent Sliding	Surface Velocity Feet/Minute	Sliding Velocity Feet/Minute
Driver	2.300	0	626	0
Driven	2.300	0	626	0
Driver	2.400	9.1	653	54
Driven	2.200	8.3	399	54
Driver	2.706	30.0	737	221
Driven	1.894	42.8	516	221
Driver	3.370	50	918	459
Driven	2.930	101.25	459	459
Driver	4.390	75	1195	896
Driven	1.909	303.3	299	896

The test procedure is to start the machine at no load and to apply the load gradually until full load is exerted on the rolls. When the rolls are ductile and when they are subjected to combined rolling and high sliding conditions, the load must be applied slowly because of the increase in tangential friction force and rate of sliding. During the tests, counter readings and any incidents are reported on data sheets. After each test, hardness of the core and surface of the roll specimen are taken and recorded. Also, the nature of the surface failure, the depth of pits and/or the thickness of flakes of sheared-off particles are noted.

Experimental Load-Stress Factors for Cylinders

The experimental load-stress factor for mating materials is determined from the loads applied on the test rolls and the radii of curvature of the rolls. This factor is, by definition,

$$K_1 = W\left(\frac{1}{r_1} + \frac{1}{r_2}\right) \qquad (7)$$

Where: K_1 = experimental load-stress factor, per inch of contact;

W = normal load on rolls, lbs. per in ch of length.

r_1 and r_2 = radii of rolls, in.

Equation (6) for the maximum specific compressive stress between two external cylinders within the elastic limit of their respective materials can be transformed to read:

$$2.857\ q_o^2 \left(\frac{1}{E_1} \quad \frac{1}{E_2}\right) = W \left(\frac{1}{r_1} \quad \frac{1}{r_2}\right)$$

With this arrangement, the left-hand side of the equation is constant for a given combination of materials, and the right-hand side is equal to the experimental load-stress factor K_1. Therefore, if the load-stress factor is known for a combination of materials, the limiting surface wear load for any two cylinders with a given length of contact can be determined.

As illustrated in Figure 8, when one of the mating materials is a ferrous ductile material, no surface breakdown should be expected after approximately 40 million cycles of repeated stress for rolling conditions. For combined rolling and sliding conditions, the number of repeated cycles of stress beyond which no surface breakdown will occur depends on the percentage sliding. For hardened steel materials subjected to rolling only, the number of cycles may be as high as 600 million.

Table 2 is a list of experimental load-stress factors at 100 million cycles of repeated stress for combinations of materials subjected to rolling and combined rolling and 9% sliding. Included in the Appendix Charts are some factors for combined rolling and 42%, 100%, and 300% sliding on the driven roll.

For numbers of cycles other than 100 million, load-stress factors can be interpreted from the load-life charts contained in the Appendix. Examination of these charts shows that the load-life curves represent probable values; exact load-stress factors may be greater or less than those listed.

Use of Experimental Load-Stress Factors for Determining Safe Wearing Load on Cam and Roll Surfaces

For cam and roll applications the following simple expression is used:

$$P = \frac{K_1 F}{\left(\frac{1}{R_1} \pm \frac{1}{R_2}\right)} \qquad (8)$$

where P = limiting surface wear load between cam and roll, lbs;
F = length of contact between cam and roll, in;
R_1 = radius of cam roll, in;
R_2 = radius of curvature of cam contour, in.

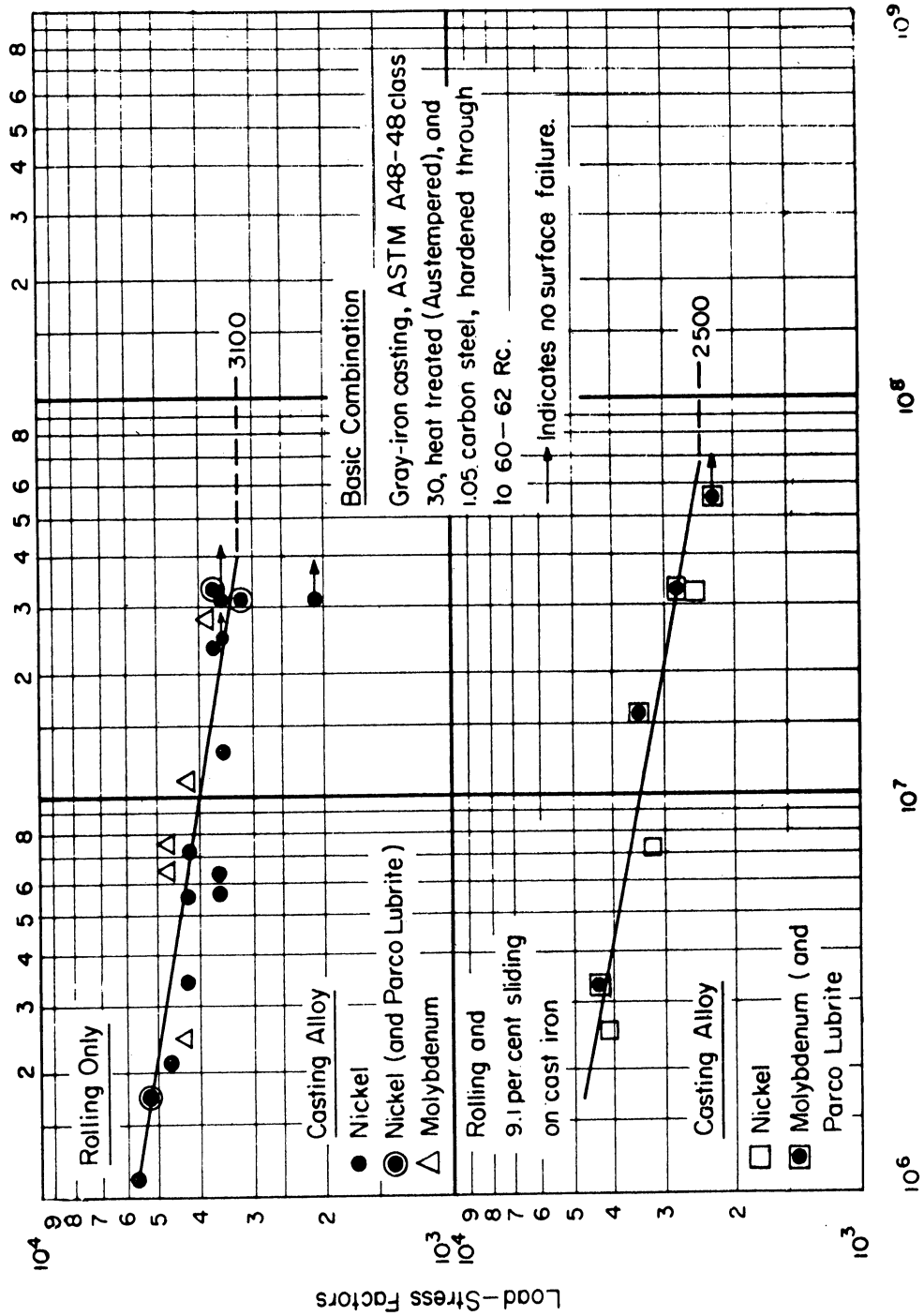

Figure 8. Fatigue Curve.

TABLE 2

COMBINATION OF MATERIALS

LIFE NO.		SLIDING FACTORS 0%	9%
	Gray iron casting, ASTM A48-48 Class 20, 130-180 Bhn and same	1300	1050
	G.M. Meehanite, 190-240 Bhn and same.	1950	1500
	Nodular iron casting, ASTM-A339-51T, Grade 80-60-03, 207-241 Bhn and same.	3400	1850
	Gray iron casting, ASTM A48-48, Class 30, heat treated (austempered), 270-290 Bhn and same.	4200	3400
	1.05 Carbon Tool Steel, Hardened Through to 60-62 Rc and:		
	Gray iron casting, ASTM A48-48, Class 20, 160-190 Bhn, phosphate coated.	1300	
	Gray iron casting, ASTM A339-51T, Grade 20, 140-160 Bhn.	1000	900
	Nodular iron casting, ASTM A339-51T, Grade 80-60-03, 207-241 Bhn.	2000	1750
	Gray iron casting, ASTM A48-48, Class 30, 200-220 Bhn.	1600	
	Gray iron casting, ASTM A48-48, Class 35, 225-255 Bhn.	2300	2100
	Gray iron casting, ASTM A48-48, Class 30, heat treated (austempered) 255-300 Bhn.	3100	2500
	Gray iron casting, ASTM A48-48, Class 30, oil quenched, 270-415 Bhn.	2200	
	S.A.E. 1020 Steel, 130-150 Bhn.	1700	1350
	S.A.E. 4150 Steel, heat treated to 270-300 Bhn, phosphate coated.	12000	7900
	S.A.E. 4150 Steel, heat treated to 270-300 Bhn.	9000	6700
	S.A.E. 4150 Steel, heat treated to 270-300 Bhn, flash chromium plated.	6300	
	S.A.E. 6150 Steel, heat treated to 270-300 Bhn.	1850	
	S.A.E. 1020 Steel, carburized to .045" depth of case, 50-58 Rc.	13000	8500
	S.A.E. 1340 Steel, induction hardened to 45-55 Rc.	10000	8000
	S.A.E. 4340 Steel, induction hardened to 50-55 Rc.	13000	9000
	S.A.E. 65 Phosphor Bronze, 67-77 Bhn.	1000	
	High strength yellow brass, extruded.	2000	
	S.A.E. 39 Cast Aluminum, 60-65 Bhn, and Gray iron casting, ASTM A48-48, Class 30, oil quenched, 340-360 Bhn.	300	
	Zinc Die casting.	320	260
	Random fibre cotton base phenolic.	1000	950
	NEMA Grade L, laminated phenolic.	880	830
	Linen base, laminated phenolic.	800	700
	Graphitized laminated phenolic.	1000	

When the cam curvature is convex, the sign is plus; when concave, the sign is minus. When R_2 is infinite, as with a cam roll on a flat surface, $P = K_1FR_1$.

The radius of curvature of the cam at the point of interest may be obtained from a layout of the cam profile, it may be calculated, or derived from charts similar to those presented by Kloomok and Muffley.

The experimental load-stress factors in Table 2 are derived from laboratory tests in which the operating conditions are nearly ideal. Those conditions are seldom duplicated in actual practice.

In cam design, misalignment and deflection of the cam roll support, backlash, restricted lubrication, variations in microstructure and hardness of the cam material, and other extraneous factors will affect the load carrying capacity of the contacting surfaces. When any of these conditions exist, the load-stress factors selected from Table 2 should be modified to suit the particulars of the application; otherwise the drive may fail prematurely.

For example, for single roll closed-track cams, the effective length of contact may be reduced because of the deflection of the cam roll support lever under load. In addition these cams must have an operating clearance, therefore impact loading of the surfaces and high percentage sliding actions may occur when the contact shifts from one side of the track to the other. Obviously, modification of the experimental load-stress factors is necessary.

On the other hand, for spring loaded peripheral cams where no backlash exists and the cam roll is lubricated and straddle mounted, the experimental load-stress factors for 9% sliding conditions in Table 2 can be used.

Experimental Load-Stress Factors for Involute Spur, Helical and Bevel Gears

In the roll tests, the rolls are driven at constant speed and controlled rolling action or constant combined rolling and sliding actions are maintained. However, in spur gear drives, because of the varying radius of curvature of the mating gear tooth profiles, the nature of the contact is rolling at the pitch line and combined rolling and variable sliding above and below the pitch line.

Therefore, to apply the experimental load-stress factors for cylinders to the equations for limiting wear loads on gears, a definite part of the profile must be selected for use as a basis of comparison.

Buckingham, for reasons outlined in his treatise, "Analytical Mechanics of Gears", selects the radius of curvature of the gear tooth profile at the pitch line, and applies there, the experimental roll test results.

He shows the relationship between the load-stress factor K used in the design of the above types of gearing and the load-stress factor K_1 obtained from the roll test to be,

$$K = \frac{K_1 \sin \phi}{4}$$

where ϕ = pressure angle of gears.

As in cam design, when applying the experimental load-stress factors to gear drives, modification is desirable for service applications which do not simulate the optimum laboratory operating conditions. For example, deflections due to overhung pinion mountings may reduce the effective width of face contact. Again, when the contact ratio approaches 1 to 1 as on spur gear pump drives the radii of curvature of the mating profiles and the per cent sliding at the tip and bottom of the active tooth profile must be considered when determining the limiting load for wear.

Influence of Several Factors on Test Results

Cold Working

The roll tests on metallic materials show that cold working of the surface lamina of materials having some degree of plasticity builds up a mechanical case which allows the surface material to carry a greater load due to the increase in hardness and physical properties of the case.

The cold working action also improves the finish of the surface layer. The improvement in surface finish and hardness on some cast iron tests, due to the cold working action is illustrated in Table 3.

Table 3

Roll Material	Hardness Core	Bhn Surface	Load-Stress Factor K_1	Per Cent Sliding	Number of Cycles	RMS Before Test	RMS After Test
Nodular C.I.	229	319	1739	0	104248000	90-120	25-55
Alloy C.I.H.T.	277	408	6087	0	4199000	100-160	25-35
Alloy C.I.H.T.	269	362	2551	50[a]	88711000	100-160	10-25
Alloy C.I.H.T.	285	362	2551	101.2[b]	51009000	100-160	15-25
Alloy C.I.H.T.	285	387	2290	303.3[b]	29204000	100-160	10-20
Alloy C.I.H.T.	293	345	1728	303.3[b]	47000000	100-160	10-15
G.M. Meehanite	170	293	1240	303.3[b]	2670000	90-120	25-45

a - Per cent sliding on driving roll

b - Per cent sliding on driven roll

Alloy C.I.H.T. Refers to Gray Iron Casting, ASTM A48-48, Class 30, heat treated (austempered), 270-290 Bhn.

Conversion Coatings

Phosphate coating by the Parco-Lubrite process has proved to be very satisfactory on gears and cams for shoe machinery. This is a conversion coating obtained by immersion for 30 minutes at 208-212°F in a proprietary solution consisting essentially of ferrous and manganese dihydrogen phosphate. Through this treatment, the surface is not only oxidized but also possesses some degree of porosity which helps to retain a lubricating film. The formation of the oxide layer on the surface tends to prevent welding between the contacting surfaces and to decrease the tangential force of friction. Furthermore, the removal of disturbed or strained layers reduces stress concentrations, and lowers the intensities of imposed stresses. It does not build up any appreciable case and its effectiveness depends a great deal on the microstructure and the hardness of the material. It is beneficial on close-grain cast iron and steel materials but has no significant influence on low grade cast iron. In practice, it is necessary to phosphate coat one of the mating members only.

Sparking has occurred in some of the roll tests in which the rate of sliding was high. It was eliminated by phosphate coating one of the rolls. The same procedure has also eliminated sparking between cast iron cams and steel rolls, and between cast iron worms and worm gears.

Speed

For metallic materials subjected to rolling conditions only, the rapidity of the cycle has no appreciable influence on surface fatigue. Similar results were obtained on roll tests in which the machine speed was varied between 1040 and 3200 RPM.

For nonmetallic materials such as laminated phenolics, the rapidity of the stress cycle is an important factor due to the high internal heat of friction and poor heat conductivity of these materials. The combination of load and speed results in roll test failures seldom encountered in cam and gear applications. These failures are typified by blistering of the surface material as shown in Figure 9.

Lubrication

No attempt has been made to evaluate the effects of various lubricants upon the resistance to fatigue of materials subjected to combined rolling and high percent sliding actions. To date surface welding has been avoided by contaminating one of the rolls by phosphate coating. However, in future tests on hardened steel rolls, the combination of high loads and high sliding velocities may necessitate the use of extreme pressure lubricants to prevent or minimize welding tendencies.

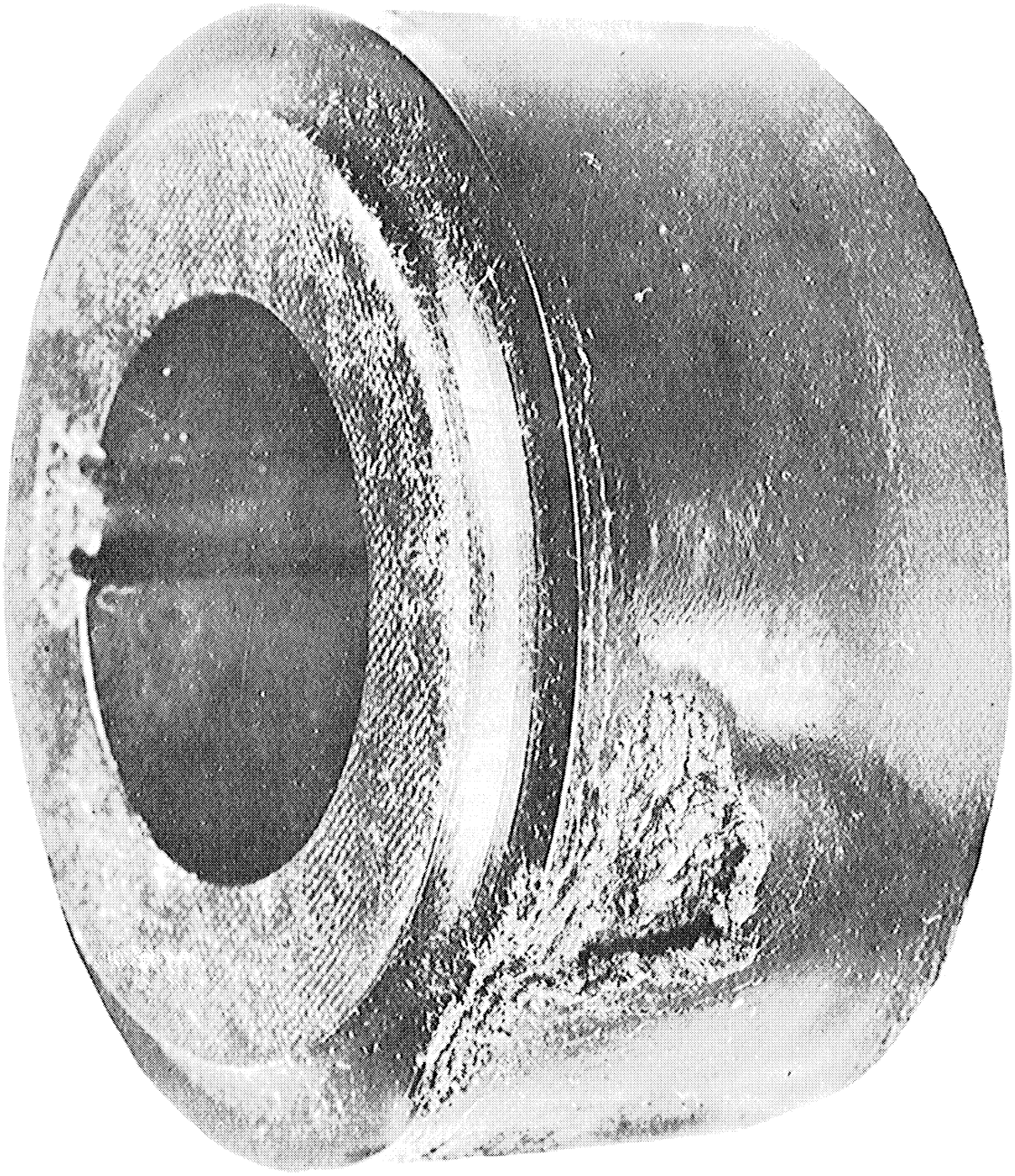

Figure 9. Blistering of the surface material.

With the advent of atomic power, designers must now consider applications in which no lubricant can be used. Therefore, to obtain some indication of the behavior of materials under this condition, some special tests were made with hardened tool steel and 17-4 PH stainless steel mating rolls. No lubricant was used and the rolls were thoroughly degreased. With the driving shaft rotated by hand, no surface damage occurred under rolling action, during 500 cycles and a maximum compressive stress of 93,500 psi, but with combined rolling and only 9% sliding of the driving roll, surface damage occurred at the end of 500 cycles and a maximum compressive stress of 30,000 psi. With combined rolling and 30% sliding, surface damage occurred within 200 repreated cycles. Again, with gross sliding that is, one roll held stationary and the other rotating, surface damage occurred immediately, although the maximum compressive stress was only 21,000 psi.

This would appear to indicate that sliding promotes early welding and scoring of dry surfaces subjected to light loads and very low sliding velocities; whereas under rolling action only, the tendency to surface weld is negligible.

Discussion of Roll Test Results

The load-stress factors for austempered Class 30 iron are higher than for any of the other cast iron materials tested. This is probably due to a change in microstructure resulting from the heat treatment. This treatment was developed in the late 1930's by E. L. Bartholomew and was based on the work done by E. C. Bain, E. S. Davenport, and others, who developed a new series of microstructures intermediate between pearlite and martensite. The heat treatment for Class 30 iron follows:

Heat to 1550 - 1600°F
Quench in salt bath at 650°F approximately
Hold 30 minutes
BHN desired 260 - 290

According to Mr. E. S. Clarke, our metallurgist, the conversion from pearlite to Austenite, no matter what the end result may be (i.e., Austenite, Bainite, tempered Martensite, etc.) results in a re-solution of carbides in a new form. With cast iron alloy, the interrupted quench heat-treatment transforms the pearlitic matrix to a Bainitic structure.

The salt bath used in this treatment refers to the use of molten anhydrous chemical compounds, as sodium chloride, sodium nitrate, barium chloride, etc. for the purpose of maintaining constant temperature baths. So-called austempering or isothermal transformation requires rapid conversion from the high or austenizing heat to a liquid medium in the 500° - 800°F range where the cast iron may transform to intermediate or Bainitic structures.

Precise metallurgical control of composition and heat treatment is essential for consistent and uniform results; otherwise poor machinability or poor wear resistance may ensue.

The load-stress factors for nodular iron, grade 80-60-03 were higher than for the other untreated irons. The load-life relationship charts for this material indicate fairly uniform microstructure of the rolls tested.

Load-stress factors for GM Meehanite are higher than those for untreated Classes 20 and 30 irons. Since this material can be austempered, it is reasonable to expect that the load-stress factors for austempered GM Meechanite would compare favorably with the factors for the austempered Class 30 iron.

Load-stress factors for Class 20 irons are less than those of any other cast iron material tested. Unlike any of the other irons, negligible improvement in surface finish and hardness was experienced from the roll tests. Also, phosphate coating did not increase the load-stress factors, and the dispersion of the roll test results indicate non-uniformity of grain structure.

Tests on carburized and induction hardened steel rolls indicate that the depth of the case should be at least twice the depth of the point of maximum shear stress. Unlike ductile materials, where the surface finish is not too critical because of the plasticity of the surface material, the degree of surface finish of hardened steels is important to prevent high local stress concentrations. Although some uncertainty exists whether or not fatigue cracks start on or underneath the loaded surfaces, the photomicrographs of a carburized steel roll, 0.020 in depth of case (Figure 10), and of a medium-carbon steel heat treated to 270-290 BHN (Figure 11) taken below the surface layer, throw some further light on this interesting phase of wear phenomena. These damaged rolls were subjected to rolling contact only. The photomicrographs show fatigue cracks below the surface layer and in the region where the shear stress is maximum. It appears that under the influence of repeated cycles of stress, the cracks grow progressively and up to the surface layer. When some of the particles break out, destructive pitting occurs.

The relatively high limiting load-stress factors for medium carbon steel heat treated to 270-300 BHN appear to be due to its cold working properties which build up a mechanical case sufficient to withstand the imposed stresses. The beneficial effect of phosphate coating is quite pronounced as evidenced by the results of the roll tests. Flash chromium plating did not increase the load-stress factors for the base material.

A few tests on SAE 6150 steel heat treated to 300-320 BHN show the load-stress factors to be similar to those for SAE 1020 steel. This high-grade steel appears to have poor resistance to surface fatigue in the 300 BHN range.

PHOTOMICROGRAPH OF A 2.300 DIA. 3/8" FACE, FINE GROUND SURFACE FINISH TEST ROLL
TAKEN NORMAL TO AND INCLUDING EDGE OF BEARING SURFACE.

100X - NITAL ETCH

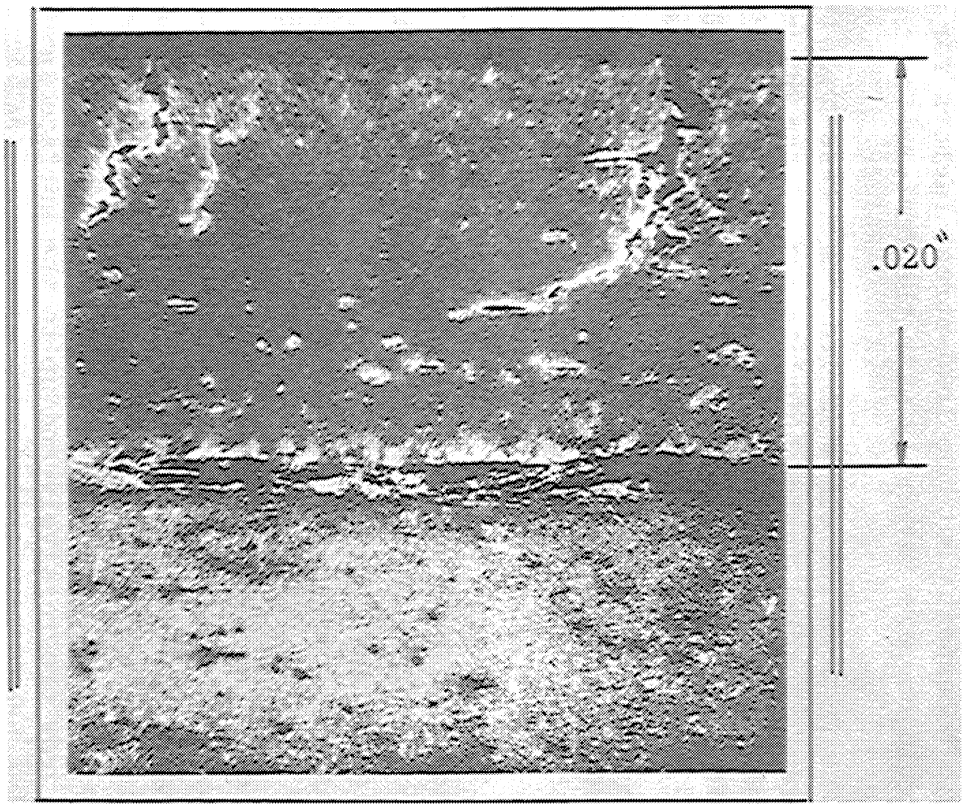

TEST RUN UNDER ROLLING CONDITION ONLY - 2340# APPLIED LOAD
SURFACE FAILURE AT 424,000 CYCLES - 1.05 HARDENED TOOL STEEL MATING ROLL.
TEST ROLL MATERIAL
LOW CARBON FREEMACHINING STEEL - CARBURIZED TO .025" DEPTH APPROX.
REHEATED TO 1425°F - 1450°F. QUENCHED IN OIL. 52-58 Rc HARDNESS

Figure 10. Photomicrograph of a carburized steel roll.

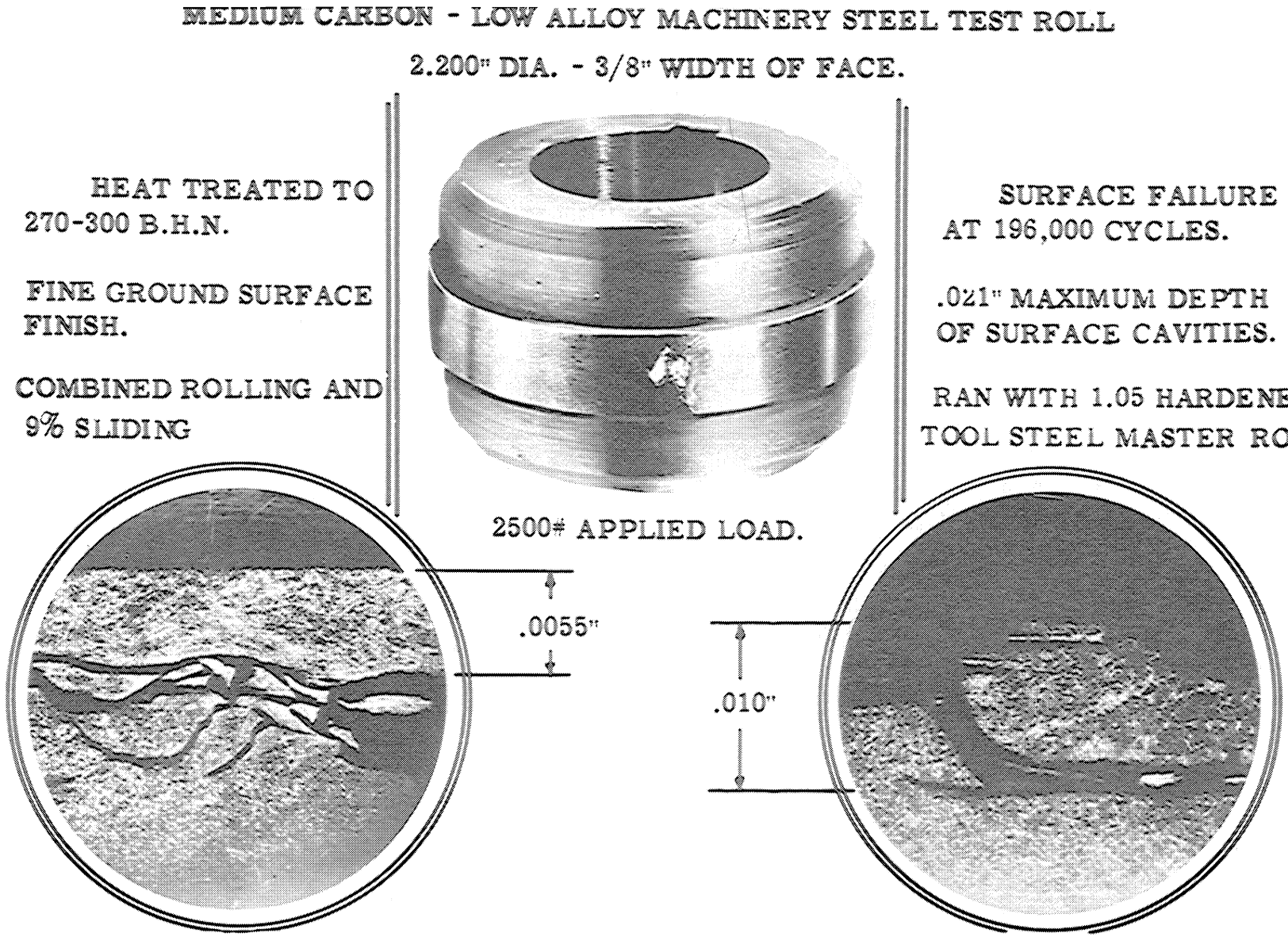

Figure 11. Photomicrograph of medium-carbon steel roll.

Tests on bronze materials have been few, and made under rolling conditions only. Some tests on austempered cast iron and bronze combinations indicate higher load-stress factors than for a combination of hardened steel and bronze. Load-stress factors for SAE 39 cast aluminum and for zinc die cast material were low and of approximately the same magnitude. Neither of these materials showed a tendency to cold-work.

Unlike metals, the load-stress factors for phenolic materials subjected to rolling action only, are affected by speed. The greater the speed the lower the limiting surface load-stress factors. The load-stress factors are further reduced when the material is subjected to combined rolling and various per cent sliding actions.

Representative load-stress factors for several laminated phenolic materials are included in the paper.

The roll tests made on these materials give some measure of the resistance to surface fatigue for given rolling speeds and for combined rolling and sliding speeds. Since the elastic deformation of laminated phenolics is many times that of metals, the load-stress factors determined from the roll test data can be directly applied in design.

In cam and gear applications the low modulus of elasticity of the non-metallic materials (5×10^5 to 10^6 lbs/sq.in) is an important factor in reducing the magnitude of impact loads.

With gears, for example, the impact load between metallic gear teeth may be many times the applied tooth load, but on nonmetallic gear teeth this impact load does not exceed twice the applied load. Impact loads on cam surfaces caused by separation between cam and cam roll are also restricted by the high elastic deformation of phenolic cam materials.

APPENDIX

Included in the Appendix are charts of the load-life relationships for the various combinations of materials listed in Table 2.

REFERENCES

1. Bartholomew, E.L., "Gray Cast Iron - A New Heat Treatment," Iron Age, August, 1940.

2. Buckingham, E., Analytical Mechanics of Gears, New York McGraw-Hill Book Company, Inc., 1949.

3. Buckingham, E., "Surface Fatigue of Plastic Materials," Trans. ASME, Vol. 66, 1944.

4. Buckingham, E., "Qualitative Analysis of Wear," Mechanical Engineering, August, 1937.

5. Buckingham, E., and Talbourdet, G.J., "Roll Tests on Endurance Limits of Materials," "Mechanical Wear," American Society for Metals, Jan., 1950.

6. Cram, W.D., "Cam Design," Third Mechanisms Conference, Purdue University, May, 1956.

7. Hertz, H., Gesammekte Werke, Vol. 1, Leipzig, 1895.

8. Kloomok, M. and Muffley, R.V., "Determination of Radius of Curvature for Radial and Swinging Follower Cam Systems," ASME Paper No. 55-SA-29.

9. Smith, J.O., and Chang Keng Lui, "Stresses Due to Tangential and Normal Loads on an Elastic Solid with Application to Some Contact Stress Problems," ASME Paper No. 52-A- 13.

10. Talbourdet, G.J., "A Progress Report on the Surface Endurance Limits of Engineering Materials, ASME Paper No. 54-LUB-14.

11. Talbourdet, G.J., "Laminated Phenolic Cams," Product Engineering, September, 1939.

12. Timoshenko, S., Theory of Elasticity, McGraw-Hill Book Co., Inc., 1934.

13. Way, Stewart, "Pitting Due to Rolling Contact," Trans. ASME, Vol 57, 1935.

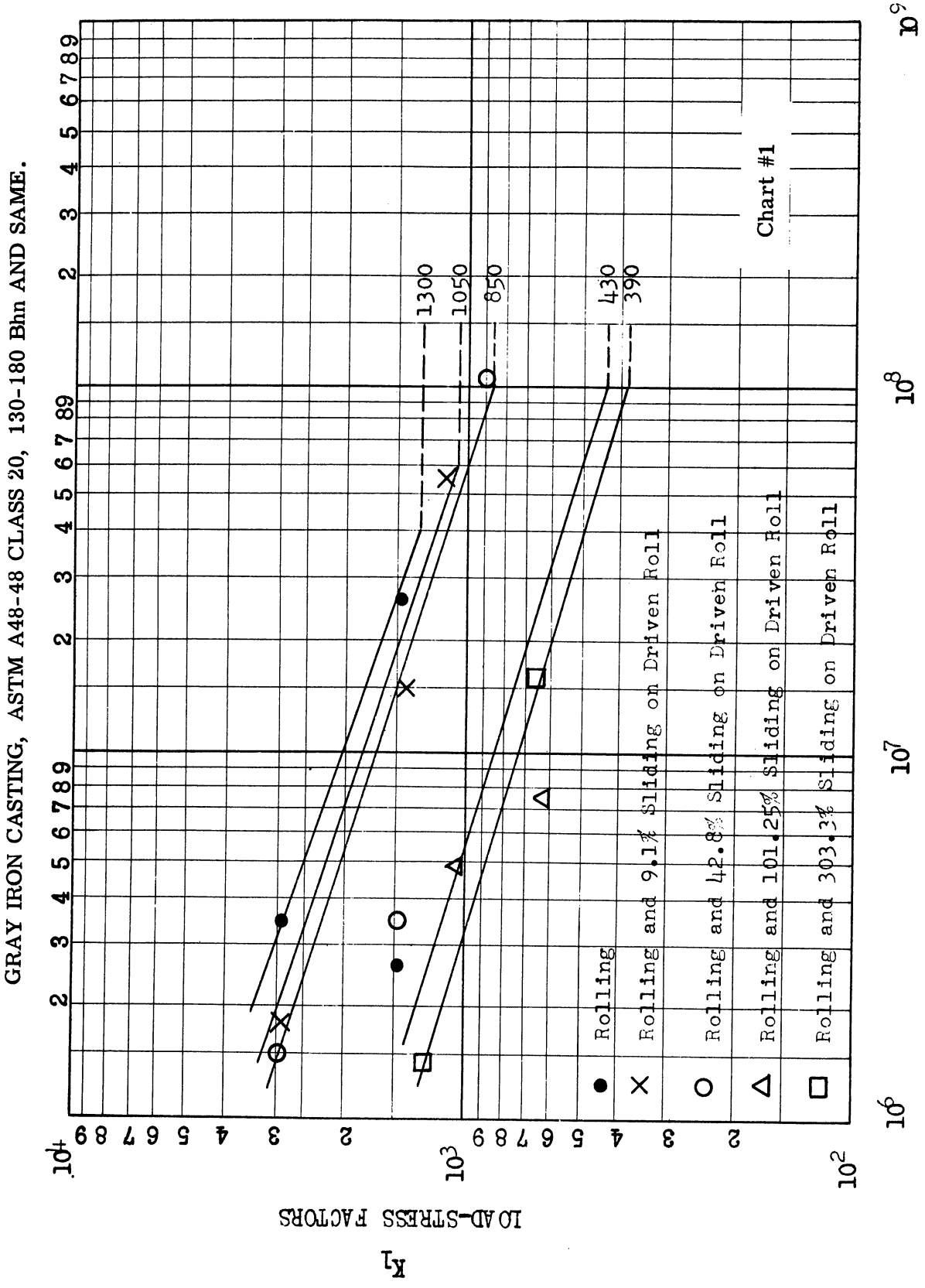

Figure 12. Fatigue curve.

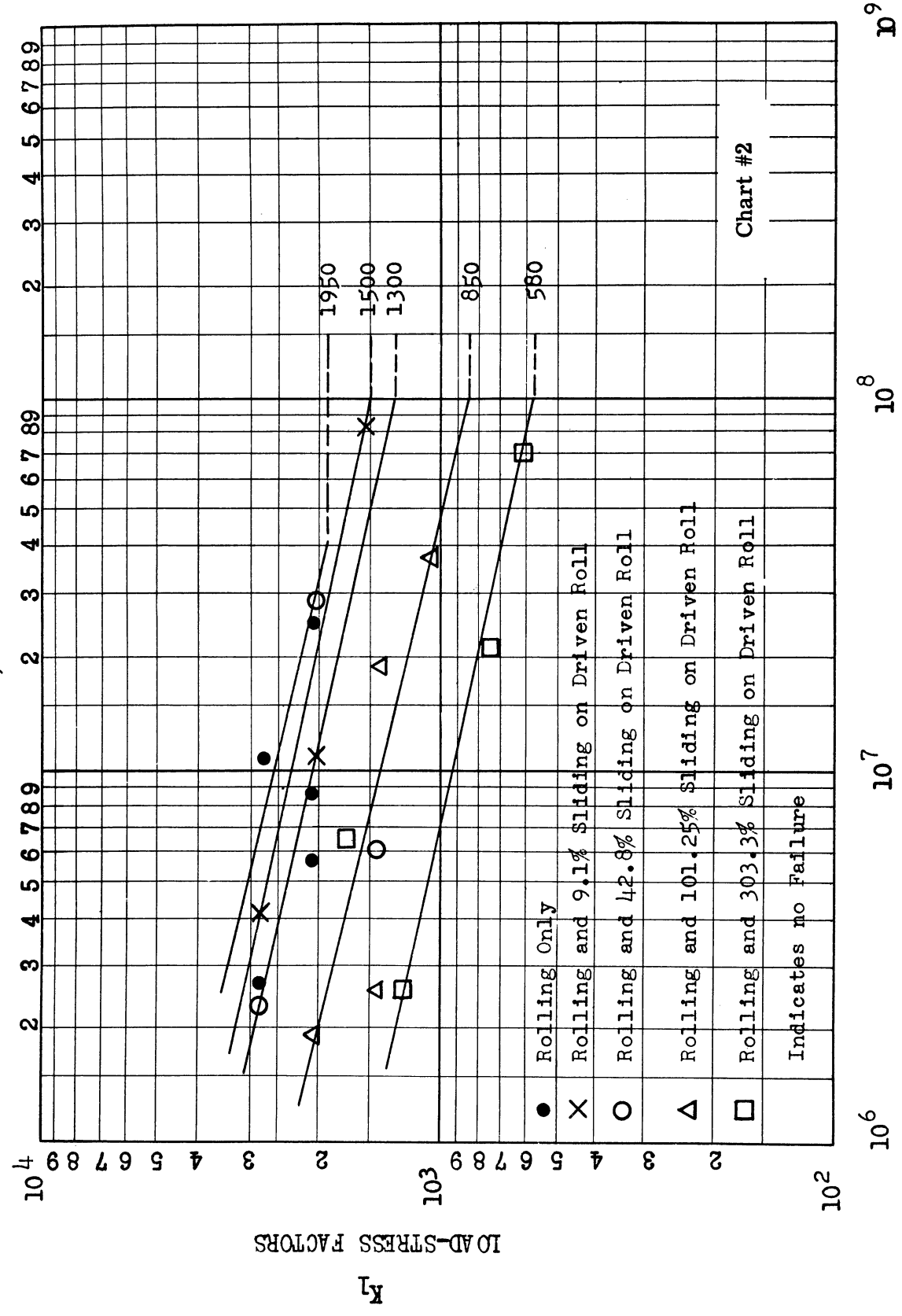

Figure 13. Fatigue curve.

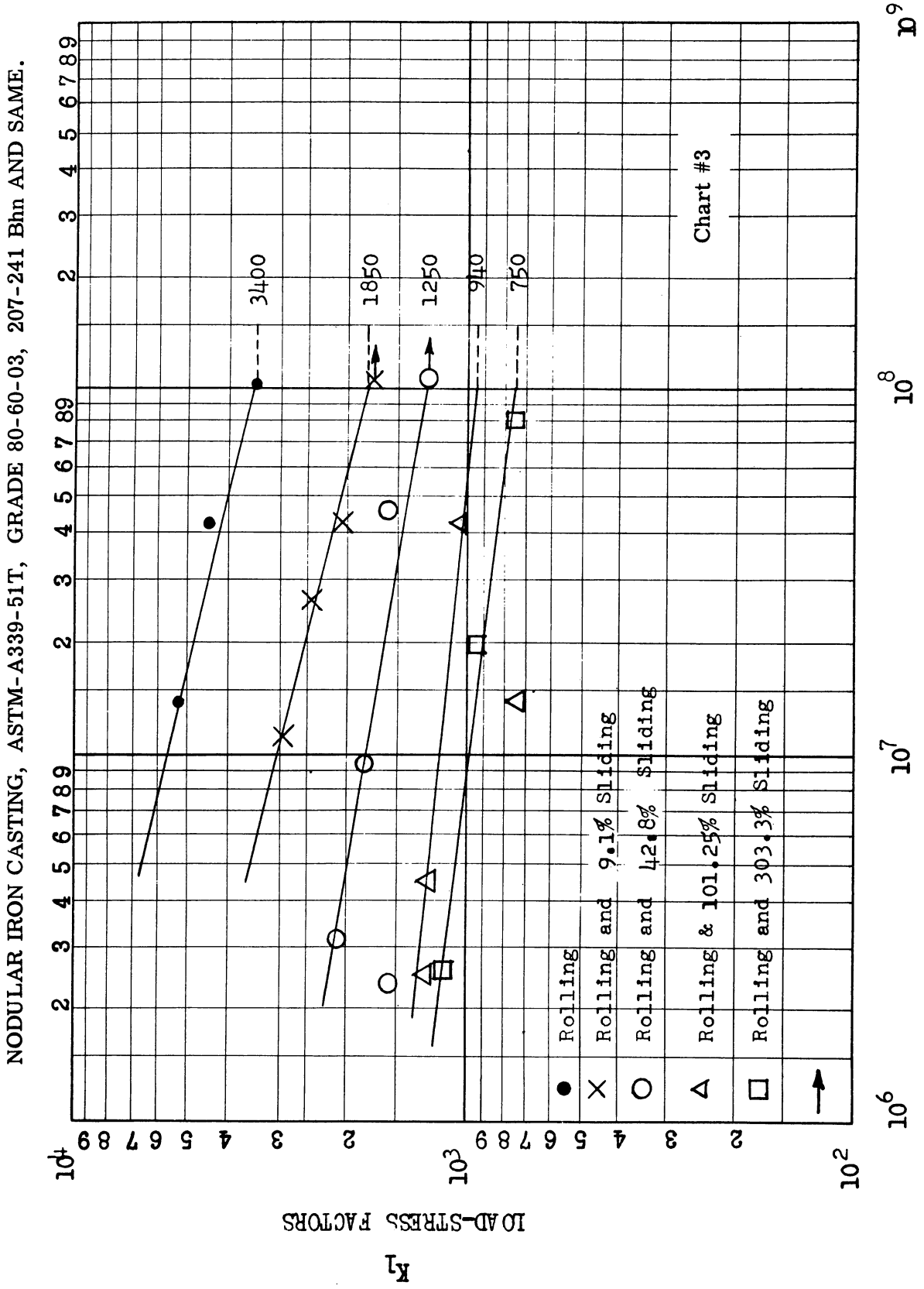

Figure 14. Fatigue curve.

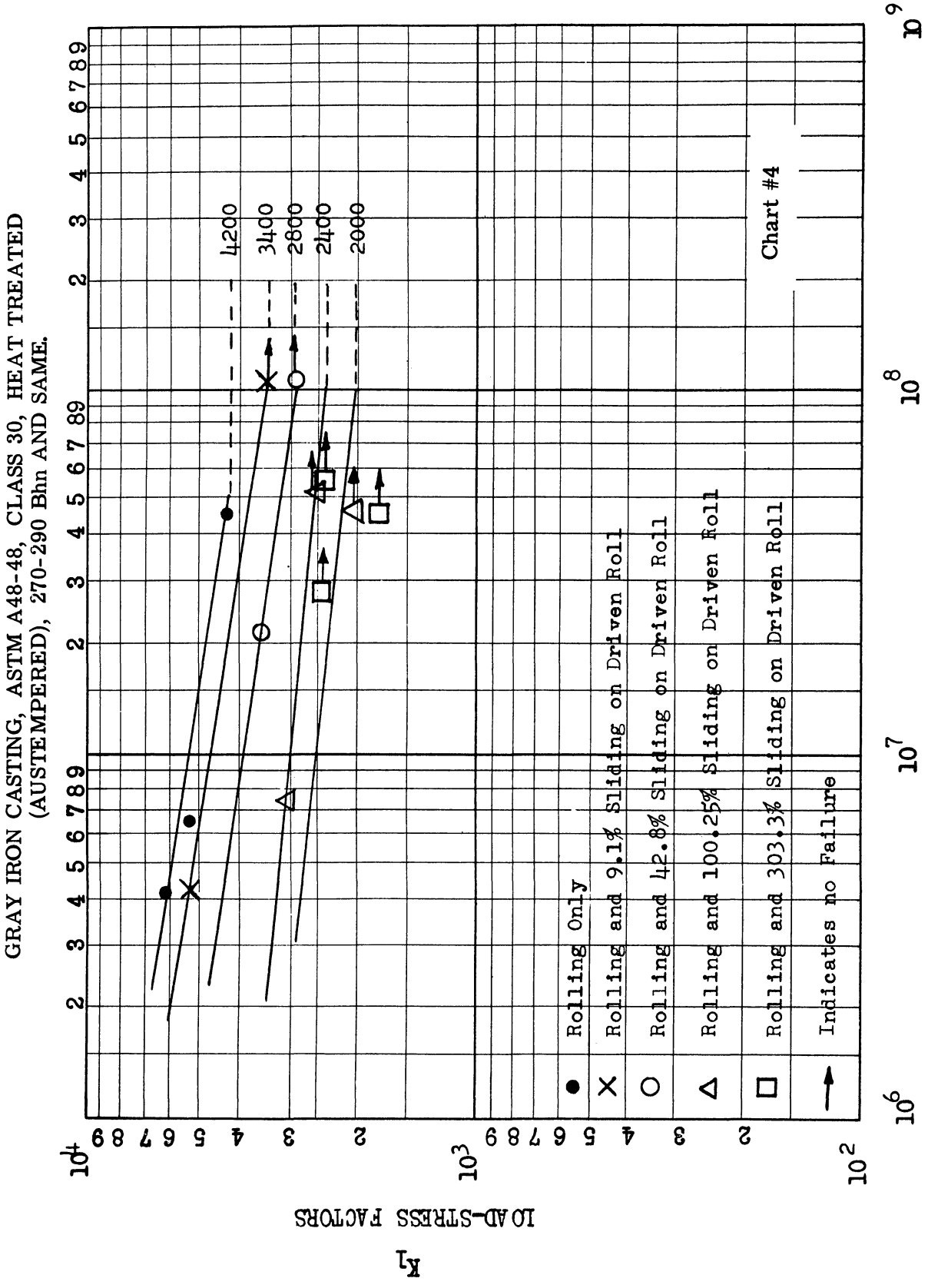

Figure 15. Fatigue curve.

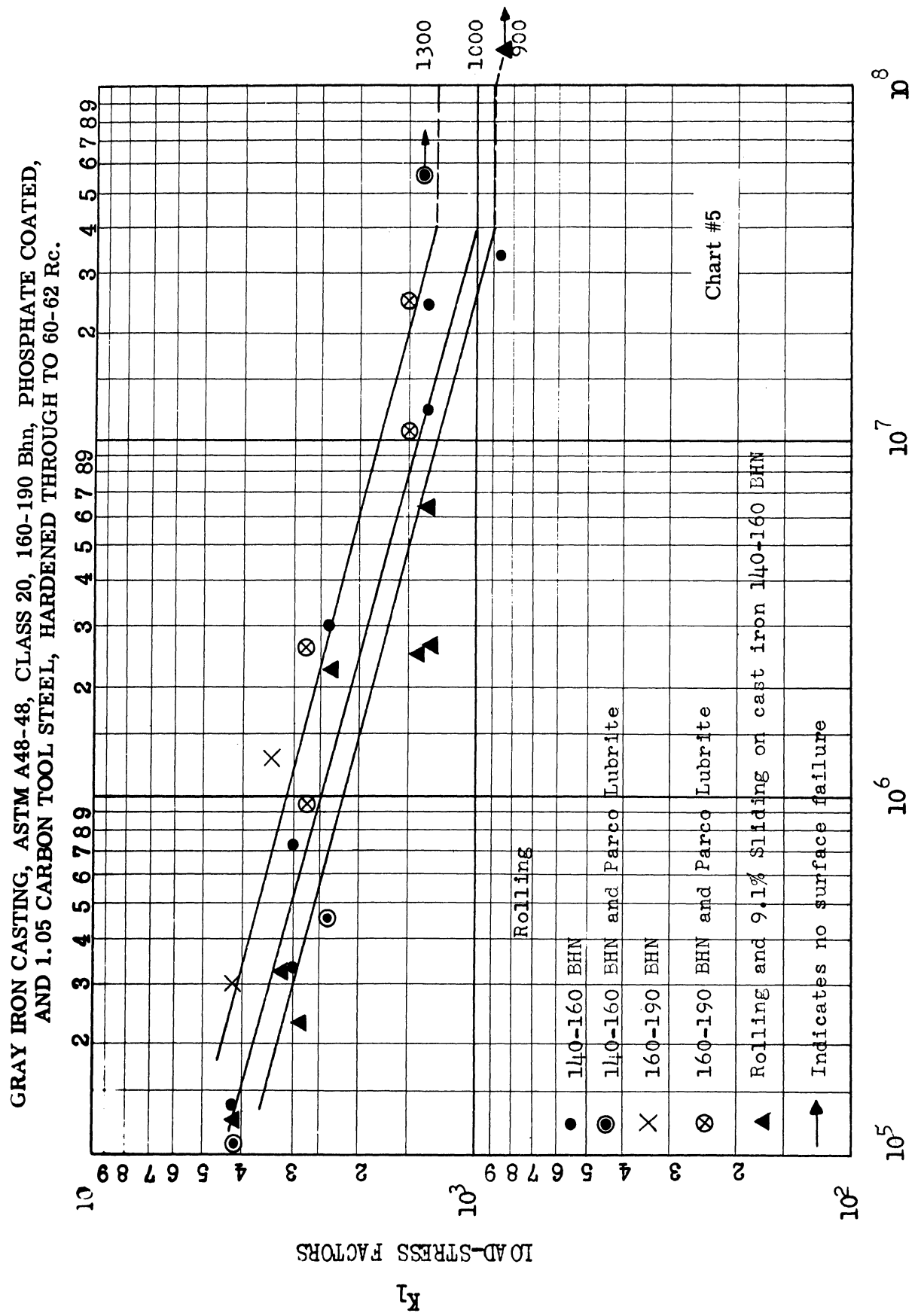

Figure 16. Fatigue curve.

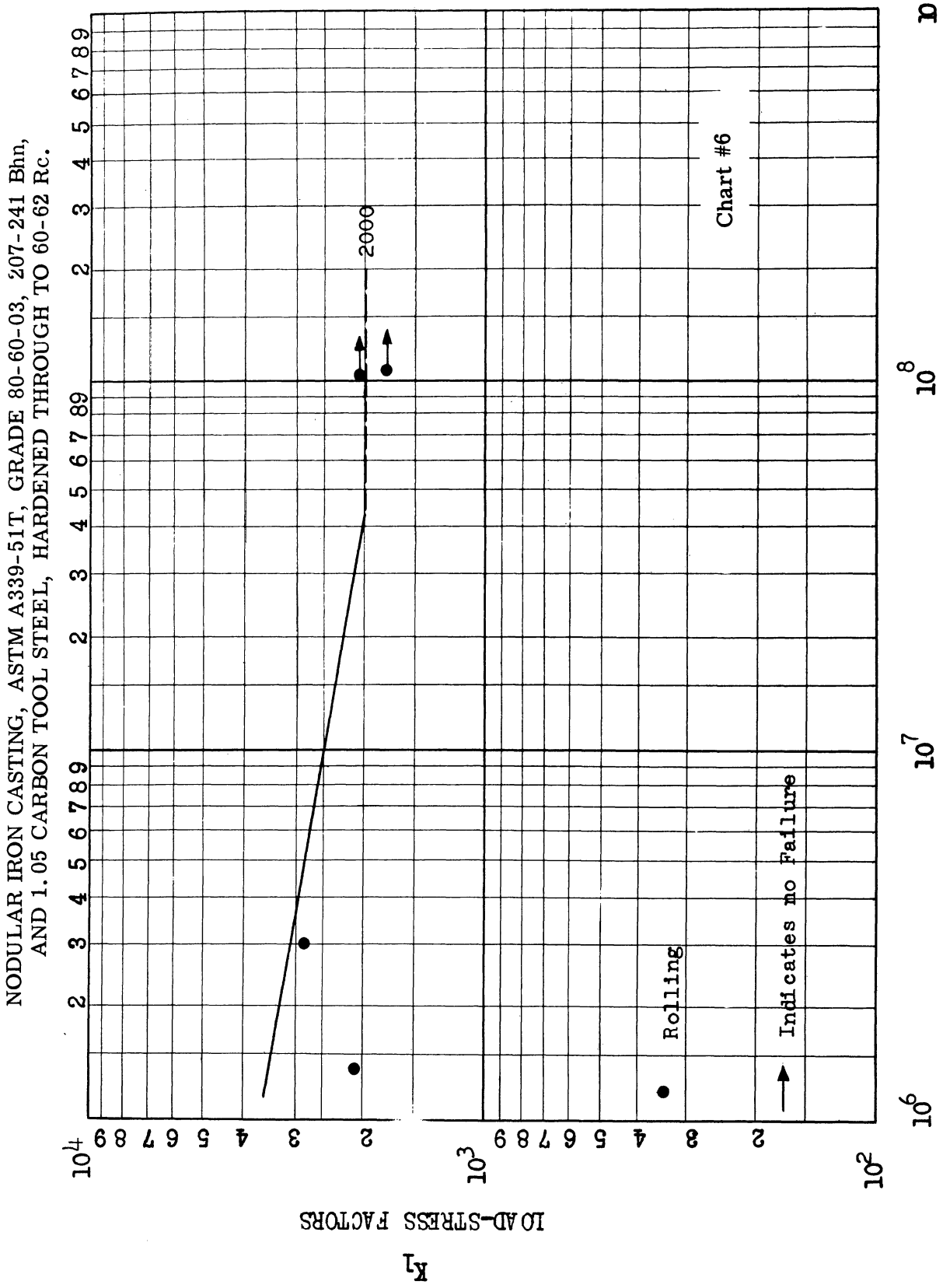

Figure 17. Fatigue curve.

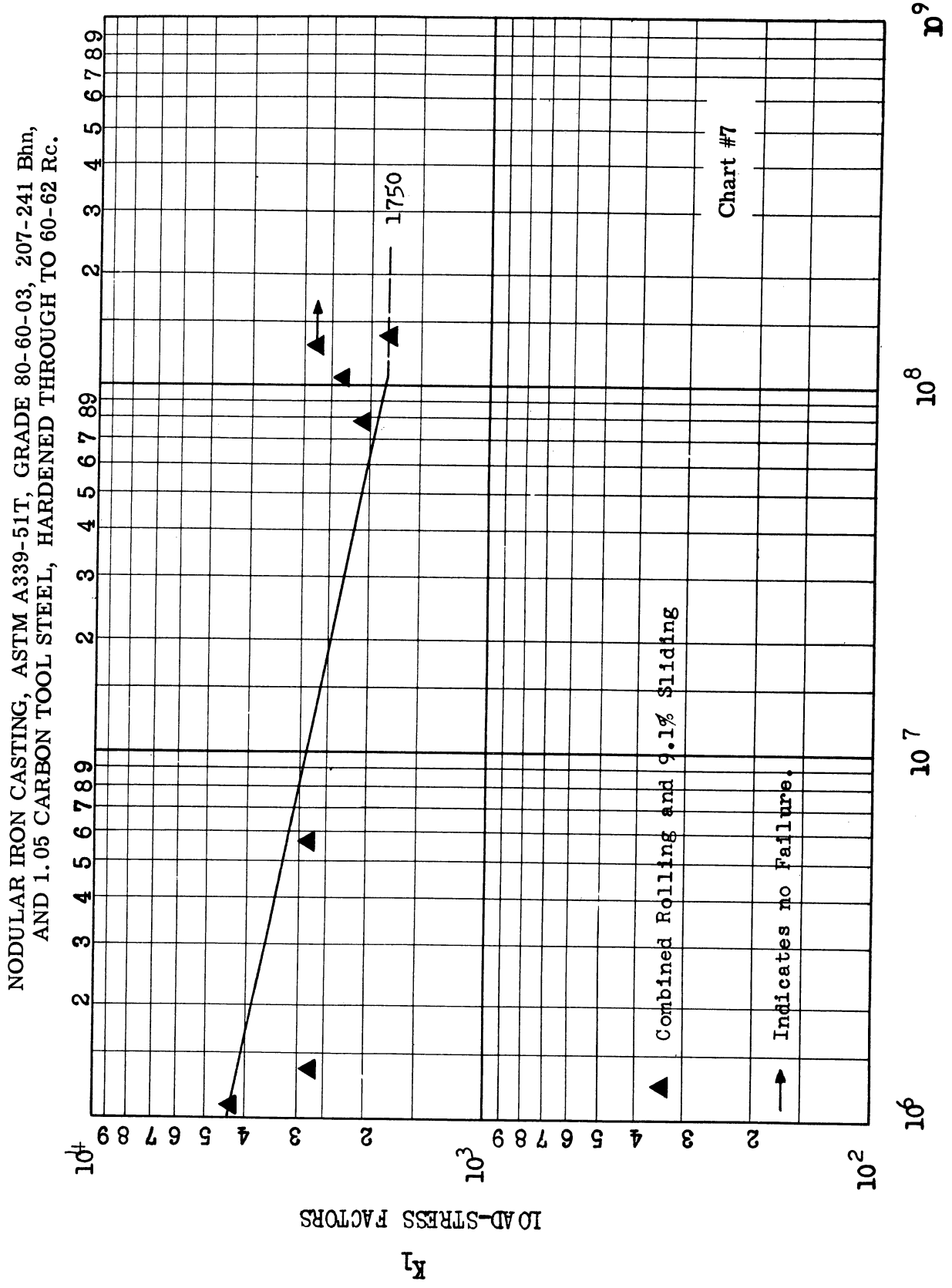

Figure 18. Fatigue curve.

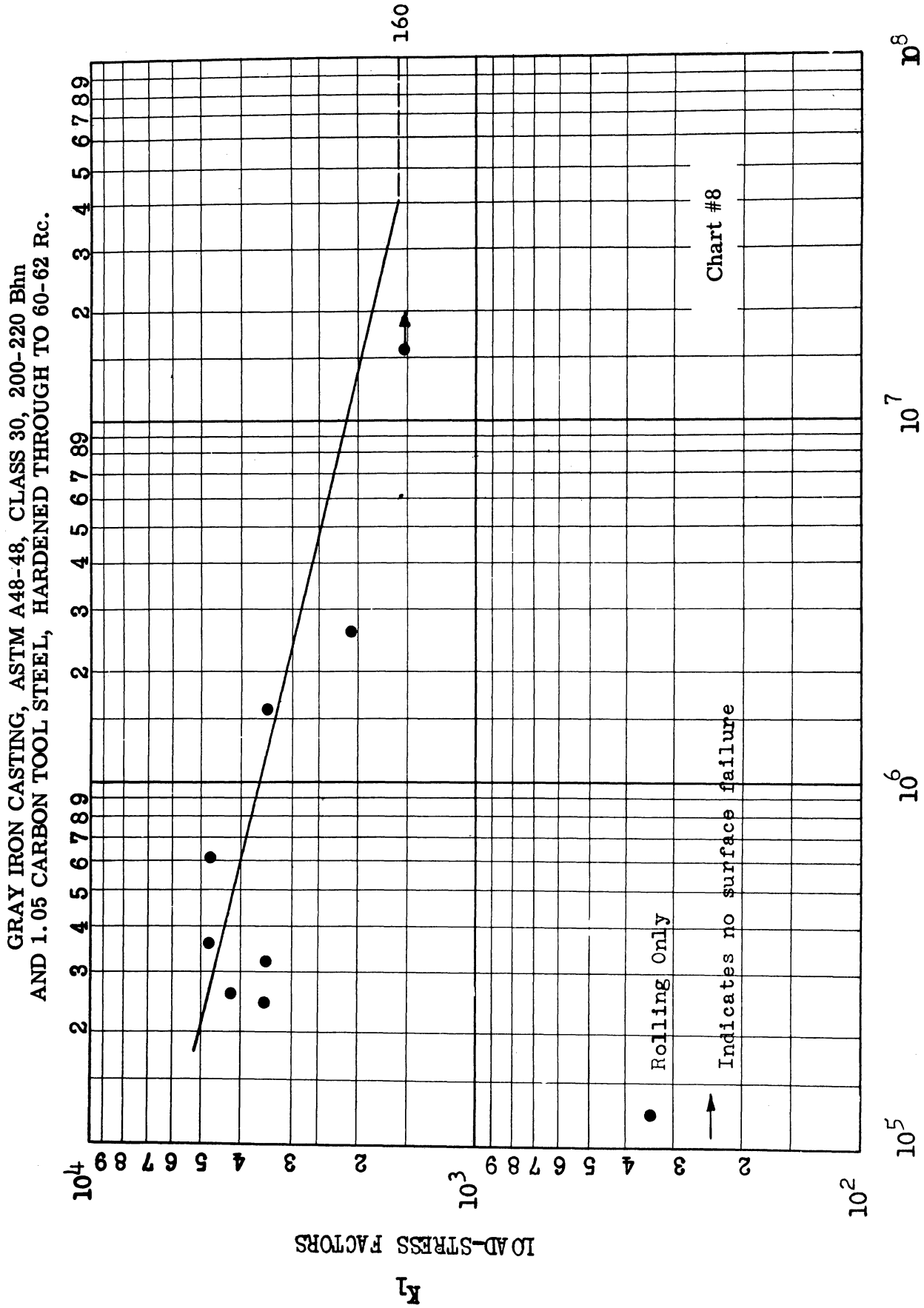

Figure 19. Fatigue curve.

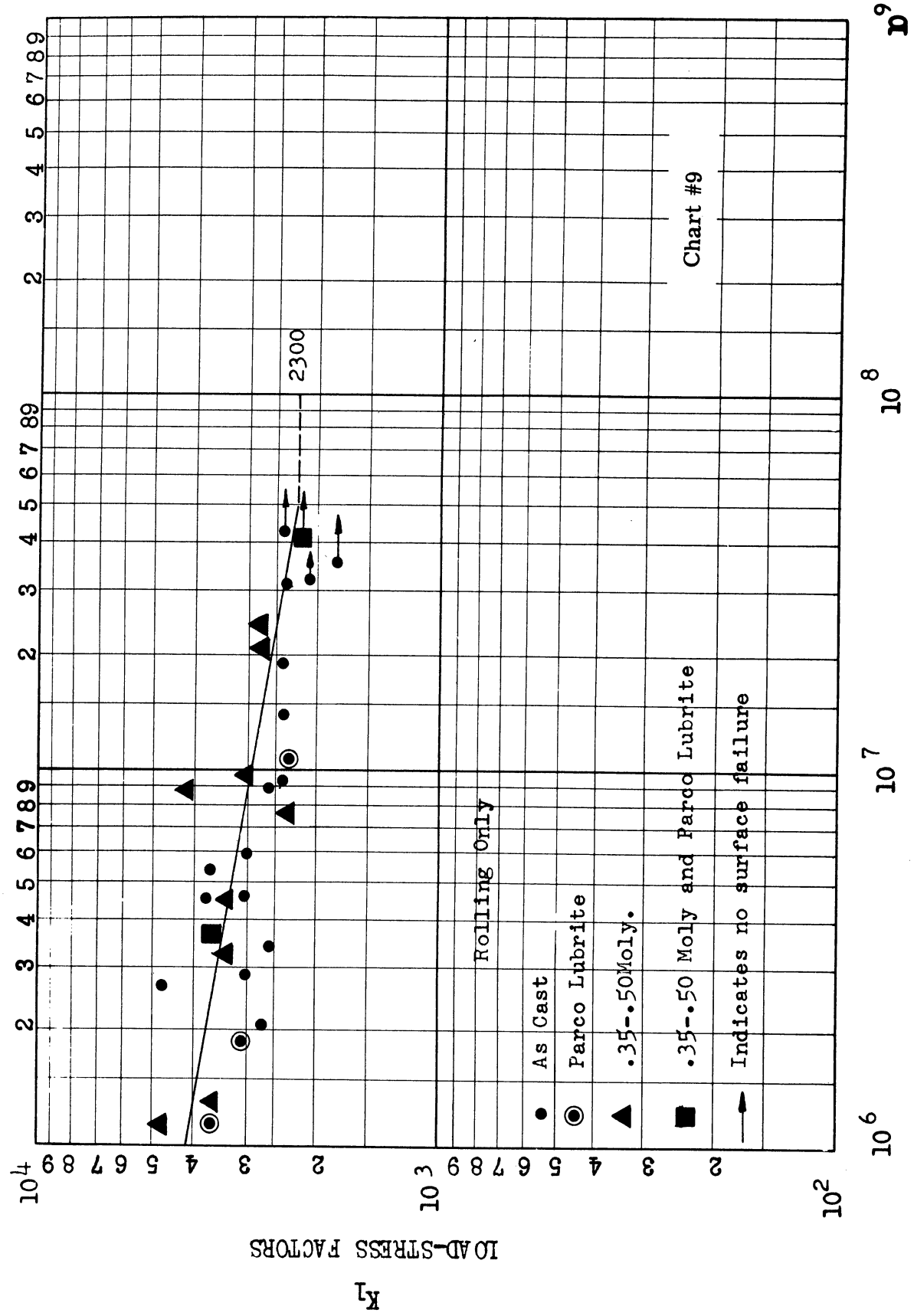

Figure 20. Fatigue curve.

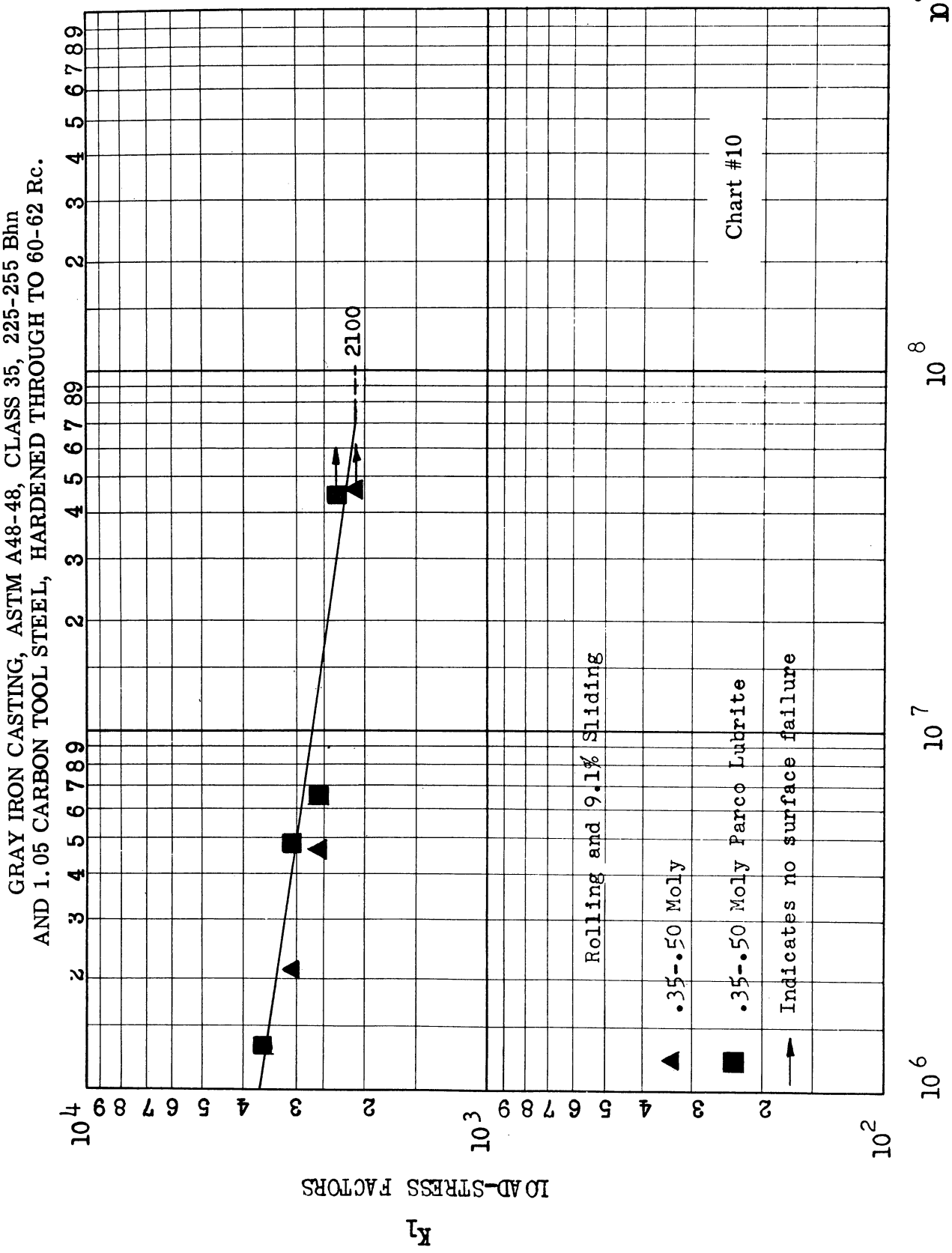
GRAY IRON CASTING, ASTM A48-48, CLASS 35, 225-255 Bhn
AND 1.05 CARBON TOOL STEEL, HARDENED THROUGH TO 60-62 Rc.
Chart #10
2100
Rolling and 9.1% Sliding
.35-.50 Moly
.35-.50 Moly Parco Lubrite
Indicates no surface failure
LOAD-STRESS FACTORS
K1
NUMBER OF CYCLES

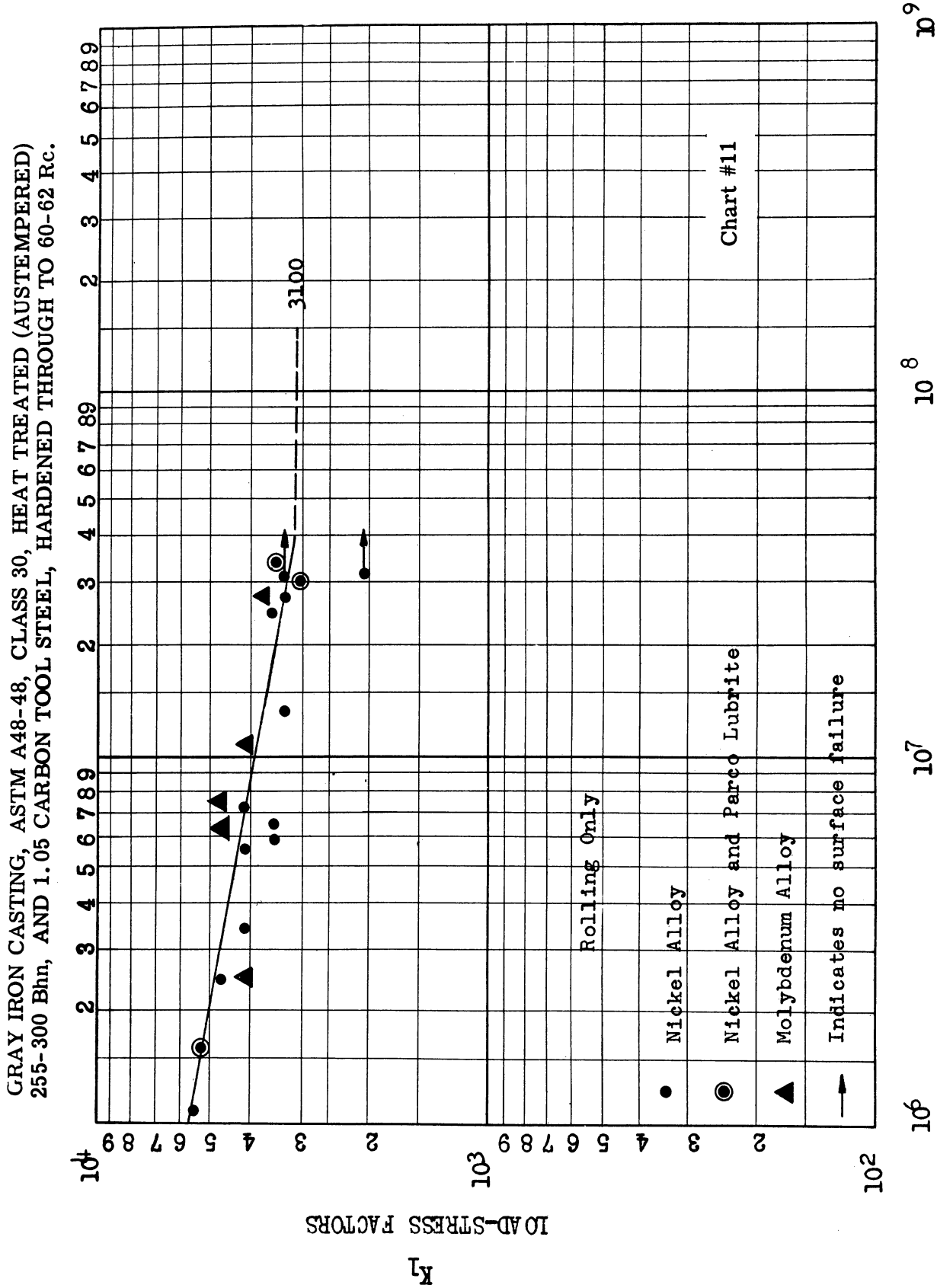

Figure 22. Fatigue curve.

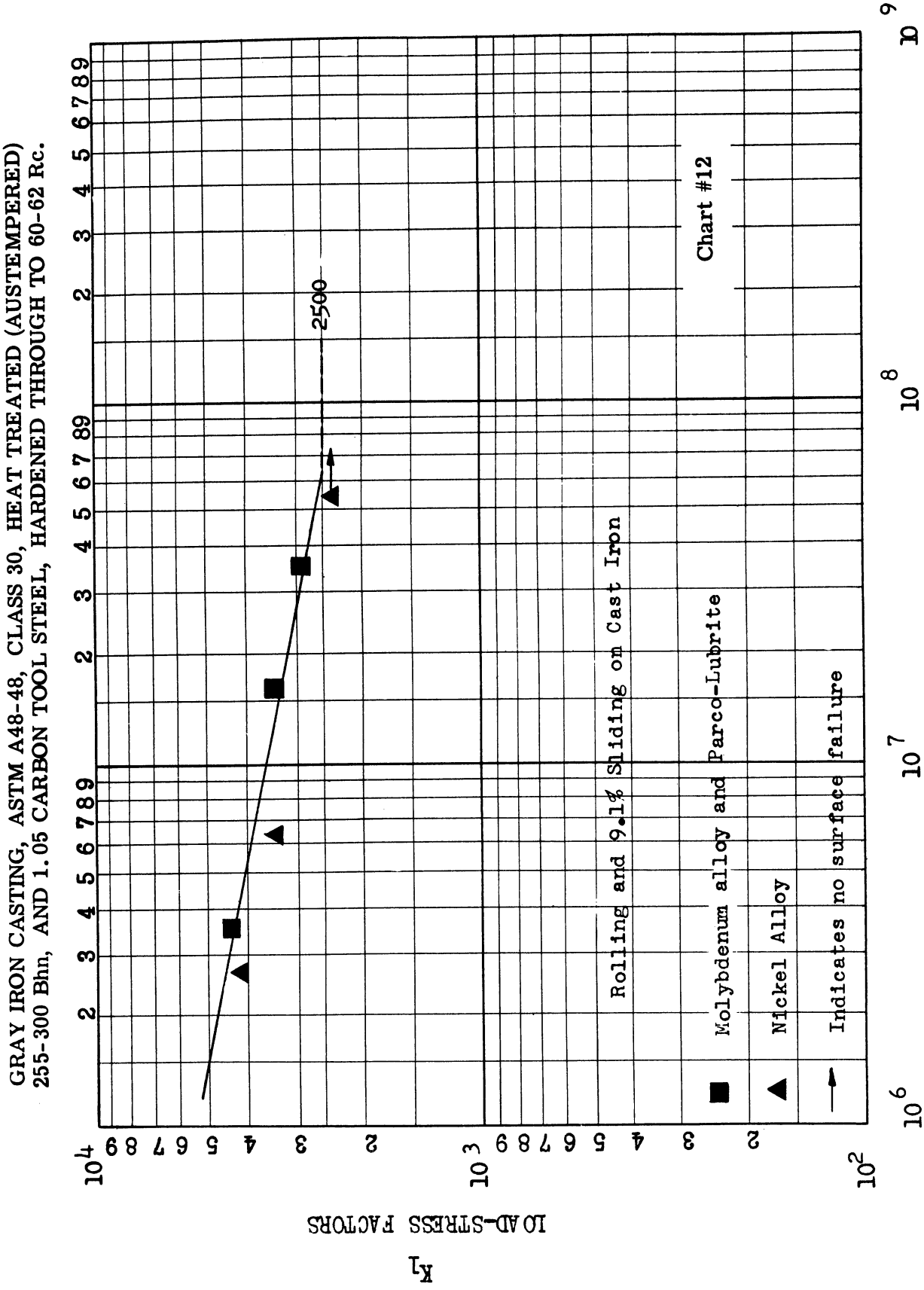

Figure 23. Fatigue curve.

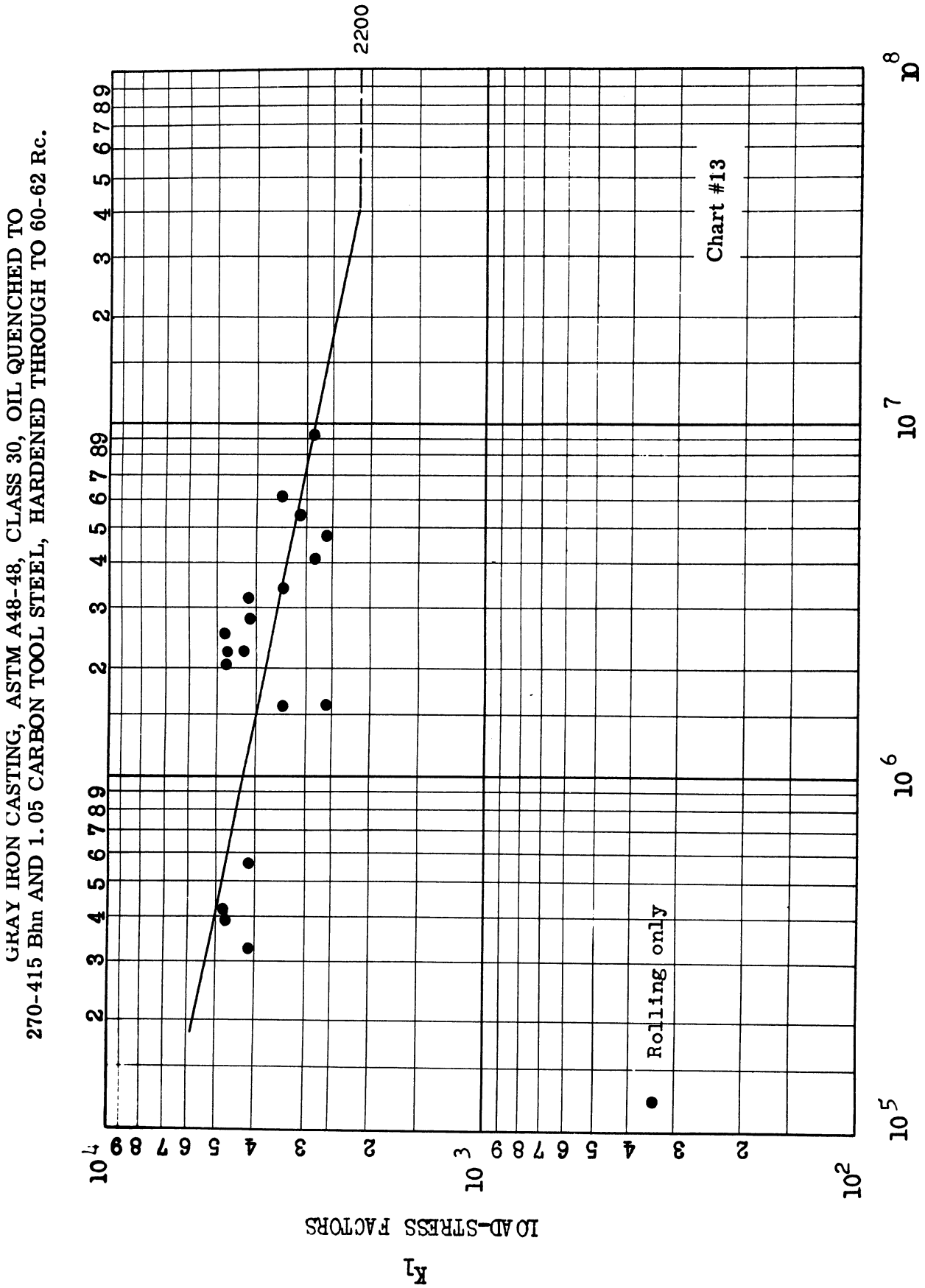

Figure 24. Fatigue curve.

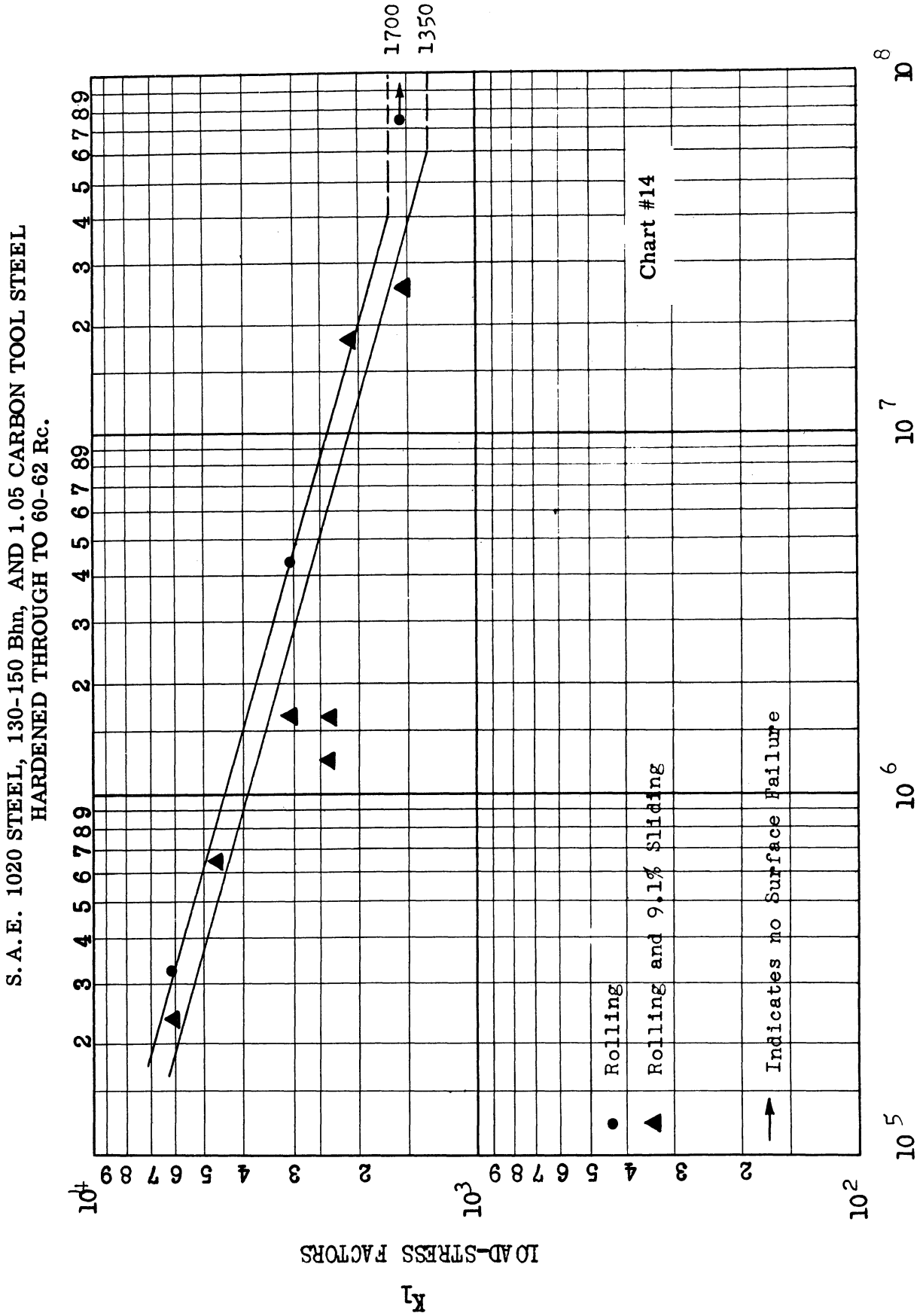

Figure 25. Fatigue curve.

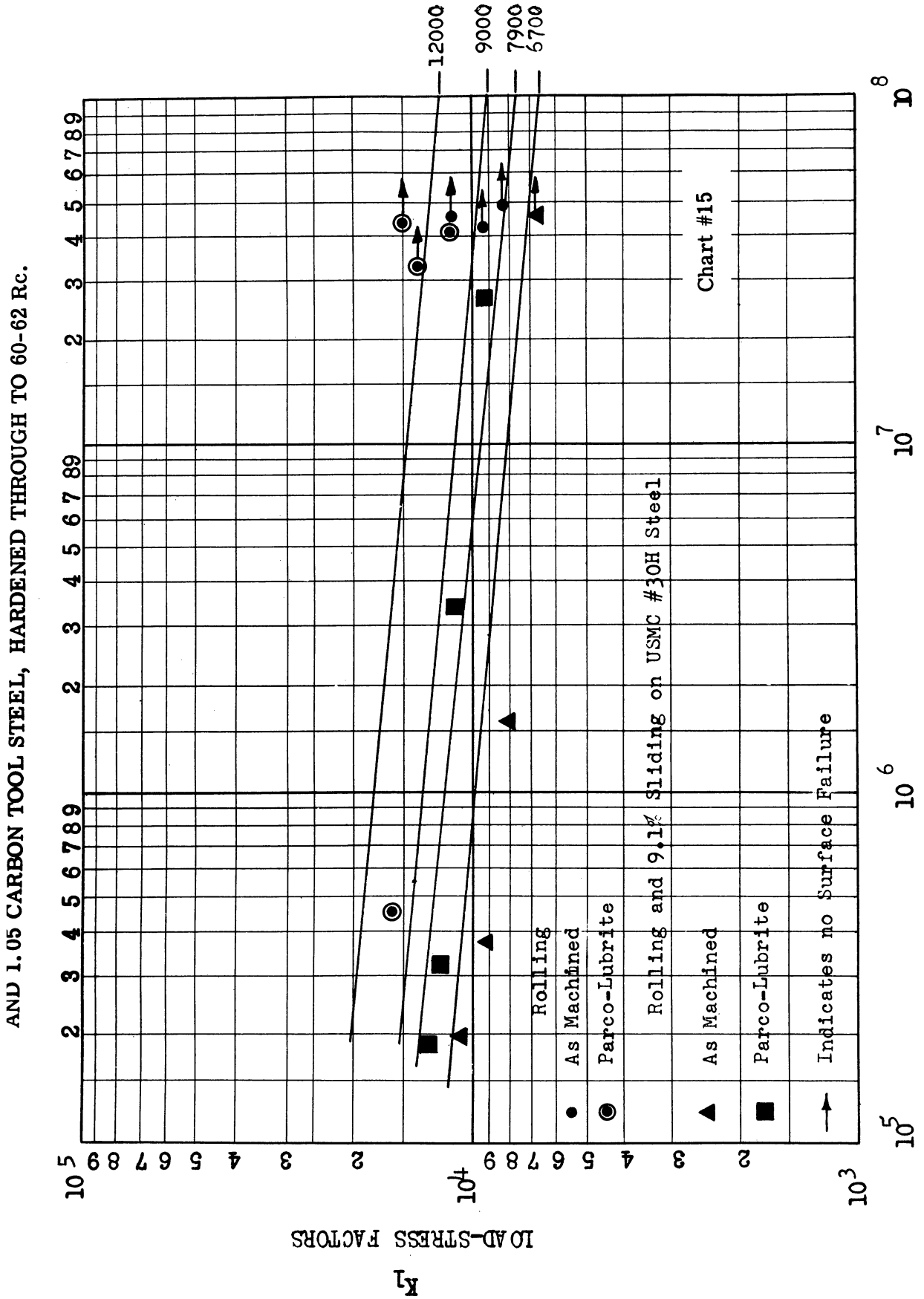

Figure 26. Fatigue curve.

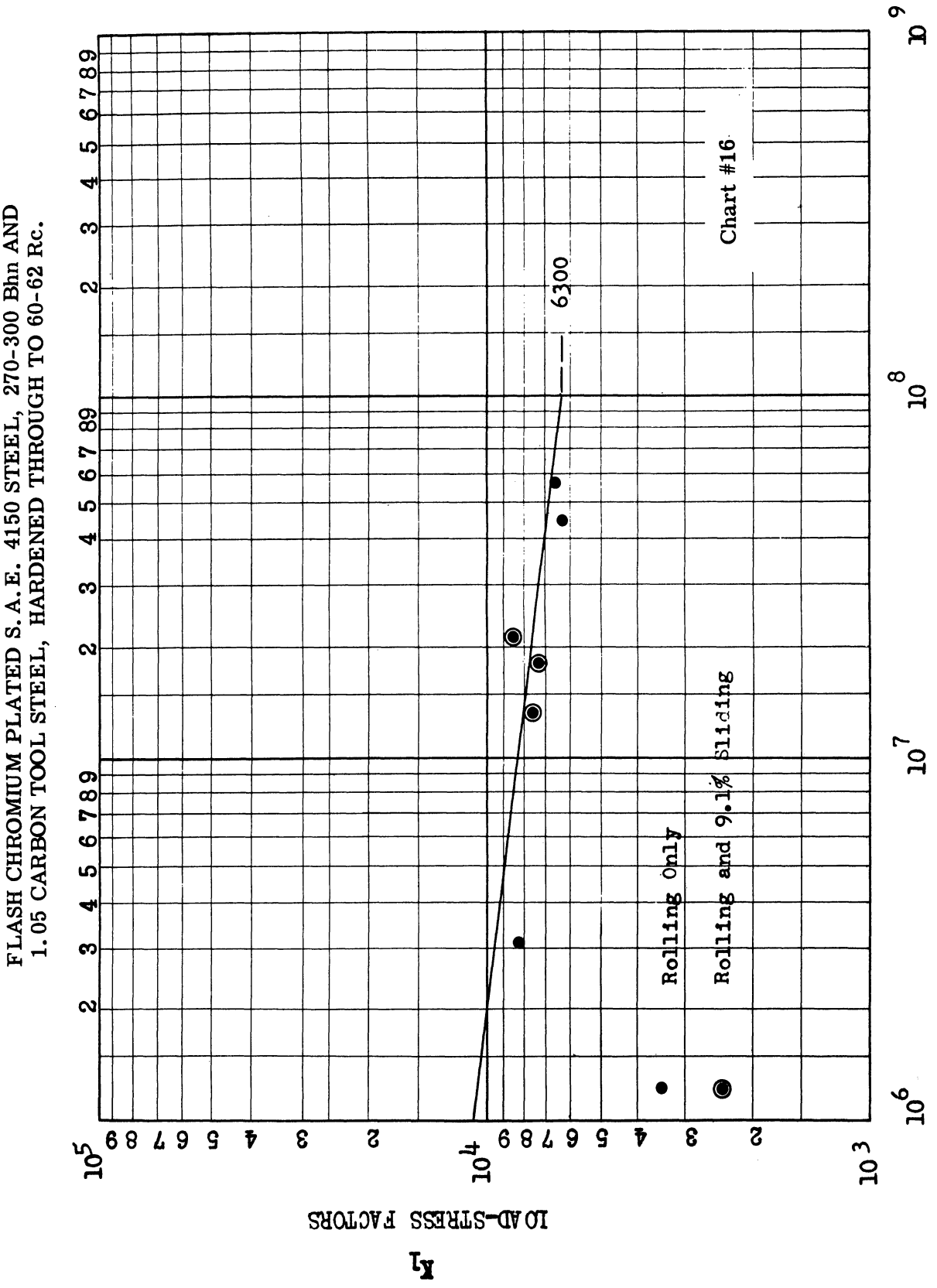

Figure 27. Fatigue curve.

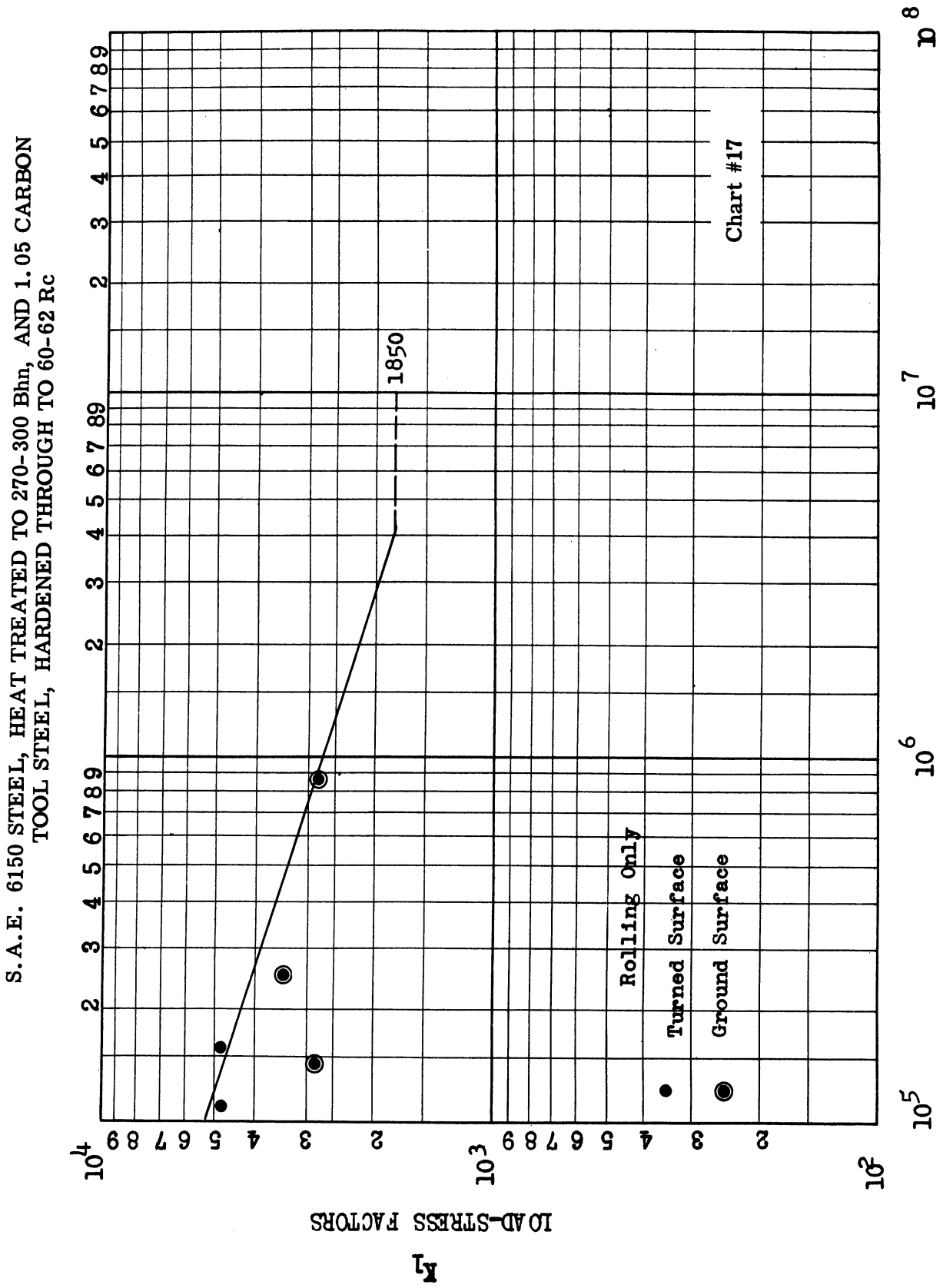

Figure 28. Fatigue curve.

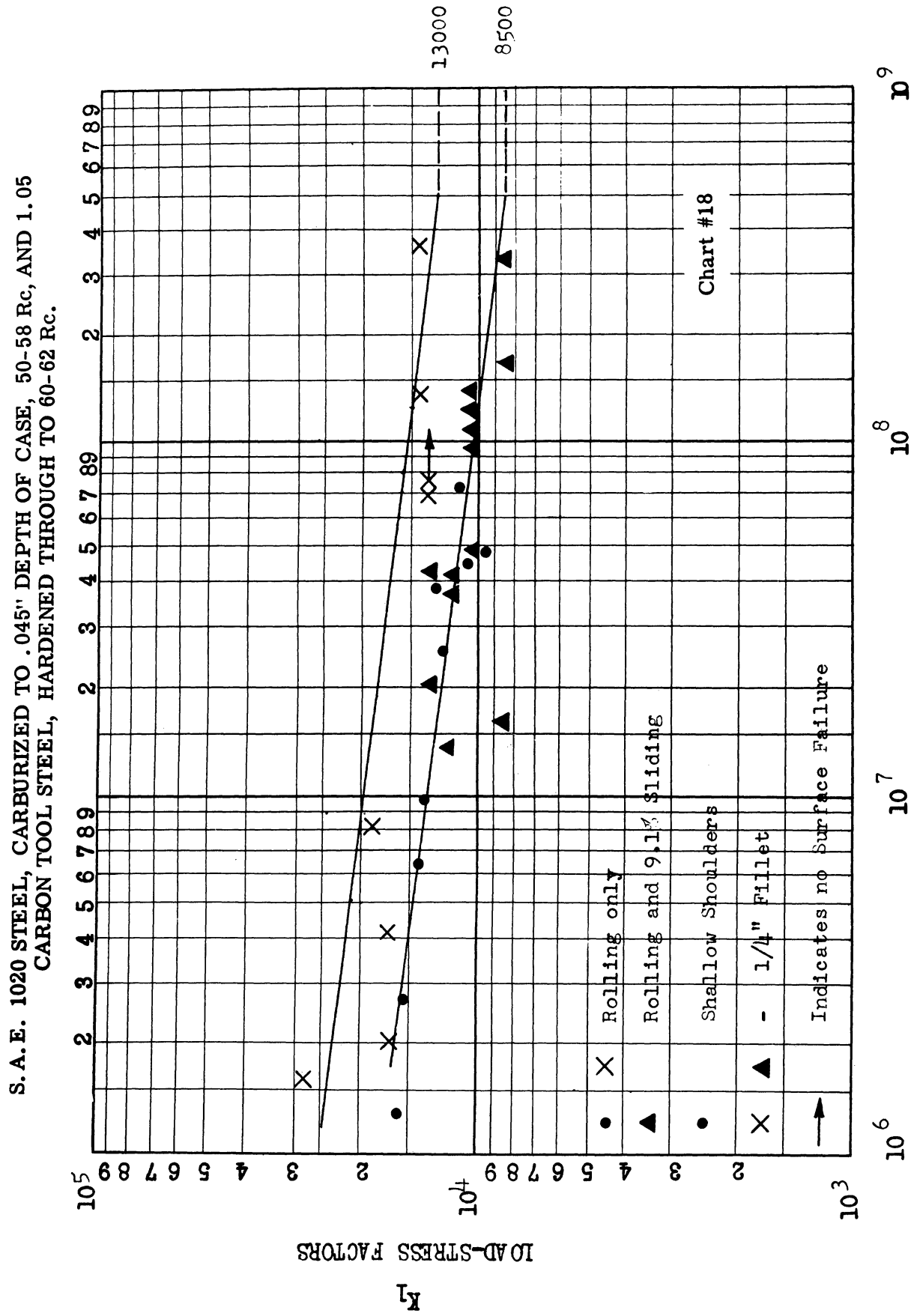

Figure 29. Fatigue curve.

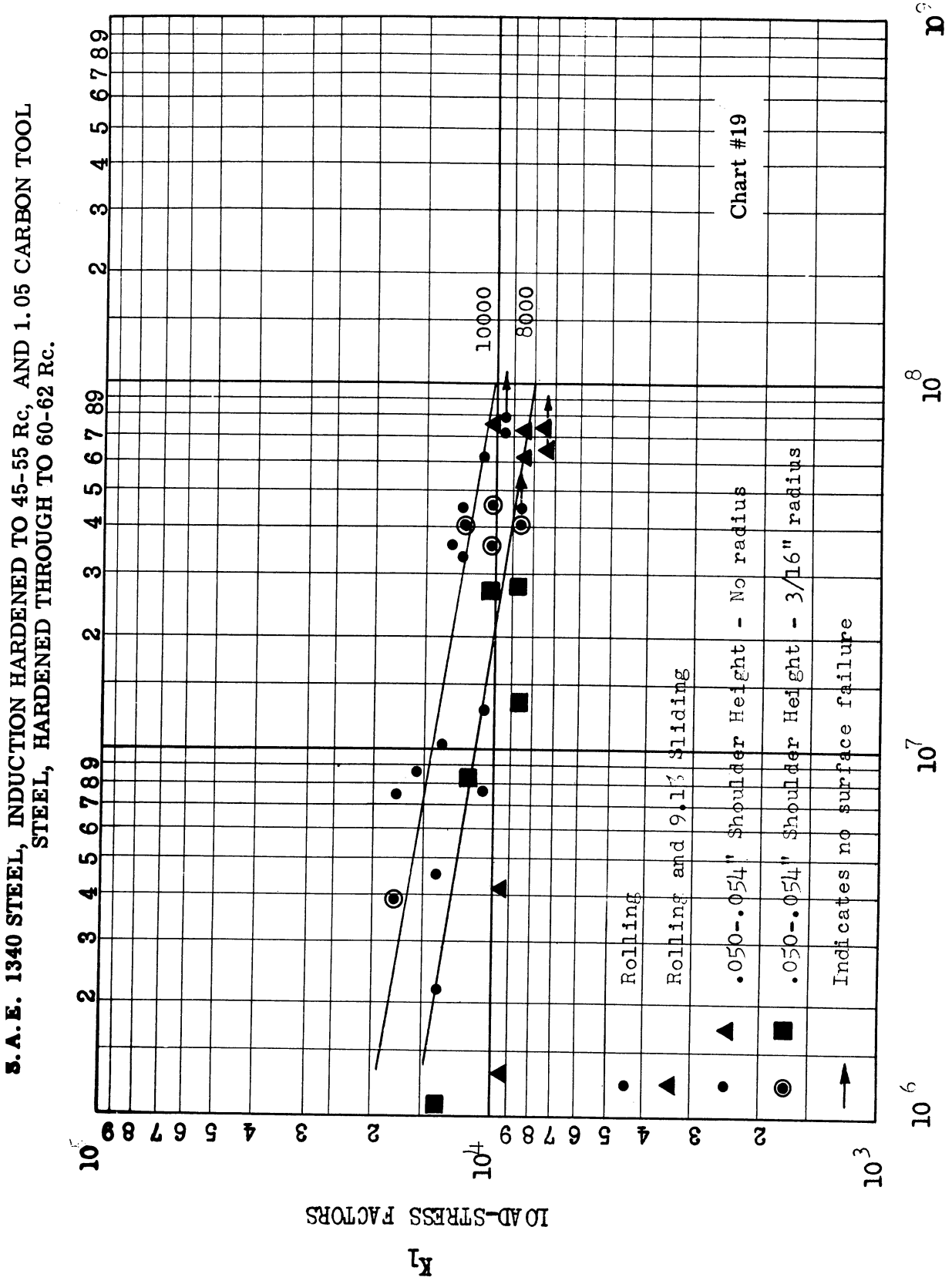

Figure 30. Fatigue curve.

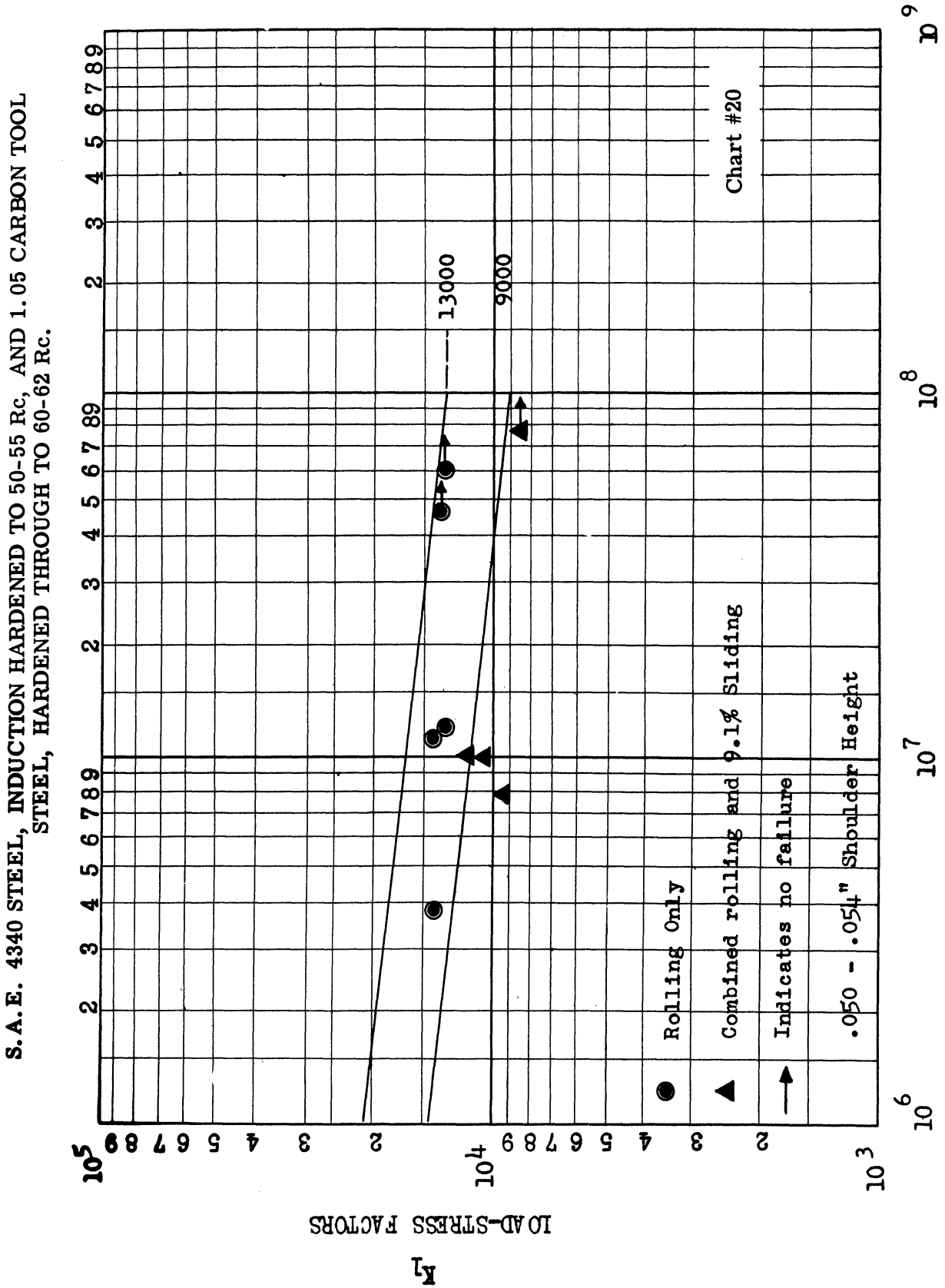

Figure 31. Fatigue curve.

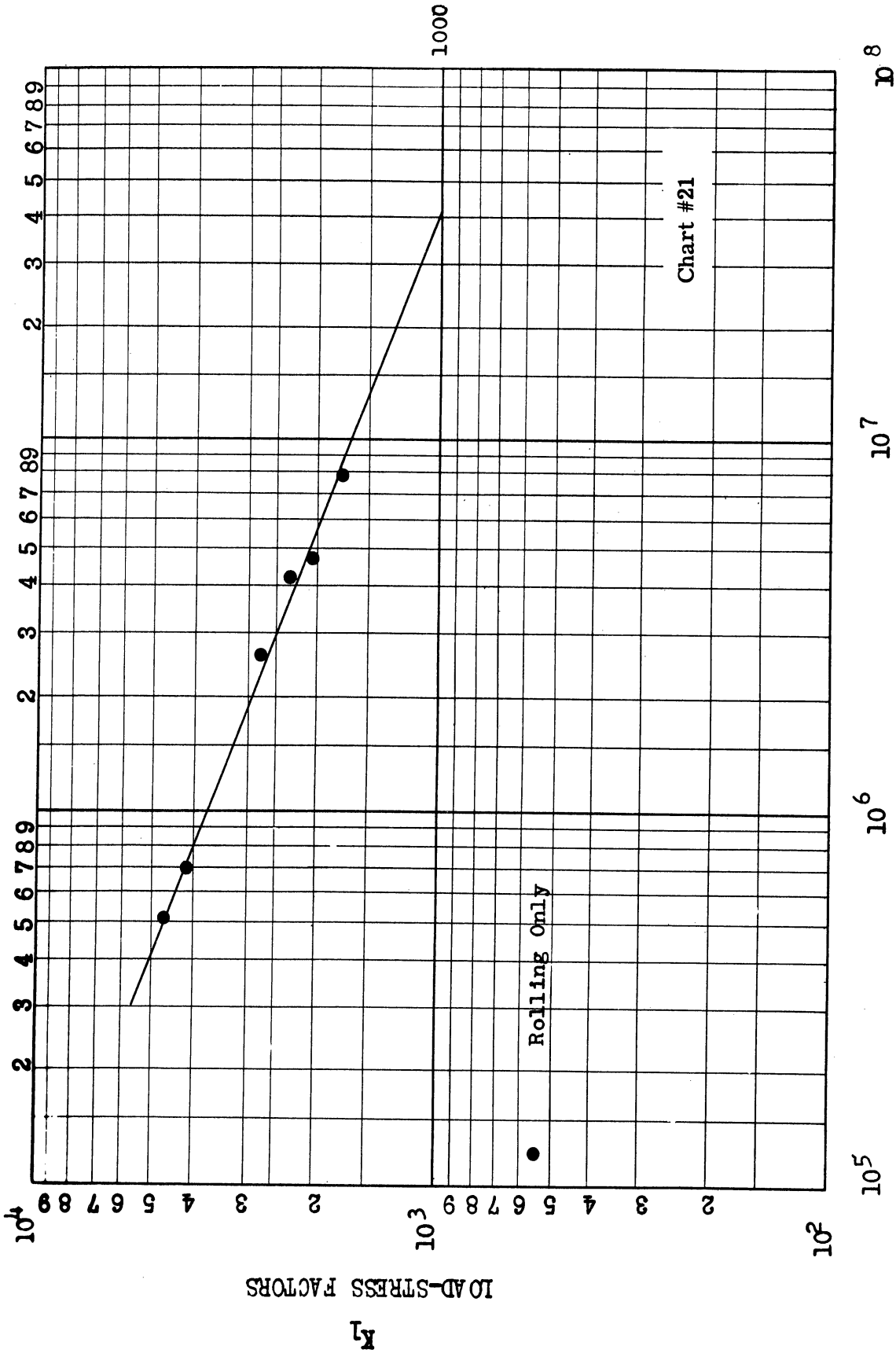

Figure 32. Fatigue curve.

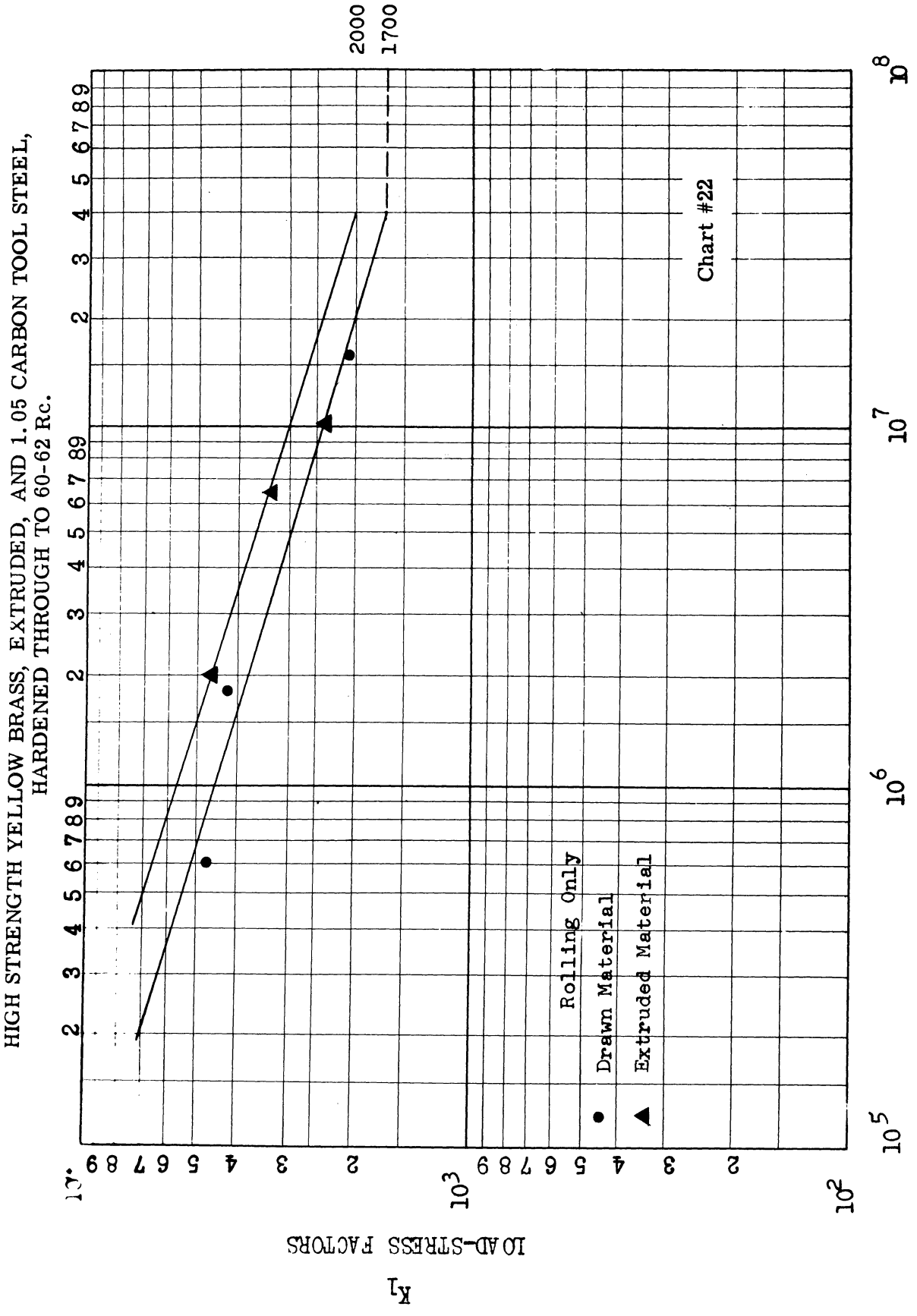

Figure 33. Fatigue curve.

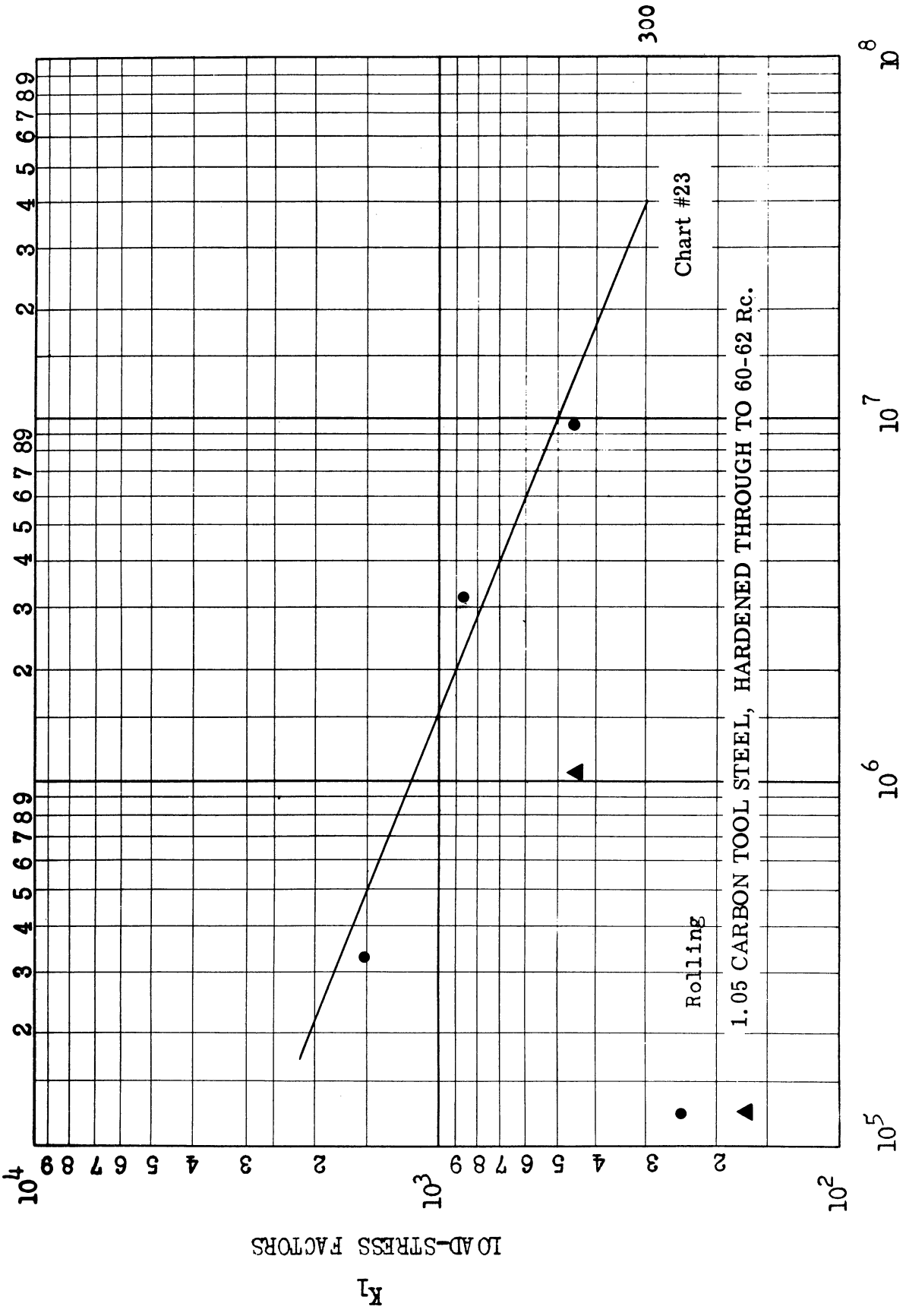

Figure 34. Fatigue curve.

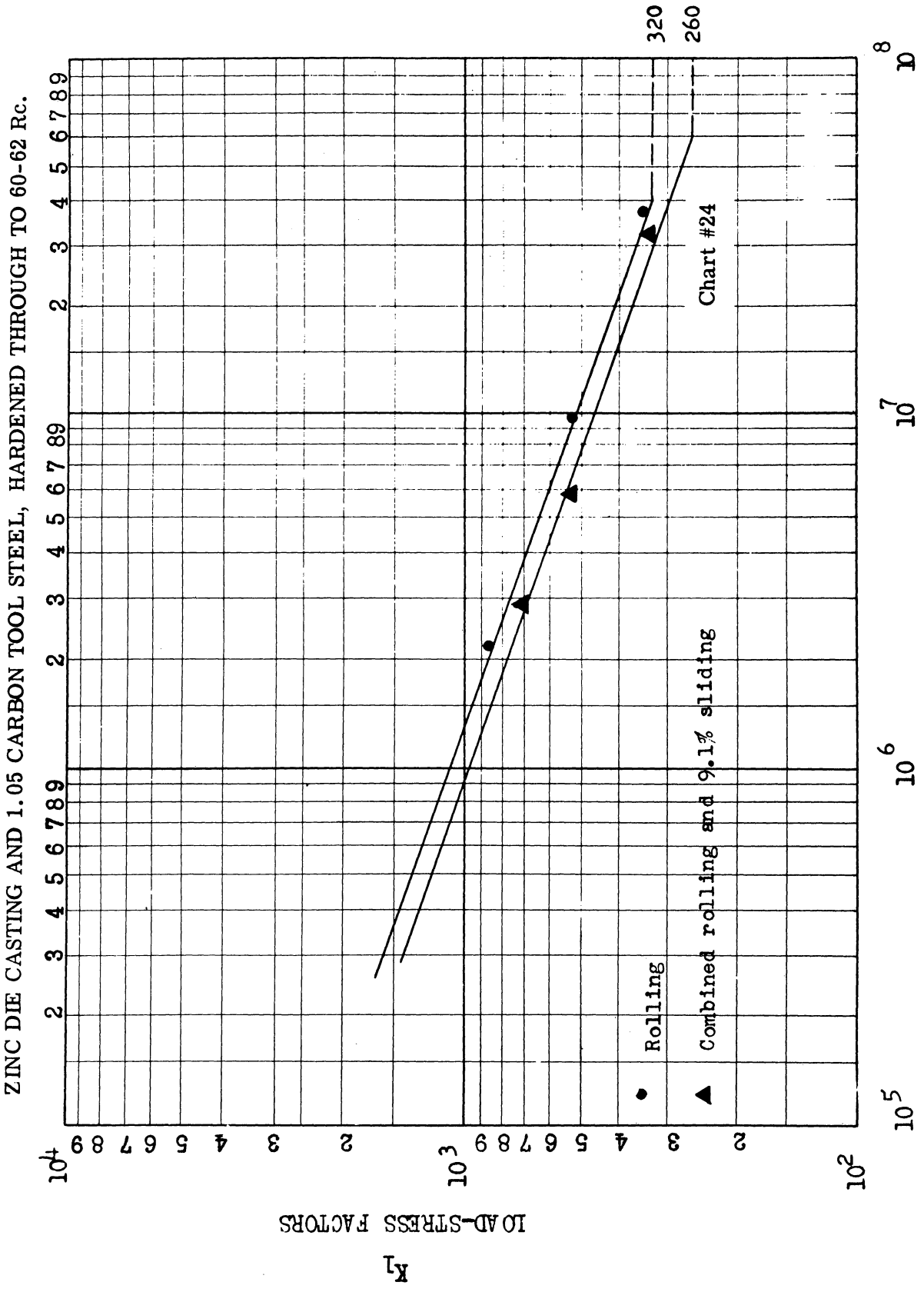

Figure 35. Fatigue curve.

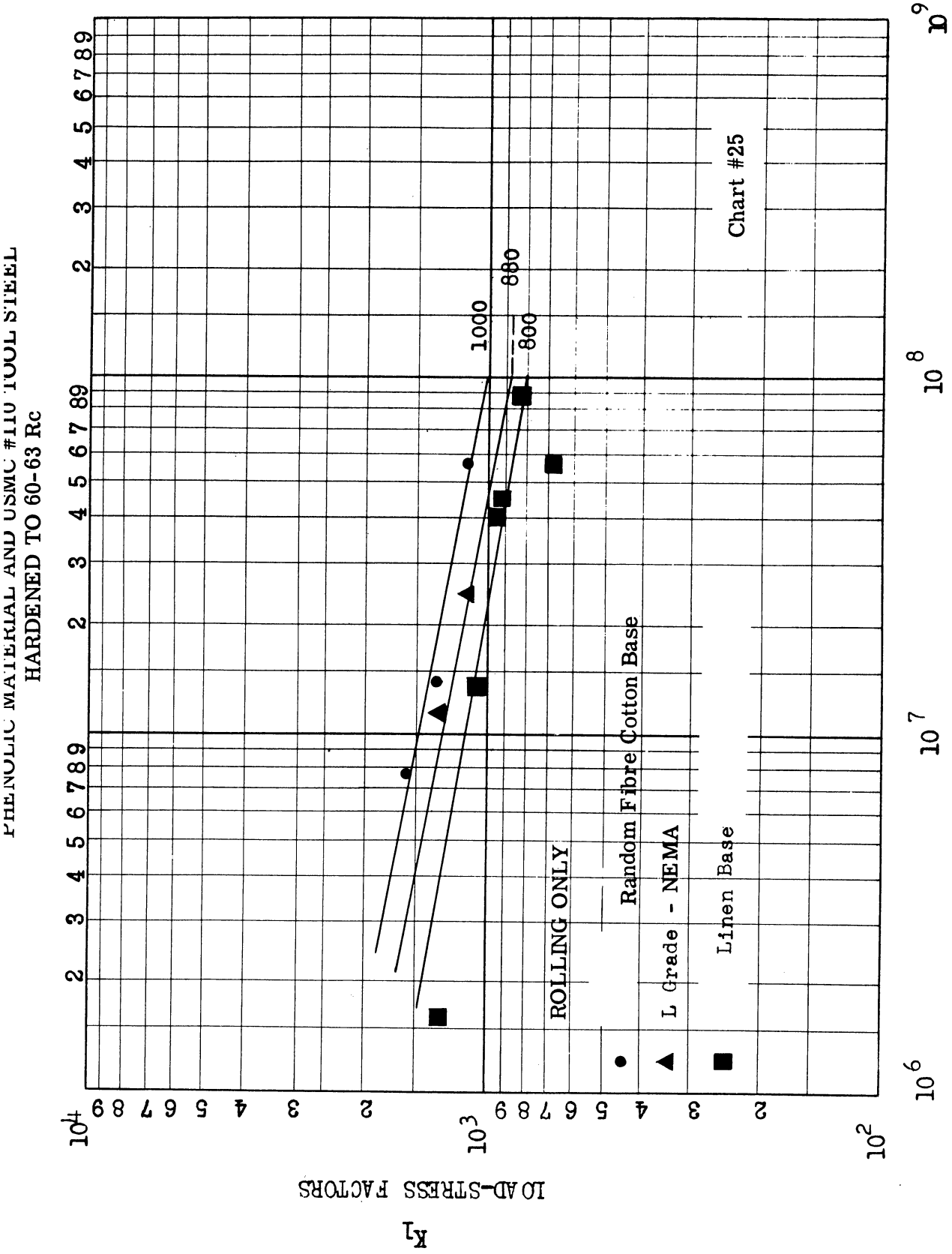

Figure 36. Fatigue curve.

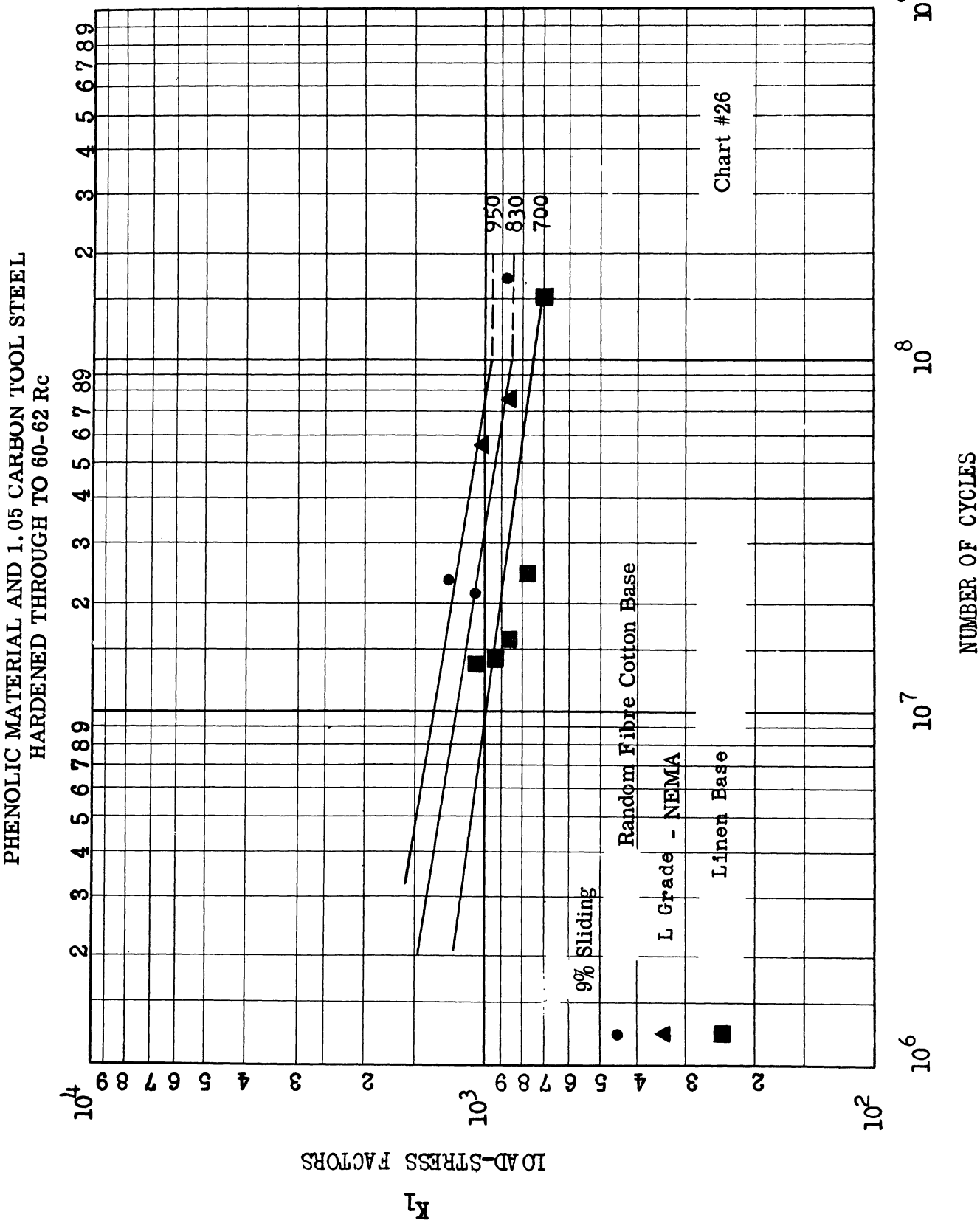
PHENOLIC MATERIAL AND 1.05 CARBON TOOL STEEL
HARDENED THROUGH TO 60-62 Rc
Chart #26
950
830
700
9% Sliding
Random Fibre Cotton Base
L Grade - NEMA
Linen Base
K_1
LOAD-STRESS FACTORS
NUMBER OF CYCLES

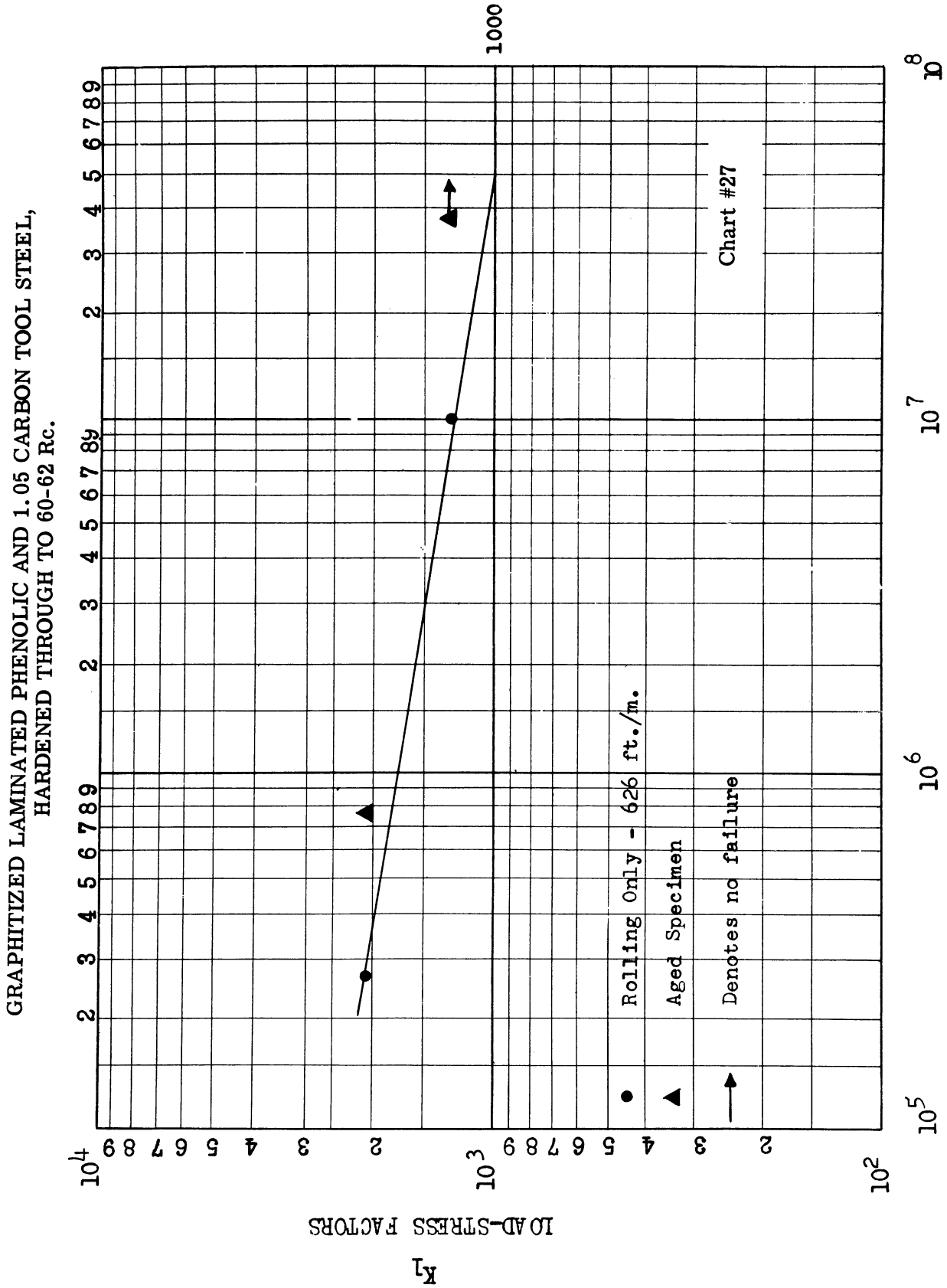

Figure 38. Fatigue curve.

SUBSURFACE FATIGUE

Horace J. Grover
Chief, Applied Mechanics Division
Mechanical Engineering Department, Battelle Memorial Institute

SUBSURFACE FATIGUE

by

Horace J. Grover

INTRODUCTION

For the purpose of this discussion, we define fatigue as the phenomenon of a metal or alloy "failing" under a number of applications of a stress whose maximum value is appreciably less than that which the metal or alloy could sustain for a single application.

Most commonly reported fatigue failures seem to start at the surface of the test-piece or machine part. However, there are situations in which failure may start subsurface, and some of these are of considerable engineering importance. Such subsurface fatigue failure is the subject of this paper. For most of the discussion, the exact meaning of the term "subsurface" will not be very important. We need not define the surface in terms of atomic distances, and may think of subsurface as usually implying at least several-thousandths of an inch below a nominal surface plane.

To permit discussion in terms of engineering interest, it will help to review some concepts concerning the stress conditions which seem to govern fatigue of metals. Most of these concepts have been developed empirically from experiments on geometrically simple test-pieces under simple nominal stress conditions. In such cases, the maximum stress is at the surface, and if the material is fairly homogeneous the fatigue failure starts at the surface.

Some Observations Concerning Surface Fatigue

Figure 1 illustrates a common method of reporting fatigue-test data. Simple test-pieces were subjected to repeated axial loading; each load varied from a maximum tension to an equal compression. The stress, plotted as ordinate, is the maximum nominal (P/A) value in the cycle. Abscissas represent cycles (to complete fracture) on a logarithmic scale. One point to be noted is the effect of a notch on the fatigue strength. This, and a great deal of other evidence, emphasizes the fact that the fatigue seems to be determined by highly localized stress conditions. This point is most important in our later consideration of subsurface fatigue.

From additional tests on similar specimens of the same material, evidence concerning the effect of mean stresses together with varying stresses may be obtained. Considering just the condition of the fatigue limit (the stress at which the S-N curve, in Figure 1, becomes essentially

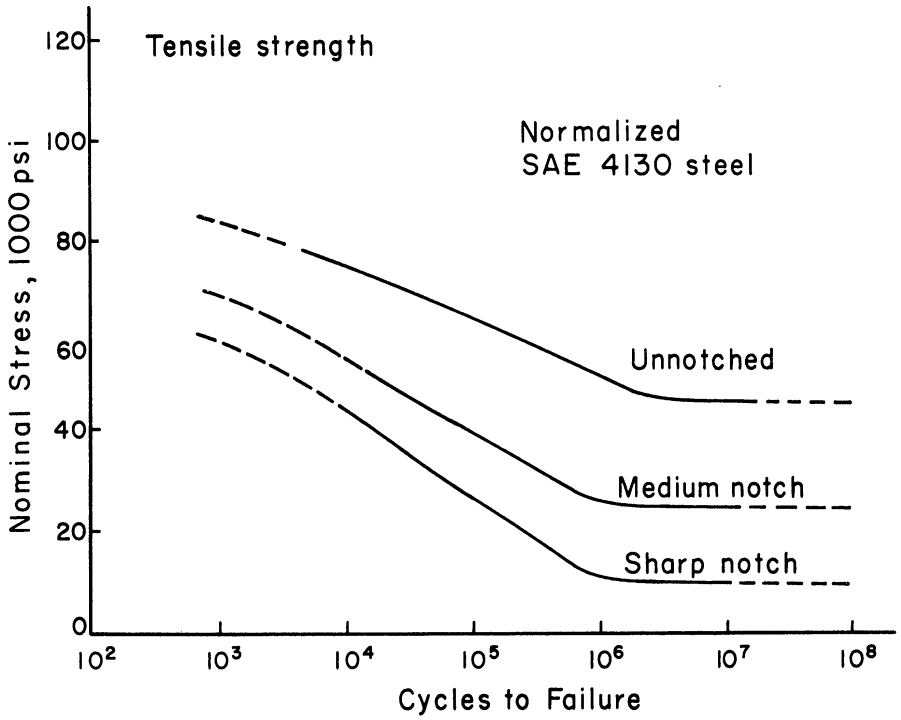

Figure 1. Tension-Compression Fatigue curves.

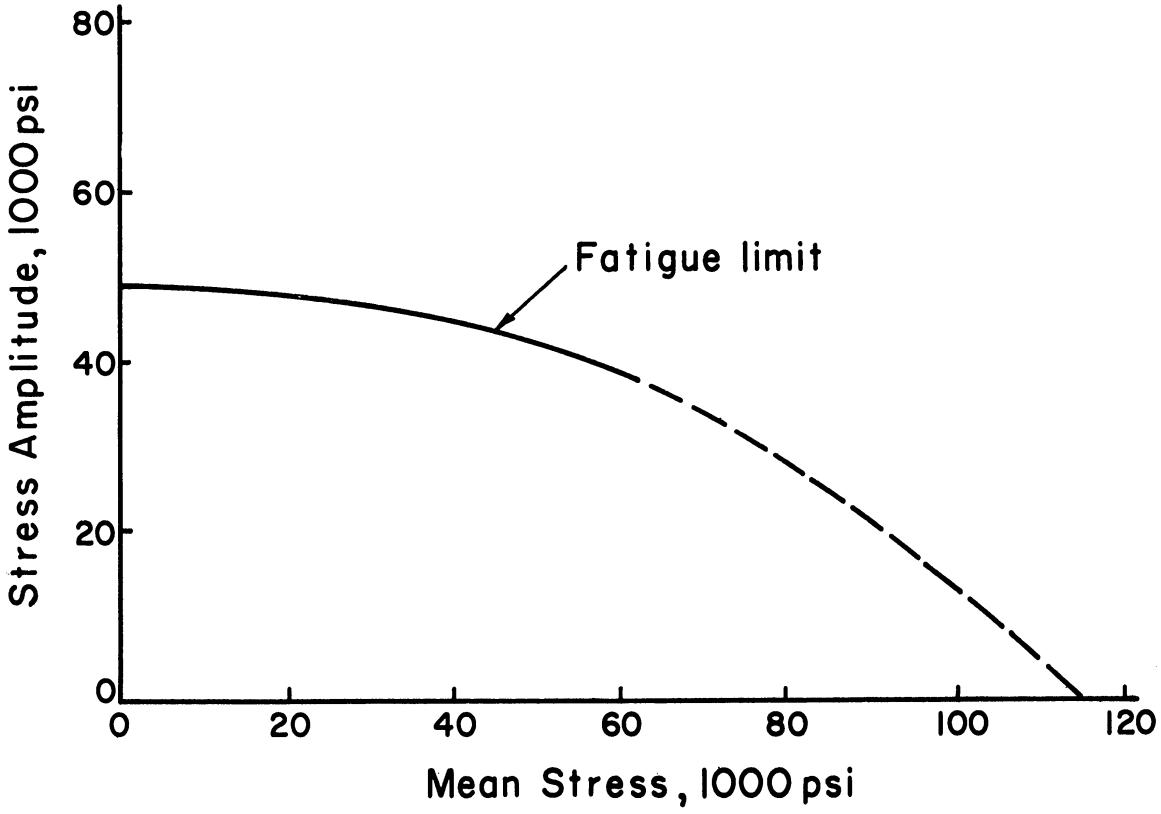

Figure 2. Fatigue diagram for normalized SAE 4130 steel.

horizontal), a plot similar to the one in Figure 2 may be derived. Few data are available in the range of mean compression. This diagram indicates that as the nominal mean stress of the loading cycle increases, the nominal alternating stress that can be withstood without failure decreases. This observation will also be of interest in connection with some subsurface failures.

Many investigators have studied the apparent effect of combined (biaxial or triaxial) stresses on fatigue. As might be expected, many of the attempts have been to find relations among fatigue-test results that would be compatible with some of the theories of static strengths. These investigations have been complicated by experimental difficulties, and the results were somewhat divergent (often affected by anisotropy of materials). However, numerous studies in bending and in torsion suggest that use of either a maximum-shear or a distortion-energy criterion of failure fits data better than use of maximum principal-stress theory. Thus, in considering subsurface fatigue, it is important to keep in mind subsurface shear stresses as well as tension or compression stresses.

One further point deserved mention. While the mechanism of fatigue is only partly understood, it is sometimes helpful to consider the process as having three steps:

1. After a number of repeated loadings, some irreversible damage occurs in a small region and, somehow, a tiny crack comes into existance.
2. Under further loadings, this crack lengthens until the part is severely weakened.
3. Finally, the process becomes catastropic and the part breaks, perhaps under a single additional cycle.

There may be important distinctions among the stress conditions most critical for each step. for example, fatigue damage in the first step might be related to the maximum shear in the local region, while for crack propagation the local tensile stresses might be more important. Final failure is often obviously influencedby the design of the part and by the characteristics of the testing machine used or by the remaining portion of the structure delivering loads to the part. These possibilities have not been wholly resolved and are difficult to study fruitfully or to discuss with generality.

Conditions For Subsurface Fatigue

With this brief background, it is interesting to speculate on the conditions under which fatigue cracks might be expected to start below the surface.

For homogeneous and isotropic materials, many conditions tend to result in surface failures. Stresses from bending and torsion are maximum at the surface. Surface roughness may impose stress concentration. The surface may be subject to corrosive attack and, in some cases, to abrasion or fretting.

However, nonhomogeneous materials may have either subsurface weakness or subsurface stress raisers, or combinations of these. Familiar examples would include subsurface inclusions and parts with special surfaces such as carburized or nitrided layers. Illustrations of some of these will be presented a little later.

For essentially homogeneous materials, some conditions may produce critical subsurface stresses. One important condition is that of local surface compression, such as under a rolling load. This situation will be an important concern later in this paper and in other discussions in this seminar. There are other conceivable situations which could give rise to subsurface stresses that would initiate fatigue. For example, combinations of centrifugal stresses and stresses from external loading might produce subsurface stress conditions that could start fatigue. Combinations of thermal and mechanical stresses can be imagined to produce critical subsurface conditions. However, situations such as these are somewhat rare in practice and have not generally been reported in the literature.

Accordingly, we will consider examples of each of these relatively common sources of subsurface origin of fatigue; 1- inclusions, 2- hardened surfaces, and 3- rolling loads.

Fatigue Originating at a Subsurface Inclusion

Figure 3 illustrates a subsurface nucleation of fatigue at an inclusion located a few thousandths of an inch below the surface of a through-hardened plate of 52100 steel. The plate was stressed in repeated reverse bending. Figure 4 shows a failure of similar appearance that occurred after repeated, but not fully reversed, bending in a shot-peened leaf spring.

Considerable analyses have been carried out on the theoretical stress concentration to be expected from simply shaped cavities or regions of different elastic properties from a base material. Fatigue tests have been run to determine the observable effect of particular types of inclusions in specific materials.[1] Such studies have resulted in recognition that many factors are involved:

1. The properties of the base materials
2. Size, distribution, and orientation of the inclusions
3. Strength properties of the inclusions
4. The nature and magnitudes of imposed stresses.

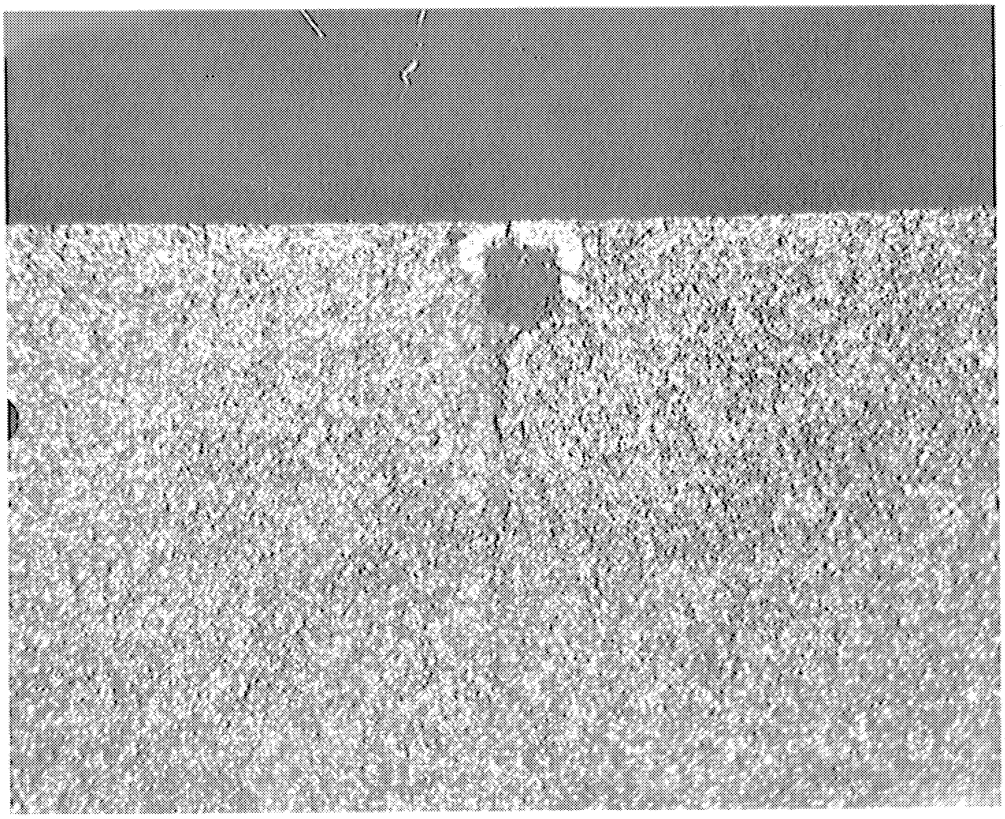

Figure 3. Subsurface-fatigue failure in through-hardened 52100 steel plate.

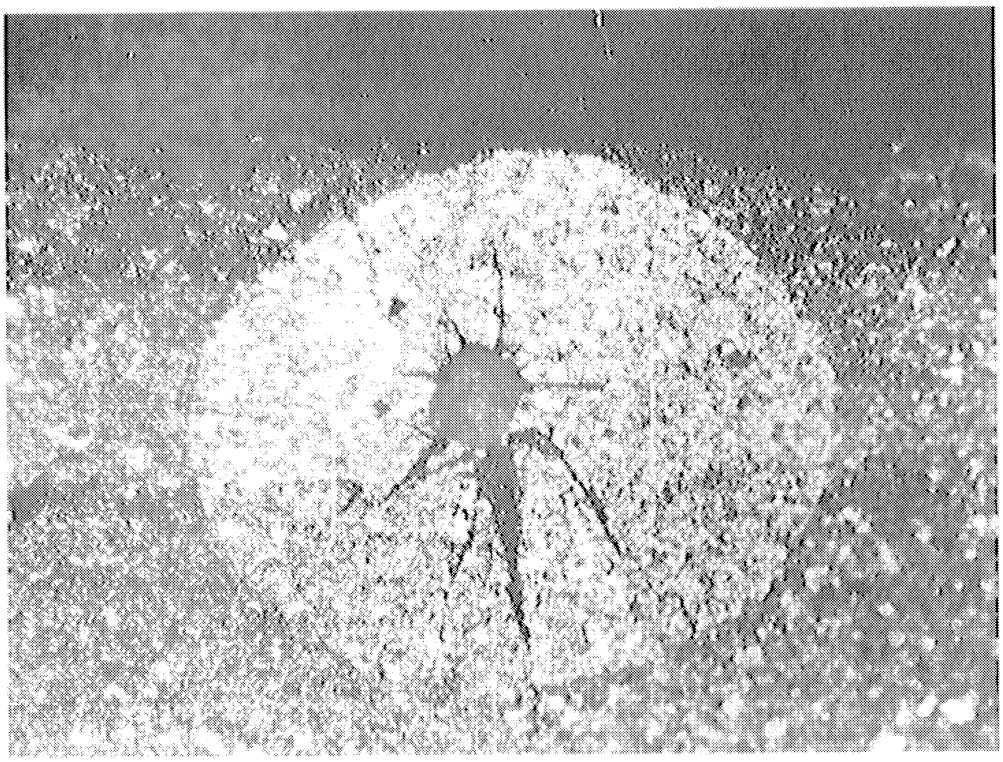

Figure 4. Subsurface-fatigue failure in shot-peened steel spring.

At present, it seems difficult to advance any general statements concerning effects of subsurface inclusions beyond the fairly obvious ones, that.

1. They can be points of weakness and of stress concentrations
2. They are especially detrimental if they are hard and non-ductile
3. They are particularly undesirable in regions of high stress.

Subsurface Fatigue of Surface-Hardened Parts

In a classic paper some years ago,[2] Woodvine noted subsurface iniation of fatigue in case-hardened test-pieces. Figure 5 (reproduced from his paper) illustrates a fatigue specimen with a "small circular white area---practically at the junction of case and core", at which "...examination indicated quite clearly that failure had commenced". For some years, similar fractures were sometimes called "Woodvine fractures".

In the more than a quarter century since such early studies of fatigue of surface-hardened parts, many investigators have noted fatigue failures starting in such transition regions between the case and core. The metallurgical details of hardening steels by carburization or by nitriding or by surface heating have been studied extensively. Many investigations have brought out the large residual stresses left after surface hardening and something about their causes.[3-4] J. Almen,[5] and later many others, emphasized the importance of such stresses on fatigue behavior and, incidentally, upon the subsurface failure frequently observed.

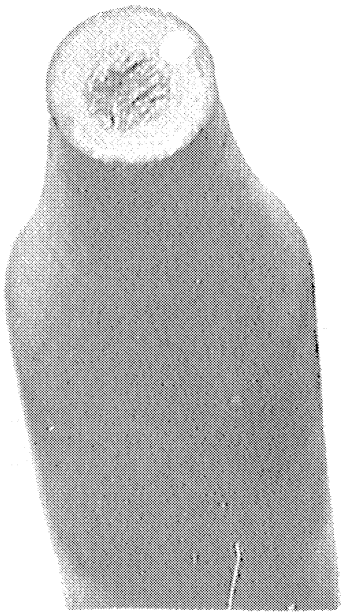

Figure 5. Subsurface-fatigue failure in a case-hardened specimen.[2]

Some of the factors involved are shown in Figures 6 and 7. Figure 6 illustrates the residual stress that might exist in a surface-hardened part; the broken lines indicate nominal stresses that would exist under a reversed-bending loading. Figure 7 shows the relationship of the stresses to the fatigue-limit conditions:

1. Curves for the fatigue-limit values are similar to the one in a previous graph (Figure 2).

2. Values for compressive mean stress have been shown as curving slightly upward in accordance with the few data available for this region.
3. Curves for case and core are estimated with account of the common indications of increasing fatigue strength with increasing hardness.

It would be expected that the fatigue strength of each region of the part would decrease from a value near the upper curve to one near the lower curve, with increasing depth below the surface---perhaps, approximately as indicated by the broken line. Fatigue failure might be expected to start in the region where the local stress in the part approached the broken line of the fatigue-limit diagram. In Figure 7, this appears to be in the neighborhood between 0.05 inch and 0.10 inch below the surface, or just below the case.

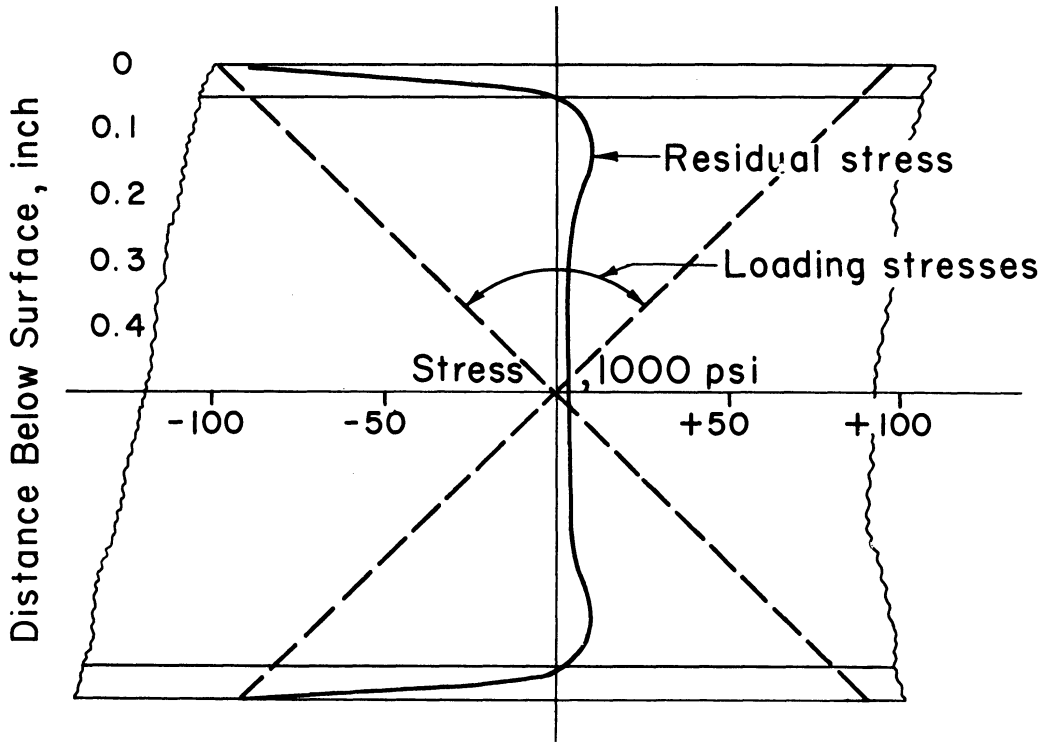

Figure 6. Schematic diagram of surface-hardened part under reversed bending.

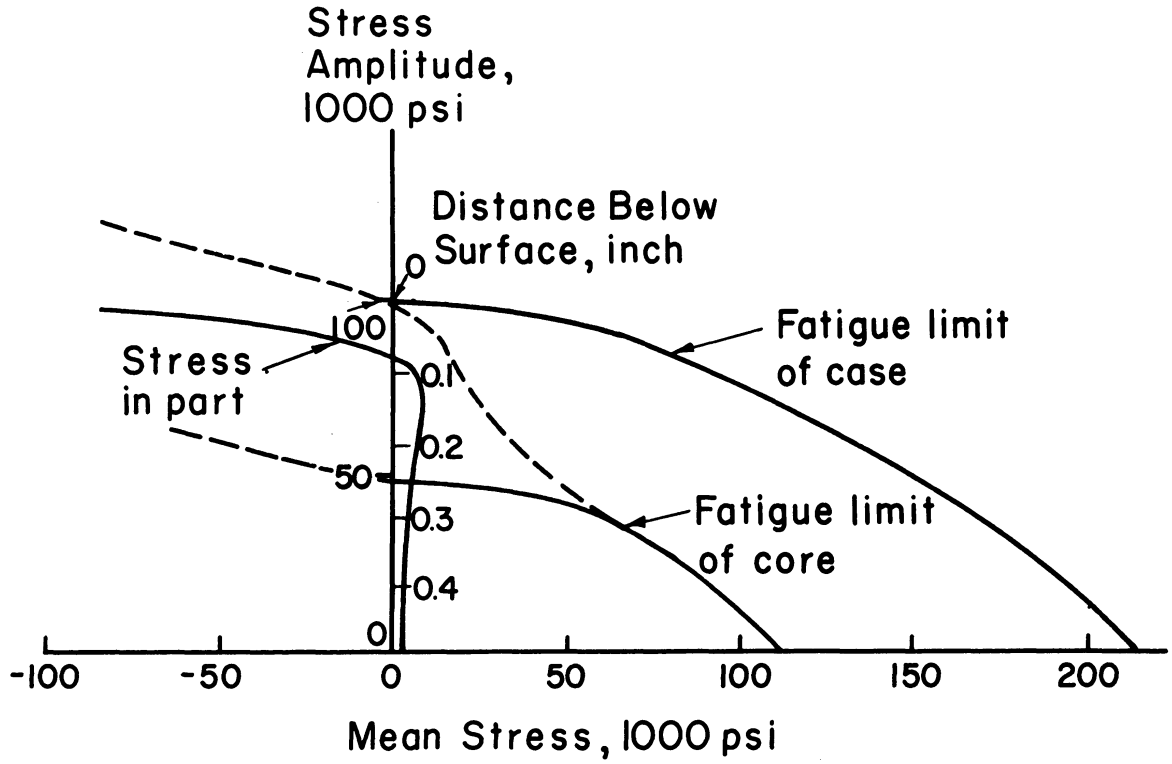

Figure 7. Schematic diagram for fatigue behavior of surface-hardened part under reversed bending.

It should be realized that the schematic diagrams in Figures 6 and 7 are only approximate indications of the complex situations probably existing. In addition to obvious simplification and license in drawing the diagrams, no account has been taken of transverse stresses, and it has been assumed that the residual-stress pattern remains unchanged during cyclic bending and can be treated as a mean stress related to observations such as those provided in Figure 2. Nevertheless, the representation provides a useful way of viewing an important factor in the fatigue behavior of surface-hardened parts, and an explanation of subsurface-failure origins in such parts.

Fatigue Under Rolling Loads

In the 19th century, H.Hertz developed stress equations for elastic bodies in contact. Others[6-7] have extended the mathematical study of such problems. If one considers a metal that is pressing on a plane of the same metal, Figure 8, it turns out that the maximum shearing stress, τ_{max}, is a distance, Z, below the surface of the plane. Approximately,

$$\tau_{max} = K_1 \sqrt{P/R} \qquad \text{and} \qquad (1)$$

$$Z = K_2 \sqrt{PR} \quad , \qquad (2)$$

where K_1 and K_2 are functions of the wheel thickness and of the elastic constants of the steel, and P is the wheel load, and R is the wheel radius. For a sphere on a plane, approximate relations are

$$\tau_{max} = K_3 \sqrt[3]{P/R^2} \qquad \text{and} \qquad (3)$$

$$Z = K_4 \sqrt[3]{PR} \qquad (4)$$

In each case, the highest stress value is at the surface of contact---but this is compression and not shear.

The following tabulation gives approximate values for a ball and for cylinders of steel on a steel plane. The values illustrate orders of magnitude that might be expected for, respectively, a ball-bearing race, a track of an overhead crane, and a rail under a locomotive driver wheel.

	Radius, in.	Width, in.	Load, lb.	Shearing Value, psi	Stress Depth, mils
Ball	0.25	-	100	135,000	5
Cylinder	8.00	1	2,000	10,000	40
Cylinder	30.00	1	40,000	24,800	243

For these items, the values imply depths of critical stress ranging from a few thousandths of an inch (through a value corresponding to a fairly deep case) to as much as a quarter of an inch. It may also be noted that shearing stresses may be very high for a small ball, and decrease with the cube root of the load, while they are lower for the large-radius cylinders and, for these, decrease as the square root of the load.

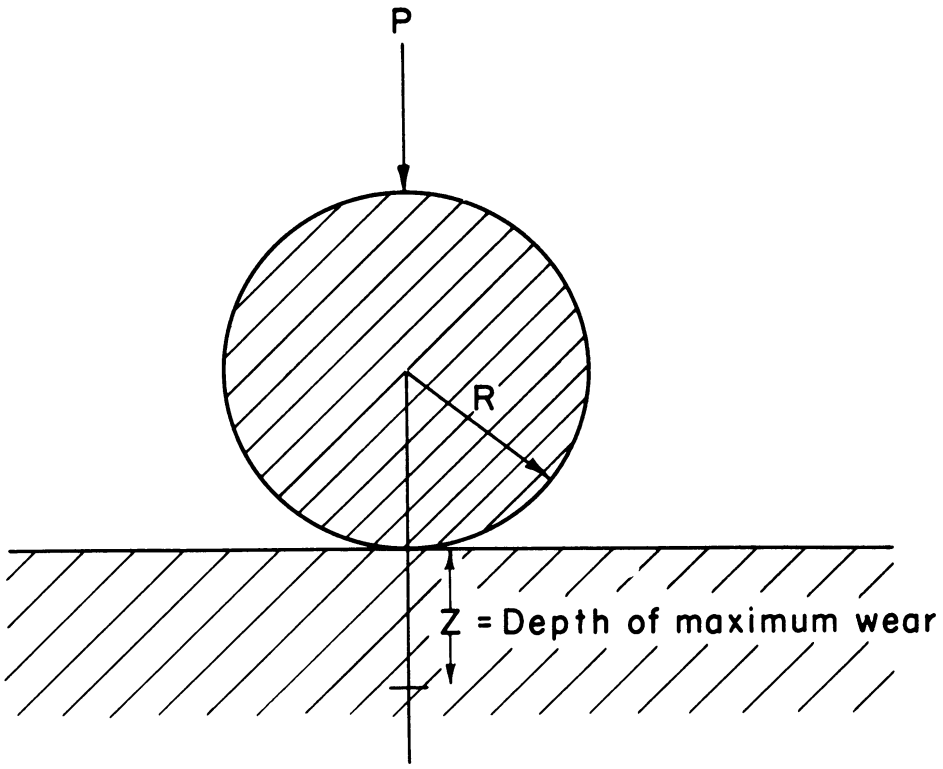

Figure 8. Subsurface shear from contact stresses.

As a ball or cylinder rolls many times over a plane surface, a subsurface region undergoes cycles of shear ranging from zero to the appropriate maximum. This situation would be expected to promote fatigue damage if the maximum shearing stress is above the fatigue limit for the material in this region. Subsurface cracks may result; and under subsequent cycles of loading, these cracks may propagate to the surface so that pitting or spalling or flaking eventually results. (It should be kept in mind that all cases of apparent spalling may not originate from subsurface fatigue.)

Figure 9 shows a typical spall in the race of a ball bearing.(15) There was reason to believe that this spalling originated from subsurface conditions under the rolling load. Balls as well as races also may have high internal-shearing stresses and may develop internal cracks. Figure 10 illustrates this.(9)

For many years, occasional "shelling" in rails have been a source of difficulty to railroads.(10 and 12) High rolling loads from driver wheels of locomotives produce surface deformation and high subsurface-shearing stresses that provide conditions for surface and subsurface cracking. Figure 11 shows a failure that occurred after many cycles of wheel loading.(13)

Rail failures have been studied extensively by the American Association of Railroads and by the American Iron and Steel Institute. Some of these studies have provided considerable information concerning subsurface-stress conditions.

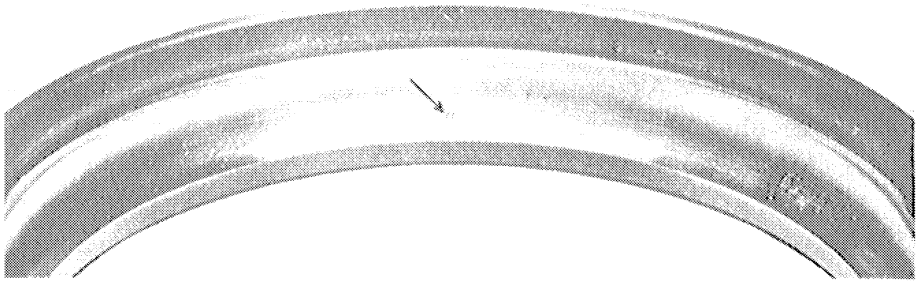

Figure 9. Spall in a ball bearing race.(15)

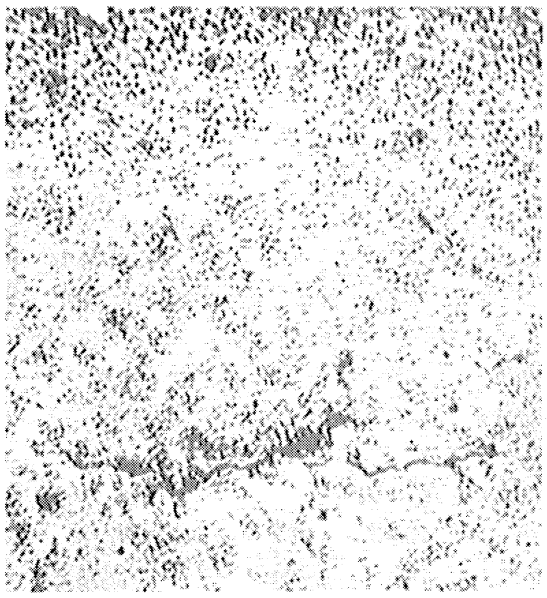

Figure 10. Fatigue failure in a ball of a ball bearing.(9)

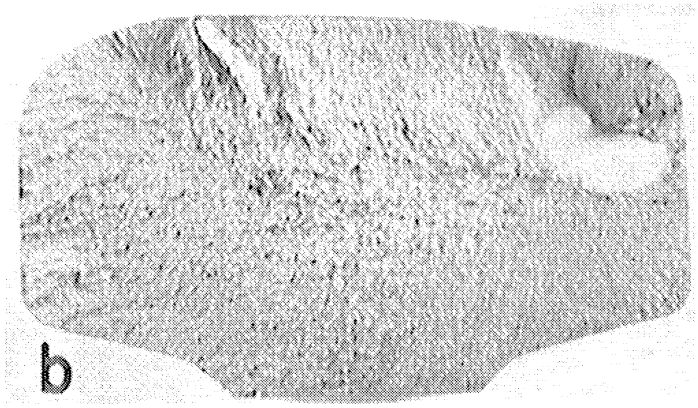

Figure 11. Fatigue failure in a railroad rail.(16)

Figure 12 shows some results (adapted from Reference 11) of a photoelastic study of a model of a rail under loading simulating a locomotive-wheel contact pressure. As would be expected under elastic conditions, there is a maximum shearing stress at a region considerably beneath the surface; the exact location could not easily by computed theoretically. The results further indicate the effect of an inclined loading to be a slight increase in the magnitude of the maximum shearing stress and a light shift of its location toward the surface.

Since both theory and photoelasticity are limited to elastic behavior and loads of rails are often sufficient to produce plastic deformation, an additional investigation studied some of the effects involved in this plastic behavior.(13) A number of rolling-load tests performed on a mild-steel bar produced some failures similar to those sometimes observed in rails. The observed failure depths were greater (by factors rangingfrom 2 to 4) than the calculated depths of maximum shearing stress on the assumption of elastic behavior. The more detrimental effect of a smaller wheel (for a fixed load) was compatible with that expected from Equation 1. Some further studies on "rails" of silver chloride provided ideas of the progressive development of subsurface plastic deformation with increasing numbers of load application. Subsurface sliplines occurred with the first few loads. With succeeding repetition of load, the density of sliplines increased and the area of observable slip widened. After many cycles, the maximum depth of slipline formation remained constant (at a value several times larger than the depth of maximum shear computed on the assumption of elasticity).

The examples described illustrate both the existence of subsurface-fatigue initiation under conditions of contact loading and some of the factors involved in such situations. Consideration of subsurface factors has also been applied to more nearly surface failures, such as pitting of gears,(14) although in such cases other items concerned with details of surface behavior are often of major importance. Some considerations along these lines will, I hope, be more fully developed in other papers in this seminar.

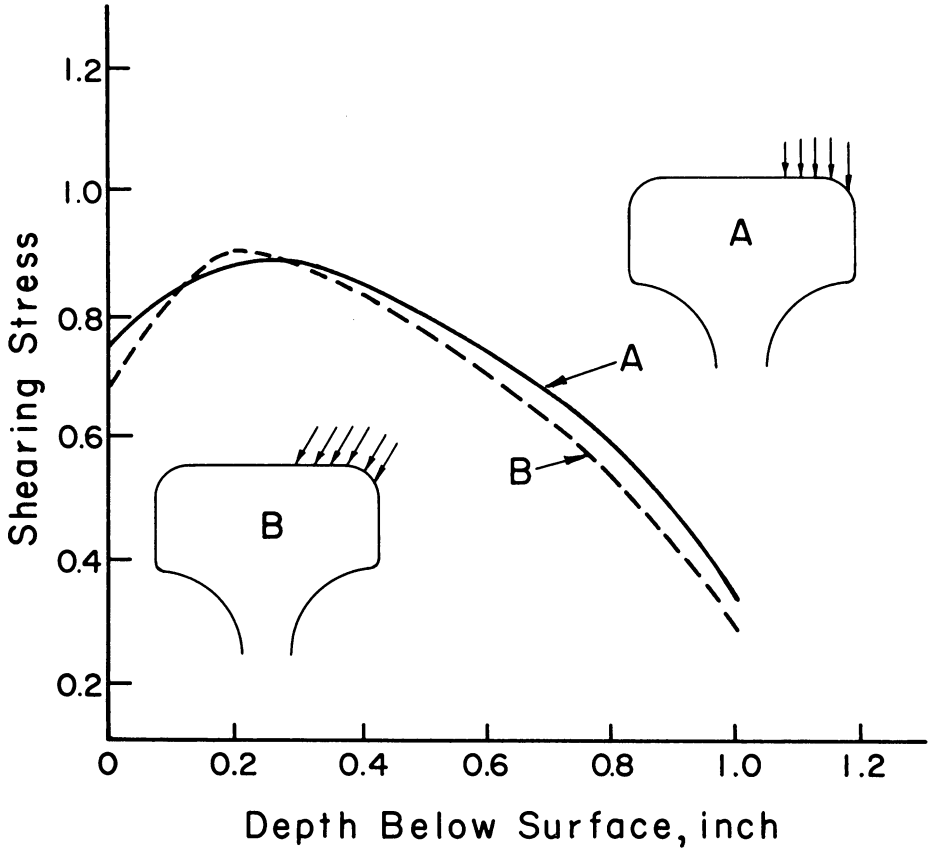

Figure 12. Results of photoelastic study of stress in rail model under (A) vertical loading and (B) inclined loading. (Adapted from Reference 11)

Concluding Remarks

The objectives of this discussion have been to stimulate thought about the conditions under which subsurface fatigue should be considered as a design contingency and to indicate some of the factors to be considered in such instances.

It has been suggested that many of the situations in which subsurface-fatigue considerations are important can be grouped in three classes.

1. Subsurface faults such as inclusions
2. Surface-hardened parts
3. Parts subjected to high contact pressures.

Examples of apparent subsurface-fatigue failure in each of these three cases have been noted.

Subsurface inclusions, seams, cracks, or other discontinuities in metal structures are particularly important when they occur in regions of otherwise high stress. Under repeated bending or torsion, faults near the surface should be especially avoided. In notched parts, particular care should be exercised near the root of the notch where a high stress concentration would be expected for a homogeneous material. In parts under rolling loads or other localized contact pressures, a subsurface region of maximum shear would be especially sensitive to internal discontinuities of metallic structure.

For surface-hardened parts, residual stresses may influence fatigue. In a shot-peened or case-hardened part, favorable surface stresses may strengthen the surface so that a region beneath this becomes the Achillean heel. In such instances, subsurface defects may be critical even under applied loading such as to produce a uniform nominal stress over the section.

Contact pressures such as those occurring in rolling loads (gears, ball bearings, wheels on tracks, etc.) may produce high surface-compressive stresses and also subsurface maximum-shearing stresses. Considerable work, both theoretical and experimental, provides fair understanding of the design factors concerned in such instances. In such cases also, subsurface defects should be avoided particularly in regions of peak stress.

REFERENCES

1. Cummings, H.N., Stulen, F.B., and Schulte, W.C., "Relation of Inclusions to the Fatigue Properties of SAE-4340 Steel," Transactions of the American Society for Metals, Vol. 49, 1957, pp. 482-511.

2. Woodvine, J.G.R., "The Behavior of Case-Hardened Parts Under Fatigue Stresses," Iron and Steel Institute, Vol. 13, 1924, pp. 197-237.

3. Koistenen, D.P., "The Distribution of Residual Stresses in Carburized Cases and Their Origin," Transactions of the American Society for Metals, Vol. 50, 1957.

4. Wishart, H.B., "Residual Stress States Produced in Metals by Various Processes," American Society for Metals, Educational Lectures on Residual Stresses, October 1951.

5. Almen, J.O., "Fatigue of Metals as Influenced by Design and Internal Stresses," American Society for Metals, Educational Lectures on Surface Stressing of Metals, February 1948.

6. Thomas, H.R., and Hoersch, V.A., "Stresses Due to the Pressure of an Elastic Solid Upon Another," Bulletin No. 212, University of Illinois, Engineering Experiment Station, 1930.

7. Smith, J.O., and Liu, C.K., "Stresses Due to Tangential and Normal Loads on Elastic Solids With Application to Some Contact Stress Problems," Transactions of the American Society of Mechanical Engineers, December 1952.

8. Jones, A.B., "Metallographic Observations of Ball-Bearing Fatigue Phenomena," ASTM Proceedings (Symposium on Testing of Bearings), Vol. 46, 1946.

9. Barwell, F.T., and Scott, D., "Effect of Lubricant on Pitting Failure of Ball Bearings: Experimental Results for Various Fluids," Engineering, July 6, 1956.

10. Baldwin, T., "Significance of the Fatigue of Metals to Railways," Institution of Mechanical Engineers and the American Society of Mechanical Engineers, Paper No. 4 of Session 9 of the International Conference on Fatigue of Metals, Vol. 2, 1956, 11 pages.

REFERENCES (CONT'D)

11. Frocht, M.M., "Three-Dimensional Photoelastic Investigation of the Principal Stresses and Maximum Shears in the Head of a Model of a Railroad Rail," AREA Bulletin, Vol. 55, 1954, pp. 854-897.

12. Keller, W.M., and Magee, G.M., "Fatigue in Railroad Equipment," Institution of Mechanical Engineers and the American Society of Mechanical Engineers, Paper No. 1 of Session 9 of the International Conference on Fatigue of Metals, Vol. 2, 1956, 5 pages.

13. Hyler, W.S., and Grover, H.J., "The Study of Simulated Rails Under Repeated Rolling Load," AREA Bulletin, Vol. 55, 1954, pp. 840-853.

14. Buckingham, E., "Surface Fatigue of Plastic Materials," Transactions of the American Society of Mechanical Engineers, Vol. 66, 1944, pp. 297-306.

15. Cordiano, H.V., Cochran, Jr., E.P., and Wolfe, R.J., "Effect of Combustion-Resistant Hydraulic Fluids on Ball-Bearing Fatigue Life," Mechanical Engineering, Vol. 77, November 1955, p. 1004.

16. Cramer, R.E., "Twelfth Progress Report on Shelly Rail Studies at University of Illinois," AREA Bulletin, Vol. 55, 1954, pp. 832-840.

RESISTANCE OF MATERIALS TO ROLLING LOADS

E. S. Rowland
Chief Metallurgical Engineer
Timken Roller Bearing Company

RESISTANCE OF MATERIALS TO ROLLING LOADS

by

E. S. Rowland

INTRODUCTION

The problem of rolling fatigue is basically a problem of stress concentrations, some of which are computable and many of which are not. The geometry which permits rolling contact inherently concentrates the load in a very small volume of metal giving rise to high stresses within that volume. Up to a point one may calculate the magnitude and distribution of stress within this small volume, but some mechanical factors concentrate the stress in a manner which cannot be calculated. Furthermore, no material is homogeneous and this lack of homogeneity produces a population of internal stress concentrations of varying severity within the material. This fact leads to the well known statistical nature of fatigue in general, and to the seemingly erratic behavior of any one steel in particular. A final factor of uncertainty is the magnitude and distribution of residual stresses left by processing and their influence on the nucleation and propagation of fatigue failures.

Metal failure by rolling fatigue is common in many industrial applications, such as rolling contact bearings, gears, cams, etc. However, the discussion in this paper will be confined to bearings and basic studies of rolling fatigue.

MATERIALS COMMERCIALLY USED IN ROLLING CONTACT BEARINGS

Historical

With very few exceptions in Europe and America, one per cent carbon-chromium through hardening steels are used for the manufacture of ball and parallel roller bearings and low carbon, case carburizing steels for tapered roller bearings. It is impossible now to be certain of the original reasons for this difference in choice of materials, but in a large measure it must be due to the difference in historical development of these bearings. The ball bearing industry was a European development and the tapered roller bearing industry, American.

The fundamental theoretical study of Hertz was followed in 1899 by the first experimental investigation of the load carrying capacity of a ball bearing by Professor Stribeck in collaboration with the German concern, Deutsche Waffenfabrik, then one of the principal ball bearing manufactures in the world. During the following years this work was

continued by Palmgren in Sweden, Mundt in Germany, and Goodman in England. By 1920 the fundamental design and basic material of the ball bearing was fairly well standardized on the continent and in America.

The concept of using tapered rollers as bearing members is unquestionably very old, but the use of this concept as the foundation of a bearing industry stems from an American patent taken out in 1898. The application envisioned for this patent was horse drawn carriages. This industry matured rapidly with the subsequent development of the motor vehicle, which necessitated the adoption of hard steel bearing materials in place of the mold steel formerly used. Because of the more complicated cross-sectional configuration of the tapered roller bearing, as compared to the ball bearing, and the shock load conditions expected in motor vehicle applications, case carburizing was considered the best means of obtaining the desired wear resistance and load carrying capacity. Case carburized materials to this day have been almost exclusively used by manufactureres of tapered roller bearings.

General

The engineering requisites for steel for rolling contact bearings are:

a. High fatigue strength.
b. High elastic strength - resistance to plastic indentation.
c. Resistance to sliding or rubbing wear.
d. Structural stability at operating temperatures.
e. A low level of non-metallic inclusions and alloy or carbide segregation which serve as internal stress concentrating factors.
f. Relative insensitivity to internal and external stress concentration.
g. Resistance to environmental chemical corrosion.

The use of 0.90 to 1.00 per cent carbon steels ensures the highest elastic and fatigue strength obtainable in steel and the excess carbides usually present at these carbon levels add some further measure of wear resistance to their already inherently good wear characteristics. The small amount of ductile austenite almost invariably retained in the microstructure is believed to provide some relief of internal and external stress concentration from inclusions, segregation, and geometry. Structural stability at operating temperatures is achieved by use of tempering temperatures in excess of operating temperatures. Resistance to chemical corrosion from an abnormal environment can usually be obtained only by resorting to more exotic bearing materials.

One of the more important metallurgical requirements, whatever steel analysis is used, is that it can be relatively free from non-metallic

inclusions and other internal stress concentration factors such as alloy and carbide segregation. Cleanliness and segregation, however, are only comparative and the steel is yet to be made that does not contain them. A low level of such internal stress concentration factors is best assured by the purchase or manufacture of bearing quality steel.

The quality standards for acceptance of bearing steels are not altogether uniform throughout the industry. Reliance is placed in macro-etch tests, non-metallic ratings, inspection of hardened and fractured surfaces and in visual examination of step-down tests by the bearing industry in judging quality of bearing materials. Differences of opinion exist among bearing manufacturers as to the limits of acceptance under each of these tests as well as the relative usefulness of the various tests. The most widely used standard for carbon-chromium ball and roller bearing steels is A.S.T.M. Specification A-295-46T. There is no corresponding specification for the case hardening steels, but comparable quality is used with proper allowance for the higher oxygen level in low carbon steels.

Chromium-Carbon Through Hardening Steels

Table 1 lists the composition of the more common ball and parallel roller bearing steels. The first two, containing .50 and 1.00 per cent chromium respectively, are used for balls and rollers and to a less degree in recent years. E-52100 is the universal high carbon bearing race material here and abroad. The remaining four steels are higher hardenability manganese-silicon and manganese-molybdenum modifications for rings of heavier cross-sectional thickness. European modifications are quite similar with manganese approaching 2.00 per cent in some Russian steels. The choice of manganese, silicon, and molybdenum is primarily based on their strong hardenability influence at high carbon levels, although manganese also aids in keeping the hardening temperatures low and silicon and molybdenum provide excellent resistance to softening at operating temperatures a little higher than normal.

These steels are melted by basic electric practice although acid open hearth practice is used on the continent for comparable compositions. Advantage is taken of the carbon-oxygen equilibrium to keep aluminum and silicon deoxidation to a minium for greater cleanliness. The grain size of these steels in the hardened condition is controlled essentially by the excess carbide particles. In fact, the hardening cycle is established and controlled largely by a fracture grain size test.

For reasons of machinability these steels must be hardened from a spheroidize annealed prior structure. The carbide size and shape in the annealed structure is closely regulated to ensure optimum machinability and a uniform response to hardening since the integrated effects of prior

Table 1

Composition of Through Hardening Bearing Steels

	C	Mn	Si	Cr	Mo
AISI E-50100	.95/1.10	.25/.45	.20/.35	.40/.60	-
AISI E-51100	.95/1.10	.25/.45	.20/.35	.90/1.15	-
AISI E-52100	.95/1.10	.25/.45	.20/.35	1.30/1.60	-
S.K.F. #1	.92/1.02	.95/1.25	.50/.70	.90/1.15	-
S.K.F. #2	.87/.97	1.40/1.70	.60/.80	1.40/1.70	-
Timken #1	.95/1.10	.60/.90	.20/.35	1.20/1.50	.20/.30
Timken #2	.95/1.10	1.05/1.35	.20/.35	1.20/1.50	.45/.55

structure, austenitizing time and temperature establish the hardenability level of these steels. Hardening temperatures of 1525 to 1575°F and tempering temperatures of 250 to 350°F are used to produce final hardnessess of 62 to 65 Rockwell "C". The hardened structure retains about 10 per cent austenite and a great many undissolved carbide particles.

Case Hardening Steels

Table 2 shows the case carburizing steels most widely used for tapered roller bearings. It is observed that they range in composition from comparatively low alloy levels to the most highly alloyed of the common carburizing steels. They are arranged in order of increasing core hardenability and hence their applications are generally in increasingly heavier section sizes. They are melted with a fine grain practice using aluminum and ferro-silicon as deoxidants. It is expected that more attention will be focused on this requirement because of the present interest in higher temperature carburization. Optimum machinability in the lower alloyed group is obtained by controlled cooling directly off the mill at a rate sufficient to cause the pro-eutectoid ferrite to be equi-axed and the remaining structure to be fine pearlite. Krupp and 3310 are traditionally normalized and given a long sub-critical temper to spheroidize the carbide and minimize martensite retention.

These steels are carburized to a surface carbon of .90 to 1.10 per cent and to a depth that varies with the section size and application. Case depths are rarely less than .025 inch measured to the 0.50 per cent carbon level and may reach as great as 0.225 inch in heavy duty industrial bearings. In general, the total carbon affected zone on both sides should not exceed one-half the minimum cross-section of the part.

Carburizing is usually done at 1650 to 1725°F and the product is then oil quenched or air cooled and reheated to 1450 to 1525°F for hardening. The double quench procedure is followed to refine the grain

size of the core, to keep both the retained austenite and residual carbides at a reasonable level, and to simplify the problem of fixture quenching of races to minimize distortion. Hardening is followed by tempering in the range 300 to 360°F.

The object in using case hardening steels is to produce a wear resistant surface of high elastic strength and a softer, shock resistant core. Hence, it is necessary that the composition of the carburizing steels be so adjusted that a proper balance be obtained between the case and core hardenability values. The aim is a case hardness of 58.0 to 62.0 Rockwell "C" and a core hardness of 25.0 to 40.0 Rockwell "C". Within these hardness ranges the case structure will contain 15 to 25 per cent austenite and the core will be essentially martensitic with a varying amount of ferrits.

Discussion

A great obstacle to evaluating materials and material structure in fatigue is that near the maximum hardness level obtainable with a given carbon content, hardness is not consistently related to fatigue strength. Styri[1], for example, has shown that the bending and torsion fatigue strength of 52100 remains essentially unchanged over a hardness range of 58.0 to 64.0 Rockwell "C". It has been observed[2] that the variation of endurance limit and elastic limit with hardness are similar, but Muir[3] has demonstrated the inconsistent relation between hardness and elastic limit. The relationship between hardness and endurance limit obtained on four steels by rotating beam tests is shown in Figure 1.

Table 2

	C	Mn	Si	Ni	Cr	Mo
AISI 8620	.18/.23	.70/.90	.20/.35	.40/.70	.40/.60	.15/.25
AISI 4617	.15/.20	.45/.65	.20/.35	1.65/2.00	-	.20/.30
AISI 4320	.17/.22	.45/.65	.20/.35	1.65/2.00	.40/.60	.20/.30
AISI 3310	.08/.13	.45/.60	.20/.35	3.25/3/75	1.40/1.75	-

There is, furthermore, little information available on the elastic strength properties of hardened steels. Effort[4] has been made in recent years to obtain such information by means of the bend test, but these results indicate that the elastic limit and yield strength in bending is higher than in simple tension. An example of this is shown

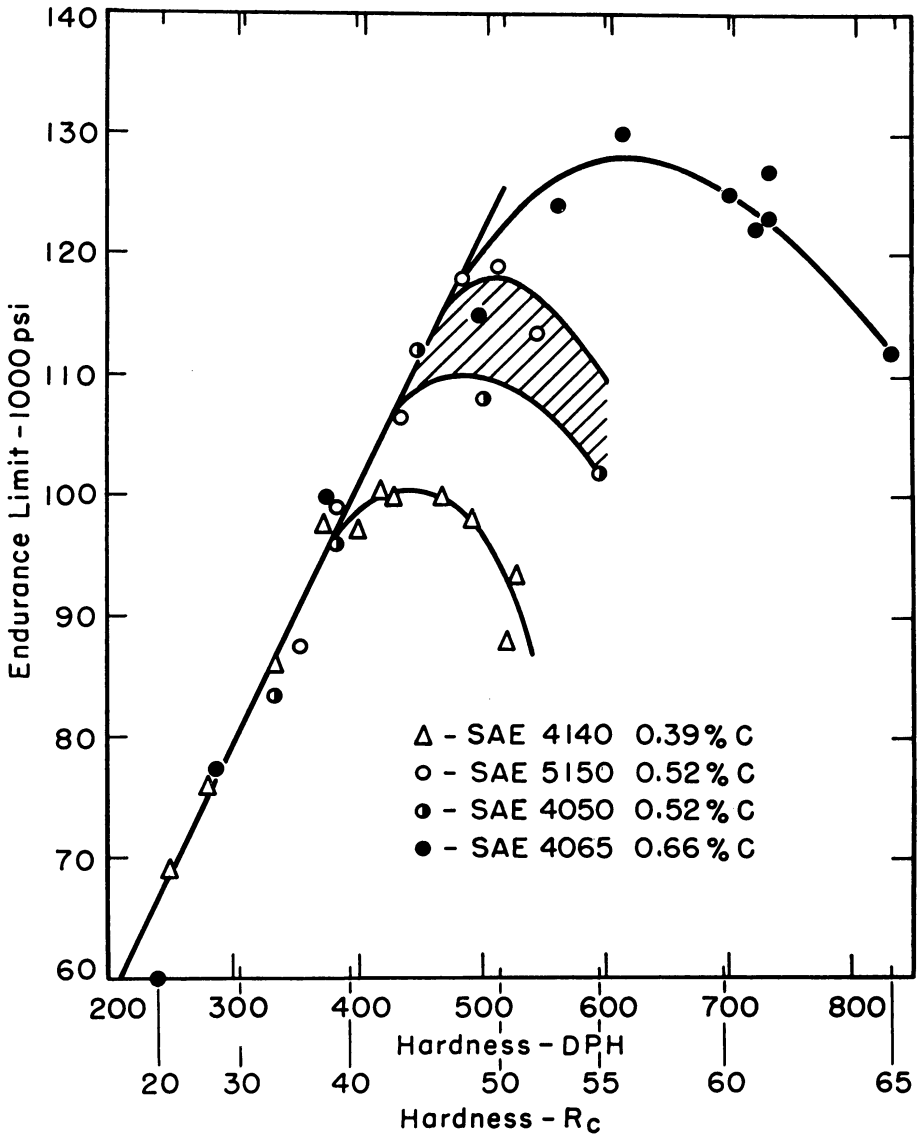

Figure 1. Effect of carbon content and hardness on endurance limit in bending. From discussion by Howard Scott (p. 145) of paper by Ross, Sernka, and Jominy. Transactions A.S.M., 1956, Vol. 48 p. 119.

for 52100 in Figure 2. Muir's elastic limit determinations were made by loading and unloading in simple tension. The quantities of retained austenite present in commercial high carbon steels may modify the relationship between elastic limit and fatigue properties.

The relationship between static properties and rolling fatigue strength is even more tenuous when we recognize that there has been no relationship established between rolling fatigue strength and other types of loading application in high carbon steels.

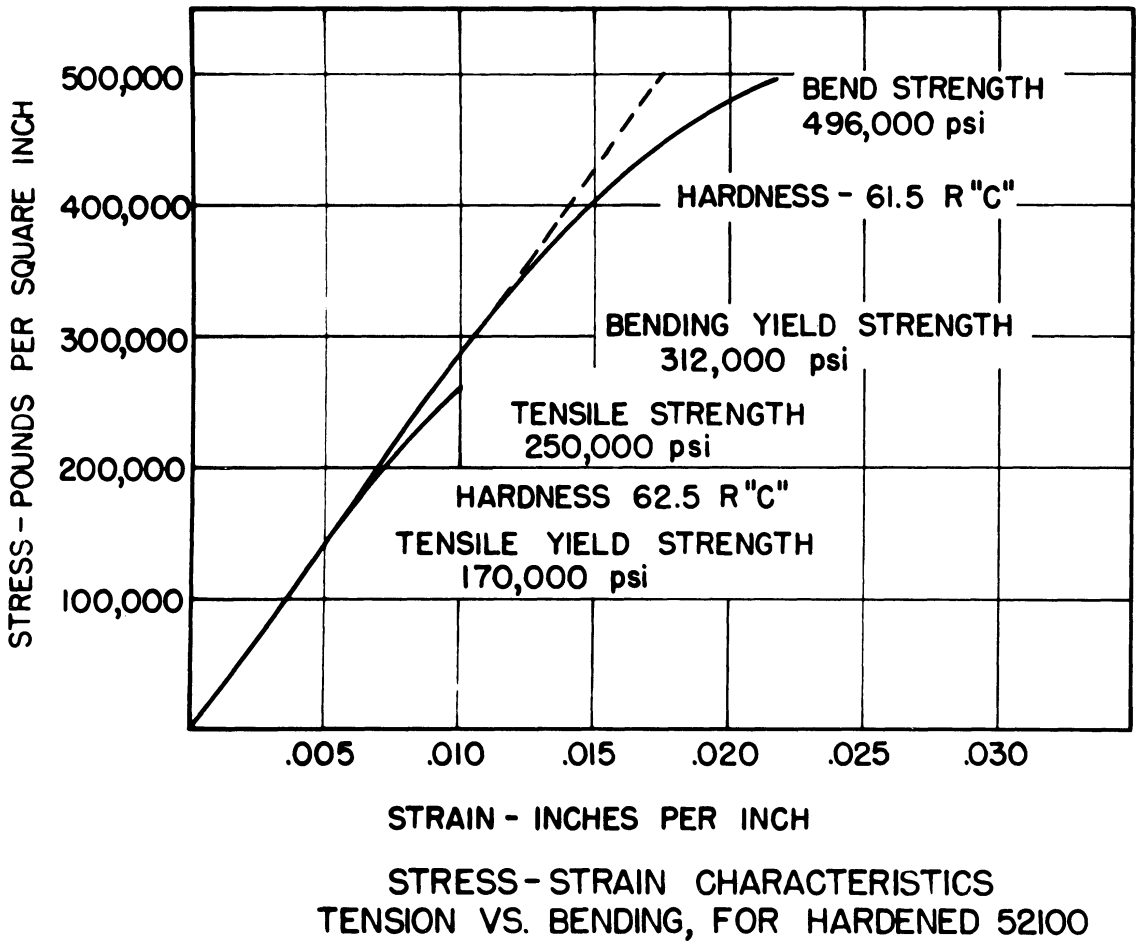

Figure 2. Comparison of tensile and bend tests of hardened 52100 steel.

CALCULATION OF STRESSES IN ROLLING CONTACT

A major characteristic of rolling fatigue is that the load is concentrated on a small area of contact between the two bodies. The shape of the area of contact is determined by the principal radii of curvature of the bodies; the size of the area is, in general, an ellipse of semi-axes a and b. The extreme shapes are obtained with a ball on a plane or another ball where a = b and the case of a cylinder on a plane or another cylinder where the contact is a rectangle of semi-width b. These various contact areas are illustrated in Figure 3.

The calculation of stress distribution within and beneath the contact area by Hertz in 1881 has since been repeated and modified by many investigators. Examples of such calculations are given in Figure 4 for the contact geometries of Figure 3. Reference(5) is an excellent guide for contact stress calculations. The accuracy of such calculations has been confirmed by photoelastic studies within the limitation of Hertz's assumptions that the materials are elastic and homogeneous. Several facts of value in the analysis of rolling fatigue which can be taken from these studies are as follows:

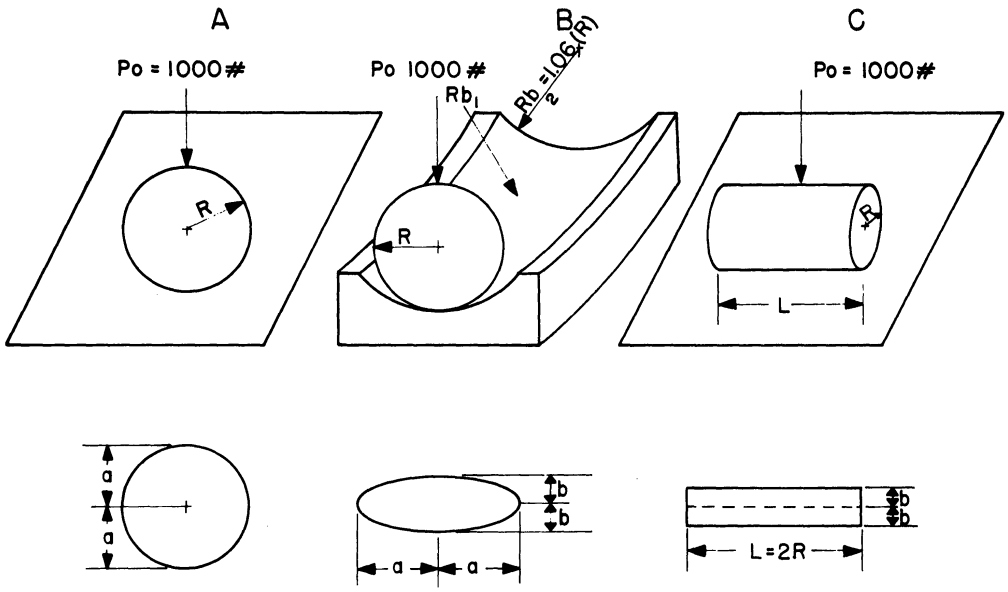

EFFECT OF CONFIGURATION OF BODIES IN CONTACT ON THE SHAPE OF THE CONTACT AREA

Figure 3. Schematic representation of various contact areas.

A	B	C
$a = b = \mu g^* = (1)(.0290)$	$a = \mu g = 2.787(.0379)$	$b = .000287\sqrt{\frac{Po}{L(\frac{1}{Ra}+\frac{1}{Rb})}}$
$b = .0290"$	$a = .1056"$	$b = .000287\sqrt{\frac{1000}{(1)(2+0)}}$
	$b = \nu g = .487(.0379)$	
	$b = .0184"$	$b = .0064"$
$P\ MAX. = \frac{3\,Po}{2\pi ab}$	$P\ MAX. = \frac{3\,Po}{2\pi ab}$	$P\ MAX. = \frac{2\,Po}{\pi Lb}$
$P\ MAX. = 570{,}000$ psi	$P\ MAX. = 246{,}000$ psi	$P\ MAX. = 99{,}300$ psi
$\tau\ MAX. = .320\ P\ MAX.$	$\tau\ MAX. = .323\ P MAX.$	$\tau\ MAX. = .30\ P\ MAX.$
$\tau\ MAX. = 182{,}000$ psi	$\tau\ MAX. = 79{,}400$ psi	$\tau\ MAX. = 29{,}800$ psi
$Z_1 = .468\,b = .0136"$	$Z_1 = .75\,b = .0138"$	$Z_1 = .786\,b = .00505"$

μ and ν are constants dependent only upon the geometry of the bodies.

$$^*g = k\sqrt[3]{\frac{Po}{\frac{1}{Ra_1}+\frac{1}{Ra_2}+\frac{1}{Rb_1}+\frac{1}{Rb_2}}}$$

Where: k = A constant depending upon the elastic constants for the bodies.
P MAX. = Maximum compressive stress in contact area.
T MAX. = Maximum shear stress in contact zone.
Z_1 = Depth to position of maximum shear stress.

Figure 4. Calculation of stresses in the contact zone when R = 0.5 inch in A, B, and C of Figure 3.

1. For static radial loading the maximum shear stress is beneath the center of the contact area at a depth proportional to the semi-minor axis of the contact ellipse. The magnitude of maximum shear stress (τ maximum) ranges from .30 to .33 times the maximum pressure (P maximum) in the center of the contact area, depending on the shape of the contact area. A typical stress distribution for static cylindrical contact is shown in Figure 5.

2. When pure rolling occurs, i.e., no tangential stress in the contact area, the maximum range (variation) of shear stress is produced at a depth closer to the surface and nearer to the edge of the contact area than the position of the maximum shear stress.[6] Radzinovsky[7] has calculated this effect for the case of cylindrical contact as shown in Figure 6. This condition places the most critical shear stress from the standpoint of fatigue in a region of lower hydrostatic stress than is present at the position of the maximum shear stress.

3. The effect of tangential stress in the contact area has been calculated and the results confirmed by photoelastic techniques. The major effect shown is that increased tangential force shifts the position of the maximum shear stress toward the surface.

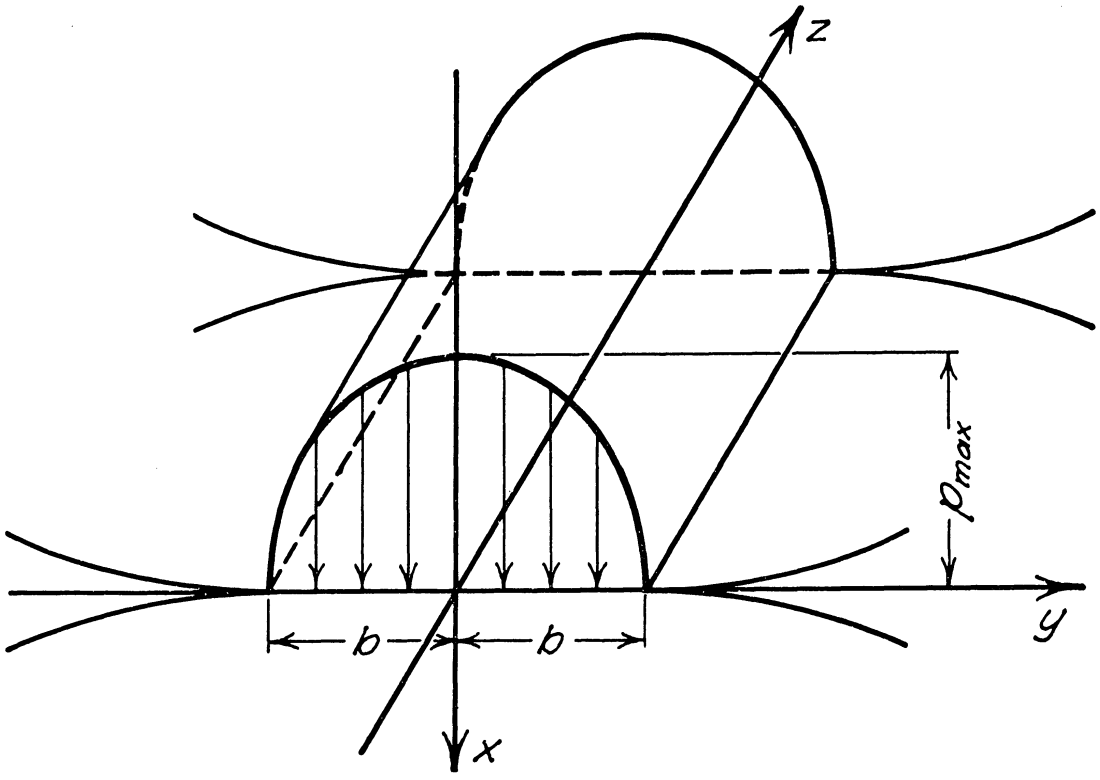

Figure 5(a). Stress distribution in the contact plane of two cylinders in pure rolling contact.

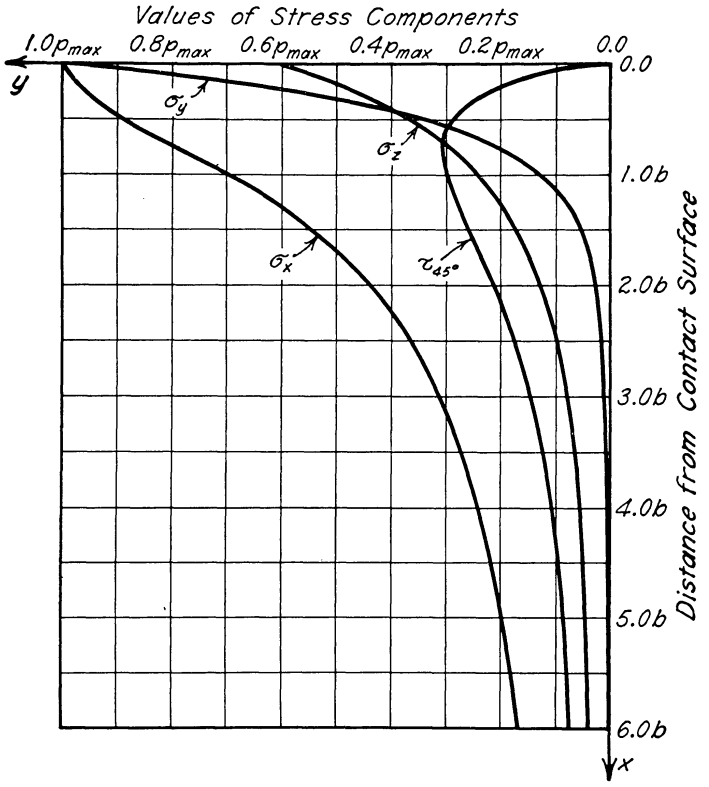

Figure 5(b). Stress distribution in depth for (a) along the X axis. (From Reference 7)

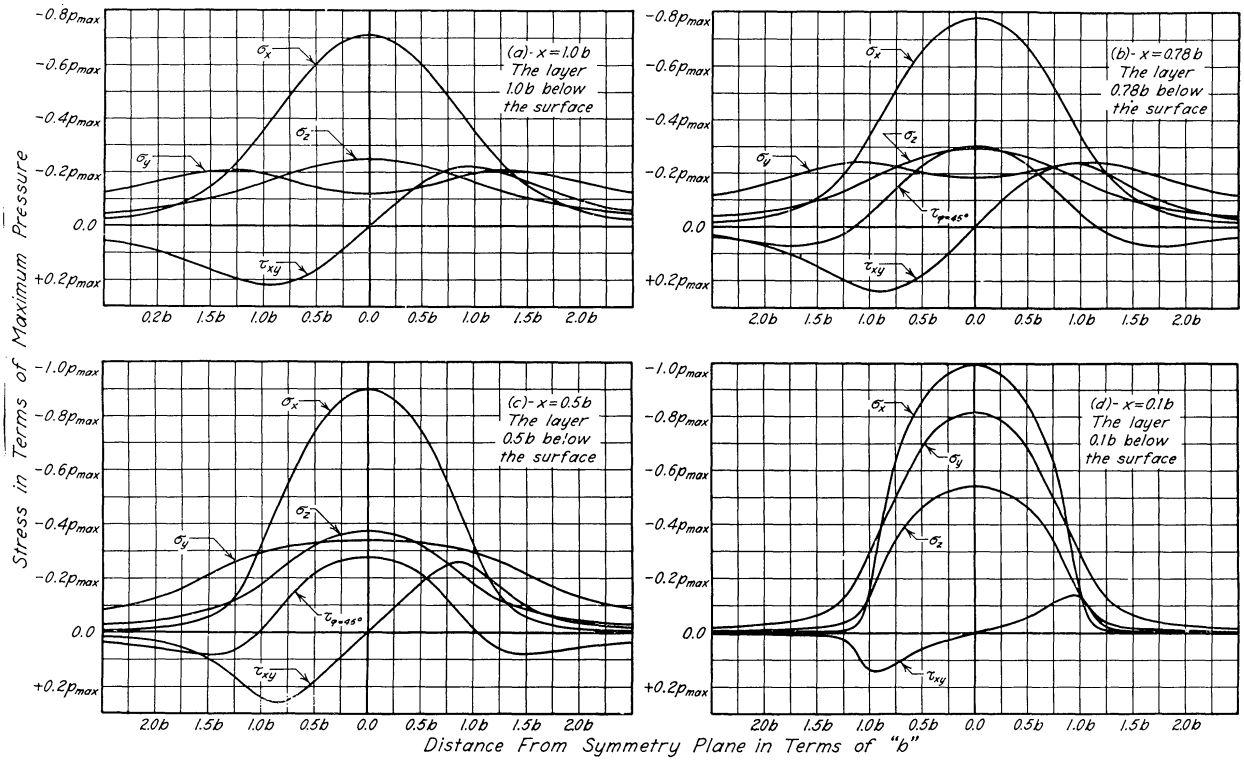

Figure 6. Variation of stress components in the contact zone as rolling occurs. (From Reference 7)

Thus rolling fatigue is a case of fatigue under combined stress where a very small volume of material is subjected to reversed shear stress while under rather high triaxial compressive stress. Tri-axial compressive stress has been shown to increase markedly the torsional fatigue strength of steel[8] so it is not surprising to find that hardened steel can sustain much higher reversed shear stresses in rolling contact than in other states of stress.

For cylindrical contact the state of stress at the ends of the contact areas cannot be calculated with the same certainty as it is within and beneath most of the contact area. The effects of undercut and roll-end geometry are thus difficult to calculate.

The designer's ability to calculate the critical stresses in rolling fatigue becomes most uncertain regarding the stress concentration effect of inhomogeneities such as non-metallic inclusions of oxides and sulfides, carbides, in the austenite-martensite aggregate of bearing steels.

Thus, since not all of the factors of stress concentration in rolling fatigue can be calculated, how may rolling fatigue results be placed on a common footing for comparison? A good compromise is to compare fatigue life as a function of P maximum for <u>similar contact geometry</u> since all of the calculable stress effects are related to P maximum by factors which depend on the geometry of contact.

In the past, when comparisons have been made for different contact configurations, the maximum shear stress, τ maximum, has been used as the basis for comparison. The recent work of Fessler and Ollerton[6], however, points out that this is unsafe because the maximum range (variation) of shear stress is related to P maximum by a different factor than is τ maximum for any given geometry, and the effect of hydrostatic stress for a given range of shear stress must be considered as well.

ROLLING FATIGUE TESTS

Bearing Life Tests

Since the rolling fatigue properties cannot be computed from easily measured mechanical properties of steels at the high hardness levels used for rolling contact bearings, numerous life tests of actual bearings have been made to determine the constants used to establish bearing ratings and to measure the effects of variations in composition, heat treatment, and other processing variables.

The statistical nature of fatigue is evident in the broad scatter of life obtained for identical bearings tested under ideal conditions. It is not unusual for the longest life in a group of 100 identical bearings to be fifty times the life of the first bearing to fail. Comparisons between bearing test groups must, therefore, be made at a constant probability of failure.

Fortunately, the life distribution conforms to the Weibull relationship[9-12], which can be written:

$$S = e^{-(\frac{l}{a})m}$$

Where S = Probability of survival of a given bearing to life "l".
e = Base of natural logarithms.
a = Constant characteristic of the life level of the sample.
m = Constant characteristic of the dispersion of life of the sample.

By testing all bearings in a test group to failure and plotting the results as shown in Figure 7 using a special probability paper on which the Weibull distribution is a straight line, the Weibull line which best fits the data can be computed by least squares. The life for any desired probability of failure can be extrapolated and the confidence limits estimated. The tests can be truncated at a considerable savings in time when 50 per cent of the bearings have failed, provided the running time of all the unfailed bearings exceeds the life for 50 per cent failure. Running a larger sample size and testing to a greater percentage of failures result in narrower confidence limits for the Weibull line but a thirty bearing sample tested to 50 per cent failure represents a good compromise of testing time versus reproducibility of results.

In nearly all bearing life tests, the time to failure is reduced by the use of higher loads and/or speeds than are normally encountered in service. The well-known inverse exponential relationship of load or stress and life has been demonstrated for ball bearings by Styri[1] up to mean Hertz compressive contact pressures in excess of 500,000 psi which is well in the range of measurable plastic deformation. The value of the exponent, x, in the equation:

$$\frac{\text{Life 1}}{\text{Life 2}} = \frac{(\text{Load 2})^x}{(\text{Load 1})}$$

has been confirmed for a very large sample of ball bearings from many manufacturers to be $2.87 \pm .35$ at 10 per cent failures and $2.80 \pm .30$ for 50 per cent failures.[13]

While the statistical analysis of bearing life test results using the Weibull distribution permits the engineer to tell whether two groups of bearings are significantly different, the broad scatter in life characteristic of rolling contact bearings continues to be a problem. Considerable effort has been expended to find ways of reducing the dispersion in bearing life. The fact that the origin of many fatigue spalls in bearings has been clearly associated with non-metallic inclusion stringers has led to the belief that a reduction in the frequency

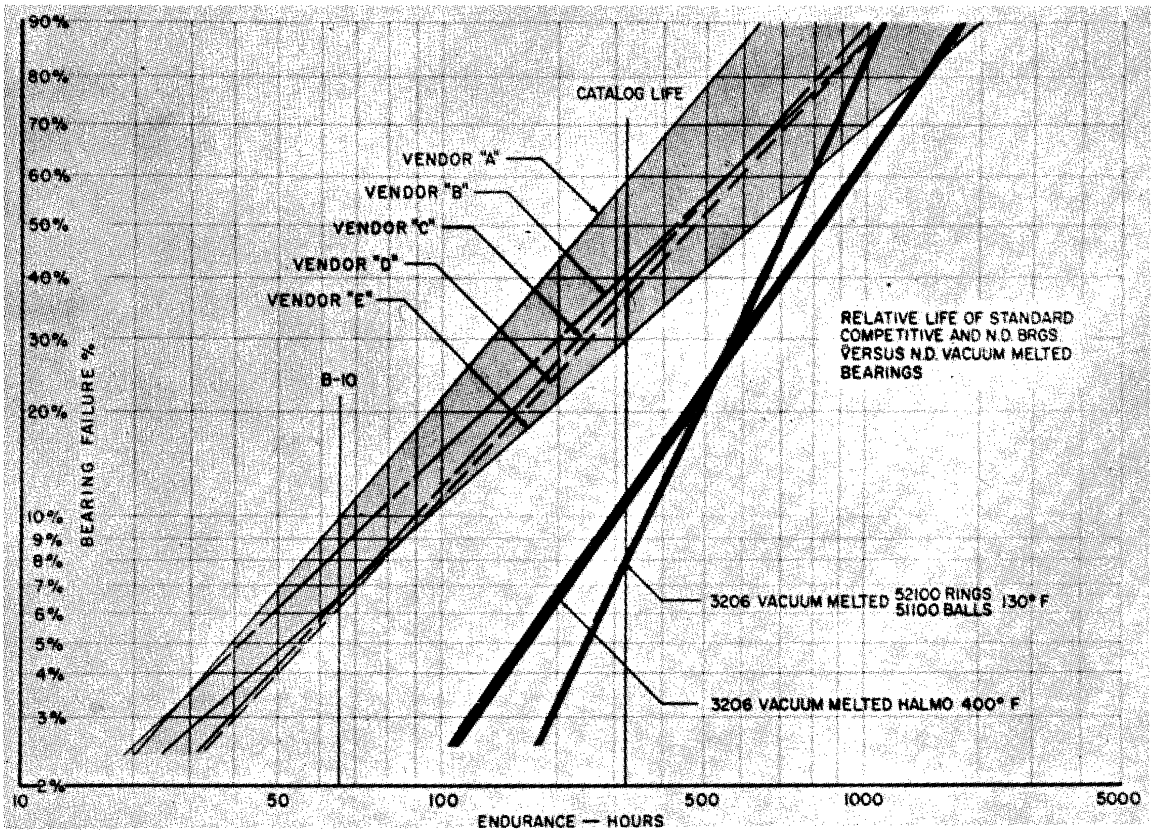

Figure 7. Weibull plot of bearing life for ball bearings made from air melted and vacuum melted steels. From "Effect of Vacuum Melting on Bearing Steels" by L.D. Cobb, S.A.E. Preprint March 1957.

and severity of such internal stress concentrations would reduce the scatter in life and increase the life for a given probability of failure.

Non-destructive tests such as magnetic particle inspection have been applied to finished parts in an effort to eliminate early failures from a given population of bearings, but without remarkable success. The data in Figure 8 show that the full range of bearing life is obtained at zero indications and the minimum time to failure is independent of the number of indications on the races. While the average life of a large group of bearings having few indications is better than the entire population, early failures have not been eliminated; their probability has merely decreased with respect to the entire population.

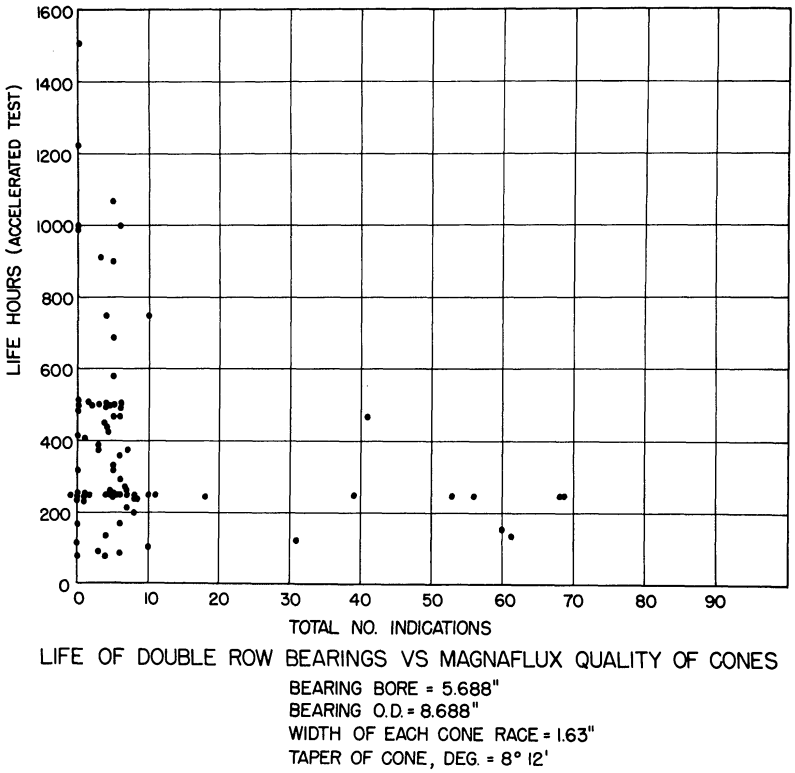

Figure 8. Data on the relationship of bearing life to magnetic particle indications on finished parts.

Simplified Rolling Contact Tests

Many attempts have been made to reduce the number of uncontrolled variables in rolling contact fatigue testing by the use of simplified test sample geometry. Several of these are described in references 14 to 20.

The recent tests at N.A.C.A. using an air-driven spin rig designed by Macks(14) for rolling contact of balls in a cylindrical raceway have shown good agreement with the bearing tests of Styri made at overlapping levels of stress as shown in Figure 9. The median life for Styri's outer races of 52100 steel is nearly coincident with the 10 per cent life for 9/16" diameter balls made of the same steel at similar hardness tested in the spin rig. The comparisons of rolling fatigue tests in Figure 9 have been made by plotting the cycles of repeated contact loading versus the value of P maximum calculated from the geometry of the rolling surfaces.

It is interesting to note that even at this high degree of overloading, the spread in bearing outer race life was about 50 to 1. More astonishing is the fact that the simple spin rig test data showed more scatter than the bearing data. This scatter for the spin rig tests

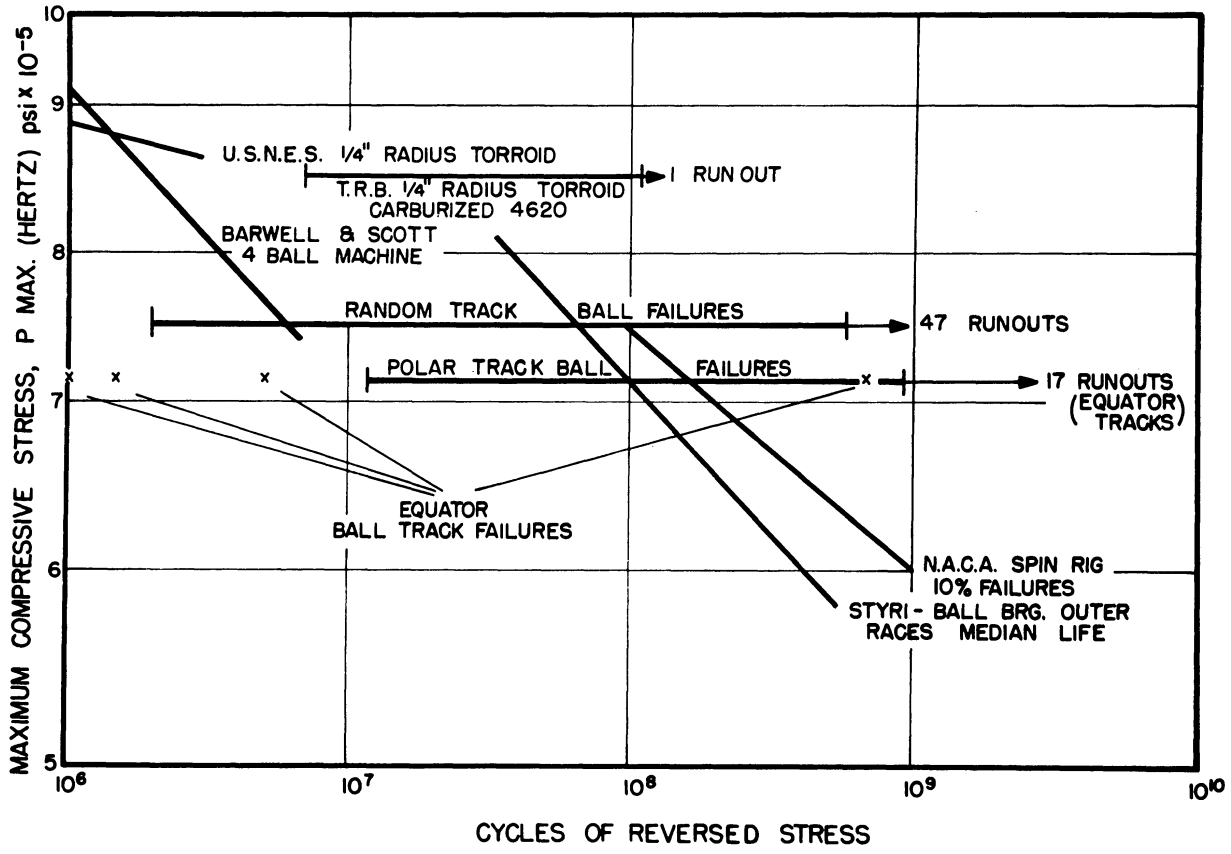

Figure 9. Maximum surface compressive stress, P maximum versus life for various rolling fatigue tests.

was greatly reduced when a group of thirteen balls were drilled to ensure that the tracks passed over the polar region of the ball.[16] The greatest scatter was shown in a group of twenty-one balls having their stressed tracks along the equator where the first five failures occurred at 1×10^6, 1.5×10^6, 5×10^6 and 700×10^6 cycles and the remainder were unfailed after 900 to 2700×10^6 cycles.

Other tests of 52100 steel balls made by Barwell and Scott[18] in an adapted Boerlage 4 ball machine are included in Figure 9 to show that not all simplified ball tests give the same results. It is likely that the displacement to much lower life is largely due to sliding in combination with rolling for the 4 ball machine tests. The 4 ball tests were also conducted at higher stress levels but the stress-life exponent is similar to those for the data of ball bearing and spin rig tests.

Results from tests of torroidal specimens in contact with cylindrical specimens of hardened 52100 steel by Gross and Greenert[20] lie between the 4 ball rig data and the spin rig data. Tests at the Timken Roller Bearing Company using carburized specimens of nickel-moly and Krupp steels with geometry similar to that of Gross and Greenert gave results near the spin rig data in the plastic range.

Tests of Buckingham and Talbourdet have shown no consistent relationship of rolling fatigue strength to hardness for high carbon steels but have provided usefull "experimental load-stress factors" for various materials in cylindrical rolling contact.[21]

Radzimovsky[7] was successful in relating the surface fatigue strength for line contact to hardness using the calculated range of maximum shear stress and a strength condition based on the Huber-Mises hypothesis. His calculated results were in good agreement with the results of Buckingham for hardnesses up to 350 Brinell. His analysis can possibly be extended to high carbon steels, when complete Goodman diagrams are available for these steels at high hardness levels.

Residual Stresses

As yet there has been no definite relationship established between residual stress and fatigue properties. The principal problem here has been the difficulty of any one laboratory studying the question on a sufficiently large scale to yield conclusive evidence. However, under the sponsorship of the SAE-ISTC Division 4 Committee on Residual Stresses, many laboratories are engaged in an extensive cooperative effort to obtain information on this point. Their report on the first stage of their investigation, the correlation of the various methods for measurement of residual stress, has been issued and work is now underway to determine the influence of residual stress on fatigue.

There is virtually nothing known about the effects of residual macro stress on rolling fatigue. Work is just beginning on the problem of measurement of micro-stresses.

Under the sponsorship of the Grinding Wheel Institue and the Abrasive Grain Association, studies have been made of grinding stresses in hardened steel[22] and their influence on bending fatigue life.[23,24] These studies indicate little effect of grinding tensile stress on fatigue life until a residual peak tensile stress of approximately 50,000 psi is approached. Above this value reduction in fatigue limit occurred whether or not the peak tensile stress was at the surface or slightly sub-surface. Upon grinding with straight grinding oil, increases up to 38 per cent in base line bending fatigue limit were observed, presumably from formation of measured residual compressive grinding stress and cold deformation.

RECENT DEVELOPMENTS IN BEARING MATERIALS

Elevated Temperature Service

Recent developments in materials for bearings have generally followed two avenues of investigation; (1) the development of steels for higher temperature applications, and (2) the use of vacuum melted steels for both room temperature and elevated temperature service.

Developments in high temperature steels for bearing races and ball or roller components can be roughly cataloged as follows:

1. The development of temper resistant steels for service up to 600°F in keeping with the pace set by lubricant manufacturers who have developed reasonably effective lubricants for short time 600°F service.
2. The development of secondary and precipitation hardening alloys and the application of available high speed tool steels for service above 600°F to roughly 1000°F to satisfy these higher temperature conditions when satisfactory lubricants or means of lubrication are made available.
3. Development and application of metallic alloys and other materials for operating temperatures above 1000°F.

Table 3 lists materials presently being applied for bearings up to 600°F. These materials are primarily E-52100 modifications which contain variable quantities of silicon and aluminum to impart higher temper resistance. Both through hardening and carburizing versions of these analyses are presently being applied. Also frequently used in this temperature range have been the high chromium stainless analyses, the 440-C and the D-1 and D-2 cold work die steels. Recently, a modified version of AISI 3310 with 5 per cent molybdenum has been introduced for bearings up to 800°F. The popularity of all of these materials is based on their comparatively good cleanliness and their relative ease of processing and lower cost.

Table 4 shows bearing materials used for service up to 1000°F. These materials exhibit high hot hardness but are more difficult to process and heat treat than those steels shown in Table 3. Furthermore, lubrication must be accomplished by gases, solid lubricants or graphite and the resistance of these steels to atmospheric oxidation at these temperatures is poor.

Table 5 lists materials presently being considered for dry operation above 1000°F. These include cobalt base and nickel base superalloys and various sintered carbide materials.

Service at elevated temperatures poses many bearing problems not commonly encountered at room temperature. These problems are two-fold, one of lubrication and the other of metallic properties.

TABLE 3

Bearing Materials for Service up to 600°F

Analysis	Manufacturer	Nominal Chemistry							Heat Treatment
		C	Mn	Si	Cr	Ni	Mo	Others	
MHT	U.S. Steel	1.00	.60	.60	1.35	-	-	1.35 Al	1550°F - Oil, 600°F Temper
TBS-600	Timken	1.00	.70	1.10	1.45	-	.30	-	1550°F - Oil, 600°F Temper
440C	Various	1.00	.50	.50	17.00	-	.50	-	1900°F - Oil, 600°F Temper
D-1	Various	1.00	.50	.50	12.00	-	1.00	-	1850°F - Oil, 950°F Temper
D-2	Various	1.50	.50	.50	12.00	-	1.00	-	1850°F - Oil, 950°F Temper
420F	Various	.30	.50	.50	13.00	-	-	-	1850°F - Oil, 600°F Temper
315*	Bower	.12	.50	.28	1.50	3.00	5.00	-	1750°F - Oil, 900°F Temper
CBS-600*	Timken	.19	.60	1.10	1.45	-	1.00	-	1525°F - Oil, 650°F Temper

* Carburizing Analysis

TABLE 4

Materials for Service from 600°F to 1000°F
Alsc Used at 600°F and Below

Analysis	Nominal Chemistry C	Mn	Si	Cr	Mo	W	Va	Heat Treatment
M-1	.80	.30	.30	4.00	8.00	1.50	1.00	2200°F - Oil 2 + 2 Temper At 1050°F
M-10	.85	.30	.30	4.00	8.00	-	2.00	"
M-50	.80	.30	.30	4.25	4.25	-	1.00	"
Halmo	.65	.30	.30	5.00	5.00	-	-	"

TABLE 5

Possible Materials for Service Above 1000°F

Stellite 19
Stellite 25
Sintered Chromium Carbide
Nickel Bonded Titanium Carbide
Inconel

Among the metal problems encountered are:

1. Reduction of load carrying capacity.
2. Accelerated wear, oxidation and corrosion.
3. Increase in galling and metal pick-up.
4. Maintenance of structural stability.
5. Size incompatibility between mating bearing parts and mountings due to differences in the temperature coefficients of expansion.

Much consideration has been given to these problems by various investigators. It is now believed that the properties and factors important in the selection and application of a steel for high temperature bearings are the following:

1. Hot hardness.
2. Recovered hardness after prolonged service.
3. Galling characteristics.
4. Coefficient of thermal expansion.
5. Corrosion resistance.
6. Cleanliness.

It is agreed that hot hardness is one of the more important properties to consider in high temperature bearing materials. It is usually considered a rough measure of the load carrying capacity of the bearing at temperature but is not always the controlling factor. Figure 10 shows the hot hardness characteristics of a number of steels considered for high temperature service. It is observed that the high speed tool steels T-1 and M-1 which normally exhibit the strongest secondary hardening also produce the highest hot hardnesses.

For ordinary operating temperature operation (150°F maximum), the effect of lubricant composition, corrosive influence and viscosity on bearing performance is usually ignored. This is reasonable since the effects are small and the lubricants used are well established and standardized. This picture changes radically at temperatures above 300°F and lubrication becomes of paramount importance in the life of bearings. Some fragmentary simulated testing data indicate a very large loss of endurance with decrease in viscosity of the lubricant. Also, the corrosive effects of some of the lubricants developed for elevated temperature service seem to affect endurance adversely.

For a time it was believed that maintenance of 60.0 Rockwell "C" at operating temperature would ensure a load carrying capacity equivalent to that of standard bearing materials at room temperature. This is now known to be unrealistic since the measured load carrying capacity of air melted M-10 and 440-C bearing materials at 60.0 Rockwell "C" were found to be approximately 60 per cent of that for 52100 bearing steel at room temperature. This is another example of the inadequacy of hardness as a

criterion of fatigue strength. Vacuum melted tool steels fare much better, by comparison, being approximately of an equal footing with 52100 steel of equivalent hardness at room temperature.

Maintenance of recovered hardness for prolonged exposure to high temperature is a measure of the structural stability of the material at temperature. Resistance to environmental corrosion is necessary, but solution of the problem is complicated by the repeated stresses of rolling contact. For example, maintenance of a passive oxide film is probably impossible. This fact would probably limit the usefulness of high chromium contents for corrosion resistance. A possible solution is the use of non-corrosive atmospheres.

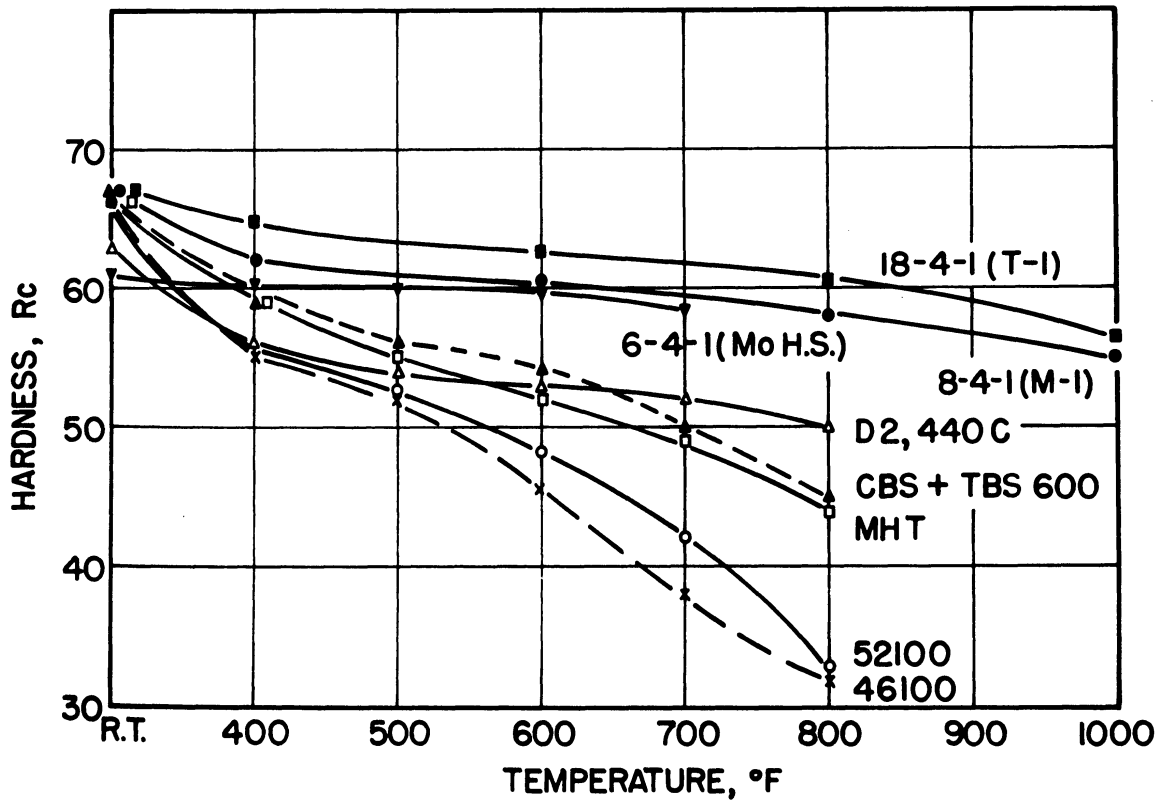

Figure 10. Hot hardness versus temperature of test. (1/2 hour at test temperature.)

Cleanliness of elevated temperature bearing steels is equally important as in standard bearing steels. However, many of the steels being applied at elevated temperatures are manufactured to the same standard of cleanliness only with considerable difficulty. In addition, many of these steels contain large segregated carbides which also serve as internal stress concentrating factors. To combat this problem two

trends are evident. Many of the more highly alloyed secondary hardening tool steels now being used at temperatures below 600°F are being replaced by lower alloy temper resistant steels. At temperatures above 600°F, where secondary hardening grades are necessary, increasing use of vacuum melting is noted.

Vacuum Melted Steel

The use of vacuum techniques in melting low alloy steels for bearing applications is a relatively recent development. The engineering advantages of vacuum melted materials have been recognized, and vacuum melted steels are under extensive investigations as bearing materials.

The processes used in producing vacuum melted bearing steels are vacuum induction melting and vacuum arc (consumable electrode) remelting. Vacuum induction melting procedures involve the variation of pressure and atmosphere during the melting, refining, and casting, while vacuum arc remelting is an operation in which an electrode is vacuum remelted in a water cooled mold. Vacuum melted metals can have superior qualities, but are very dependent upon the quality of the melting materials and the control of the melting techniques.

One advantage to be gained by vacuum melting is the improvement in inclusion ratings as measured by magnetic particle and microscopic methods. It is apparent that steel cleanliness is closely related to the oxygen content, and the decrease in oxygen level on vacuum melting is reflected by an improvement in steel cleanliness. Vacuum melting does not significantly change the sulfur content of a steel, but the type and distribution of the sulfides may be altered by vacuum remelting. The curves of Figure 11 compare the inclusion size distributions of an air melted and vacuum remelted nickel-moly steel. These data indicate a significant improvement in the cleanliness of bearing steels by vacuum remelting.

The evidence concerning the effect of vacuum melting by either method on bearing performance is just beginning to trickle in. In general, the influence has been favorable as Cobb's data of Figure 7 show. It will be some time, however, before sufficient data are accumulated to accurately assess the extent of this generally favorable development.

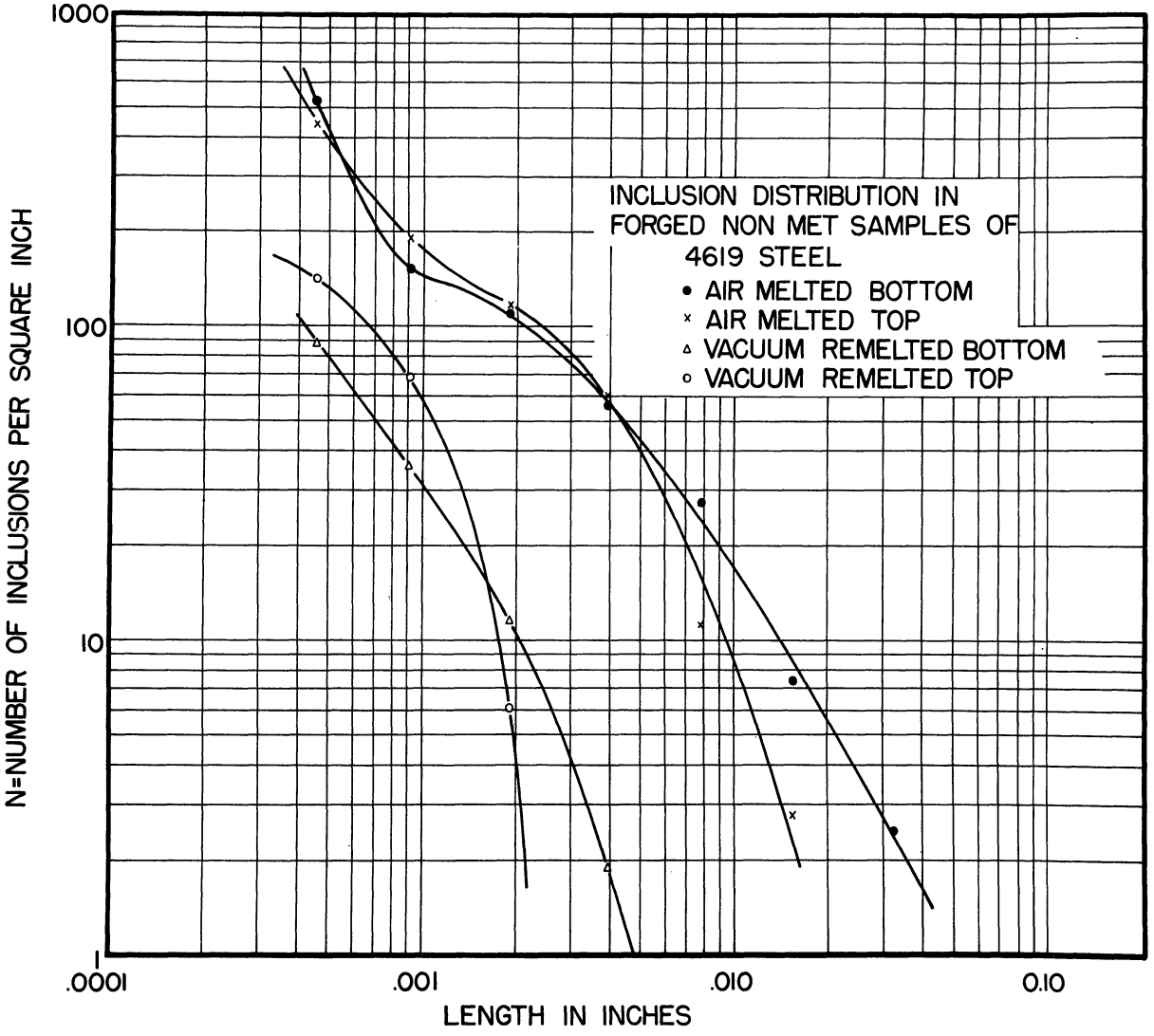

Figure 11. Distribution of oxide inclusion stringer lengths for consumable electrode vacuum remelted 4619 steel compared with corresponding samples from the basic electric arc melted electrode.

REFERENCES

1. Styri, H., "Fatigue Strength of Ball Bearing Races and Heat Treated 52100 Steel Specimens," Proceedings of A.S.T.M., Vol. 51, 1951, p. 682.

2. Shih, C.H., Averbach, B.L., and Cohen, M., "Some Effects of Silicon on the Mechanical Properties of High Strength Steels," Transactions of A.S.M., Vol. 48, 1956 p. 86.

3. Muir, H., Averbach, B.L., and Cohen, M., "The Elastic Limit and Yield Behavior of Hardened Steels," Transactions of A.S.M., Vol. 47, 1955 p. 380.

4. Hamaker, J.C., Strang, V.C., and Roberts, G.A., "Bend Tensile Relationships for Tool Steels at High Strength Levels," Transactions of A.S.M., Vol. 49, 1957 pp. 550-575.

5. Jones, A.B., "Analyses of Stresses and Deflections," New Departure Engineering Data, New Departure Division, General Motors Corporation, Bristol, Connecticut, 1946.

6. Fessler, H. and Ollerton, E., "Contact Stresses in Toroids Under Radial Loads," British Journal of Applied Physics, Vol. 8, October 1957 pp. 387-393.

7. Radzimovsky, E.I., "Stress Distribution and Strength Condition of Two Rolling Cylinders Pressed Together," University of Illinois Engineering Experiment Station Bulletin Series No. 408, Vol. 50, No. 44, 1953.

8. Crossland, B., "Effect of Large Hydrostatic Pressures on the Torsional Fatigue Strength of an Alloy Steel," Proceedings of the International Conference on Fatigue of Metals, London, September 1956 p. 138.

9. Weibull, W.A., "A Statistical Distribution Function of Wide Applicability," Journal of Applied Mechanics, Vol. 18, No. 3, September 1951 p. 293.

10. Gumbel, E.J., "Statistical Theory of Extreme Values and Some Practical Applications," National Bureau of Standards, Applied Mathematics, Series No. 33, 1954.

11. Johnson, L.G., "The Merdian Ranks of Sample Values in Their Population With an Application to Certain Fatigue Studies," Industrial Mathematics, Vol. 2, 1951 p. 1.

REFERENCES (CONT'D)

12. Johnson, L.G., "Ball Bearing Engineers Statistical Guide Book," New Departure Division, General Motors Corporation, Bristol, Connecticut, April 1957.

13. Lieblein, J. and Zelen, M., "Statistical Investigation of the Fatigue Life of Deep Groove Ball Bearings," Journal of Research of the National Bureau of Standards, Vol. 57, No. 5, November 1956, Research Paper 2719 p. 273.

14. Macks, E.F., "The Fatigue Spin Rig - A New Apparatus for Rapidly Evaluating Materials and Lubricants for Rolling Contact," Lubrication Engineering, Vol. 9, No. 5, October 1953 p. 254.

15. Butler, R.H., and Carter, T.L., "Stress Life Relation of the Rolling Contact Fatigue Spin Rig," N.A.C.A. Technical Note 3930, March 1957.

16. Butler, R.H., Bear, H.R., and Carter, T.L., "Effect of Fiber Orientation on Ball Failures Under Rolling Contact Conditions," N.A.C.A. Technical Note 3933, February 1957.

17. Carter, T.L., "Effect of Temperature on Rolling Contact Fatigue Life With Liquid and Dry Powder Lubricants," N.A.C.A. Technical Note 4163, January 1958.

18. Barwell, F.T., and Scott, D., "Effect of Lubricant on Pitting Failure of Ball Bearings," Engineering, July 6, 1956 p. 9.

19. Gross, M.R., "Laboratory Evaluation of Materials for Marine Propulsion Gears," Proceedings of A.S.T.M., Vol. 51, 1951 p. 701.

20. Greenert, W.J. and Gross, M.R., "Basic Information on the Bearing Properties of Various Materials in Liquid Metals," E.E.S. Report 090014A, U.S. Naval Engineering Experiment Station, Annapolis, Maryland, 19 February 1954.

21. Cram, W.D., "Practical Approaches to Cam Design," 3rd Conference on Applied Mechanics, Machine Design, November 1, 1956 p. 100.

REFERENCES ON RESIDUAL STRESS

22. Letner, H.R., "Residual Grinding Stresses in Hardened Steel," Transactions A.S.M.E., Vol. 77 p. 1089 (1955).

23. Tarasov, L.P., and Grover, H.J., "Effects of Grinding and Other Finishing Processes on the Fatigue of Hardened Steel," Proc. A.S.T.M., Vol. 50 p. 668 (1950).

24. Tarasov, L.P., Hyler, W.S., and Letner, H.R., "Effect of Grinding Conditions and Resultant Residual Stresses on the Fatigue Strength of Hardened Steel," 1957 A.S.T.M. preprint No. 65.

ACKNOWLEDGEMENT

Much of the preparation of this paper was due to the considerable efforts of A. L. Christenson, Dr. W. E. Littmann, R. A. Bloom and C. F. Jatczak of the author's laboratory. Their help is gratefully acknowledged.

PITTING OF GEAR TEETH

J. D. Graham
Chief Materials Engineer
International Harvester Company

PITTING OF GEAR TEETH

by

J. D. Graham

A discussion of any phenomenon involved with the stress state of gear teeth in action should be approached with great care and with full appreciation of how little we know. To begin with, the fundamentals of gear design are in themselves quite involved. The unavoidable dimensional variations produced even in the manufacture of precision gearing complicate the picture severely. When consideration is given to the elastic deflections resulting from applied loads, both in the gear itself and in its supports, the area of "intelligent guesswork" grows rapidly. To this must then be added our very great ignorance of the residual stresses existing in most gear teeth from heat treatment or grinding, combined with the extreme difficulty of accurately evaluating the distribution of applied stress in such a complicated structure. It is little wonder that there is considerable divergence of opinion as to the mechanism by which the surface damage called "pitting" is produced.

Let us take a brief look at the principal types of gear wear, using the illustrations adopted as standard by the American Gear Manufacturers Association for convenient comparison (1).

Adhesive Wear - called scoring, galling, or scuffing, in which welding of surface asperities takes place due to failure of lubricating film, primarily brought about by high temperature, pressure, and sliding velocity, is illustrated in Figure 1.

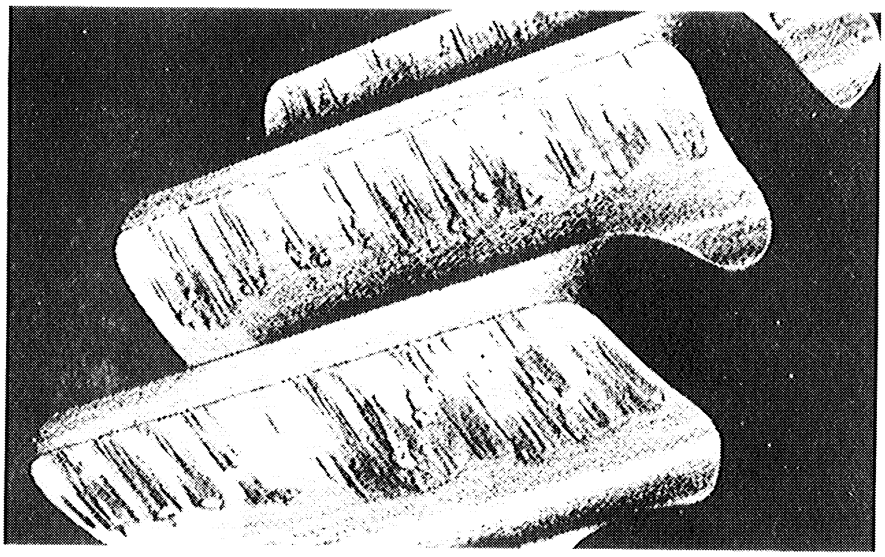

Figure 1. Adhesive wear - severe scoring.(AGMA).

Abrasive or Cutting Wear - in which foreign particles carried in the oil gouge metal out of the surface, is shown in Figure 2.

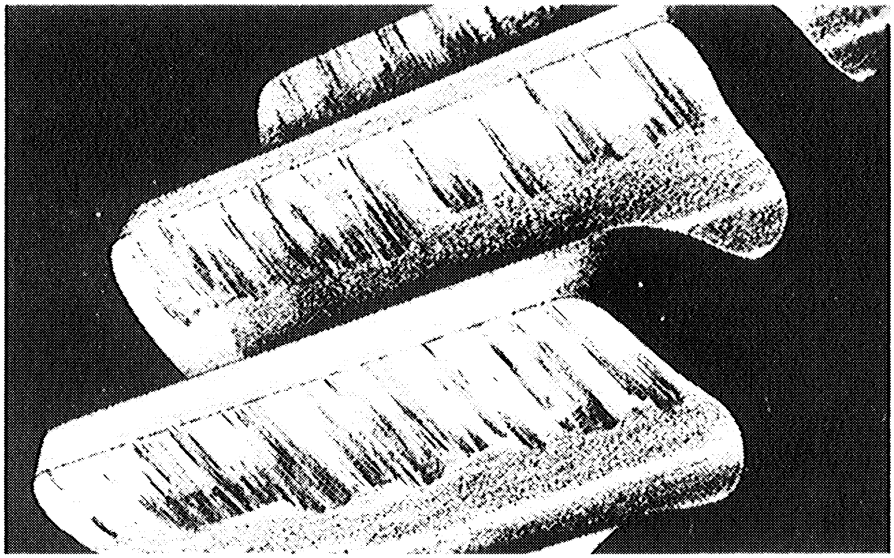

Figure 2. Abrasive wear.(AGMA).

Corrosive Wear - in which material is removed chemically by improper lubricant, moisture, or other corrosive influence may appear as shown in Figure 3.

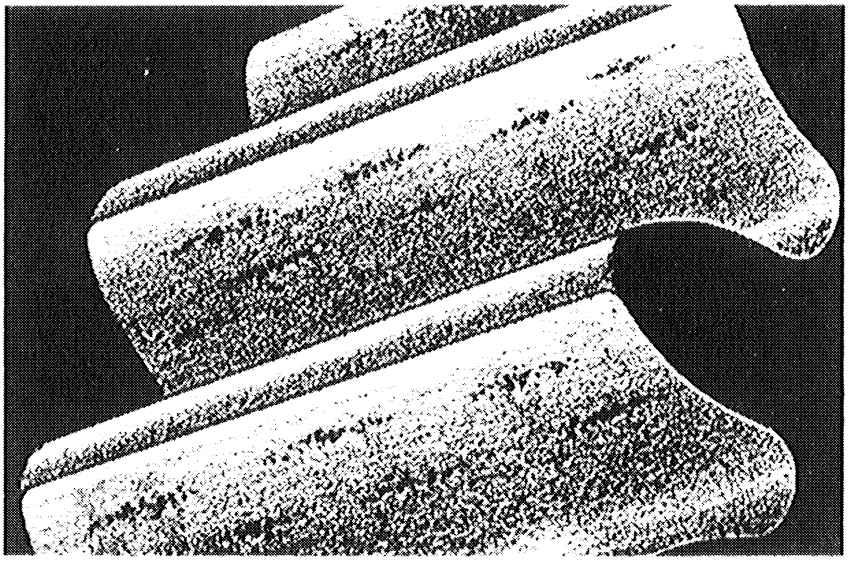

Figure 3. Corrosive wear.(AGMA).

Surface Fatigue - in which repeated surface loads cause fatigue cracks which may progress to surface deterioration is shown in Figure 4. Pitting and spalling fall in this category.

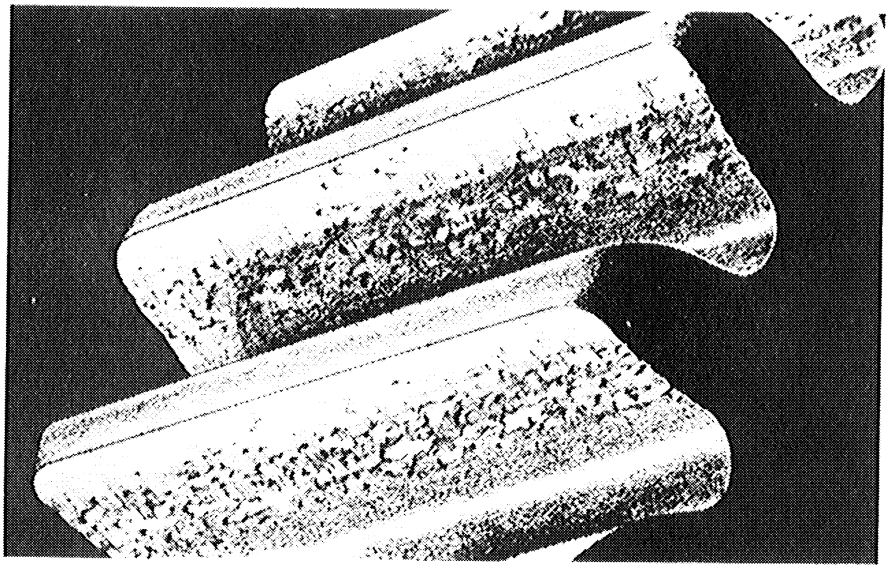

Figure 4. Destructive pitting.(AGMA).

This brief review of gear wear is included here to accent the difference between pitting or spalling and the other wear mechanisms -- the presence of a fatigue factor, by which the stresses induced by rolling or sliding contact, or both, eventually cause fatigue failure. Thus, in contrast to the other types of wear, these failures are not measured in terms of volume of metal removed, but rather in number of cycles and the load required to produce the phenomenon.

The Nature of Pitting Failure

Stresses Producing Pitting. The stresses involved in fatigue of gear surfaces arise from the relative rolling and sliding actions of the mating teeth. These actions vary continuously as tooth contact progresses through it cycle, and are very different with gears of different design. The most useful tool in analyzing these stresses is the technique of photoelastic stress analysis, by which studies are made of plastic models under applied loads, viewed with polarized light in such a way that dark lines, or "fringes" surround areas of equal stress. Such a study of a gear tooth is shown in Figure 5 and indicates the location and distribution of the compressive stresses arising at the contact face as well as the bending stresses at the root radius. The stresses in any

Figure 5. Photoelastic fringe pattern of plastic model of 1.5 long addendum 7 pitch spur pinion tooth loaded at the pitch line.

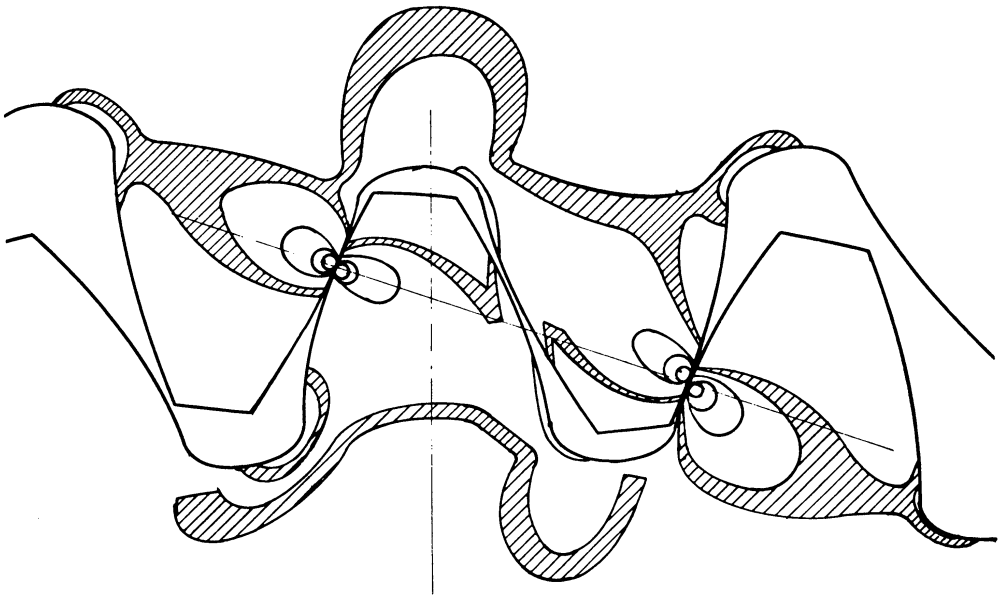

Figure 6. Photoelastic pattern of a pair of gears under load.(Buckingham).

are proportional to the number of fringes crossed from the area marked "0" (essentially no stress). Unfortunately the fringes at the extreme contact surface are shadowed in this figure. These surface stresses can be seen in Figure 6, a somewhat exaggerated drawing prepared by Buckingham (2) showing the actual stress distribution. Maximum shear stress exists slightly below the surface. Distribution of shear stress near the tooth surface both with and without the added complication of sliding forces is graphically illustrated in Figure 7 from Burwell (3). This actually is a graphic illustration of the formula derived by Hertz in 1881 which, in modified form, is universally used to calculate these gear tooth contact stresses, called "Hertz Stresses". Compressive stress is, of course, maximum at the surface, but metals do not fail by compression itself. The maximum shear stress exists roughly 0.010" to 0.012" below the surface in ordinary gearing.

The sliding action, which accompanies rolling over most of the tooth profile (in some cases over all of it) adds additional complications in the form of compressive and tensile stresses preceding and following the sliding contact. Figure 8 from Dudley (4) shows these stresses, and other influences on the stress picture.

Still another stress influence is the elastic wave which precedes and follows the area of contact, which is in effect bulging of the surfaces from the adjacent compressed area. These bulges subject the surface to repeated reversals of bending stress as the contact area passes.

The relative influence of these various factors on the surface material depends upon gear design, speed, load, lubrication, surface condition, and many other factors.

Sub-Surface Fatigue. As discussed above, the Hertz stress results in maximum shear stress somewhat below the surface (at a depth approximately 40% of the contact band width), and equal to about 30% of the Hertz stress. Under certain conditions, this stress exceeds the endurance limit of the material and with repeated cycling a fatigue crack forms parallel to the surface, gradually increases, and eventually finds its way to the surface. The small piece thus isolated breaks out and a pit is formed. Because the pit formation is the result of fatigue failure, a gear may run for some time before evidence of pitting appears.

A great deal of simulated gear testing has been done with carburized rolls. Figure 9 illustrates a fatigue crack below a carburized surface subjected to severe rolling load in such test work by Buckingham and Talbourdet (5). In this test, maximum shear stress was developed at a depth of 0.015", and the crack appeared at the juncture of case and core, 0.020" from the surface (still in the high stress area). Figure 10 shows a somewhat different configuration of subsurface cracking of a gear tooth surface (Rockwell C 61) heavily loaded and beginning to fail by pitting. In this case the cracks are near the surface, whereas the case depth is 0.032".

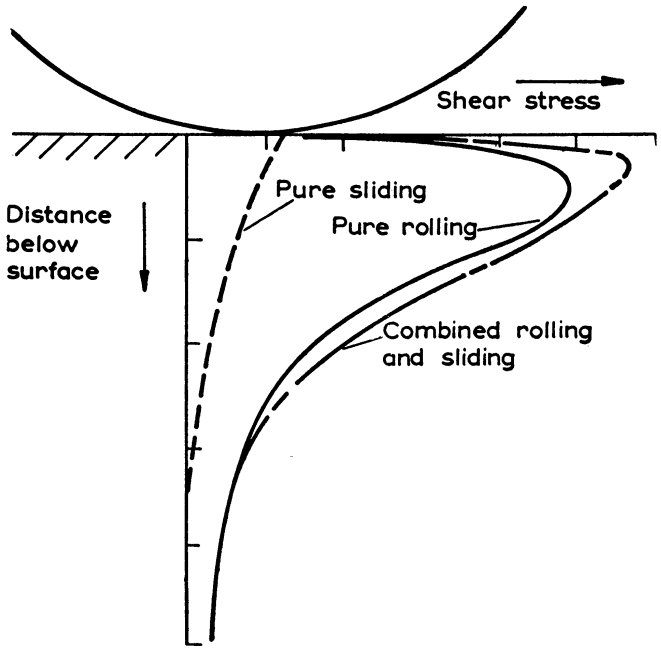

Figure 7. Magnitude of shear stress at various depths directly below the point of contact of two hard surfaces, in rolling, sliding, and combined contact.(Burwell).

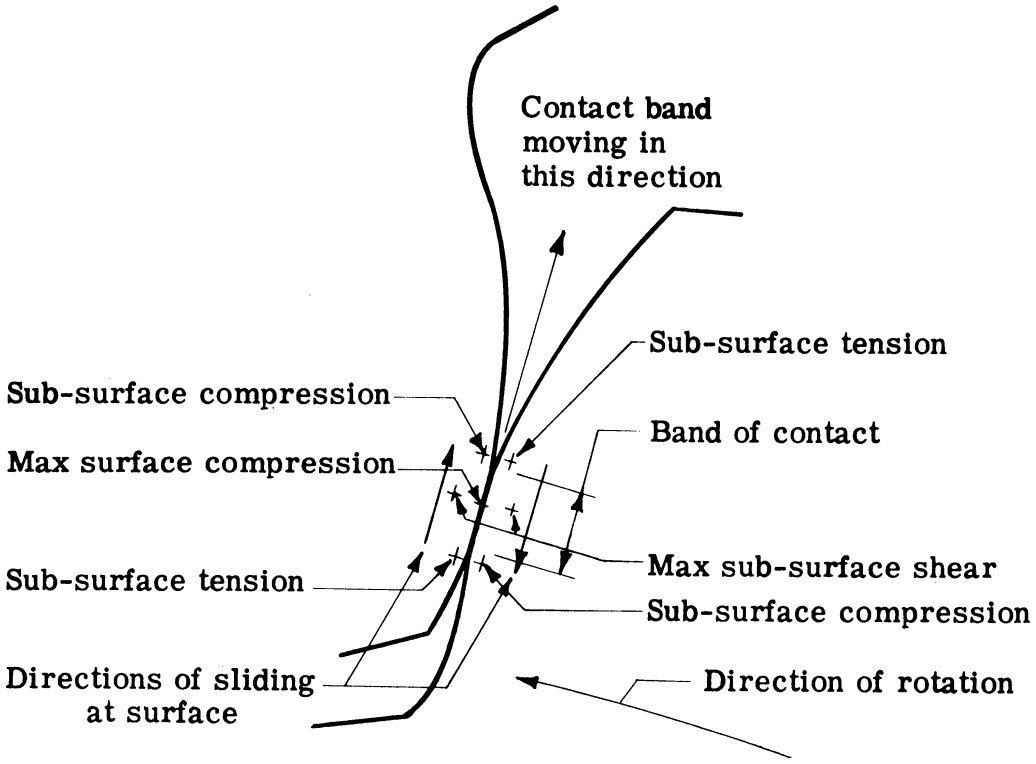

Figure 8. Stress in region of contact of mating gear teeth.(From Dudley).

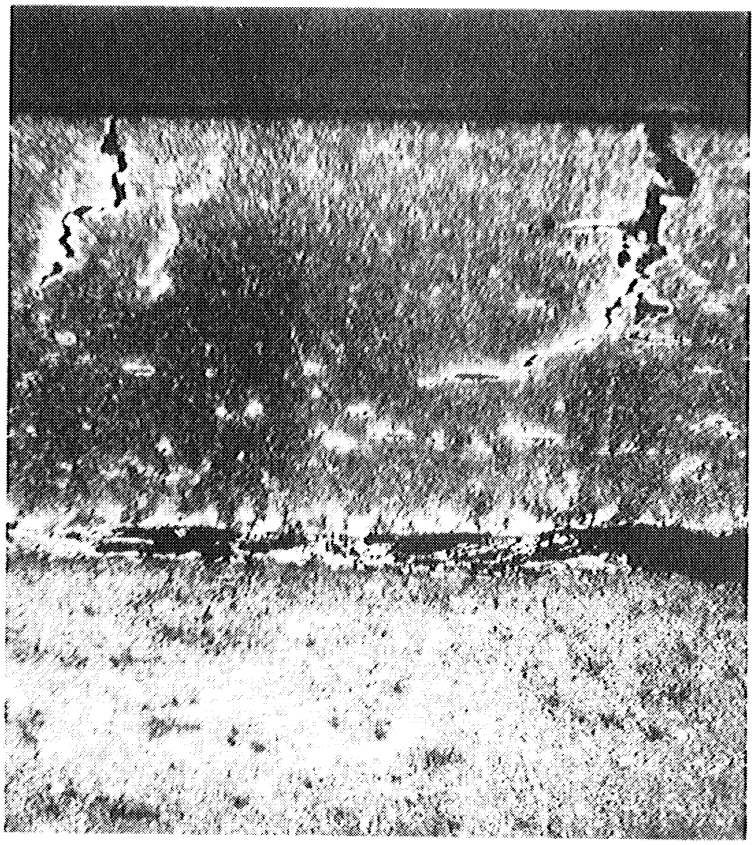

Figure 9. Horizontal crack and cracks normal to surface of carburized and hardened roll subjected to heavy rolling load, surface hardness Rockwell C 52-58.(Buckingham and Talbourdet). Magnified 100 diameters.

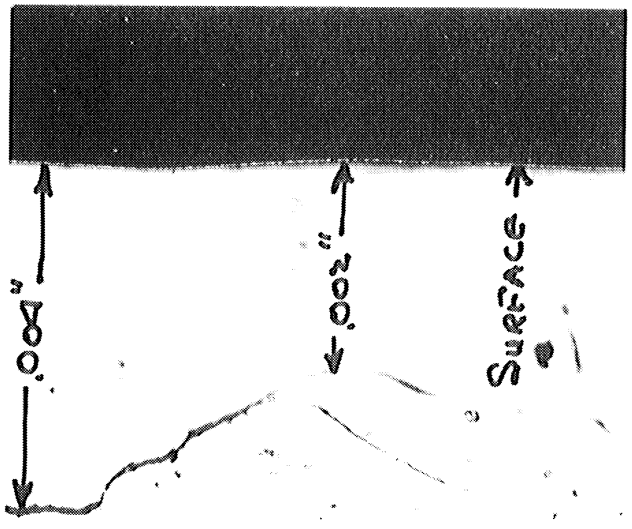

Figure 10. Sub-surface cracks in truck transmission gear adjacent to severe pits. Magnified 500 diameters.

Surface Cracks. Sometimes under the complicated reversals of stress along the surface, fatigue cracks develop normal to the surface. Two of these cracks may be seen in Figure 9, which are beginning to propagate parallel to the surface. It may be seen that under varying stress conditions this could lead to very slight or very deep pits. A mechanism for accelerated propagation of such cracks was advanced by Stewart Way (6), in which the lubricating oil forms a hydraulic wedge under the action of the rolling surfaces, and the surface crack is forced to grow. This theory assumes the presence of surface cracks sloping in the direction of rolling. Timoshenko (7) has expanded on this theory to describe the formation of V-shaped pits with the apex pointing opposite to the direction of rolling. Figure 11 and Figure 12 show the presence of such pits on both gear and pinion surfaces, pointing in the direction predicted by Timoshenko.

Surface Flow. In the case of soft gears, plastic flow of the surface material on case hardened gears of full hardness. Almen (8) and others have shown that plastic flow of the surface always occurs to some extent under load even though the effects are not obvious and the gear teeth are very hard. Figure 13 shows clear evidence of such flow at the surface of a carburized spiral bevel gear tooth hardened to Rockwell C 62.

Surface flow may influence pitting in opposite ways. Such deformation produces severe stresses which, in combination with the other stresses involved, may induce fatigue at varying depths below the surface. It has also been suggested (9) that this surface deformation may prevent pitting or stop its progress by developing an area of compressive residual stress just below the surface through which a fatigue crack starting normal to the surface cannot propagate.

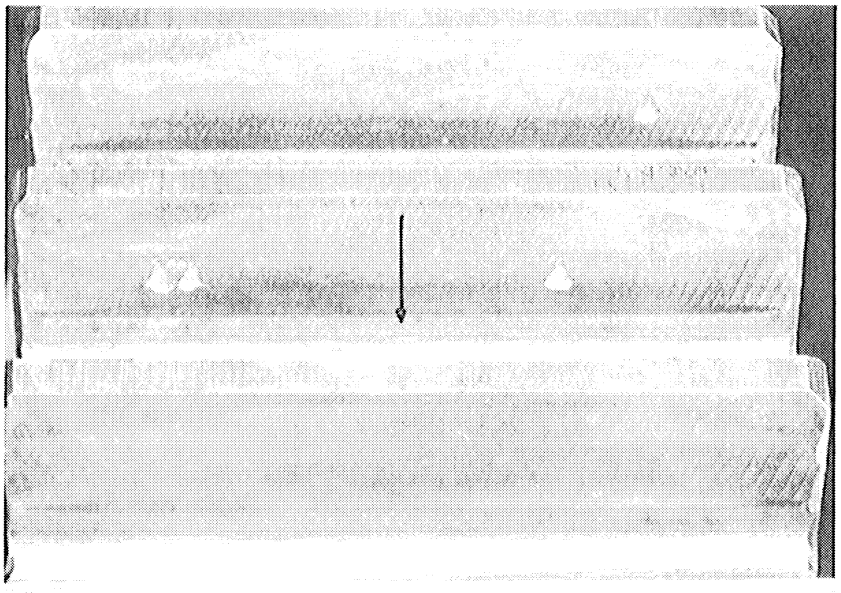

Figure 11. Heavy drive gear showing arrowhead pits pointing towards tip of gear (arrow indicated direction of rolling).

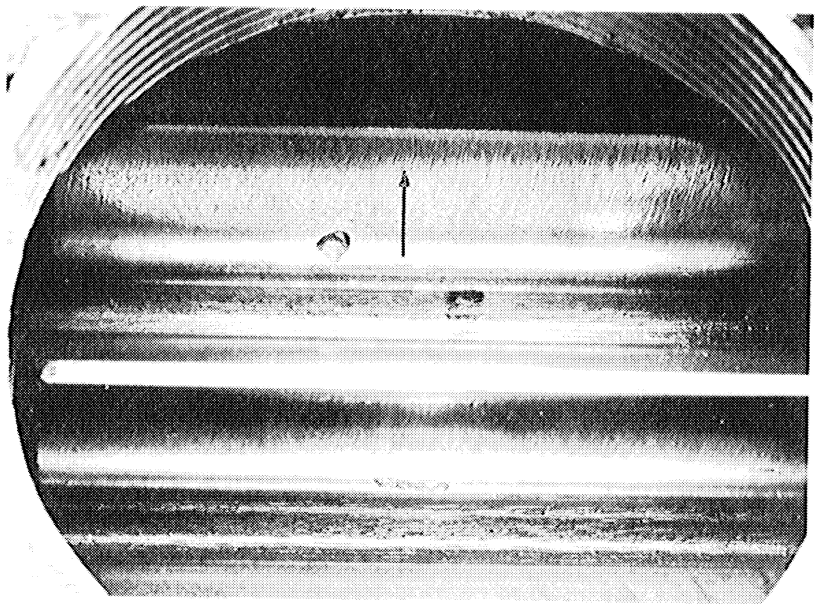

Figure 12. Heavy drive pinion seen through hole in housing showing arrowhead pit pointing to root (arrow indicated direction of rolling).

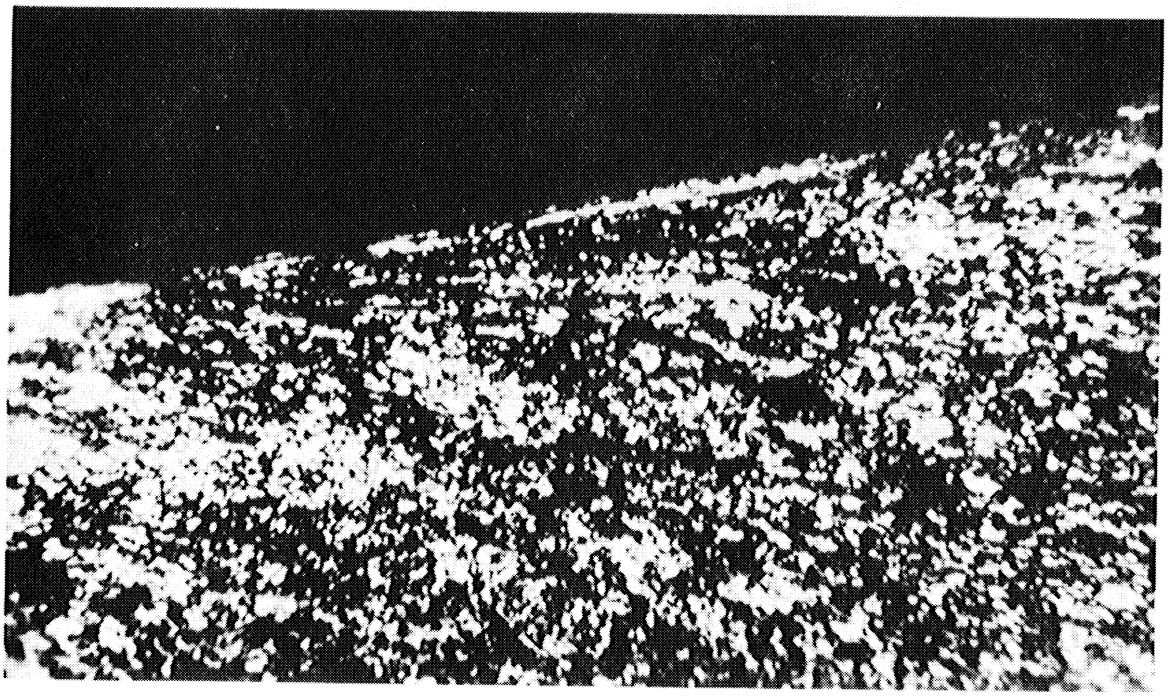

Figure 13. Surface of spiral bevel gear showing plastic flow in spite of hardness of Rockwell C 62.(Almen). Magnified 1500 diameters.

Gear Tooth Pitting. A typical example of pitting in automotive gearing is shown in Figure 14, a tractor sprocket drive pinion. Until recently this type of gear failure was not of major concern except in special instances. When pitting did occur it generally led to noise rather than breakdown. Over the last ten years, however, the power transmitted by gear trains in many applications has steadily increased, and steps have been taken to increase the resistance of gear teeth to bending failure. As a result gears are carrying more and more load, and Hertz stresses have steadily risen. Failures of the type shown in Figure 15 are becoming more of a problem. This fracture initiated from the stress concentration at the pitting slightly below the pitch line. Figure 16 shows a closer view of the fracture in which the progress of fatigue from the surface pit is obvious. Another example of the same type of failure is shown in Figure 17. Pitting may also progress to complete disintegration of the tooth surface, as shown in Figure 18.

Gear tooth pitting may usually be classified in one of two ways: progressive or "destructive" pitting, and initial or "Incipient" pitting.

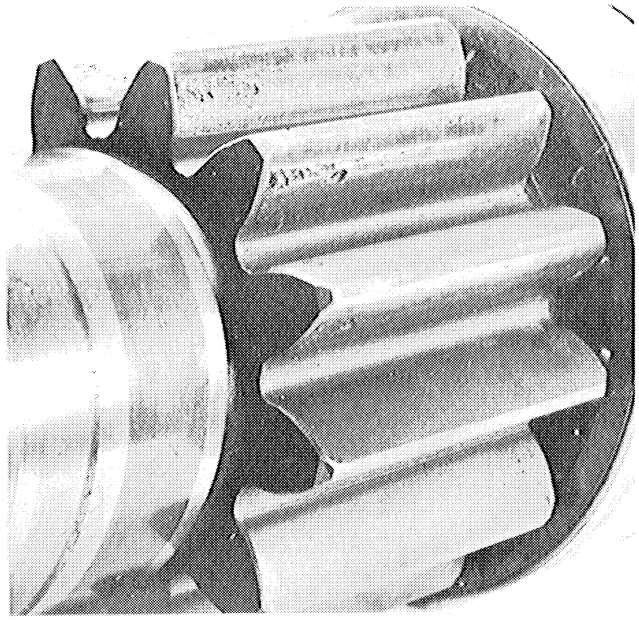

Figure 14. Tractor final drive pinion pitting failure.

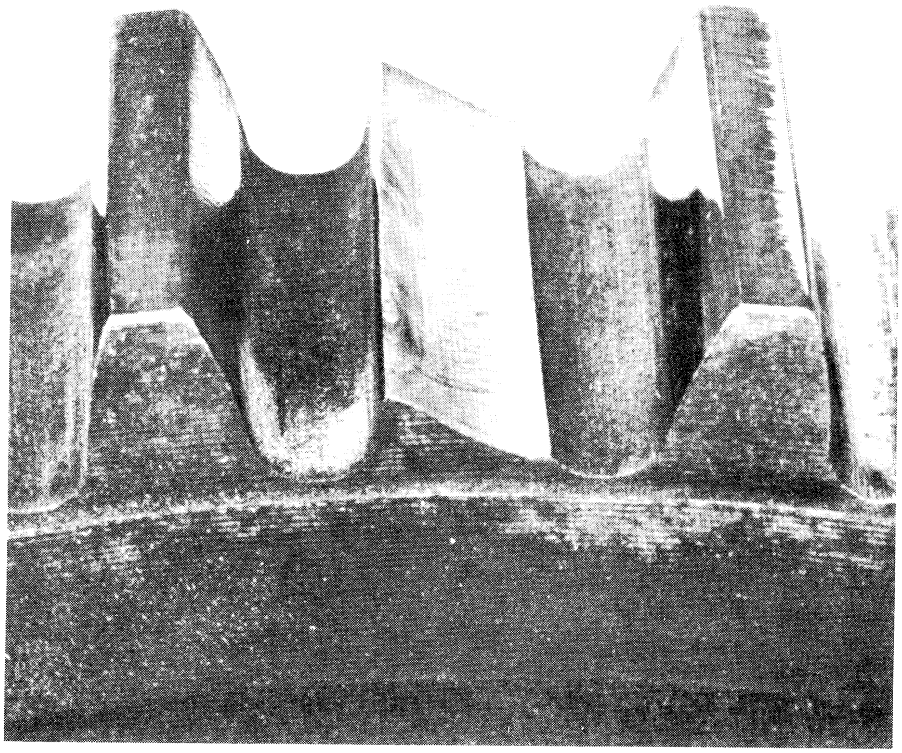

Figure 15. 6 Pitch transmission gear showing fatigue failure of tooth originating in pit at tooth surface.

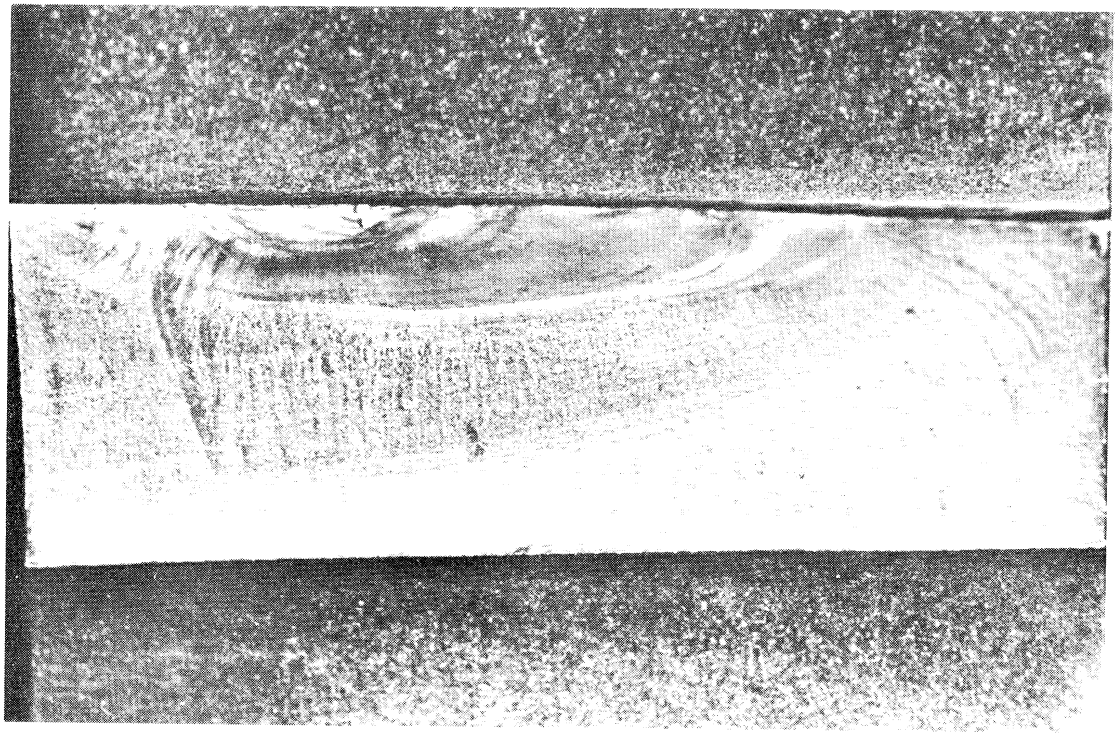

Figure 16. View of fracture surface in Figure 15. Magnified 6 diameters.

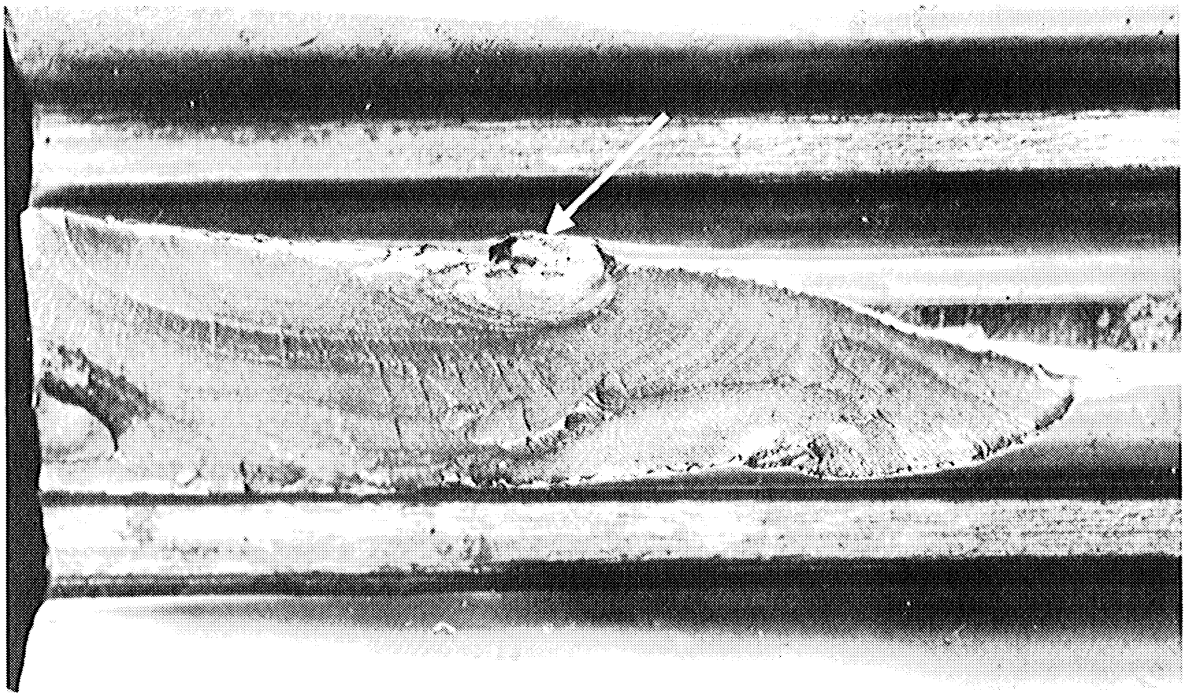

Figure 17. Fatigue fracture originating in pit at tooth surface.

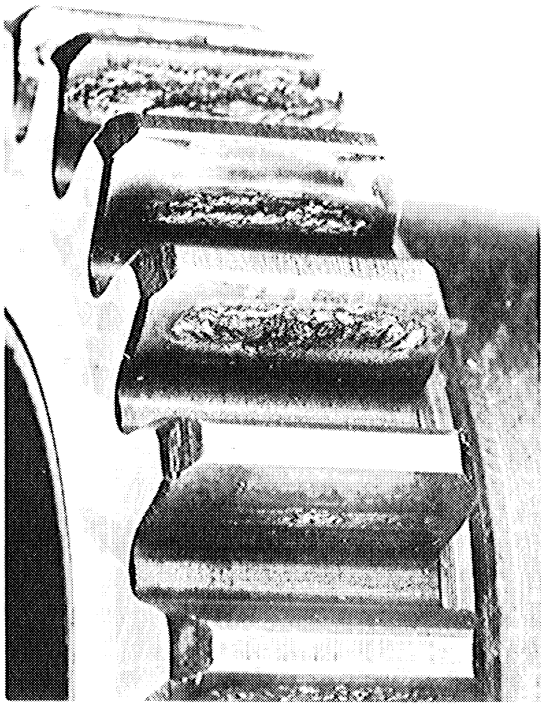

Figure 18. Transmission gear showing severe surface deterioration.

Incipient Pitting. This form of surface failure consists of very small pits which do not progress beyond the initial stage, and frequently "heal over" due to slight surface removal by normal wear. Such pitting is seen on the surface of a hypoid pinion in Figure 19. After a few more hours of wear this pitting will probably disappear. There is strong evidence that this type of pitting originates at the surface as described under "Surface Cracks". The failure to progress may be due to residual stresses slightly below the surface as discussed under "Surface Flow". Compressive stress or increased strength that could limit the progress of these cracks can also result from previous treatment of the gear.

Destructive Pitting. This failure may originate from either sub-surface or surface fatigue, depending on the circumstances involved. In either event the characteristic is continued development of more and deeper pits, which eventually lead to failure from fracture of the tooth or complete disintegration of the surface, if sufficient cycles are involved. Figure 20 shows a gear in which three subsequent teeth demonstrate severe pitting, heavy spalling and pitting, and complete tooth destruction. It is obviously destructive pitting with which we are concerned.

Overcoming Pitting Failure

In the effort to design and manufacture gear trains to carry greater loads, the ultimate limitation is pitting. Many factors are known which can protect gear teeth from bending fatigue failure, including gear design to reduce bending stresses, and material selection and processing techniques to increase fatigue resistance. Definite limitations exist, however, in our ability to design and make gear teeth to carry high surface loads. Within these limitations, there are many factors which can be controlled to prevent pitting, and these will now be discussed.

Accuracy of Gear Teeth. Gear teeth are very complicated geometrical designs, which, if perfectly formed and completely rigid, would transmit loads smoothly and efficiently. Neither of these conditions can exist. Gears are subject to dimensional variations in manufacture, and gear teeth and mounting mechanisms are subject to elastic deformation when loaded. The result is that power transmission through a pair of mating gears is actually a series of pulses, partly the result of transmitted load and partly the forces required to constantly accelerate or decelerate the mating gears in relation to each other to accommodate irregularities in conjugate action. The total load developed in this way is called dynamic load, and may be several times as great as that required for the transmission of power. In fact under certain circumstances the dynamic load may be sufficient to cause pitting or bending failure while little or no load is being transmitted.

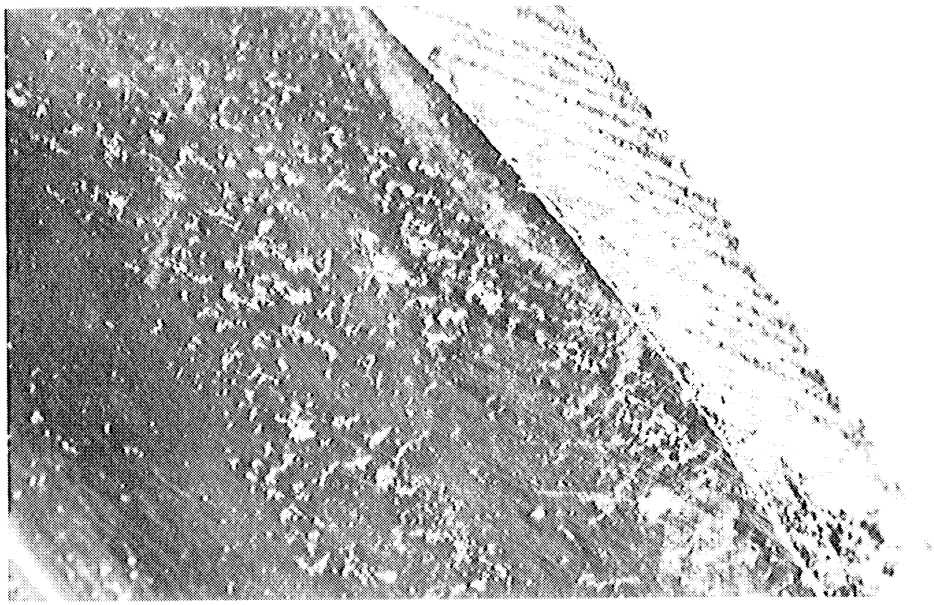

Figure 19. Hypoid pinion exhibiting incipient pitting, which will disappear with continued running.

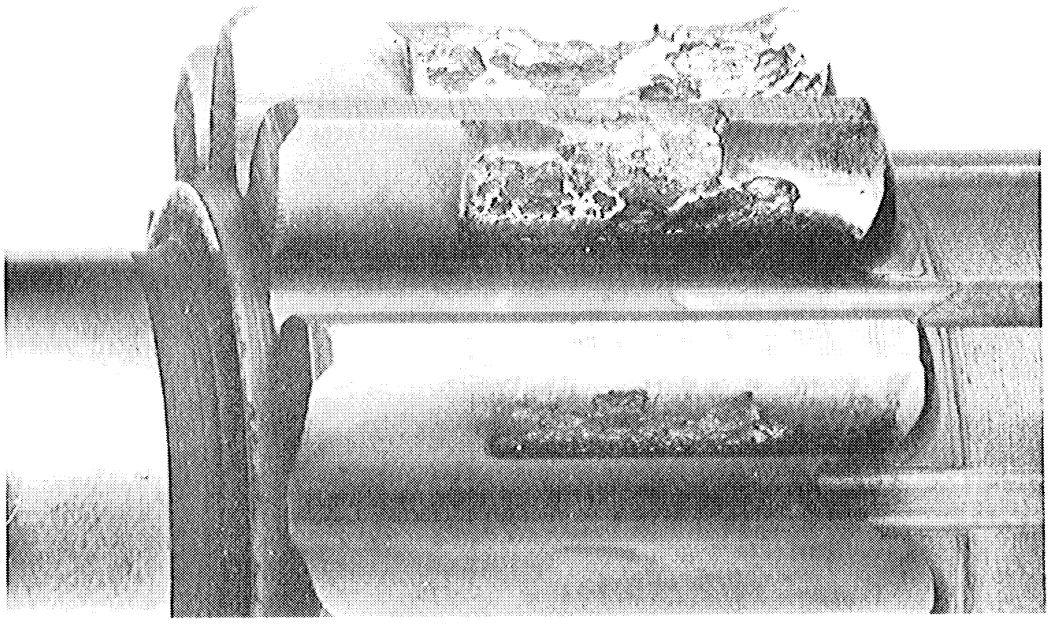

Figure 20. Drive pinion showing on successive teeth severe pitting, heavy spalling and pitting, and complete tooth destruction.

The following information compiled by Buckingham (2) on a typical six pitch gear pair with average manufacturing errors, under different transmitted loads at 2000 r.p.m. will illustrate this point:

Dynamic Load
(Pounds at Pitch Line)

Horsepower Transmitted	Due to Power Transmission	Due to Accelerating Forces	Total
100	1350	1228	2578
50	675	1087	1762
0	0	925	925

This data should adequately accent the importance of accurate gear manufacture to tolerances as close as the economic circumstances permit, often supplemented by intentional modification of gear tooth form to accomodate unavoidable elastic deformations.

Surface Finish. In somewhat the same general area but on a microscopic scale, surface roughness can contribute drastically to tooth surface loading. In mating of rough surfaces the compressive contact is carried by a small fraction of the normal area, and actual Hertz stresses increase drastically. Fortunately these irregularities usually wear off or plastically deform to give better contact before surface fatigue is initiated, but in this process involute accuracy may be lost.

Gear Design Changes. Any changes which reduce Hertz stresses, and in some cases changes that reduce sliding velocity, will help prevent pitting. Such changes must always be made by competent gear designers who are aware of the many factors involved.

Increase of pressure angle will reduce Hertz stress, if not carried too far, and is sometimes employed to overcome pitting. Bending strength of the teeth is also increased, but supporting beard loads are aggravated due to greater separating forces.

Decrease in circular pitch (more teeth) reduces contact stresses by more "overlap" -- more than one tooth in contact a greater percent of the time. In most gears this will not help pitch line pitting since only one tooth is in contact near this point.

One of the basic problems of involute geometry is the high contact stress and high sliding velocity as the base circle is approached. When pinions with few teeth are cut, initial contact with the gear occurs very close to the base circle, and pitting and other wear troubles are invited. A common remedy is the use of a long and short addedum system,

which basically means increasing the OD of the pinion and decreasing the OD of the gear while keeping the pitch circle the same. This moves the active involute farther from the base circle eliminating pinion undercutting, and increasing both tooth strength and pitting resistance of the pinion. If the gear becomes the driver, however, the reverse becomes true, therefore a long and short addendum system should not be used with reversing drives without careful consideration.

Profile Modifications. It has already been mentioned that elastic deflection of gear teeth may cause serious trouble under high loads. This deflection actually permits the gear to lag slightly behind the pinion so that as the next gear tooth approaches contact its edge tends to dig into the pinion tooth at its base instead of smoothly assuming its share of the load. This produces very severe stresses and may cause pitting. Another common result of tooth interference is uncontrolled wear at this point which gradually shifts the abnormally severe stresses along the line of contact to the point where only one tooth carries the load, where pitting then takes place.

Modification of the involute profile to compensate for this deflection (and at the same time, for unexpected manufacturing errors) is common practice in heavy duty gearing. This modification often takes the form shown in Figure 21 which is a representation of a typical involute profile chart of a gear tooth in which tip interference had been experienced. A straight line represents a perfect involute, and the heavy line in this example shows the use of proper profile over the dedendum* and part of the addendum, with a modification to relieve the outer portion of the profile. Such modification maybe used on the tip of the gear, the addendum of both gear and pinion, the addendum and dedendum of the pinion, or other combinations depending on the gear design, application, and experience. Tooth deflection is sometimes compensated for by slightly decreasing the pressure angle of the pinion, which actually amounts to relieving the involute surface in a gradual manner, the modification being zero at the tip and becoming maximum at the start of active profile (end of active profile towards the root).

The amount and kind of modification necessary to best achieve proper operation is found by trial and error. It must be remembered that since these steps are taken primarily to correct for elastic deformation, the correction must not be designed for a specific load condition, and proper compensation will not be obtained under other loads.

Crowing and Taper. Lack of parallelism of mating gear teeth due to mounting deflections or tooth errors causes the contact to localize near one end of the teeth and abnormally high contact stresses result. This is probably the greatest single cause of pitting, and also the most obvious. Figure 14 clearly shows end loading.

---

* The dedendum is that portion of active involute profile extending from the start of active profile to the pitch line, and the addendum extends from the pitch line to the tip.

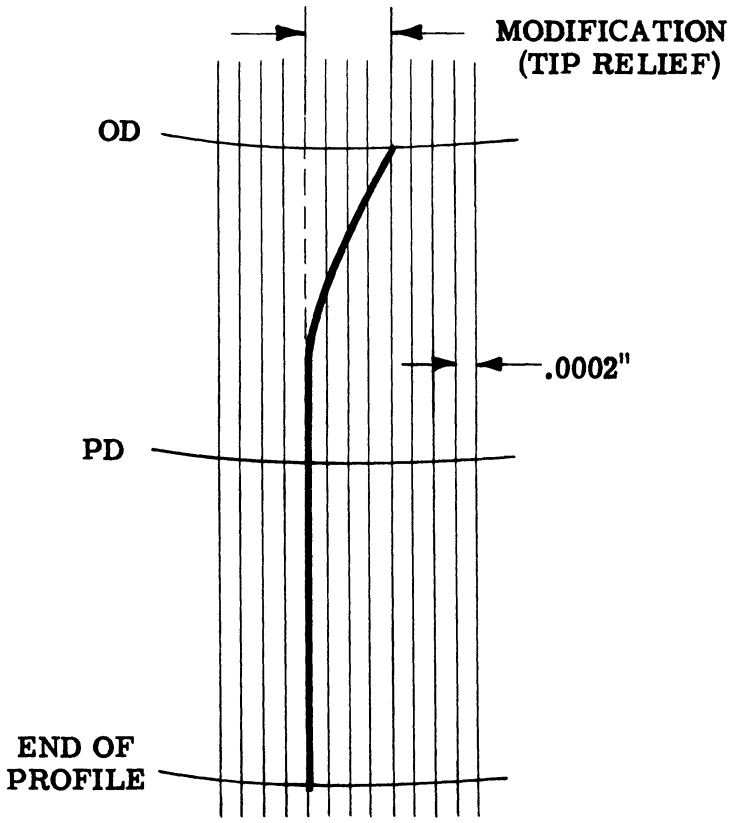

Figure 21. Typical modified involute profile to avoid tip interference.

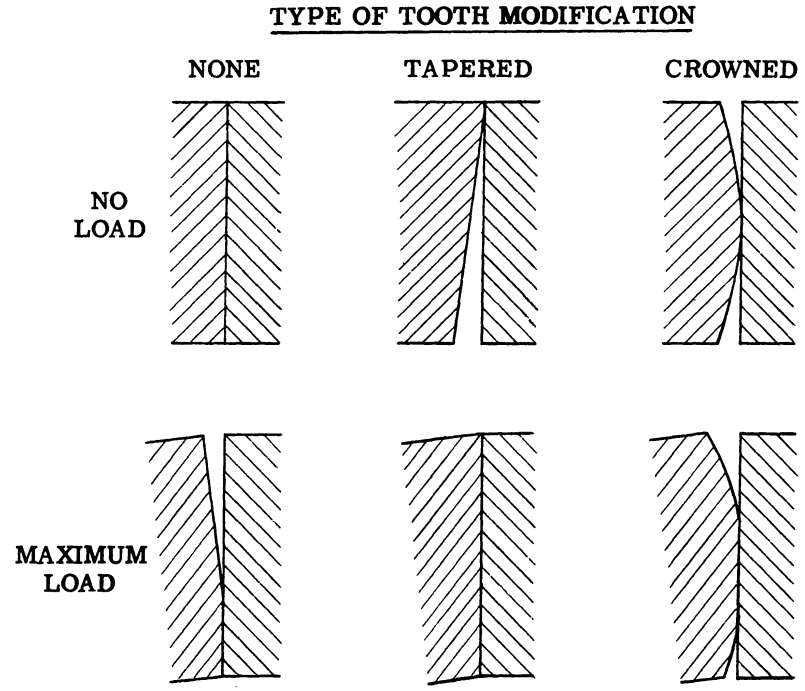

Figure 22. Illustration of effect of taper and crown modification to overcome end loading caused by misalignment.

When unpredictable variations in parallelism are encountered, crowning may be employed. In spur gears this consists in putting a very slight arc in an axial direction on the tooth faces, so that contact is kept away from the ends of the tooth. If misalignment occurs under load, the crowned tooth still maintains tangent contact with its mate, instead of end contact.

Figure 22 is a greatly exaggerated illustration of taper and crown modifications. The left hand pair show schematically unmodified tooth surfaces which, under load, are subject to axial misalignment with resulting narrow contact at one end of the teeth causing severe overloading. The middle figures represent a taper correction, which produces end contact at light loads but under full load adequately compensates for misalignment. The right hand figures represent crowning, in which the contact area moves in one direction or the other depending on the deflection and misalignment. Note that the width of contact of the crowned surface under load is much more than that of the unmodified surfaces. As in profile modification, great care must be taken to use only enough crown or taper, since improper use of either of these modifications can result in overload surfaces or tooth breakage.

Metallurgical Factors. The pitting resistance of the material in a pair of gear teeth increases, in general, with fatigue strength, but no simple relationship exists. Ductility may permit the removal of surface errors by plastic deformation, thus reducing Hertz stress concentration before pitting can begin. Choice of gear materials is also greatly influenced by bending strength problems, welding tendency, machinability, and other factors (10).

Many tests have been run with gears or with simulated gears (roll tests) comparing the surface fatigue resistance of various materials. While considerable variation exists between the calculated results in different test areas (particularly where the tests are on actual gears) these tests have yielded much valuable comparative information.

In general, increasing hardness increases resistance to pitting. At the same time increased strength reduces the tendency for an imperfect surface to adjust itself by wear or surface flow, and thus reduce localized contact pressures. This has given rise to the fairly common practice of requiring that the pinion, which makes more revolutions, be made as hard as possible, and the gear somewhat softer to allow for "run-in". Thus the choice of hardness is closely tied in with the loads that are to be transmitted and the accuracy and surface finish of the teeth.

The importance of hardness is illustrated by the teeth shown in Figure 23 from a seven pitch pinion which has been run 100 million cycles at a Hertz stress of 190,000 psi. This pinion was made from a 0.47% carbon steel and induction hardened to a pitch line surface hardness of about Rockwell C 56. Considerable pitting has occured, although the pitting has not changed materially from that which was present at 40 million cycles. The same pinion design made from a low alloy carburized and hardened to Rockwell C 62 carried 100 million cycles at

220,000 psi without pitting. A wealth of field service experience backs up the statement that the above difference is not due to the differences in alloy or carbon content of the surface, or the method of processing, but to the difference in surface hardness.

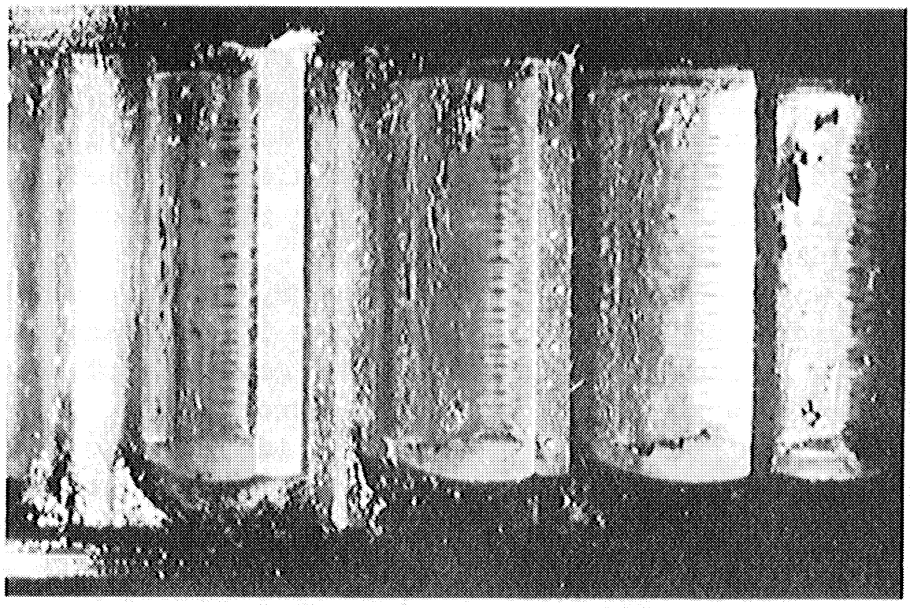

Figure 23. 7 Pitch pinion induction hardened and tempered to Rockwell C 56, run 100 million cycles at 190,000 psi Hertz stress.

With light case gears (0.030" effective case or less) pitting resistance may be affected by case depth. Buckingham (5) has pointed out that heavily loaded gear teeth should be carburized and hardened to an effective case depth at least twice the depth of maximum shear stress. Obviously the transition from case to core in the area of high stress will be more dangerous with very low core strength. The relationship of case depth and core strength of case hardened gear teeth is a very complex subject, however, it is of primary interest in relation to bending strength and deep spalling problems. For pitting resistance it is sufficient to say that where light case gears are experiencing pitting failure, increase of case depth or core hardness, or both, may provide a cure. (10) (11)

The influence of inclusions in the steel on pitting is well known in relation to roller and ball bearing surfaces. Very little work has been done on this factor in gear teeth. However, the nature of pitting failure is such that "dirty" steel would obviously promote failure under certain conditions.

Lubrication. The influence of lubrication on pitting is a controversial problem giving rise to conclusive proof of opposite statements by different authorities. This obviously arises from the fact that pitting may originate in several different ways and may proceed to tooth destruction under different influences. Where considerable sliding action is present, lubrication has been proven to have an influence on pitting. The proper choice of lubricant depends upon the surface finish of the gear teeth, the gear design, and loading.

Tests with a large number of truck transmission gears comparing pitting performance with a standard EP lubricant and a special lubricant, proved a definite difference in the load that could be carried without pitting. Apparently the better lubricant reduced the surface stresses resulting from sliding action.

Stewart Way in 1935 introduced his theory of hydrodynamic crack propagation mentioned earlier, stating that pitting cannot occur in the absence of a lubricant. Since heavy duty gears cannot be operated without lubrication we must put up with this problem.

Coatings. As pointed out earlier, pitting is often a race between wear or plastic flow which tend to reduce localized contact pressure on the one hand, and pitting fatigue damage on the other. Thus, any influence that will help avoid surface damage briefly until some adjustment can take place may relieve pitting. Phosphate coating and copper plating have both shown excellent results. However, care must be taken to avoid the damage of hydrogen embrittlement in any plating process. Fatigue tests have shown serious damage to bending fracture resistance accompanying copper plating of gear teeth.

Pitting Problems

So far we have discussed the major factors that should be reviewed in analyzing pitting problems or in designing gear trains to avoid pitting. A brief look at some typical examples will help to show the application of these factors.

"Bull" Gear and Pinion. Illustrated in Figure 24 is a gear pair that involves several of the facotrs discussed. This 4 pitch gear pair has experienced pitting on one end of the gear after 1150 hours of field use. It is immediately obvious that the load is not uniformly distributed since pitting has taken place only on one end of the gear teeth. The gear has pitted and the pinion has not, due to the difference in hardness (pinion, Rockwell C 62; gear, Rockwell C 52).

This end loading is caused by mounting deflections for which a taper of about 0.016" in tooth thickness had been provided in the pinion. Obviously a slight increase in taper is called for, or an increase in the rigidity of the mounting structure.

The hardness of the gear could be increased to improve the surface fatigue strength. This increase should only be sufficient to prevent pitting, and still allow as much local deformation as possible to relieve localized stresses from tool marks and minor mismating of involute profiles. Gear hardness can safely be somewhat lower than pinion hardness since fewer cycles are run by the gear.

Actually, the hardness of the gear was increased to Rockwell C 57 by induction hardening, and pitting was effectively controlled. Excessive taper in a long addendum pinion can result in a very thin tooth tip, so no further taper modification was made.

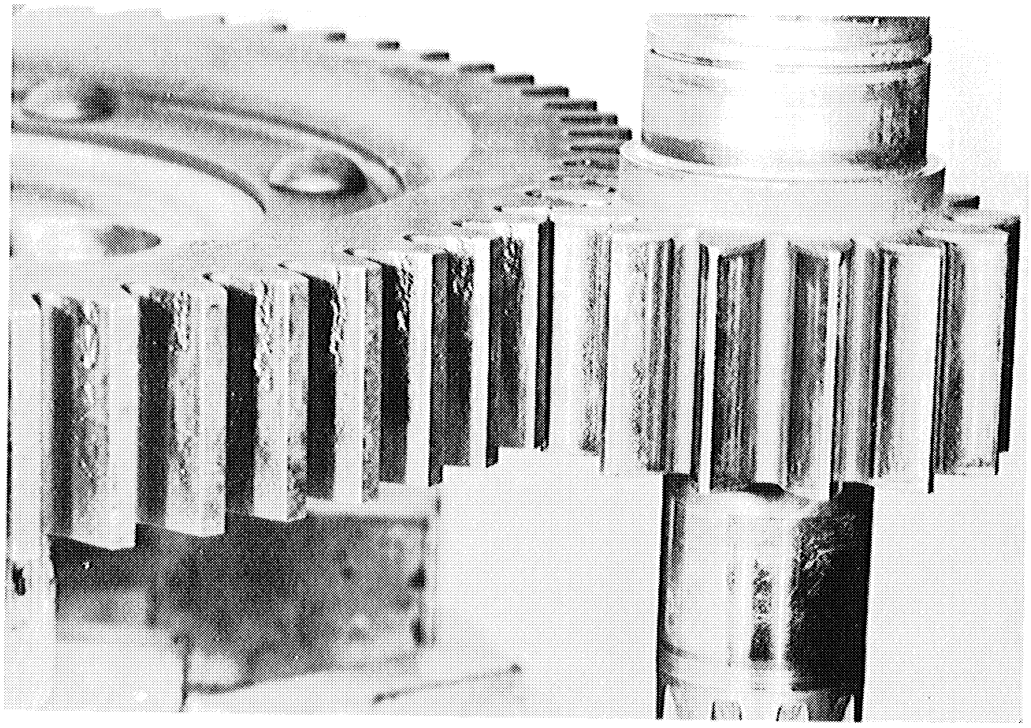

Figure 24. Farm tractor bull gear and pinion showing end contact and pitting. Pinion carburized and hardened to Rockwell C 62. Gear furnace hardened and drawn to Rockwell C 52. 1150 hours of heavy field use. 4 Pitch, long and short addendum system.

Sprocket Drive Pinion. This is a 2-1/2 pitch spur pinion which carries a very heavy load and has an interesting history of development, much of which illustrates the principles discussed in this paper. The pinion is pictured in Figure 14. Both pinion and gear are medium carbon steel, heat treated by induction. The pinion was 8645 and the gear a modified C-1045.

Preliminary development started with a pinion hardness about Rockwell C 55-57. Continued efforts to improve pitting and breakage resistance of this pinion included tapering and crowning to relieve end loading; a change in material and hardness technique to reduce residual stress and increase hardness (Rockwell C 58-60); shot peening; and a slight reduction in mating gear hardness (to Rockwell C 53-54). Pressure angle was changed from 22 degrees to 25 degrees. Changes also involved improving mounting structurerigidity, which permitted a reduction in the amount of taper and crown.

Test work was carried out in a typical "four-square" opposed transmission unit pictured in Figure 25.

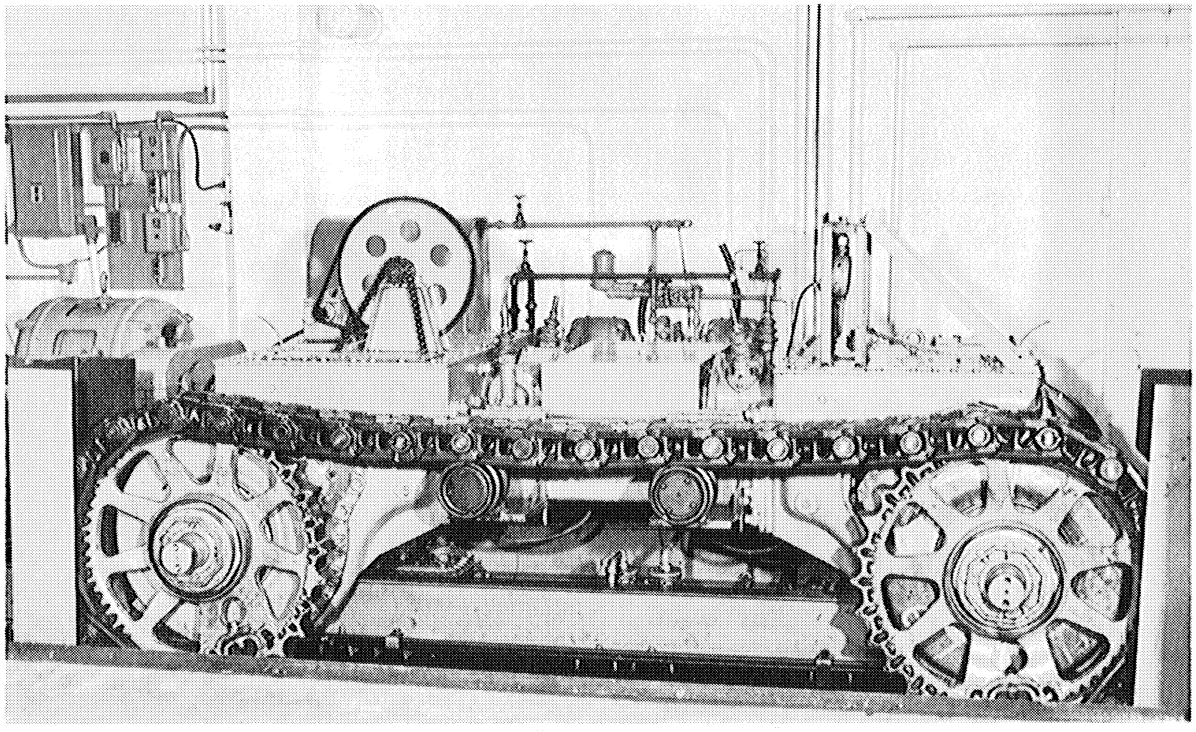

Figure 25. Four-square test machine for endurance testing of heavy duty gearing. This machine provides internal loading of two drives against each other, permitting loads in excess of twice the maximum field load.

One type of failure is shown in Figure 26 in which fatigue fracture of a tooth has originated in severe pitting of the tooth face.

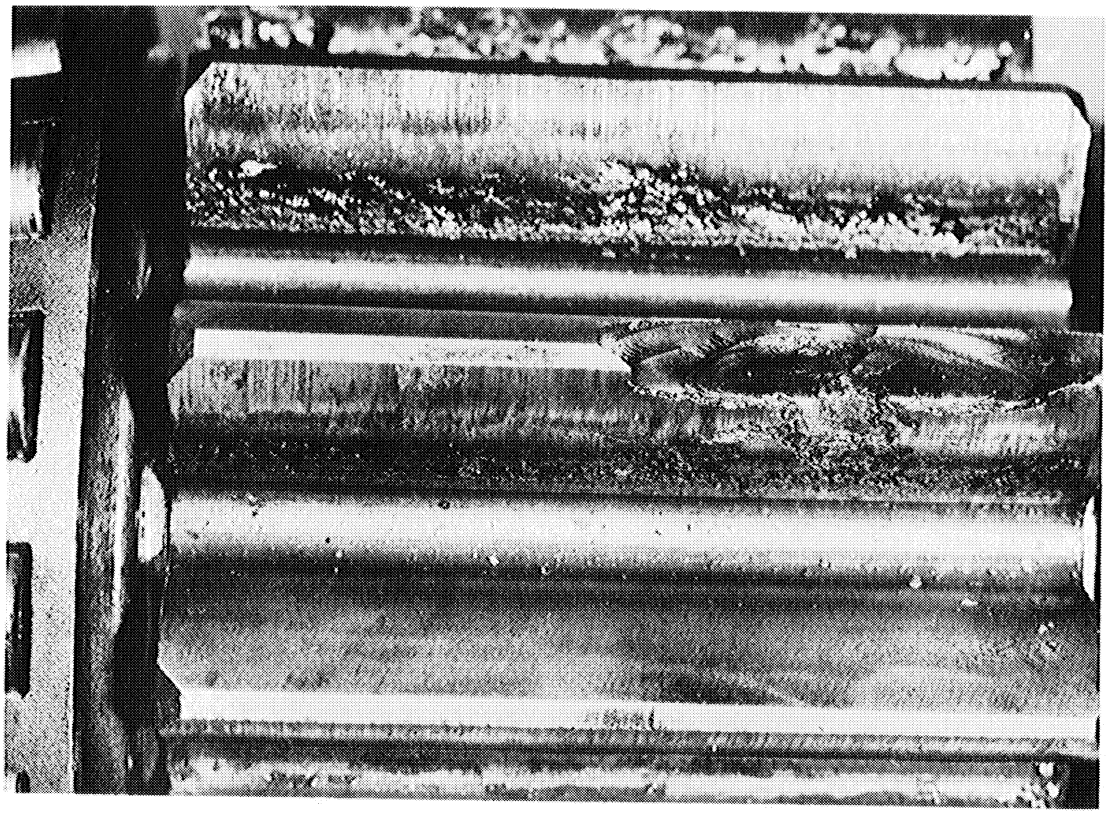

Figure 26. Sprocket drive pinion showing fatigue fracture originating from severe pitting.

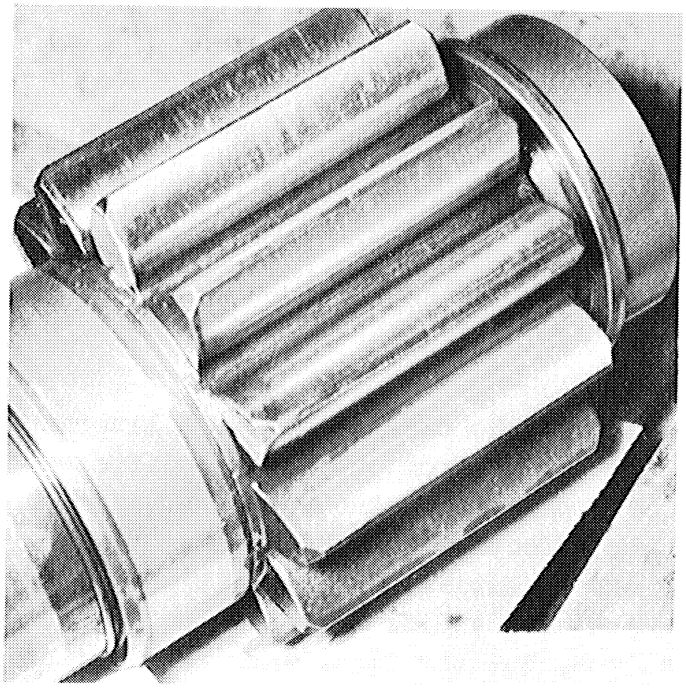

Figure 27. Sprocket drive pinion showing excellent condition after testing.

Typical of the results of the changes that were made is the pinion shown in Figure 27 which was subject to 800 hours of heavy testing compared with the pinion in Figure 14 which had been tested for 311 hours at comparable load.

Hypoid Pinion. The pinion illustrated in Figure 28 is typical of pitting problems on hypoid pinions. This pinion is made of alloy carburizing steel, carburized and marquenced to a surface hardness of Rockwell C 60. Pitting has occured at the heel contact. This type of gear must be cut with abnormal tooth contour to allow for changes during heat treatment. Investigation showed that compensation in cutting did not match the actual change that took place, with the result that heavy contact occurred at the location of pits.

Figure 28. Pitting of hypoid pinion.

Conclusion

It is obvious that the conflicts in the literature as to the theory of pitting failure arise from the several different mechanisms by which failure can take place. Fortunately the various controls outlined are all reasonably effective and a knowledge of the particular mechanism involved is not essential to a cure.

Simulated tests have yielded much valuable information on the subject of surface fatigue, but the final answer to suitability of a gear set must be obtained from actual service.

REFERENCES

1. American Gear Manufacturers Association, "Standard Nomenclature - Gear Tooth Wear and Failure," A.G.M.A., Pub. 110.02, December, 1951.

2. Buckingham, Earle, "Operational Stresses in Automotive Gears," SAE Quarterly Transactions, Vol. 5, pp. 43-55, January, 1951.

3. Burwell, John T. Jr., "Survey of Possible Wear Mechanisms," Wear Vol. 1, No. 2, pp. 137-139, October, 1957.

4. Dudley, Darle W., Practical Gear Design, McGraw-Hill, 1954.

5. Buckingham, Earle and Talbourdet, G. J., "Recent Roll Tests on Endurance Limits of Materials," Mechanical Wear (Symposium), ASM, 1950.

6. Way, Stewart, "Pitting Due to Rolling Contact," Transactions, American Society of Mechanical Engineers, Vol. 57, June, 1935.

7. Timoshenko, S., "Strength of Materials," Part II, pp. 505-509, Von Nostrand, 1956.

8. Almen, J. O., "Surface Deterioration of Gear Teeth," Mechanical Wear (Symposium), ASM, 1950.

9. Almen, J. O., "Fatigue Failures Are Tensile Failure," Product Engineering, March, 1951.

10. Buckingham, Earle, "Analytical Mechanics of Gears," pp. 508-526, McGraw-Hill, 1949.

11. Powell, Bever, and Floe, "Surface Fatigue of Carbo-Nitrided Steel," Metal Progress, March, 1958.

THE IMPORTANCE OF SURFACE TEMPERATURE TO SURFACE DAMAGE

B. W. Kelly
Staff Research Engineer
Caterpillar Tractor Company

THE IMPORTANCE OF SURFACE TEMPERATURE TO SURFACE DAMAGE

by

B. W. Kelly

INTRODUCTION

One of the most difficult forms of failure of machine parts to examine and understand is that of surface damage, for it is a function of so many forms of activity that occur on, in and under the surface proper. One cannot within the scope of any reasonable length paper, deal with more than one of these variables, and in this consider only a few forms of failure. The subject chosen for this discussion is the variable of surface temperature, that which is primarily caused by friction heating.

This will be a qualitative analysis. Although a thorough study of the subject requires a fair amount of theoretical background, it is felt that the thermal characteristics that are created during friction heating are not well understood by the engineer and that a qualitative feeling for at least the principles involved can be useful and develop a respect for the importance of this subject to the damage of surfaces.

The report will deal principally with two forms of failure -- scoring and pitting. The application will be primarily to very hard surfaces, such as those that are found on gears, anti-friction bearings, camshafts, etc.

PRINCIPLES

For this discussion, several assumptions are made. The first is that perfect thermal contact occurs between the two parts that are involved. There are no serious errors in this assumption, providing the thickness of the oil film between the two mating parts is not great enough to allow a significant temperature differential or that the quantity of lubricant will not materially remove heat directly from the contact area. Perfect thermal contact means, therefore, the temperature on one of the inner faces can be assumed to be the same as the temperature on its mating surface, and the total primary dissipation of heat is into the two elements in contact and not through the lubricant in the contact area. The second assumption that should be made here is that the bulk temperature of the two parts in contact is stable. In other words, the

amount of heat being removed by external dissipation is equal to the heat input due to friction. Here again, the assumption is valid in many practical applications for machine elements. A third assumption is that the velocity of the surfaces is sufficiently high so that the temperature that occurs in contact will not significantly precede the area of contact. This velocity is not actually very high; and even though on an existing part it is somewhat less than required, the error is still small.

These principles have been set forth by Professor H. Blok in 1937,[1] and later in an excellent discussion of the dissipation of frictional heating.[2] It would be pointless to discuss them further here, but for those who are more interested in the subject, the articles mentioned should be required background reading.

The assumptions that have been made can be readily fulfilled in the case of cylinders, such as those shown in Figure 1, pressing together with a rectangular shape contact area and having rotation velocities V_1 and V_2. The band of contact of width b, constitutes the shape of the heat source. The heat intensity which is proportional to the friction at each point in the contact pressure set forth in the elastic analysis by Hertz.[3] Actually Blok's approximate solution, which will be used here, assumes a parabolic distribution for mathematical simplification, but this produces an insignificant error. The distribution of temperature at the surface shown in Figure 2 is of interest and importance. A lag in the maximum temperature point occurs in this case about midway between the center of contact and the trailing edge. The reader will later see that this trailing characteristic is important in the consideration of thermal stresses.

SCORING

Scoring of surfaces is gradually becoming more recognized as a direct function of surface temperature.

In the case of unlubricated surfaces this temperature is generally considered to be the softening or melting point of the materials. In the case of solid lubricant films, it is directly related to the softening point of these films.[4] More recently it has been found that surface temperatures far lower than melting points of the materials in the surfaces bring about the onset of scoring of liquid lubricated surfaces.[5] It is, as a result, becoming more recognized that non-reactive (no extreme pressure additives) mineral oils and very likely most other commercial oils and synthetics[6,7] have a critical temperature beyond which they are no longer capable of satisfactory lubrication. Many speculations on the exact mechanism over which the temperature has control have been made. The most promising of these hypotheses perhaps is one concerning the failure of the adsorption characteristics of the oil,

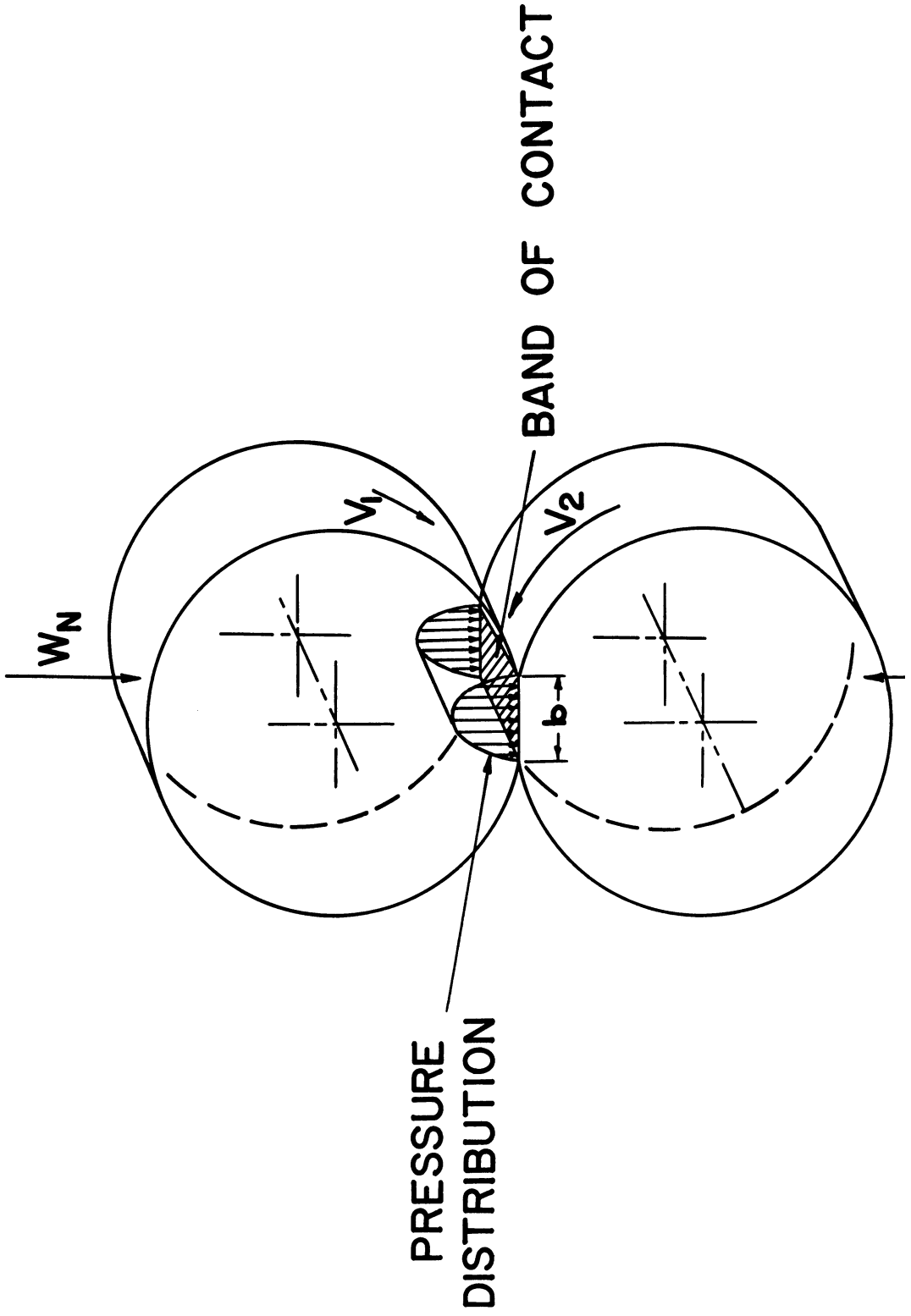

Figure 1. Contact conditions.

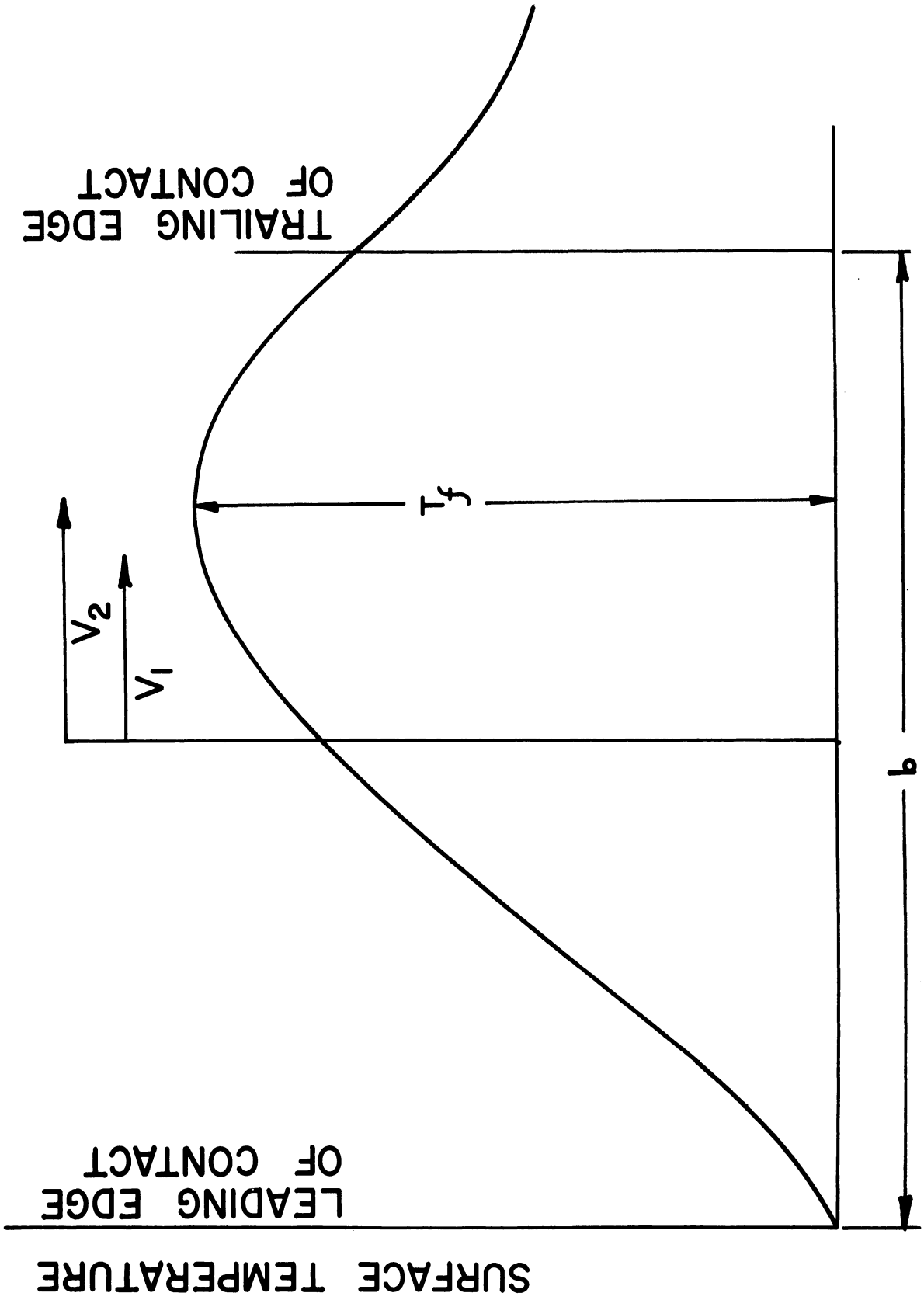

Figure 2. Shape of surface temperature rise in band of contact.

called desorption. Roughly this may be looked upon as the failure to "wet" the surface.

Scoring takes on different appearances, which are principally functions of the characteristics of the material, its surface characteristics and the lubricant. The carburized and hardened surface scored in a non-surface reactive mineral oil is badly torn and appears "roped" as in Figure 3. The same material scored in an extreme pressure (EP) lubricant appears softer with more material flow. Very likely, the lack of tearing which occurs with EP oil is associated with the protective contamination of the surface by the additives and the higher surface temperature required to produce the failure. This same appearance, although to a lesser extent, will frequently be seen to occur on a surface which has been treated, such as one which has been Parko-Lubrited.

With regards to the maximum mean temperature due to frictional heating, T_f, Figure 2, that is produced, a qualitative examination of the formula derived by Blok will be revealing. The formula is shown below:

$$T_f = K \frac{f \; W_n \; (V_1 - V_2)}{(C_1 \sqrt{V_1} + C_2 \sqrt{V_2}) \sqrt{\frac{b}{2}}}$$

K	=	Constant (1)
f	=	Coefficient of friction
W_n	=	Normal load per unit length
V_1 and V_2	=	Surface velocities
C_1 and C_2	=	Constants of material which include thermal conductivities, specific heats and densities
b	=	Width of band of contact
T_f	=	Maximum mean surface temperature (sometimes called "flash temperature".)

It is important to notice the velocity relationship that is obvious in the formula. From any given condition, if V_1 and V_2 are increased but the difference remains the same, then the resulting temperature, which is frequently called temperature flash, is reduced. This fact has been often overlooked in previous scoring criteria, such as PV and PVT, which are proportional to the heat intensity but not the surface temperature.

It will be found that if V represents the sliding velocity or the difference between V_1 and V_2, then the scoring resistance will vary as $\sqrt{V}$. This velocity relation has been used, for instance, by T. B. Lane(8) to further verify the temperature criteria for scoring on gears.

Another interesting relation is found between maximum Hertz pressure, P_o, see Figure 1, and temperature. It can be shown for instance that the maximum surface temperature varies as $P_o^{3/2}$ instead

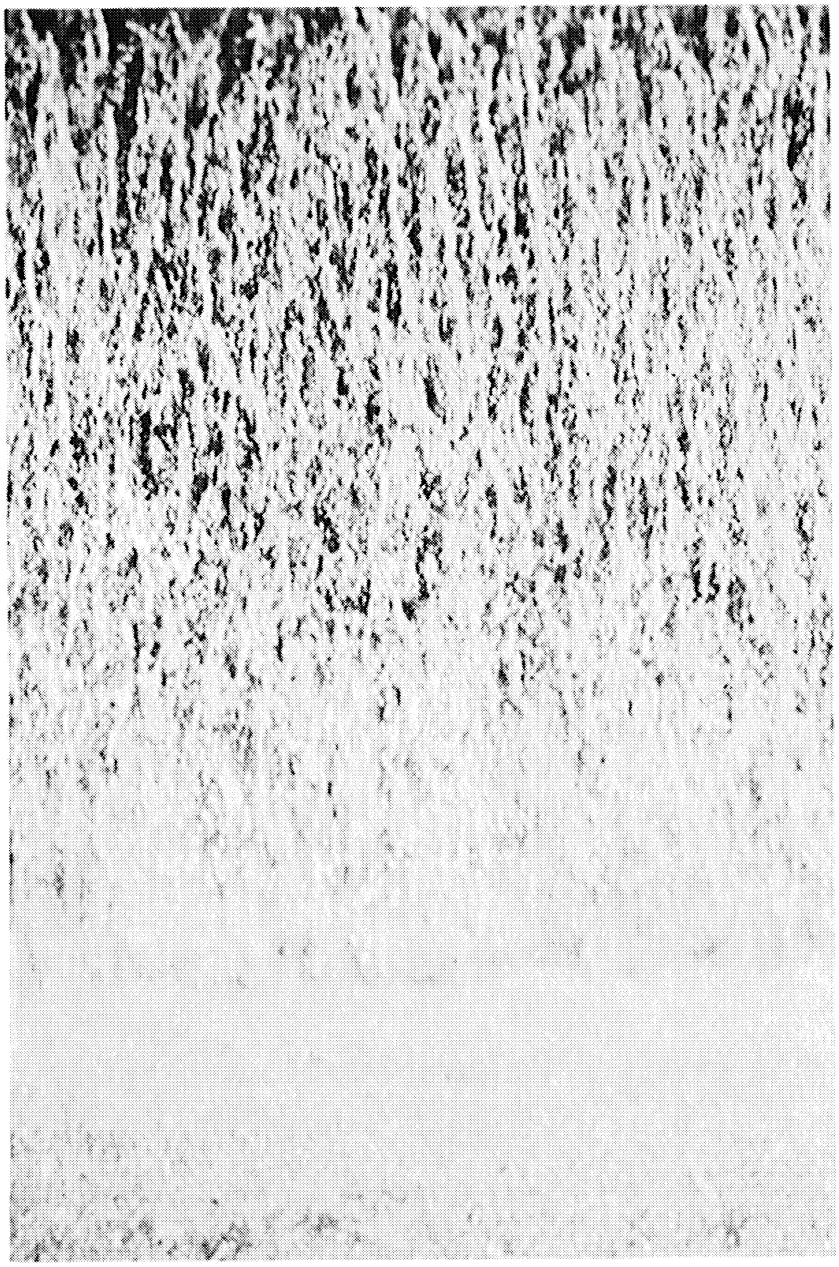

Figure 3. Scoring of carburized and hardened gears in straight mineral oil.

of directly proportional to P_o for a fixed values of V and geometry such as the roller radii. Increases in radii of curvature will, however, affect the surface temperature much less than might be expected and as in the case of gears where the use of larger radii of curvature such as in the adoption of higher pressure angles, will frequently be accompanied by higher values of V which can easily create no improvement in surface temperature and scoring resistance at all.

In a previous publication on gear tooth scoring,(9) the author showed the distribution of the load and speeds on gear teeth, and a formula was presented based on the temperature flash formula but which included an empirical factor of surface roughness. An assumption was made that the coefficient of friction was a constant for all of the tests. It was recognized at the time that it introduced elements which were foreign to the fundamental nature of the formula.

Since this work, investigations into the coefficient of friction as influenced by velocity have allowed us to use the formula below with improved success. Allowing for the similarity of material and simplifying, the formula can be written as:

$$T_T = T_B + K \frac{f\ W_n\ (\sqrt{V_1} - \sqrt{V_2})}{\left(1 - \frac{S}{50}\right)\sqrt{b/2}}$$

T_T = Total surface temperature
T_B = Bulk stable temperature of the part
S = Surface finish r.m.s. micro inches

It is apparent that we have not yet been able to remove the empirical value of S for surface finish. The work on the coefficient of friction is not complete, and it may be found that the surface finish will affect this value strongly.

As might be anticipated the coefficient of friction is reduced as the velocities increase; thereby giving more advantage to the higher speed gears than would have been predicted by the previous formula, which assumed friction was constant.

The reader will find additional verification to the critical temperature criteria throughout the literature.(10)(8) It is important to note that the proponents of this hypothesis are increasing as time goes on.

Pitting and Thermal Stresses

A second serious form of failure on surfaces is pitting. The literature is full of descriptions of this fatigue phenomena, and a considerable number of opinions have been expressed in lectures and over conference tables as to whether pitting originates as a surface or

subsurface failure. Blanket statements, of course, cannot be made since each form is a result of the stress system, the material strength, the residual stresses, lubricant characteristics, etc. and surface temperatures which produce thermal stresses.

Although it is beyond the scope of this paper to discuss in detail various forms of pitting failure, it is advisable that a brief description of some types be given so that the thermal stress problem be associated with one form in a clear fashion.

A typical example on gears, for instance, is the pitting that occurs on machinable hardness members such as Figure 4. The pits are generally not very deep and have a characteristic "scooped-out" appearance as if a small radius peen had been driven into the surface. Such pits, in the opinion of the author, are principally due to the maximum subsurface shear stresses[11, 12, 13] as illustrated in Figure 5. A similar form of pitting occurs frequently on through-hardened parts, particularly those such as anti-friction bearings on which the frictional tangential forces are low.[14]

Another form of subsurface initiation of a surface failure often mistaken for pitting is "case crushing". The initial stage of the failure appears simply as surface cracks seen in Figure 6. Within a very short time, often only a few cycles of load application, the surface appears as in Figure 7. The failure originates in the junction between the case and core as shown in Figure 8 and is due primarily to the deeper shears below the maximum as shown in Figure 9. Such failures are normally caused by too thin a case such as on the nitrided gear tooth in Figure 10 or too soft a core on carburized and hardened parts.

The form of pitting least explainable but most common is that which originates at the surface of very hard members. The appearance of such pits is shown in Figure 11 with the characteristic spalling in a fan shape pattern from the pits at the apex of the fan. Careful observation of the initiation and development of such pits in laboratory test machines show that they do start from the surface as shown in the cross section and metallographic photograph, Figures 12 and 13. It is the author's view that these too are a direct result from the stress conditions in the contact area even though increased attention is being given to physico-chemical effects of lubricants. Nevertheless, more recent examinations in the field of stress and stress distribution in and below the surface can be combined with what we will consider thermal effects.

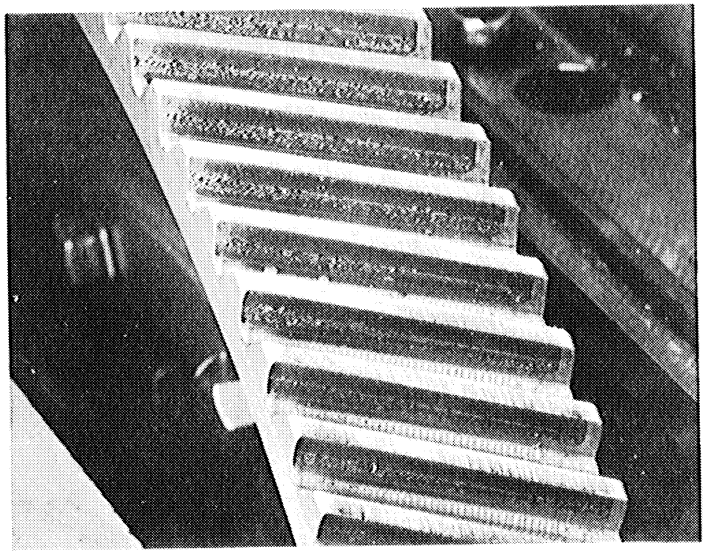

Figure 4. Pitting of machinable hardness gear.

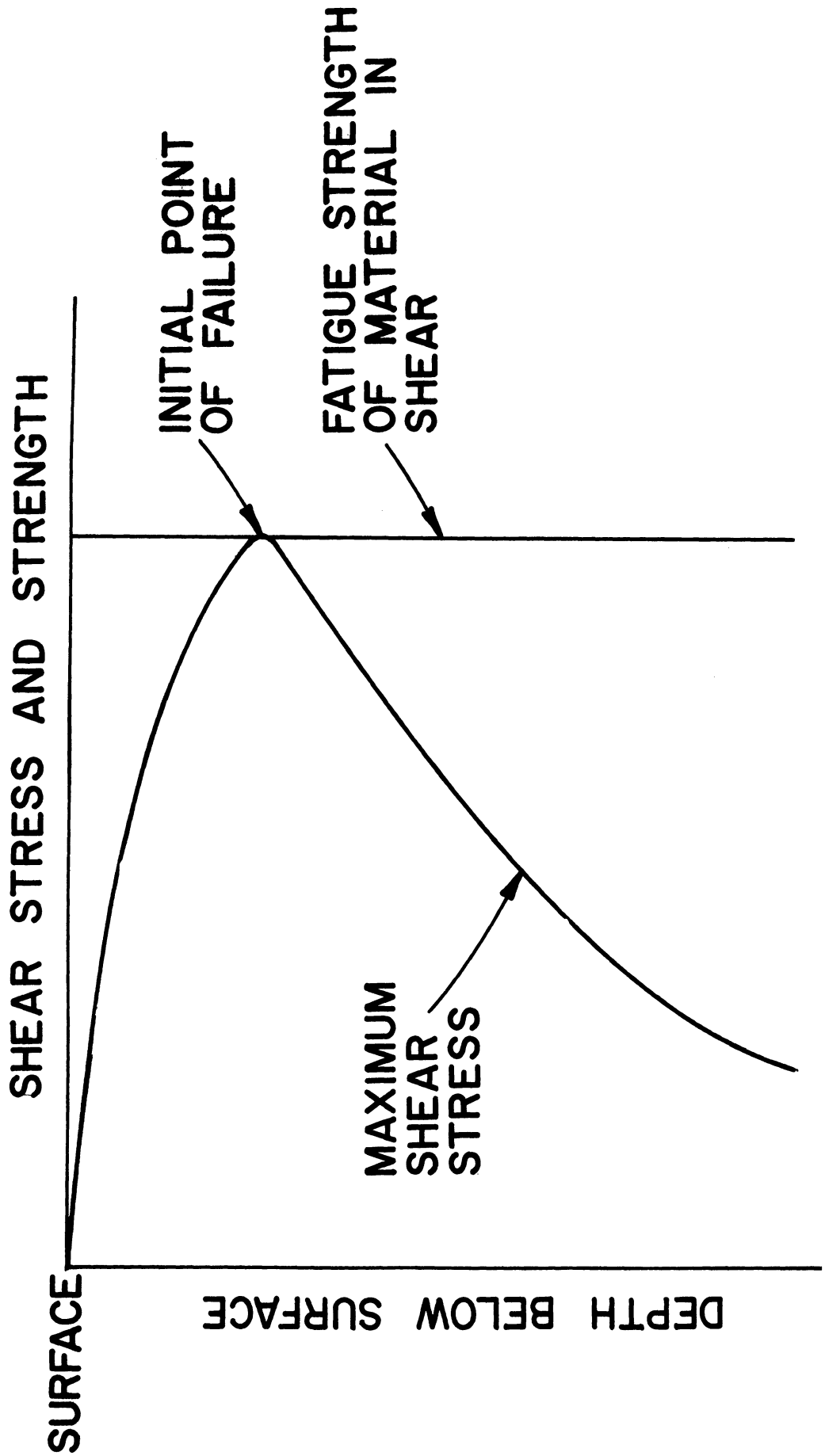

Figure 5. Failure conditions for pitting failure of mild steel.

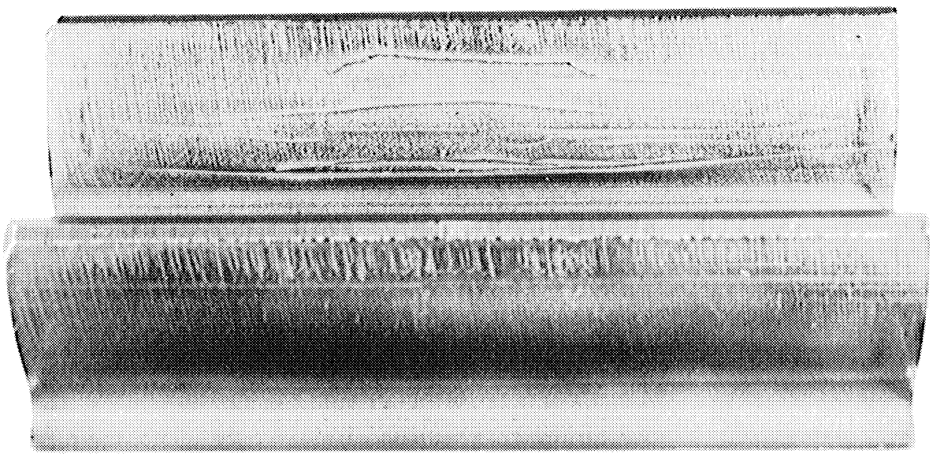

Figure 6. Initial appearance of case crushing on carburized and hardened gear.

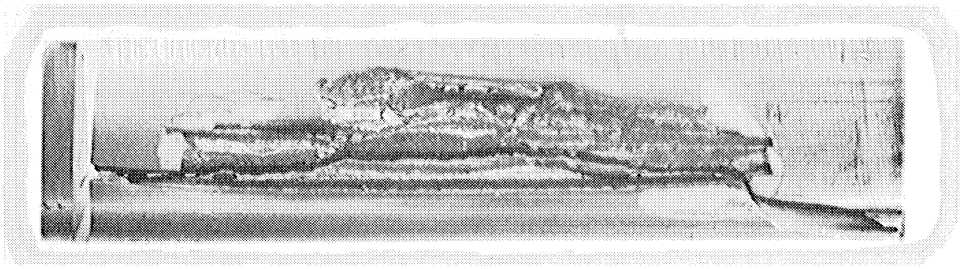

Figure 7. Final stage of case crushing.

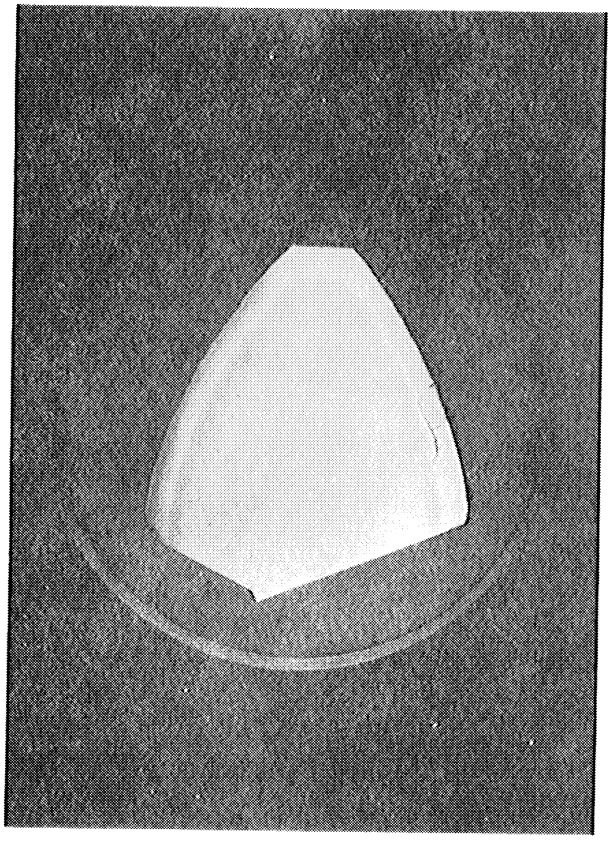

Figure 8. Initial cracks at junction of case and core.

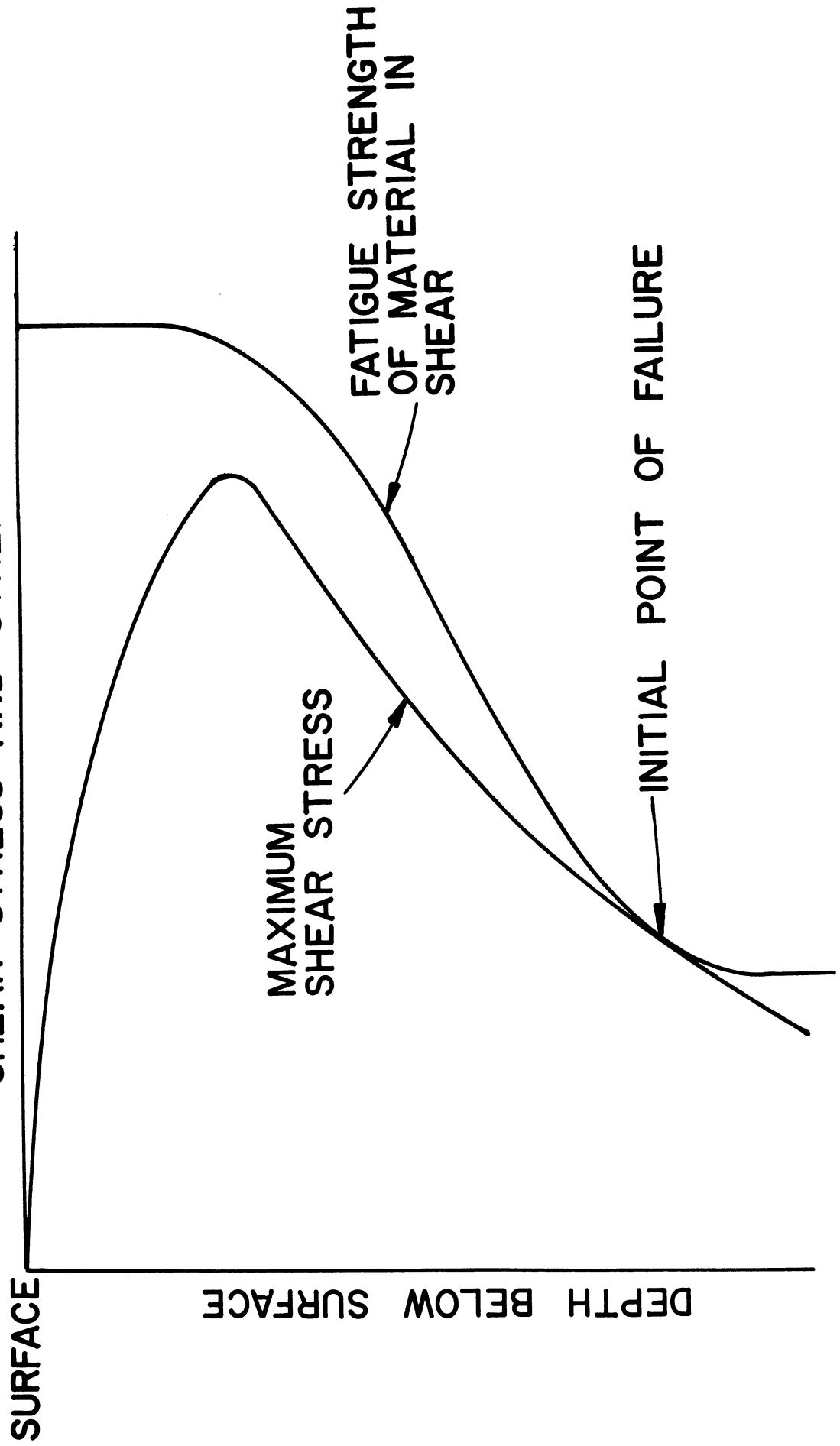

Figure 9. Failure conditions for case crushing of case hardened parts.

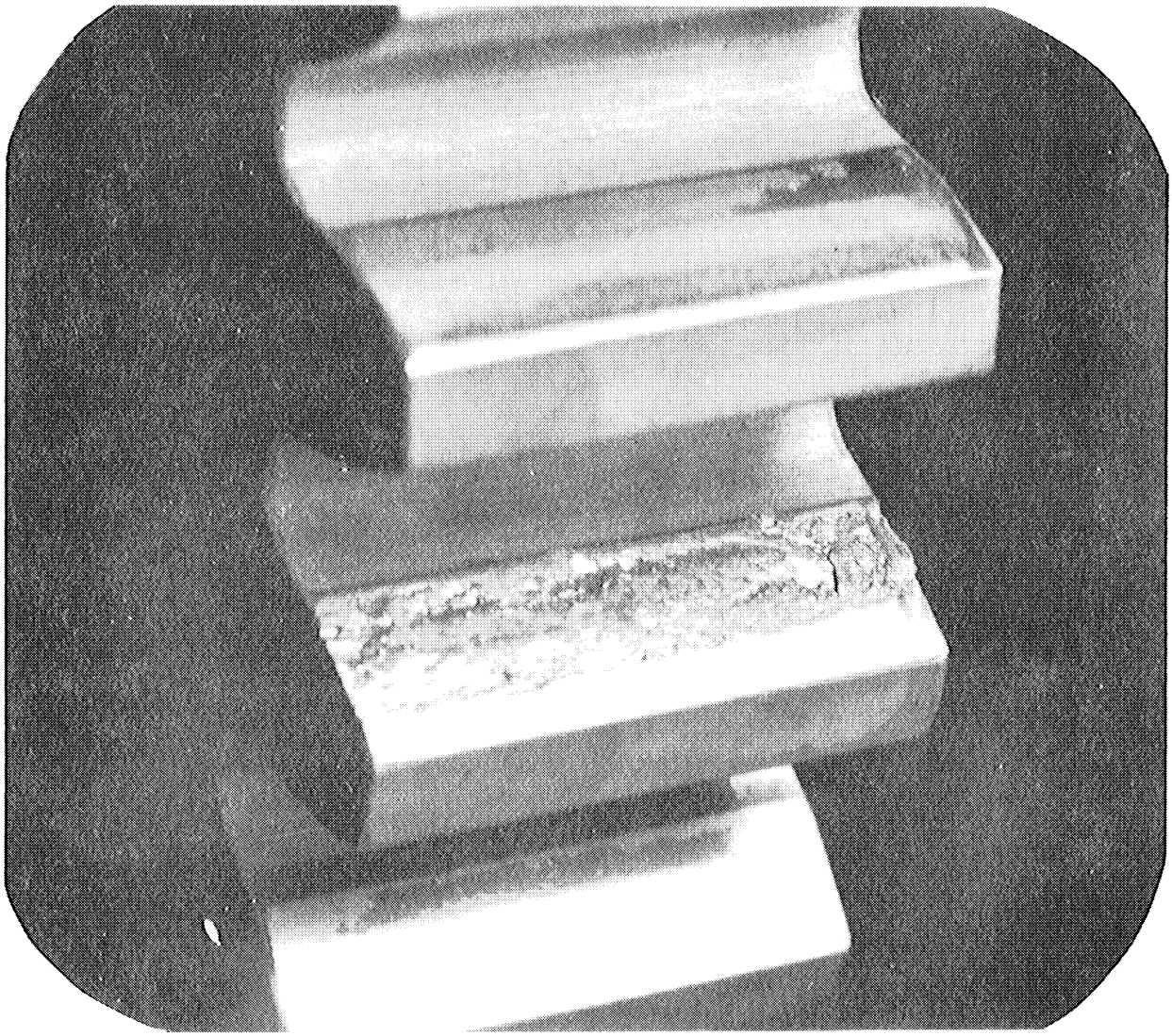

Figure 10. Case crushing of a nitrided gear.

Figure 11. Conventional pitting of carburized and hardened gear.

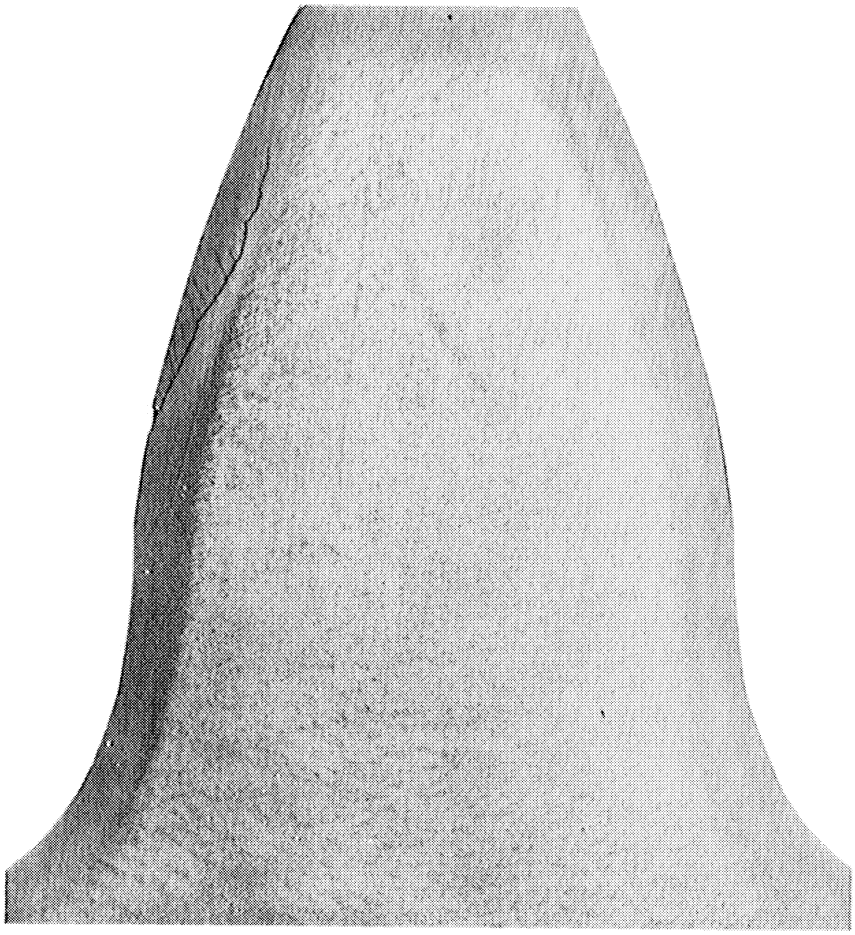

Figure 12. Propagation pattern of conventional pitting.

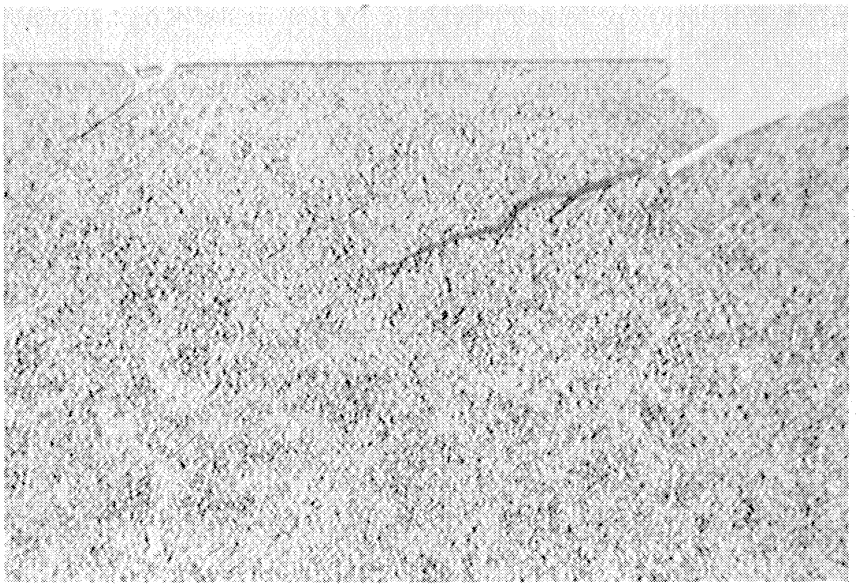

Figure 13. Surface initiation of conventional pits. 500x.

If the coefficient of friction is 1/9 or greater, the maximum shearing stress occurs at a point in the surface rather than below without consideration of thermal effects. This was shown by Smith and Liu[15] and shortly thereafer by H. Poritsky,[16] who although using different methods of analysis came to the same conclusion.

Smith and Liu's examination which was more complete with a coefficient of friction of 1/3 pointed out the importance of maximum and range of shearing stress on a given plane in the surface. It was shown that the maximum shear stress was equal in their case to 0.43 times the maximum Hertz pressure, P_o, and the maximum range of shear was 63% of the maximum pressure.

Since shears and ranges of shears in the complex problem of contact stresses are difficult to discuss except in lengthy detail, it will serve our purpose well to describe at this time normal stresses and draw implications from them with a brief note on corresponding shear stresses later. For instance, in the case of a tangential load caused by a friction coefficient of 1/3 the stress σ_x parallel to the surface and in the plane of rotation, and its range are shown in Figure 14. It will be noted that instead of the normal Hertz stress of P_o, the maximum normal compressive stress is now equal to 1.2 P_o with an actual tensile stress at one edge of the ellipse of contact pressure equal to .67 P_o. This reversal of stress from compression to tension should be kept in mind since it is important in the formation and propagation of a fatigue crack on the surface.

The major difficulty in applying such analyses successfully to a well lubricated machine element is the large friction necessary for significant increases of stress to appear. It will be shown, however, that thermal stresses make frictional effects more pertinent on such parts.

In order for the reader to recognize the existence of thermal stresses, it is necessary to examine the temperatures below the surface. These will show the necessary temperature differences or thermal gradients. In order to assign some quantities to the figures to be discussed, an example which involves the contact pressures and other values in Figure 15 will be used. Figure 16 shows the calculated temperatures that are developed in this case, not only on the surface, but below the surface. Note that the temperature at about .005"below the surface where the maximum surface temperature has occurred is only 1/5 that of the maximum, constituting a reduction of over 350°F in the thin surface material.

Without becoming involved in the mathematics of this work, a little qualitative study will show that if the surface material is at a higher temperature than the sub-surface material, then attempts of the surface to expand against the restraining sub-surface material will produce surface compressive stresses, σ_T, which are approximately proportional to the surface temperature. It is understandable furthermore that they are primarily compressive in all directions, parallel to

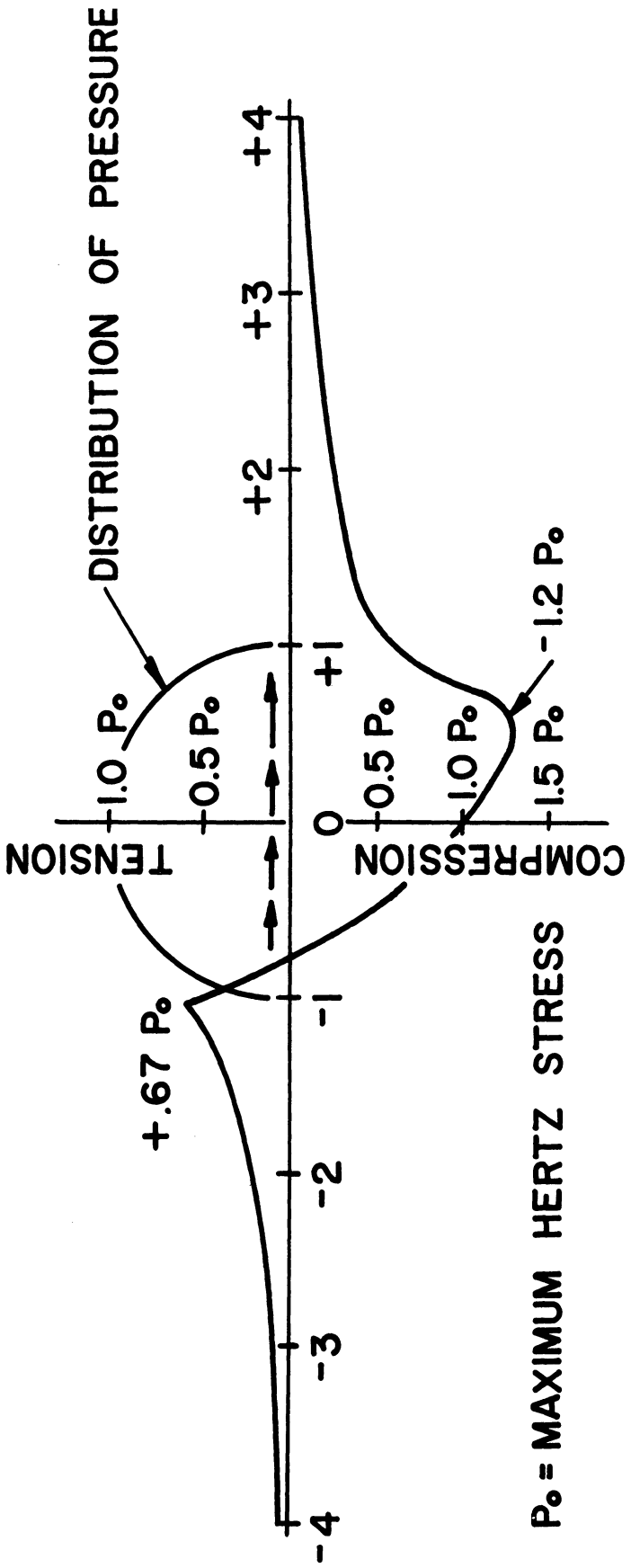

Figure 14. Range of values of σ_x with $\mu = 1/3$.

RADII OF ROLLERS	2.00 & 4.00 INCHES
V_1	100 IN./SEC.
V_2	150 IN./SEC.
LOAD W_N	23,000 LB. IN.
COEFFICIENT OF FRICTION	0.1
SPECIMENS	STEEL ON STEEL

Figure 15. Data for quantitative study.

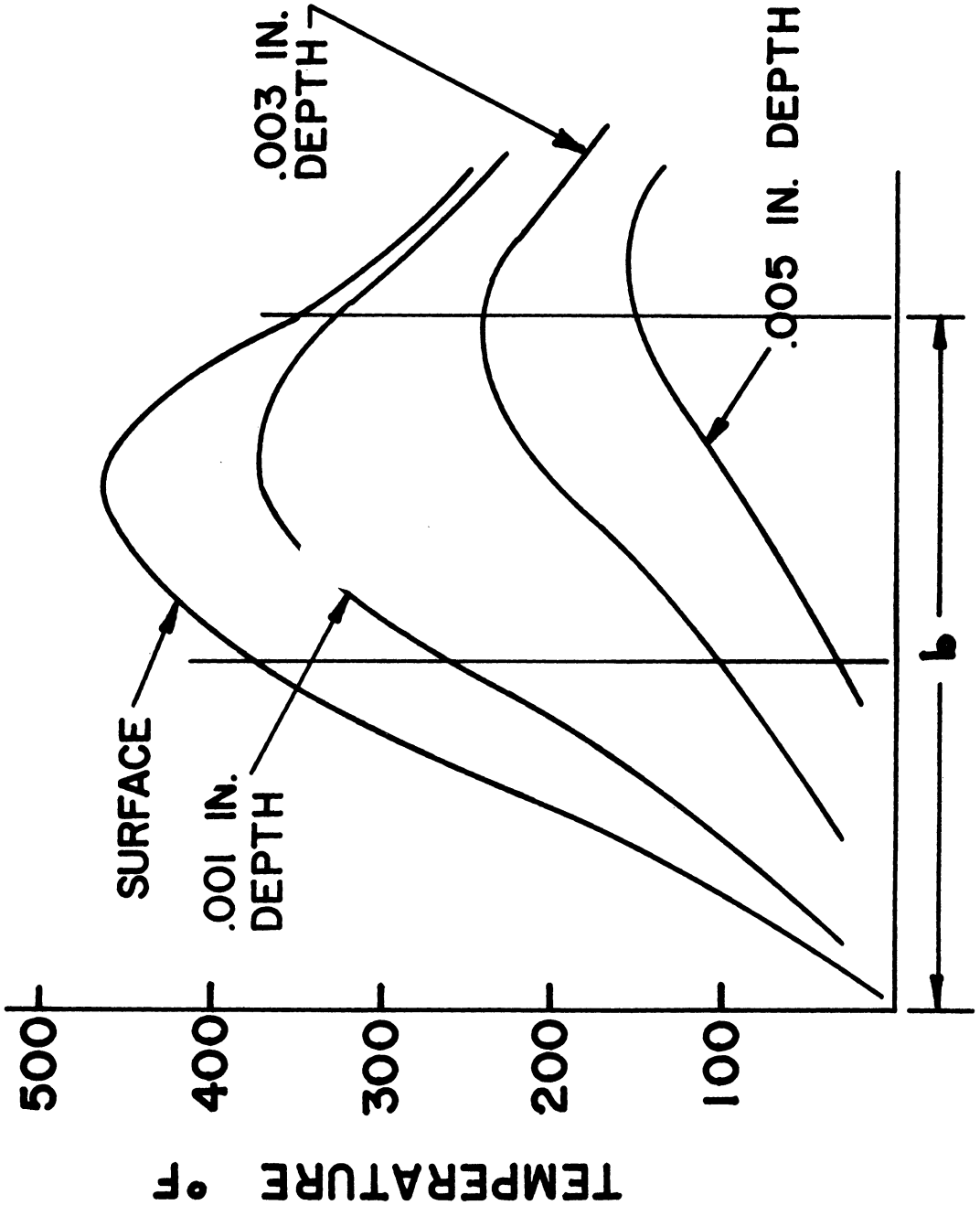

Figure 16. Temperature flash on and below surface.

the surface but, of course, are zero normal to the surface because of the lack of restraint in this direction.

The stresses that are thus produced in our example are illustrated in Figure 17.

The effect created by super-imposing the thermal stresses on the normal stress system, σ_x, for a negative sliding member versus one in positive sliding is of considerable interest. Negative sliding occurs on the slower of the two members, such as the upper cylinder illustrated in Figure 1. This action takes place in the dedendum area of a driving gear (the working surface below the pitch line), the wheel of a braking locomotive or the rotating cam follower of the camshaft. It is well known that the dedendum of the driving gear will pit more readily than the surface above it on the same profile. Also it has been found that an alloy iron camshaft will run with a stronger hardened steel tappet which could be considered in negative sliding, but a hardened steel shaft will not run satisfactorily with an alloy iron tappet.(17) Stewart Way suggested in 1935(18) that this was principally due to the action of the lubricant which on the slow speed member became trapped in micro-surface cracks, and under the compression of applied load, developed a hydraulic pressure of sufficient magnitude to extend the crack as shown in Figure 18. This explanation is reasonable once cracks are present, however, in most cases, one is hard pressed to find surface cracks which could be propagated in this manner. For instance, examinations of positive sliding members have not generally shown such cracks, which could initiate the propagated fracture as explained by Way.

However, if the steps are examined of super-imposing the stresses σ_x and σ_T that are created during contact, we can see the results of compressive and tensile stresses as they occur on both the negative and positive sliding members, as shown in Figures 19 and 20 for the data shown in Figure 15. Included in the charts is the semi-elliptical distribution of compressive stress as shown by Hertz, and also the distorted pattern of the ellipse which is caused by the frictional forces. These surface tangential forces cause the maximum compressive stresses on the negative sliding member to trail the centerline of contact. If the thermal stresses that are developed are now super-imposed, the trailing characteristic of these can add materially to the maximum stresses that occur on the negative sliding member, Figure 19, but they do not add as strongly to those stresses created on the positive sliding member, Figure 20. Moreover the tensile stress is retained on the negative sliding member, but it has been eliminated on the positive sliding member by thermal compression. Such an examination concludes that the range of normal maximum stresses in compression on the surface of the negative sliding member is greater than that produced on the positive sliding member, in the case of our example by almost 20%.

As was mentioned previously because of the complex triaxial stress conditions during contact, a thorough examination must include

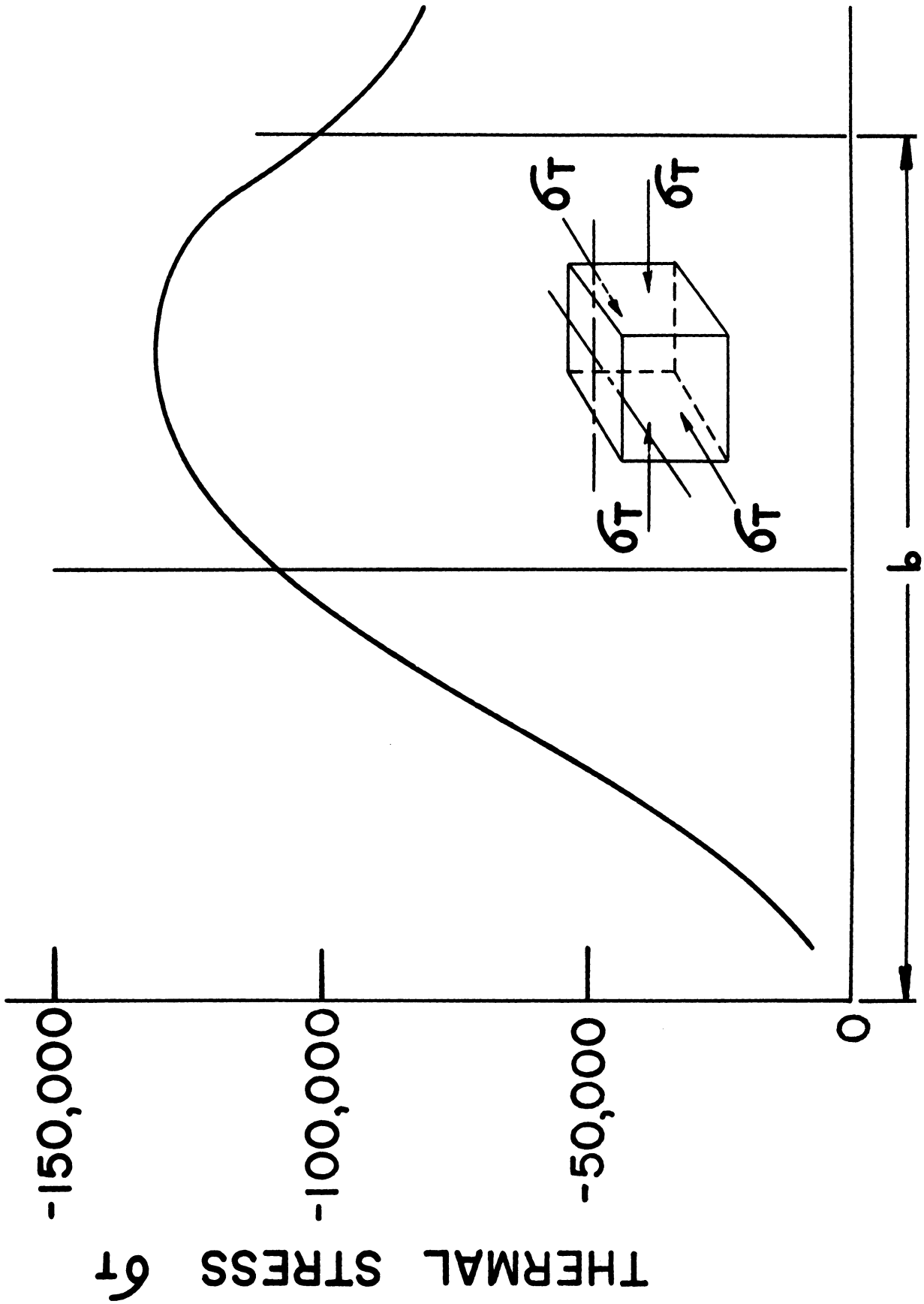

Figure 17. Thermal Stresses in Surface.

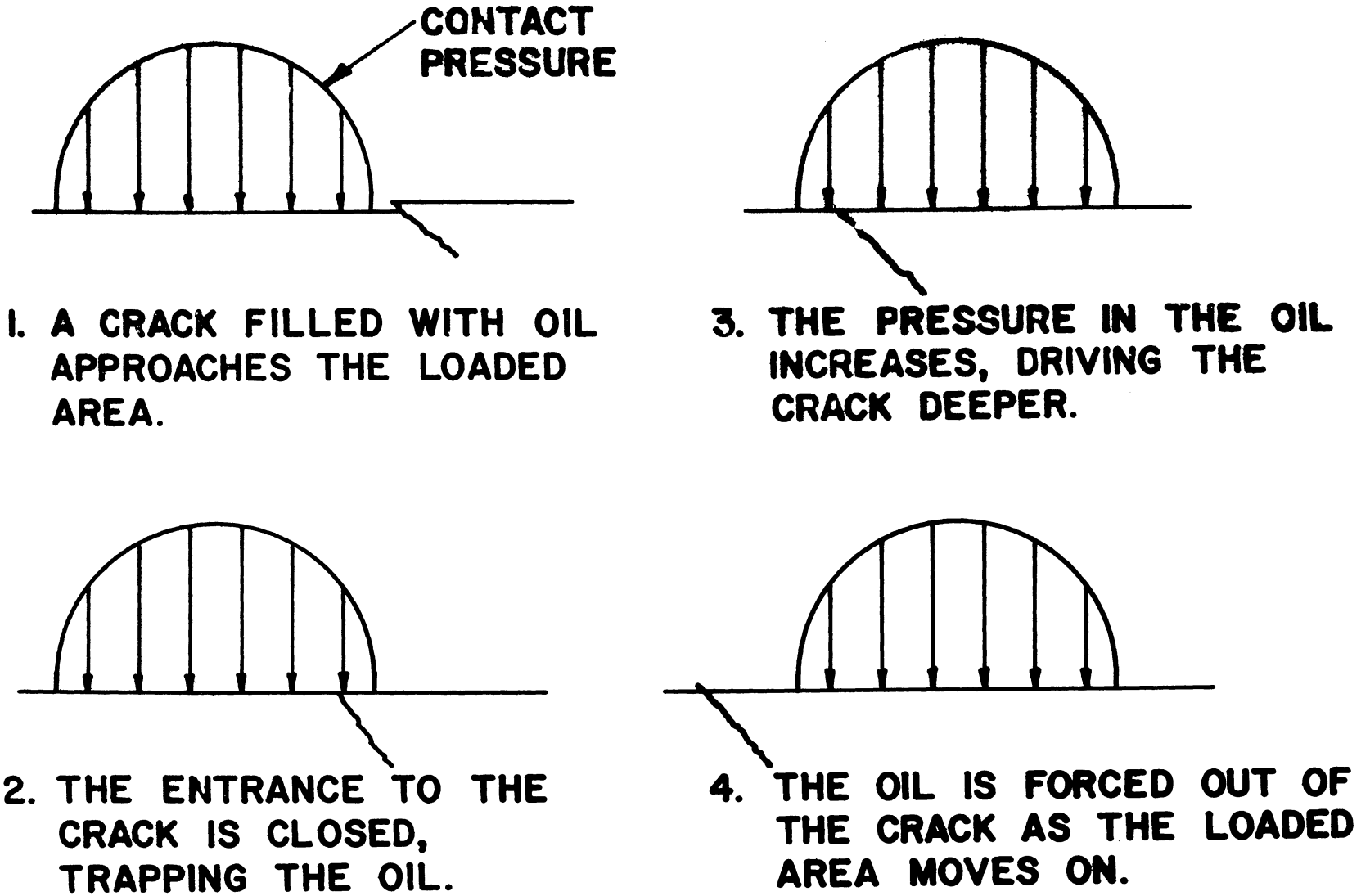

Figure 18. Way's Theory of Hydodynamic Propagation of Surface Fatigue Cracks by Lubricant.

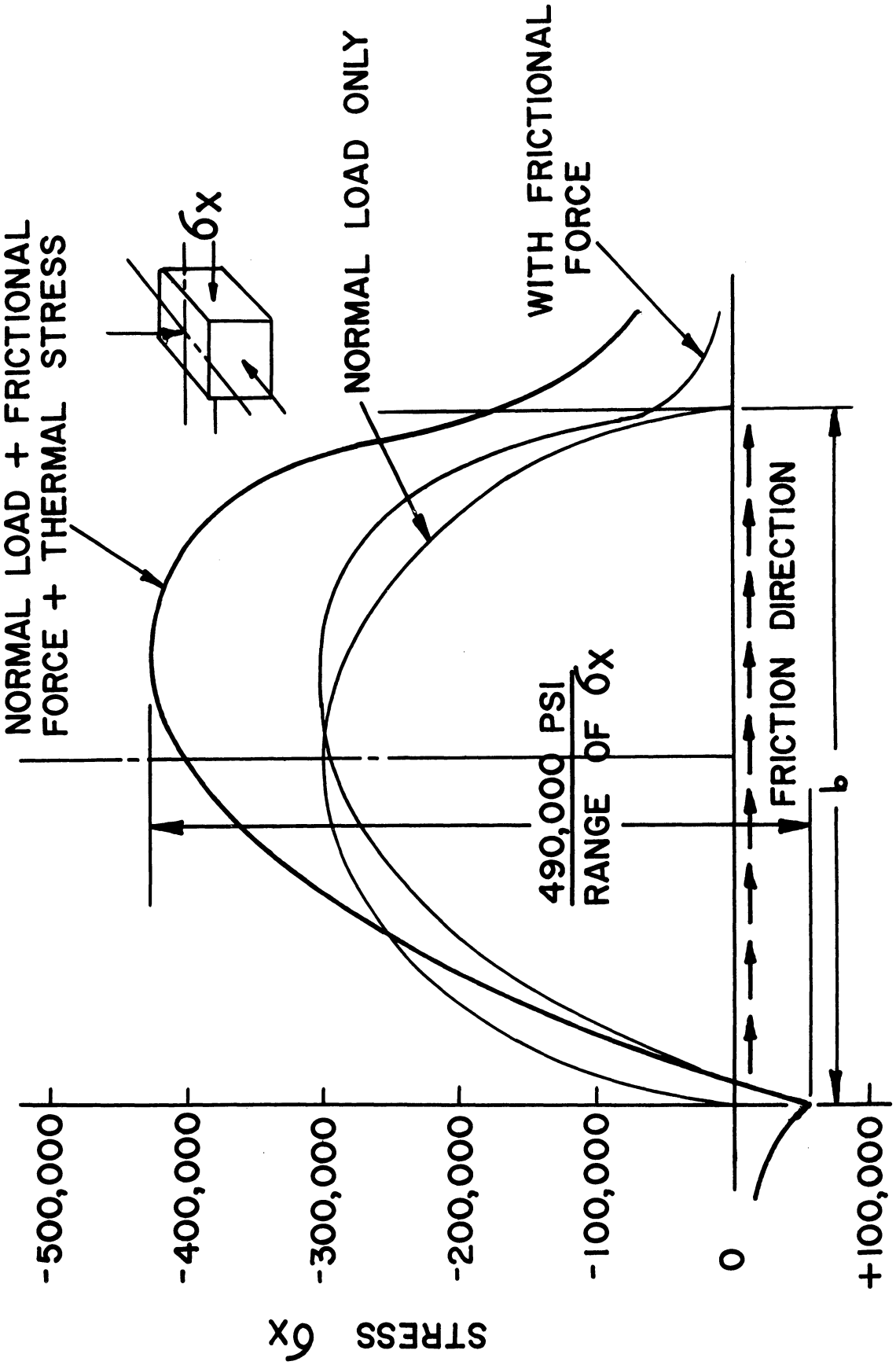

Figure 19. Stress Range of σ_x on Member in Negative Sliding.

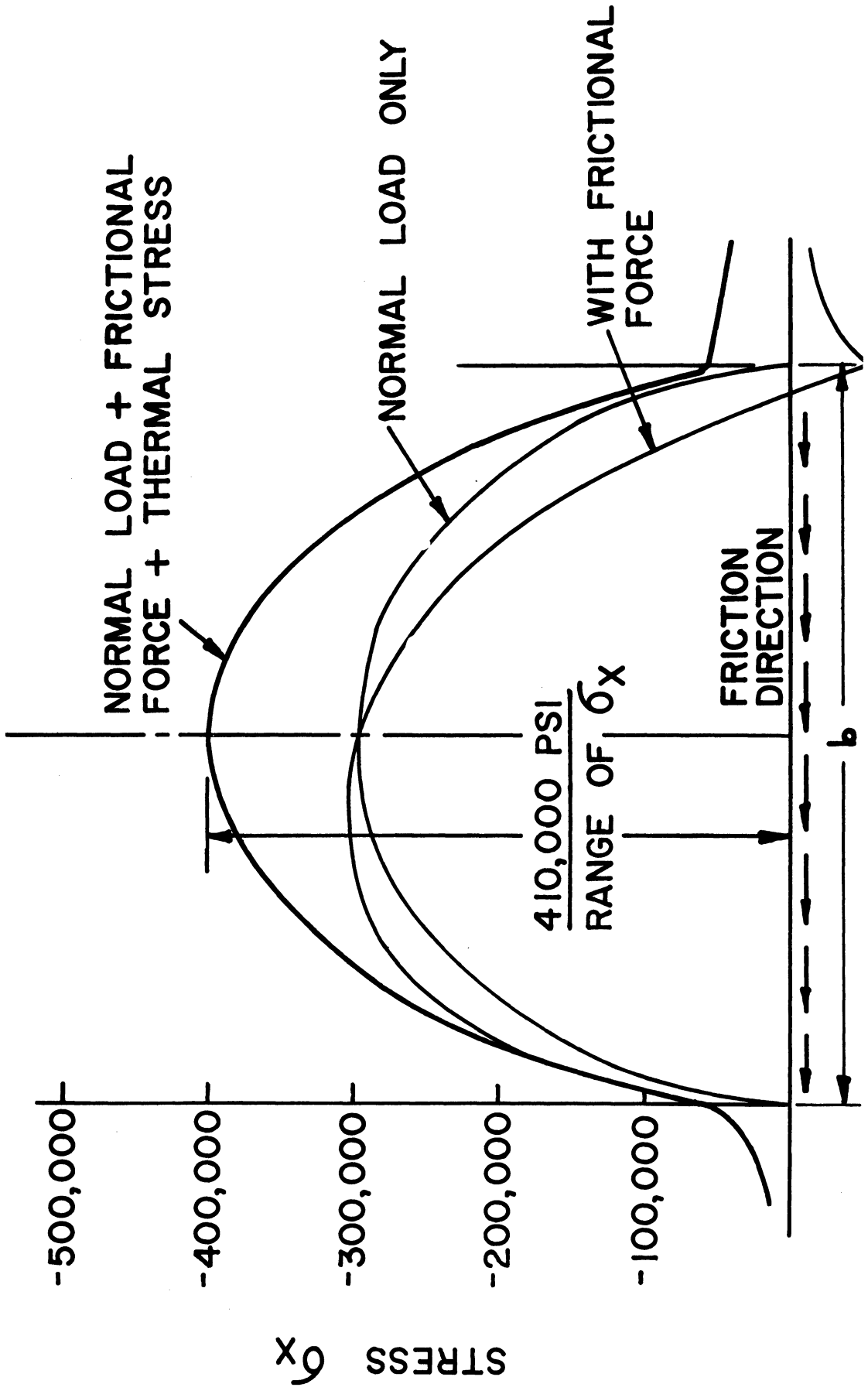

Figure 20. Stress Range of σ_x on Member in Positive Sliding.

the examination of shear stresses and ranges of shear on fixed planes as the contact load passes over. This is true because no failure will occur under even very high compression of a hydrostatic nature (equal compression in all directions). One must, therefore, look for large differences in compression which are capable of producing high enough shearing stresses to fail the material.

Investigations of this type can be conducted as mathematical tensor analysis or by the use of Mohr Circles.[19] The work reported here was aided by the use of an automatic digital computer. A number of planes were examined for maximum shear and ranges of shear which are shown in Figure 21, for the negative sliding surface. The angle which each plane makes with the surface in contact is illustrated simply by the position of each small plane on a quadrant representing as its surface all possible angles which could be examined. The magnitude of the maximum shears is shown on each small plane. The maximum range of shear was found to be about 0.394 times the maximum Hertz stress or 118,000 psi which occurred on the same plane showing the maximum shear of 95,000 psi. It is reasonable that shears of this magnitude which are subject to some reversal will cause fatigue fracture of even the strongest commercially used steels.

Considerable study must be given to qualitatively understand the physical causes of the stresses in each of the planes. However, it is particularly interesting to note that many of the planes illustrate shear stresses which are very close to the maximum. In a case such as this where the shear stresses are large in many planes, it is not difficult to surmise why even very hard steels, which are not generally considered to be ductile, will flow at the surface. Such surface metal flow is frequently seen on hypoid gears,[20,21], for instance, where thermal stresses can play an important part because of high sliding velocities even though the coefficient of friction is not exceptionally high.

The examination made in this report is admittedly abbreviated at this time. Its content is to impress upon the engineer the importance of increased studies on the effect of surface temperatures not only on scoring and pitting, but also on wear of various forms. It is felt that studies of this nature combined with further studies on the coefficient of friction will bring about increased understanding of surface damage, which in turn will bring about increased efficiency in the attention to surface damage problems.

Particular acknowledgment is due Professor H. Blok who, through private communications, provided us with the exact temperature flash formula and suggested E. Melan's[21] approach to thermal stresses. The author also acknowledges the mathematical assistance of W. P. Evans and E. D. Eyman of the Caterpillar Research Department.

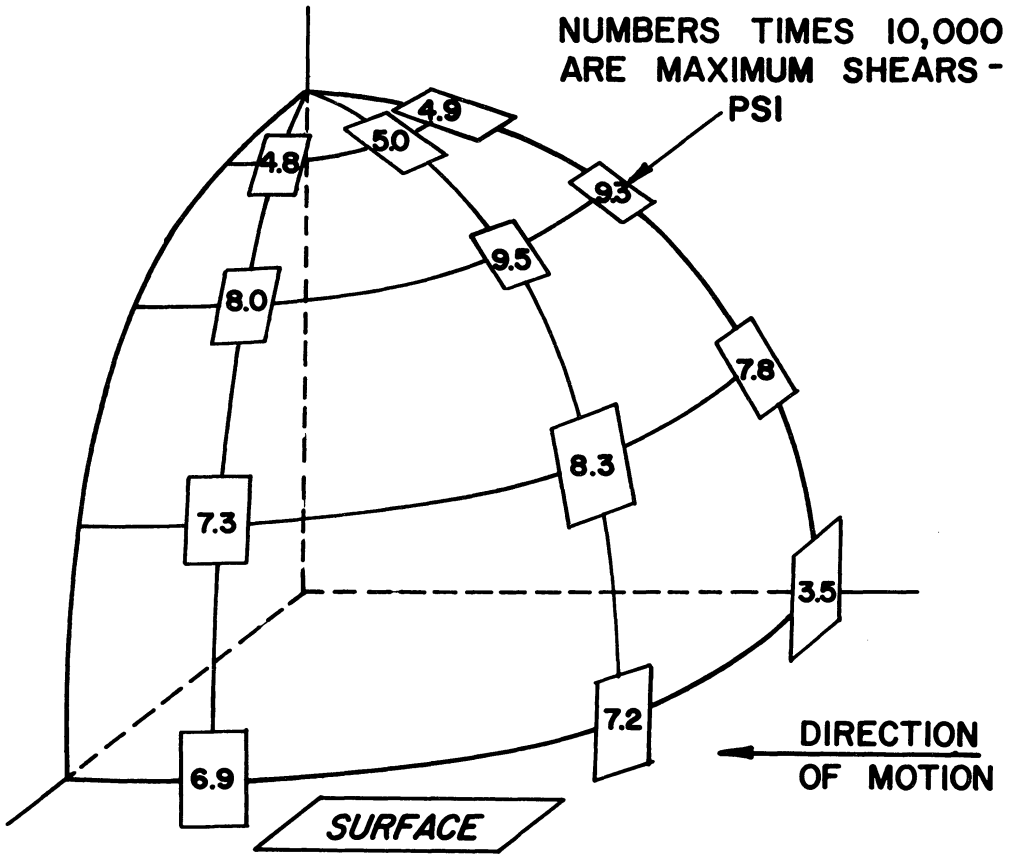

Figure 21. Maximum Shear Stresses Occurring at Various Angles to Surface in Thermal Stress Example.

REFERENCES

1. Blok, H., "Les Temperatures de Surface dans les Conditions de Graissage sans Pression Extreme," Second World Petroleum Congress, Paris, June 1937.

2. Blok, H., "The Dissipation of Frictional Heat," Applied Scientific Research, Sect. A, Vol. 5, 1955.

3. Hertz, H., "Gesammelte Werke," English Translation in Miscellaneous Papers, 1896, Leipzig, Germany, Vol.1, 1895.

4. Bowden and Tabor,"Friction and Lubrication of Solids," Oxford University Press, 1950.

5. Rabinowitz, E., and Tabor, D., Proc. Roy. Soc., 2084 455, (1951).

6. Murray, Johnson, and Bisson, Lubrication Engineering 10, 193, (1954).

7. Cowley, Ultee and West, "Influence of Temperature on Boundary Lubrication," ASLE Reprint 56LC-18, 1956.

8. Lane, T.B., and Hughes, J.R., "A Practical Application of the Flash-Temperature Hypothesis to Gear Lubrication," Proc. Third World Petroleum Congress, the Hague, 1951, Sect. 7.

9. Kelley, B.W., "A New Look at the Scoring Phenomena of Gears," SAE Transactions, Vol. 61, 1953.

10. Thomas, H.R., and Hoersch, V.A., "Stresses Due to the Pressure of One Elastic Solid on Another," University of Illinois Bulletin No. 212.

11. Dudley, D.W., "Practical Gear Design," McGraw Hill Publishing Co., 1954.

12. Seely and Smith, "Advanced Mechanics of Materials," John Wiley & Sons, Pub. 1952.

13. Radzimovsky, E.I., "Stress Distribution and Strength Condition of Two Rolling Cylinders Pressed Together," Univeristy of Illinois Bulletin No. 408.

14. Barwell, F.T., "The Effect of Lubrication and Nature of Superficial Layer After Prolonged Periods of Running," Properties of Metallic Surfaces, Inst. of Metals Report, 1953.

15. Smith and Liu, "Stresses Due to Tangential and Normal Loads on an Elastic Solid with Application to Some Contact Stress Problems," ASME Paper No. 52-A-13, 1952.

16. Poritsky, H., "Stress and Deformations Due to Tangential and Normal Loads on an Elastic Solid with Applications to Contact of Gears and of Locomotive Wheels," Journal of Applied Mechanics, Trans. ASME, Vol. 72, 1950.

17. "What We Know About Cam and Tappet, Materials, Design, Lubrication," SAE Journal, Sept., 1955.

18. Way, Stewart, "Pitting Due to Rolling Contact," Journal of Applied Mechanics, Vol. 2, 1935.

19. Zizicas, G.A., "Representation of Three-Dimensional Stress Distribution by Mohr Circles," ASME Journal of Applied Mechanics, Vol. 22, June 1955.

20. Almen, J.O., "Surface Deterioration of Gear Teeth," Mechanical Wear, A.S.M., 1950.

21. Barwell, F.T., "Wear of Metals," Journal of the Institute of Metals, Feb. 1958.

22. Melan, E., Ingenieur-Archiv, Vol. 20, 1952.

GALVANIC CORROSION

F. L. LaQue
Vice-President, Development and Research Division
International Nickel Company

by

F. L. LaQue

Since this is the only paper in the present series to be devoted to corrosion, the term "Galvanic Corrosion" as it appears in the title will be used in a broader sense than is sometimes the case. Ordinarily, galvanic corrosion is the accelerated attack which results from the flow of current between dissimilar metals in electrical contact in a liquid capable of conducting current. However, all corrosion that occurs in a conducting liquid is considered to result from a flow of electricity from one metal surface to another even when the surfaces are on the same metal. to this extent, all corrosion might be called galvanic Although in this discussion the field will be extended beyond couples of dissimilar metals, it will be limited to instances where the anodes and cathodes in the corrosion current circuit will be readily recognizable and where either the anode or cathode, or both, can be well defined as to location and may be of substantial area. This will include "galvanic" action as it is related to corrosion in or around crevices and pitting. From the practical point of view, inclusion of these several forms of corrosive attack will serve to cover a large portion of difficulties likely to be encountered as a result of corrosion.

Galvanic Corrosion

What will be discussed under this heading will be what is usually referred to when the term 'galvanic action' is used in its narrowest sense. Conditions necessary for galvanic action are:

1. A combination of dissimilar metals having a difference in solution potential in the corrosive environment.
2. A metallic connection between the dissimilar metals capable of permitting a flow of electrons from one metal to another.
3. An ionized liquid capable of conducting electric current between the dissimilar metals.

If any of these conditions is lacking, there will be no galvanic action. For example, there could be no galvanic action involving a bronze shaft passing through a rubber bearing in a steel strut attached to a wooden hull immersed in sea water. The potential difference of about 0.3 volt between the steel and the bronze would satisfy condition 1, the sea water would provide the conductive ionized liquid required by condition 3, but the rubber bearing, being a good electric insulator,

would interrupt the metallic path for electrons required by condition 2, so that no galvanic action would be possible in this case. However, if the hull were made of steel instead of wood, the metallic electrical path might be completed from the strut to the bronze shaft through the steel hull and through the engine and its support which would likely be in electrical contact with the hull through the engine bed supports and with the shaft through the transmission couplings.

Condition 2, therefore, provides a most effective means of avoiding galvanic corrosion by insulating one metal from another by whatever means may be most appropriate and convenient. For example, in the case cited, it would be possible to insulate the bronze shaft from the steel strut and the steel hull by the use of an insulting shaft coupling in which there would be an insulating gasket between the coupling faces, insulating sleeves around the shanks of the coupling bolts and insulating washers under the bolt heads or nuts. Similar devices for interrupting a metallic path for current flow can be readily worked out to deal with any combination in which it is desirable to avoid an opportunity for galvanic corrosion.

Condition 1 requires the existance of a difference in potential between the dissimilar metals. This condition is practically always satisfied since even small variations in the composition of metal will give rise to potential differences in most environments. These potential differences in most environments. These potential differences can vary between a few millivolts, e.g., between copper steel and plain carbon steel, or can be well over a volt, e.g., between magnesium and copper in sea water.

The difference in potential that can develop is determined not only be the metals in the couple but by the corrosive characteristics of the liquid with which they are in contact. In extreme cases, the direction as well as the magnitude of the potential difference may change. For example, in most waters, zinc is less noble than iron and a galvanic current will flow from the zinc to the iron through the water. However, there are some waters (especially when they are hot) in which zinc will develop a surface film which will make it more noble than iron, so that the galvanic current will flow from the iron to the zinc.(1)

Rather than to try to measure potential differences between a great number of possible combinations of metals in a particular environment, it is simpler to measure the potential of each of them with reference to some common bench mark or standard of potential. These potential standards can be hydrogen on platinum in contact with a standard acid solution or, more commonly, an electrode system having a stable and reproduceable potential such as mercury in contact with mercurous chloride in potassium chloride (calomel half cell), silver in contact with silver chloride or copper in contact with saturated copper sulfate.

For convenient reference, the potentials of some of these standard reference electrodes or half cells relative to a standard hydrogen electrode are shown in Table 1.

Table 1

Hydrogen Potentials of Half-Cells

Half-Cell	Potential in Volts
Saturated Calomel	0.2415
Normal Calomel	0.2800
Tenth Normal Calomel	0.3337
Silver:Silver Chloride	0.2222
Copper:Copper Sulfate (Sat.)	0.3160

An idea of the range of potential of some common metals and alloys with reference to a calomel half cel made up with saturated potassium chloride in flowing sea water is given in Table 2.

The potentials shown in Table 2 are what is called open circuit potentials - that is the potential that exists when no current is flowing from one metal to another. It is possible, therefore, to calculate what potential difference would exist between any pair of metals shown in Table 2 by subtracting the potential of one metal from that of the other. for example, the open circuit potential difference between zinc and copper would be 0.67 volt, and the galvanic current would tend to flow through the salt water from the zinc to cause galvanic acceleration of corrosion of the zinc and galvanic reduction in corrosion of the copper. On the other hand, the open circuit potential between copper and a stainless steel passive type 316 would be 0.31 volt with current tending to flow from the copper to the stainless steel so as to accelerate corrosion of the copper.

As mentioned previously, it would be necessary to make similar open circuit potential measurements in all solutions of interest in order to determine the potential differences that might exist in dissimilar metal couples. Many such studies have been made with results reported in the technical literature.(2) On the basis of such observations, plus a good deal of practical experience, it has been possible to arrange many common metals and alloys in what might be called a general galvanic series as covered by Table 3.

It is not possible to assign values to the potentials of the metals in this series since these values will vary from one corrosive solution to another. However, the relative positions of the metals are likely to be as shown in the table for most commonly encountered environments. Therefore, as a guide to probable galvanic behavior, it may be assumed that when any two metals are combined in a galvanic couple, the

Table 2

Potentials of Some Common Metals and Alloys
in Flowing Sea Water at 25°C. (77°F.)

Metal	Stea Poter Negati Satur Calc Half (
Zinc	1.(
Aluminum (Alclad 3S)	0.9
Aluminum 3S-H	0.
Aluminum 61 S-T	0.
Aluminum 52 S-H	0.
Cast iron	0.(
Carbon Steel	0.
Stainless steel type 430 (17 per cent chromium)[a]	0.
Ni-Resist cast iron (20 per cent nickel)	0.
Stainless Steel type 304 (18 per cent chromium, 8 per cent nickel)[a]	0.
Stainless steel type 410 (13 per cent chromium)[a]	0.
Ni-Resist cast iron (30 per cent nickel)	0.
Ni-Resist cast iron (20 per cent nickel + copper)	0.
Naval rolled brass	0.
Yellow brass	0.
Copper	0.
Red Brass	0.
Composition G bronze	0.
Admiralty brass	0.
90-10 cupro nickel (0.8 per cent iron)	0.
70-30 cupro nickel (0.06 per cent iron)	0.
70-30 cupro nickel (0.47 per cent iron)	0.
Stainless steel type 430 (17 per cent chromium)[a]	0.
Nickel	0.
Stainless steel type 316 (18 per cent chromium, 12 per cent nickel, 3 per cent molybdenum)[a]	0.
Inconel	0.
Stainless steel type 410 (13 per cent chromium)[a]	0.
Titanium (commercial)	0.
Silver	0.
Titanium (high purity from iodide)	0.
Stainless steel type 304 (18 per cent chromium, 8 per cent nickel)[a]	0.
Hastelloy C	0.
Monel	0.
Stainless steel type 316 (18 per cent chromium, 12 per cent nickel, 3 per cent molybdenum)[a]	0.

[a] The stainless steels as a class exhibited erratic potentials depending on the incid of pitting and corrosion in the crevices formed around the specimen supports. The values listed represent the extremes observed and due to their erratic nature shoul not be considered as establishing an invariable potential relationship amongst the alloys covered.

Table 3

Galvanic Series

CORRODED END (anodic, or least noble)
Magnesium
Magnesium alloys
Zinc
Aluminum 2S
Cadmium
Aluminum 17ST
Steel or Iron
Cast Iron
Chromium-iron (active)
Ni-Resist*
18-8 Chromium-nickel-iron (active)
18-8-3 Chromium-nickel-molybdenum-iron (active)
Lead-tin solders
Lead
Tin
Nickel (active)
Inconel (active)
Brasses
Copper
Bronzes
Copper-nickel alloys
Monel
Silver solder
Nickel (passive)
Inconel (passive)
Chromium-iron (passive)
18-8 Chromium-nickel-iron (passive)
18-8-3 Chromium-nickel-molybdenum-iron (passive)
Silver
Graphite
Gold
Platinum
PROTECTED END (cathodic, or most noble)

*Reg. U.S.Pat. Off.

galvanic corrosion current will flow through the solution from the one higher in the list to the one lower in it, and this will cause accelerated corrosion of the metal higher in the list and will lead to reduced corrosion or galvanic protection of the metal lower in the list. In a general way, the galvanic effect will increase with the spread between the two metals in the galvanic series. For example, there is likely to be more galvanic corrosion of steel coupled to bronze than of steel coupled to Ni-Resist cast iron.

The metals included in the galvanic series shown in Table 3 are divided into groups. They may shift their relative potentials or positions within a group, but are unlikely to shift from one group to another except in the special cases of alloys (e.g., stainless steels) that may be either active or passive depending on the environmental conditions.

Stainless steels exhibit a passive potential in solutions where they resist corrosion. The active potential of a stainless steel is observed when it is being corroded by its environment. Such active potentials are usually confined to limited areas, as within pits or in crevices and are encountered in solutions such as salt water in which conditions for maintaining passivity are of a borderline nature. Under these circumstances, there is a galvanic cell with the corroding metal within a pit or crevice acting as anode and the inert metal around the pit or crevice acting as cathode. The open circuit potential of such a cell can be as great as between ordinary steel and passive stainless steel. Thus, the principal effect of a combination involving partically active stainless steel and a more noble metal such as copper is for the copper to supplement the passive portion of the stainless steel surface in promoting galvanic corrosion within the pit or crevice. Similarly, if the couple should involve a metal like ordinary steel having about the same potential as the active stainless steel, the effect would be to reduce the rate of pitting or crevice corrosion either by counteracting galvanic effect or by polarizing the passive stainless steel cathode so as to reduce the difference in potential between the pit or crevice and the surrounding surfaces. Where the environment is of a borderline nature as to its passivating effect, it is prudent to assume that the stainless steel will act galvanically at its active potential when its area is relatively small as compared with that of the other in the couple and at its passive potential when its area is relatively large. This would lead to the conclusion that it would be as dangerous to use a stainless steel bolt in a brass plate as to use a brass bolt in a stainless steel plate in salt water.

It is generally safer to use combinations of metals from within any group than to mix metals from different groups. This general rule is subject to considerable modification when effects of relative areas are taken into account, as will be discussed later, and will not apply where extreme differences in relative areas may exist. Extra caution

will be required even with small potential differences or differences in position in the series when the area of the metal higher in the list is relatively very small. Galvanic corrosion may be negligible where the area of the metal higher in the list is relatively very large, even though the potential difference or distance apart in the series is also large.

Up to now, the discussion has been based principally on potential differences and especially on differences in potential as measured on open circuit with no current flowing. As soon as current begins to flow, reactions at the surface of both metals in a galvanic couple will tend to reduce the open circuit potential. This may be the result of an accumulation of corrosion products around the less noble metal (the anode of the galvanic current circuit) and an accumulation of hydrogen or other products of the reaction at the more noble metal (the cathode of the galvanic corrosion circuit). These effects are called polarization of the galvanic cell, divided between that at the anode (anodic polarization) and that at the cathode (cathodic polarization). Without going into a detailed discussion of the nature of polarization and the many polarization reactions that may be important, it will suffice for the present purpose to point out that polarization at the anode shifts it potential closer to that of the cathode and polarization at the cathode shifts its potential closer to that of the anode, so that the initial potential difference may be eliminated at some value of current flow which becomes the limiting amount that can be generated in a particular galvanic couple.

Since the extent of polarization is determined by the amount of current that leaves or enters a particular area, the shifts in potential just mentioned are determined by the anodic and cathodic current densities rather than simply by the total amount of current flowing. Depending on the natures of the metals and the corrosive media and incidental conditions of exposure with respect to such factors as aeration, temperature and velocity (agitation), the magnitude of the galvanic current may be controlled by anodic polarization (anodic control), cathodic polarization (cathodic control), both anodic and cathodic polarization (mixed control), or where there is neither anodic nor cathodic polarization, by the electrical resistance of the galvanic circuit (resistance control). These several possibilities are shown diagramatically in Figure 1.

Cathodic polarization control is encountered most frequently with galvanic couples of a common metals and alloys in environments of greatest interest, such as waters, soils, and atmospheres.

Cathodic polarization by the most common reactions is reduced by the presence of oxygen which is, therefore, a potent cathodic depolarizer, and, for the same reason, a potent accelerator of galvanic action. Thus, galvanic action is likely to be greatest in highly aerated solutions and is increased also by velocity effects or agitation which allow more

oxygen to reach the cathodic surfaces and also reduce anodic polarization by removing protective corrosion products as fast as they are formed. These considerations suggest obvious steps, such as oxygen elimination and reduction in turbulence or velocity of flow that may be taken to reduce galvanic corrosion.

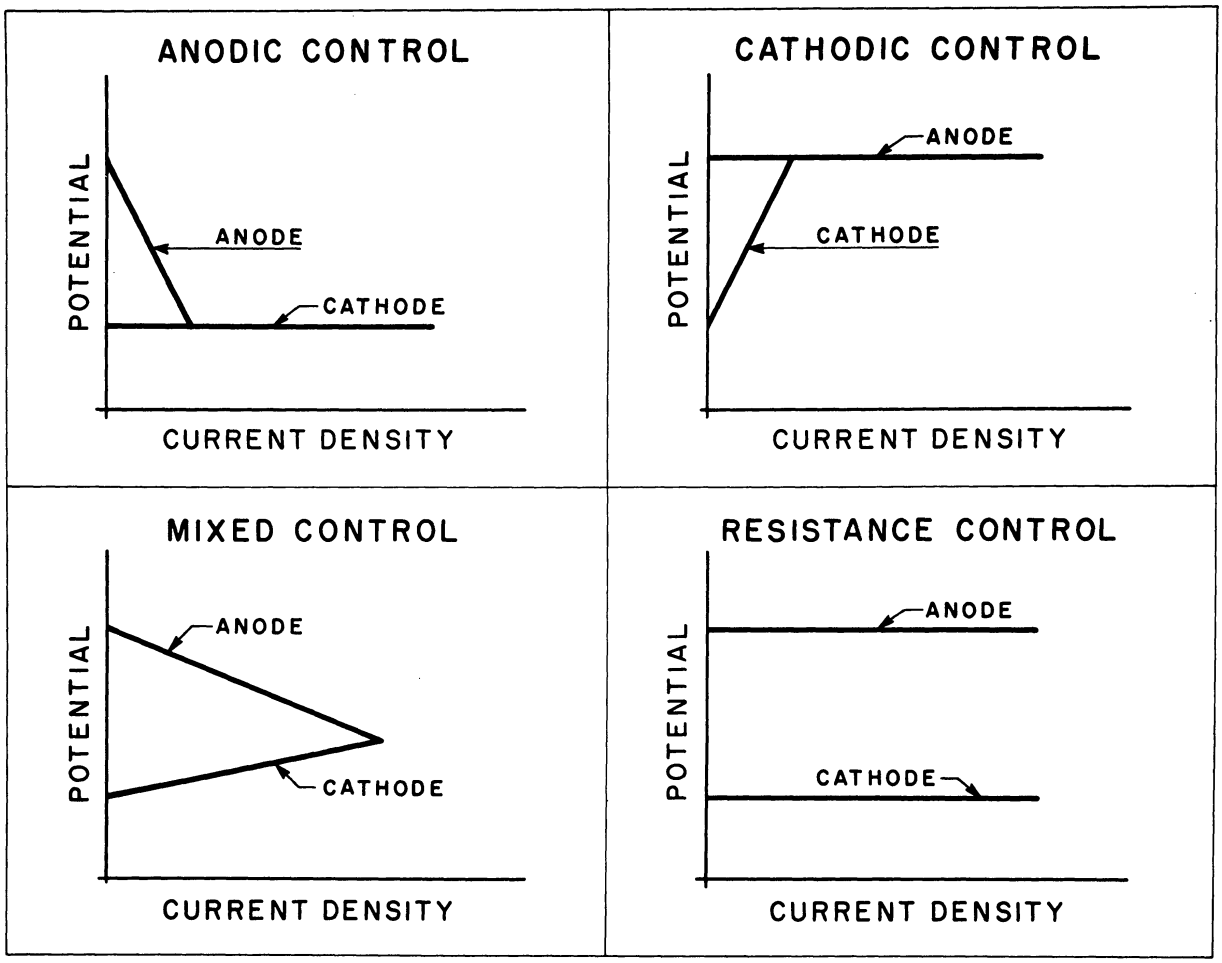

Figure 1. Polarization control of corrosion.

It is possible also to achieve anodic polarization by appropriate action. For example, iron can be made considerably more noble by the addition of chromate to water, as shown in Figure 2.(3) Thus, by induced extreme anodic polarization, galvanic potential differences can be eliminated and galvanic action brought under control.

Certain organic inhibitors have a strong effect in increasing cathodic polarization, while still others form films on metal surfaces which introduce enough resistance into the galvanic circuit to be effective in stifling galvanic action. It is possible, therefore, to control galvanic action by the use of appropriate inhibitors, as in automotive cooling systems.(4)

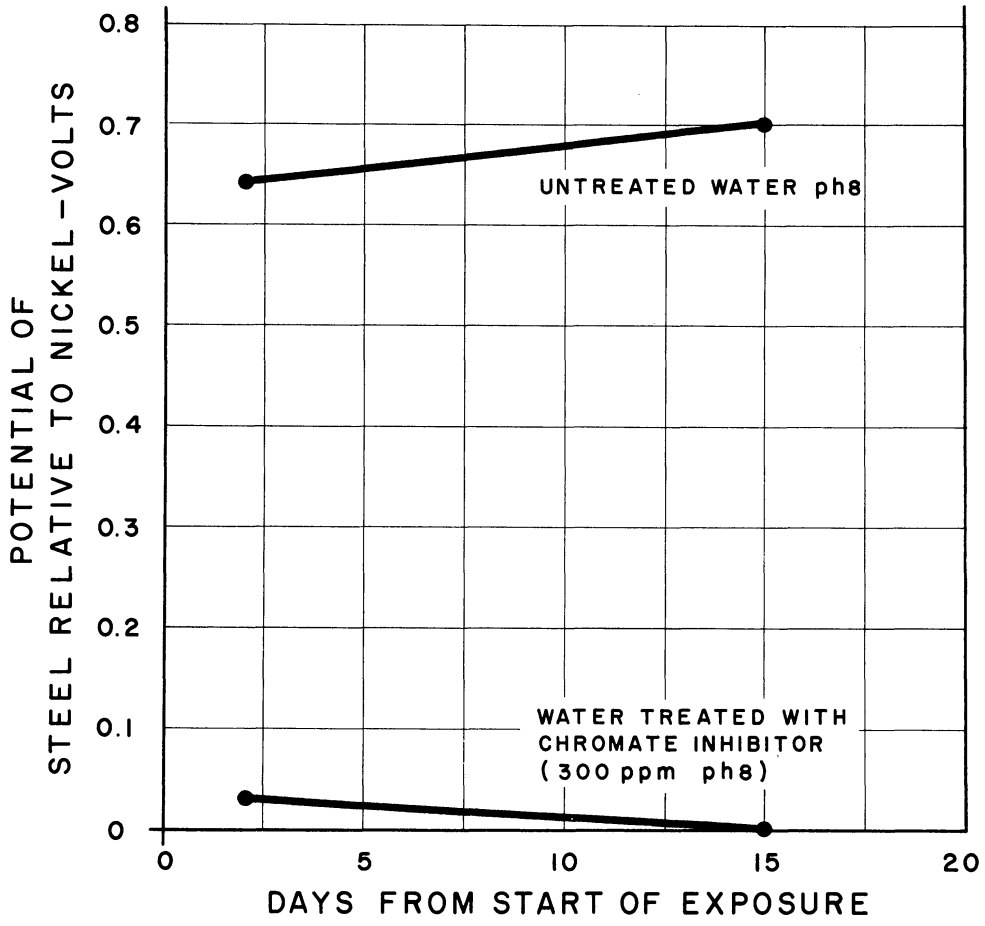

Figure 2. Effect of chromate in reducing galvanic potential in water.

Reference was made previously to the importance of current density with regard to polarization and to the frequency with which cathodic polarization becomes the principal controlling factor in galvanic action. From this, it follows that if the area of the anode remains constant and if there is little or no anodic polarization (as is frequently the case), the extent of galvanic corrosion of the anodic metal of the couple will be influenced greatly by the area of the cathodic metal. As the area of the cathode is increased, the cathodic current density will decrease and with it, the extent of cathodic polarization, so that a relatively high potential difference will be maintained. Furthermore, the larger the cathode, the more accessible it will be to oxygen and other depolarizing influences which will supplement the effect of the low cathodic current density in maintaining conditions that can aggravate galvanic corrosion.

This principal can be illustrated by results of experiments with couples of iron and copper in a salt solution.(5) The area of the iron was kept constant, while that of the copper in several couples was made larger and larger, with results shown in Figure 3, where the corrosion of the iron is shown to be a direct function of the area of the copper with which it was coupled. It should be noted also that the open circuit potential difference between the iron and the copper was the same in the couple where the area of the copper was smallest as in the couple where the area of copper was largest. Thus, determination of open circuit potentials provides no measure of galvanic effects which are controlled by the amount of current that can flow under the conditions established by polarization effects rather than by the potential difference that exists before any current flow and resulting polarization have occurred.

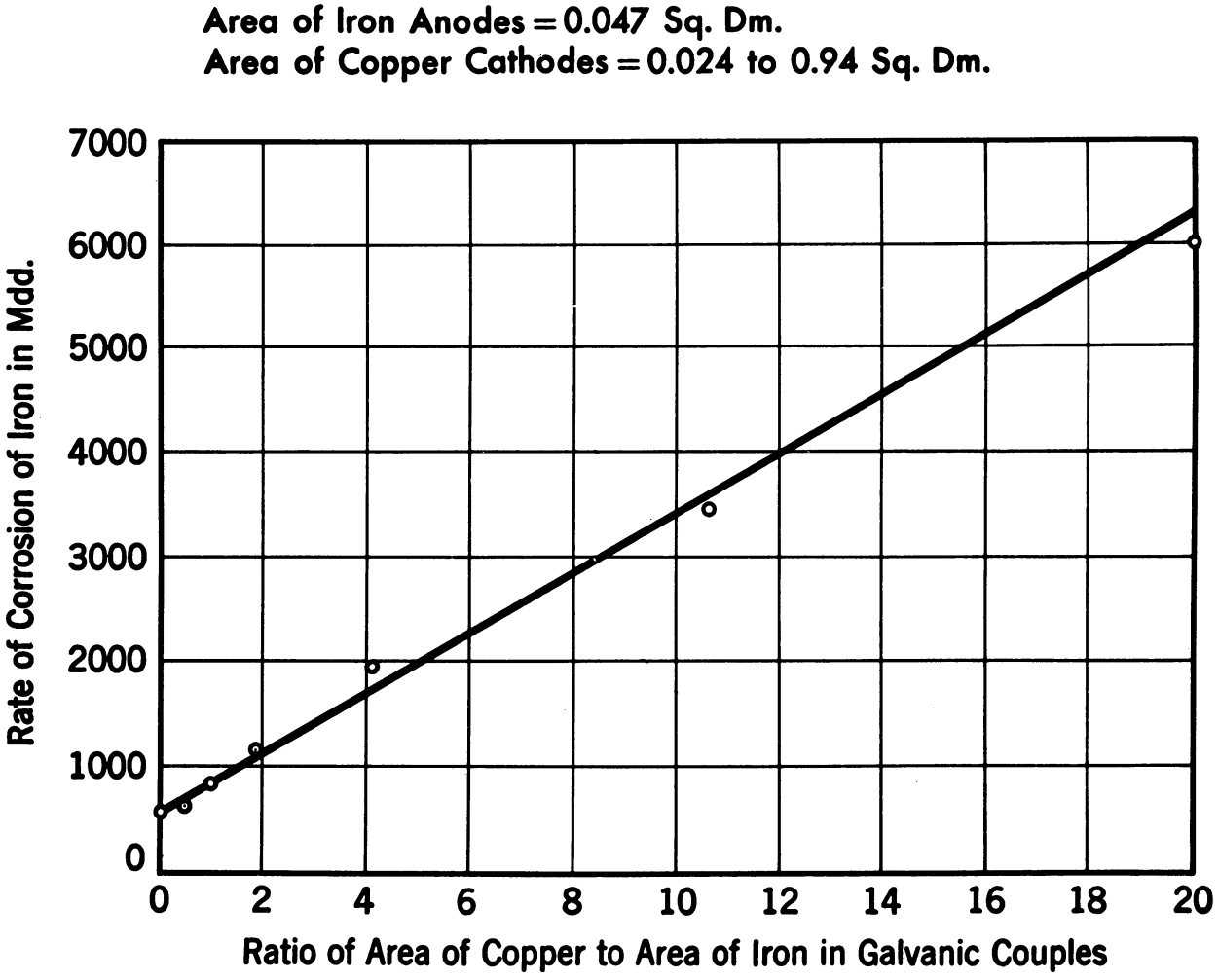

Figure 3. Effect of area of copper cathode on galvanic corrosion of iron anode in aerated 3% sodium chloride.

It is evident, therefore, that where cathodic polarization is the principal determinant of sustained current flow, a large area of cathode relative to the area of the anode will result in undesirably high concentrated galvanic corrosion of the anode, while a very small area of cathode relative to the area of the anode may result in so little galvanic action distributed over the large anode as to be insignificant. This is illustrated in Figure 4 by a practical example comparing steel rivets in copper plates and copper rivets in steel plates after immersion in sea water. The metals are the same in each case, but the destruction of the steel rivets associated with the large copper cathode, in the one case, demonstrates the danger of a relatively large cathode, while the insignificant effect of the copper rivets in the steel plate, shows how a relatively small cathode can be tolerated.

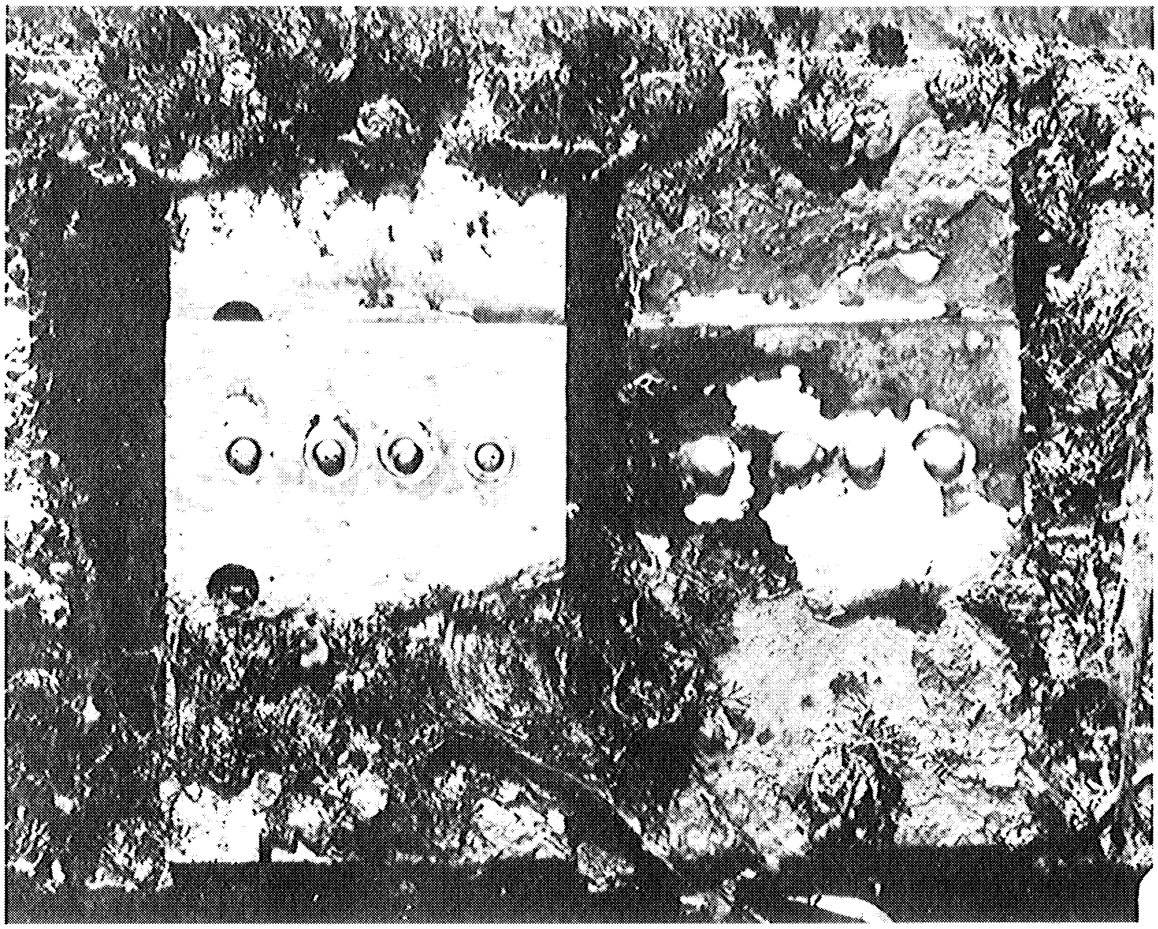

Figure 4. Left: Steel rivets in copper plate.
Right: Copper rivets in steel plate.

These same considerations are significant with respect to the use of paint or other insulating coatings for the control of galvanic action.[6] If a coating is applied to the anode of a galvanic couple,

it is essential that the coverage be complete and remain complete; otherwise, the effect of the coating will be to concentrate the galvanic effect at the bare spots and thus lead to a very high anodic current density with consequently severe localized corrosion. On the other hand, if a coating is applied to the cathodic member of the couple, a failure to achieve or maintain complete coverage will be very much less serious. If 99% coverage of the cathode is achieved, the galvanic effect will be reduced proportionately, and may remain tolerable with much less coverage of the cathode. Consequently, when coatings are used to control galvanic action, the cathode should be coated as well as, or instead of, the anode. The general order of preference in the use of coatings would be:

1. Coat both metals.
2. Coat the more noble metal only.
3. Leave both metals bare.
4. Coat the less noble metal only.

Distribution of Galvanic Corrosion

In addition to polarization effect, the overall electrical resistance of the galvanic circuit will have an influence on the magnitude and especially on the distribution of the galvanic action. Outside of insulators introduced into the galvanic circuit either accidentally or deliberately, the electrical resistance of the metallic portion of a galvanic circuit is usually negligible. The resistance of the electrolyte is much more important and will usually determine the areas of the dissimilar metals that will participate in the galvanic couple action. The laws of current flow and distribution are such that the galvanic action may be concentrated near the junction of dissimilar metals which touch each other along a line contact, as when one metal butts against or overlays another. Deepest attack will occur right at the contact and taper off further from it, either abruptly or gradually, depending on the conductivity of the electrolyte, and the area of the liquid path or paths through which current can flow. In a large volume of liquid, having a good conductivity, such as sea water, the galvanic currents can spread over larger areas and there may be only slight concentration of galvanic action along a line of contact. On the other hand, in a limited volume of fresh wate of low conductivity, the galvanic effect may be concentrated at the joint and decrease sharply within a short distance from it,[7] as illustrated by Figure 5, showing the distribution of galvanic corrosion of a steel plate in the vicinity of a nickel plate in contact with the steel in tap water.

The dimensions and shape of the electrolytic path are also important. This is illustrated by experiences with small diameter tubes and pipes carrying sea water. Galvanic effects will ordinarily not extend more than about two pipe diameters inside a tube or pipe carrying sea water. This limits the areas that can participate in galvanic effects

in such assemblies, and also limits the locations in which any increase or decrease in corrosion can properly be attributed to galvanic action.

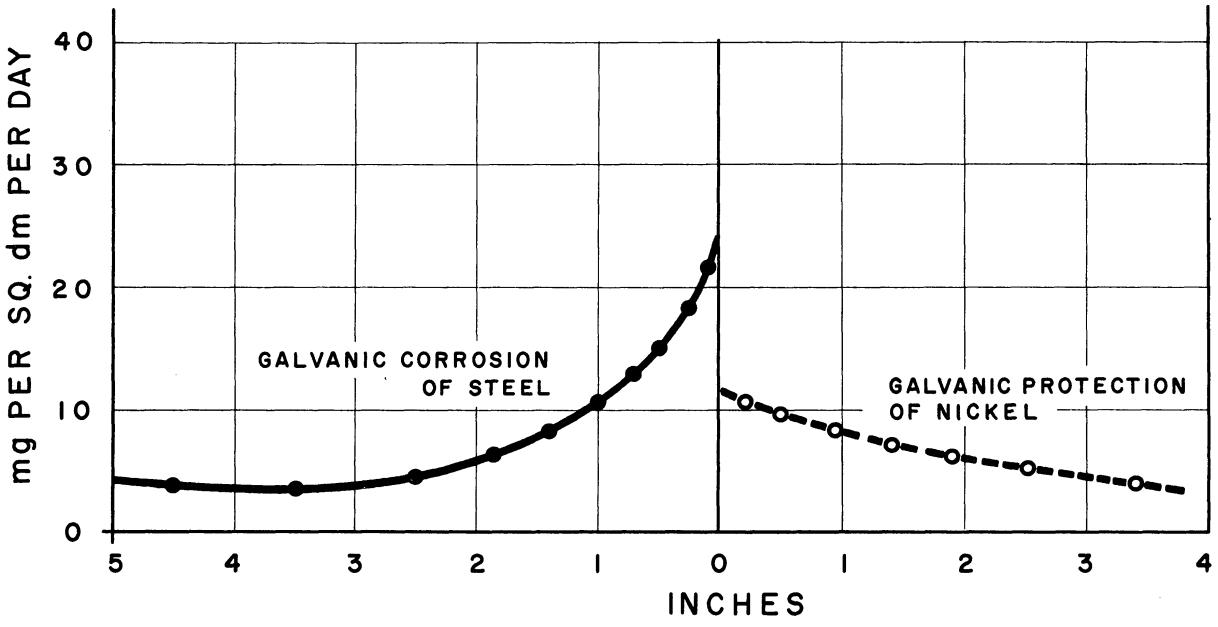

Figure 5. Distribution of galvanic effects from line of contact of steel and nickel in water.

In couples exposed to the atmosphere, the high electrical resistance of the thin film of rain or condensed moisture that forms the electrolyte in possible galvanic couples, limits the distribution of galvanic action to the immediate vicinity of the contact. This is illustrated by Figure 6 which shows galvanic corrosion of magnesium in contact with steel exposed to the salt atmosphere at Kure Beach. It will be noted that galvanic corrosion of the magnesium was confined to a region not more than 1/4 inch from the edge of the steel, and the steel was likewise protected by the magnesium in an equally narrow region. This leads to the feasibility of avoiding galvanic corrosion in combinations of metals exposed to the atmosphere when drainage prevents pocketing of liquids by using insulating washers that will extend at least 1/4 inch away from the edge of either metal, and thus increase the resistance of the electroyte path sufficiently to practically eliminate galvanic effects.

Similarly, gaskets and compounds used to seal crevices between overlapping dissimilar metals can be effective not only in excluding the electrolyte, but also in avoiding action near the overlapping edges, if the compounds or fabrics used are made to extend a quarter inch or so beyond the edge of the laps.

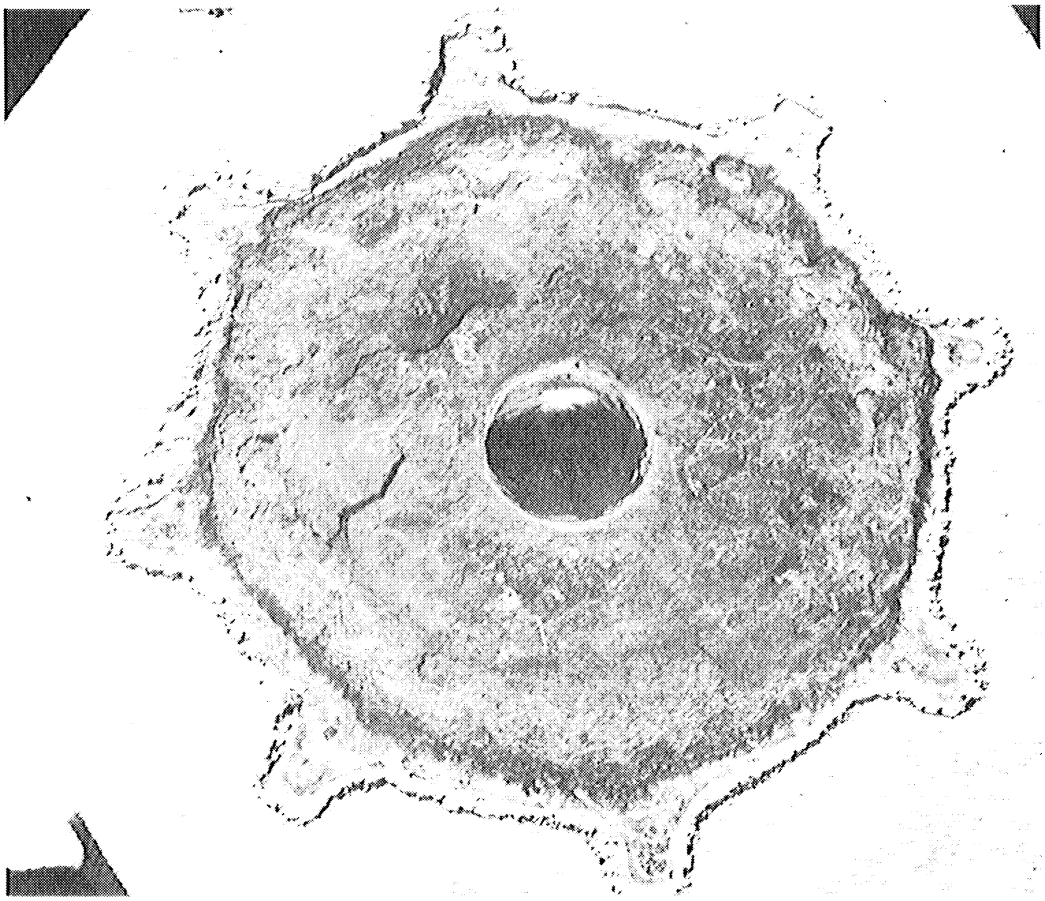

Figure 6. Galvanic corrosion of magnesium casting in contact with steel hub exposed in marine atmosphere for nine years.

A peculiar form of what may be called galvanic corrosion is that due to the electrolyte deposition or "cementation" of a metal in solution onto the surface of a less noble metal with which the solution comes into contact. For example, water which passes through a copper or brass piping system may pick up a small smount of copper as a corrosion product in solution. If this water subsequently comes into contact with a less noble metal such as zinc in a galvanized steel hot water tank or aluminum used for a similar purpose, the copper will plate out on the zinc or aluminum, while an equivalent amount of zinc or aluminum

will be taken into solution or corroded. Corrosion of the zinc or aluminum will be aggravated further by the galvanic action that will follow between the deposited copper and the adjacent zinc or aluminum. A minute concentration of copper, e.g., less than 0.1 part per million is sufficient to make water severly corrosive to aluminum. This effect cannot be avoided by providing electrical insulation between the copper and aluminum portions of the water system. The only remedies other than to avoid the use of aluminum downstream of sources of copper corrosion products would be to treat the water for removal of copper before it comes into contact with the aluminum. In atmospheric exposures, it is wise to avoid circumstances where corrosion products from copper or high-copper alloys might drip or be washed over associated aluminum surfaces.

An appended chart based on experiences with galvanic couples in sea water may be used as a practical guide for estimating the probable direction and extent of galvanic corrosion in couples of several common metals and alloys. This chart takes into account the effects of relative areas and effects of activity and passivity as discussed previously.

Crevice Corrosion

Wherever a crevice exists between overlapping metal surfaces or between a metal and some substance resting on it, there is an opportunity for accelerated corrosion either within the crevice or just outside it. The basic cause of such accelerated corrosion is the difference in the nature of the environment within a crevice as compared with the environment outside it. The difference can be in such details as:

1. The concentration of dissolved oxygen.
2. The concentration of metallic ions.
3. The concentration of dissolved salts.
4. The hydrogen ion concentration or pH.

For this reason, the several possible sources of corrosion currents involved in crevice corrosion are called concentration cells or, sometimes when the concentration of dissolved oxygen is of prime importance, differential aeration cells.

The classic example of a metal ion concentration cell that causes corrosion is represented by a copper alloy tie rod embedded in acid soaked wood in a tank haolding acid for descaling steel.(8) This is illustrated by Figure 7. Copper in corrosion products can escape fairly readily from those surfaces of the tie rod that are close to joints in the wood, but dissolved copper accumulates along the rod away from the joints. This gives rise to a situation where the metal ion concentration of the electrolyte near the joints is much less than elsewhere along the rod. Since the potential of the copper alloy is higher where the concentration of copper ions is lower, as shown by the data in Table 4, the surfaces near the joints act as anodes in a sort of galvanic cell with the cathodes being located away from the joints.

SEA WATER CORROSION OF GALVANIC COUPLES

Legend

- □ The corrosion of the metal under consideration will be reduced considerably in the vicinity of the contact.
- ○ The corrosion of the metal under consideration will be reduced slightly.
- △ The galvanic effect will be slight with the direction uncertain.
- ◬ The corrosion of the metal under consideration will be increased slightly.
- ▲ The corrosion of the metal under consideration will be increased moderately.
- ● The corrosion of the metal under consideration will be increased considerably.

S Exposed area of the metal under consideration is small compared with the area of the metal with which it is coupled.

E Exposed area of the metal under consideration is approximately equal to that of the metal with which it is coupled.

L Exposed area of the metal under consideration is large compared to that of the metal with which it is coupled.

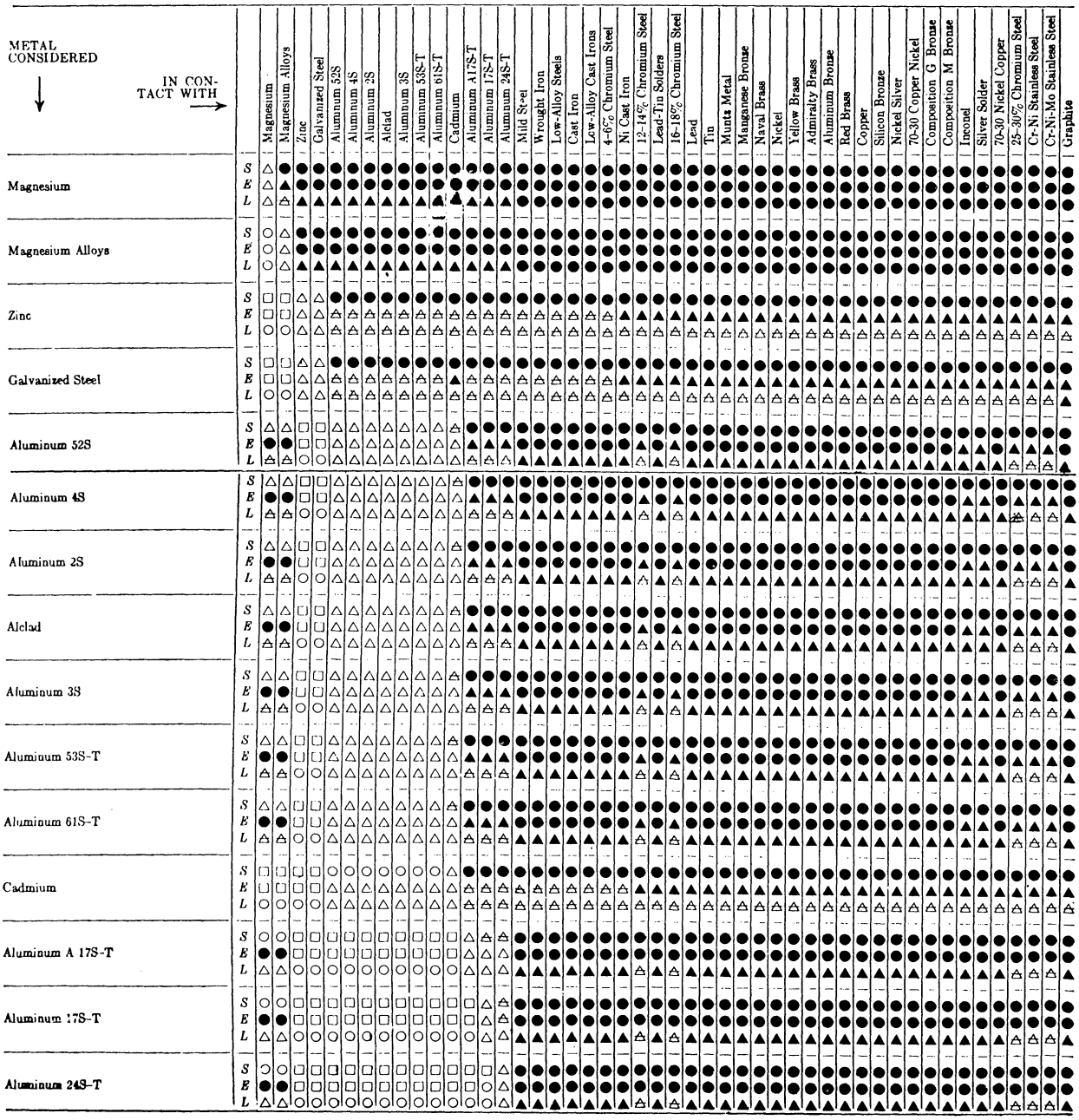

SEA WATER CORROSION OF GALVANIC COUPLES — *Continued*

Legend

□ The corrosion of the metal under consideration will be reduced considerably in the vicinity of the contact.
○ The corrosion of the metal under consideration will be reduced slightly.
△ The galvanic effect will be slight with the direction uncertain.
▲ The corrosion of the metal under consideration will be increased moderately
● The corrosion of the metal under consideration will be increased considerably.

S Exposed area of the metal under consideration is small compared with the area of the metal with which it is coupled.
E Exposed area of the metal under consideration is approximately equal to that of the metal with which it is coupled.
L Exposed area of the metal under consideration is large compared to that of the metal with which it is coupled.

METAL CONSIDERED ↓ / IN CONTACT WITH →		Magnesium	Magnesium Alloys	Zinc	Galvanized Steel	Aluminum 52S	Aluminum 4S	Aluminum 2S	Alclad	Aluminum 3S	Aluminum 53S-T	Aluminum 61S-T	Cadmium	Aluminum A17S-T	Aluminum 17S-T	Aluminum 24S-T	Mild Steel	Wrought Iron	Low-Alloy Steels	Cast Iron	Low-Alloy Cast Irons	4-6% Chromium Steel	Ni Cast Iron	12-14% Chromium Steel	Lead-Tin Solders	16-18% Chromium Steel	Lead	Tin	Muntz Metal	Manganese Bronze	Naval Brass	Nickel	Yellow Brass	Admiralty Brass	Aluminum Bronze	Red Brass	Copper	Silicon Bronze	Nickel Silver	70-30 Copper Nickel	Composition G Bronze	Composition M Bronze	Inconel	Silver Solder	70-30 Nickel Copper	25-30% Chromium Steel	Cr-Ni Stainless Steel	Cr-Ni-Mo Stainless Steel	Graphite
Mild Steel	*S*	□	□	□	□	□	□	□	□	□	□	□	□	□	□	□	△	▲	●	●	●	●	●	●	●	●	●	●	●	●	●	●	●	●	●	●	●	●	●	●	●	●	●	●	●	●	●
	E	□	□	□	□	□	□	□	□	□	□	□	□	□	□	□	△	△	▲	▲	▲	▲	▲	▲	▲	▲	▲	▲	▲	▲	▲	▲	▲	▲	▲	▲	▲	▲	▲	▲	▲	▲	▲	▲	▲	▲	▲
	L	○	○	○	○	○	○	○	○	○	○	○	○	○	○	○	△	△	△	△	△	△	△	△	△	△	△	△	△	△	△	△	△	△	△	△	△	△	△	△	△	△	△	△	△	△	△	△
Wrought Iron	*S*	□	□	□	□	□	□	□	□	□	□	□	□	□	□	□	△	△	●	●	●	●	●	●	●	●	●	●	●	●	●	●	●	●	●	●	●	●	●	●	●	●	●	●	●	●	●	●
	E	□	□	□	□	□	□	□	□	□	□	□	□	□	□	□	△	△	△	△	△	▲	▲	▲	▲	▲	▲	▲	▲	▲	▲	▲	▲	▲	▲	▲	▲	▲	▲	▲	▲	▲	▲	▲	▲	▲	▲
	L	○	○	○	○	○	○	○	○	○	○	○	○	○	○	○	△	△	△	△	△	△	△	△	△	△	△	△	△	△	△	△	△	△	△	△	△	△	△	△	△	△	△	△	△	△	△	△
Low-Alloy Steels	*S*	□	□	□	□	□	□	□	□	□	□	□	□	□	□	□	□	□	△	□	△	▲	●	●	●	●	●	●	●	●	●	●	●	●	●	●	●	●	●	●	●	●	●	●	●	●	●	●
	E	□	□	□	□	□	□	□	□	□	□	□	□	□	□	□	□	□	△	△	△	▲	▲	▲	▲	▲	▲	▲	▲	▲	▲	▲	▲	▲	▲	▲	▲	▲	▲	▲	▲	▲	▲	▲	▲	▲	▲
	L	○	○	○	○	○	○	○	○	○	○	○	○	○	○	○	○	○	△	△	△	△	△	△	△	△	△	△	△	△	△	△	△	△	△	△	△	△	△	△	△	△	△	△	△	△	△	△
Cast Iron	*S*	□	□	□	□	□	□	□	□	□	□	□	□	□	□	□	□	△	●	△	●	▲	●	●	●	●	●	●	●	●	●	●	●	●	●	●	●	●	●	●	●	●	●	●	●	●	●	●
	E	□	□	□	□	□	□	□	□	□	□	□	□	□	□	□	□	□	△	△	△	▲	▲	▲	▲	▲	▲	▲	▲	▲	▲	▲	▲	▲	▲	▲	▲	▲	▲	▲	▲	▲	▲	▲	▲	▲	▲
	L	○	○	○	○	○	○	○	○	○	○	○	○	○	○	○	○	○	△	△	△	△	△	△	△	△	△	△	△	△	△	△	△	△	△	△	△	△	△	△	△	△	△	△	△	△	△	△
Low-Alloy Cast Iron	*S*	□	□	□	□	□	□	□	□	□	□	□	□	□	□	□	□	□	△	△	▲	●	●	●	●	●	●	●	●	●	●	●	●	●	●	●	●	●	●	●	●	●	●	●	●	●	●	—
	E	□	□	□	□	□	□	□	□	□	□	□	□	□	□	□	□	□	△	△	△	▲	▲	▲	▲	▲	▲	▲	▲	▲	▲	▲	▲	▲	▲	▲	▲	▲	▲	▲	▲	▲	▲	▲	▲	▲	▲
	L	○	○	○	○	○	○	○	○	○	○	○	○	○	○	○	○	○	△	△	△	△	△	△	△	△	△	△	△	△	△	△	△	△	△	△	△	△	△	△	△	△	△	△	△	△	△	△
4–6% Cr Steel	*S*	□	□	□	□	□	□	□	□	□	□	□	□	□	□	□	□	□	▲	□	▲	△	●	●	●	●	●	●	●	●	●	●	●	●	●	●	●	●	●	●	●	●	●	●	●	●	●	●
	E	□	□	□	□	□	□	□	□	□	□	□	□	□	□	□	□	□	▲	○	△	▲	▲	▲	▲	▲	▲	▲	▲	▲	▲	▲	▲	▲	▲	▲	▲	▲	▲	▲	▲	▲	▲	▲	▲	▲	▲
	L	○	○	○	○	○	○	○	○	○	○	○	○	○	○	○	○	○	△	○	△	△	△	△	△	△	△	△	△	△	△	△	△	△	△	△	△	△	△	△	△	△	△	△	△	△	△	△
Ni Cast Iron	*S*	□	□	□	□	□	□	□	□	□	□	□	□	□	□	□	□	□	□	□	□	△	●	●	●	●	●	●	●	●	●	●	●	●	●	●	●	●	●	●	●	●	●	●	●	●	●	●	●
	E	□	□	□	□	□	□	□	□	□	□	□	□	□	□	□	□	□	□	□	□	△	▲	▲	▲	▲	▲	▲	▲	▲	▲	▲	▲	▲	▲	▲	▲	▲	▲	▲	▲	▲	▲	▲	▲	▲	▲	▲
	L	○	○	○	○	○	○	○	○	○	○	○	○	○	○	○	○	○	○	○	○	△	△	△	△	△	△	△	△	△	△	△	△	△	△	△	△	△	△	△	△	△	△	△	△	△	△	△
12–14% Chromium Steel	*S*	□	□	□	□	□	□	□	□	□	□	□	□	□	□	□	□	□	□	□	□	□	△	▲	●	▲	▲	●	●	●	●	●	●	●	●	●	●	●	●	●	●	●	●	●	●	●	●	●
	E	□	□	□	□	□	□	□	□	□	□	□	□	□	□	□	□	□	□	□	□	○	△	▲	▲	▲	▲	▲	▲	▲	▲	▲	▲	▲	▲	▲	▲	▲	▲	▲	▲	▲	▲	▲	▲	▲	▲
	L	○	○	○	○	○	○	○	○	○	○	○	○	○	○	○	○	○	○	○	○	○	△	△	△	△	△	△	△	△	△	△	△	△	△	△	△	△	△	△	△	△	△	△	△	△	△	●
Lead-Tin Solders	*S*	□	□	□	□	□	□	□	□	□	□	□	□	□	□	□	□	□	□	□	□	□	△	△	△	△	△	△	△	△	△	△	△	△	△	△	△	△	△	△	△	△	△	△	△	△	△	△	●
	E	□	□	□	□	□	□	□	□	□	□	□	□	□	□	□	□	□	□	□	□	□	△	△	△	△	△	△	△	△	△	△	△	△	△	△	△	△	△	△	△	△	△	△	△	△	△	△	▲
	L	○	○	○	○	○	○	○	○	○	○	○	○	○	○	○	○	○	○	○	○	○	△	△	△	△	△	△	△	△	△	△	△	△	△	△	△	△	△	△	△	△	△	△	△	△	△	▲
16–18% Chromium Steel	*S*	□	□	□	□	□	□	□	□	□	□	□	□	□	□	□	□	□	□	□	□	□	□	△	△	△	●	●	●	●	●	●	●	●	●	●	●	●	●	●	●	●	●	●	●	●	●	●	●
	E	□	□	□	□	□	□	□	□	□	□	□	□	□	□	□	□	□	□	□	□	○	○	△	△	△	△	▲	▲	▲	▲	▲	▲	▲	▲	▲	▲	▲	▲	▲	▲	▲	▲	▲	▲	▲	●
	L	○	○	○	○	○	○	○	○	○	○	○	○	○	○	○	○	○	○	○	○	○	○	△	△	△	△	△	△	△	△	△	△	△	△	△	△	△	△	△	△	△	△	△	△	△	△	●
25–30% Chromium Steel	*S*	□	□	□	□	□	□	□	□	□	□	□	□	□	□	□	□	□	□	□	□	□	□	△	□	△	△	□	□	□	●	●	●	●	●	●	●	●	●	●	●	△	□	△	●	●	●	●	●
	E	□	□	□	□	□	□	□	□	□	□	□	□	□	□	□	□	□	□	□	□	□	□	△	△	△	○	○	○	○	○	○	○	▲	▲	▲	▲	▲	▲	▲	▲	▲	▲	▲	▲	▲	▲	●
	L	○	○	○	○	○	○	○	○	○	○	○	○	○	○	○	○	○	○	○	○	○	○	△	○	△	△	○	○	○	△	△	△	△	△	△	△	△	△	△	△	△	△	△	△	△	△	●
Austenitic Cr-Ni Stainless Steel	*S*	□	□	□	□	□	□	□	□	□	□	□	□	□	□	□	□	□	□	□	□	□	□	△	□	△	△	□	□	□	●	●	●	●	●	●	●	●	●	●	●	△	△	●	●	●	●	●	●
	E	□	□	□	□	□	□	□	□	□	□	□	□	□	□	□	□	□	□	□	□	□	□	△	□	△	△	○	○	○	○	○	▲	▲	▲	▲	▲	▲	▲	▲	▲	▲	▲	▲	▲	▲	▲	●
	L	○	○	○	○	○	○	○	○	○	○	○	○	○	○	○	○	○	○	○	○	○	○	△	○	△	△	○	○	○	△	△	△	△	△	△	△	△	△	△	△	△	△	△	△	△	△	●
Austenitic Cr-Ni-Mo Stainless Steel	*S*	□	□	□	□	□	□	□	□	□	□	□	□	□	□	□	□	□	□	□	□	□	□	△	□	△	△	□	□	□	●	●	●	●	●	●	●	●	●	●	●	△	□	△	●	●	●	●	●
	E	□	□	□	□	□	□	□	□	□	□	□	□	□	□	□	□	□	□	□	□	□	□	△	□	△	△	○	○	○	○	○	▲	▲	▲	▲	▲	▲	▲	▲	▲	▲	▲	▲	▲	▲	▲	●
	L	○	○	○	○	○	○	○	○	○	○	○	○	○	○	○	○	○	○	○	○	○	○	△	○	△	△	○	○	○	△	△	△	△	△	△	△	△	△	△	△	△	△	△	△	△	△	▲
Lead	*S*	□	□	□	□	□	□	□	□	□	□	□	□	□	□	□	□	□	□	□	□	□	□	△	△	△	△	△	△	△	△	△	△	△	△	△	△	△	△	△	△	△	△	△	△	△	△	△	●
	E	□	□	□	□	□	□	□	□	□	□	□	□	□	□	□	□	□	□	□	□	□	□	△	△	△	△	△	△	△	△	△	△	△	△	△	△	△	△	△	△	△	△	△	△	△	△	△	▲
	L	○	○	○	○	○	○	○	○	○	○	○	○	○	○	○	○	○	○	○	○	○	○	△	△	△	△	△	△	△	△	△	△	△	△	△	△	△	△	△	△	△	△	△	△	△	△	▲
Tin	*S*	□	□	□	□	□	□	□	□	□	□	□	□	□	□	□	□	□	□	□	□	□	□	△	△	△	△	△	△	△	△	△	△	△	△	△	△	△	△	△	△	△	△	△	△	△	△	△	●
	E	□	□	□	□	□	□	□	□	□	□	□	□	□	□	□	□	□	□	□	□	□	□	△	△	△	△	△	△	△	△	△	△	△	△	△	△	△	△	△	△	△	△	△	△	△	△	△	▲
	L	○	○	○	○	○	○	○	○	○	○	○	○	○	○	○	○	○	○	○	○	○	○	△	△	△	△	△	△	△	△	△	△	△	△	△	△	△	△	△	△	△	△	△	△	△	△	▲

SEA WATER CORROSION OF GALVANIC COUPLES — *Continued*

Legend

□ The corrosion of the metal under consideration will be reduced considerably in the vicinity of the contact.
○ The corrosion of the metal under consideration will be reduced slightly.
△ The galvanic effect will be slight with the direction uncertain.
⏢ The corrosion of the metal under consideration will be increased slightly.
▲ The corrosion of the metal under consideration will be increased moderately.
● The corrosion of the metal under consideration will be increased considerably.

S Exposed area of the metal under consideration is small compared with the area of the metal with which it is coupled.
E Exposed area of the metal under consideration is approximately equal to that of the metal with which it is coupled.
L Exposed area of the metal under consideration is large compared to that of the metal with which it is coupled.

METAL CONSIDERED ↓ / IN CONTACT WITH →		Magnesium	Magnesium Alloys	Zinc	Galvanized Steel	Aluminum 52S	Aluminum 4S	Aluminum 2S	Alclad	Aluminum 3S	Aluminum 53S-T	Aluminum 61S-T	Cadmium	Aluminum A17S-T	Aluminum 17S-T	Aluminum 24S-T	Mild Steel	Wrought Iron	Low-Alloy Steels	Cast Iron	Low-Alloy Cast Irons	4–6% Chromium Steel	Ni Cast Iron	12–14% Chromium Steel	Lead-Tin Solders	16–18% Chromium Steel	Lead	Tin	Muntz Metal	Manganese Bronze	Naval Brass	Nickel	Yellow Brass	Admiralty Brass	Aluminum Bronze	Red Brass	Copper	Silicon Bronze	Nickel Silver	70-30 Copper-Nickel	Composition G Bronze	Composition M Bronze	Inconel	Silver Solder	70-30 Nickel Copper	25-30% Chromium Steel	Cr-Ni Stainless Steel	Cr-Ni-Mo Stainless Steel	Graphite
Muntz Metal	*S*	□	□	□	□	□	□	□	□	□	□	□	□	□	□	□	□	□	□	□	□	□	□	▲	▲	●	▲	▲	△	□	●	△	●	●	●	●	●	●	●	●	●	●	●	●	●	●	●	●
	E	□	□	□	□	□	□	□	□	□	□	□	□	□	□	□	□	□	□	□	□	□	□	⏢	⏢	⏢	⏢	⏢	△	⏢	⏢	△	⏢	⏢	⏢	⏢	⏢	⏢	⏢	⏢	⏢	⏢	⏢	⏢	⏢	⏢	⏢	●
	L	○	○	○	○	○	○	○	○	○	○	○	○	○	○	○	○	○	○	○	○	○	○	△	△	⏢	△	△	△	△	⏢	△	⏢	⏢	⏢	⏢	⏢	⏢	⏢	⏢	⏢	⏢	⏢	⏢	⏢	⏢	⏢
Manganese Bronze	*S*	□	□	□	□	□	□	□	□	□	□	□	□	□	□	□	□	□	□	□	□	□	□	▲	▲	●	▲	▲	□	△	●	□	●	●	●	●	●	●	●	●	●	●	●	●	●	●	●	●
	E	□	□	□	□	□	□	□	□	□	□	□	□	□	□	□	□	□	□	□	□	□	□	⏢	⏢	⏢	⏢	⏢	○	△	⏢	△	⏢	⏢	⏢	⏢	⏢	⏢	⏢	⏢	⏢	⏢	⏢	⏢	⏢	⏢	⏢	●
	L	○	○	○	○	○	○	○	○	○	○	○	○	○	○	○	○	○	○	○	○	○	○	△	△	△	△	△	△	△	△	△	△	△	△	△	△	△	△	△	△	△	△	△	△	△	△	△	△
Naval Brass	*S*	□	□	□	□	□	□	□	□	□	□	□	□	□	□	□	□	□	□	□	□	□	□	▲	▲	●	▲	▲	△	●	△	△	●	●	●	●	●	●	●	●	●	●	●	●	●	●	●	●
	E	□	□	□	□	□	□	□	□	□	□	□	□	□	□	□	□	□	□	□	□	□	□	⏢	⏢	⏢	⏢	⏢	⏢	⏢	⏢	⏢	⏢	⏢	⏢	⏢	⏢	⏢	⏢	⏢	⏢	⏢	⏢	⏢	⏢	⏢	⏢	▲
	L	○	○	○	○	○	○	○	○	○	○	○	○	○	○	○	○	○	○	○	○	○	○	△	△	△	△	△	△	△	△	△	△	△	△	△	△	△	△	△	△	△	△	△	△	△	△	△	△
Nickel	*S*	□	□	□	□	□	□	□	□	□	□	□	□	□	□	□	□	□	□	□	□	□	□	⏢	△	⏢	△	△	□	□	□	△	●	●	●	●	●	●	●	●	●	●	●	●	●	●	●	●	●
	E	□	□	□	□	□	□	□	□	□	□	□	□	□	□	□	□	□	□	□	□	□	□	○	△	○	△	△	○	○	○	△	△	⏢	⏢	⏢	⏢	⏢	⏢	⏢	⏢	⏢	⏢	⏢	⏢	⏢	⏢	▲
	L	○	○	○	○	○	○	○	○	○	○	○	○	○	○	○	○	○	○	○	○	○	○	△	△	△	△	△	△	△	△	△	△	△	△	△	△	△	△	△	△	△	△	△	△	△	△	△	▲
Inconel (13% Cr, 6.5% Fe, Bal. Ni)	*S*	□	□	□	□	□	□	□	□	□	□	□	□	□	□	□	□	□	□	□	□	□	□	□	△	□	△	△	□	□	□	△	●	●	●	●	●	●	●	●	●	●	●	●	●	●	●	●	●
	E	□	□	□	□	□	□	□	□	□	□	□	□	□	□	□	□	□	□	□	□	□	□	□	○	△	○	△	△	○	○	○	△	△	⏢	⏢	⏢	⏢	⏢	⏢	⏢	⏢	⏢	⏢	⏢	⏢	⏢	⏢	▲
	L	○	○	○	○	○	○	○	○	○	○	○	○	○	○	○	○	○	○	○	○	○	○	△	△	△	△	△	△	△	△	△	△	△	△	△	△	△	△	△	△	△	△	△	△	△	△	△	▲
Yellow Brass	*S*	□	□	□	□	□	□	□	□	□	□	□	□	□	□	□	□	□	□	□	□	□	□	△	▲	●	▲	▲	□	□	▲	△	●	●	●	●	●	●	●	●	●	●	●	●	⏢	●	●	●	●
	E	□	□	□	□	□	□	□	□	□	□	□	□	□	□	□	□	□	□	□	□	□	□	⏢	⏢	⏢	⏢	⏢	○	○	○	△	⏢	⏢	⏢	⏢	⏢	⏢	⏢	⏢	⏢	⏢	⏢	⏢	⏢	⏢	⏢	●
	L	○	○	○	○	○	○	○	○	○	○	○	○	○	○	○	○	○	○	○	○	○	○	△	△	△	△	△	○	○	△	△	△	△	△	△	△	△	△	△	△	△	△	△	△	△	△	⏢
Admiralty Brass	*S*	□	□	□	□	□	□	□	□	□	□	□	□	□	□	□	□	□	□	□	□	□	□	□	▲	●	▲	▲	□	□	□	□	△	□	●	●	●	▲	●	●	●	□	⏢	●	●	●	●	●	●
	E	□	□	□	□	□	□	□	□	□	□	□	□	□	□	□	□	□	□	□	□	□	□	○	⏢	⏢	⏢	⏢	○	○	○	○	△	○	⏢	⏢	⏢	⏢	⏢	⏢	⏢	⏢	⏢	⏢	⏢	⏢	⏢	▲
	L	○	○	○	○	○	○	○	○	○	○	○	○	○	○	○	○	○	○	○	○	○	○	○	△	△	△	△	○	○	○	△	△	△	△	△	△	△	△	△	△	△	△	△	△	△	△	△
Aluminum Bronze	*S*	□	□	□	□	□	□	□	□	□	□	□	□	□	□	□	□	□	□	□	□	□	□	□	▲	●	▲	▲	□	□	□	△	▲	△	●	●	●	▲	●	●	●	△	▲	●	●	●	●	●	●
	E	□	□	□	□	□	□	□	□	□	□	□	□	□	□	□	□	□	□	□	□	□	□	○	⏢	△	△	△	○	○	○	△	○	⏢	⏢	⏢	⏢	⏢	⏢	⏢	⏢	⏢	⏢	⏢	⏢	⏢	⏢	▲
	L	○	○	○	○	○	○	○	○	○	○	○	○	○	○	○	○	○	○	○	○	○	○	○	△	△	△	△	○	○	○	△	○	△	△	△	△	△	△	△	△	△	△	△	△	△	△	⏢
Red Brass	*S*	□	□	□	□	□	□	□	□	□	□	□	□	□	□	□	□	□	□	□	□	□	□	□	▲	▲	▲	▲	□	□	□	□	△	▲	▲	▲	●	▲	▲	□	▲	●	●	●	●	●	●	●
	E	□	□	□	□	□	□	□	□	□	□	□	□	□	□	□	□	□	□	□	□	□	□	○	△	△	△	△	○	○	○	○	△	○	△	△	△	△	⏢	⏢	⏢	⏢	⏢	⏢	⏢	⏢	⏢	⏢	▲
	L	○	○	○	○	○	○	○	○	○	○	○	○	○	○	○	○	○	○	○	○	○	○	○	△	△	△	△	○	○	○	○	△	○	△	△	△	△	△	○	△	△	△	△	△	△	△	△
Copper	*S*	□	□	□	□	□	□	□	□	□	□	□	□	□	□	□	□	□	□	□	□	□	□	□	▲	▲	▲	▲	□	□	□	□	□	□	□	△	△	△	●	△	△	□	△	●	●	●	●	●	●
	E	□	□	□	□	□	□	□	□	□	□	□	□	□	□	□	□	□	□	□	□	□	□	○	△	△	△	△	○	○	○	○	○	△	○	△	△	△	⏢	△	△	○	△	⏢	⏢	⏢	⏢	⏢	▲
	L	○	○	○	○	○	○	○	○	○	○	○	○	○	○	○	○	○	○	○	○	○	○	○	△	△	△	△	○	○	○	○	○	○	○	△	△	△	△	△	△	○	△	△	△	△	△	⏢
Silicon Bronze	*S*	□	□	□	□	□	□	□	□	□	□	□	□	□	□	□	□	□	□	□	□	□	□	□	▲	▲	▲	▲	□	□	□	□	△	□	△	△	△	△	●	△	△	□	⏢	●	●	●	●	●	●
	E	□	□	□	□	□	□	□	□	□	□	□	□	□	□	□	□	□	□	□	□	□	□	○	△	△	△	△	○	○	○	○	○	○	△	△	△	△	⏢	△	△	○	△	⏢	⏢	⏢	⏢	⏢	▲
	L	○	○	○	○	○	○	○	○	○	○	○	○	○	○	○	○	○	○	○	○	○	○	○	△	△	△	△	○	○	○	○	○	○	○	△	△	△	△	○	△	△	△	△	△	△	△	⏢
Nickel Silver	*S*	□	□	□	□	□	□	□	□	□	□	□	□	□	□	□	□	□	□	□	□	□	□	□	⏢	□	⏢	⏢	□	□	□	□	△	□	△	△	△	△	▲	△	△	□	⏢	●	●	●	●	●	●
	E	□	□	□	□	□	□	□	□	□	□	□	□	□	□	□	□	□	□	□	□	□	□	○	△	○	△	△	○	○	○	○	○	○	△	△	△	△	△	⏢	⏢	○	△	⏢	⏢	⏢	⏢	⏢	▲
	L	○	○	○	○	○	○	○	○	○	○	○	○	○	○	○	○	○	○	○	○	○	○	○	△	○	△	△	○	○	○	○	○	○	△	△	△	△	△	△	△	○	△	△	△	△	△	⏢
70–30 Copper Nickel	*S*	□	□	□	□	□	□	□	□	□	□	□	□	□	□	□	□	□	□	□	□	□	□	□	⏢	□	△	△	□	□	□	□	□	□	□	□	□	□	□	△	△	□	△	□	●	●	●	●	●
	E	□	□	□	□	□	□	□	□	□	□	□	□	□	□	□	□	□	□	□	□	□	□	○	△	○	△	△	○	○	○	○	○	○	○	○	○	○	○	△	△	○	△	⏢	⏢	⏢	⏢	⏢	▲
	L	○	○	○	○	○	○	○	○	○	○	○	○	○	○	○	○	○	○	○	○	○	○	○	△	○	△	△	○	○	○	○	○	○	○	○	○	○	○	○	△	○	△	△	△	△	△	△
Composition G Bronze (88% Cu, 2% Zn, 10% Sn)	*S*	□	□	□	□	□	□	□	□	□	□	□	□	□	□	□	□	□	□	□	□	□	□	□	⏢	□	△	△	□	□	□	□	□	□	□	□	□	△	△	△	△	△	□	△	●	●	●	●	●
	E	□	□	□	□	□	□	□	□	□	□	□	□	□	□	□	□	□	□	□	□	□	□	○	△	○	△	△	○	○	○	○	○	○	○	○	○	○	○	△	△	○	△	⏢	⏢	⏢	⏢	⏢	▲
	L	○	○	○	○	○	○	○	○	○	○	○	○	○	○	○	○	○	○	○	○	○	○	○	△	○	△	△	○	○	○	○	○	○	○	○	○	○	○	○	△	○	△	△	△	△	△	△
Composition M Bronze (88% Cu, 3% Zn, 6.5% Sn, 1.5% Pb)	*S*	□	□	□	□	□	□	□	□	□	□	□	□	□	□	□	□	□	□	□	□	□	□	□	⏢	□	△	△	□	□	□	□	□	□	□	□	□	△	△	△	△	△	□	△	●	●	●	●	●
	E	□	□	□	□	□	□	□	□	□	□	□	□	□	□	□	□	□	□	□	□	□	□	○	△	○	△	△	○	○	○	○	○	○	○	○	○	○	○	△	△	○	△	⏢	⏢	⏢	⏢	⏢	▲
	L	○	○	○	○	○	○	○	○	○	○	○	○	○	○	○	○	○	○	○	○	○	○	○	△	○	△	△	○	○	○	○	○	○	○	○	○	○	○	○	△	○	△	△	△	△	△	△

SEA WATER CORROSION OF GALVANIC COUPLES — *Continued*

Legend

□ The corrosion of the metal under consideration will be reduced considerably in the vicinity of the contact.
○ The corrosion of the metal under consideration will be reduced slightly.
△ The galvanic effect will be slight with the direction uncertain.
⏢ The corrosion of the metal under consideration will be increased slightly.
▲ The corrosion of the metal under consideration will be increased moderately.
● The corrosion of the metal under consideration will be increased considerably.

S Exposed area of the metal under consideration is small compared with the area of the metal with which it is coupled.
E Exposed area of the metal under consideration is approximately equal to that of the metal with which it is coupled.
L Exposed area of the metal under consideration is large compared to that of the metal with which it is coupled.

METAL CONSIDERED ↓ / IN CONTACT WITH →		Magnesium	Magnesium Alloys	Zinc	Galvanized Steel	Aluminum 52S	Aluminum 4S	Aluminum 2S	Alclad	Aluminum 3S	Aluminum 53S-T	Aluminum 61S-T	Cadmium	Aluminum A17S-T	Aluminum 17S-T	Aluminum 24S-T	Mild Steel	Wrought Iron	Low-Alloy Steels	Cast Iron	Low-Alloy Cast Irons	4-6% Chromium Steel	Ni Cast Iron	12-14% Chromium Steel	Lead-Tin Solders	16-18% Chromium Steel	Lead	Tin	Muntz Metal	Manganese Bronze	Naval Brass	Nickel	Yellow Brass	Admiralty Brass	Aluminum Bronze	Red Brass	Copper	Silicon Bronze	Nickel Silver	70-30 Copper Nickel	Composition G Bronze	Composition M Bronze	Inconel	Silver Solder	70-30 Nickel Copper	25-30% Chromium Steel	Cr-Ni Stainless Steel	Cr-Ni-Mo Stainless Steel	Graphite
Silver Solder	*S*	□	□	□	□	□	□	□	□	□	□	□	□	□	□	□	□	□	□	□	□	□	□	□	□	○	□	□	□	□	□	□	□	□	□	□	□	□	△	△	△	△	△	⏢	⏢	⏢	●
	E	□	□	□	□	□	□	□	□	□	□	□	□	□	□	□	□	□	□	□	□	□	□	○	○	○	□	□	□	○	△	○	△	○	○	○	○	△	△	△	△	△	△	⏢	⏢	⏢	⏢
	L	○	○	○	○	○	○	○	○	○	○	○	○	○	○	○	○	○	○	○	○	○	○	△	△	△	△	△	△	△	△	△	△	△	△	△	△	△	△	△	△	△	△	⏢	⏢	⏢	⏢
70-30 Nickel-Copper	*S*	□	□	□	□	□	□	□	□	□	□	□	□	□	□	□	□	□	□	□	□	□	□	□	□	□	□	□	□	□	□	□	□	□	□	□	□	□	□	□	□	□	△	⏢	⏢	⏢	●
	E	□	□	□	□	□	□	□	□	□	□	□	□	□	□	□	□	□	□	□	□	□	□	○	○	○	□	□	□	○	○	○	○	○	○	○	○	○	○	○	○	○	○	△	△	△	⏢	⏢
	L	○	○	○	○	○	○	○	○	○	○	○	○	○	○	○	○	○	○	○	○	○	○	○	○	○	○	○	○	○	○	○	○	○	○	○	○	○	○	○	○	○	○	△	△	△	△	⏢

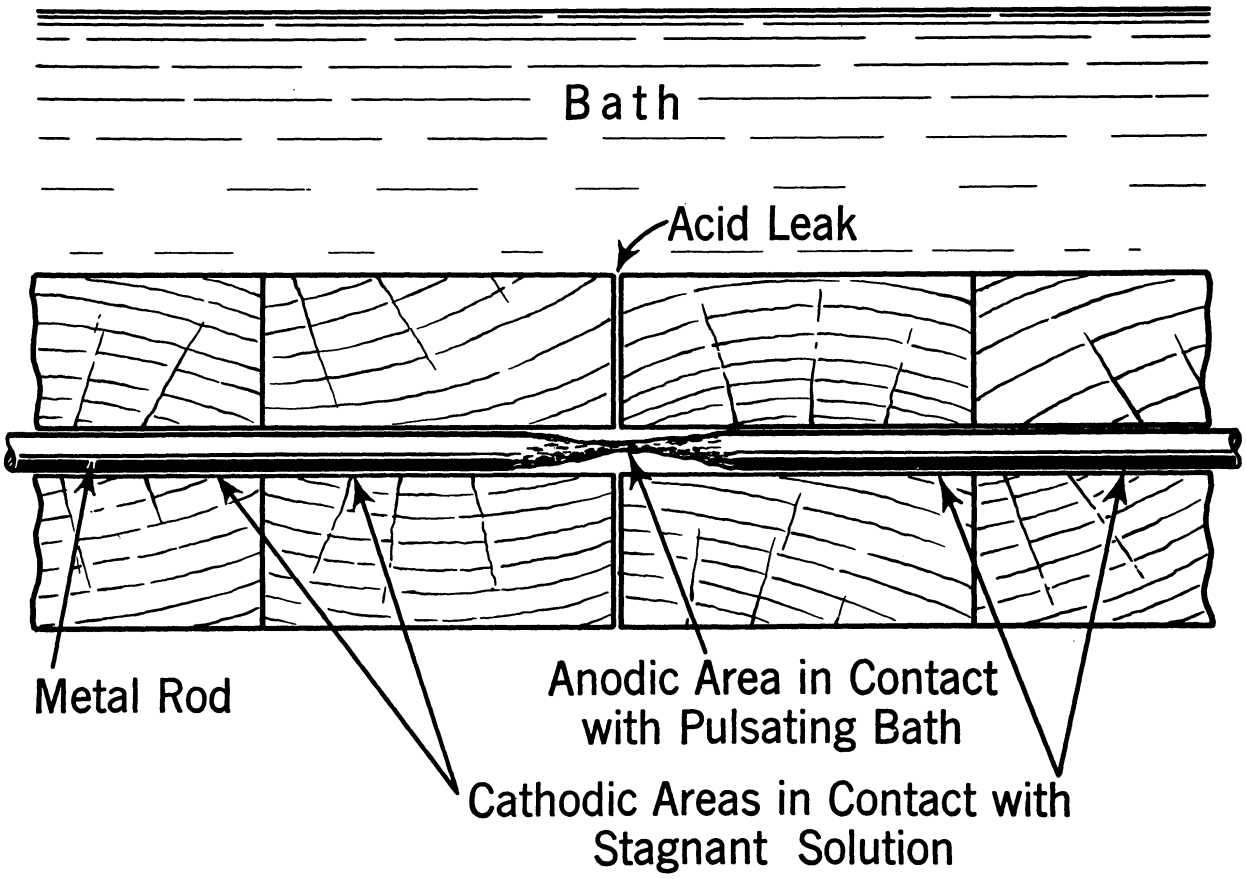

Figure 7. Concentration cell corrosion of tie rod in acid pickling tank.

Table 4

Potentials of Copper-Ion Concentration Cells

Concentration of Copper in Solution in Contact with Copper Anode	Concentration of Copper in Solution in Contact with Copper Cathode	Potential Difference in Millivolts Theoretical - Observed	
0.01 Normal	0.1 Normal	28	31
0.001 Normal	0.1 Normal	58	59
0.0001 Normal	0.1 Normal	92	99

The best remedy for this sort of corrosion difficulty is to avoid the crevices in the first place, but where, as in the example cited, this is not possible, favorable steps would be:

1. To reduce washing out of corrosion products by keeping the rods tightened so as to close up the joints.
2. Use alloys showing minimum susceptibility to metallic ion concentration cell effects, e.g., high nickel alloys are generally better than high copper alloys.

Differential aeration or oxygen concentration cells are encountered more frequently than metal ion concentration cells. Tendency to such aeration cell action is indicated in a rough way by the position of the metals in the standard electro-motive series of the elements, and generally, also by position in the galvanic series already shown in Table 3. Metals towards the top of the series are generally more susceptible to differential aeration cells than those towards the bottom. This is also true of alloys that develope oxide films that make them passive or more noble than their principal costituents, e.g., the stainless steels. In the case of such alloys which may exhibit a broad range of solution potentials between their active and passive states, as already discussed, the differential aeration cell may become a much more powerful active-passive cell. Here, the surfaces within the crevice are starved of the oxygen necessary for the maintenance of passivity, while those surfaces outside the crevice having relatively free access to oxygen remain passive. The result is a powerful galvanic cell with the anode within the crevice and the cathode outside. The driving potential can be over half a volt. Like other galvanic cells, these active-passive cells obey the same general laws with respect to potential gradient, resistance and polarization effects. This includes area effects. As might be anticipated, the greatest corrosion damage within a crevice occurs when the area of the passive cathode outside the crevice is relatively large. This was demonstrated[9] in experiments with crevice couples of Type 430 stainless steel assembled as shown in Figure 8 and exposed to sea water for 87 days. Figures 9 for

weight losses and 10 for depth of attack within the crevices are very similar to Figure 3 for iron-copper couples and show that corrosion in a crevice involving an active-passive cell effect is proportional to the exposed area of passive alloy outside the crevice. This principle applies as well to other differential aeration cell situations. An example of crevice corrosion of a cast iron cylinder liner coller with salt water is shown in Figure 11. Here the anodic crevice was formed by a gasket used to seal the liner in the cylinder block.

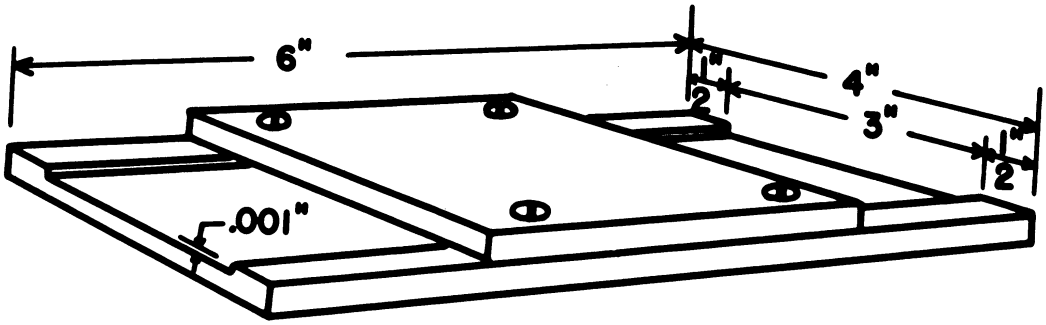

Figure 8. Specimen used for studying area effects in crevice corrosion.

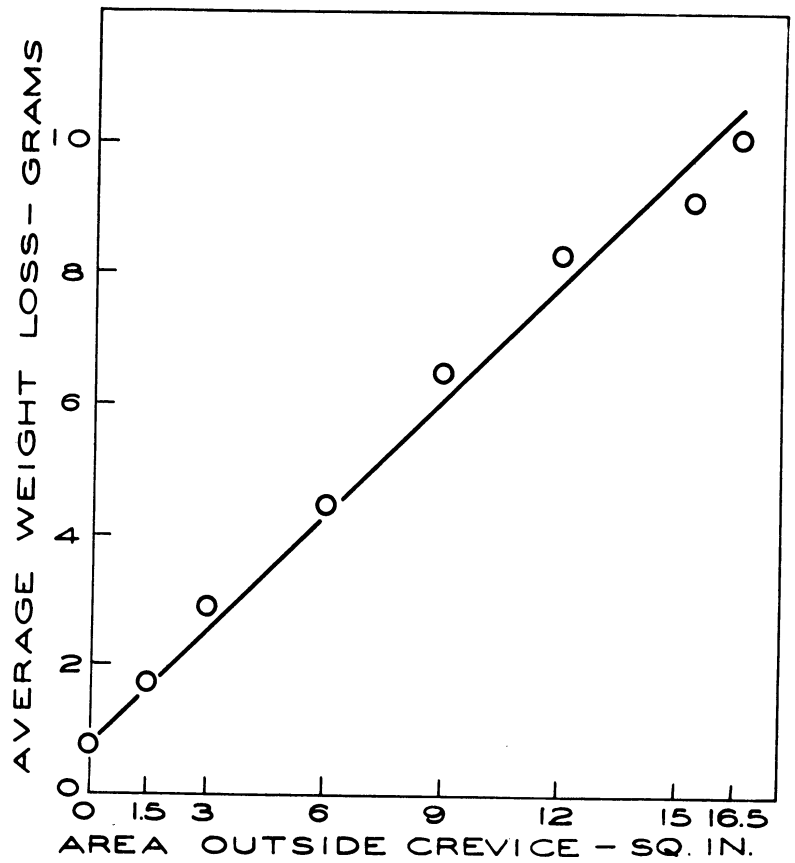

Figure 9. Average weight loss of specimens versus area of specimen outside the crevice.

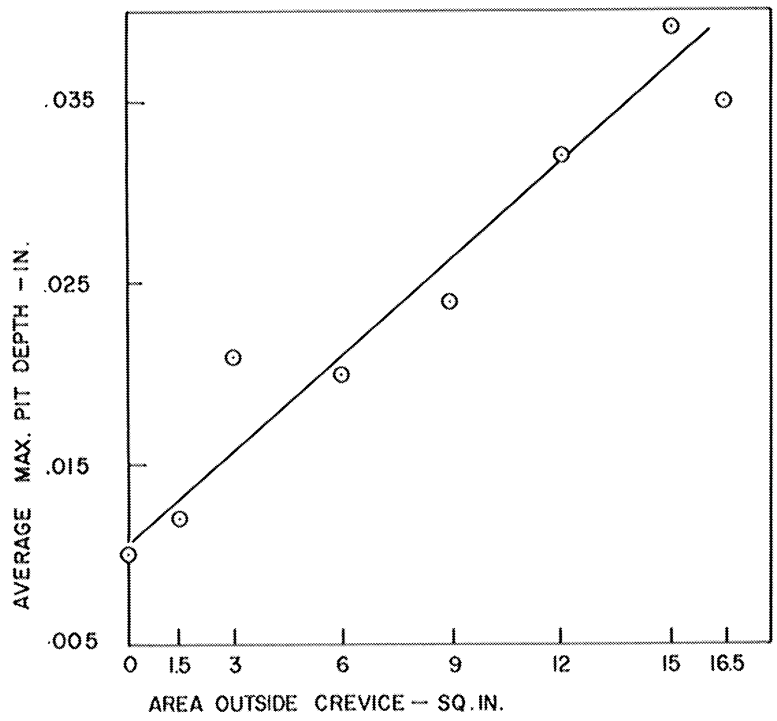

Figure 10. Average maximum pit depth within the crevice versus area of specimen outside the crevice.

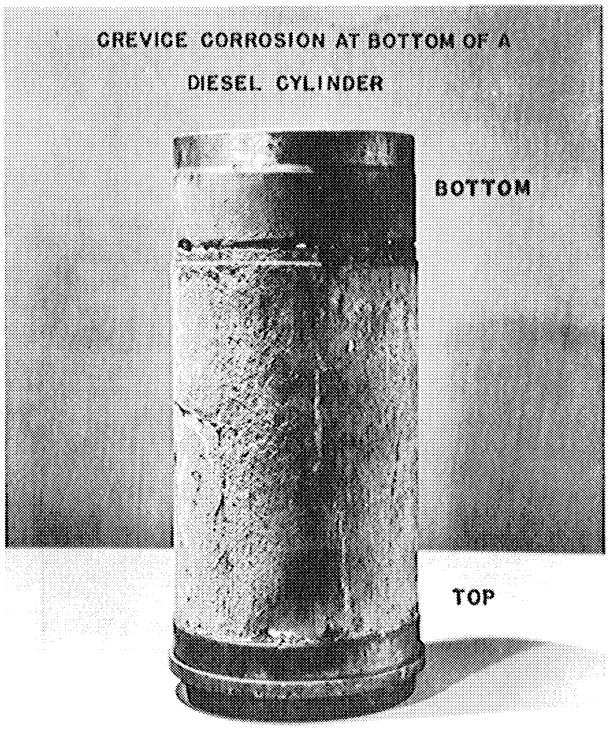

Figure 11. Crevice Corrosion at bottom of a diesel cylinder.

The best way to avoid differential aeration crevice corrosion is to avoid crevices, as by:

1. Using butt joints instead of lap joints.
2. Sealing lap joints if they must be used.
3. Keeping surfaces clean and free from partially adherent deposits - this may be accomplished by periodic scrubbing or by maintaining the flow of liquids at a high enough velocity to prevent any solids (including corrosion products) from adhering to the metal surface.
4. Avoiding contact with porous substances that can act like poultices, e.g., insulation, gaskets, packing, etc.
5. Use of passivating compounds in packings where this is possible.
6. Where crevices cannot be avoided, use alloys showing minimum susceptibility to crevice corrosion. For example, in the copper-nickel alloy system, the nickel rich alloys are more susceptible to differential aeration cell effects than the copper rich alloys. On the other hand, the latter are more susceptible than the former to metal ion concentration cells.However, since the location of the anodes is within the crevice in the one case (differential aeration cell) and outside the crevice in the other (metal ion cell), the two types of cell tend to counteract each other in the nickel-copper alloys. This makes the copper-nickel alloys containing around 30% nickel or 10% nickel with about 1% iron particularly resistant to crevice corrosion effects.

While all stainless steels are more or less susceptible to crevice corrosion, the resistance to such attack varies through wide limits. The straight chromium stainless steels are most susceptible, while the more higly alloyed chromium-nickel-stainless steels are much less susceptible and especially when they contain extra amounts of nickel and molybdenum. An approximate order of merit of alloys in the general class of stainless steels in resisting crevice corrosion is as follows - the best being at the top of the list and the worst at the bottom.

1. Hastelloy C
2. Ni-o-nel
3. Carpenter 20
4. Type 317
5. Type 316
6. Type 310
7. Inconel
8. Type 309
9. Types 302, 304, 321, 347
10. Type 446
11. Type 431
12. Type 430
13. Type 430F
14. Type 410
15. Type 416

Pitting

Pitting may be considered to be a special form of galvanic corrosion where the anode is within the pit and the cathode is a surface outside the pit. Pits may represent also a special case of crevice corrosion and be initiated by the concentration cell effects discussed with respect to this form of corrosion. Frequently, the corrosion products that accumulate within a pit change the chemical nature of the environment, e.g., so as to make it more acid and thus tend to keep a pit in an active state so that corrosion will proceed at a rate that may sometimes accelerate as corrosion products accumulate. By and large, the remarks made with respect to crevice corrosion apply to pitting as well and need not be repeated in detail. Pitting has received a great deal of study by many investigators (10-13) whose writing should be consulted for detailed information with respect to particular metals and alloys.

Charts showing the graphical treatment of the behavior of galvanic couples were reprinted with permission from H. H. Uhlig, Editor, Corrosion Handbook, John Wiley and Sons, Inc.

REFERENCES

1. Hoxeng, R.B., and Prutton, C.F., Corrosion, 5, 10, 330.

2. LaQue, F.L., and Cox, G.L., Proc. Am. Soc. Test. Mat., 40, 670, 1940.

3. Darrin, Marc, Ind. and Eng. Chem., 37, 45, 8, 741.

4. Daugherty, M.W., and Koenig, R.F., S.A.E. Paper, 339, Summer Meeting, June, 1949.

5. Wesley, W.A., Proc. Am. Soc. Test. Mat. 40, 690, 1940.

6. Seagren, G.W., and LaQue, F.L., Corrosion, 3, 97, 1947.

7. Copson, H.R., Trans. Electrochem. Soc., 84, 71, 1943.

8. McKay, R.J., Trans. Am. Electrochem. Soc., 41, 201, 1922.

9. Ellis, O.B., and LaQue, F.L., Corrosion, 7, 11, 362, 1951.

10. Uhlig, H.H., Trans Am. Inst. Min. and Met., Eng., 140, 411, 1940.

11. May, R., Journal Inst. Met., 82, 65, 1953.

12. Aziz, P.M., and Godard, H.P., Ind. and Eng. Chem., 44, 1791, 1952.

13. Streicher, M.A., Journal Electrochem. Soc., 103, 375, 1956.

ACCELERATED CAVITATION RESEARCH

William J. Rheingans
Manager, Hydraulic Department
Allis-Chalmers Manufacturing Co.

ACCELERATED CAVITATION RESEARCH

by

William J. Rheingans

INTRODUCTION

An accelerated cavitation machine of the vibratory type was constructed by the Research Laboratory of the Allis-Chalmers Mfg. Co. in 1948 and was placed in operation in September of that year. It has been in continous use ever since for making hundreds of tests on a large variety of materials to determine their relative resistance to cavitation and has also been used for making investigations of some of the phenomena of cavitation and pitting.

These tests supplement the accelerated cavitation tests made during the years 1934 to 1937 by J. M. Mousson(1) and S. Logan Kerr(2) who tested about all the materials available at that time which were suited for use on hydraulic machinery. The development of new materials and new techniques for the application of materials since 1937, some of which have unusually high resistance to pitting or other advantages when used where cavitation occurs, indicated the necessity for continous research of this type and resulted in the construction of the accelerated cavitation machine discribed in this article.

HISTORY OF CAVITATION

The following is a brief history of cavitation and the problems which brought about the development of accelerated cavitation machines.

Cavitation as used throughout this article is defined as the formation of voids within a body of moving liquid (or around a body moving in liquid) when the particles of liquid fail to adhere to the boundaries of the passageway. This occurs when there is insufficient internal pressure to overcome the inertia of the particles and force them to take sufficiently curved paths along a boundary which has a change or variation in shape.

Cavitation affects the operation of hydraulic machinery in various ways. It can cause a loss of power and efficiency by increasing resistance to the flow. It can produce noise and vibration and it can produce pitting which is defined as the actual erosion of material subjected to cavitation.

The phenomenon of cavitation was anticipated as early as 1754 by Leonhard Euler(3) in his theory on hydraulic turbines when he noted that an insufficient pressure in a perfect liquid can cause a divergence between theory and experiment and can result in zero resistance.

Some of the practical aspects of cavitation were first noted in connection with ship propellers operating at high speeds. Sidney W. Barnaby and Mr. Thorncroft, in a paper presented to the Institution of Civil Engineers in London in 1895, mentioned the occurance of a new phenomenon during propellor trials of HMS Daring.(4) They noted the formation of cavities in water which tended to become filled with water vapor. This condition was held responsible for waste of power and other difficulties. About the same time Chas. A. Parsons(5) verified this by tests on the SS Turbina where loss of power on the first stream turbine driven propellers was traced to cavitation.

The first recorded indication that cavitation produced erosion or pitting of materials was in an article published in 1907 by W. Wagenbach(6), in which he described how the Francis turbine runners of the Jaice hydroelectric works in Bosnia failed after a few weeks operation in 1890. The runners were so badly eroded by cavitation that they had to be replaced. After this there were numerous reports of pitting, both on hydraulic turbine runners and on ship propellers.

However, the wide variation in the resistance of different materials, to pitting is a phenomenon that was first discovered during the 1920's. It is probable that prior to this period some engineers may have suspected such variations but there is no record of any published information on actual comparative tests.

J. Ackert in his handbook published in 1926(7), reported the relative resistance of cast iron, cast steel and bronze to erosion or pitting.

In 1924 the Allis-Chalmer Mfg. Co. fastened 15 patch plates of various types of materials to the back sides of the buckets near the discharge edge on a cast iron Francis runner furnished for the Isle Malign Plant in Quebec. An inspection of this runner after three and one half years of operation showed that patch plates of stainless steel resisted pitting to a remarkable degree as compared to the cast iron in the runner and as compared to other materials used in the remainder of the patch plates. About this time similar experiments with various materials including stainless steel were being made on hydraulic turbine runners in a number of other power plants. However, it was soon realized that using different types of material in a hydraulic turbine and then waiting a number of years for an answer was not a very satisfactory method of determining the degree of resistance to pitting of these materials. The time interval was entirely too long, and there was no satisfactory method for comparing materials tried in one turbine with those tried in another.

Therefore, starting about 1932 several types of machines were developed which were capable of producing accelerated cavitation whereby the resistance of various metals to pitting could be determined accurately under laboratory control within a reasonable period of time.(8)

The earlier machines used the principal of passing water at a high velocity through a restricted area, followed by a sudden enlargement. This was known as the venturi tube type of machine.

In 1935, Dr. J. C. Hunsacker and Dr. H. Peters of Massachusetts, Institute of Technology developed the vibratory method of accelerated cavitation.(9,10) This is the method used for tests described in this article.

CAVITATION MACHINE

Figure 1 shows a schematic layout of the vibratory type of accelerated cavitation machine.

The apparatus follows the general description by S. Logan Kerr(2). It consists of a vacuum tube oscillator which produces an alternating magnetic field through the nickel tube. When the frequency of the magnetic field is the same as the natural longitudinal frequency of vibration of the nickel tube, the tube will vibrate at maximum amplitude in the longitudinal direction.

The test specimen Figure 2 is attached to the end of the tube and immersed in the test fluid to a depth of 1/8 in. Since the test fluid heats rapidly during a test run and since the rate of pitting varies considerably with the temperature of the fluid, the beaker containing the test fluid is set in a running water bath to maintain a constant temperature of 76 deg. plus or minus 1 deg.

Since the frequency and amplitude of vibration of the test specimen have considerable effect on the rate of pitting, provisions are made to control these quantities at all times. The frequency of course is determined by the length of the nickel tube. The vacuum tube oscillator circuit is tuned to the natural frequency of the nickel tube. All tests are made at a frequency of 6500 cycles per second this being the natural frequency of vibration of the nickel tube 12 in. long, with test button attached.

An electric strain gauge is attached to the nickel tube to measure the amplitude of longitudinal vibration. It is calibrated at frequent intervals by measuring the actual movement of the test specimen by means of a stroboscopic light and microscope with micrometer scale. All tests are made with an amplitude of vibration of .0034 in. In this paper, the amplitude of vibration refers to the total travel of the test specimen. The criterion for rate of pitting is the loss of weight of the test specimen.

Method of Testing

As a check on the relative performance of the vibratory machine, it was decided to use a brass test specimen as a standard to be tested at frequent intervals. By comparing the rate of pitting of the

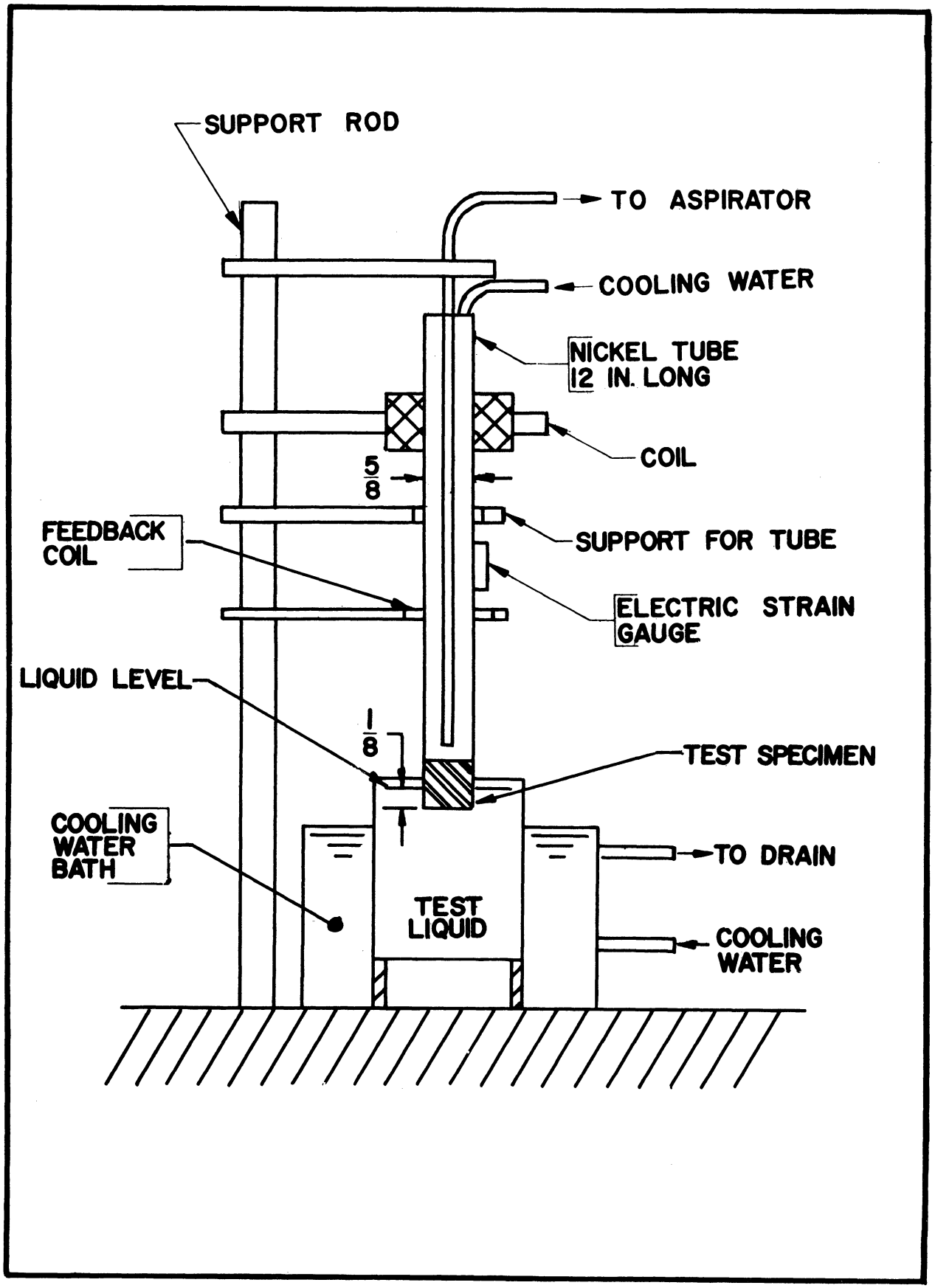
SUPPORT ROD
TO ASPIRATOR
COOLING WATER
NICKEL TUBE
12 IN. LONG
COIL
5/8
FEEDBACK
COIL
SUPPORT FOR TUBE
ELECTRIC STRAIN
GAUGE
LIQUID LEVEL
1/8
TEST SPECIMEN
COOLING
WATER
BATH
TO DRAIN
TEST
LIQUID
COOLING
WATER

Figure 1.

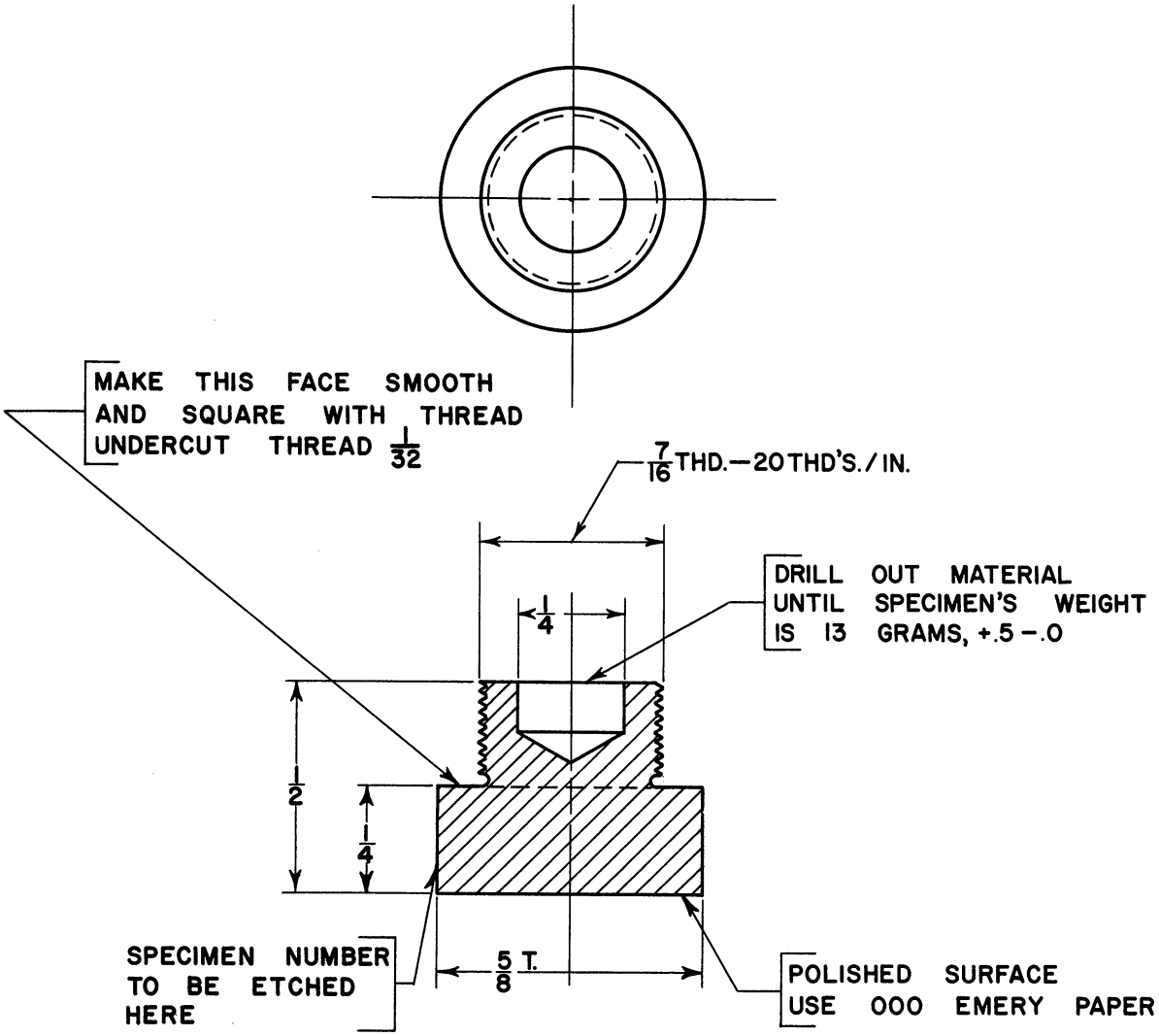
MAKE THIS FACE SMOOTH AND SQUARE WITH THREAD UNDERCUT THREAD 1/32
7/16 THD.—20 THD'S./IN.
DRILL OUT MATERIAL UNTIL SPECIMEN'S WEIGHT IS 13 GRAMS, +.5 −.0
1/4
1/2
1/4
SPECIMEN NUMBER TO BE ETCHED HERE
5/8 T.
POLISHED SURFACE USE 000 EMERY PAPER

Figure 2.

various standard specimens, any serious deviation in the relative performance of the apparatus becomes apparent immediately.

At first cast bronze was used for this purpose. However, it was found that this material would pick up water and actually increase in weight during the first 30 minutes of testing. The standard test specimen was then changed to rolled brass, ASTM Specifications B-16-44, which gave satisfactory results.

However, since most materials, particularly cast materials have a tendency to pick up some moisture during the course of a 2 hour cavitation test, all of the test specimens are placed in boiling water for 30 minutes, before being tested and before being weighed.

All of the test specimens are carefully adjusted to the same weight within 1/2 gram. They are all weighed accurately to the nearest 1/10 milligram in a chemical balance scale. All specimens are weighed every 30 minutes during the test. It was found that the rate of loss of some of the metals increases for the first 60 to 90 minutes but after that period the loss approaches a fairly constant rate. The length of each test was therefore limited to 120 minutes. Figure 3 shows how the rate of loss of metal varied with time. It was observed in several instances that a highly polished specimen had a slower rate of pitting during the first 60 minutes of testing than the same material with a dull finish. However, by the end of a 120 minute test the highly polished specimen would be pitting at the same rate as the duller specimen.

Effect of Amplitude of Vibration

An interesting series of tests was made on several materials to determine the effect on the rate of pitting by changing the amplitude of vibration of the test specimen. The construction of the accelerated cavitation machine made it possible to control the amplitude of vibration by controlling the power output of the vacuum tube oscillator. The amplitude was measured by means of the electric strain gauge fastened to the nickel tube. This strain gauge was calibrated at frequent intervals by means of a microscope micrometer. During these tests the frequency of vibration was the same as for all the tests described in this paper, namely 6,500 cycles per second.

Figure 4 shows how the amount of pitting decreased as the amplitude was decreased. There was very little difference in the rate of pitting between .0030 inches and .0035 inches amplitude. For this reason an amplitude of .0034 inches was selected for all the standard tests made on different materials to determine their relative resistance to pitting. Thus a slight variation in amplitude for different tests had very little effect on the relative rate of pitting of the test specimens.

The results of these tests indicate that a certain amplitude of vibration of the test specimen is needed to produce actual pitting, and that the magnitude of the amplitude required varies for different metals.

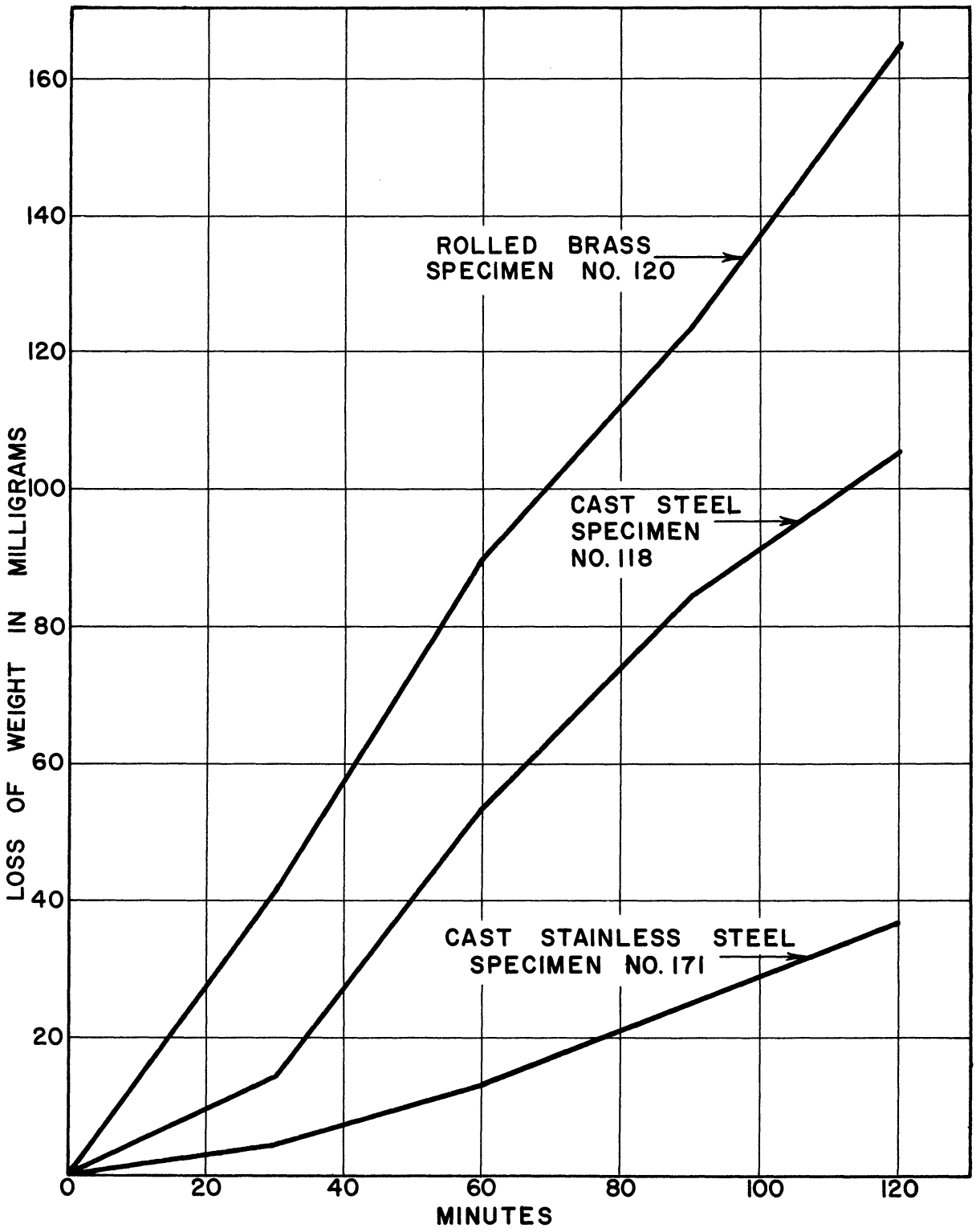
ROLLED BRASS
SPECIMEN NO. 120
CAST STEEL
SPECIMEN
NO. 118
CAST STAINLESS STEEL
SPECIMEN NO. 171
LOSS OF WEIGHT IN MILLIGRAMS
MINUTES
0
20
40
60
80
100
120
140
160

Figure 3.

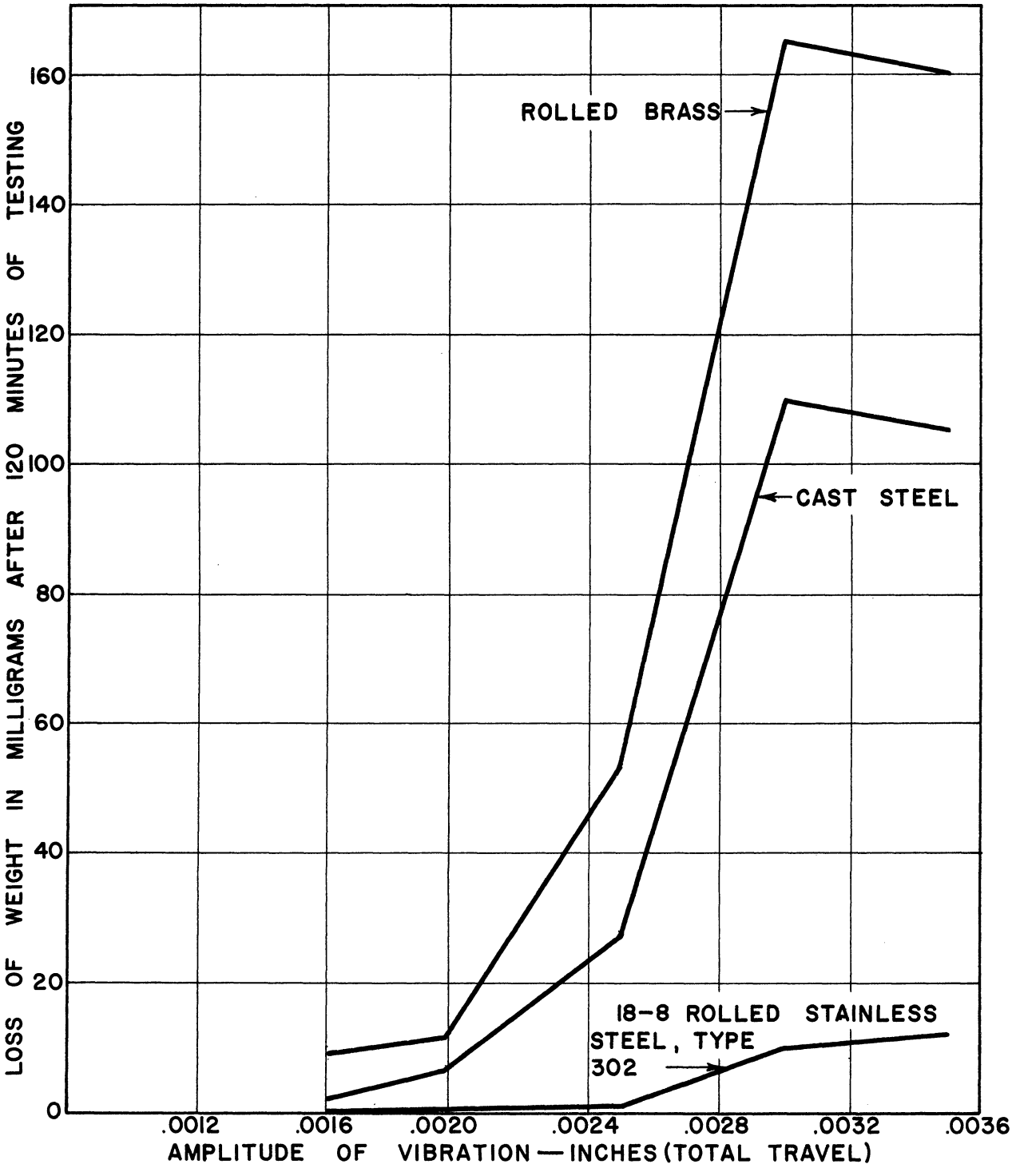
LOSS OF WEIGHT IN MILLIGRAMS AFTER 120 MINUTES OF TESTING
160
140
120
100
80
60
40
20
0
ROLLED BRASS
CAST STEEL
18-8 ROLLED STAINLESS STEEL, TYPE 302
.0012
.0016
.0020
.0024
.0028
.0032
.0036
AMPLITUDE OF VIBRATION — INCHES (TOTAL TRAVEL)

Figure 4.

The 18-8 rolled stainless steel type 302 required an amplitude of .0025 inches before pitting became appreciable. The cast steel specimen showed very little pitting below .0016 inches amplitude, and the brass specimen probably would have stopped pitting below .001 inches if the tests had been carried to such low values.

Apparently there is a difference in the minimum force required to produce pitting on different materials and changing the amplitude of vibration seems to change the forces that produce pitting. This experimental data corresponds to some of the field results, where cast iron or cast steel which pitted rapidly was replaced with stainless steel which did not pit at all under the same operating and cavitation conditions.

Just what the forces are that are created by the vibrating specimen and that produce pitting is still open to speculation. The maximum velocity of the test specimen when vibrating at 6,500 cycles per second, with an amplitude of .0034 inches is only 5.8 feet per second as computed from the sine wave formula

$$V = FA$$

Where V = Maximum Velocity
F = Frequency
A = Amplitude (full travel)

This velocity is much too low to produce any impact forces sufficient to cause pitting. However, the acceleration of the test specimen is quite high. At .0034 inches amplitude of vibration the maximum acceleration is 7,300 G's or about 235,000 ft. per second. It is possible that this high rate of acceleration is responsible for the forces that produce pitting.

The most logical explanation is the theory by R. T. Knapp and A. Hollander[11] that bubbles form in the cavitation region where the absolute pressure drops below the vapor pressure of the surrounding liquid. They actually demonstrated by high speed moving pictures that cavitation bubbles form in the liquid and then collapse at velocities up to 800 feet per second, depending upon the size of the bubble. These extremely high velocities of collapse produce pressures of approximately 50,000 pounds per square inch, but only over a microscopically small area.

Observation of the test specimens after having been tested at various amplitudes of vibration showed that the pitted area on the bottom of the button, and the depth of pitting decreased with a decrease in amplitude. One of the reasons why the depth of pitting decreases with a decrease in amplitude is apparent when observing the test fluid in stroboscopic light. As the amplitude is decreased the size of the vapor bubbles that form beneath the button also decrease. According to the theory of collapse of a vapor bubble, the smaller the bubble the smaller the velocity of collapse and therefore the smaller the pressures produced.

The reason for the decrease in pitted area with a decrease in amplitude is also apparent from observation of the test fluid under stroboscopic light. As the amplitude decreases the area covered by vapor bubbles also decreases. This is probably due to the lower vacuums produced under the test button at lower amplitudes, and therefore the formation of vapor bubbles over a large area is prevented by the surrounding pressure.

Further tests are being made in an attempt to determine what forces are being produced under the vibrating test specimen, or what is actually taking place that produces the pitting.

EFFECT OF SUBMERGENCE IN TEST LIQUID

Another series of tests was made to determine the effect on the rate of pitting of various depths of submergence of the test specimen in the fluid. Tests were made on brass and on 18-8 cast stainless steel at various depths of submergence from 1/8 in. to 2 in.

The results of these tests are shown in Figures 5 and 6. With the rolled brass specimen the material removed increased 25% with an increase of submergence from 1/8 in. to 2 in. With the 18-8 cast stainless steel specimen the material removed decreased 60% with an increase of submergence from 1/8 in. to 2 in.

On both the brass and the stainless steel the area of the pitted surface on the specimens increased with an increase in submergence. However, on the brass the depth of pitting remained about the same for all depths of submergence while on the stainless steel the depth of pitting decreased as the submergence was increased. Figure 7 is a photograph showing the pitting of brass and stainless steel at 1/8 in. submergence and at 2 in. submergence.

The reason why only the central portion of the specimen is erroded or pitted is not quite clear. As the test specimen vibrates, vapor bubbles form near the center of the bottom of the button and flow downward to the bottom of the container in a continuous stream. Figure 8 shows this action with a test specimen vibrated in oil. Air bubbles are also visible in the liquid. Apparently air is being drawn down along the side of the test button from the surface of the liquid. This air flows underneath the button to prevent formation of the vapor bubbles at the outer edges. As the depth of submergence of the test specimen is increased, the quantity of air drawn from the surface decreases, thereby permitting the formation of larger pitted areas on the test specimen. This flow of air is not visible on any of the photographs, but close observation with stroboscopic light indicates that air is actually being drawn from the surface of the liquid to the bottom of the vibrating test specimen.

The reason why the brass specimens pitted to the same depth at all depths of submergence and why the pitting on stainless steel decreased

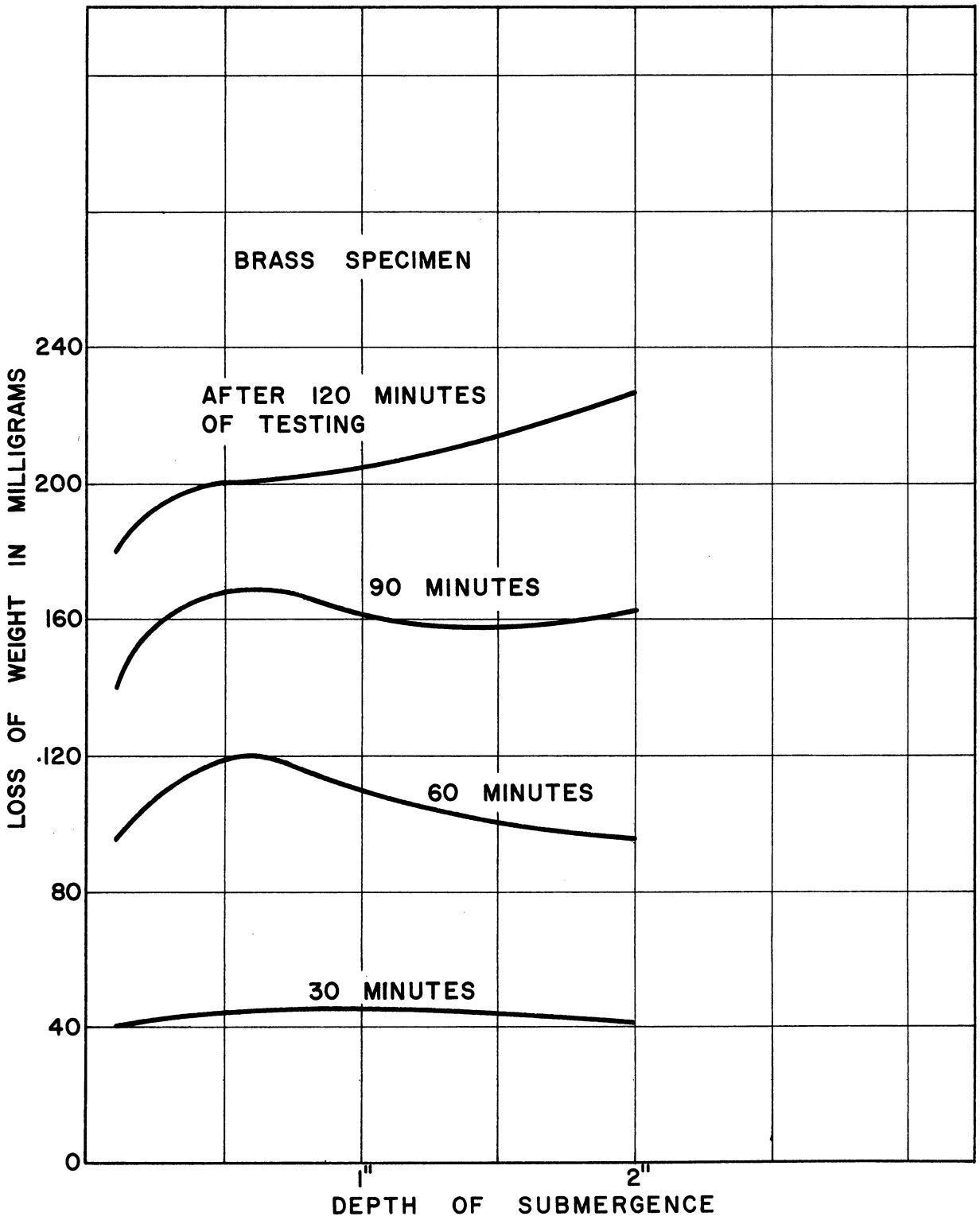
BRASS SPECIMEN
AFTER 120 MINUTES
OF TESTING
90 MINUTES
60 MINUTES
30 MINUTES
LOSS OF WEIGHT IN MILLIGRAMS
240
200
160
120
80
40
0
1"
2"
DEPTH OF SUBMERGENCE

Figure 5.

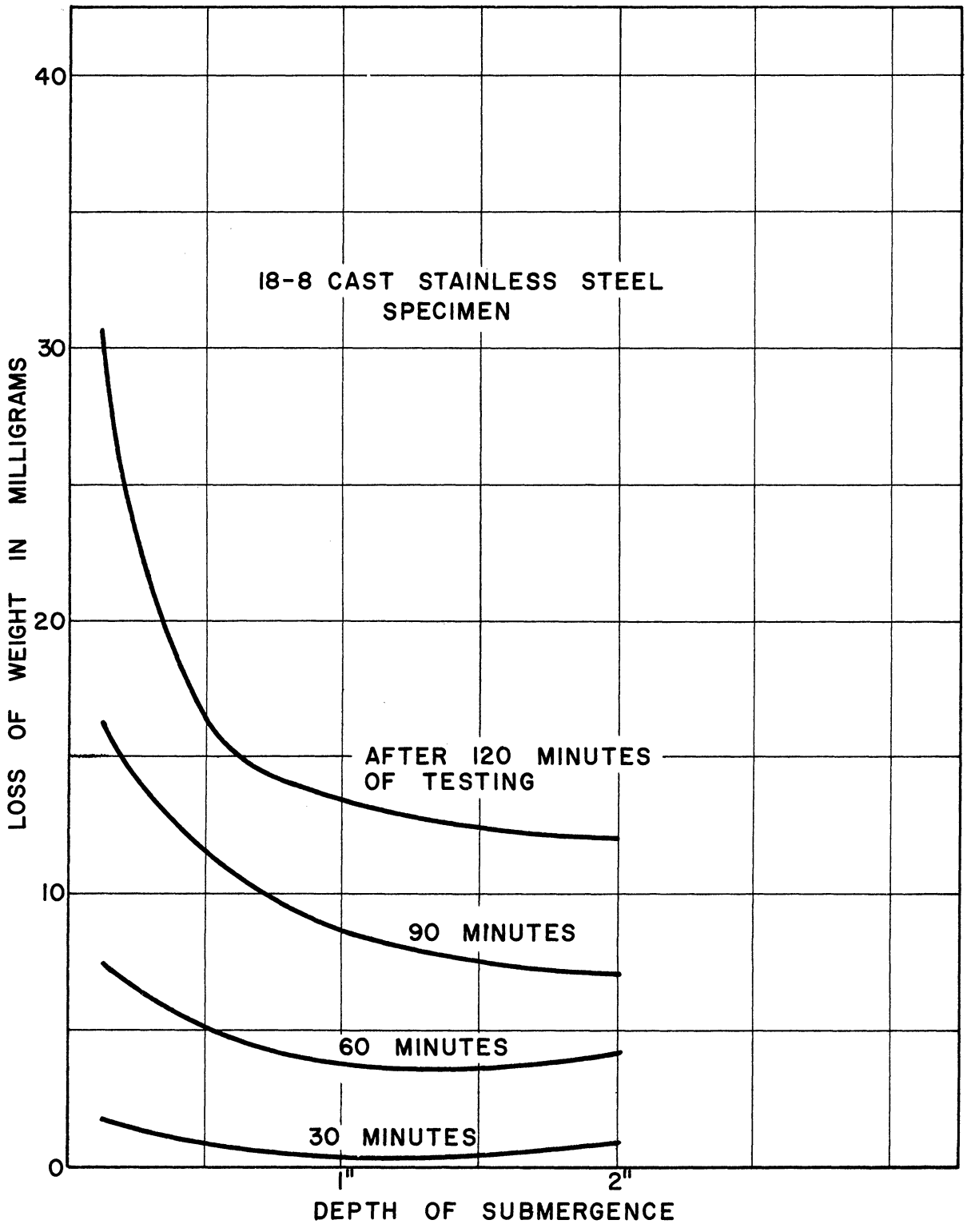
18-8 CAST STAINLESS STEEL
SPECIMEN
LOSS OF WEIGHT IN MILLIGRAMS
40
30
20
10
0
AFTER 120 MINUTES
OF TESTING
90 MINUTES
60 MINUTES
30 MINUTES
1"
2"
DEPTH OF SUBMERGENCE

Figure 6.

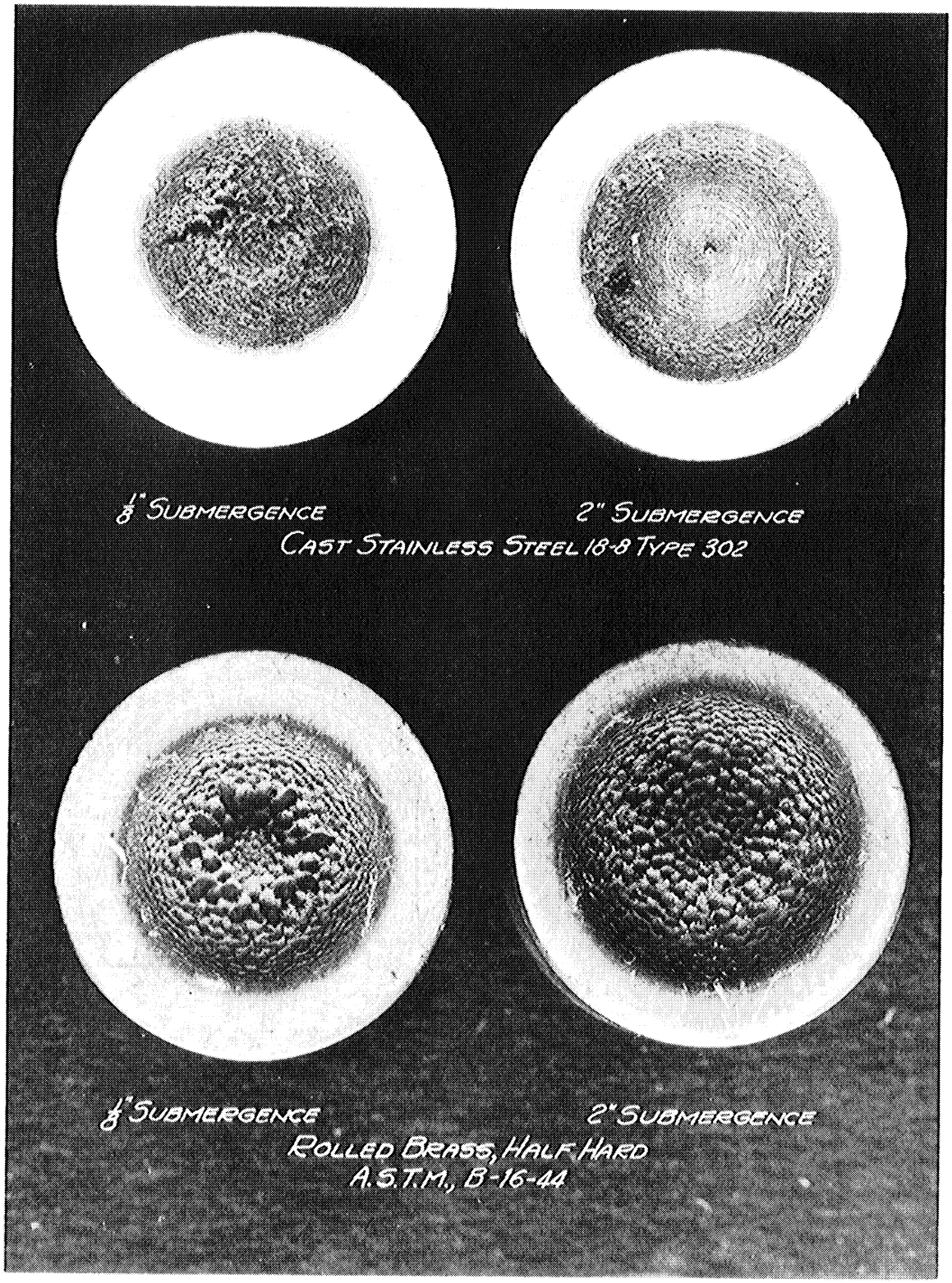
1/8" Submergence
2" Submergence
Cast Stainless Steel 18-8 Type 302
1/8" Submergence
2" Submergence
Rolled Brass, Half Hard
A.S.T.M., B-16-44

Figure 7.

Figure 8. Pattern of flow under cavitation specimen, specimen vibrating 6,500 cycles per second through distance of .00342" in mineral seal oil. Allis-Chalmers cavitation laboratory. 8/29/49.

with an increase of depth, cannot be explained readily. It might be expected that pitting would decrease with increased submergency because with increased pressure, the formation of vapor bubbles decreases. It is possible that the severity of cavitation actually did decrease with an increase in submergence, but that the brass specimen was so susceptible to cavitation, that it was not very sensitive to a change in the cavitation forces, whereas the stainless steel was probably close to the borderline between pitting and not pitting and was therefore sensitive to any slight differences in the cavitation forces such as would occur due to an increase in the depth of submergence. This is similar to what occurred when the amplitude of vibration was decreased as shown in Figure 5.

EFFECT OF DIFFERENT TEST LIQUIDS

One of the most interesting series of tests was made using different test liquids. Most of the standard tests to determine the relative resistance of different materials to pitting have been made in distilled water. S. Logan Kerr made some tests using salt water[2] which showed very little difference in the rate of pitting as compared to fresh water.

The present series of tests used liquids such as sulphuric acid, hydrochloric acid, oils and water treated with a chromate inhibitor. The materials tested were brass, stainless steel, cast steel and special cast irons.

Table 1 lists the results of tests on various cast irons when tested in distilled water and in water treated with chromate ($Na_3 CrO_4$). The chromate solutions were alkaline, having a PH number of 8.6.

The purpose of these tests was to determine whether addition of an inhibitor such as chromate to water would reduce pitting. With the exception of the heat treated low alloy cast iron, none of the test results indicated that addition of chromate increased the resistance to pitting any appreciable amount.

However, since the Brinell hardness was determined for all of the test specimens it was noted that the loss of metal of the various materials after 120 minutes of testing varied with hardness. This is shown in Figure 9 and despite the fact that this curve represents cast iron with various chemical compositions, there is a definite relation between hardness and resistance to pitting.

Table 2 lists the results of tests on half hard rolled brass bar stock using various solutions of sulphuric and hydrochloric acid and also oils. The first group of tests seemed to indicate that the greater the concentration of sulphuric acid the greater the resistance to cavitation. In the second series however, where both the water and the acid solutions were wetted to give approximately the surface tensions of the oils used, there seemed to be very little difference in the resistance

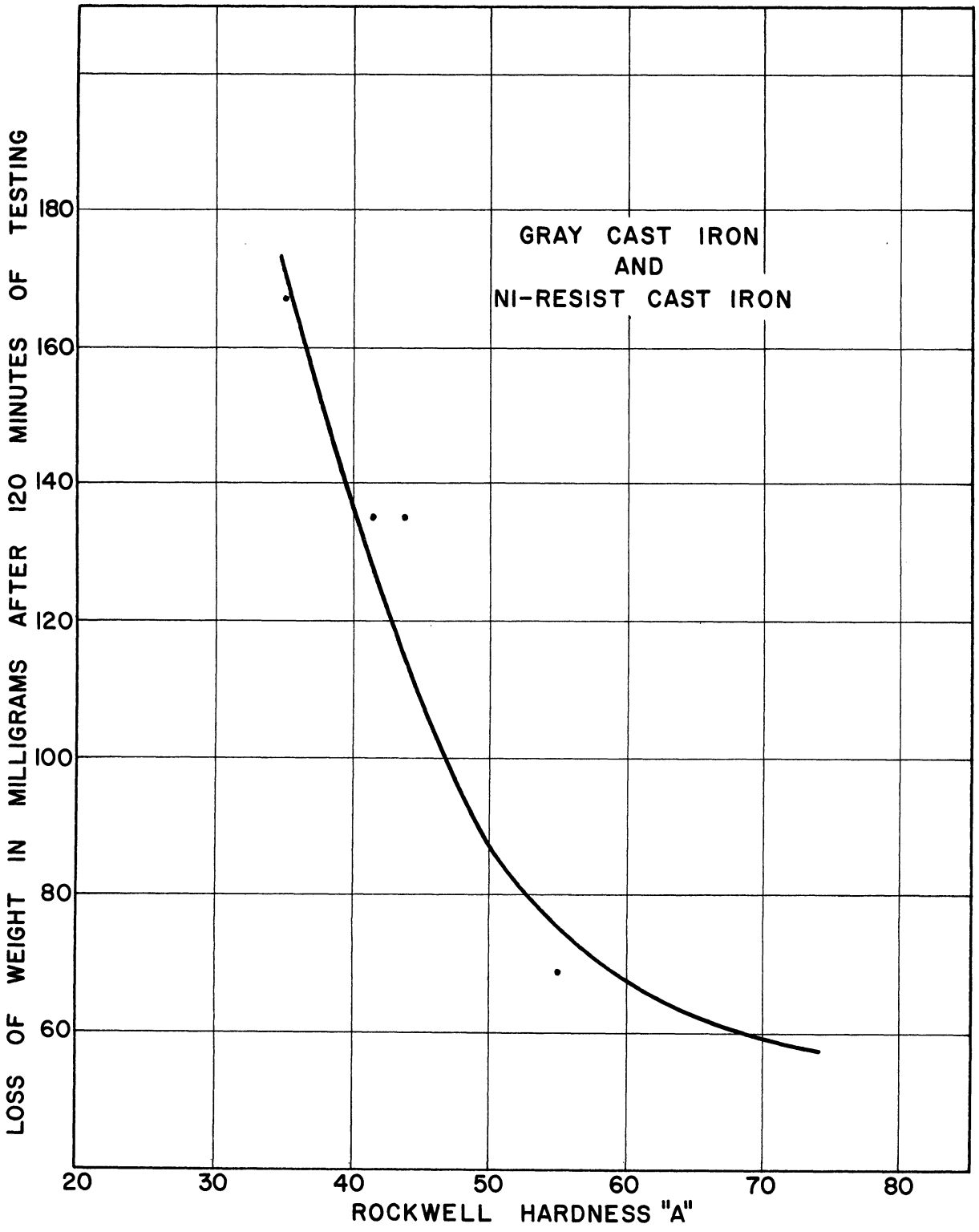
GRAY CAST IRON
AND
NI-RESIST CAST IRON
LOSS OF WEIGHT IN MILLIGRAMS AFTER 120 MINUTES OF TESTING
180
160
140
120
100
80
60
20
30
40
50
60
70
80
ROCKWELL HARDNESS "A"

Figure 9.

TABLE 1

Effect on Inhibitor in Test Liquid on Resistance to Pitting

Material	Test Liquid	Total loss in MG in 120 min.
Low Alloy Gray Iron, as cast - Rockwell A55	Water (distilled)	68
Low Alloy Gray Iron, as cast - Rockwell A55	0.2% Chromate ($Na_3 CrO_4$) 99.8% Water PH = 8.6	67
Low Alloy Gray Iron, as cast - Rockwell A55	0.4% Chromate ($Na_3 CrO_4$) 99.6% Water PH = 8.6	67
Low Alloy Gray Iron, Heat Treated - Rockwell A71	Water (distilled)	59
Low Alloy Gray Iron, Heat Treated - Rockwell A71	0.2% Chromate ($Na_3 CrO_4$) 99.8% Water PH = 8.6	36
Low Alloy Gray Iron, Heat Treated - Rockwell A71	0.4% Chromate ($Na_3 CrO_4$) 99.6% Water PH = 8.6	31
Type 1 Ni-Resist - Rockwell A43	Water (distilled)	136
Type 1 Ni-Resist - Rockwell A43	0.2% Chromate ($Na_3 CrO_4$) 99.8% Water PH = 8.6	115
Type 1 Ni-Resist - Rockwell A43	0.4% Chromate ($Na_3 CrO_4$) 99.6% Water PH = 8.6	122
Type 2 Ni-Resist - Rockwell A35	Water (distilled)	166
Type 2 Ni-Resist - Rockwell A35	0.2% Chromate ($Na_3 CrO_4$) 99.8% Water PH = 8.6	166
Type 2 Ni-Resist - Rockwell A35	0.4% Chromate ($Na_3 CrO_4$) 99.6% Water PH = 8.6	181
Type 3 Ni-Resist - Rockwell A42	Water (distilled)	133
Type 3 Ni-Resist - Rockwell A42	0.2% Chromate ($Na_3 CrO_4$) 99.8% Water PH = 8.6	130
Type 3 Ni-Resist - Rockwell A42	0.4% Chromate ($Na_3 CrO_4$) 99.6% Water PH = 8.6	115

TABLE 2

Rolled Brass Bar Stock,
ASTM, B-16-44, Half Hard
Cu. 60%, Zn. 27% PB. 3%, 90 Brinell

Test Liquid	PROPERTIES OF LIQUID		Total loss in MG in 120 min.
	Vapor Pressure ft H_2O	Surface Tension dynes/-cm.	
Water (distilled)	1.1	76.5	190
5% H_2SO_4, 95% H_2O	.8	76.1	174
25% H_2SO_4, 75% H_2O	.7	71.2	154
50% H_2SO_4, 50% H_2O	.3	65.5	77
Water (wetted to reduce surface tension)	1.1	34.6	145
25% H_2SO_4, 75% H_2O (wetted)	.7	32.0	166
5% HCL, 95% H_2O (wetted)	-	49.1	156
25% HCL, 75% H_2O (wetted)	-	41.0	164
MINERAL SEAL OIL	-	32.3	1.2
MINERAL SEAL OIL & CHLOROFORM	-	31.5	39
TRANSFORMER OIL Spec. N-2698, Sun Oil Co. T-92304-6199 Sun X 2587	-	34.7	4.7
ETHYL ALCOHOL	2.6	21.7	17.7
CARBON TETRACHLORIDE	5.1	-	18.7
CHLOROFORM	9.0	26.7	18.0
ACETONE	10.2	23.3	12.3
TURPENTINE	0.2	27.1	4.6

to pitting between distilled water and various concentrations of acid. The biggest variation was found when oil was used as the test liquid. The results showed that there was a marked drop in loss of weight of the test specimen when vibrated in either mineral seal oil or transformer oil. A test was also made mixing the mineral seal oil with chloroform to increase the specific gravity and decrease the viscosity, bringing these values closer to that for water. This mixture showed an increase in the loss of weight of the test specimen.

Table 3 lists the results of tests on cast stainless steel, type 302. Again the acid solutions showed no marked increase or decrease but the test in the seal oil showed a big decrease in pitting.

TABLE 3

Cast Steel, Fed. Spec. QQ-S-681 b
Class 2 Med.

Test Liquid	PROPERTIES OF LIQUID		
	Vapor Pressure ft H_2O	Surface Tension dynes/-cm.	Total loss in MG in 120 min.
Water	1.1	76.5	104.4
25% H_2SO_4, 75% H_2O (wetted)	.7	32.0	155.5
25% HCL, 75% H_2O)(wetted)	-	41.0	146.0
MINERAL SEAL OIL & CHLOROFORM	-	31.5	6.9
ETHYL ALCOHOL	2.6	21.7	6.6
CARBON TETRACHLORIDE	5.1	-	1.6
CHLOROFORM	9.0	26.7	2.0
ACETONE	10.2	23.3	1.3
TURPENTINE	0.2	27.1	0.6

Table 4 lists the results of tests on cast steel. These tests indicate a definite increase in loss of weight with the acid solutions. However, the acid solutions have a corrosive effect on cast steel and can cause an appreciable loss of weight due to corrosion alone, during the two hour test period. This static loss of weight of the test specimens in the acid solutions is shown in Table 5. The brass and stainless steel loss due to corrosion is neglibible. However, when the static loss due to corrosion for cast steel is subtracted from the loss of weight of the test specimens, as determined during the cavitation tests, there again is an indication that the acid solutions do not effect the resistance to pitting.

The general conclusion from all of these tests is that acid solutions do not change the cavitation forces, and there is some evidence that the greater the acid concentration the smaller the amount of pitting. On the other hand when the test specimens are vibrated in oil, alchohol and other liquids the weight loss is greatly reduced. The explanation for

TABLE 4

Cast Stainless Steel, Type 302
18% Cr, 8% Ni, 0.11% C

Test Liquid	PROPERTIES OF LIQUID		Total loss in MG in 120 min.
	Vapor Pressure ft H_2O	Surface Tension dynes/-cm.	
Water (distilled)	1.1	76.5	35
25% H_2SO_4, 75% H_2O (wetted)	.7	32.0	25
25% HCL, 75% H_2O (wetted)	-	41.0	48
MINERAL SEAL OIL & CHLOROFORM	-	31.5	2.1

TABLE 5

Loss of Weight of Test Specimens Due to Corrosion When Immersed Statically in Test Liquid for 120 Minutes

Material	Test Liquid	Loss of Weight in MG in 120 min.
Rolled Brass, ASTM, B-16-44--Half Hard	25% H_2SO_4, 75% H_2O	0.3
	50% H_2SO_4, 50% H_2O	2.2
Cast Stainless Steel--Type 302	25% H_2SO_4, 75% H_2O	6.5
	25% HCL, 75% H_2O	5.2
Cast Steel--QQ-S-681b, Class 2 Medium	25% H_2SO_4, 75% H_2O	51.8
	25% HCL, 75% H_2O	67.3

this phenomena probably lies in the correlation between the rate of pitting, and the vapor pressure, and surface tension of the liquid. Plotting the rate of pitting against the vapor pressure with liquids of approximately equal surface tension showed a definite relationship. This is similar to the relationship Mousson(1) and Nowotny(13) found in their tests when changing the temperature of the water. Figure 10.

The experiments by Mousson were confined to the lower temperatures and vapor pressures, whereas Nowotny covered the entire range of temperature from freezing to boiling. The increase in rate of pitting with increase in temperature at the lower temperatures and the reduction in rate of pitting with higher temperatures as found by Nowotny seem to indicate that the vapor point, and the outside pressure are determining factors. This is indicated by the conditions of stability of the vapor bubbles whose collapse produce the mechanical forces that cause pitting erosion. For equilibrium of a vapor bubble we have

$$P_i = P_e - \frac{2S}{r}$$

Where:

P_i = internal pressure
P_e = external pressure
s = surface tension of the liquid
r = radius of the bubble

For boiling liquid the internal pressure is equal to the vapor pressure which is equal to the external pressure (where the liquid is boiled in an open container the external pressure is equal to the atmospheric pressure or $P_i = P_v = P_e$ where P_v = vapor pressure). Under this condition the bubble continues to grow (r approaches infinity) and finally explodes. Since there is no possibility for the bubbles to collapse, the destructive forces are absent. Therefore, with the stability of the bubbles decreasing with decreasing pressure differences ($P_e - P_v$) and on the other hand with an increase in the number of bubbles and their collapse with increasing vapor pressure (increasing temperature) the relation between temperature and rate of pitting is indicated. Nowotny demonstrated this by making tests on aluminum test specimens in various alcohols and benzenes, the boiling points of which were between 68 deg. and 136 deg. C. He found that at the boiling point, $P_e = P_v$, the test samples were not damaged regardless of the liquid used.

Nowotny also demonstrated that by keeping the liquid at constant room temperature, which was equivalent to keeping the vapor pressure constant, but changing the external pressure P_e, the limiting condition $P_e - P_v$ in general governed the rate of erosion. For high external pressures where the differential pressure $P_e - P_v$ was large, the test specimens were badly eroded. For low external pressures where the pressure differentials were small, $P_e - P_v = 0$, no damage was visible.

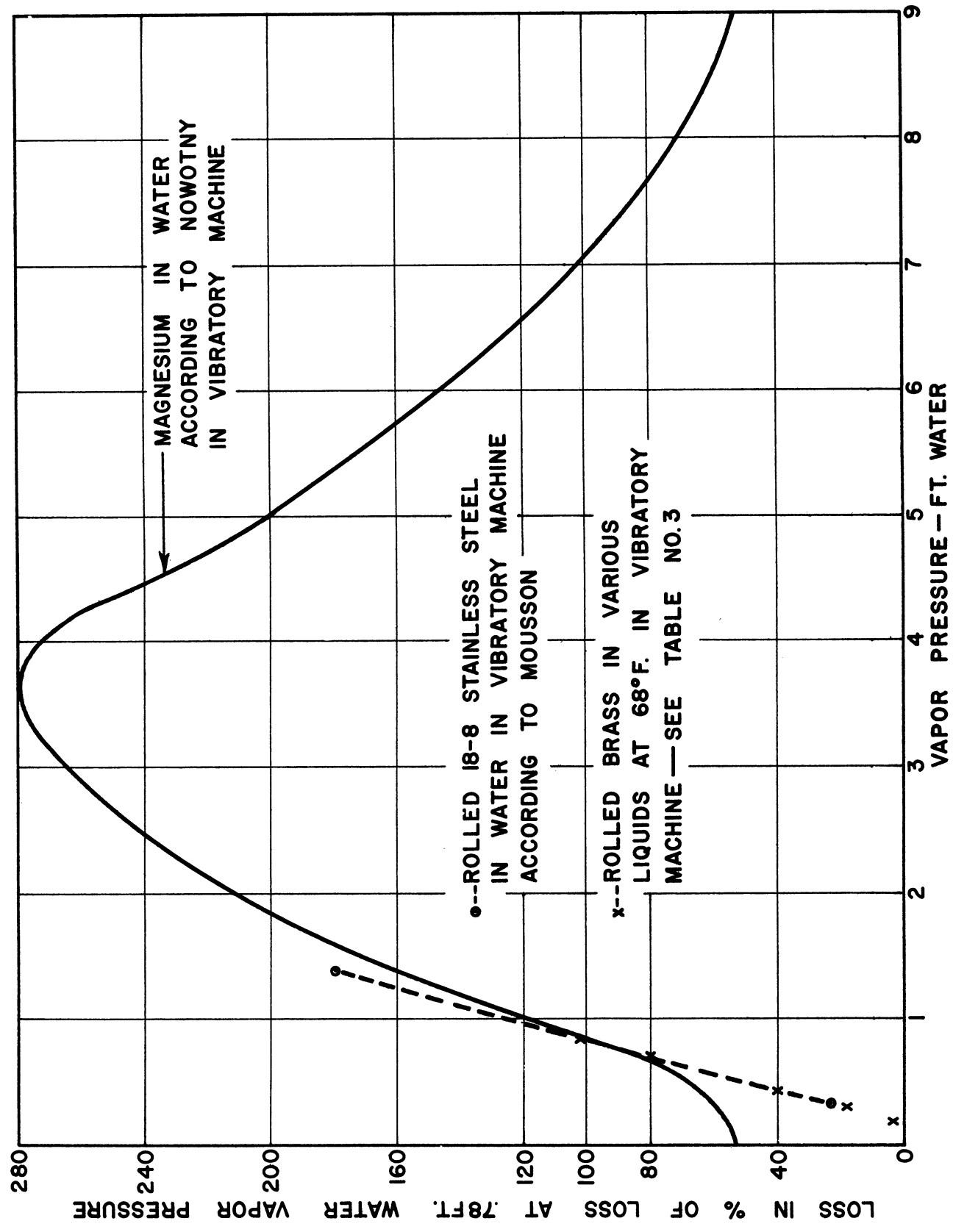
LOSS IN % OF LOSS AT .78FT. WATER VAPOR PRESSURE
VAPOR PRESSURE—FT. WATER
MAGNESIUM IN WATER ACCORDING TO NOWOTNY IN VIBRATORY MACHINE
●--ROLLED 18-8 STAINLESS STEEL IN WATER IN VIBRATORY MACHINE ACCORDING TO MOUSSON
x--ROLLED BRASS IN VARIOUS LIQUIDS AT 68°F. IN VIBRATORY MACHINE—SEE TABLE NO.3
0
40
80
100
120
160
200
240
280
1
2
3
4
5
6
7
8
9

Figure 10.

As a further check, tests were made with the water at 100°C (boiling) but with an external pressure P_e of 2 atmospheres. This again produced pitting of the test specimen, which was quite natural since $P_e - P_v$ was greater than zero.

All these tests indicate definitely that the destruction by cavitation does not depend merely on water hammer but depends upon bubble formation because with the vibratory machine, the liquid impact does not change with a change in external pressures P_e. The tests also indicate the reason for the various rates of pitting when using different liquids with different vapor pressures, as shown in Tables 2, 3, and 4.

All of this adds to our knowledge of the Mechanics of Cavitation and shows that there is a definite similarity between the cavitation produced by Mousson with a Venturi type of machine and the cavitation produced with the vibratory machine used by the Author.

The tests with various liquids as shown in Tables 2, 3, and 4 also seem to show that the surface tension of the liquid has an important influence on the degree of pitting. The greater the surface tension S The greater the damage. This is indicated by the nature of the bubble mechanism. The capillary energy of the bubble, $E = 4\pi (r_o)^2 S$, which released during the collapse of the bubble is a measure of the attack of each individual bubble. r_o denotes the radius of the bubble before collapse. However, further investigations along these lines are necessary before a relationship between surface tension and rate of pitting can be definitely established.

PITTING RESISTANCE OF VARIOUS MATERIALS

Tables 6 to 19 list practically all of the materials tested in the accelerated cavitation machine. These materials were tested at a depth of immersion of 1/8 in. in distilled water at 6500 cycles per second with a total travel amplitude of .0034 inches.

Cast and Rolled Stainless Steels

Table 6 lists tests on a number of cast stainless steels, which indicate quite a variation in resistance to pitting. Even cast stainless steels of the same type but cast in different foundries show considerable variation in their resistance to pitting. For example cast stainless steel type 302, which contains 18% chrome and 8% nickel showed losses of 12, 22 and 35 milligrams as furnished by 3 different foundries. This is a maximum variation of 300% in the resistance to pitting. Some of these variations may be due to the materials being cast for various purposes. Other causes for variations are the carbon content of the steel, where the specifications for a particular type permit a wide variation in carbon. The heat treatment of the casting and the hardness of the material also effect its resistance to pitting.

TABLE 6

Cast Stainless Steel

Specimen No.	MATERIAL Cr %	Ni %	C. %	Heat Treatment	Type	Furnished by	Brinell Hardness	Total loss in MG in 120 min.
159	18	8	0.12	As Cast	302	Midvale	-	12
103	18	8	0.12	As Cast	302	Midvale	-	13
137	27	10	0.26	As Cast	312	-	-	13
234	28	8	0.31	As Cast	-	American Brake Shoe	229	13
231	19	8	0.12	2050°F 1/2 Hr.	-	American Brake Shoe	156	17
228	19	9	0.06	2050°F 1 Hr.	-	American Brake Shoe	156	19
230	18	9	0.07	2000°F 1/2 Hr.	-	American Brake Shoe	136	19
229	18	9	0.04	2000°F 1/2 Hr.	-	American Brake Shoe	146	22
106	18	8	0.10	As Cast	302	Boney Floyd	-	22
107	17	12	0.10	-	316	-	-	24
233	18	14	0.08	2050°F 1 Hr.	-	American Brake Shoe	149	28
139	21	10	0.11	As Cast	307	-	-	31
168	18	8	0.11	As Cast	304	Allegheny Ludlum	-	33
167	18	8	0.11	As Cast	302	Allegheny Ludlum	-	35
232	18	10	0.07	2050°F 1/2 Hr.	-	American Brake Shoe	170	47
169	-	-	-	As Cast	327	Allegheny Ludlum	-	53

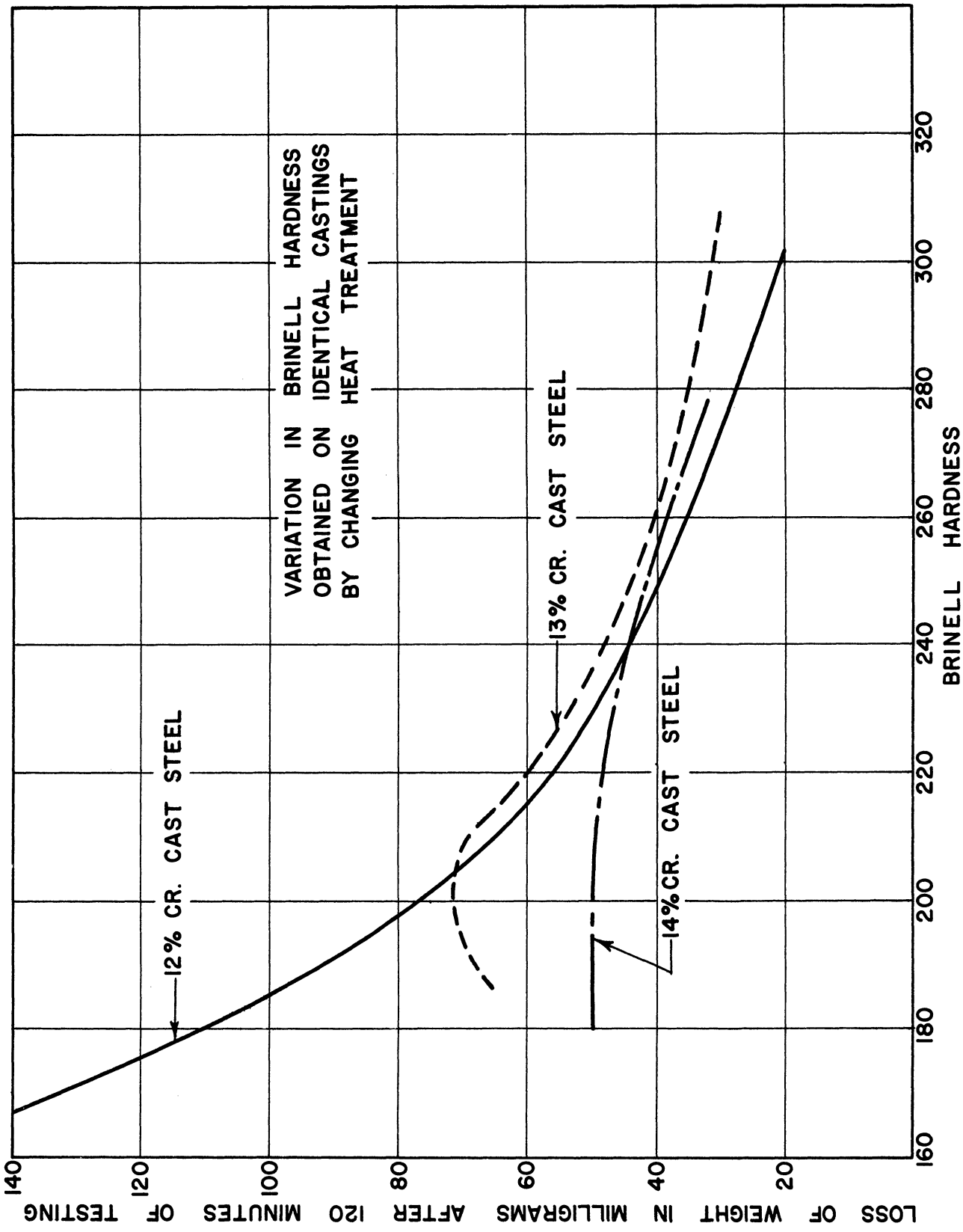
VARIATION IN BRINELL HARDNESS
OBTAINED ON IDENTICAL CASTINGS
BY CHANGING HEAT TREATMENT
12% CR. CAST STEEL
13% CR. CAST STEEL
14% CR. CAST STEEL
LOSS OF WEIGHT IN MILLIGRAMS AFTER 120 MINUTES OF TESTING
BRINELL HARDNESS
20
40
60
80
100
120
140
160
180
200
220
240
260
280
300
320

Figure 11.

TABLE 7

Cast Chrome Stainless Steel

Specimen No.	Material	Cast by	Brinell Hardness	Total loss in MG in 120 min.
182	12.0% Chrome	Ohio Steel	302	20
108	12.0% Chrome, 0.10% C	-	-	22
196	13.0% Chrome	Allegheny Ludlum	306	25
207	13.1% Chrome	Ohio Steel	269	29
208	14.3% Chrome	Ohio Steel	269	34
212	14.0% Chrome	Ohio Steel	269	34
171	13.0% Chrome, 0.12% C	Allegheny Ludlum	-	38
213	14.1% Chrome	Ohio Steel	223	46
205	13.4% Chrome	Ohio Steel	223	47
194	13.0% Chrome	Allegheny Ludlum	235	49
209	14.3% Chrome	Ohio Steel	223	49
210	14.1% Chrome	Ohio Steel	187	50
195	13.0% Chrome	Allegheny Ludlum	241	51
181	12.0% Chrome	Ohio Steel	225	54
193	13.0% Chrome	Allegheny Ludlum	229	57
170	13.0% Chrome, 0.12% C	Allegheny Ludlum	-	59
206	13.2% Chrome	Ohio Steel	187	64
192	13.0% Chrome	Allegheny Ludlum	207	70
180	12.0% Chrome	Ohio Steel	167	141

Table 7 lists the results of tests on 12%, 13%, and 14% chrome cast steels with varying Brinell hardness. Figure 11 shows the loss in milligrams during a two hour test in the accelerated cavitation machine plotted against Brinell hardness, where both the 12% and 13% chrome steel test specimens were taken from the same castings, and the variation in Brinell hardness was obtained entirely by changing the heat treatment of the two materials. These tests show the large effect that hardness of a material has on its resistance to pitting.

The large variations in resistance to pitting of the different cast stainless steels indicate the necessity for constant checks on such material when used in hydraulic machinery to assure that the desired resistance to pitting is being obtained.

TABLE 8

Rolled Annealed Stainless Steels

Specimen No.	Material	Total loss in MG in 120 min.
105	18% Cr., 8% ni, 0.12% C., Type 302	8.0
157	18% Cr., 8% ni, 0.12% C., Type 302	32

Table 8 lists the results of tests on rolled annealed stainless steel. The wide variation in resistance to pitting of the two rolled stainless steels of the same type is another reason for the necessity for making careful accelerated cavitation tests on all materials of this type before using them for the purpose of resisting pitting.

Welded Steels

Table 9 lists the results of tests on various welded materials. These tests also show a wide variation in resistance to pitting depending upon the type of material used.

Some of these materials such as Lincoln Abrasoweld showed a very high resistance to pitting. However, the Abrasoweld has such a high Brinell hardness that it is nearly impossible to grind or machine and its use is therefore quite limited. The tests indicated that the 16% chrome 7% nickel stainless steel also had very high resistance to pitting. This material can be ground and machined without too much difficulty.

Table 10 shows the results of tests on welded stainless steels when welded to 12% chrome either preheated or not preheated. These tests show that preheating of the base metal has very little effect on the resistance to pitting of the welded deposit.

In recent years there has been some difference of opinion among engineers as to the type of stainless steel welding rod to be used in prewelding or repairing hydraulic machinery for protection against the effects of pitting (erosion) due to cavitation. The most important differences have been concerned with the composition of the welding rod, the number of layers of weld to be used, the amount of dilution of the weld deposit with the base metal and the effect of the presence of columbium in the weld rod.

To answer these questions, two series of tests (specimens 198 to 204, and specimens 235 to 242) were made on various combinations of stainless steel weld deposits. The results of these tests are shown in Table 11.

TABLE 9

Welded Materials

Specimen No.	Material	Brinell Hardness	Total loss in MG in 120 min.
248	Lincoln Abrasoweld	320	2.5
249	Arcos Chromend (16% Cr---7% Ni)	275	8.5
136	16% Cr, 7% Ni	-	9.4
250	Crucible steel---Rezistal WH	177	11
135	19% Cr, 9% Ni---Cb	-	13
252	Smith Co.---Smithway (18% Cr, 8% Ni)	137	23
251	Smith Co.---Smithway 159 (25% Cr, 20% Ni)	133	25
15	Lincoln A5	-	27
16	Stelco 604	-	27
254	Lincoln Stainweld D (25% Cr, 20% Ni)	145	27
256	Victor (G.E. Co.) W2310	136	29
258	Victor (G.E. Co.) W-23-8	134	31
257	Victor (G.E. Co.) W2310 Cb	142	32
134	19% Cr, 9% Ni---Cb	-	36
132	25% Cr, 12% Ni---Cb	-	36
14	130x INCO Monel	-	37
255	Crucible steel---Rezistal KA2S (19% Cr, 9% Ni)	134	37
245	Arcos Chromend K (19% Cr, 9% Ni)	130	38
247	Lincoln Stainweld A-7 (18% Cr, 8% Ni)	140	40
246	Lincoln Stainweld A5-Cb (18% Cr, 8% Ni)	133	41
133	25% Cr, 12% Ni---Cb and 19% Cr, 9% Ni---Cb	-	41
17	Lincoln Aerisweld AE-124K	-	55
253	International Nickel, Monel 140-x	116	89

TABLE 10

Welded Stainless Steel on 12% Chrome Steel

Specimen No.	Material	Brinell Hardness	Total loss in MG in 120 min.
	Effect of Preheat on Base Metal		
188	18% Cr, 8% Ni on 12% Cr. Cast Steel Preheated to 600°F	186	7.6
186	18% Cr, 8% Ni on 12% Cr. Cast Steel--- No Preheat	195	7.8
187	18% Cr, 8% Ni, on 12% Cr. Cast Steel Preheated to 400°F	195	8.0
184	12% Cr, on 12% Cr. Cast Steel Preheated to 400°F	360	13
185	12% Cr, on 12% Cr. Cast Steel Preheated to 600°F	352	14
183	12% Cr, on 12% Cr. Cast Steel--- No Preheat	347	16.8

Since the investigation was primarily concerned with the prewelding and repair of hydraulic turbine runners, cast steel was selected for the base metal in the preparation of the test specimens.

These tests specimens were made by applying the stainless steel weld deposits to bars 10 in. long by 2-1/2 in. wide by 1 in. thick, cast separately with steel conforming to Federal Specifications QQ-S-681-b, Class 2, medium, which is commonly used for hydraulic turbine runner castings.

Six types of standard commercial stainless steel weld rods as purchased from the Arcos Corporation, 1500 So. 50th St., Philadelphia, Pa. were used as follows:

Type 301, grade, 17% Cr, 7% Ni
Type 308, grade, 18% Cr, 8% Ni
Type 309, grade, 25% Cr, 12% Ni
Special, grade, 17% Cr, 7% Ni, 1% Cb
Special, grade, 18% Cr, 8% Ni, 1% Cb
Special, grade, 25% Cr, 12% Ni, 1% Cb

The chromium and nickel percentages refer to the commercial weld rod designation and do not refer to the chemical analysis of the weld deposit.

TABLE 11

Welded Stainless Steel

Specimen No.	MATERIAL		Brinell Hardness	Total loss in MG in 120 min.
	1st Layer of Weld	2nd or Final Layer Weld		
	1st SERIES			
203	17% Cr, 7% Ni, Type 301		308	10
201	18% Cr, 8% Ni, Type 308		160	23
198	25% Cr, 12% Ni, Type 309		145	26
204	17% Cr, 7% Ni, Type 301	17% Cr, 7% Ni, Type 301	255	6
199	25% Cr, 12% Ni, Type 309	18% Cr, 8% Ni, Type 308	145	31
202	18% Cr, 8% Ni, Type 308	18% Cr, 8% Ni, Type 308	151	33
200	25% Cr, 12% Ni, Type 309	17% Cr, 7% Ni, Type 301	175	35
	2nd SERIES			
237	17% Cr, 7% Ni, Type 301	17% Cr, 7% Ni, Type 301	196	7.2
241	17% Cr, 7% Ni, 1% Cb	17% Cr, 7% Ni, 1% Cb	355	11
236	18% Cr, 8% Ni, Type 308	17% Cr, 7% Ni, Type 301	167	14
235	18% Cr, 8% Ni, Type 308	18% Cr, 8% Ni, Type 308	166	19
242	17% Cr, 7% Ni, Type 301	18% Cr, 8% Ni, Type 308	161	19
238	25% Cr, 12% Ni, Type 309	18% Cr, 8% Ni, Type 308	166	20
240	18% Cr, 8% Ni, 1% Cb	18% Cr, 8% Ni, 1% Cb	185	23
239	25% Cr, 12% Ni, 1% Cb	18% Cr, 8% Ni, 1% Cb	168	27

After the test specimens were welded, they were ground to a smooth finish. The Brinell hardness of each specimen was then determined. For the first series of tests, standard bend tests were made on each of the test specimens, and a chemical analysis was made of chips taken from the uppermost weld deposit of each specimen.

The results of the accelerated cavitation tests on the 1st series of specimens show that two layers of type 301 stainless steel welds have considerably greater resistance to pitting than any of the other combinations of welds. These tests also show that two layers of weld give greater resistance to pitting than one layer.

Table 12, shows the chemical analysis of the uppermost layer of the weld deposit on the test specimens of the 1st series of tests. This table shows that there is considerable dilution of the weld deposit when placed upon the base metal. Another interesting observation is that the weld deposit with an actual content of 16% chrome and 6-1/2% nickel has the highest resistance to pitting. Welds with chrome and nickel contents above and below these figures seem to be more susceptible to cavitation. This is in general accordance with the test results obtained by J. M. Mousson(1) as well as with test results on various welded materials as listed in Table 9.

The bend tests made on the welded bars of the 1st series of specimens indicated that the use of only one layer of type 301 weld deposit resulted in lower bend angles, and therefore lower ductility than with one layer of either type 308 or type 309. The bend tests also indicated that two layers of weld regardless of the combination, resulted in definitely higher bend angles and therefore greater ductility than 1 layer of any type of weld deposit. The bend angles obtained with two layers of weld indicated satisfactory ductility considering the fact that the weld is a protective coating and not subject to high stresses.

Since there was considerable variation in the resistance to pitting of the various weld combinations in this 1st series of tests, it was decided to conduct a second series of tests, using various combinations of welds, as well as making tests on stainless steel deposits made with weld rods containing from 0.8 to 1.0% columbium.

The first series of tests had indicated that two layers of weld had a higher resistance to pitting, and had greater ductility than one layer. Also from the practical standpoint, two layers of weld deposit are always desirable for prewelding and repairs so as to insure a thorough coverage of the surface being prewelded or repaired. Therefore, all test specimens in the second series of tests had two layers of weld.

The results of the accelerated cavitation tests on this second series of specimens 235 to 242 are shown in Table 11. The 2nd series again indicates that two layers of 17% Cr, 7% Ni, type 301 stainless steel weld have a greater resistance to pitting than any other combination of weld deposits. The addition of columbium did not increase the resistance to pitting of any of the types of weld rods tested. No was there any

TABLE 12

Chemical Analysis of Test Specimens

Specimen No.	WELD ROD MATERIAL		Chromium	Nickel	Total Carbon
	1st Layer of Weld	2nd Layer of Weld (final layer)			
203	17% Cr, 7% Ni, Type 301		12.48	4.90	.09
201	18% Cr, 8% Ni, Type 308		16.45	7.80	.10
198	25% Cr, 12% Ni, Type 309		16.90	11.20	.12
204	17% Cr, 7% Ni, Type 301	17% Cr, 7% Ni, Type 301	15.80	6.50	.05
199	25% Cr, 12% Ni, Type 309	18% Cr, 8% Ni, Type 308	19.85	10.30	.06
202	18% Cr, 8% Ni, Type 308	18% Cr, 8% Ni, Type 308	19.56	9.70	.07
200	25% Cr, 12% Ni, Type 309	17% Cr, 7% Ni, Type 301	17.12	7.80	.10

Cast steel used for base metal.

indication that the addition of columbium made the welding process easier. In fact the presence of columbium sometimes makes welding with stainless steel rod quite difficult. Columbium also seems to have the effect of greatly increasing the hardness of the 17% Cr, 7% Ni, weld deposit as shown in Table 11. This makes it difficult to machine and grind.

Although two layers of 17% Cr, 7% Ni, type 301 stainless steel weld show a very high resistance to pitting, it has several undesirable characteristics when welded directly to a mild carbon steel base. The stainless steel weld has a tendency to dilute with the carbon steel until it is no longer austenitic. It thus may form a boundary layer of martensite steel between the base metal and the weld which is extremely hard and brittle. If subjected to high stresses, cracks may develop in the martensite boundary layer and spread into both the welded surface and the base material.

However, further tests and experimental data will be required before definite conclusions can be made regarding such characteristics.

Welds with higher chrome and nickel contents have less tendency to form such a martensite boundary layer. 25% Cr, 12% Ni, stainless steel weld as a first layer should eliminate the possibility of a martensite boundary layer, if proper welding technique is used. However, the use of 25% Cr, 12% Ni, as a first layer and 17% Cr, 7% Ni, as a second layer does not have the high resistance to pitting that two layers of 17% Cr, 7% Ni have. It is possible that by using 25% Cr, 12% Ni for a first layer and then using two layers of 17% Cr, 7% Ni, a higher resistance will be obtained. Tests along these lines are now being made.

The conclusions that can be made based on the two series of tests are as follows:

1. Two layers of weld give better protection and have greater resistance to pitting than one layer of weld deposit.
2. The use of 25% Cr, 12% Ni, type 309 stainless steel as a first layer of weld tends to reduce the resistance to pitting of the weld deposits.
3. The addition of columbium to the weld rods has no beneficial effects as far as resistance to pitting is concerned.
4. Two layers of 17% Cr, 7% Ni, type 301 stainless steel weld gives the greatest resistance to pitting.
5. If the weld will be subjected to high stresses, 25% Cr, 12% Ni, type 309 stainless steel should be used as a first layer so as to prevent the formation of a martensite boundary subject to the formation of cracks.

Based upon these conclusions it is recommended that two layers of 17% Cr, 7% Ni, type 301 stainless steel weld rods be used for pre-welding and repairing all hydraulic turbine machinery subject to strong pitting due to cavitation, where the welds and the base materials are not subject to high stresses. Where high stresses exist, it is recommended that 25% Cr, 12% Ni, type 309 stainless steel be used for a first layer. The use of weld rods containing columbium is not recommended.

It is interesting to note that for all the welded materials listed in Tables 9, 10 and 11, there is a definite relationship between resistance to pitting and hardness, even though a wide variety of materials was used. This is shown in Figure 12. For a Brinell hardness between 130 and 180 there is apparently quite a variation in the resistance to pitting depending upon the type of material used. However, the general trend seems to be the harder material, the greater the resistance to pitting. There also seems to be a definite upper limit in this respect. In other words any increase in Brinell hardness beyond 200 to 240 does not materially increase the resistance to pitting.

Sprayed Stainless Steels

Table 13 lists the tests on various sprayed stainless steels. These tests indicate that although some of the sprayed stainless materials had a resistance about equal to cast steel, others pitted very rapidly. These differences are probably largely due to the method of application of the sprayed metal which accounts for the variance in field reports as to their effectiveness. Quite a number of the test specimens had to be scrapped before the two hour test period was completed because the sprayed metal would separate from the base. The high acceleration (about 7,300 G's) of the vibratory test is a severe test on the adhesion of the metal.

TABLE 13

Sprayed Stainless Steels

Specimen No.	Material	Total loss in MG in 120 min.
12	Metco Metcaloy No. 2	72
11	Metco Metcaloy No. 1	98
112	18% Cr, 8% Ni, Type 302	187
116	13% Cr, Type 420	192
179	Metcaloy No. 2	216

If the sprayed material is carefully applied it seems to have about the same resistance to pitting as cast steel, but considerably less resistance than a properly welded stainless steel. In general the application of sprayed metal is cheaper than welding with mild or stainless steel, and it sometimes proves to be a satisfactory means of repair where pitting is not very severe, and where speed of application and low initial costs are a factor.

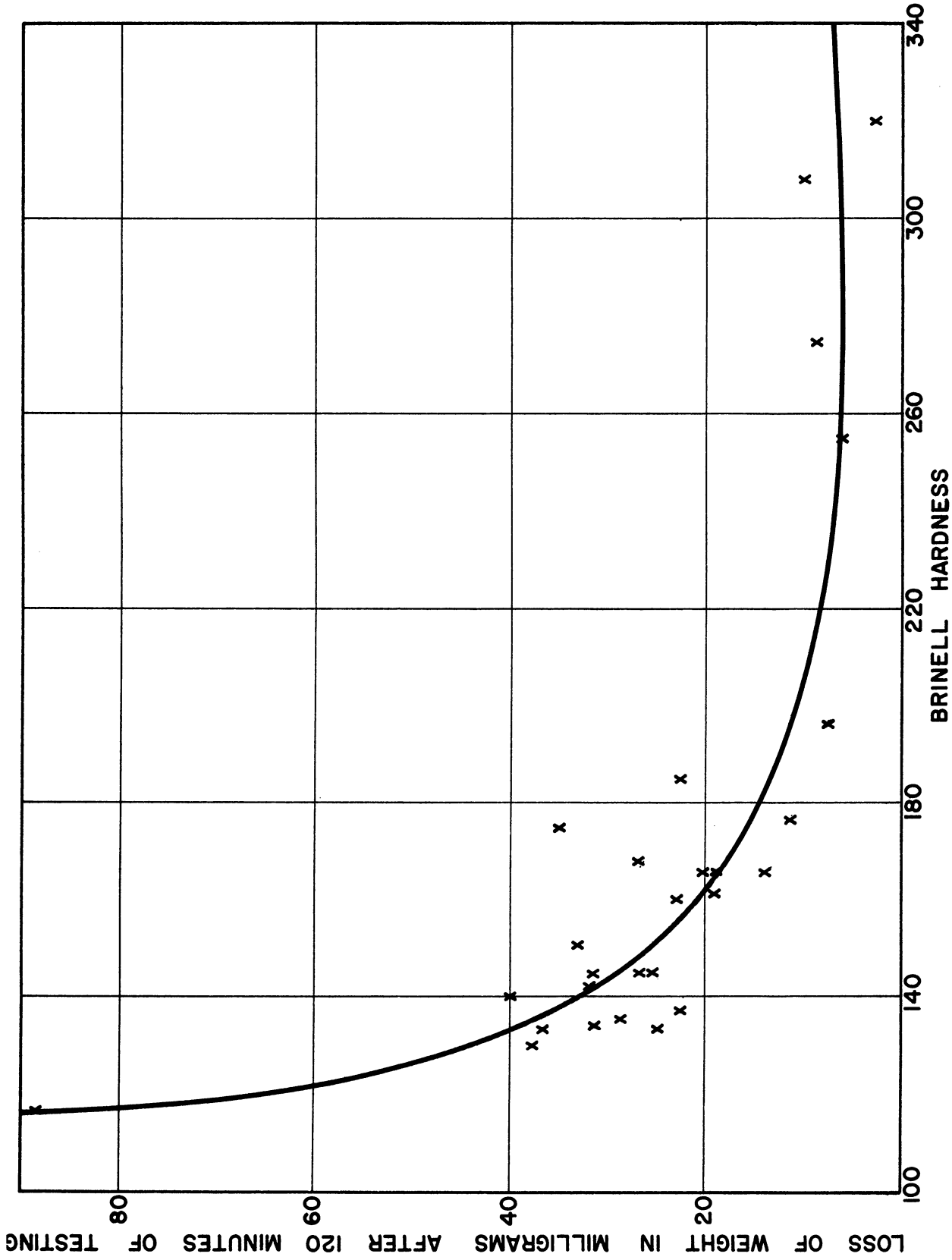
LOSS OF WEIGHT IN MILLIGRAMS AFTER 120 MINUTES OF TESTING
20
40
60
80
100
140
180
220
260
300
340
BRINELL HARDNESS

Figure 12.

Cast Steels

Table 14 lists the results of tests on the cast steel most commonly used for hydraulic turbine runners. The tests on three castings from three different foundries do not show any appreciable variation.

TABLE 14

Cast Steels

Specimen No.	Material	Total loss in MG in 120 min.
178	Fed. Spec. QQ-S-681 b Class 2 Medium	88
158	Fed. Spec. QQ-S-681 b Class 2 Medium	104
118	Fed. Spec. QQ-S-681 b Class 2 Medium	105

AMPCO Bronzes

Table 15 lists an interesting series of tests on Ampco bronzes. Ampco is the trade name for a bronze with an aluminum content varying from 10% to approximately 14%. The Brinell hardness increases as the aluminum content increases. The results of the tests on the cast bronzes show that some of them have twice the resistance to pitting compared to the best stainless steel castings. The welded bronzes also show a remarkable resistance to pitting. Figure 13 shows photographs of cast and welded Ampco bronze test specimens. Figure 14 shows how the resistance to pitting of these materials varies with hardness. This curve shows that while the resistance to pitting increases with hardness there is a maxiumum point beyond which resistance to pitting decreases with increased hardness. This same trend can be noticed for welded materials of all types shown in Figure 12. The maximum hardness for best resistance to pitting seems to be about the same for both groups of materials.

Unfortunately there is very little information as to how these bronzes either cast or welded stand up under field conditions, which is really the final criterion. In one instance bronze patch plates were alternated with ordinary bronze on the back sides of the blades of a hydraulic turbine runner. After a period of operation the ordinary bronze patch plates had pitted to a considerable extent, while the Ampco bronze showed very little signs of pitting. Several Ampco bronze runners have been manufactured and are now in operation, but the period of operation has not been long enough to determine their resistance to pitting under field conditions.

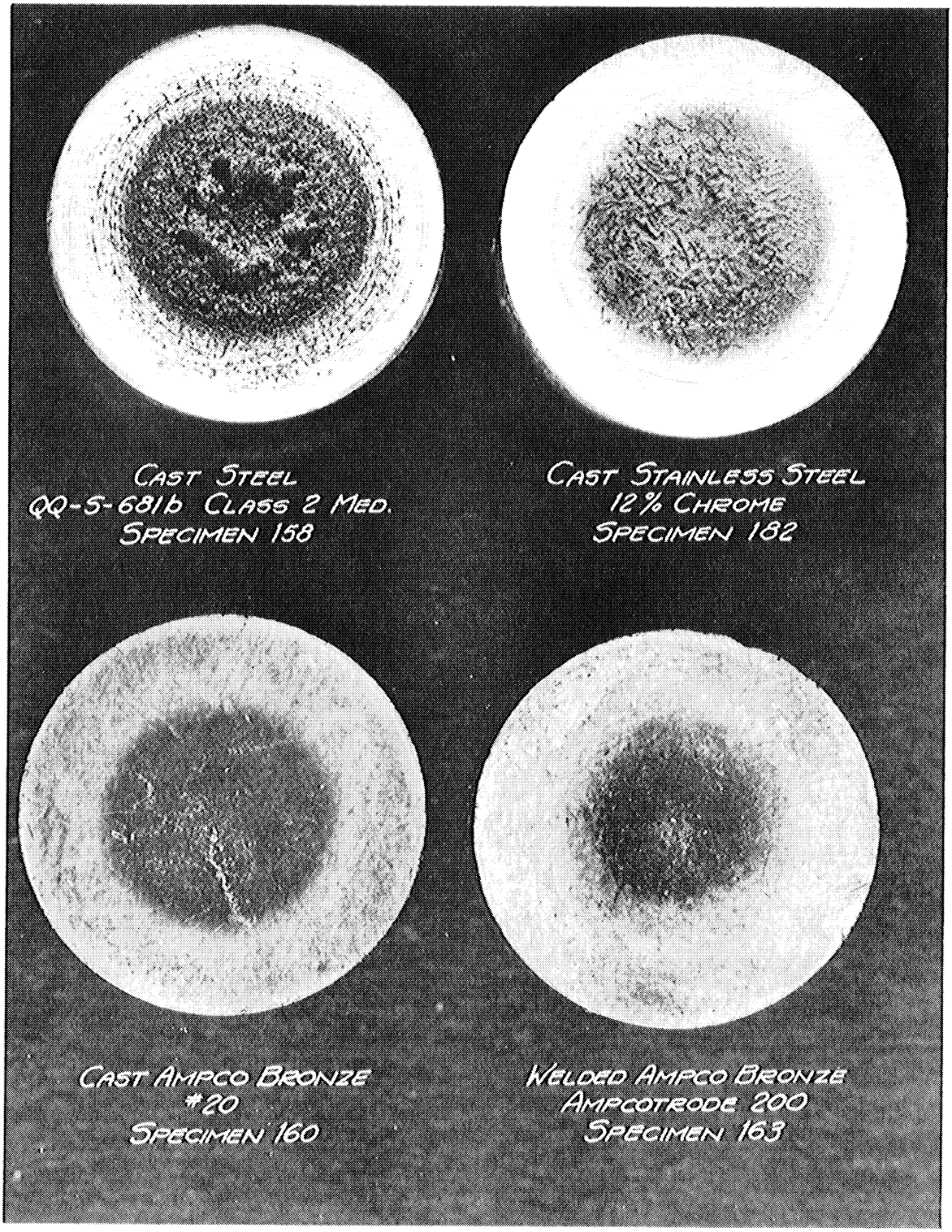
CAST STEEL
QQ-S-681b CLASS 2 MED.
SPECIMEN 158
CAST STAINLESS STEEL
12% CHROME
SPECIMEN 182
CAST AMPCO BRONZE
#20
SPECIMEN 160
WELDED AMPCO BRONZE
AMPCOTRODE 200
SPECIMEN 163

Figure 13.

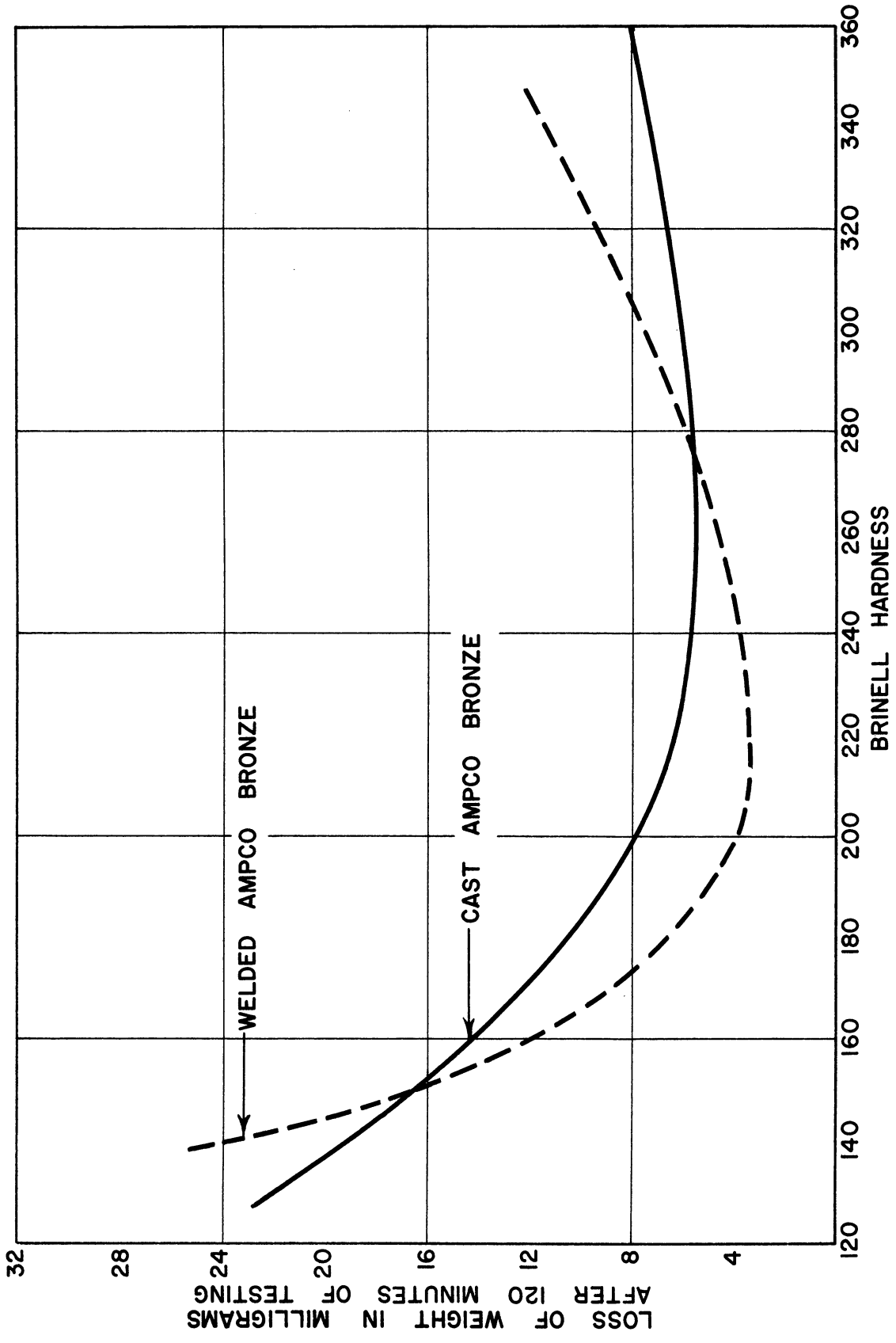
LOSS OF WEIGHT IN MILLIGRAMS
AFTER 120 MINUTES OF TESTING
32
28
24
20
16
12
8
4
120
140
160
180
200
220
240
260
280
300
320
340
360
BRINELL HARDNESS
WELDED AMPCO BRONZE
CAST AMPCO BRONZE

Figure 14.

Certainly the tests of the Ampco bronzes in the accelerated cavitation machine warrant experimenting with this material in field installations.

TABLE 15

Bronzes

Specimen No.	Material	Total loss in MG in 120 min.
	AMPCO ROLLED BRONZES (Furnished by Ampco Co.)	
111	Ampco No. 18 (extruded) Brinell 190	12
	AMPCO CAST BRONZES (Furnished by Ampco Co.)	
160	Ampco No. 20 Brinell 235	5.8
161	Ampco No. 21 Brinell 285	6.2
162	Ampco No. 22 Brinell 340	9.5
125	Ampcoloy 46 Brinell 190	9.9
124	Ampco No. 18 Brinell 170	12
121	Ampcoloy A3 Brinell 130	22
	WELDED AMPCO BRONZES (Furnished by Ampco Co.)	
163	Ampcotrode 200 on SAE 1010 steel, Brinell 220	3.2
164	Ampcotrode 250 on SAE 1010 steel, Brinell 260	5.3
126	Ampcotrode 160 on SAE 1010 steel, Brinell 185	5.2
127	Ampcotrode 160 on Ampco 18, Brinell 185	5.9
165	Ampcotrode 300 on SAE 1010 steel, Brinell 320	9.5
128	Ampcotrode 160 on Ampcoloy 46, Brinell 180	20
123	Ampcotrode 10 on SAE 1010 steel, Brinell 140	24
122	Ampcotrode 10 on Ampcoloy A3, Brinell 140	31

Colmonoy

Table 16 lists tests made on welded Colmonoy. The tests show that some types of welded Colmonoy have a high resistance to pitting.

Table 17 lists Colmonoy sprayed onto a base and then fused on at a temperature of 1850 deg.F. These tests show that some of these materials also have a high resistance to pitting.

TABLE 16

Welded Colmonoy

Specimen No.	Material	Total loss in MG in 120 min.
	(Colmonoy furnished by Wall Colmonoy Co.)	
148	Colmonoy WER-100 Arc Welded	6.0
145	Colmonoy No. 6 Arc welded	8.4
129	Colmonoy---2 layers gas welded	19
130	Colmonoy---1 layer gas welded	23
147	Colmonoy No. 5 arc welded	23
146	Colmonoy No. 4 arc welded	29

TABLE 17

Colmonoy Sprayed and Then Fused to Base

Specimen No.	Material	Total loss in MG in 120 min.
144	Colmonoy No. 6	8.0
156	Colmonoy No. 6	9.5
143	Colmonoy No. 5	16
141	Colmonoy No. 4	30
151	Colmonoy, Sweat-on-Paste, Arc Application	30
150	Colmonoy, Sweat-on-Paste, QXI-ACETYLENE APPLICATION	34

Colmonoy is a trade name for a material consisting primarily of iron, nickel, chromium, borium, silicon and carbon. Before applying Colmonoy as a spray, the base metal is thoroughly grit blasted. The Colmonoy is then sprayed uniformly over the grit blasted area to a thickness of approximately .060 in. The sprayed area is then heated with an

oxy-acetylene flame or in a heat treating furnace to a temperature of 1850 deg.F. Colmonoy has the property of becoming very plastic at this temperature thereby fusing itself to a grit blasted area.

The author knows of no field tests on this material but based on the results in the accelerated cavitation machine, it merits consideration. One advantage is the ease of application, whereby the material is sprayed on and then fused with a torch or in an oven. However, the fusing process presents the problem of possible distortion of the base metal. The cost of the Colmonoy material may also be a detriment to its general use to prevent pitting.

Several test buttons were prepared by spraying Colmonoy to a base, but eliminating the fusing process. It was impossible to obtain any pitting data on these specimens because the sprayed material separated from the base during the vibration tests.

Thiokol Rubber

Table 18 lists tests made on Thiokol rubber sprayed on various materials used for a base. The test specimens were prepared by the U.S. Navy. The loss of weight of the test specimens is not a very satisfactory means for determining the relative resistance of rubber because of its low specific gravity compared to metal. However, visual inspection of the test specimens indicated that the rubber overlay gave considerable resistance to pitting. Figure 15 shows a photograph of several of the rubber overlays after two hours testing in the accelerated cavitation testing machine. These photographs show how the center of the rubber overlay is eroded down to the base metal. The composition of the base metal apparently has very little influence on the resistance of the rubber to pitting, as is indicated in Table 18.

TABLE 18

Thiokol Rubber

Specimen No.	Material	Total loss in MG in 120 min.
Navy	(Furnished by U. S. Navy)	
No. 2	Flame sprayed on stainless steel	26
No. 4	Flame sprayed on stainless steel weld inlay	28
No. 10	Flame sprayed on manganese bronze	30
No. 8	Flame sprayed on mild welded steel	31
No. 6	Flame sprayed on mild steel	33

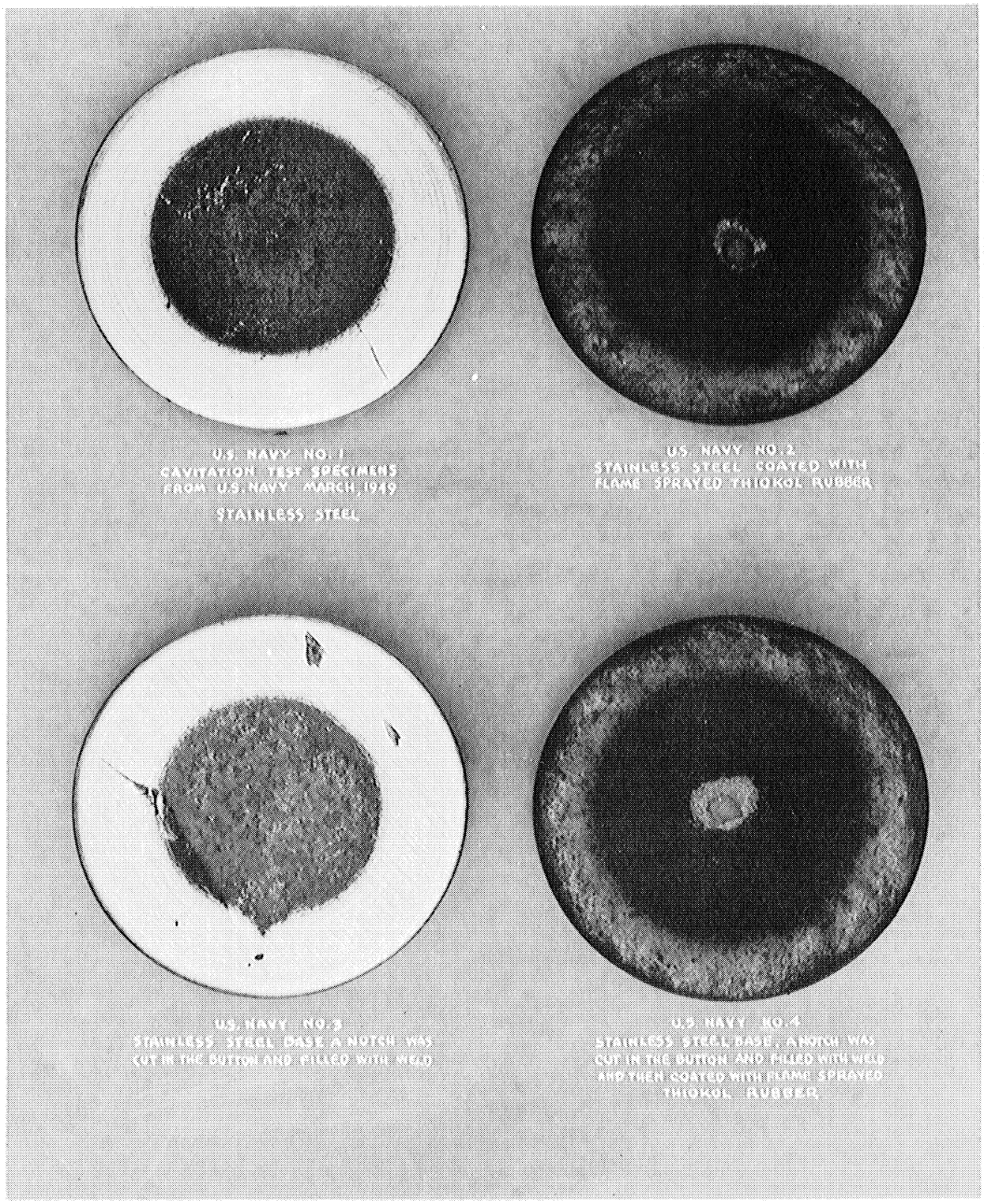
U.S. NAVY NO. 1
CAVITATION TEST SPECIMENS
FROM U.S. NAVY MARCH, 1949
STAINLESS STEEL
U.S. NAVY NO. 2
STAINLESS STEEL COATED WITH
FLAME SPRAYED THIOKOL RUBBER
U.S. NAVY NO. 3
STAINLESS STEEL BASE, A NOTCH WAS
CUT IN THE BUTTON AND FILLED WITH WELD
U.S. NAVY NO. 4
STAINLESS STEEL BASE, A NOTCH WAS
CUT IN THE BUTTON AND FILLED WITH WELD
AND THEN COATED WITH FLAME SPRAYED
THIOKOL RUBBER

Figure 15.

The U. S. Navy has used this rubber overlay with considerable success on propeller shafts, rudders and struts of navy vessels where pitting was being encountered. One of the important features of the successful use of rubber overlays is proper application. The U. S. Navy sand blasts the base metal to obtain a clean surface. The metal is heated to a temperature somewhat above the surrounding air temperature. The rubber is then sprayed on with a gun using the powder and gun developed by the Schori Process Corporation.

The results of the tests in the accelerated cavitation machine and the results obtained by the Navy under actual operating conditions, indicate that it might be desirable to investigate the performance of this rubber when used for hydraulic machinery parts subject to pitting.

Miscellaneous Materials

Table 19 lists some miscellaneous materials tested in the accelerated cavitation machine. This table shows that Stellite has by far the greatest resistance to pitting of all of the materials tested, which agrees with the results obtained in other accelerated cavitation machines.

The Stellite used in the present test was a rolled material consisting of 55% cobalt, 33% chrome, and 6% tungsten with a Brinell hardness of about 410. The Stellite was brazed to the base metal with silver solder. Stellite can be obtained as a casting and can also be applied by welding. Its disadvantage for ordinary hydraulic machinery is its high cost, and the difficulty of machining and grinding it because of its extreme hardness. However, it has been used successfully for steam turbine blading where the erosion problems are somewhat similar to pitting in hydraulic turbines.

The other materials (specimens 217, 214 and 215) which show such a high resistance to pitting are all special alloy tool steels with a hardness which makes them unsuited for ordinary hydraulic turbine parts. They have their place however for special applications.

TABLE 19

Miscellaneous Materials

Specimen No.	Material	Brinell Hardness	Total loss in MG in 120 min.
Special	Stellite, Haynes No. 6, Rolled	410	0.6
217	Vascaloy---Ramet, Tangtung-G	640	1.6
216	Ohio Die	601	2.5
214	Nestro	668	4.6
215	Vasco Supreme	657	6.2
166	Nitraloy---Holcomb No. 218	-	14
Navy No. 9	Manganese Bronze	-	80
Navy No. 7	Welded Mild Steel	-	97
Navy No. 5	Mild Steel	-	107
119	Brass, 70% Co, 30% Zn	-	156
120	Rolled Brass B-16-44-Half Hard Bar Stock used for Standard Check of Cavitation Machine, Cu 60%, Zn 27%, Pb 3%	90	162

CONCLUSIONS

The tests on variation in amplitude of vibration, on variation in depth of submergence and with various liquids, answered some of the questions regarding the phenomena of cavitation. Although these tests were not always conclusive, they indicated the type of additional investigations that should be made.

The standard accelerated cavitation tests were made mostly on standard trade materials to determine the qualities of materials readily available to the industry. These tests showed the following:

1. That new materials such as the Ampco bronzes, Colmonoy and Thiokol rubber are constantly being developed which might be suitable for hydraulic machinery and might have a distinct advantage over the materials now in use.
2. That the practical application of the materials, such as number of layers to be used when making repairs by welding or when prewelding, influences the resistance to pitting whereas preheating the base metal has very little effect on on the resistance.
3. That hardness has a definite effect on resistance to pitting regardless of the material being used.
4. That it is important to make constant accelerated cavitation tests on the special materials, particularly stainless steels, to insure obtaining the desired resistance to pitting.

The results of all of the tests showed that the accelerated cavitation machine is a very useful machine to:

1. Make further investigations on the phenomena of cavitation.
2. Test new materials and new techniques of application of materials for their relative resistance to pitting.
3. Test samples of all special materials to determine their resistance to pitting to avoid the wide variation of these qualities when the materials are obtained from different sources.

Although items 2 and 3 constitute practically a full time test program for an accelerated cavitation machine, any suggestions as to how it can be used for advancing the knowledge of the mechanics and phenomena of cavitation and pitting are welcomed.

ACKNOWLEDGMENTS

All of these accelerated cavitation tests were made possible through funds provided by the Allis-Chalmers Manufacturing Company. The Research Laboratory of the Company built the cavitation machine and kept it in operation. The tests were made under the direction of the Hydraulic Department.

The Ampco bronze test specimens were provided by the Ampco Metal Company, Milwaukee, Wisconsin.

The Colmonoy specimens were furnished by the Wall Colmonoy Corporation, Detroit, Michigan.

Cast stainless steel specimens were provided by Allegheny Ludlum Steel Corporation, Brackenridge, Pennsylvania, Ohio Steel Foundry Company, Lima, Ohio and Midvale Company, Midvale, Pennsylvania.

The Thiokol rubber specimens were supplied by the Material Laboratory, New York Naval Shipyard, Naval Base Station, Brooklyn, New York.

The Cast iron specimens for the tests with the chromate inhibitor were supplied by the International Nickel Company, New York, New York.

The author is indebted to those companies for making the facilities available for the tests, for furnishing test specimens and for permission to publish the test results.

BIBLIOGRAPHY

1. Mousson, J. M., "Pitting Resistance of Metals Under Cavitation Conditions," Trans. A.S.M.E. July, 1937, Paper, HYD-59-5.

2. Kerr, S. Logan, "Determination of the Relative Resistance to Cavitation Erosion by the Vibratory Method," Trans. A.S.M.E. July, 1937, Paper, HYD-59-5.

3. Euler, Leonhard, "Theorie plus complete des machines qui sont mises in mouvement par la reaction de l'eau," (More complete theory of machines driven by Hydraulic Recation), Historie de L'Acadomie Royal, Berlin, 1754.

4. Barnaby, Sydney W., "On the Formation of Cavities in Water by Screw Propellers at High Speeds," Trans. Inst. Naval Arch. London, Vol. 39, 1897.

5. Parsons, Charles A., "The Application of the Compound Steam Turbine to the Purpose of Marine Propulsion," Trans. Inst. Naval Arch. London, Vol. 38, 1897.

6. Wagenbach, W., "Beitiage zur Berechnung und Konstrucktion von Wassertrubinen," (Contribution to the Calculation and Construction of Hydraulic Turbines), Zeirschrift fur das Gesamte Turbinenwesen, Berlin, 28 June, 1907, No. 18.

7. Ackert, J., "Kavitation," (Cavitation), Handbuck der Experimtalphysik, Leipzig, Vol. 4, Part 1, 1926.

8. Schroter, Hellmut, "Korrosion durch Kavitation in einem Diffusor," (Erosion by Cavitation in a Diffusor), Zeitschrift des Vereines deutscher Ingenieure, Berlin, 21, May, 1932 Vol. 76, No. 21.

9. Gaines, Newton, "A Magnetostriction Oscillator Producing Intense Audible Sound and Some Effects Obtained," Physics, Vol. 3, 1932, pp. 209-229.

10. Hunsaker, J. C., "Progress Report on Cavitation Research at Massachusetts Institute of Technology," Trans. A.S.M.E., Vol. 57, 1935, Paper, HYD-57-11.

11. Knapp, R.T. and Hollander, A., "Laboratory Investigations of the Mechanism of Cavitation," Trans. A.S.M.E., July, 1948, Paper No. 47-A-150.

BIBLIOGRAPHY (CONT'D)

12. Weyl, W. A. and Marbae, E. C., "Some Mechano---Chemical Properties of Water," publication NAVEXOSP-571, Office of Naval Research.

13. Nowotny, Dr. Hans, "Destruction of Materials by Cavitation," V.D.I., Vol. 86, May 2, 1942, pp. 269-283.

14. Poulter, T. C., "Mechanism of Cavitation-Erosion," Journal of Applied Mechanics, March, 1942.

ADDITIONAL REFERENCES

Ackeret, J., "Kaviation und Kavitationskorrosion," Hydromechanische Problem des Schiffsantriebs, 1932, pp. 227-240.

Balhan, J., "The Cavitation-Erosion of Ship's Propellers," The Engineers' Digest, May, 1953, p. 163.

Beeching, R., "Selecting Alloys to Resist Cavitation Erosion," Product Engineering, January 1948, pp. 110-113.

Chambers, L.A., "Emission of Visible Light from Cavitated Liquids," Journal of Chemical Physics, May, 1937, pp. 290-292.

Copson, H.R., "Effects of Velocity on Corrosion by Water," Industrial and Engineering Chemistry, Vol. 44, August, 1952, p. 1745.

Crewdson, E., "Cavitation," Engineer, January 23, 1953, pp. 122-123.

Daily, J.W., "Cavitation Characteristics and Infinite Aspect Ratio Characteristics for a Hydrofoil Section," Trans. A.S.M.E., Vol.71, 1949, p. 269.

Eisenberg, Phillip, "A Brief Survey on the Progress of the Mechanics of Cavitation," Navy Department, David Taylor Model Basin, Washington, D. C., Report 842, 1953.

Eisenberg, P., "On the Mechanism and Prevention of Cavitation," Report No. 712, David W. Taylor Model Basin, Washington, D. C..

Ellis, A.T., "Observations on Cavitation Bubble Collapse," California Institute of Technology, Hydrodynamics Laboratory Report No. 21-12, December, 1952.

Ellis, A.T., "Production of Accelerated Cavitation Damage by an Acoustic Field in a Cylindrical Cavity," California Institute of Technology, Hydrodynamics Laboratory Report No. 21-14, September, 1955.

Föttinger, Dr. Ing. Hermann, "Untersuchungen über Kavitation und Korrosion bei Turbinen, Turbopumpen und Propellern," Hydraulische Probleme, 1926, pp. 14-64, 107-110.

Harvey, E.N, McElroy, W.D., and Whiteley, A.H., "Cavity Formation in Water," Journal of Applied Physics, Vol. 18, February, 1947, p. 162.

ADDITIONAL REFERENCES (CONT'D)

Horton, "The Effect of Intermolecular Bond Strength on the Onset of Cavitation," Journal of the Accoustical Society of American, May, 1953.

Jost, "Explosion and Combustion Processes in Gases," McGraw-Hill Book Co., Inc., New York, N. Y., p. 275.

Knapp, R.T., "Cavitation Mechanics and Its Relation to the Design of Hydraulic Equipment," James Clayton Lecture, Proc. of the Institution of Mechanical Engineers, series A, Vol. 166, 1952, pp. 150-163.

Meier, Dipl. Ing. A.,"Kinematics of Piston Slap," Society of German Engineers.

Numachi, F. and Kurokawa, T., "The Effect of Air Content on the Appearance of Cavitation in Distilled, Salt, and Sea Water," Translation and Commentary, Ordnance Research Laboratory, Pennsylvania State College, Pa., 1946.

Pond, H.L. and Eisenberg, Phillip, "Water Tunnel Investigations of Steady State Cavities," Navy Department, David Taylor Model Basin, Washington, D. C., Report 668, 1948.

Raven, F.A., Feiler, A.M., and Jespersen, Anna, "An Annotated Bibliography of Cavitation," Navy Department, David Taylor Model Basin, Washington D. C., Report R-81, 1947.

Rayleigh, Lord, "On the Pressure Developed in a Liquid During the Collapse of a Spherical Cavity," Philosophical Magazine, series 4, Vol. 34, 1917, pp. 94-98.

Rheingans, W.J., "Prevention and Reduction of Cavitation and Pitting in Hydraulic Turbines," Allis Chalmers Engineering Bulletin No. 11, Milwaukee, 1949.

Rouse, Hunter and McNown, J.S., "Cavitation and Pressure Distribution," State University of Iowa, Bulletin 32, No. 42, 1948.

Stahl, H.A. and Stepanoff, A.J., "Thermodynamic Aspects of Cavitation in Centrifugal Pumps," Mem. ASME, Ingersoll Rand Company, Phillipsburg, N.J., 1955, ASME Diamond Jubilee Annual Meeting Paper No. 55-A-136.

Stepanoff, A.J., "Cavitation in Centrifugal Pumps," Transactions, American Society of Mechanical Engineers, Vol. 67, 1945, pp. 539-552.

ADDITIONAL REFERENCES (CONT'D)

Speller, F.N., "Memo on Cavitation," A.S.T.M. Bulletin No. 133, March, 1945, pp. 21-22.

Speller, F.N., and LaQue, F.L., "Water Side Deterioration of Diesel Engine Cylinder Liners," The International Nickel Company, Inc., New York City, 1950.

Ware, M., Taylor, R.E., and Witzky, J., "The New Packard Light Weight Diesel Engine," Society of Automotive Engineers National Diesel Engine Meeting, Paper presented November 3, 1953.

Watson, R., "Cavitation in Centrifugal Pumps," Proceedings of the 3rd National Conference in Industrial Hydraulics, Armour Research Foundation, Chicago, Ill., p. 60.

Knapp, R.T., "Recent Investigations of the Mechanics of Cavitation and Cavitation Damage," The American Society of Mechanical Engineers, Paper No. 54-- A-106 presented November - December 3, 1954.

Abstract

This paper describes water-tunnel investigations into the mechanics of "fixed" type cavitation and into the probable mechanism through which this type causes material damage. High-speed motion pictures were used to study the cavity mechanics, and indications of the damage pattern were obtained by measuring the pitting rate on soft aluminum test specimens. Information was obtained on the frequency and intensity of the damaging blows, the distribution of damage in relation to the area covered by the cavitation, and the variation of the intensity of cavitation with velocity.

Margulis, W., McGowan, J.A., and Leith, W.C., "Cavitation Control Through Diesel Engine Water Treatment," SAE, presented June 3-8, 1956.

Abstract

It has been found that by means of magnetostrictive cavitation testing, it is possible to duplicate the conditions that lead to deterioration of the water side of diesel engine cylinder liners. In order to obtain accurate results it is necessary that conditions of temperature and pressure that are present in the water system by duplicated on the laboratory facility. It has been shown that increasing water pressure will definitely inhibit the erosive action of cavitation. Changes in operating temperatures will have less predictable results. The use of a chromate type corrosion inhibitor is effective in decreasing cavitation within concentration limits of 1000 to 2000 ppm. Soluble oil water treatments are also effective in concentrations between one-half and two percent. Boron nitrate type corrosion inhibitors are ineffective in combating cavitation.

Schrader, Alan R., "Investigation of Cavitation Erosion in Diesel Engine Coolant Systems at the U. S. Naval Engineering Experiment Station," SAE, presented June 3-8, 1956.

Abstract

Two phases of the U. S. Naval Engineering Experiment Station's current investigation of cavitation erosion in diesel engine coolant systems are described. The first phase is concerned with accelerated cavitation tests as conducted with a magnetostriction apparatus. Various materials and test arrangements were included in the studies. The second phase of the investigation covered the measurement of cylinder liner and block vibration in diesel engines wherein cavitation erosion damage was known to exist. This analysis indicated that the principal source of vibrational energy in the area of cavitation damage was the resonant vibration of the cylinder liners as excited by the impacts of piston slap and cylinder firing pulses.

Sutton, G.W., "A Photoelastic Study of Strain Waves Caused by Cavitation," American Society of Mechanical Engineers, Paper No. 57--APM-15, July 24, 1956.

Abstract

Ultra-high-speed photoelastic techniques have been applied to a study of the transient stresses and strains in a photoelastic plastic when subject to cavitation. A photocell, used to detect the transient strains, indicated that the time duration of the strains was about 2 microsec. Using an ultra-high-speed motion-picture camera, ultrasonic cavitation bubbles have been photographed collapsing on the surface of a photoelastic specimen, and the resulting strain wave in the solid has been photographed. The dynamic properties of a photoelastic material have been obtained in order to permit quantitative interpretation of the transients. This has indicated that the stresses due to cavitation may be as high as 2 x 10^5 psi. The photoelastic plastic, CR-39, was found to exhibit strain birefringence, and its strain-optic constant was found to be independent of the rate of loading.

Taylor, Irving, "Cavitation-Pitting by Instantaneous Chemical Action from Impacts," The American Society of Mechanical Engineers, Paper No. 54--A-109, presented November 28-December 3, 1954.

Abstract

The author contends that certain extremely reactive unstable substances are produced locally in water and some other liquids, at the instant of final cavity collapse, by cavitational impacts. These substances complete subsequent chemical reactions in a few millionths of a second. They may react with each other or with the liquid itself, and disappear by reforming into stable liquid. Those that are very close to a solid wall at the instant of their creation, however, can just as well react chemically with the solid. These reactions occur so quickly that even in a very fast-flowing liquid, the evidence (pitting) may be localized within an inch downstream of the main impact point. The paper represents an idea rather than new experimental data, the conclusions being stated in the form of contentions. The author, however, presents an analysis of known data upon which these contentions are based.

Trock, Bernard, "A Study of Cavitation Erosion," SAE, presented June 3-8, 1956.

Abstract

Cavitation-erosion is a peculiar form of corrosion or pitting which occurs on the water side of Diesel Engine cylinder liners, on hydraulic turbines, on centrifugal pumps and on high-speed ship propellers causing extensive and costly damage. As a result it has been the subject of numerous investigations. Despite these studies its mechanism is still unknown although it has been established that the following factors affect the pitting rate of the metals: (a) Hardness, (b) Porosity and surface discontinuities, (c) Viscosity, temperature and molecular size of the contacting liquid, (d) Amplitude of vibration, and (e) the addition of corrosion inhibitors. Some recent experimental data which illustrates some of the above effects is included.

FRETTING AND FRETTING CORROSION

J. R. McDowell
Research Engineer
Westinghouse Electric Company

FRETTING AND FRETTING CORROSION

by

J. R. McDowell

INTRODUCTION

Fretting or fretting corrosion can be thought of as a special type of wear leading generally to corrosion products the production of which has been accelerated by mechanical means. It is always characterized by minute reciprocating motion between the wearing materials which are held together by a normal force. Typical examples of mechanical assemblies which are subject to this type of wear or deterioration are press fits or bolted assemblies where vibration or repeated mechanical straining of the parts cause them to have this required relative though minute motion while some load normal to the motion is applied. The resulting damage may vary from only a discoloration of the mating surfaces to the wearing away of a sixteenth inch of material. The surface may show the formation of an abundance of corroded materials or merely a heavily galled appearance with little oxide debris. The frequency, total number of cycles, amount of motion, normal pressure, physical characteristices of the mating materials, and environmental conditions will all contribute to the results.

Historically the first mention of the observation of the phenomenon was made by Eden, Rose, and Cunningham[1] in 1911. It was not until 1927, however, that Tomlinson[2] wrote the first published report of an investigation of the subject and the name he gave to it in a later paper[3] has remained. The first reference to this type of wear in America was called false brinelling by J. O. Almen[4] in a report of the effects of a long list of lubricants rated as to their ability to prevent fretting corrosion. His paper cited a classic example of the damage that can be caused. The wheel bearings of automobiles shipped by rail to the West Coast were pitted at the spots where the balls or rollers had rested while the vibration caused by the rail joints had produced very slight movement at these points. The bearings had to be replaced. Autos that had been jacked off their wheels were much less effected as were those shipped in the summertime.

Another serious example of trouble caused by fretting corrosion is the rotor-head bearings of helicopters which prompted the formation of laboratory and service evaluation panels on the subject of fretting corrosion in 1950 by the Coordinating Research Council, Inc. Airframe Lubricants Group at the request of the United States Air Force. The S.A.E. committee S-2 (helicopters) also set up a special project in 1947 to study the phenomenon.

Many examples could be cited from the literature of the deleterious effect of fretting corrosion on machine parts, but it seems only necessary to point out the most common places where it may be expected. As already suggested, bearings in general which do not rotate but oscillate or are subject to vibration in place are particularly susceptable. Press fits where gears, bearings, wheels, etc. are mounted on shafts that rotate are very likely to fret at the points where the shaft is alternately stressed between tension and compression inside the fitted member. Jaws and chucks of rotating machinery tend to fret in the same manner against the pieces they hold during rotation or vibration. Gear tooth spline couplings which by their nature allow slight alternating axial movement between the teeth are very prone to fret. Bolted assemblies subject to vibration, where one of the members is stressed by alternating loads causing that member to move with respect to its mount the small amount required by its elastic deformation, will fret at the mating surfaces. Considerable work has been done in the past 20 years since Tomlinson's second paper in 1938. A summary of what has been learned will be outlined in some detail.

Effect of Motion

Tomlinson[2] in his first paper demonstrated that a single stroke of a bar across a plate could produce oxide debris and score marks where contact was accomplished. To support his molecular attrition theory for fretting corrosion he presents photographs of fretting at motions of 6.5×10^{-8} inches which he felt was about the threshold of fretting. Most of his measurements were for very small motions the exact amplitude of which seemed to have little effect. He did show that motion was necessary, however. In his second paper[3] the effect of a high surface elasticity was noted to be about one tenth the shear modulus of the base material. This had to be passed before motion actually took place.

Uhlig et al[5] used motions from $.5 \times 10^{-3}$ inches to 9×10^{-3} inches showing a linear relationship for weight loss directly proportional to the amount of motion, Figure 1. Halliday and Hirst[6], using motion from $20\mu = .8 \times 10^{-3}$ inches to $150\mu = 5.6 \times 10^{-3}$ inches, claimed a sudden increase in the volume of wear at the value of 4×10^{-3} inches. The curve, however, does not seem consistent with the plotted points. Their reasoning was based partially on the fact that high electrical resistance was maintained between the specimens at low amplitudes whereas at the higher values metal-to-metal contact was encountered similar to the low resistance if the first few cycles of every test before any debris separated the sliding pieces. They theorized that more severe wear was therefore taking place. The design of the test pieces in the two investigations was different. That of Uhlig et al. tended to trap the debris while the Halliday and Hirst design allowed free escape, thus possibility accounting for the discrepancy. Investigations at the

Westinghouse Research Laboratories indicate no sudden rise in wear rate at motions up to 5×10^{-3} inches.

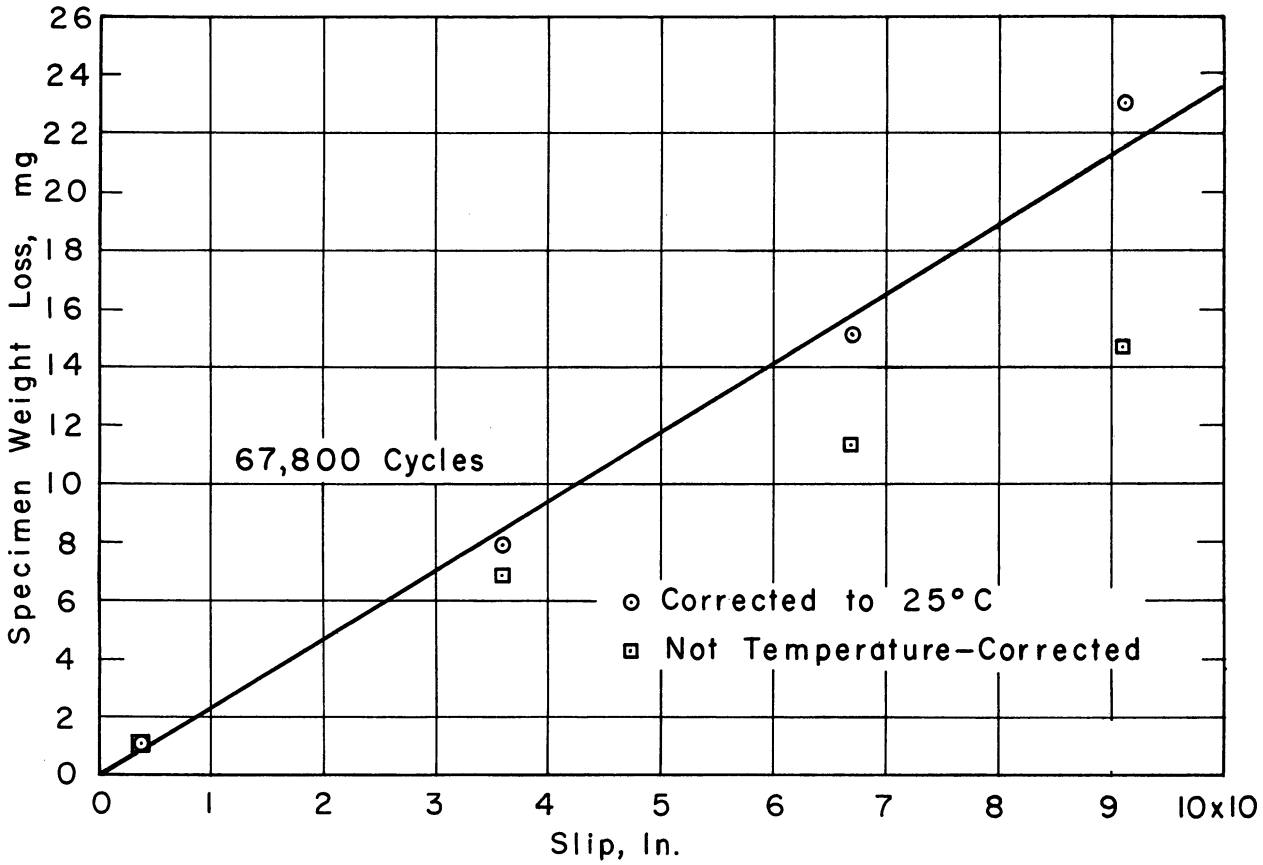

Figure 1. Effect of relative slip on fretting of mild steel in dry air. Pressure, 5,300 psi; frequency, 540 cpm. Reprinted from H.H. Uhlig, I. Ming Feng, W.D. Tierney, and A. McCellan, "A Fundamental Investigation of Fretting Corrosion," NACA Technical Note 3029, December, 1953.

Effect of Pressure

Tomlison[3] claimed no effect due to pressure. His contention was based on the visual examination of the wear caused by a spherical surface oscillating on a flat specimen. The Hertz stress would be much higher at the inner edge of the fretted band than on the outside circumference. The fretting looked quite uniform across this band width. No actual measurement was made.

Uhlig et al in their first report[7] showed a curve of increasing wear with pressure up to a point where it dropped off again, Figure 2. The drop was due to a decrease in motion resulting from the fact that elastic motion of the apparatus increased with load thus reducing the remainder for a given setting of the machine. Later[5] Figure 3, they

show a curve of continually increasing wear with pressure when the motion was held at a constant value. Wright[8] gives a similar curve of linear increase of column damage with increased pressure.

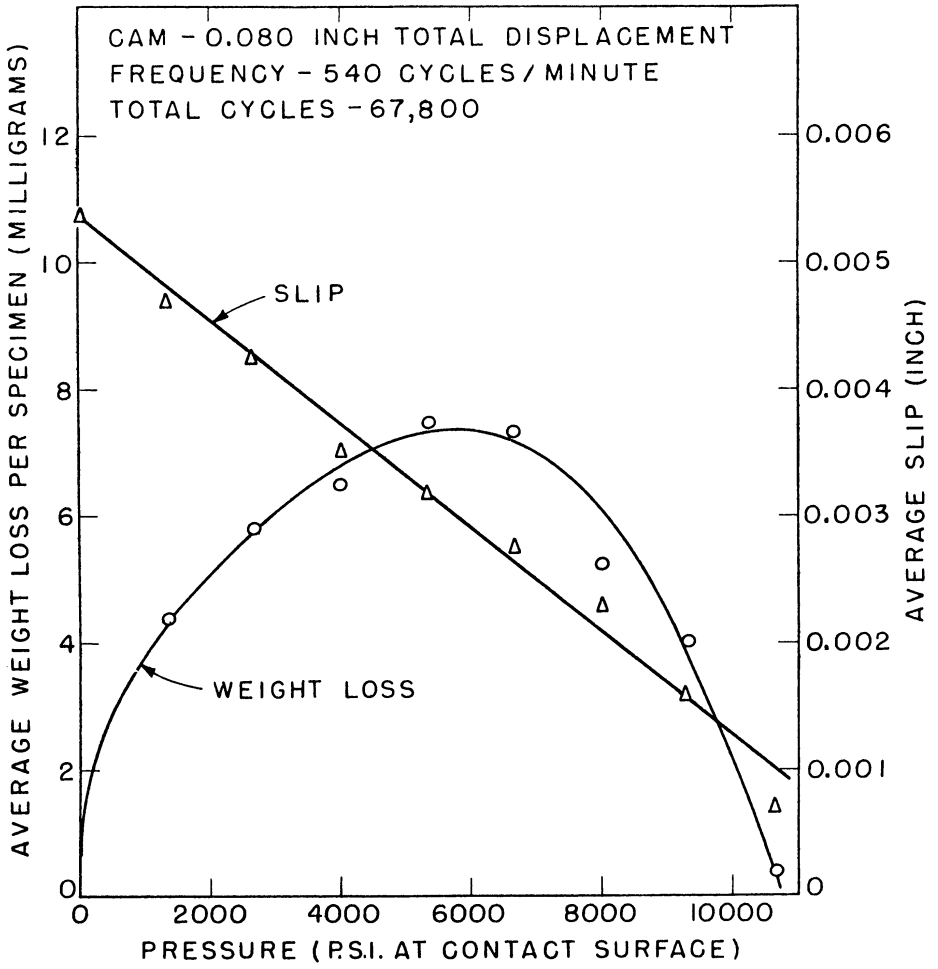

Figure 2. The effect of pressure (load) on weight loss and slip. Reprinted from H.H. Uhlig, W.D. Tierney, and A. McCellan, "Test Equipment for Evaluating Fretting Corrosion," ASTM Special Technical Publication No. 144, June, 1952.

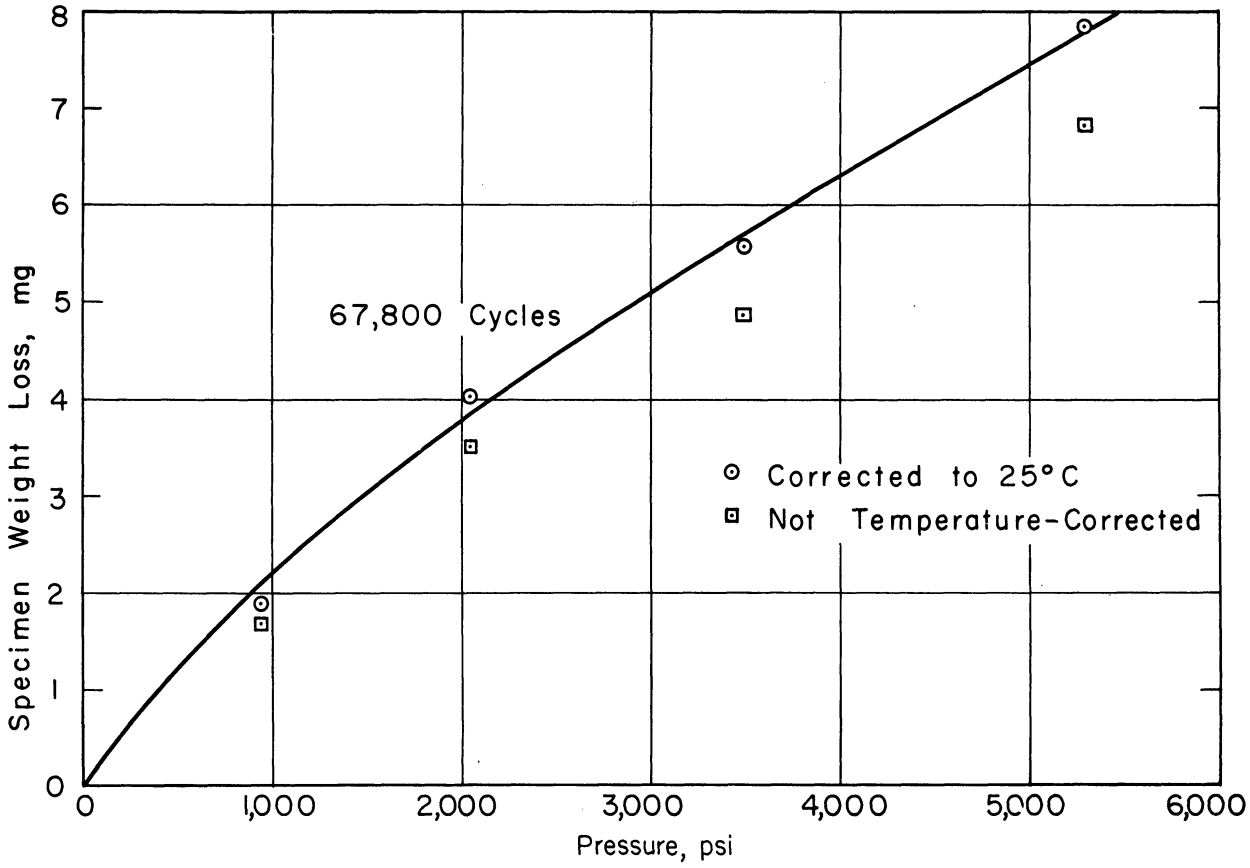

Figure 3. Effect of pressure (load) on fretting of mild steel in dry air. Frequency, 540cpm; slip, 0.0036 inch. Reprinted from H.H. Uhlig, I. Ming Feng, W.D. Tierney, and A. McCellan, "A Fundamenatal Investigation of Fretting Corrosion," NACA Technical No. 3029, December, 1953.

Photographs of two phenolic resin bonded cloth filled plastic specimens are shown in Figure 4 tested at Westinghouse in which the effect of increased load can clearly be seen in the amount of increased fretting of the tool steel mating specimen.

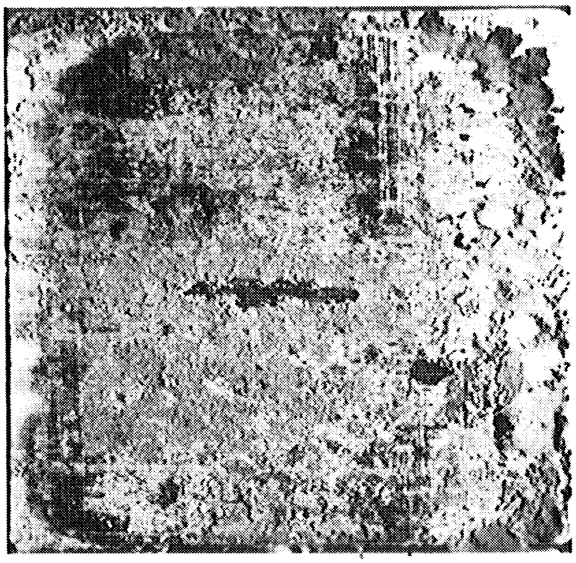

LOAD 26 LB.
MOTION .005 IN.

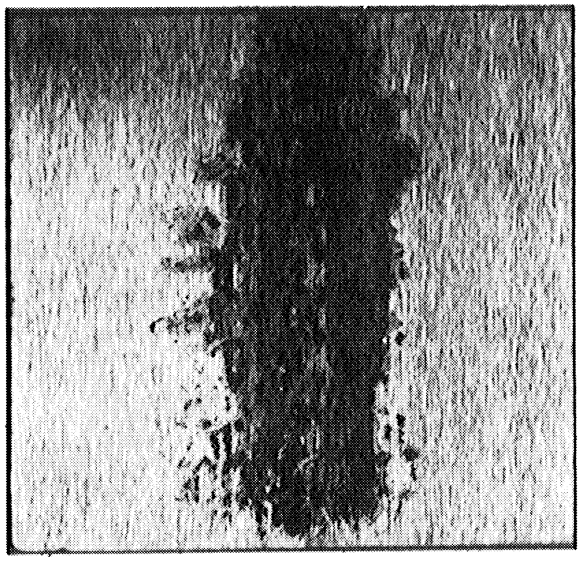

LOAD 26 LB.
MOTION .001 IN.

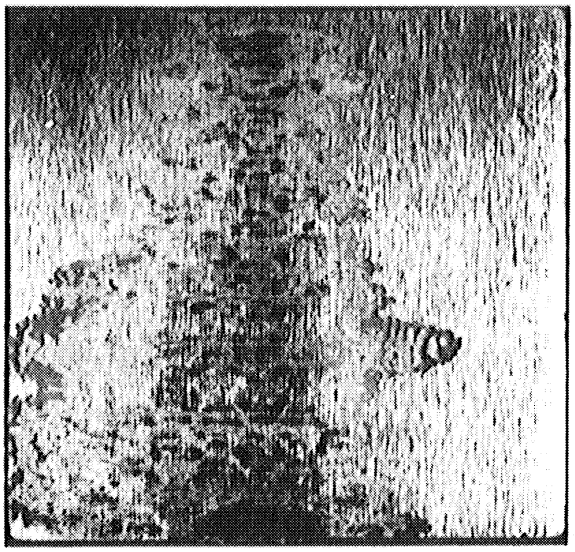

LOAD 6 LB.
MOTION .005 IN.

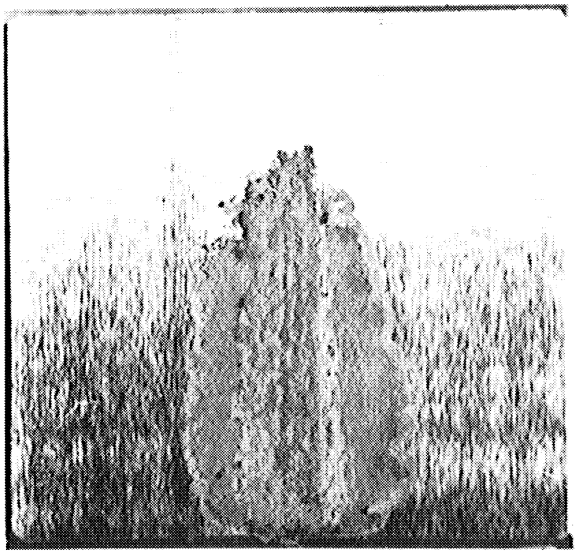

LOAD 6 LB.
MOTION .001 IN.

Figure 4. Photographs of steel specimens in contact with cloth filled phenolic resin plastic showing relative effect of load and motion in laboratory atmosphere.

Effect of Number of Cycles

It is unanimously agreed that fretting damage increases with the number of cycles. The rate of increase varies depending on the material, hardness, hardness of the oxide, and motion. It should be stated that most of the variables which effect the amount of fretting or fretting corrosion are interdependent, and it is erroneous to assume that each can be treated as a separate factor. Under somewhat similar conditions this can be done, but care should be taken in so doing.

There is generally a run-in period during which the rate is more rapid. Uhlig[5] reported a value of 150,000 cycles for this period after which the rate was very uniform. Wright[8] also shows linear curves. Halliday and Hirst[6] show that the variation in the coefficient of friction causes erratic results during the early stages and that as this period is passed the rate settles down to a more uniform value. As will be brought out later the manner in which the wear is taking place either by metal-to-metal contact at isolated points, grinding or rolling action of powdered oxide debris, or large area metal-to-metal contact has considerable effect on the wear rate. Figure 5 shows the wear curves tested at Westinghouse of increase in fretting area with time. The depth of deep pits formed by some materials is not taken into account and, therefore, the volume loss would give slightly different values. With aluminum, particularly, this is true. The erratic early stages of these curves are very noticeable. The curves of Figure 5 were obtained by separating the specimen at intervals during the test life and photographing the upper specimen. They were then replaced as carefully as possible without disturbing the debris and the test continued . A series of such photographs is shown in Figure 6. The curve resulting is shown in Figure 7.

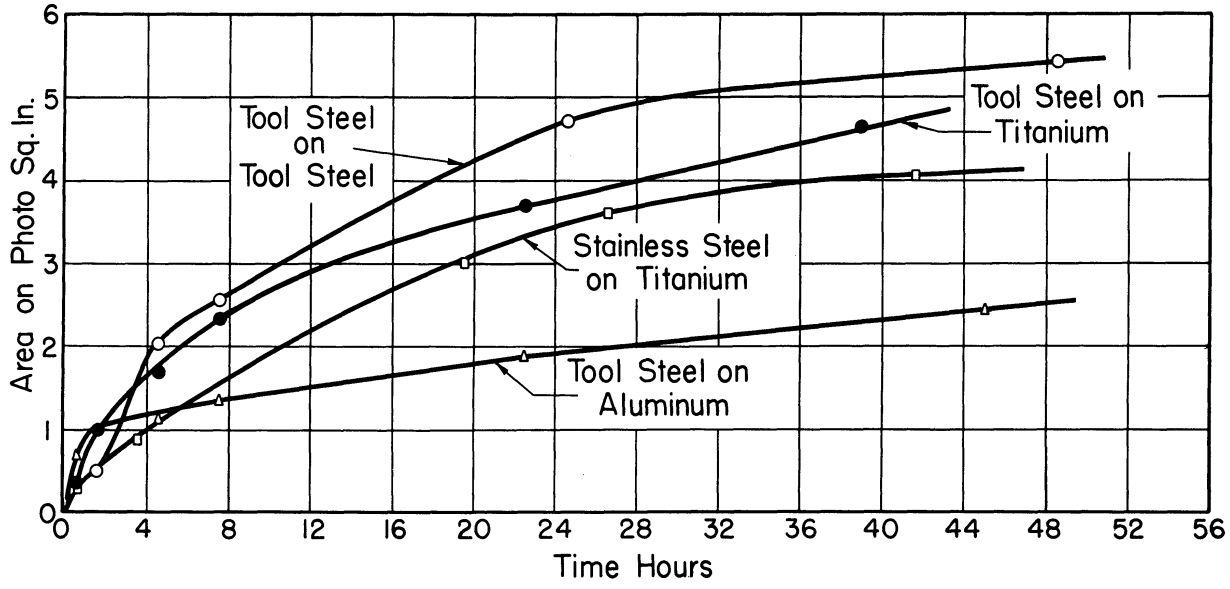

Figure 5. Curves of fretted area with time of four different combinations of materials. Motion, .002 inch; Load, 46 lbs; Nominal initial pressure, 1840 psi, frequency, 1170 cpm.

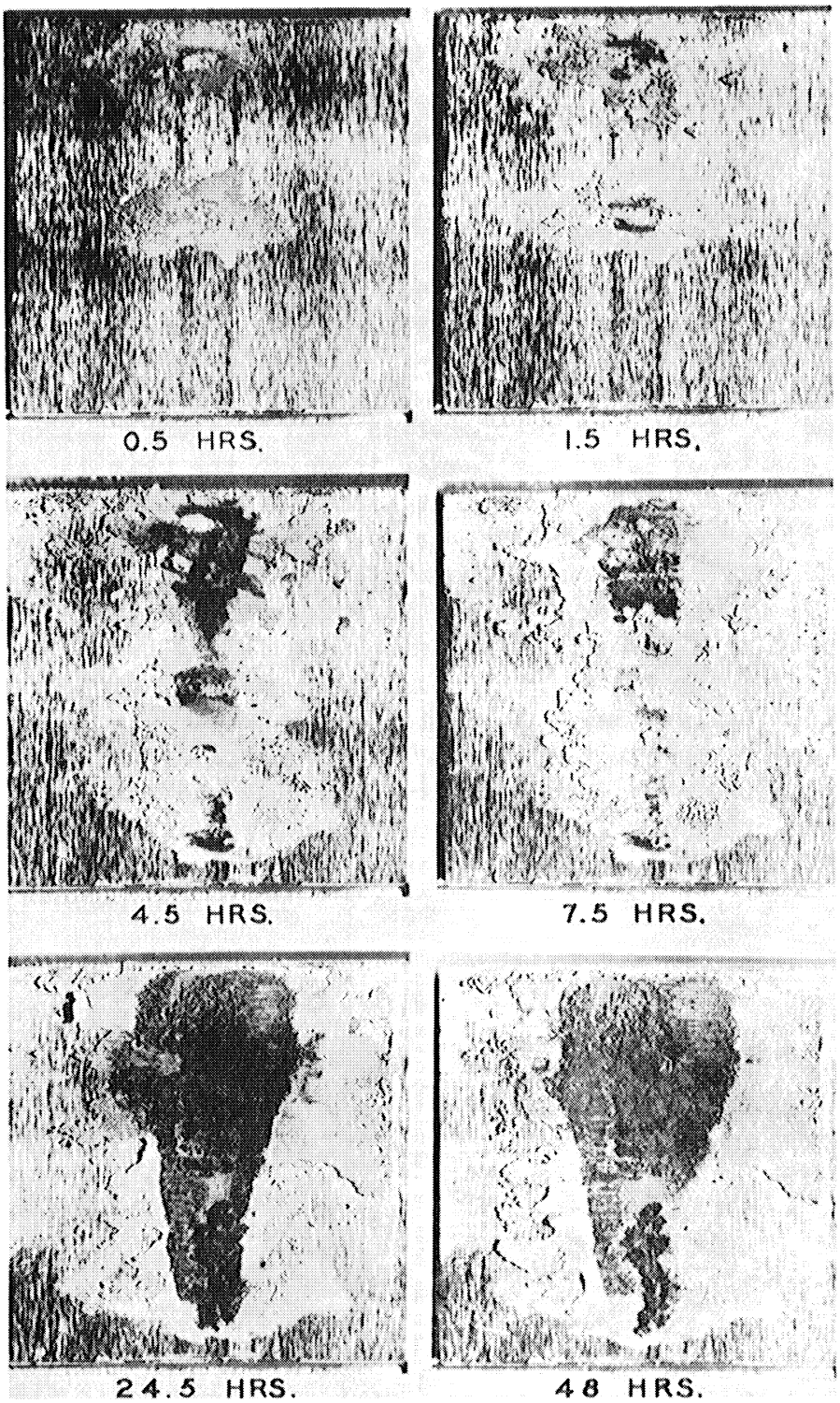

Figure 6. Photographs of a specimen of tool steel fretted against another tool steel specimen in laboratory atmosphere at the indicated stages of its test life. Motion, .00216 inches; Nominal initial pressure 1840 psi; frequency, 1170 cpm.

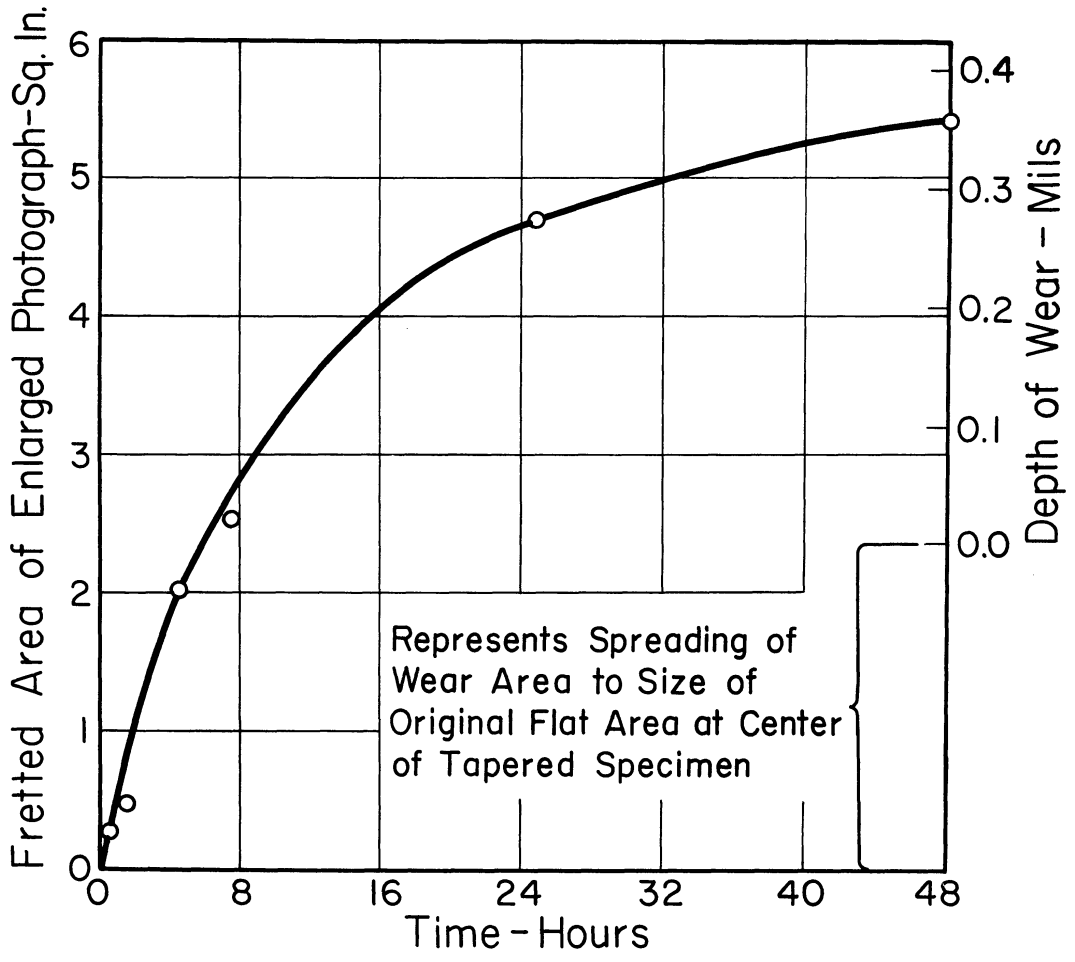

Figure 7. Fretting wear of tool steel on tool steel.

Effect of Frequency

Under atmospheric conditions a frequency effect should be expected since a chemical action is taking place in the oxidation of the metal involved. Uhlig[5] presents data to support this showing a decrease of fretting with rising frequency. The effect seems most active at values below 1,000 cycles per minute and at larger amplitudes of motion. In his theory for fretting for which he has developed an emperical expression the chemical phase becomes more important at lower frequencies. Using an inert atmosphere the effect vanishes. Tests made at Westinghouse[9] showed no frequency effect but they were all above 850 cycles per minute which would agree with Uhlig's findings.

Effect of Hardness

Generally speaking harder materials will tend to be less susceptable to fretting corrosion. This is not universally true, however. Tomlinson[3] showed hard steel and chrome plate to be less susceptable than mild steel. Almen[4] and the author[9] present further evidence of this effect under atmospheric conditions. The author[10] in an investigation of hardened steels in an oil bath found that hard steels tended to have heavier or deeper scoring and galling wear unless a chemical change such as nitriding altered the surface structure. Dies[11] stated that the hardness of the oxide played an important role in the process and that the same wear rates were observed for both a mild steel and a nitrided steel when rubbed against a chromium steel. He showed, however, the beneficial effect of nitrided steel against hard steel when compared with stainless steel or aluminum against hard steel. Sakmann and Rightmere[12] also state that the hardness of the oxide is an important property but that the worst combination is one in which both metal and oxide are hard. Lead, for instance, being soft, allows the hard oxide particles to be imbedded in it, and shows up well in fretting resistance against steel.

Godfrey[13] lists the nonmetals directly in their order of increasing hardness (mica, lucite, glass, quartz, and ruby) as also their order of increasing resistance to fretting.

Effect of Temperature

Uhlig et al[5] present data in the range of temperature from -125° C to +150° C. For short time tests 67,800 cycles little change was observed as to fretting tendencies. At longer times a decrease in weight loss with increasing temperature up to 0° C was observed. In both cases a sizable drop in wear occurred reaching a minimum at about 100° C. The curve for wear rate rose again at higher temperatures. His explanation suggests the possibility of greater adsorption of gasses at low temperatures.

The suggestion is continually being made that high local temperatures are responsible for the debris formed during fretting corrosion. Many investigators have shown that the energy dissipated is extremely low and with measurements of this surface temperature demonstrate that high local temperatures are not present during fretting corrosion.

Coefficient of Friction

Weismantle[14] presents a chart listing by coefficient of friction a number of bonded dry film lubricants and their associated ability to prevent fretting corrosion. The low friction materials are definitely superior in this respect. Teflon has been shown to be very good as a fretting inhibitor if high pressures do not prevent its use. Godfrey and Bisson[15] show the effectiveness of the low coefficient of friction of MoS_2 as a fretting inhibitor. The softness of MoS_2 (1 to 1.5 on Mohs's scale) may also contribute to its effectiveness.

Curves of the coefficient of friction of steel, or steel with time are shown by Halliday and Hirst[6] in which initially low values with the first cycle suddenly rise to very high values as the initial oxide film is broken. As metal-to-metal contact continues at sufficient points this value remains high with high normal loads until sufficient oxide debris is accummulated to separate the surfaces. At low normal loads the coefficient of friction does not get much higher than 0.2, then drops to the same low values finally reached by the higher normally loaded tests. This final value is of the order of .05 or lower and is reached after about 10 minutes indicating a lubricating characteristic of the debris. They suggest that the oxide rolls as little pebbles under the load thus approaching rolling friction. They found by electron microscopic examination that the debris became finer as the tests progressed. The author would suggest that this is not true of some materials as there is definite evidence in tests conducted at Westinghouse that certain materials such as stainless steel, aluminum, and magnesium tend to compact the oxide along with loose metallic debris, and that the coefficient of friction will begin to approach the value for the initial oxides of the metals. Compacted iron oxide has also been observed in many cases.

Effect of Humidity

Three known references show some discrepancy as to the exact effect of humidity, but all show a general tendency toward the alleviation of fretting at higher humidities. Uhlig[5] gives a straight line relationship from 0 to 100% humidity with a reduction in weight loss of about half at 100% as compared to the weight loss at 0%. Wright[8] used humidities of 0, 45% and 100%. His curves are reproduced in Figure 8. Godfrey[16] found a peak high wear rate at 30% humidity in the unlubricated state. The general trend was to a lower wear rate at high humidities for both lubricated and unlubricated conditions using mineral oil for the lubricant. His data does not show the high per cent variation that the other two investigators have shown. The explanation offered by Uhlig and Wright is that the moisture acts as a lubricant or helps carry away debris. The author would also suggest that at high

humidities $Fe_2O_3 \cdot H_2O$ may form, which is about one point on the Mohs's scale of hardness softer than Fe_2O_3, and that the abrading factor may thereby be lowered at high humidities.

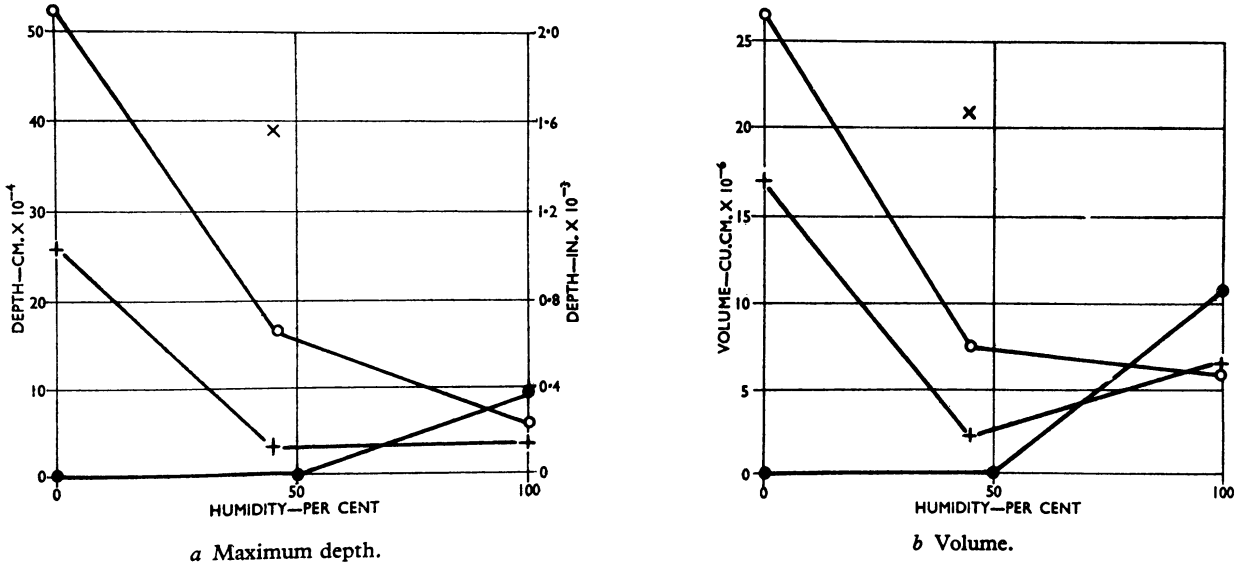

a Maximum depth.

b Volume.

Figure 8. Variation of Fretting Corrosion with Humidity.
x Nickel against steel, 50,000 oscillations
o Chromium against steel, 50,000 oscillations
+ Steel against steel, 50,000 oscillations
● Gold against steel, 100,000 oscillations
Reprinted from K.H.R. Wright, "An Investigation of Fretting Corrosion," Proc. Inst. of Mech. Eng., Vol. 1B, 1952-53, page 561.

Effect of Lubrication

The effect of dry lubricants has already been mentioned as beneficial under the heading of coefficient of friction. Oil and grease lubrication is also a very effective method of reducing fretting corrosion. The added advantage of such lubricants is that if fluid enough they limit the supply of oxygen which reduces or eliminated the role which oxidation plays in this phenomenon.

In a study of 39 lubricants including water, Almen[4] stated that the viscosity was the predominant characteristic that influenced their rating. The very fluid materials sealed the fretting area from access of oxygen and gave the best protection. This was the reason for the severe fretting of the automobile wheel bearings during winter shipment. The thick grease provided very little protection.

Herbeck and Strohecker[17] found that shear-susceptible greases will work down and minimize fretting corrosion regardless of initial consistency but again that feedability is the prime factor in reducing fretting.

Even a little oil will reduce fretting corrosion by a considerable amount over dry conditions. A striking example is shown in Figure 9 of tests run at Westinghouse. Tomlinson[3] indicated that surfaces initially smeared with oil did not fret as readily as dry surfaces. Godfrey[16] made a series of fretting tests of a steel ball which had a small drop of oil surrounding the area of contact with a flat surface. As fretting progressed the debris began to soak up the lubricant, and it finally reached an "unlubricated" state where the curve of wear area with time suddenly changed to a much steeper slope.

The author[10] found that the fretting when completely immersed in oil is reduced to metal-to-metal contact with resultant welding. Very little oxide debris is formed. The surfaces become very rough as metal is transferred back and forth between the mating surfaces and it has the appearance of galling.

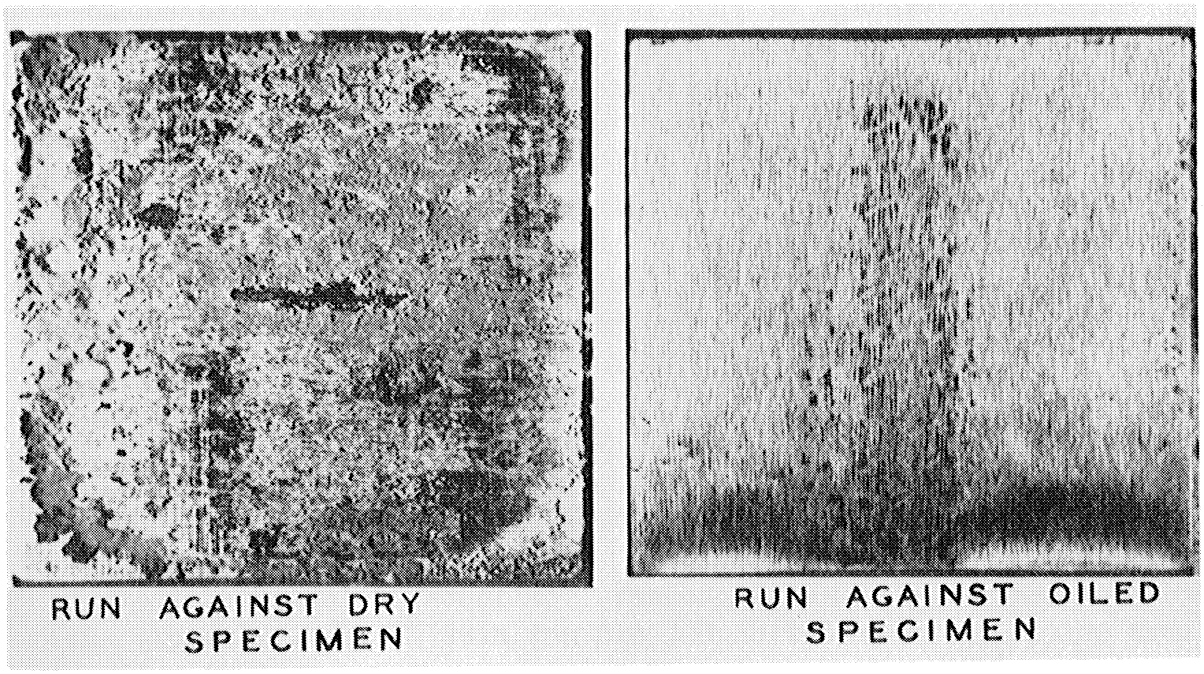

Figure 9. Photographs of two steel specimens rubbed against cloth filled phenolic resin plastic specimens. One mating plastic specimen was given a couple of drops of oil, the other was dry. Motion, .005 inch; Nominal pressure, 1000 psi; No. of cycles, 3.37 million.

Effect of Vacuum and Inert Atmosphere

It has been shown very conclusively that oxidation plays an important role in fretting corrosion. Many tests in vacuum, nitrogen, helium, and hydrogen have shown a marked decrease in the resulting wear. The change from air to nitrogen reported by Uhlig et al[5] resulted in a reduction in fretting to 1/4 the weight loss. Some work by Rosenberg and Jordan(18) shows that even in hydrogen atmosphere oxides are formed. The adsorbed and absorbed oxygen is adequate to provide some oxidation products. Sakmann and Rightmere[12] present photographs showing the effect of degassing the mating surfaces by an electrical discharge just prior to testing while in the vacuum chamber. This degassing seemed to apply only to steel surfaces. Copper and aluminum did not show the corresponding reduction in amount of debris of the degassed specimens of these materials.

The exclusion of air to the fretting area seemed to be the best explanation of the results of a test at Westinghouse(9) where the surfaces had been previously coated with rubber cement. The cement had apparently extruded from the bearing area but remained at the edges to seal it from the atmosphere. Very little fretting resulted.

Identification

There is no absolute formula by which it may be determined whether two worn and corroded surfaces were worn by fretting or by some other mechanism. An analysis of the possibility of reciprocating minute motion should first be made to determine if such motions do or did exist between the parts involved. There have been some cases of repeated normal motion between surfaces which produced fretting debris. An unpublished report of The National Physical Laboratory, Engineering Department, in England, by S.L. Smith, G.A. Tomlison, and R.C.A. Thurston gives photographs of fretting between two steel balls of equal diameter which were loaded against each other with an alternating force. The area of contact thus became greater or less as the load alternated. The motion would thus be normal to the surface with no theoretical possibility of sliding. The area which was beyond the smallest contact area and within the largest contact area fretted. Similar fretting was reported by Kennedy(19) in a device of the same type as an incidental result of work on contact fatigue.

An abundance of red Fe_2O_3 oxide debris of steel surfaces coming from a joint or crack is a very good sign that fretting corrosion is occurring. Fe_3O_4 can be the product if a limited supply of oxygen is available. Likewise, $Fe_2O_3 \cdot H_2O$ can result when humidity is high. An analysis of the debris will help, but environmental conditions should be kept in consideration.

A close examination of the fretted area for markings which might indicate reciprocating sliding will aid to identify such motion. The photograph of Figure 10 is of a specimen of nitrided steel that has been in contact with another hard nitrided surface while in an oil bath. The little ripples of the fretted area are of the same dimension as the amount of motion indicating that a hard high shot of one surface was rubbing back and forth in a groove in the mating surface.

If shafts are breaking in fatigue within press fits, a close examination of the surfaces should be made for the possibility of fretting corrosion being responsibile for initiating the crack.

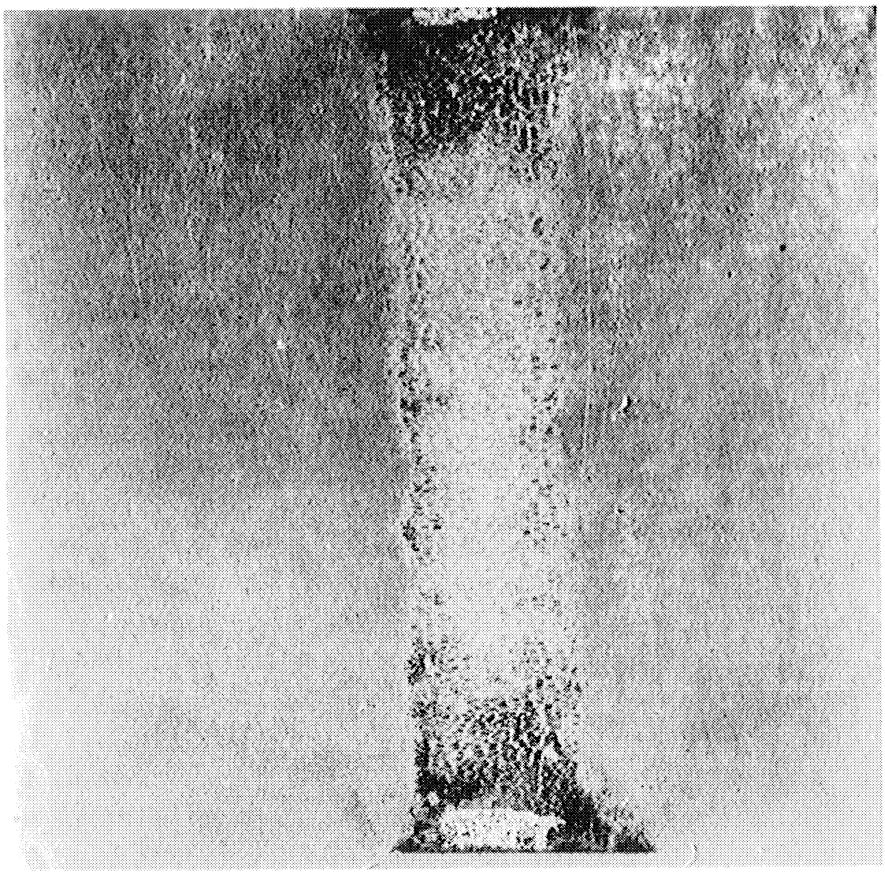

Figure 10. Photograph of nitrided tool steel fretted against a nitrided tool steel in an oil bath. Motion, .0048 inch; Nominal pressure, 5,850 psi; No. of cycles, 5.05 million.

Theories of the Mechanism of Fretting Corrosion

Tomilnson(2) presented the first theory of molecular cohesion. He felt that since the phenomenon continued down to motions of 6×10^{-8} that surface molecules were coming close enough to be plucked out by tangential motions of this order of magnitude. The loose particles then oxidized immediately upon being removed from their base metal. He did not entirely rule out some kind of surface fatigue, however, particularly with his second paper when he measured the very low surface modulus of shear.

Godfrey(13) stated that the fretting always began with the removal of loose powder of the virgin material which later oxidized in progressive stages till the final product was $Fe_2O_3 \cdot H_2O$. He agreed with Tomlinson essentially except as to the necessity for molecular dimensions. He also made a point of the fact that a single stroke in one direction did all the necessary damage to be called fretting corrosion and it would just be repeated with successive cycles.

Sakmann and Rightmere showed rather conclusively, however, that oxidation plays an important role in fretting corrosion. Their tests of the various materials in vacuum and helium atmospheres showed very definite decreased wear rates where oxygen is absent. They suggest that the hardness of the oxide make it act as an abrasive. Uhlig[20][5] presents a mechanism for fretting corrosion. A hypothetical surface is shown sketched as a series of saw teeth or contacting asperities of two mating surfaces. When one rubs on the other the oxide surface is broken and a clean metal surface is exposed behind. Oxygen or air immediately adsorbs to the clean surface and begins to form an oxide. The added energy of sliding aids the formation of the oxide which is then removed by the next reversal. Whether the oxide forms before being wiped off or whether virgin material with adsorbed gasses adhearing to it is wiped off to for the oxide later is uncertain. He presents the empirical equation

$$W\ (\text{total}) = (k_o\ L^{1/2} - k_1\ L)\ \frac{C}{f} + k_2\ lLC$$

where W is specimen weight loss - milligrams, L is the load - psi. C is the number of cycles, f is the frequency - cps, l the slip - in, and k_o, k_1, and k_2 are constants. The constants for his data are $k_o = 5.05 \times 10^{-6}$, $k_1 = 1.51 \times 10^{-8}$, and $k_2 = 4.16 \times 10^{-6}$.

Feng and Rightmere[21] present an independent slightly different view. They suggest that the asperities initially shear each other off their adjoining metal bases forming pieces of loose debris. This debris accumulates at low points until it fills up these spaces. It is then ground up gradually changing to oxidized particles. These accumulations of oxidized particles continue to grind out pits but the wear action becomes slower as more and more particles form. They then spill out into open spaces till the entire area becomes covered with this oxidized material. They do not agree with Tomlinson, contending that an oxide covered surface should not readily adhear by molecular attraction to an adjoining surface. Further, the particles are much larger than molecular. They did agree with Godfrey in that they felt welding even on a larger scale would not be conducive to the formation of loose particles.

E.E. Wisemantle in an unpublished Westinghouse report of the work leading to reference 14 suggested a surface fatigue effect as though the asperities were little cantilever beams subjected to very high plastic fatigue strains. These would then break off and the action continue much as Feng and Rightmere suggest.

The author would rather take sides with the British authors Halliday and Hirst[6] whose measurement of the initial variation of the coefficient of friction as well as electrical resistance measurements indicate definite welding of the metal surfaces after breaking up the initial oxide, coating by plastic flow. These roughened surfaces then grind up loose metallic debris which gradually forms the oxides that are responsible for the lower wear rate of oxide pebbles that continue to gradually grind away the surface at low amplitudes and pressures. At high amplitudes (.016 inches) they show that this film of debris is not sufficient to separate the surfaces and that much more rapid wear will result.

Preventative Measures

The most obvious solution is to prevent relative motion or at least reduce it. This can be done by designing a more rigid mount or by making clamps extremely tight. The insertion of a rubber gasket between the surfaces to take up the motion elastically was found most effective at Westinghouse.

Reducing the friction by dry lubricants or by low friction inserts such as Teflon will reduce fretting.

Flooding the area with a lubricant or the sealing of the area with rubber cement or other sealing material to exclude the atmosphere will reduce fretting corrosion.

Increasing the abrasion resistance of the surfaces will help. Nitriding, chrome plating, shot peening, flame-plating, spray metal coating all have beneficial effects. For fatigue purposes, Horger and Buckwalter[22] found this to be effective.

For roller or ball bearings an increased in amplitude of oscillation allows the bearing to be lubricated properly.

REFERENCES

1. Eden, E.M., Rose, W.N., Cunningham, F.L., "The Endurance of Metals: Experiments on Rotating Beams at University College, London, Proc. I. Mech. Eng., part 4, 1911, p. 839.

2. Tomlinson, G.A., "The Rusting of Steel Surfaces in Contact," Proc. Roy. Soc. A., Vol. 115, 1927, pp. 472-483.

3. Tomlinson, G.A., Thorpe, P.L., Gough, H.J., "An Investigation of Fretting Corrosion of Closley Fitting Surfaces," Proc. Inst. of Mech. Eng., Vol. 141, 1939, pp. 223-249.

4. Almen, J.O., "Lubricants and False Brindling of Ball and Roller Bearings," Mechanical Engineering, Vol. 59, 1937, pp. 415-422.

5. Uhlig, H.H., Feng, I.M., Tierney, W.D., and McCellan, A., "Fundamental Investigation of Fretting Corrosion," NACA Technical Note 3029, December, 1953.

6. Halliday, J.S., and Hirst, W., "The Fretting Corrosion of Mild Steel," Proc. of the Roy. Soc. A., Vol. 236, No. 1206, August 2, 1956, pp. 411-425.

7. Uhlig, H.H., Tierney, W.D., and McClellan, A., "Test Equipment for Evaluating Fretting Corrosion," ASTM Special Technical Publication No. 144, June, 1952.

8. Wright, K.H.R., "An Investigation of Fretting Corrosion," Proc. Inst. of Mech. Eng., Vol. 1 B, 1952-53, pp. 556-574.

9. McDowell, J.R., "Fretting Corrosion Tendencies of Several Combinations of Materials," ASTM Special Technical Publication No. 144, June 1952

10. McDowell, J.R., "Fretting of Hardened Steel in Oil," Paper No. 56LC9 Joint Lubrication Conference of the ASME-ASLE, October 9, 1956. (To be published in ASLE Transaction, Vol. 1, No. 2, October, 1958).

11. Dies, Kurt, "Fretting Corrosion a Chemical-Mechanical Phenomenon," The Engineer's Digest (American Edition), Vol. 2, No. 1, January, 1945, p. 14.

12. Sakmann, B.W., and Rightmire, B.G., "An Investigation of Fretting Corrosion Under Several Conditions of Oxidation," NACA Technical Note No. 1492.

13. Godfrey, Douglas, "Investigation of Fretting Corrosion by Microscopic Observation," NACA Technical Note No. 2039, February, 1950.

14. Weismantle, E.E., "Friction and Fretting with Solid Film Lubricants," Lubrication Engineering, Vol. 11, No. 2, March-April, 1955, pp. 97-100.

15. Godfrey, Douglas, and Bisson, Edmond E., "Effectiveness of Molybdenum Disulfide as a Fretting Corrosion Inhibitor,"NACA Technical Note 2180, September, 1950.

16. Godfrey, Douglas, A Study of Fretting Wear in Mineral Oil," Lubrication Engineering, Vol. 12, No. 1, January-February, 1956, pp. 37-42

17. Herbek, Jr. E.W. and Strohecker, R.F., "Effect of Lubricants in Minimizing Fretting Corrosion," ASTM Special Technical Publication No. 144, June, 1952.

18. Rosenberg, S.J., and Jordan, L., "The Influence of Oxide Films on the Wear of Steels," Transactions, Am. Soc. of Metals, Vol. 23, No. 3, September, 1935, pp. 577-613.

19. Kennedy, N.G., "Fatigue of Curved Surfaces in Contact Under Repeated Load Cycles," Proc. International Conference on Fatigue of Metals, 1956, Inst. of Mech. Eng., September 1956, pp. 282-289.

20. Uhlig, H.H., "Mechanism of Fretting Corrosion," Journal of Applied Mechanics, Vol. 21, No. 4, December, 1954, p. 401.

21. Feng, I.M., and Rightmire, B.G., "The Mechanism of Fretting," Lubrication Engineering, Vol. 9, No. 3, June, 1953, p. 134.

22. Horger, O.J., and Buckwalter, T.V., "Fatigue Strength of 2 Inch Diameter Axles with Surfaces Metal Coated and Flame Hardened," Proc. ASTM, Vol. 40, 1940, pp. 733-745.

OTHER REFERENCES

1. Anonymous, "Fretting to Fretting Corrosion," Lubrication, Published by the Texas Co., Vol. 41, No. 8, August, 1955.

2. Bailey, John M., and Godfrey, Douglas, "Coefficient of Friction and Damage to Contact Area During the Early Stages of Fretting. II-Steel, Iron, Iron Oxide, and Glass Combinations," NACA Technical Note 3144, April, 1954.

3. Campbell, W.E., "The Current Status of Fretting Corrosion," ASTM Special Technical Publication No. 144, June, 1952.

4. Fenner, A.J., Wright, K.H.R., Mann, J.Y., "Fretting Corrosion and Its Influence on Fatigue Failure," Proc. Int. Conf. on Fatigue of Metals, 1956, Inst. of Mech. Eng., 1956, pp. 386-393.

5. Fink, M., "Wear Oxidation, A New Component of Wear," Trans. Am. Soc. Steel Treating, Vol. 18, July-December, 1930, pp. 1026-1034.

6. Godfrey, Douglas, and Bailey, John M., "Coefficient of Friction and Damage of Contact Area During the Early Stages of Fretting. I-Glass, Copper, or Steel against Copper," NACA Technical Note 3011, September, 1953.

7. Gray, H.C., and Jenney, R.W., "An Investigation of Chafing on Aircraft Engine Parts," SAE Journal, Vol. 52, No. 11, November, 1944, pp. 511-518.

8. Horger, O.J., "Fatigue of Large Shafts by Fretting Corrosion," Proc. of International Conference on Fatigue of Metals, 1956, Inst. of Mech. Eng., 1956, pp. 352-360.

9. Morton, Hudson T., "Friction Oxidation," The Fafnir Bearing Co., 1946.

10. Oding, I.A., and Ivanova, V.S., "Fatigue of Metals Under Contact Friction," Proc. of International Conference on Fatigue of Metals, 1956, Inst. of Mech. Eng., 1956, pp. 408-413.

11. Rahm, Adolph R., and Wurster, Harry F., "Fretting Corrosion in Aircraft Accessories," Lubrication Engineering, Vol. 7, No. 1, September, 1951, pp. 22-28, 40.

12. Roehner, T.G., and Armstrong, E.L., "Fretting Corrosion Studies with a Modified Fafnir Machine," The Institute Spokesman, Vol. XVI, No. 3, June, 1952, p. 8.

13. Sachs, G., and Stefan, P., "Chafing Fatigue Strength of Some Metals and Alloys," Trans. A. S. M. , Vol. 29, No. 2, June, 1941, pp. 373-399.

14. Waterhouse, R.B., "Fretting Corrosion," Inst. of Mech. Eng., Vol. 169, No. 59, 1955, pp. 1157-1172.

CORROSION AT HIGH TEMPERATURES

M. J. Tauschek
Chief Engineer, Valve Division
Thompson Products, Inc.

CORROSION AT HIGH TEMPERATURES

by

M. J. Tauschek

INTRODUCTION

The problem of corrosion of metals at high temperatures usually resolves itself into gross oxidation of the alloy--usually, because other forms of corrosion can and do occur. This type of corrosion is most often encountered in internal combustion heat engines, including the gasoline, diesel and gas turbine types. Here oxygen resulting from excess air charging or from incomplete combustion of the air is the principal corrodant on the hot gas side of the engine. The same generalization applies to high temperature heat exchangers, consider as a class to include steam boilers and nuclear reactor exchanger loops. Corrosion in such apparatus is complicated by the presence of frequent galvanic couples in their construction, by trace contaminants dissolved in the heat exchanger fluids and by the fact that these apparatus operate under static stress. Nevertheless, the same general considerations that control corrosion in heat engine service apply also, with some reservations, to heat exchanger corrosion. Therefore, this summary will concern itself only with the problem of corrosion in heat engines.

The theory underlying high temperature oxidation of metals is well developed and the processes controlling such oxidation reasonably well understood. However, actual corrosion problems are invariably so complex that they cannot be adequately handled from a purely analytical standpoint. Real problems of this nature are attacked empirically, with various types of accelerated laboratory tests being used to provide quantative data. The theory is used to predict and interpret qualitative trends in engine relationships.

In this summary, the underlying theory will be described first, followed by a number of examples of corrosion on gasoline engine exhaust valves to illustrate the various points. This will be followed by a description of the accelerated laboratory test techniques now used in industry. The summary will be completed with a few comments on metallurgy of alloys for corrosion resistance.

BASIC THEORY

High temperature oxidation of metals is controlled by thin surface films of corrosion products. When a clean metal specimen is exposed to a corroding atmosphere, corrosion initially proceeds at a very rapid rate. As corrosion products are formed, these cling to the metal specimen, sheilding it from the corrodant and limiting further corrosion.

Typical surface films which form on metals and metal alloy are shown in Figure 1. Two types are possible, those having an excess of metal ions in the film structure (metal-excess film) and those having a deficiency of these ions (metal-deficit film). These films have a gross shielding action but on an atomic scale are not impervious to metal ions. Metal ions can migrate through the film, interstitially in the metal-excess film and by jumping successively to vacant lattice sites in the metal-deficit film. Consequently corrosion proceeds even with a tightly adherent film, although at a vastly reduced rate as compared to a clean metal specimen.

The concept of surface films comprised of corrosion products enables us to explain many empirical observations relating to the corrosion rate. First, the corrosion rate will be related to the concentration of metal ions in the surface film. This characteristic depends on the properties of the metal or alloy that is corroding. Second, the thickness of the corrosion film will determine the rate at which metal ions can diffuse through the film and the thickness, in turn, depends on how long the specimen has been exposed to corroding conditions. Third, any factor such as temperature or electric potentials which influence the rate of diffusion of the metal ions through a given film will directly affect the rate of corrosion.

The concept of surface films has permitted the derivation of a number of laws relating to corrosion rates. At high temperatures, only two of these laws are of any importance--the parabolic and linear rate laws illustrated in Figure 2. The parabolic rate law applies to materials such as chromium and high chromium alloys, which form dense, tightly adherent, cohesive surface films of chrome oxide. Such alloys have corrosion products of a greater specific volume than the parent metal. As corrosion proceeds the surface film becomes increasingly thicker, thus reducing the rate of corrosion. It can be shown analytically and has been confirmed empirically that the rate of corrosion is proportional to the square root of the time and therefore corrosion will proceed along a parabolic curve. The ordinate of this curve represents the thickness of the surface film, the loss in weight of the parent metal or the gain in weight of the parent metal plus the corrosion products. The rate of corrosion at any point is proportional to the slope of the curve at that point.

For metals and alloys which do not form protective films, the linear rate law applies. These alloys are characterized by those where the specific volume of the corrosion products is less than that of the parent metal or by those such as molybdenum where the corrosion products are volatile at high temperatures. Even though these materials may have inherent resistance to oxidation as far as the clean specimen is concerned, the corrosion rate is constant and independent of time and corrosion proceeds unabated. The corrosive loss from such metals and alloys after long exposure at high temperatures will be considerably larger than those which form protective surface films and thus alloys which follow the linear rate law are not satisfactory for high temperature service.

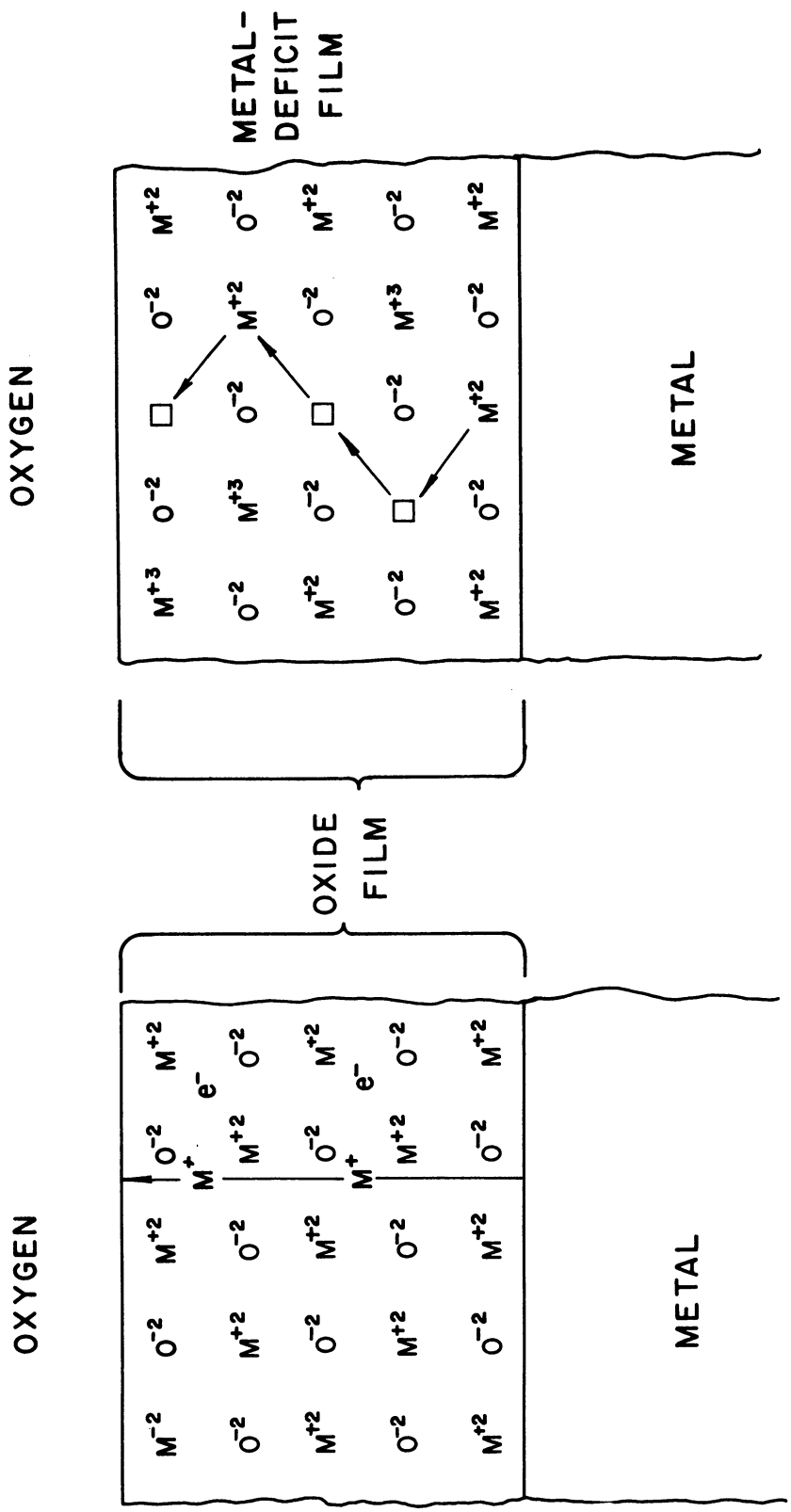

Figure 1. Formation of Surface Films on Corrosion-Resistant High-Temperature Alloys

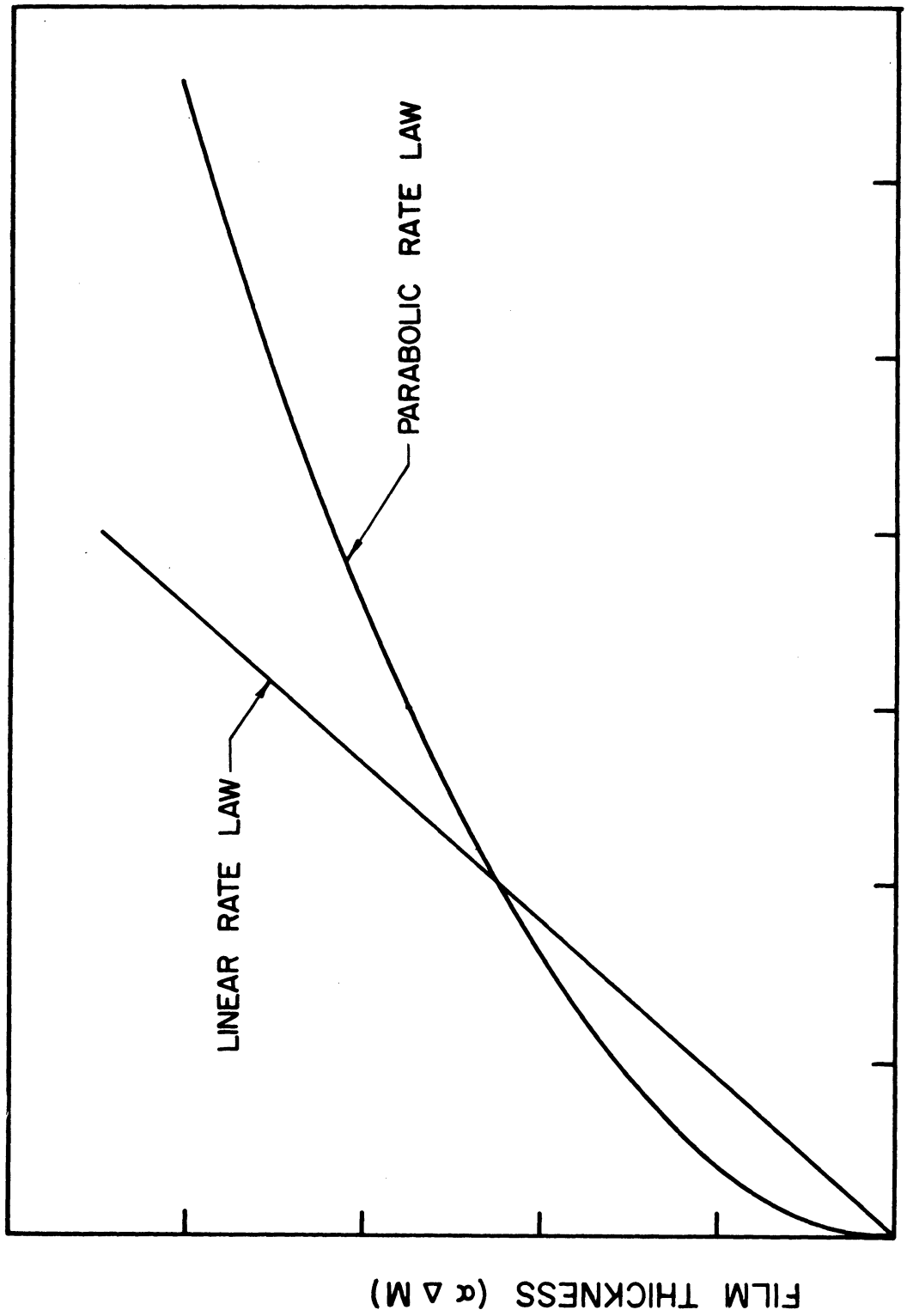

Figure 2. Oxidation Rate Laws Controlling Corrosion at High Temperatures.

In practice the tight cohesive surface layers described under the parabolic rate law are the exception rather than the rule. The specific volume of the corrosion products is different than that of the parent metal and as a result the surface films are under a certain amount of stress. As surface film build-up progresses these stresses lead to various forms of defects in the film, such as the pores, cracks and blisters illustrated in Figure 3. These defects impair the shielding ability of film and increase the corrosion rate. The defects are ordinarily self-healing since, as rupturing of the surface film and scaling occur, additional corrosion products are formed to fill the voids. Corrosion then proceeds at some rate intermediate between the parabolic and linear rates, depending on the nature and extent of the defect.

INFLUENCE OF ENVIRONMENT ON CORROSION

In high temperature corrosion problems the most important variable is that of temperature. It is quite essential that the importance of temperature by itself be fully appreciated. Corrosion rates vary exponentially with temperature to such an extent that a small change in temperature can overshadow any other change in the corroding system.

Most corrosion reactions, being kinetic processes, follow Arrhenius's equation:

$$K = k_1 e^{-\frac{k_2}{T}}$$

T = Absolute temperature
e = Base of Naperian logarithms
k_1, k_2 = Constants

In this equation K is the rate constant or the factor that determines the rate at which the corrosion reaction will proceed. The plot of K as a function of T becomes a straight line on semi-logarithmic coordinates. Figure 4 shows data for the oxidation of magnesium illustrating this relationship and showing good agreement with experimental data. The important point, however, is the marked variation in the corrosion rate with temperature. A change of 100 F degrees in the temperature changes the corrosion rate by a factor of 10:1. The extreme importance of temperature in controlling corrosion reactions is thus well established.

Figure 5 illustrates the temperature dependence of the corrosion rate for a very complex reaction involving the metal oxide corrosion of exhaust valve alloys. The metal oxide used in this test is solid up to about 1650° F and liquid from there on. Again, the valve alloys are complex alloys made up of iron, chromium, nickel, molybdenum with carbon and silicon additions. Here the corrosion rate does not show good agreement with the theory, probably because a number of complex reactions are occuring simultaneously rather than the simple oxidation considered in the preceding example. Nevertheless, the temperature dependence of the

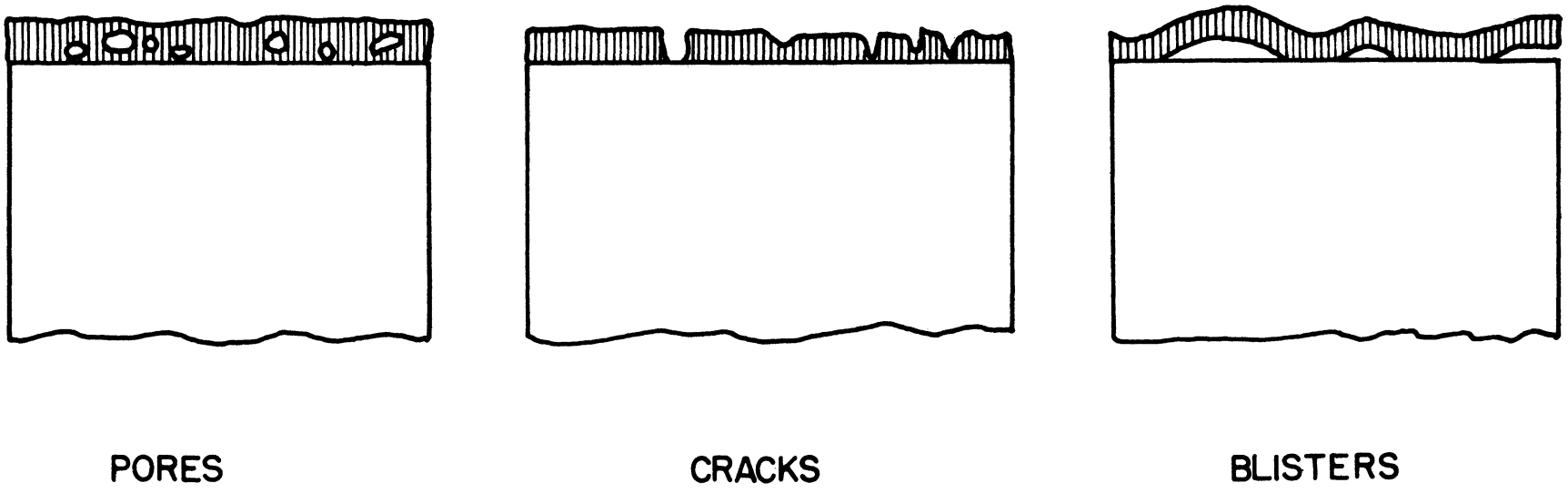

Figure 3. Imperfect Oxide Films Formed at High Temperatures.

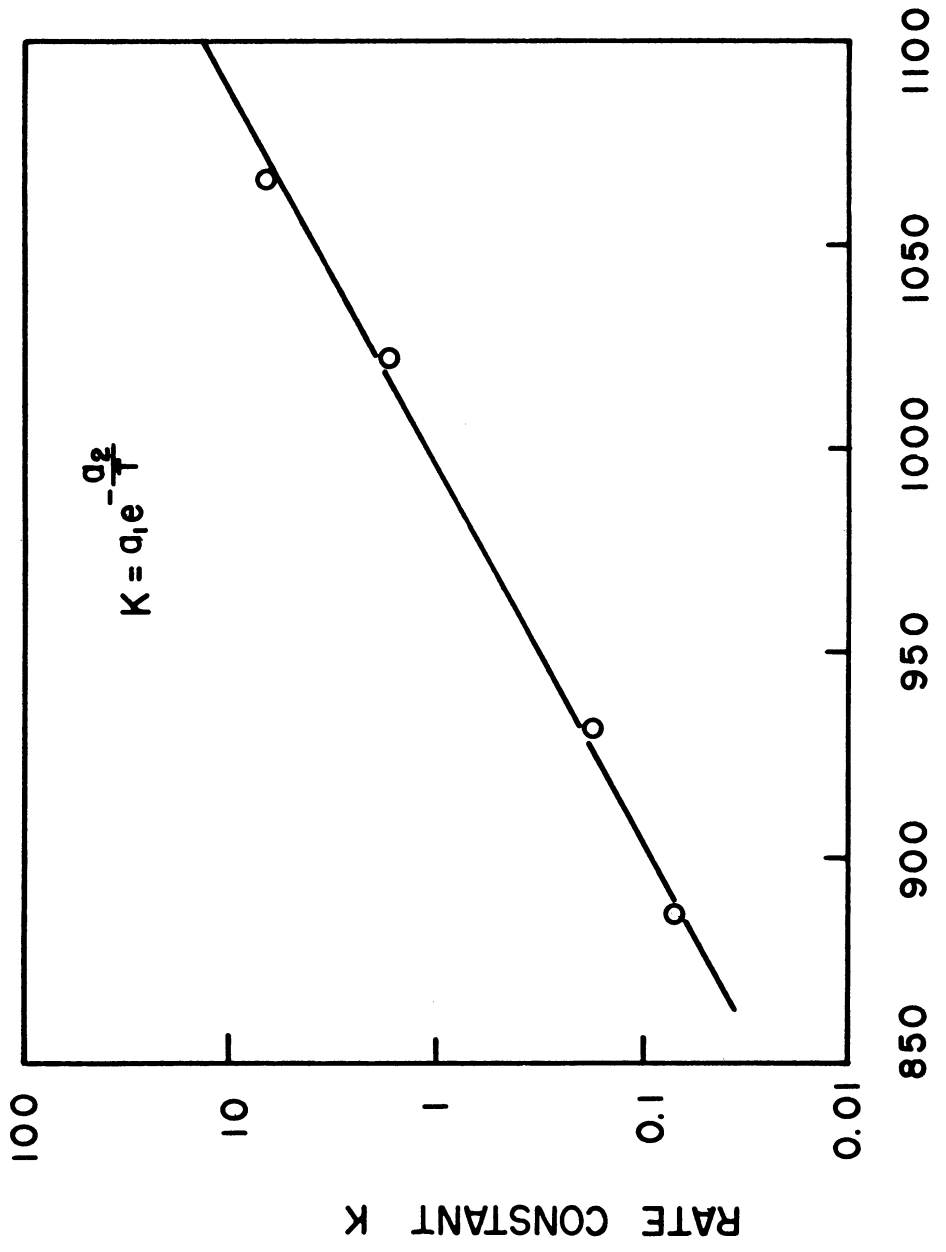

Figure 4. Effect of Temperature on the Rate of Oxidation of Magnesium.

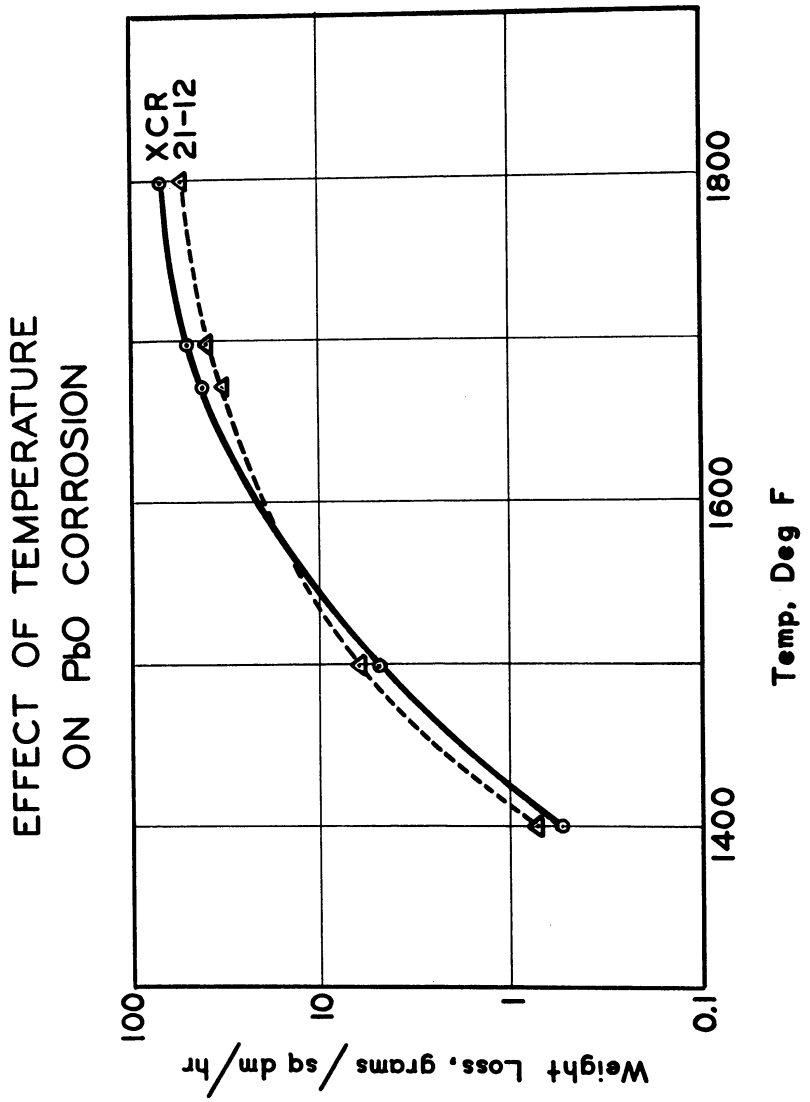

Figure 5. Effect of temperature on the metal oxide corrosion of typical exhaust valve alloys.

corrosion rate is of roughly the same order of magnitude as that described previously. In the temperature range of from 1400 to 1500° F, the 100° F temperature increment varies the corrosion rate by a factor of 10.

Another factor controlling the corrosion rate is the chemical environment surrounding the controlling material. Obviously no corrosion can occur if no corrodants are present. In high temperature corrosion reactions the presence of free uncombined oxygen is the critical factor. Figure 6 illustrates data showing the rate of corrosion penetration on the underhead of automotive exhause valves as a function of the amount of oxygen in the exhaust gases. Varying the mixture strength to the engine changes the amount of oxygen remaining in the exhaust gases and the shape of the corrosion curve is quite similar to that of the residual oxygen curve. Corrosion of this sort is therefore proportional to the amount of corrodant in the environment and usually, though not always, varies in direct proportion to the corrodant concentration.

METAL OXIDE CORROSION

Recently a great deal of attention has been focused on corrosion resulting from metal oxides in the products of combustion of heat engine fuels. These oxides result from the presence of lead in automotive gasolines and of vanadium in diesel and gas turbine fuels. These metal oxides, as well as certain others, have a considerable influence in accelerating corrosion reactions.

Two reasons exist for this effect. First, the metal oxides can react with a protective film formed on high temperature alloys to destroy and disrupt this film. For example, lead oxide in the presence of oxygen can react with the protective chrome oxide film on exhaust valve steels according to the following equation:

$$2\ Cr_2O_3 + 6\ PbO + 3\ O_2 \rightarrow 2\ Pb_3Cr_2O_9$$

Thus the protective film is disrupted or destroyed and corrosion prodeeds unabated. Similar reactions are possible with oxides of vanadium and molybdenum. It is not necessary that the metal oxides have any interaction with the parent alloy itself. The disruption of the surface film is sufficient to allow the parent alloy to oxidize at a substantially increased rate.

A second mechanism by which the metal oxides accelerate corrosion is their function as an electrolyte. The conductivity of these materials is high at elevated temperatures, even in the solid state, and comparable to that found for aqueous solutions at room temperature. As an example, Figure 7 shows the electrical conductivity of lead oxide as a function of temperature. Consequently, these materials form electrolytic cells with the corroding metal or alloys at any discontinuity that might occur on the corroding alloy, such as those characterized by welding junctions, by metallurgical discontinuities or by the presence of stress.

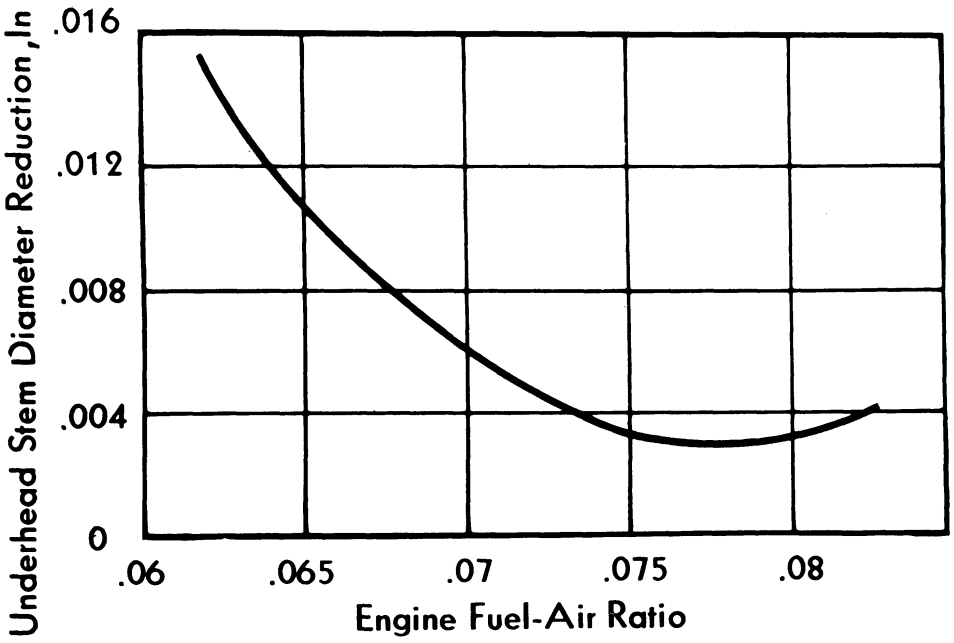

Figure 6. Effect of chemical composition of environment in controlling corrosive attack on the stems of gasoline engine exhaust valves.

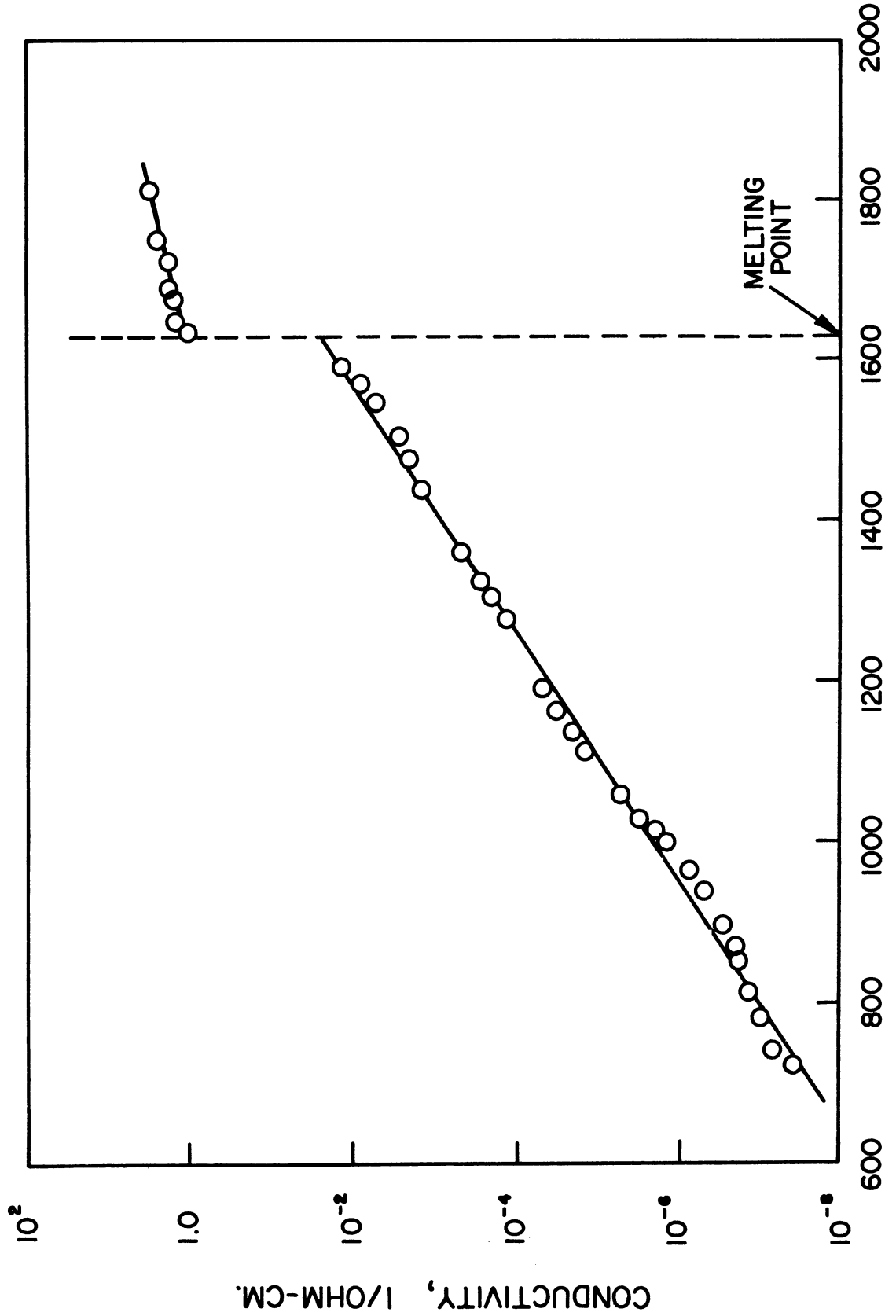

Figure 7. Electrical Conductivity of Lead Oxide as a Function of Temperature in the Solid and Liquid States.

REAL CORROSION PROBLEMS

In actual practice real corrosion problems become exceedingly complex. An example of the sort of complexity encountered is shown in Figure 8 for internal combustion engine exhaust valves. First, the temperature varies over the valve and since oxidation reactions depend primarily on the temperature, consequent variations in the corrosion rate can be anticipated. Again the valve is exposed to an environment containing oxygen and metal oxides as well as metal halides, sulfates and phosphates arising from additives or impurities in the fuel and oil. Various materials are used to make up the valve configuration and the juncture between these various materials represent galvanic couples, which in the presence of an electrolyte can cause localized corrosion. Finally the valve is subjected to cyclic stress which also exerts an influence on corrosion. Each of the foregoing factors play an important part in determining how and at what rate the valve will corrode.

Figure 9 shows the temperature distribution on a typical 4-stroke cycle engine valve. This distribution is determined by the thermal conductivity of the valve and the rate of heat flow into and out of the valve at its various surface locations. The pattern is typical of that encountered on all such valves. The temperature at the valve face is about 1150°F. Temperature gradients exist across the top of the valve head, reaching a maximum of approximately 1300°F in the center of the head, and down the valve stem, reaching 1350°F at a point approximately where the projected face angle intersects the valve stem. Because of the pronounced influence of temperature on the rate of corrosion, it would be anticipated that accelerated corrosion would be found in the center of the valve head and on the valve stem in the underhead area. Figure 10 shows the top head of an exhaust valve after a period of operation in the engine. Corrosion in the outer half of the head diameter is so retarded that the original machining marks on the top of the head are still visible. On the other hand, corrosion in the center half of the head is accelerated to the point where deep pits appear in the valve, particularly at the very center of the head. This corrosion pattern correlates very nicely with temperature distribution on the valve head. A similar situation exists on the valve stem as shown in Figure 11. Here the valve originally had a straight stem blending into the radius leading to the valve face. Extended operation in the engine has caused corrosion to occur in the high temperature area of the stem, again in proportion to the temperature.

The presence of dissimilar materials used in valve construction creates galvanic couples as shown in Figure 12. Corrosion at the face of a valve is a very serious matter since this induces leakage and subsequent valve failure. For this reason, many valves use a welded-on layer of highly corrosion-resistant alloy at the valve face. The welded junction where this alloy layer joins the base material of the valve and the seating contact between the alloy layer and the valve seat both constitute galvanic couples. It is expected that accelerated localized corrosion

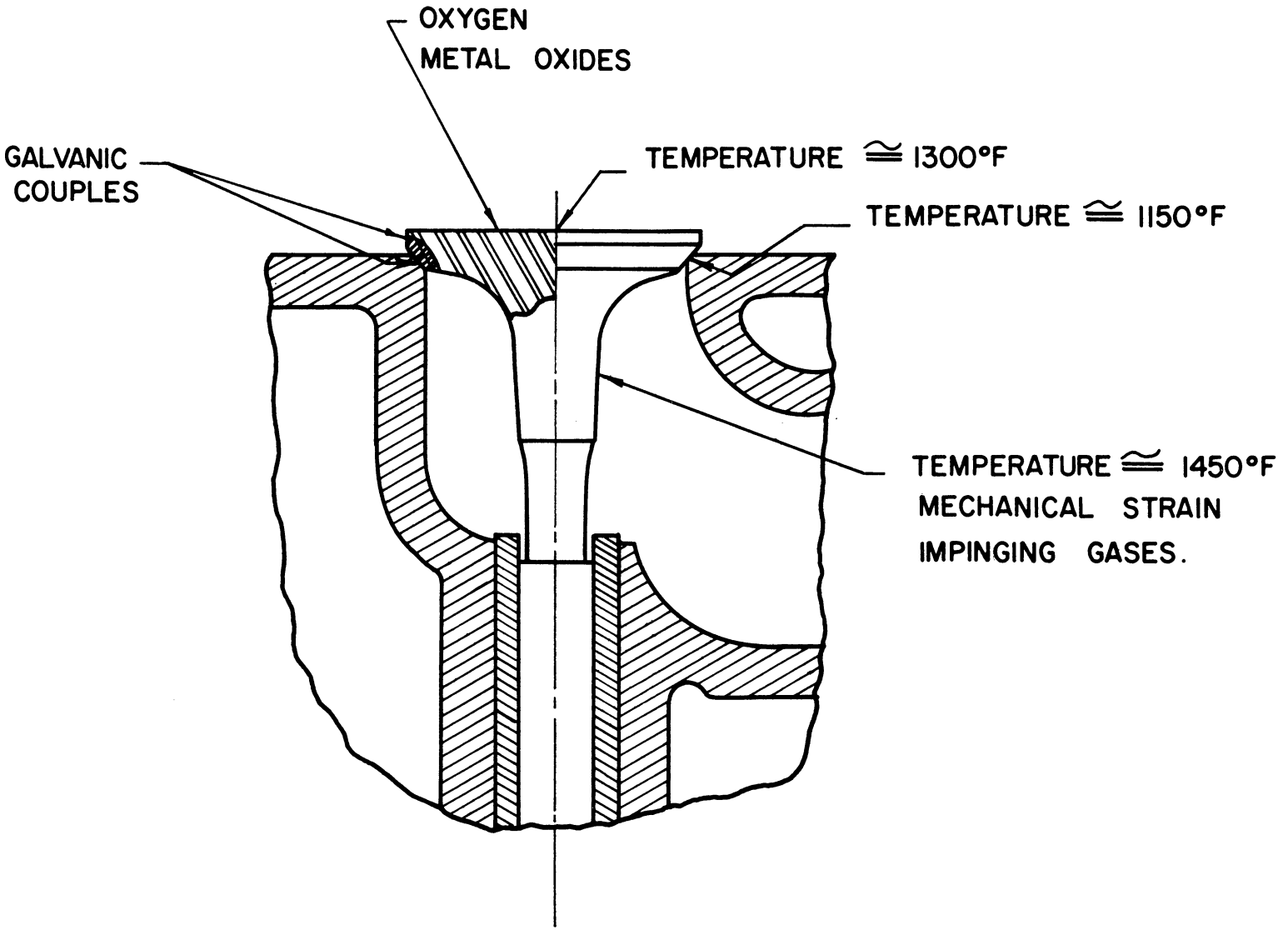

Figure 8. Environmental Factors Contributing to Corrosion on a Gasoline Engine Exhause Valve.

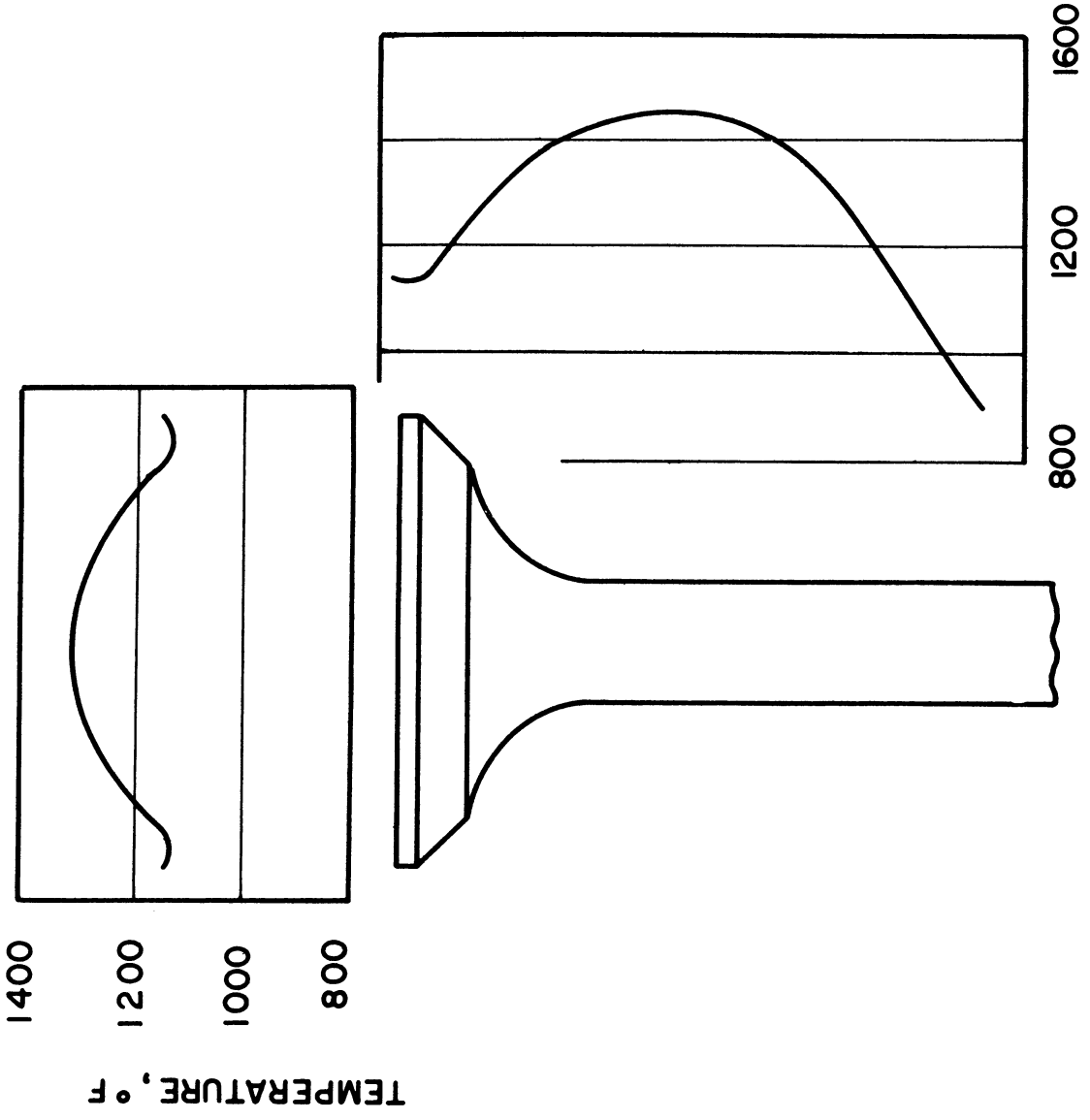

Figure 9. Variation in Temperature Encountered on a Typical Gasoline Engine Exhaust Valve.

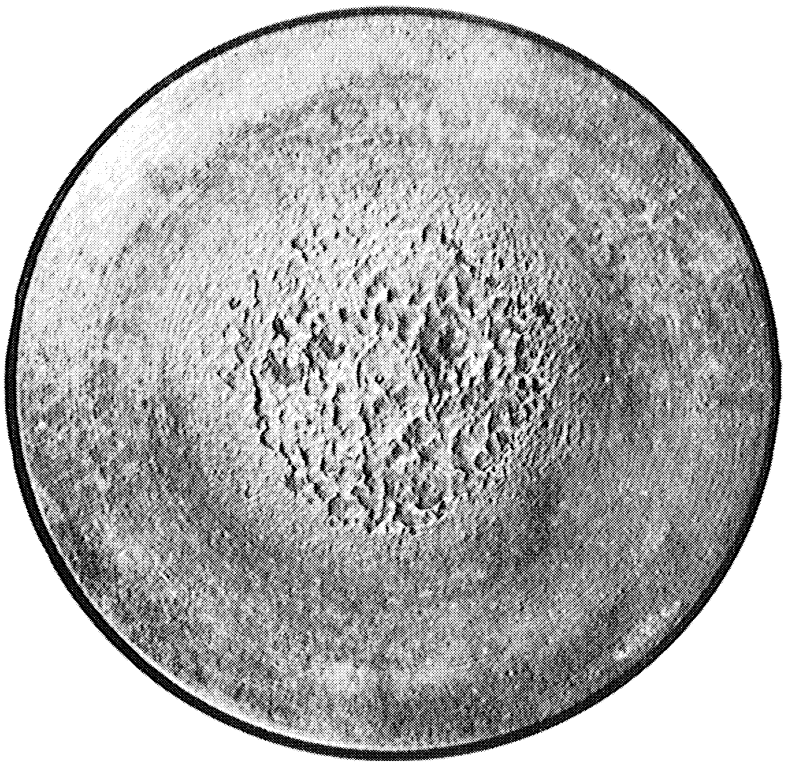

Figure 10. Distribution of corrosive attack conforming to temperature pattern on exhaust valve top-of-head.

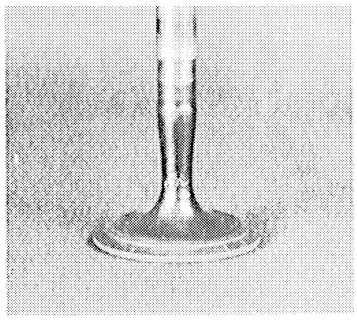

Figure 11. Localized corrosive attack on high temperature area on exhaust valve stem.

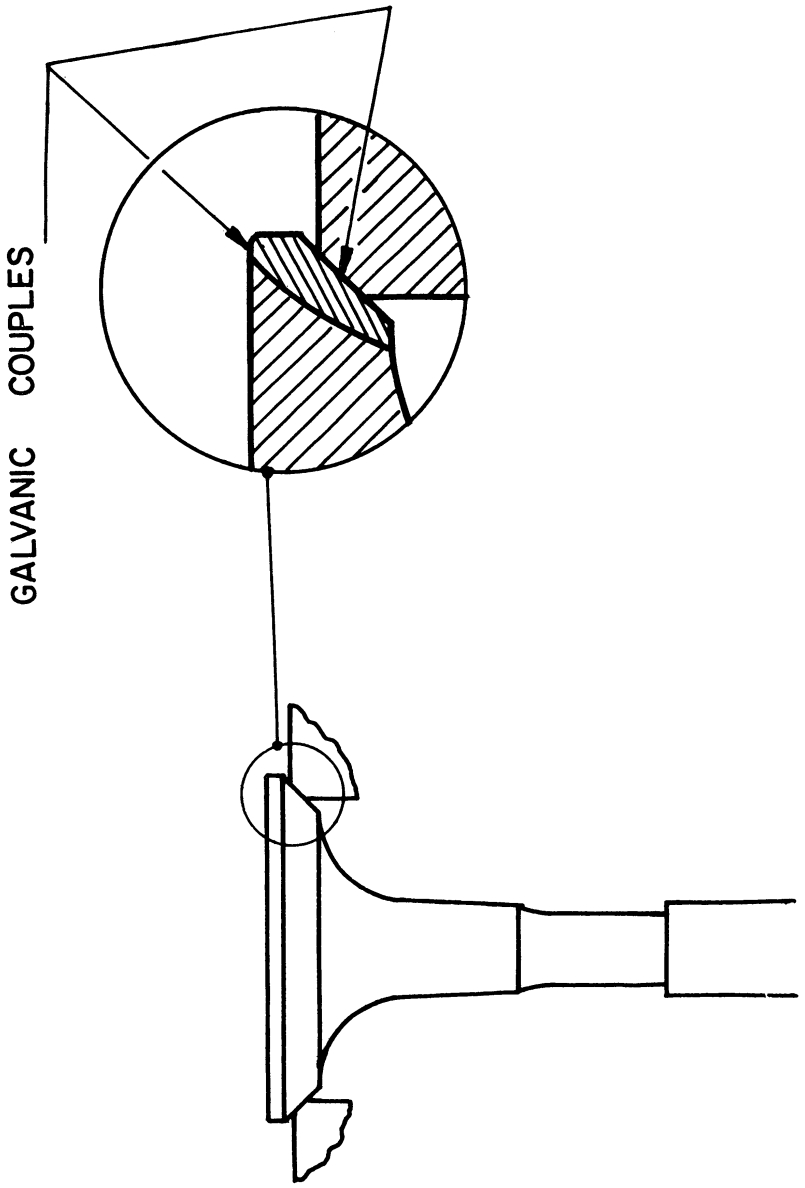

Figure 12. Galvanic Couples on Alloy-Faced Exhaust Valves Resulting from Contact of Dissimilar Materials.

would occur at these points. Figure 13 shows the type of corrosion encountered at the juncture on the top of the valve head where the alloy layer joins the base material. The base material, being less corrosion resistant than the seating face, preferentially corrodes. Corrosion is most pronounced and penetration most deep at the juncture between the two materials and diminishes as the distance from the juncture increases. Figure 14 shows the parallel situation occurring at the valve face. It is important to note that corrosive attack is confined to that portion of the face in contact with the valve seat. Because important temperature differentials do not exist across the face, localized corrosion of this sort can only be explained on the basis of galvanic action. The corrosion resistance of the valve face is vastly greater than that of the seat, however, the seat operates at a temperature of from 600 to 800°F whereas the valve face operates in the 1200 to 1300°F range. For this reason, the valve face preferentially corrodes and the seat ordinarily is not damaged. It is conceivable that with a good enough valve facing alloy and a poor enough seat material, galvanic corrosion could be transferred from the valve face to the seat.

It should be pointed out that factors other than gross junctions between dissimilar materials can cause galvanic corrosion. Thus, metallurgical discontinuities or areas of varying stress are in themselves sufficient to set up galvanic cells. For example, wrought nickel base alloys hardened by titanium frequently pit where the titanium stringers run to the surface. These same alloys in the cast condition or in the wrought condition without the titanium do not suffer pitting type corrosion. Again, since the electrical potential of a stressed material is different from that of the same material in the free state, sharp stress gradients can cause galvanic corrosion. Experiments in our laboratory have shown that in general the presence of stress does not influence the overall rate of corrosion but that the juncture between the stressed and unstressed materials will suffer localized attack.

In contrast to static stress, dynamic stress plays a far different role in controlling corrosion. Corrosion such as that shown in Figure 11 occurs on a part of the exhaust valve subjected to a cyclic stress. The origin of these stresses is in the tensile loads and bending moments imposed upon the valve underhead section at the time of valve seating. The resultant strain is believed to cause ruptures in the surface film overlaying the material, permitting accelerated corrosion through the ruptures as illustrated in Figure 15. The strain on the valve is proportional to a number of geometrical factors in the engine and may vary widely from valve to valve. Similarly, experience has shown that this underhead corrosive attack is sporadic and irreproducible and apparently a function of uncontrollable variations in the valve installation. Admittedly, high temperature areas occur on this part of the valve which in themselves contribute markedly towards the extent of corrosion. Yet the variations in corrosive attack that have been experienced are such that they cannot be explained on the basis of temperature alone.

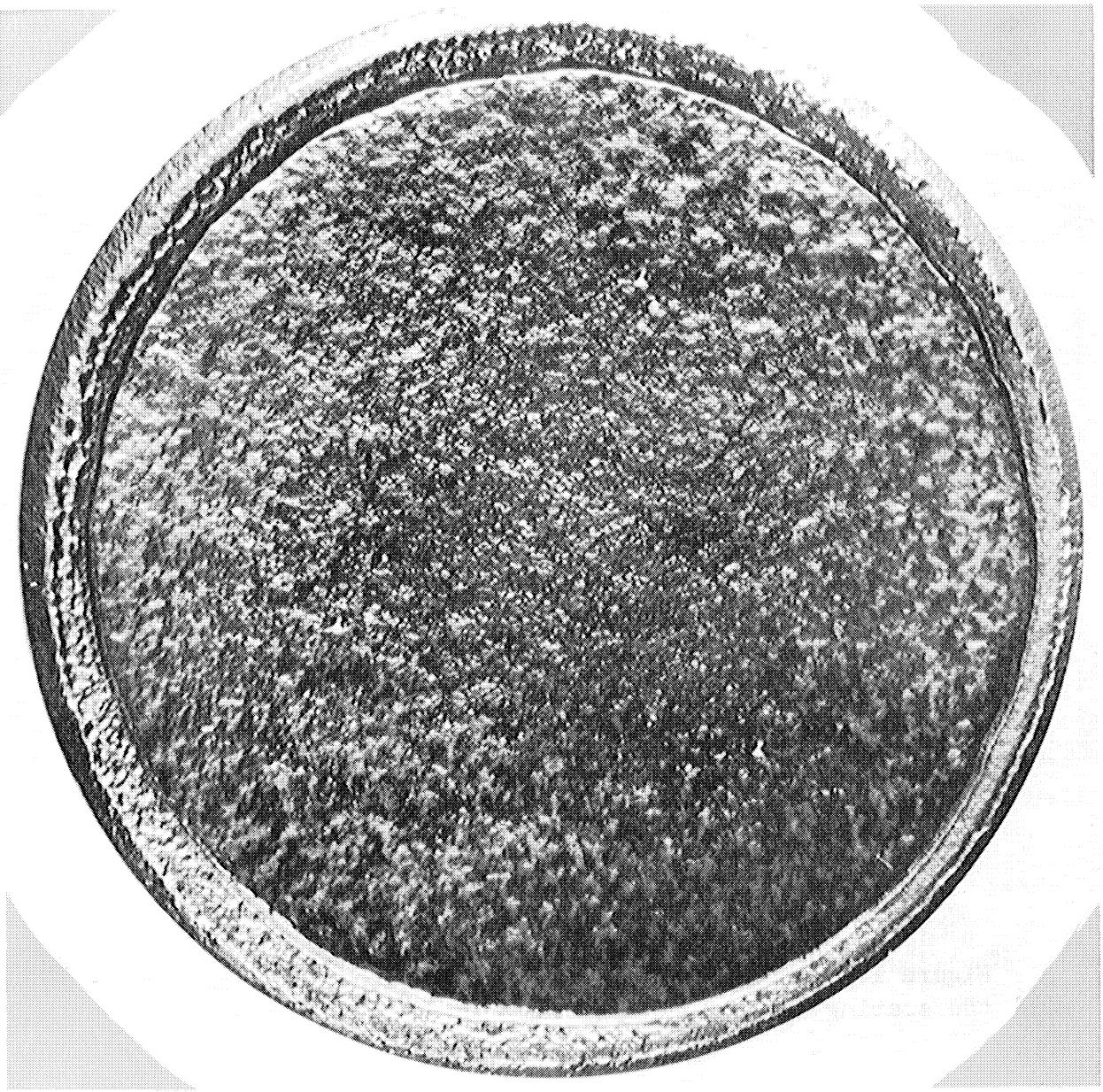

Figure 13. Accelerated galvanic corrosion occurring at the juncture of the facing and base alloys on exhaust valves.

Figure 14. Accelerated galvanic corrosion occurring within the seating area of exhaust valves.

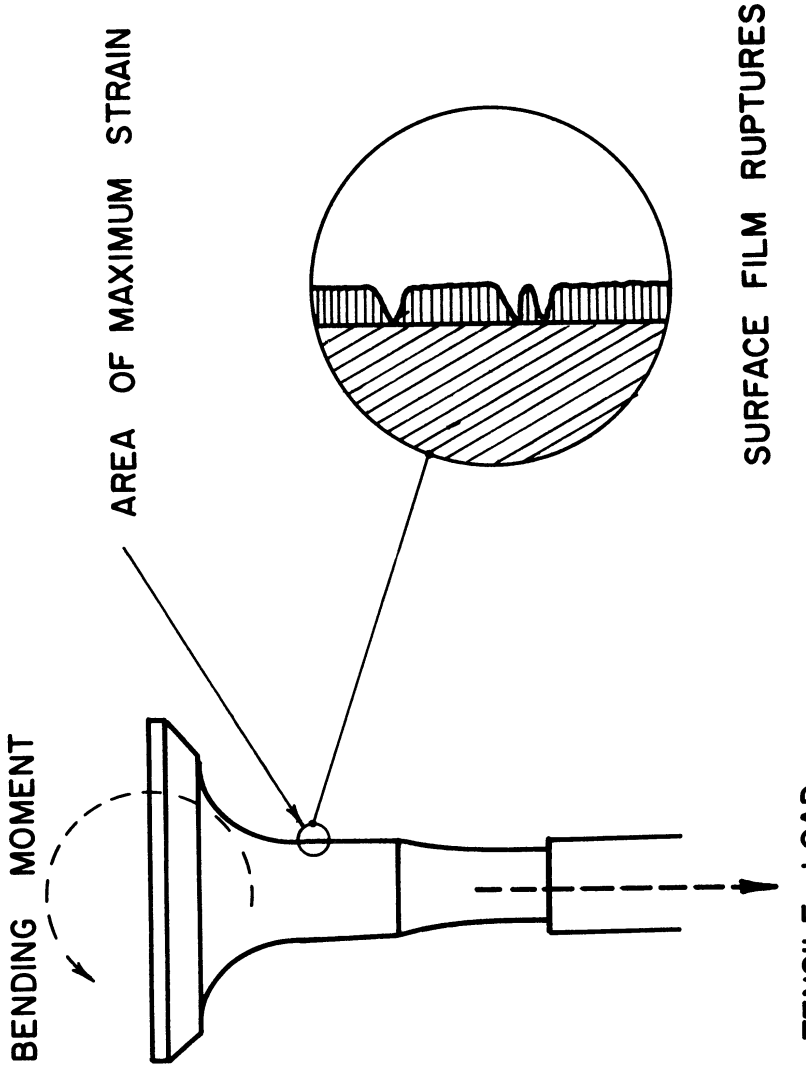

Figure 15. Postulated Effect of Underhead Strain on Exhause Valve in Rupturing Surface Film and Accelerating Corrosion.

It is therefore believed that the theory relating to surface film ruptures because of strain is operative on the underhead of the valve.

LABORATORY CORROSION TESTS

Because of the complex nature of actual corrosion problems these cannot usually be handled on a purely analytical basis. Resort is then made to laboratory testing of two basic types; (a) service testing, (b) accelerated laboratory test procedures. Service tests have the advantage of being the most accurate and reliable but are usually costly and time consuming. Simple laboratory bench tests can be used, particularly for screening purposes, to study alloys or environmental factors and by proper choice of test variables corrosion can be accelerated to achieve considerable information in a short period of time.

As in any other type of accelerated testing, there is always the danger that the circumstances under which corrosion occurs can be changed to such an extent that the results of the accelerated tests are no longer valid nor applicable to the service problem. Many of the tests currently used in industry have been criticized on this point, and some justly so. Nevertheless, the accelerated test offers so versatile a tool to the engineer or metallurgist that its economic value cannot be overlooked. It is not necessary that a test procedure duplicate exactly the conditions encountered in service. To do so would make the test unduly complicated and cumbersome. However, it is essential that the degree of correlation between the laboratory test and service performance be established early in the testing procedure and that the limitations of the accelerated test be fully appreciated. In this way it can be used as a valuable screening tool, reserving service testing only for the more promising solutions to the particular corrosion problem at hand.

The types of accelerated corrosion tests that can be set up are unlimited. In their simplest form these tests can be conducted by putting a sample in the furnace at a predetermined temperature, leaving it there for a certain time interval, and examining it visually for corrosion at the end of the test. Most industrial tests are a bit more sophisticated. In their most common form a specimen of the alloy under study is placed in the corroding environment at a predetermined temperature for a predetermined length of time. The extent of corrosion is determined by measuring the change in weight of the specimen. If the corrosion products adhere to the specimen and are not lost during testing, the gain in weight may be used. If, on the other hand, some corrosion products are lost, then the specimen is cleaned at the end of the test and the loss in weight taken as the index of corrosion. Less frequently the corrosive penetration or change in size of the specimen may be used as an index. A more refined version of the simple weight change experiment is conducted by suspending the specimen from a balance

in the corrosive environment. In this way the rate of corrosion as well as the gross overall weight change can be determined. Such tests however have the disadvantage of being harder to control and reproduce and consequently most industrial tests ignore the rate for the sake of simplicity.

A typical example of one such test is that used for evaluating the corrosive tendencies of valve alloys, as illustrated in Figure 16. A cylindrical specimen of the alloy to be tested is placed in a magnesia crucible together with 40 grams of lead oxide. The crucible is then placed in an electric muffle furnace and heated to 1675°F for one hour. The atmosphere in the furnace may either be air or a gas mixture of carbon monoxide, carbon dioxide, nitrogen and water vapor selected so as to simulate the composition of exhaust gases ordinarily found during engine operation. At the completion of the test, the specimen is cooled, electrolytically cleaned and its weight loss determined. The weight loss per unit surface area is then used as a means of expressing the relative corrosive tendency of the alloy.

The use of this test implies that exhaust valves fail through straightforward metal oxide corrosion. The temperatures employed in the test are higher than those experienced in engine operation. This serves two purposes; first, to insure that the metal oxide is liquid during the test and second, to accelerate the test and obtain reasonable information during the one hour test duration. There is an implied assumption in this test procedure that the effect of temperature on corrosion rate will be roughly proportional for all alloys tested.

Because of the differences between this test procedure and the actual circumstances surrounding a valve in an engine, it is reasonable to inquire whether the test accurately predicts valve alloy performance. Figure 17 shows data comparing the weight loss as measured in a crucible test to the weight loss of valves actually operated in dynamometer engines. The circular data points are those for chrome-nickel-manganese alloys currently used in the construction of exhaust valves for which the correlation is reasonably good. The two square data points show two chrome-manganese experimental steels. With this class of materials, good correlation between the laboratory test and the engine test cannot be obtained and such steels cannot be rated on the basis of the laboratory test alone. Figure 18 shows similar data taken from engines operated in every day commercial trucking service. In this chart the service life of the valve alloy expressed in terms of mileage to burning failure is shown as a function of the weight lost for the same alloy in the laboratory crucible test. Each data point represents tests for 24 valves in order to insure statistical reliability in the data. The vertical bars running through the data points illustrate the extremes in valve life encountered in service. Again reasonabley good correlation is obtained. The data point marked "A" is that for one of the chrome-manganese series of steels which previously exhibited lack of correlation in the laboratory test. That marked "B" is for a valve

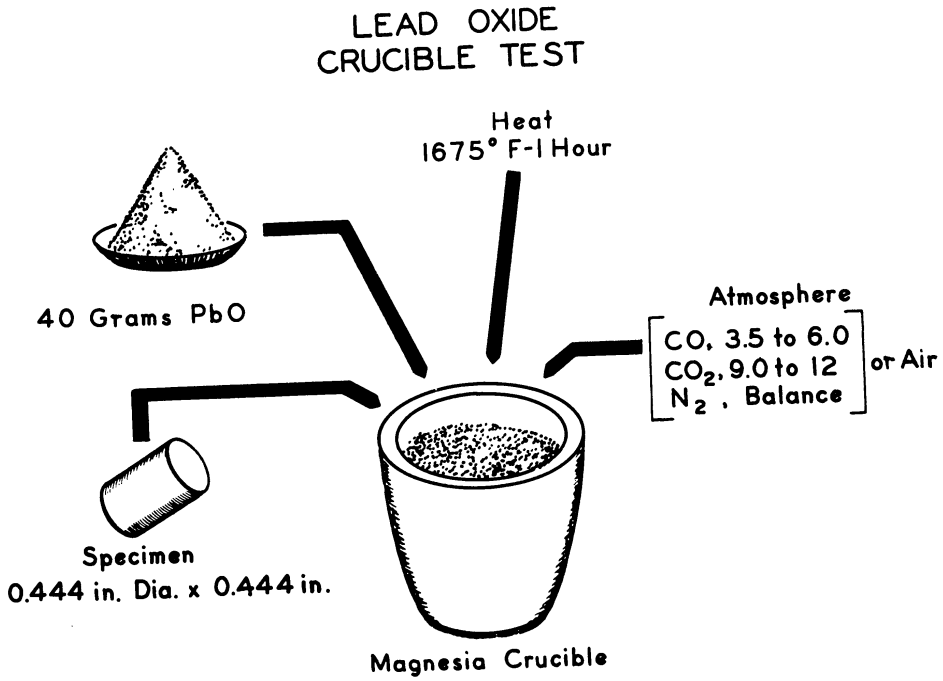

Figure 16. Laboratory Test Used to Determine the Resistance of Alloys to Corrosive Attack by Metal Oxides.

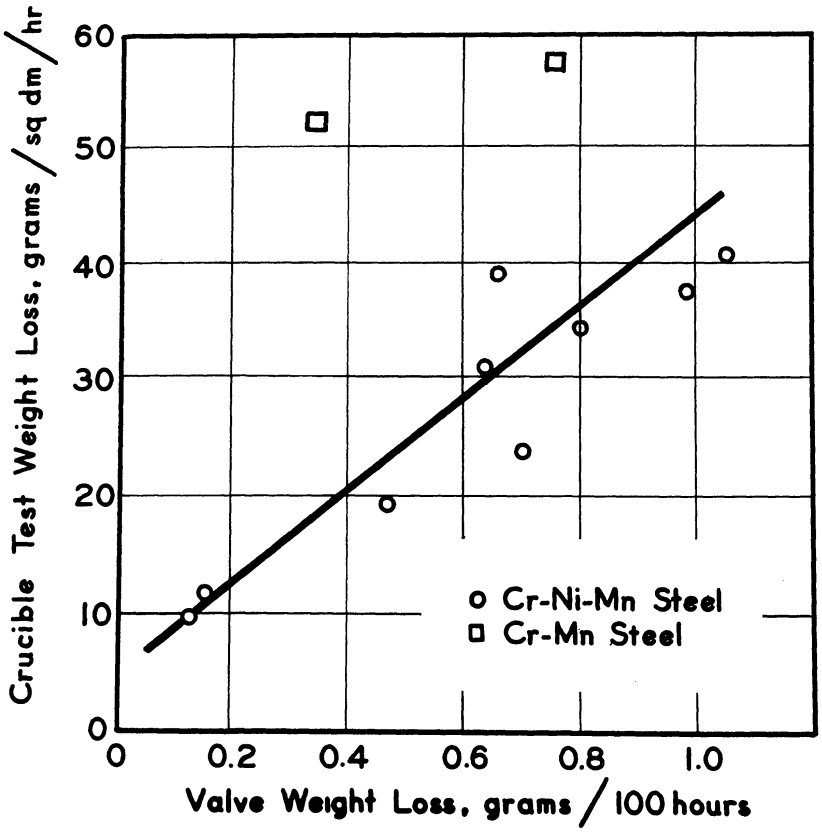

Figure 17. Correlation of Laboratory Test With Dynamometer Experience in Engines.

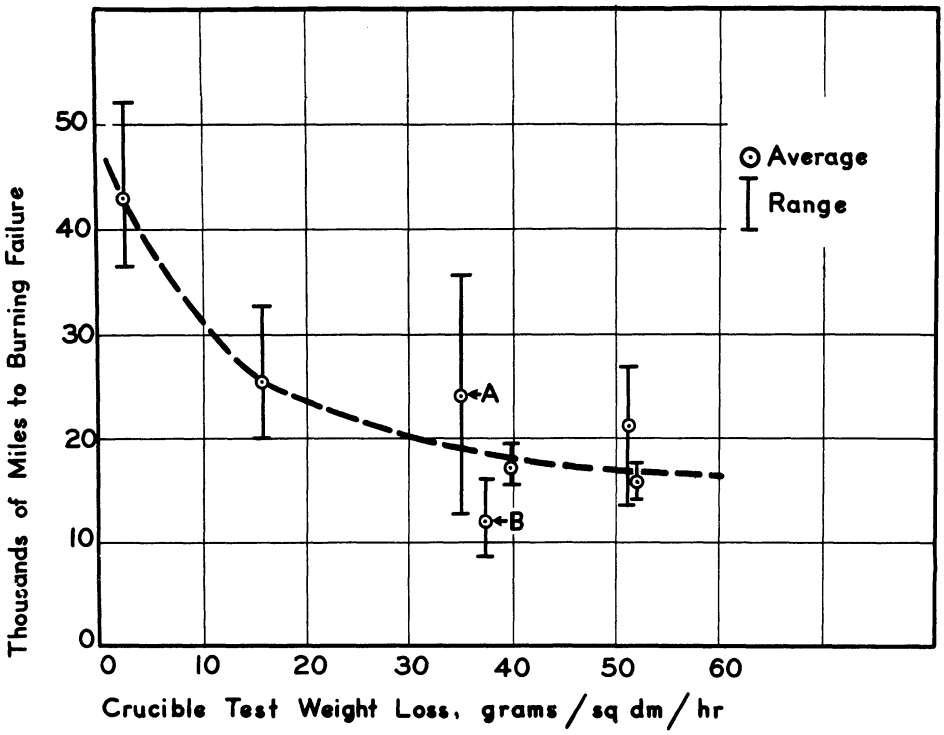

Figure 18. Correlation of Laboratory Tests With Field Service Experience in Engines.

alloy having particularly unsatisfactory physical properties which contributed to early failure in service.

Correlation to the extent just described is about all that can be expected from simple accelerated tests. Past efforts to improve the accuracy of such testing (for example, the laboratory metal oxide test) have usually resulted in complicating the test procedure and extending the time intervals without any improvement in accuracy. In order for such tests to be useful and valuable to the engineer, they must be kept in their simplest possible form. A clear understanding and appreciation of their limitations will then permit them to be most intelligently applied.

ALLOYS FOR HIGH TEMPERATURE SERVICE

Most all alloys intended for high temperature service must have many properties in addition to corrosion resistance. Those which are statically or dynamically loaded must have requisite hot creep and fatigue strength. Alloys subjected to shock load must also have high temperature impact strength. When contacting or wearing surfaces are involved, the alloy must have good hot hardness as well as scuff, wear and abrasion resistance. Again, the forming processes used to manufacture such components must be considered and the alloy must have castability, weldability, machinability, forgeability as determined by these processes. As a result, corrosion resistance is only one of many properties sought in a high temperature alloy. Frequently, other considerations are dominant and the corrosion resistance is consequently compromised. Occasionally it becomes necessary to obtain corrosion resistance through the use of welded overlays or surface coatings in order that materials of more desirable properties may be used for the basic structure of the component in question.

Alloys intended for high temperature service almost invariably contain substantial concentrations of chromium. The reason for this is that chromium forms a cohesive tightly adherent oxide film, protecting the alloy by virtue of this coating. Figure 19 shows weight loss data for chromium-containing iron-base alloys and illustrates the effect of chrome in alleviating corrosion. The value of chromium diminishes as the concentration of this element is increased. Iron-base alloys with chromium above about 25% cannot be wrought. Again, high chromium concentrations produce undesirable brittleness in high temperature alloys. For these reasons most commercial heat resistant alloys contain chromium concentrations of 15 to 25%.

The effect of nickel is similar to an additive to that of chromium as shown in Figure 20. These data are for a 20% chromium alloy. Nickel concentrations of from 20 to 40% can profitably be used to reduce the corrosion rate. In high temperature service, nickel-base alloys are frequently used in preference to those containing iron because

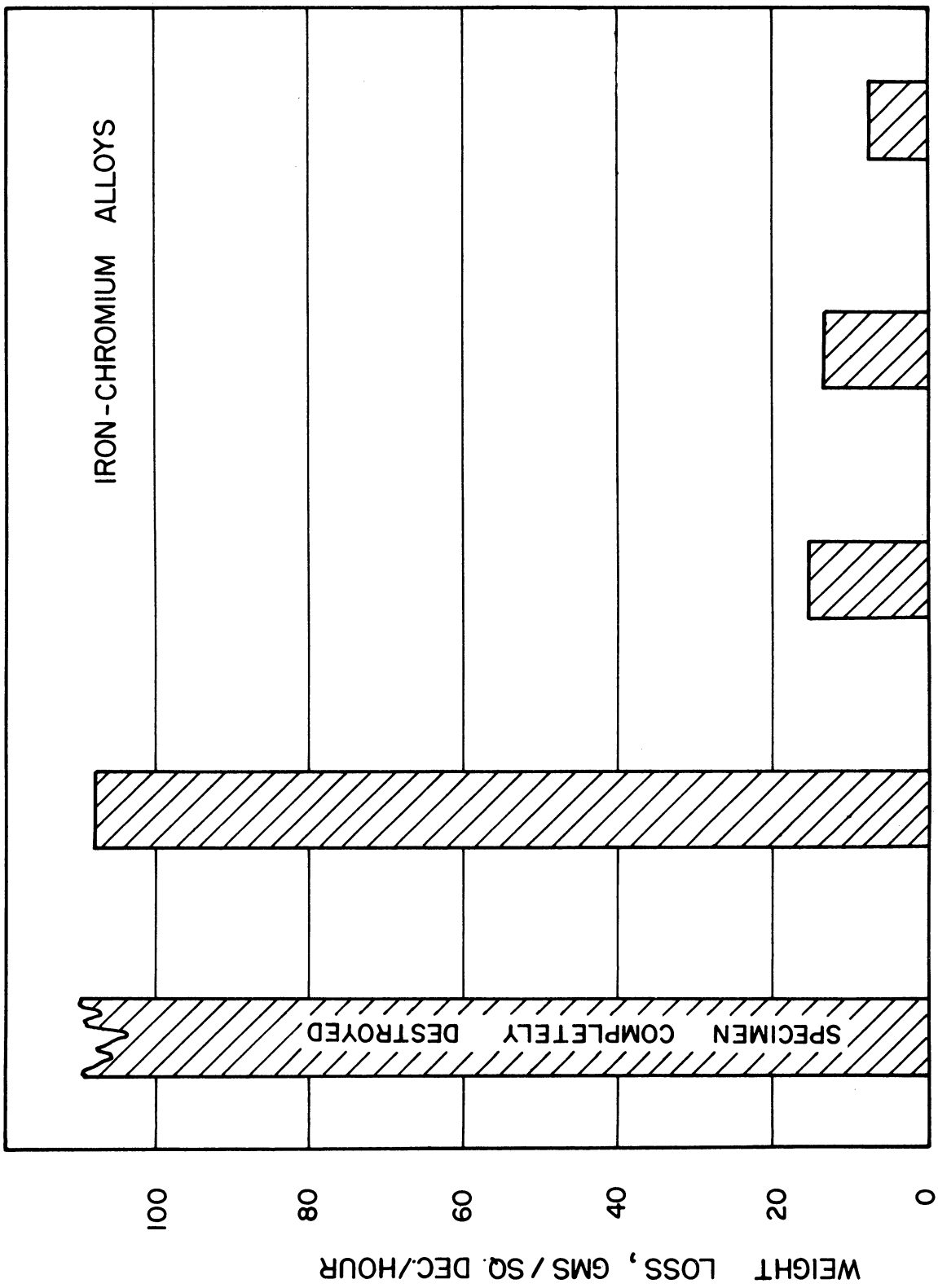

Figure 19. Effect of Chromium on the Metal-Oxide Attack of Chromium-Iron Alloys.

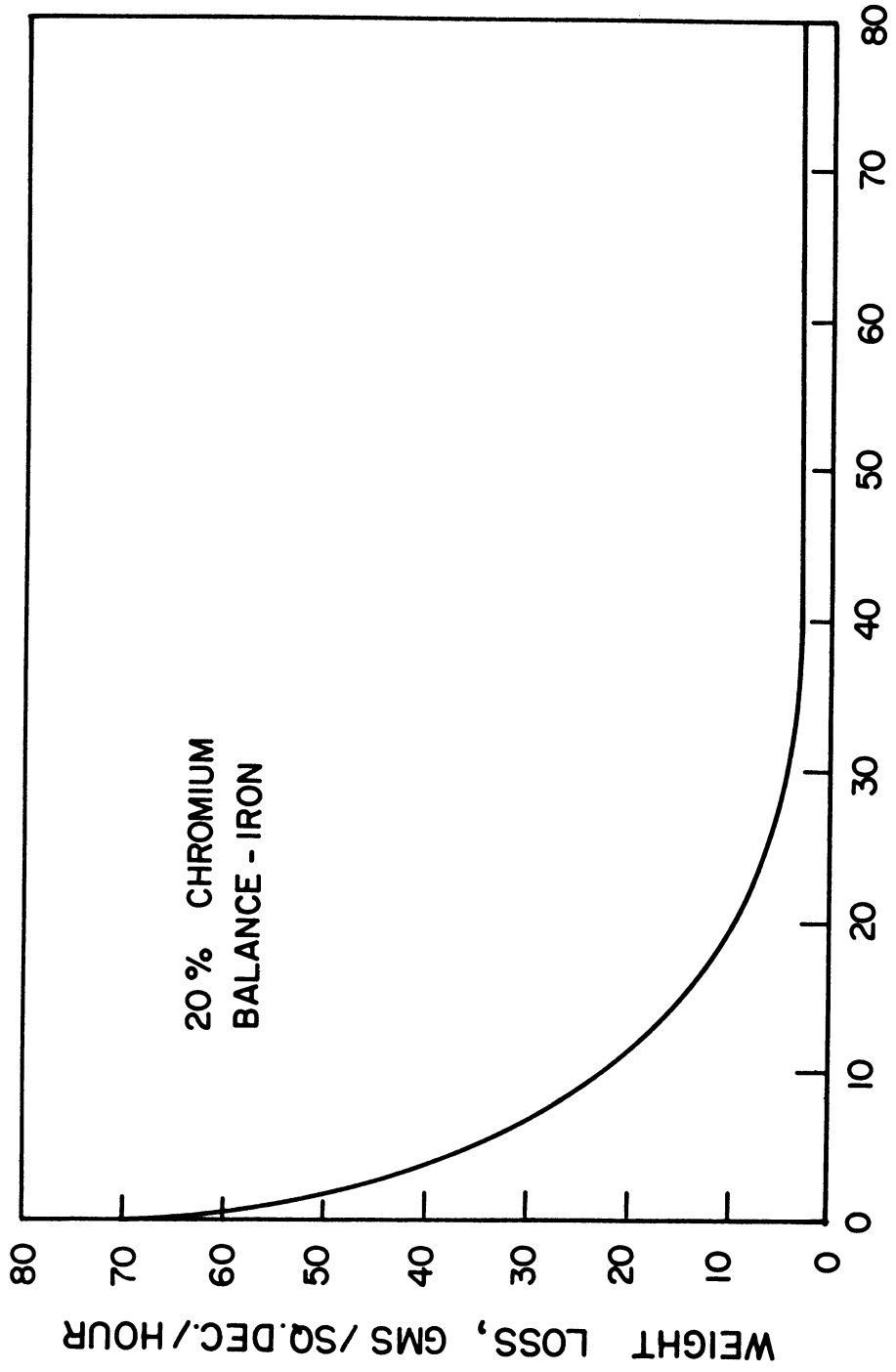

Figure 20. Effect of Nickel on the Metal Oxide Attack of Chromium-Iron-Nickel Alloys.

of the higher hot strength of such alloys. The replacement of all the iron with nickel does not impair the corrosion resistance.

Similar trends can be developed for all the remaining important alloy ingredients in high temperature materials. Inasmuch as the effect of these ingredients will vary widely depending upon the specific circumstances, i.e. the temperature, the corroding medium and the alloy in which they are used, it is important that these trends be obtained for circumstances closely paralleling the anticipated service usage. A vast wealth of information exists in the literature on the effect of these alloying agents. Considerable discretion is required before this information can be used to compound corrosion-resistant alloys for a specific application.

One important point that must be considered in corrosion-resistant alloys is the effect of minor alloying elements or even impurities on the corrosion rate. For example, silicon in concentrations of 1 to 3% is frequently used to improve the corrosion resistance of alloys exposed to pure oxidizing conditions. Silicon under these circumstances has considerable effectiveness in reducing oxidation. In the presence of metal oxides, however, the silicon preferentially reacts with the metal oxide leading to accelerated corrosion as shown in Figure 21. The mechanism involved in this type of corrosion is not clearly understood although its effect has been substantiated and repeatedly shown in a number of alloys, both iron and nickel base. It appears from the curve that about 0.5% silicon represents stoichiometric proportions for the reaction with the metal oxide, and the importance of reducing or eliminating silicon from the analysis is clearly shown. Similar effects can be shown for other trace elements in valve alloy analyses, particularly aluminum in the nickel-base alloys.

It is interesting to note in the present example that the effect of silicon in metal oxide corrosion of valve alloys was unrecognized for many years. Data taken in the range of 0.5 to 4.0% silicon served to indicate that high silicon additions were beneficial to the analysis. It was not until silicon-free analyses were actually tested that the true effect of silicon was recognized. It is therefore quite important that the effect of all the elements in a high temperature alloy be known and that these elements be controlled within a desirable range. Again, as a word of caution, such elements must be controlled in the preliminary testing leading to the development of an alloy. Uncontrolled variations in silicon in a valve alloy, for example, can completely dominate other intentional variations in the analysis and confuse the test results to the point where they are worthless.

SUMMARY

The problem of high temperature corrosion of metals and metal alloys is mainly one of gross oxidation. The theory controlling such oxidation processes is well developed but because actual corrosion

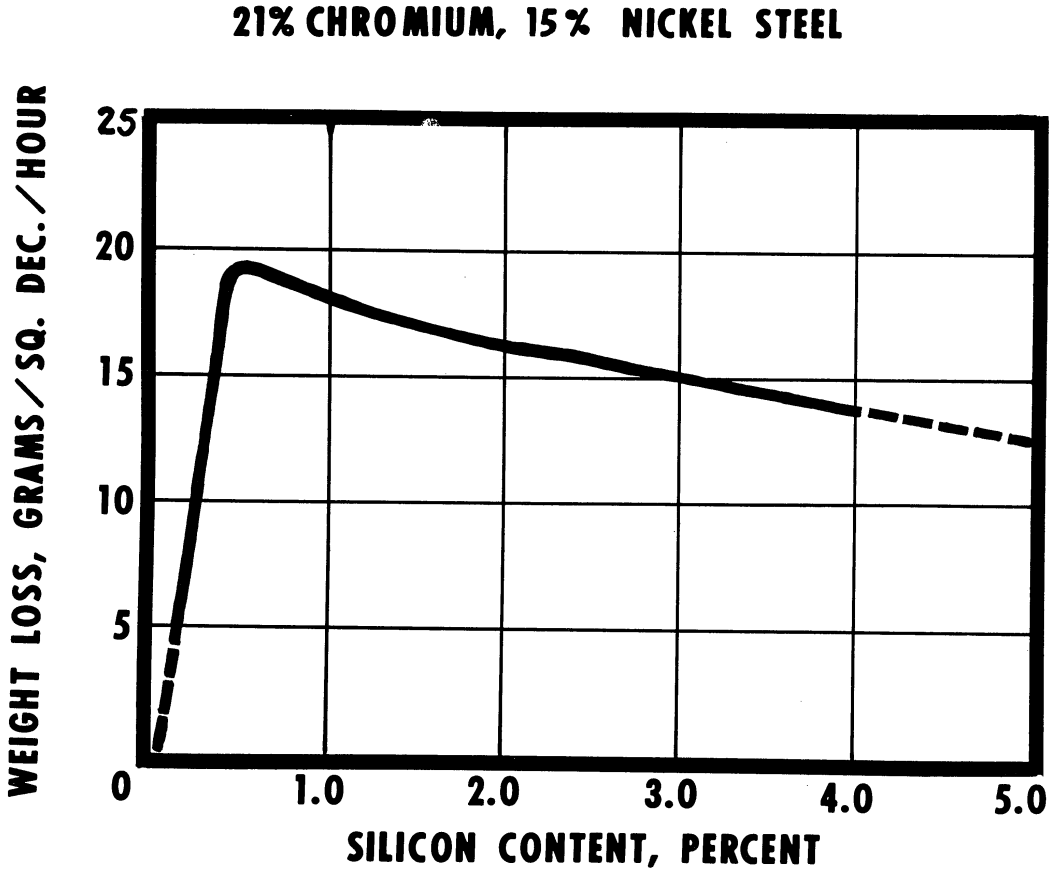

Figure 21. Effect of Silicon on the Metal-Oxide Attack of a 21% Chromium, 15% Nickel Valve Alloy.

problems become so complex these are usually solved empirically rather than analytically. Frequent recourse is made to accelerated laboratory tests which are used mainly for screening purposes followed by service testing of the most desirable alternatives.

Alloys used for high temperature service generally are rich in chromium because of its ability to form protective chromium oxide surface films. The corrosion resistance of these alloys is also improved by large additions of nickel. Considerable care must be taken in the control of minor alloying ingredients and impurities in order that these do not impair the corrosion resistance.

BIBLIOGRAPHY

1. "Symposium on Corrosion of Materials at Elevated Temperatures," ASTM, 1951, (STP 108), 121 pages.

2. Kubaschewski, O. and Hopkins, B. E., Oxidation of Metals and Alloys, Academic Press, 1953, 239 pages.

3. Speller, Frank, Corrosion: Causes and Prevention, 3rd Edition, McGraw-Hill, 1951, 686 pages.

4. Uhlig, H., Corrosion Handbook, Wiley, 1958, 1188 pages.

5. Simnad, M. T., "Diffusion and Oxidation of Metals," Industrial and Engineering Chemistry, Part 2, 48, Annual Review 1955, March 1956, 586-610.

6. Simnad, M. T., "Diffusion and Oxidation of Metals," Industrial and Engineering Chemistry, Part 2, 49, Annual Review 1956, March 1957, 617-626.

7. Smeltzer, W. W. and Everett, L. H., "Oxidation of Metals," Industrial and Engineering Chemistry, Part 2, 50, Annual Review 1957, March 1958, 496-502.

ABRASIVE WEAR OF METALS

T. E. Norman
Metallurgical Engineer
Climax Molybdenum Company

ABRASIVE WEAR OF METALS

by

T. E. Norman

Introduction

This paper will deal with the various types of abrasive wear which occur at normal temperatures as a result of dynamic contacts between metallic wearing surfaces and abrasive particles or fragments. These types of abrasive wear occur in a wide variety of operations, which include mining, earthmoving, minerals beneficiation, chemical processing, agriculture, foundry, brick and ceramic manufacture, power production and many other operations in the basic industries. The annual cost of replacing worn parts subject to abrasive wear is a major expense in many of these industires. Consequently, increasing attention is being devoted to ways and means of reducing this wear by the development of better abrasion resistant materials and by better choice of the materials now available.

The author's experience with abrasion resistant materials has been largely in the mining, minerals beneficiation and earthmoving industries. Abrasive wear occurs under a rather wide variety of conditions in these industries. The performance of abrasion resistant ferrous alloys in these industries should, therefore, assist in the development and selection of abrasion resistant materials for use in many of the industries where abrasive wear is a problem

Types of Abrasive Wear

While the conditions under which abrasive wear occur vary widely with each application, it has been observed that these conditions can generally be classified into three distinct types as proposed and defined by Avery[1]. These types are as follows:

1. Gouging abrasion, usually with impact.
2. High stress or grinding abrasion.
3. Low-stress scratching abrasion or erosion.

Sometimes more than one of these types of wear will occur simultaneously on a wearing part, but usually the type which predominates can be recognized. This allows an appropriate and economical selection of material to be made for each specific application. It is important to recognize that a material which is most suitable for one of these

three types of abrasion may be inferior or uneconomical when used in one or both of the other types of abrasion.

Gouging abrasion implies a condition where rocks or other coarse abrasive materials cut into a wearing surface with considerable force to tear off relatively large particles of metal from this wearing surface. Sometimes these gouging forces are applied at relatively low velocity, as in the case of a shovel dipper digging into a rock pile, while in other cases, they may be applied at high velocity, as in the case of the hammers or breaker bars in an impact type pulverizer. The mechanism of metal removal appears to be closely similar to that produced by machining with a cutting tool or abrasive wheel. Under these circumstances, a material which is known to be difficult or impossible to machine should offer good resistance to gouging abrasion. Actual service experience tends to confirm this.

Many conditions of gouging abrasion also involve severe impact. Under these circumstances, the practical choice of a suitable material to resist this abrasion frequently involves a compromise selection in which a material is chosen which has less than optimum abrasion resistance, combined with adequate impact strength. Austenitic manganese steel represents such a compromise and is probably the most widely used material for conditions involving gouging abrasion.

Figure 1 shows a "folding type" scraper for underground mining operations, together with some of the rock which this scraper handles. This is a good example of a part subject to gouging abrasion.

High stress or grinding abrasion occurs when two wearing surfaces rub together in a gritty environment with sufficient force to produce a crushing action in the mineral particles or other abrasive entrapped between these two surfaces. Quartz and silicate minerals are the most common materials which produce the wear resulting from these abrasive forces. While the nominal loads per unit of surface area may appear to be low, the actual stress which acts on microscopic areas, as a result of indentation or scratching by the abrasive, is quite high. Some comprehension of the unit stresses involved can be obtained from the fact that quartz grains are capable of indenting or scratching the hardest types of steel. The unit stresses are, therefore, probably above 300,000 psi. Such high unit stresses are capable of causing micro-spalling or fracturing of brittle constituents, such as coarse carbides, which may exist in the structure of some wear-resistant alloys.

Ball mill grinding provides one of the principal applications where high stress abrasion occurs. Other industrial applications exist where dirt and grit are unavoidably trapped between two bearing surfaces, such as in conveyor chains and sprockets, open gears and exposed parts of earthmoving equipment.

Figure 1. View of a 6 foot wide "folding type" ore scraper in folded position. The edges and corners of the wearing blade and the back of the scraper are subject to severe gouging abrasion by the broken ore which this scraper handles.

Figure 2 shows the interior of a large ball mill used for ore grinding. The balls and liners in this mill wear away relatively rapidly due to high stress abrasion. Their wear rates are within the ranges listed for items 2-a and 2-b in table 1 and are approximately equal to the wear rates shown for items 2-a and 2-b in table 2.

Low stress scratching abrasion or erosion involves surface contact, with some degree of velocity, between relatively freely moving abrasive particles and a wearing surface. The forces are seldom high enough to cause much crushing or breaking of the abrasive grains. These grains are most frequently suspended and carried in a fluid such as air or water, or in some cases they are given velocity and produce wear by their own weight, as in the case of sand sliding down a shute.

In most cases of erosive wear, the abrasive particles are small so that impact forces on the wearing part are usually negligible. Exceptions to this may occur where tramp iron or other large pieces of material become mixed with the abrasive particles. Usually, however, it is permissible to use relatively brittle materials to resist erosive wear. This is fortunate, since our most erosion-resistant materials are usually relatively brittle. One notable exception to this is soft rubber, which yields elastically under the action of low and medium velocity abrasive grains. Consequently, it shows excellent resistance to erosive wear in certain applications.

Figure 3 shows a view of a spiral-type sand classifier. As the spirals rotate slowly to convey a mixture of sand and water up an inclined trough, erosive wear is produced on the face and edge of the wear shoes, which must be replaced periodically when they are worn down to about 1/4 inch thickness.

Typical Wear Rates in Each Type of Abrasive Wear

Table 1 provides an approximate guide to the rates at which an abrasion resistant part may wear in each type of abrasion. These wear rates will vary considerably depending on the composition and structure of the material used in the wearing part. For the data in table 1, the wear rates are given for only one of the materials more commonly used in each type of abrasion. In later sections of this paper, comparative wear rates obtained from other materials will be given.

The wear rates in table 1 are based on the maximum rate at which metal is removed normal to the wearing surface of a part. It is given in mils (thousandths of an inch) per hour. For instance, on a chute liner this rate would be in terms of loss of thickness per hour, while on a dipper tooth it would be the rate at which the point wears away, or loss of length per hour. On a grinding ball it would represent loss of radius per hour or one-half the loss in diameter.

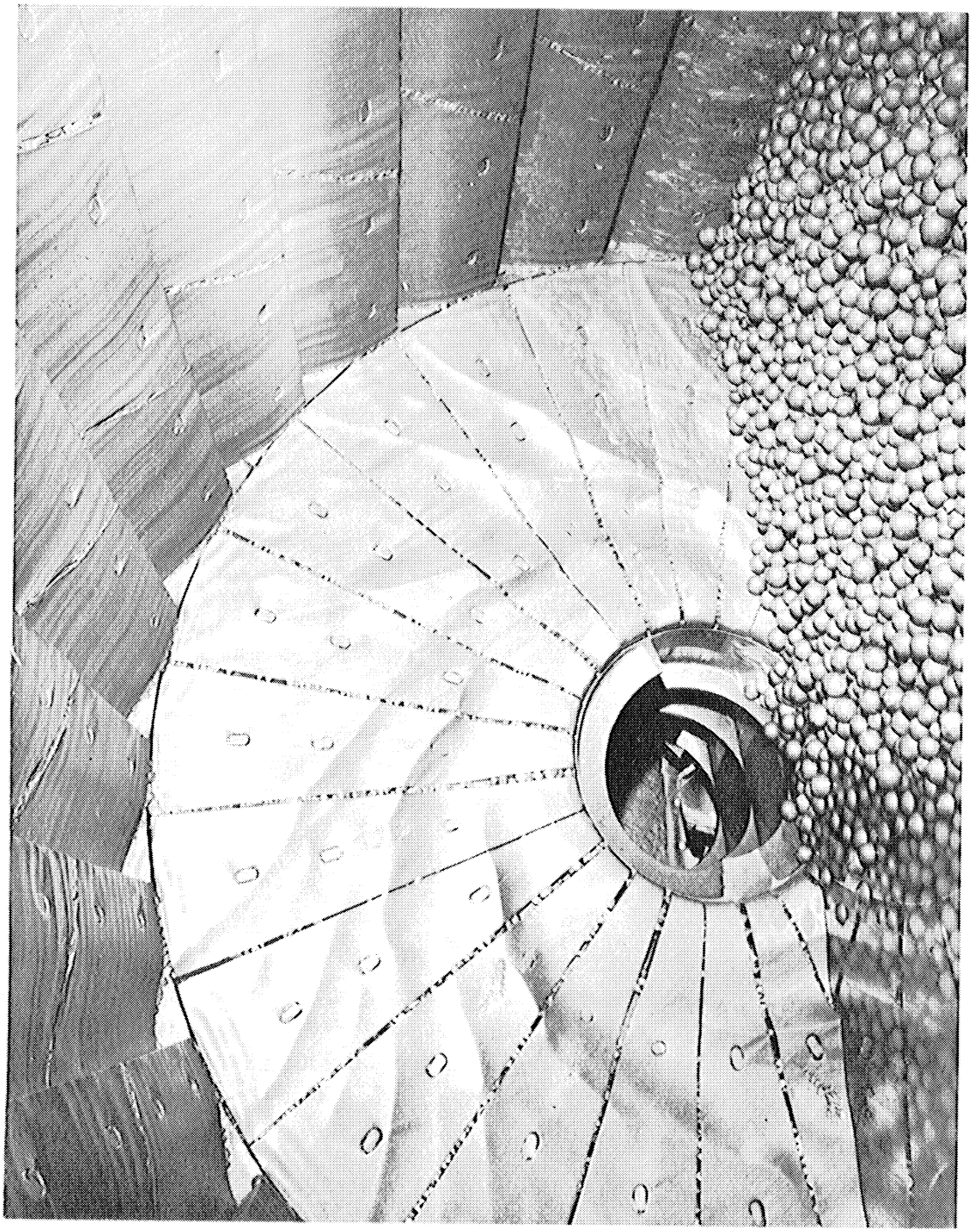

Figure 2. Interior view of a 13 foot diameter ball mill showing partially worm end and shell liners.

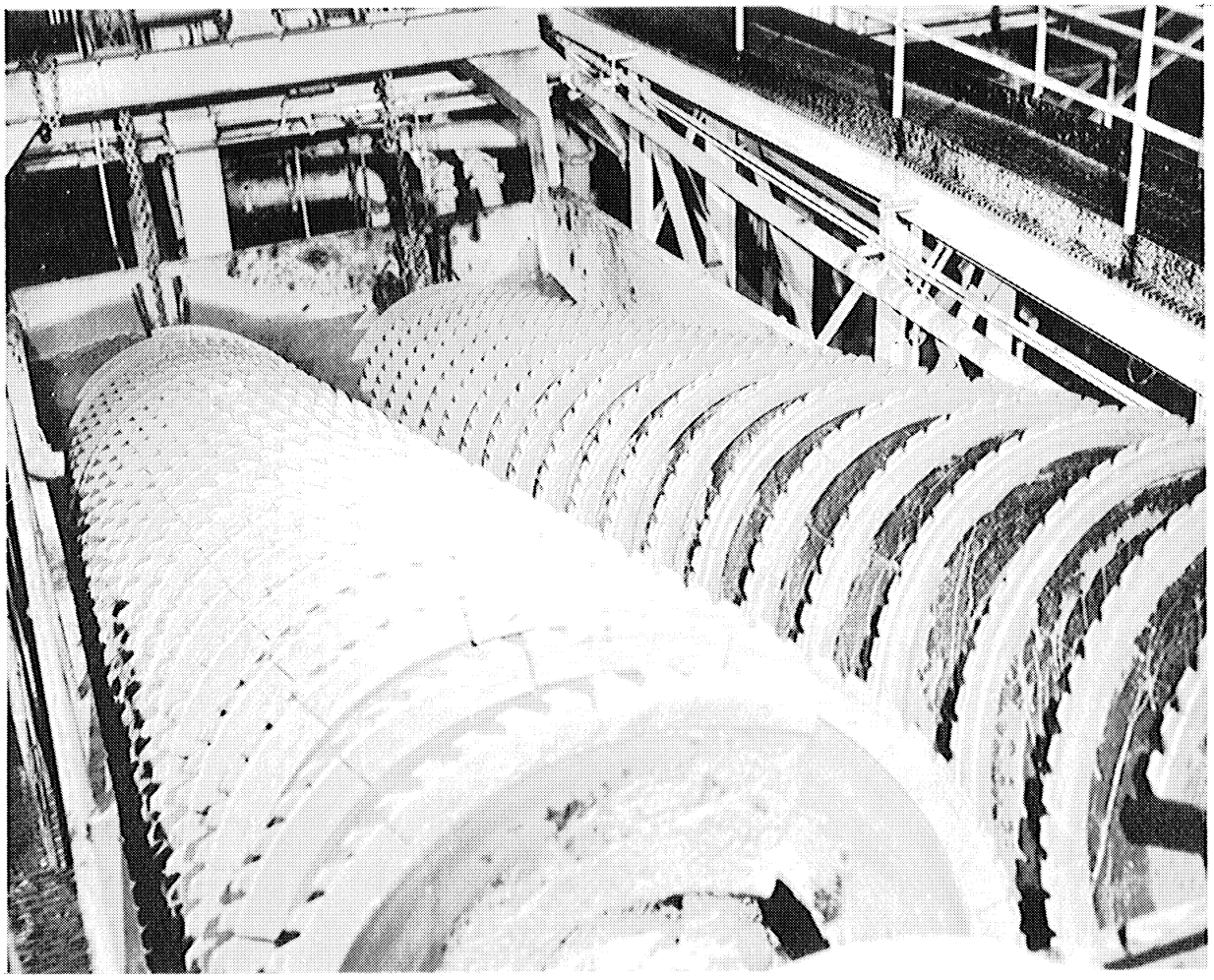

Figure 3. View of a screw-type sand classifier. Each sprial rotates to move coarse settled sand up an inclined trough. Wear occurs on the edge and face of the alloy white iron shoes mounted on the perhiphery of each spiral.

Table 1

Typical Rates of Wear in Various Types of Abrasive Wear

Application	Wear Rate* (Mils per Hour)
(1) Austenitic Manganese Steel in Gouging Abrasion	
(a) Hammers in impact pulverizers	5 to 1000
(b) Shovel dipper teeth	5 to 500
(c) Wearing blades on coarse ore scrapers	5 to 100
(d) Ball mill scoop lips	3 to 15
(e) Crusher liners for crushing siliceous ores	2 to 20
(f) Chute liners handling coarse siliceous ores	0.1 to 10
(2) Low-Alloy High Carbon Steel in High Stress (Grinding) Abrasion	
(a) Rod and ball mill liners in siliceous ores	0.5 to 5.0
(b) Grinding balls in wet grinding siliceous ores	0.15 to 0.45
(c) Grinding balls in wet grinding raw cement slurries	0.05 to 0.15
(d) Grinding balls in dry grinding cement clinker	0.005 to 0.015
(3) Pearlitic White Iron in Low-Stress Abrasion (Erosion)	
(a) Sandblast nozzles	100 to 1000
(b) Sandslinger liners	50 to 250
(c) Pump runner vanes pumping abrasive mineral slurries	0.1 to 5.0
(d) Agitator and flotation impellers in abrasive mineral slurries	0.05 to 1.00
(e) Screw type classifier wear shoes in sand slurries	0.05 to 0.20

* Wear rate is based on rate of metal removal normal to the wearing surface of the part.

Wear Rates in Gouging Abrasion-- In general, the wear rates in mils per hour for gouging abrasion tend to be higher than in grinding or in erosive wear, with the exception of erosive wear by abrasives contacting wearing surfaces at high velocities. It should be appreciated, however, that for gouging abrasion, a large tonnage of material may be handled per unit of wearing surface, so that the weight or volume of metal worn away per ton of material handled may be quite small, compared to grinding abrasion, where intimate contact is required between each particle or fragment of the abrasive and the wearing surfaces which grind this abrasive.

As is indicated in item 1-a in table 1, hammers for impact pulverizers may wear away quite rapidly. This is particularly true when hard siliceous ores are pulverized in an impact type crusher. When the wear rate is as high as 1000 mils (i.e. one inch), per hour, this would normally be considered excessive, since it would require such frequent changing of hammers that use of an impact pulverizer would be impractical under these conditions. Normally the use of impact type pulverizers is confined to the crushing of the softer ores and minerals such as limestone, coal and phosphate rock where rates of wear are reasonably low. Wear rates on these hammers can also be substantially reduced by applying suitable hard facing alloys or by brazed-on tungsten carbide. This is a commonly-used procedure, but even such methods of protection have not solved the wear problem when impact crushers are used for the harder types of ore.

Shovel dipper teeth (item 1-b) normally wear at rates near the lower end of the range indicated in table 1. However, rates as high as 500 mils per hour have been experienced in the handling of the hard taconite ores which are now being mined on the Iron Ranges in Minnesota and Michigan. Since this requires very frequent changing of the dipper teeth, steps have been taken to reduce this wear rate by redesign of the tooth, combined with either the use of a hard facing alloy or a harder, more wear-resistant steel for a tooth material. Rapid wear is still a problem here, however, and the development of still more wear-resistant materials for these teeth would be welcomed.

The rates of wear on wearing blades for coarse ore scrapers, as given in item 1-c, are believed to be typical of most experience in the mining industry. Again, these rates will depend to a large extent on the character of the ore being handled. As an example, the wear rate on the edge of the scraper blade shown in figure 1 is within a range of 10 to 50 mils per hour of operation.

The rate shown in 1-d for ball mill scoop lips is typical of the experience in a number of ore grinding operations at ore concentrating plants in the Western States. While the wear rate is relatively moderate and allows the lips to be used for periods ranging from one month to three or four months, an improvement in this life would be highly desirable, since changing of these lips usually involves the

shutting down of a large high production unit for replacement of a relatively small part. Obviously, under such circumstances a considerably higher price per pound could be justified for a material in these lips if the new material would give substantially longer life. Usually some impact is involved in this scoop lip service, so any new material for these lips must have a combination of good impact resistance along with good abrasion resistance.

The crusher liners used for crushing siliceous ores, as listed in item 1-e, are usually made as large castings and account for a very substantial proportion of the manganese steel used for the mining and minerals processing industries. A wear rate of two to five mils per hour is normal for most siliceous ores, with the exception of the hard taconite ores which have been producing wear rates as high as 20 mils per hour. When it is realized that a wear rate of 20 mils per hour gives these large castings a useful life of only about 200 hours, it becomes obvious that this constitutes a serious wear problem. Consequently, considerable effort and expense can be justified to try to develop better wearing materials for such crusher liners. Since considerable impact is involved in this service, there are very definite limitations in the types of material which can be considered for these crusher liners.

The chute liners which are used to handle coarse siliceous ores (item 1-f) are normally expected to last for at least several months and preferably for several years. A wide range in wear rates occurs on these due to variations in character and velocity of the ore being handled. A wear rate of 1 mil per hour, which quite possibly is near the average, would give a 2" thick chute liner a service life of 2,000 operating hours, which is quite reasonable when it is considered that many of these chute liners are exposed to this wear for only a fraction of the total time that they are in service. However, when the wear rate on these liners is as high as 10 mils per hour, this usually produces an excessively short life, in which case steps are taken to improve this life either by use of more wear-resistant materials or by changing the service conditions under which this chute liner is operating.

Wear Rates in High Stress (Grinding) Abrasion-- In grinding abrasion, the wear rates in mils per hour tend to be relatively low, but since large surface areas are involved, the wear rate in pounds per ton of material ground is relatively high and constitutes one of the major items of expense in ore processing operatiions. The rates of wear in ore and mineral grinding operations have been determined quite accurately at many grinding operations. Probably at least 90% of such rates will fall within the limits shown for items 2-a to 2-d in table 1.

For the rod and ball mill liners listed as item 2-a, a wear rate of about one mil per hour is reasonable and probably represents near-average experience. With such a rate, a set of liners 4" thick

would last 4,000 hours. However, if operating conditions in the grinding mill are such that a wear rate of 5 mils per hour is experienced, this would involve changing the liners every 800 hours. Such frequent changes would be considered excessive in most grinding operations, so when wear rates approach this upper limit, steps are usually taken to reduce this rate either by changes in operating conditions, liner design, or liner material.

The wear rates on grinding balls when grinding various types of abrasive, as listed under 2-b, 2-c and 2-d, provide a good indication of how the types of abrasive influence wear rates in grinding service. The marked reduction in wear rate when a change is made from wet grinding to dry grinding in cement plants has been the object of considerable speculation. It has been suggested by a number of investigators that this reduction in wear rate is due to a lack of corrosion on the ball surfaces under the dry grinding conditions. The author cannot agree with this, however, and does not feel that much of the ball wear in normal wet grinding operations, which is usually in neutral or alkaline pulps, is due to corrosion. These rates of ball wear in wet grinding can be substantially changed by changes in the microstructure and carbon content of the ferrous alloys used for these balls. This indicates that the balls resist wear largely as a result of certain physical properties of the alloy rather than as a result of chemical films produced on the surface of the balls. Also, if corrosion were a major factor in producing wear of these balls, it should be possible to reduce their wear rate very substantially merely by increasing their chromium content to within the ranges most commonly used in stainless steels and irons. However, it has been the author's observation that wear rates in commerical wet grinding operations are relatively insensitive to such changes in the chromium content of the balls, provided that this change in chromium content does not produce a substantial change in the microstructure of the balls. For example, in commerical wet grinding mills, martensitic 0.2 to 2% chromium steels show about the same or only slightly faster wear rates than martensitic 10 to 20% chromium steels of equivalent carbon content. It seems most probable, therefore, that the wear in wet grinding mills is due largely to physical forces which remove particles of metal rather than chemical films from the ball surface. It is the author's belief that when the change is made to dry grinding, a change in the character of these physical forces occurs which, in turn, results in the substantial reduction in the rates of wear produced on the ball surfaces.

Some further discussion of this controversial question occurs in the author's discussion of Ellis'[4] wear tests, and also in the paper on ball wear by Wesner, Pobereskin and Campbell[3].

Wear Rates in Low Stress Abrasion (Erosion)-- Rates of wear in low stress abrasion are largely dependent on such factors as velocity, sharpness and hardness of the abrasive and the hardness of the constituents in the

structure of the abrasion-resistant alloy. Since severe impact seldom exists with this type of abrasion, a wide choice of materials is available. Unalloyed or low alloy pearlitic types of white iron have been extensively used in this service since they have relatively good resistance to erosive wear (compared to most steels) along with a low first cost. However, under the action of high velocity abrasives, the rates of wear on pearlitic white iron are still excessively high, as may be seen from items 3-a and 3-b. In these applications the answer has been to change to more wear-resistant materials, such as boron carbide for sand blast nozzles and the high chromium white irons or high carbon, high chromium toolsteels for sandslinger liners.

In the cases where pealitic white irons wear at rates of 5 mils per hour or less, sufficient life can be obtained from parts of this material to permit its practical usage. However, even in such parts, it has generally become economical to use a more wear-resistant material, which usually involves a substantially higher first cost. One reason for this is that under conditions of erosive wear, the change to a more wear-resistant material usually involves a very substantial degree of improvement in life of a part. This has been nicely demonstrated by Avery[1] in his laboratory comparisons of various materials in each of the three types of abrasion. It has been well confirmed by the author's own tests on wearing parts used in the pumping, agitation and conveying of ground ore-water mixtures.

Typical Rates of Wear Per Ton of Ore In Mining and Concentrating Operations

In the mining and concentration of low-grade siliceous ores, a consumption of from 1 to 3 pounds of steel and iron per ton of ore treated is about normal. Most of this consumption is the result of abrasive wear. Table 2 shows some actual and more or less typical wear rates experienced in the various major items of equipment. It may seen from this table that the grinding operation is responsible for a major portion of this wear.

The crushing operation is usually the next most important consumer of wearing parts. On the other items, wear rates can vary considerably at each mining operation, depending on mining methods and equipment used. For instance, at an open pit mining operation, consumption of scraper parts would be replaced by such items as dipper teeth and the track pads for the crawler tracks on earthmoving equipment. Also in the concentrating plant, the type and consumption of parts subject to erosive wear may vary widely. Substantial variations from the data in table 2 may also occur in grinding abrasion, if rod mills are used along with ball mills for the grinding operation.

Table 2

Typical Rates of Wear in the Mining, Crushing and Concentration of a Siliceous Ore

Application	Wear Rate* Lb per ton
(1) Austenitic Manganese Steel in Gouging Abrasion	
(a) Underground ore scrapers	0.025
(b) Crusher liners	0.110
(c) Chute liners handling coarse ore	0.010
(d) Ball mill scoop lips	0.005
Total for gouging wear	0.150
(2) Low-Alloy High Carbon Steel in Grinding Abrasion	
(a) Grinding balls	1.40
(b) Ball mill liners	0.18
Total for grinding wear	1.58
(3) White Iron in Low Stress Abrasion (Erosion)	
(a) Classifier wear shoes	0.025
(b) Chute liners for fine ore	0.010
(c) Flotation cell impellers and liners**	0.030
(d) Sand pump wearing parts**	0.005
(e) Rods for rod-deck screens	0.003
Total for erosive wear	0.073
Total consumption of wearing parts	1.803

* This is a gross wear rate which includes the weight of the parts when worn out.

** Molded soft rubber may replace white iron in some of these parts.

While consumption of wear resistant materials for some of the items listed in table 2 may appear to be quite low, it should be realized that replacement of these items may involve the shut-down of an important production unit with consequent loss of production. Under such conditions it becomes quite important to devote considerable attention to ways and means of improving the life of these relatively minor wearing parts.

Influence of Hardness of the Abrasive Mineral on Wear Rates

In the field of mineralogy, it is generally accepted that a mineral surface can be scratched only by a substance harder than the mineral itself. Conversely, it is reasonable to expect that a mineral would have to be harder than the wearing surface of a homogeneous abrasion-resistant alloy, before it could scratch or produce appreciable wear on this alloy. To a large extent this appears to be true, though a small amount of wear still occurs even when relatively soft minerals rub against very hard wear-resistant materials. There is, however, usually a very marked drop in the wear rate when the hardness of the abrasive mineral is less than that of the material which it is abrading.

In general, the hard minerals such as silicon carbide, alumina, and quartz tend to produce high wear rates and less spread in the relative wear rates of different ferrous alloys than the softer minerals such as feldspar and calcite. This is indicated by the data from many investigators.(1)(2)(4)(5)(6)(7) Some further indication of this is provided by the results shown in figure 4. To obtain the data for this study, various groups of marked grinding balls were run in a 3 ft. diameter pilot plant ball mill for a number of 24 hour periods. Wear rates of the various groups of marked balls, when grinding three relatively pure minerals of different hardness, under closely controlled conditions, were determined. For each test the abrasive mineral, which was about pea size, was fed to the mill (and discharged from it) at a constant rate of 390 lb. of mineral plus 130 lb. of water per hour. The wear rates shown in figure 4 for a 0.80% carbon steel at three hardness levels are typical of the results obtained.

It can be seen from figure 4 that in grinding quartz, which is approximately as hard as the martensitic steel and definitely harder than pearlitic steels, the wear rates of the three steels are relatively close to each other, with a spread of only 25% between the hardest and softest steel. In grinding feldspar, which is definitely softer than the martensitic steel, but harder than the pearlitic steels, a spread of over 100% exists between the two types. This is due to the marked drop in wear rate of the martensitic steel when it is grinding a mineral softer than itself. Under these circumstances, the martensitic balls become highly polished while the pearlitic steels maintain a dull, scratched finish.

In grinding calcite, which is softer than all three steels, the wear rates of all three are very low, though there is still a spread of over 100% in relative wear rates of the martensitic and pearlitic types.

A very similar trend has been observed in grinding commercial ores or minerals.(2) In grinding high quartz ores, a small spread in relative wear rates has been obtained between the martensitic and pearlitic steels, while in grinding high feldspar ores, the martensitic steels

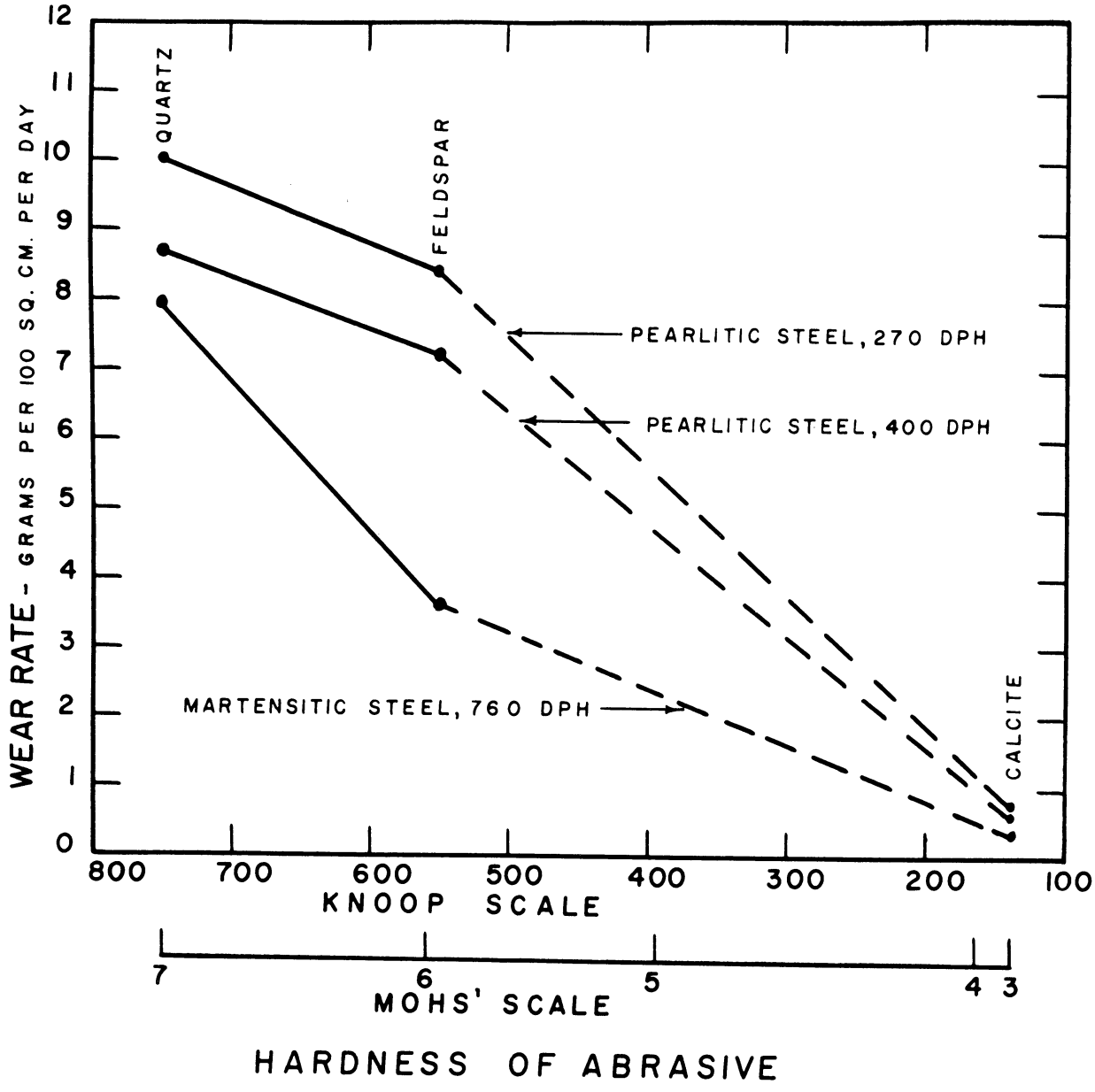

Figure 4. Influence of hardness of the abrasive mineral on the wear rate of 0.80% carbon steel grinding balls at three hardness values.

(and martensitic white iron) show much greater superiority. Ores with a high iron oxide content produce results similar to high feldspar ores, due probably tc the fact that hematite and magnetite have approximately the same mineralogical hardness as feldspar.

Cement clinker acts like calcite on the wear rate of steel grinding balls. The wear rates for all types of steel are very low, while at the same time a pearlitic steel will wear from two to four times as fast as a martensitic steel.

It may be interesting to note that calcite in these tests acted more like a lubricant than as an abrasive. The wear rates of the three groups of steel balls in water alone were about twice their wear rates in the calcite and water mixtures.

It is unfortunate that similar wear tests were not run with minerals whose hardness is between 6 and 3 on the Mohs' scale. This might move the points where the lines for the two pearlitic steels change their slope. For this reason the points between the feldspar and calcite wear rates have been connected with broken lines.

Comparative Wear Rates of Some Commonly Used Materials in Each Type of Abrasion

Reliable quantitative data on the relative performance of the commonly used abrasion-resistant materials in specific types of commercial service are still quite scarce. However, by combining the quantitative information which is available with the somewhat more extensive information of a qualitative nature, it is usually possible to develop some sort of merit rating for the various materials which are being considered for a specific part in a specific service. The results from the extensive laboratory tests on wear-resistant materials as reported by Avery[1] and a number of others[5][6][7][8], appear to correlate well in most instances with actual results obtained in service from each of the three types of abrasion. When using these laboratory results as a guide, however, it is necessary to be sure that the abrasive conditions produced in the laboratory are at least similar to those imposed on the wearing part in actual service.

The discussions and tables which follow in this section are based largely upon the author's own field tests and observations on wearing parts used in the mining, crushing, and concentration of a siliceous type of ore at Climax, Colorado. While the list of available materials which might be considered for each application is not complete, it is hoped that a sufficient variety and range of materials have been tested to at least serve as a guide to the selection of suitable alloys for parts used in each of the three types of abrasion.

Gouging Abrasion

Table 3

Approximate Order of Merit and Relative Wear Rates of Some Materials Used to Resist Gouging Abrasion

Item No.	Material	Relative Wear Rate* (Approximate Range)
1	Sintered tungsten carbide**	0.5 - 5
2	High chromium white irons**	5 - 10
3	"Martensitic" Ni-Cr white iron**	10 - 20
4	Martensitic steel, 1.0% carbon**	20 - 30
5	Pearlitic white iron**	25 - 50
6	Martensitic steel, 0.2 to 0.3% carbon	25 - 50
7	Austenitic manganese steel	30 - 50
8	Pearlitic low-alloy steel, 0.7% carbon, 400 B.H.N.**	30 - 60
9	Pearlitic unalloyed steel, 0.7% carbon, 250 B.H.N.	50 - 70
10	As-rolled or normalized 0.2% carbon steel	100

* Approximate wear rates are based on limited data from various sources. Due to the wide variety of service conditions in which gouging abrasion occurs, some relative wear rates may be outside of the ranges indicated.

** When these materials are used under high impact conditions, they must be well supported by a tough steel backing. Under such conditions, they are normally used as brazed-on inserts or as welded-on hard-surfacing deposits.

Table 3 lists the approximate order of merit and relative wear rates of some materials used to resist gouging abrasion. This table is based largely on the author's results and observations from tests on such parts as percussion type rock drill bits, wearing blades for ore scrapers, chute liners handling coarse ore, crusher liners and lips for ball mill scoop feeders. In each of these applications, wear is believed to occur principally by the gouging type of abrasion. Due largely to the nature of the operating conditions under which such gouging abrasion occurs, it has been considerably more difficult to evaluate the relative merits of different materials in this type of service than in the types of service involving high stress or erosive wear. Also, because of the high impact frequently associated with gouging abrasion, the choice of materials which can be considered for

comparative tests is correspondingly limited. The order of merit and the range of relative wear rates in table 3 are, therefore, largely of a qualitative or approximate nature.

The sintered tungsten carbide listed under item 1 in table 3 is used to resist gouging abrasion in such parts as rock drilling bits, wearing edges of the hammers in impact-type pulverizers, and various miscellaneous applications where relatively small areas of wearing surface are exposed to extremely abrasive conditions. There is no doubt that it deserves its present position at the top of the list in resisting this abrasion. The approximate relative wear rate given is based largely on the performance of tungsten carbide inserts in percussion type rock bits where it usually has shown from about 25 to 50 times the wear resistance of martensitic high carbon steel. While this tungsten carbide is generally considered to be a relatively brittle material, it shows surprisingly good impact resistance when used as small inserts, provided these inserts are well supported by brazing onto a tough and fairly hard steel backing.

For resistance to gouging abrasion, the high chromium white irons (item 2) are probably most commonly used in the form of a hard facing material applied to a tougher steel backing. For example, various modifications of the high chromium white iron compositions are frequently applied as welded hard facings to the wearing surface of manganese steel hammers used in impact pulverizers. In the author's tests, these high chromium white irons have also shown outstanding service when used as castings in chute liners exposed to severe abrasion by coarse ore. They have relatively good toughness for a white iron material and may be used in service involving moderate impact.

The martensitic nickel-chromium types of white iron (item 3) are being used in gouging service in such applications as chute liners handling coarse ore, provided these liners are not subject to severe impact. This type of material has also been used as a hard facing alloy, though not as extensively as the high chromium white iron compositions.

The martensitic high carbon steels (item 4) have been rather extensively used in rock drilling bits, coal cutters and other relatively small parts where abrasion occurs principally due to gouging. In some parts this steel is in the form of a carburized and hardened case on low carbon steel. In other usage, a steel of about this carbon content, when suitably alloyed to produce a martensitic structure, is used as a welded hard facing deposit on a tougher steel backing. To some extent, at least, these high carbon martensitic steels are being replaced by tungsten carbide inserts. These high carbon martensitic steels are seldom suited to use in the entire body of large parts, such as heavy castings, for service involving gouging abrasion because of their inadequate impact resistance and tendency to retain high residual stresses which produce premature failure from cracking.

The pearlitic white irons (item 5) have been used rather extensively in chute liners, small crushing rolls, and certain other parts where gouging without severe impact was involved. The relatively low first cost of these pearlitic types of iron has been a point in their favor, even though their wear resistance and toughness was not as good as the white irons represented by items 2 and 3. During recent years, however, the increase in cost of all types of white iron parts, together with the added cost of labor and shut-down time for their replacement, has frequently shifted the economic advantage to the use of the high chromium or martensitic white irons represented by items 2 and 3.

The martensitic low-alloy steels containing about 0.2 to 0.3% carbon (item 6) have been increasing rapidly in popularity during recent years for many applications involving gouging abrasion. In wrought form they are most commonly used as rolled plate in chute liners, mine car and ore truck body liners[9], and wearing parts for earthmoving equipment. In cast form, steels of this type are used for dipper teeth, bulldozer corner bits, and other such items used principally in earthmoving equipment. Cast steel of this type may also be used in some wearing parts for crushing and pulverizing equipment and in chute liners subject to fairly high impact.

Austenitic manganese steel (item 7), is probably the most extensively used material for applications involving gouging abrasion. The high toughness, freedom from high residual stresses in large castings, and ready availability have made this austenitic manganese steel the usual choice for castings subject to wear by gouging abrasion. It is also used to some extent in wrought form. It normally lends itself well to weld repair or build-up by hard facing, though suitable precautions should be taken to guard against excessive weld embrittlement.

The pearlitic medium to high carbon low alloy steels, (item 8), have been used to some extent as castings to resist gouging abrasion. For pure gouging service they do not appear to have any particular advantage over austenitic manganese steel and have the disadvantage of substantially less toughness. However, conditions may exist where a combination of gouging abrasion plus high stress or low stress abrasion may occur, in which case the pearlitic low alloy steel may show definitely better wear resistance than the austenitic manganese steel.

The pearlitic high carbon unalloyed steels (item 9) are used principally in wrought form for such applications as ore bin chute liners, grizzley rails, and crusher rolls. While many of these applications involve the use of special shapes, there are also many others where the steel is used in the form of railroad rails. While this steel is listed near the bottom of table 3 in relative wear resistance, it has the advantage of low cost and ready availability, together with a reasonable degree of impact resistance, which makes it suitable and economical for many applications.

The low carbon unalloyed mild steels (item 10) are at the bottom of the list in order of relative wear resistance, but nevertheless have been frequently used in applications involving gouging abrasion because of ready availabiltiy and low cost, along with good toughness and ease of fabrication. In applications where wear occurs relatively slowly so that frequent replacement is not a problem, this low carbon steel may still be an economical choice. However, where periodic replacement of the part due to wear is necessary, it has usually been economical to use a more wear-resistant material, such as item 6 or one of the white iron compositions.

In table 3 the author has listed item No. 10 as the standard material for comparative purposes and nominally assigned it an abrasion factor of 100. It is interesting to compare the results from this table with the laboratory results reported by Avery on a number of similar materials tested in a gouging wear test (reference 1, page 24). Relatively good correlation exists between Avery's results with an alundum grinding wheel and the author's ratings from actual commercial service in various types of gouging abrasion.

High Stress Grinding Abrasion

Large tonnages of ferrous alloy materials are consumed under conditions of high stress grinding abrasion in the various types of grinding mills. Ball mills, which are used to grind most metallic ores and many non-metallic minerals, account for a major portion of this consumption. Rod mills, which use rods in place of balls for grinding in the relatively coarse size range, also consume important tonnages of these ferrous alloys. Probably, however, in the case of rod mills, a combination of gouging abrasion and high stress grinding abrasion exists.

The wear resistance of most ferrous alloys is very largely governed by their microstructure and carbon content. This applies to all types of abrasion. In grinding abrasion, it is further indicated by the author's tests that the structure of the matrix has a much greater influence on relative wear resistance than the distribution or quantity of any primary or secondary carbides which may be present. In general, a high carbon martensitic matrix provides optimum wear resistance. A hard (350 to 500 BHN), high carbon pearlitic matrix might be listed as next in order of relative wear resistance. A bainitic matrix is usually inferior to a "hard" pearlite even though the hardness of the bainite may exceed that of the pearlite. The softer grades of pearlite might be listed next in order of wear resistance, followed by mixtures of pearlite and ferrite, with low carbon ferritic structures at the bottom of the list.

Ferrous alloys with a high carbon, austenitic matrix require special consideration since their wear resistance may vary from that of a high carbon martensite down to that of relatively soft pearlite. This

wear resistance of the austenite is governed largely by its composition, particularly with respect to carbon and austenite-stabilizing alloying elements. This will be discussed further in a later section of this paper.

In all grinding mills the principal consumption of materials by wear occurs in the grinding media itself, which may be balls, rods, or in some cases, pebbles. Because of the high tonnages which are consumed, materials for grinding balls have been studied and compared rather extensively by both large and small scale test procedures.(2)(3)(4)(10)(11)(12) Since large scale tests require large tonnages of balls and long periods for comparative testing of different materials, the author has devised and used a small scale test procedure which compares small groups of marked balls which are all run at one time in commercially operating ball mills.(2) The balls in each group are given distinctive identification marks and their wear rates are compared to that of 0.80% carbon low alloy martensitic steel balls.

Table 4 summarizes the relative wear rates obtained from nine different types of material which were tested by the author as marked balls in a number of ball mill grinding operations. The materials are listed in their approximate order of wear resistance. Items 2, 3, 4, 5, 6 and 8 represent materials which are commercially used for grinding balls. Items 1 and 7 are seldom if ever used for grinding balls because of their high alloy content and relatively high cost, while item 9 would not be considered for commercial use because of its poor wear resistance.

Where comparisons are available, the results in table 4 from the small scale, "short time" tests show excellent correlation with the results from large scale tests where hundreds of tons of balls were run over long periods of time. It is obvious from table 4 that for a proper comparison, a small scale test on any material should be run in the same mills and abrasive as the large scale tests. This is further indicated by the results of Wesner, Pobereskin and Campbell(3) from their small scale tests on ball wear in cement mills.

The results in table 4 illustrate the marked influence which the hardness of the abrasive has on relative wear rates. In general, the spread in relative wear rates for the various materials is substantially less when grinding hard ores high in quartz content than it is when grinding softer minerals such as feldspar, hematite and cement clinker. A possible explanation for this is presented in the author's discussion of figure 4.

Liners for ball and rod mills are next in importance to grinding media insofar as consumption in high stress abrasion is concerned. Normally these liners are made from relatively large castings or wrought steel shapes, which introduce the important factor of heavy section into any consideration of suitable ferrous alloys for the liner material. While good wear resistance may be obtained from grinding balls by the use of relatively low alloy compositions, coupled with heat treatments

Table 4

Relative Wear Rates of 3 Inch Diameter Grinding Balls When Grinding Various Ores and Minerals

Mill Location				Climax, Colo.	Garfield, Utah	Ajo, Ariz.	Cooley, Minn.	Golden, Colo.	Portland, Colo.
Type of Ore or Product Ground				Molybdenum	Copper	Copper	Iron	Feldspar	Cement
Principal Abrasives (In order of importance)				Quartz & Feldspar	Quartz & Feldspar	Quartz & Feldspar	Hematite & Quartz	Albite & Orthoclase	Cement & Clinker
Item No.	Material	Carbon %**	Hardness BHN***	Wear Rates Relative to 0.80% Carbon Martensitic Low Alloy Steel*					
1	High carbon-chromium toolsteel	2.15	615	92	-	-	55	-	-
2	Martensitic Cr-Mo high carbon steel	1.20	652	97-99	89-96	-	78-88	-	-
3	"Martensitic" Ni-Cr white iron	3.20	615	95-104	90-95	84-87	62-67	72	Broke
4	Low alloy martensitic steel (Std)	0.80	652	100	100	100	100	100	100
5	Pearlitic Cr-Mo high carbon steel	1.20	460	104-107	105-106	121-128	114-115	189	-
6	Pearlitic unalloyed steel	0.75	375	115-118	118	131-133	-	244-264	366
7	Austenitic manganese steel	1.15	200	124-130	-	154-155	-	364	-
8	Pearlitic white iron, chill cast	3.00	477	Broke	136-139	168-185	148-160	247	-
9	C-1020 steel, forged, air cooled	0.20	130	205	-	-	-	-	-

* Relative wear rates are based on a nominally assigned factor of 100 for item 4. The best wearing materials have the lowest wear rates. All grinding was in wet slurries with the exception of cement clinker. Where a range in wear rates is given, it indicates that two or more groups of the same type of material were tested.

** The carbon contents listed are approximate or nominal values.

*** Most of the hardness values given were converted from an average of Rockwell C readings.

which use rapid quenching procedures, the attainment of comparative structures and wear resistance in a liner will normally require a more highly alloyed composition and less drastic quenching procedures. The less drastic type of quench is required to avoid quench cracks or high residual stresses in the heavy sections and more complicated shapes required for liners.

Table 5 lists the relative wear rates obtained on a number of types of materials which have been or are being used in ball and rod mill liner service. The wear rates listed for these materials were obtained by comparative wear tests on large diameter marked balls when they were all run at one time in commercially operating ball mills grinding siliceous ore at Climax, Colorado.

Table 5

Relative Wear Rates of Some Materials
for Grinding Mill Liners in High Stress Abrasion
(Grinding a Siliceous Ore at Climax, Colorado)

Item No.	Material	Hardness* Rc	Relative Wear Rate
1	High chromium white iron (15% Cr 3% Mo)	66	89
2	High chromium white iron (27% Cr)	64	98
3	Martensitic 1% carbon Cr-Mo steel**	55	100 (Std)
4	"Martensitic" Ni-Cr-Mo white iron, chill cast	59	107
5	Martensitic 0.7% carbon Cr-Mo steel	58	111
6	"Martensitic" Ni-Cr white iron, chill cast	55	116
7	Martensitic 0.4% carbon Cr-Mo steel	55	120
8	Pearlitic 0.8% carbon Cr-Mo steel	39	127
9	Austenitic manganese steel	49	138
10	Pearlitic low chromium white iron	48	195
11	Normalized 1020 steel	65 Rb	225

* Hardnesses from the average of Rockwell hardness readings on the worn surface after service in the ball mill. On materials with austenite in their structure, this surface hardness is usually substantially higher than the hardness of the material below the cold worked surface.

** This "standard" material contained 1.0% carbon, 0.8% manganese, 6.0% chromium, 1.0% molybdenum and was hardened by an air quench from 1900 F.

Details of the test procedure are given in a previous paper by the author(13). These large diameter test balls, because of their size and heat treatment, had structures practically identical to those obtained from heavy section liners made from the same materials. The relative wear rates given in table 5 are within close limits of accuracy (plus or minus 1%), due to the fact that each material was exposed to the same amount of abrasion for the same period. Where comparisons are available, these wear rates on the marked large diameter balls correlate very well with the relative wear rates established for the same materials when used in actual liners for these same mills. Because of this, this "marked ball" test has become a very convenient tool for evaluation of new liner materials or for a study of the effects of variables in composition, heat treatment or structure.

Figure 5 illustrates how this marked ball test might be used in a study of certain variables in ferrous alloys. The data for the curve in figure 5 were obtained from martensitic steels of various carbon contents by using the same procedure and comparative standard as was used to obtain the data for table 5. The importance of using high carbon contents to improve relative wear rates (lower abrasion factors) is well illustrated by this curve.

In general, the spread in relative wear rates of various materials when exposed to grinding abrasion by hard ores or minerals does not tend to be as great as occurs in either gouging wear or erosive wear. For softer ores or minerals, such as feldspar or cement clinker, a larger spread than that indicated in table 5 will probably exist for the various materials. This is well illustrated by the results from the author's tests on materials for grinding balls. (Figure 4 and table 4).

The choice of a suitable and economical material for grinding mill liners, from the list given in table 5, depends on many factors which require a balancing of the relative abrasion resistance of the material against its first cost, relative toughness, frequency of replacement and availability. While the materials represented by items 1 and 2 stand at the top of the list in so far as their abrasion resistance is concerned, their relatively high alloy content and first cost may limit their use to a relatively few mills where conditions are such that these materials show a high degree of superiority over the lower alloyed or lower cost compositions. Also, items 1 and 2 may have insufficient toughness for use in some applications, though it should be pointed out that these two alloys have much better toughness than the low alloy types of white iron.

The materials represented by items 3, 4, 5 and 6 in table 5 have been used commercially for mill liners to a much greater extent than items 1 and 2. While their high hardness and relatively low toughness have limited their field of application to some extent, they have shown a combination of moderate first cost, ready availability

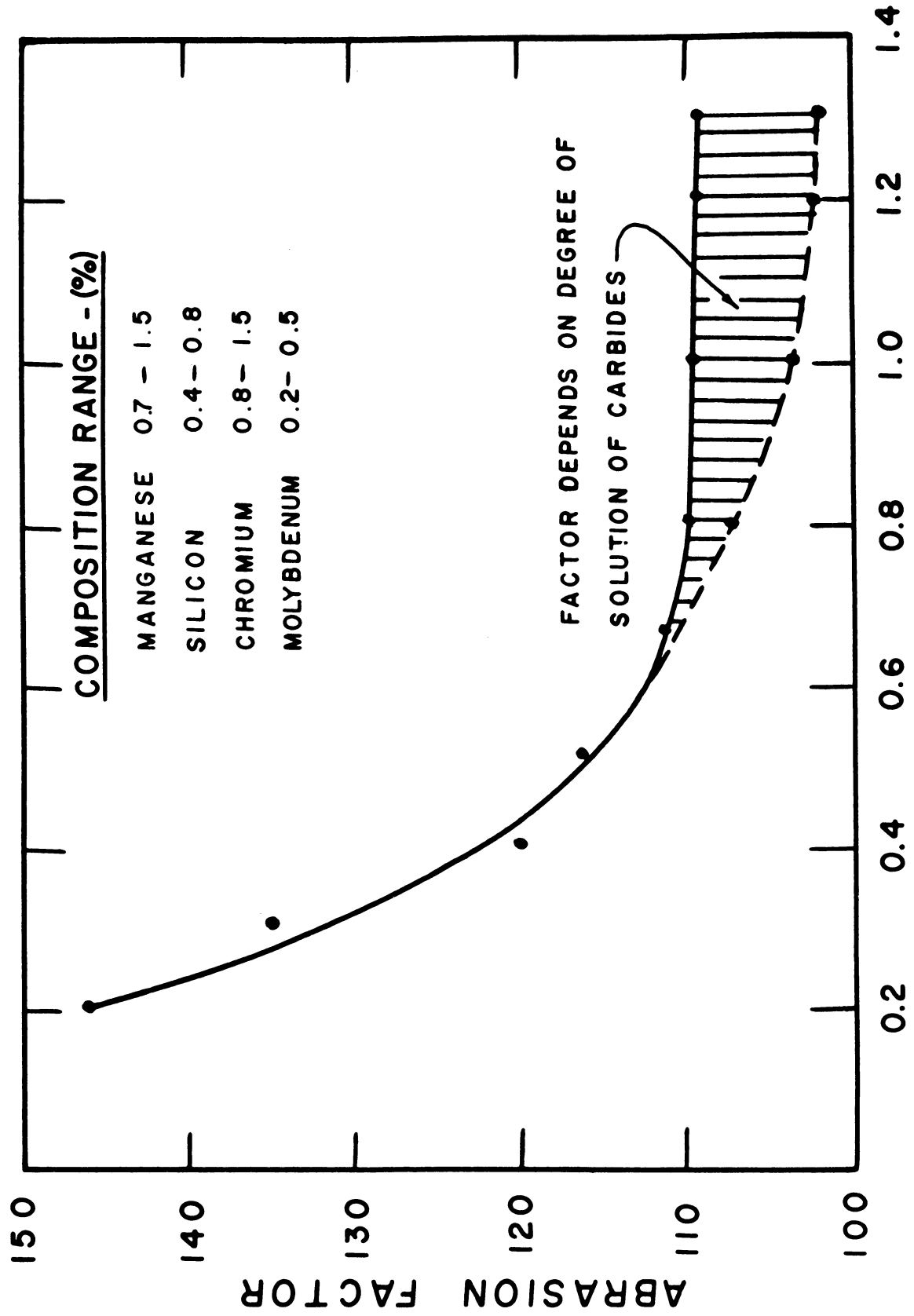

Figure 5. Influence of carbon content on the wear rates of martensitic cast steels when grinding a siliceous ore at Climax, Colorado.

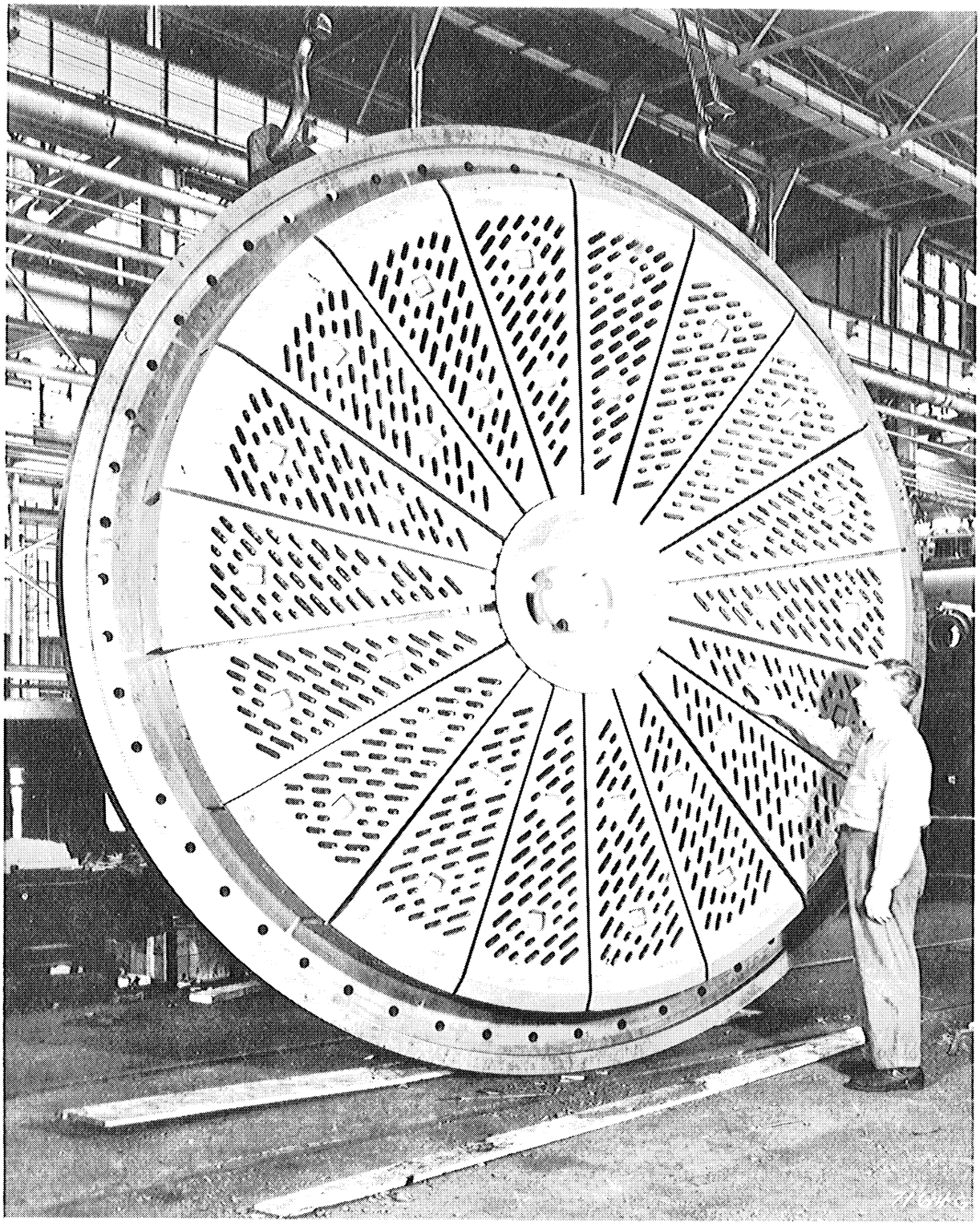

Figure 6. Picture of a ball mill discharge grate assembly. Pearlitic, medium to high carbon, low-alloy steels are well adapted and are extensively used in castings for grate assemblies such as this.

and a sufficient degree of toughness to make them popular for many grinding mill liners.

The 0.4% carbon martensitic steel (item 7) has relatively good toughness compared to the materials preceding it in the list, but due to its lower carbon content, it has shown somewhat less wear resistance in the author's tests. Material of this type has not yet been extensively used in grinding mill liners, so a full evaluation of its possibilities cannot be made at this time.

The pearlitic high carbon chrome-moly steel (item 8) has become a popular material for grinding mill liners. Its moderate first cost, ready availability, fairly good toughness, and consistent performance in service have been advantages in its favor. Due to its lower hardness and pearlitic structure, mill liners made from this type of steel are much less likely to contain high residual stresses than the martensitic steels. This is particularly important in heavy section castings where high residual stresses may cause premature failure from cracking and breakage.

Austenitic manganese steel (item 9) was one of the original materials extensively used for grinding mill liners and is still used in a number of mills, particularly where a high degree of impact is involved. While this type of steel shows poorer wear resistance than the compositions preceding it in the list, the additional toughness obtainable from the austenitic mangnaese steel provides a factor of safety which makes the use of this material a logical choice where impact conditions are unusually severe for grinding mill service. It should be pointed out, however, that for most grinding mill service, the high toughness of the austenitic manganese steel is not needed.

The pearlitic low chromium white iron type of material (item 10) has been used extensively for grinding mill liners in low impact service, where it is capable of standing up without serious spalling or breakage. The principal advantages of this pearlitic type of white iron have been low first cost and ready availability. However, at the present time this pearlitic white iron has been largely displaced by the more wear-resistant liner materials listed above it in table 4.

Low carbon steel similar to item 11 is seldom, if ever, used commercially for grinding mill liners at the present time, due to its inferior wear resistance. However, the material is listed in table 4 since it provides a good indication of the results which might be obtained from relatively soft, low carbon steel of this type.

More complete discussions of the various materials commercially used for grinding mill liners are given in other papers by the author.[13][14]

Erosive Wear

Materials which best resist erosive wear generally have a very high hardness or a high proportion of hard constituents such as

carbides in their structure. One exception to this is soft rubber, which yields elastically under the impact of the abrasive grains, provided the velocity, size and sharpness of these grains are not too great. The ferrous alloys used to resist erosive wear normally have a high carbon content, which is preferably up in the white iron range of compositions. Certain parts having very light sections, such as screen wire and screen rods, which are not adaptable to production in the form of castings, are usually made from a high carbon grade of steel and are preferably hardened to the maximum hardness at which they can be used without premature failaure from breakage.

In most conditions of erosive wear, the wearing parts are exposed to very little impact. This permits the use of relatively hard and brittle materials. If impact does occur in combination with erosion, it is obvious that one of the tougher grades of steel must be used for the part, though in this case its wear resistance and life can frequently be improved by the use of erosion-resistant hard facing alloys or possibly by protecting the wearing surface of the part by the use of brazed-on tungsten carbide or some other hard material of this type.

Table 6

Relative Wear Rates of Various Materials in Erosive Service
(Handling Slurries of Ground Siliceous Ore at Climax, Colo.)

Item No.	Material	Relative Wear Rate* Classifier Wear Shoes	Sand Pump Impellers	Flotations Cell Impellers
1	High chromium white iron (15% Cr, 3% Mo)	28	-	-
2	High chromium white iron (27% Cr)	48	30	27
3	Molded soft natural rubber	-	33	46
4	"Martensitic" Ni-Cr white iron	80	88	-
5	Pearlitic low chromium white iron (Std)	100	100	100
6	Martensitic 1.5% carbon steel	180	122	-

* Relative wear rates are based on a nominal rate of 100 for the pearlitic white iron in each type of service. Rates are based on the reciprocal of time required to "wear out" each part. For instance, a material with a wear rate of 28 will last about 3 1/2 times as long as material with a wear rate of 100.

Table 6 lists the relative wear rates of six materials used to resist erosive wear in the handling of slurries of ground siliceous ore at Climax, Colorado. In this service the high chromium types of white

iron (items 1 and 2) have been most outstanding and were actually superior to molded rubber (item 3) under these conditions. The martensitic nickel-chromium type of white iron (item 4) was only moderately better than a pearlitic type of white iron (item 5) in this service. Possibly this can be explained by the fact that the hardness of the carbides in the structure of item 4 was not much, if any, greater than the hardness of the carbides in the structure of item 5. The importance of having hard carbides present is illustrated by item 6, which had a hard, martensitic matrix but relatively few carbides in its structure. As a consequence, this martensitic steel did not even show as good wear resistance as a pearlitic white iron.

Table 7 lists the relative wear rates of a number of types of hardened steel used in erosive service for the screening of crushed siliceous ore at Climax. The screens used for this purpose are of the rod deck type, in which individual rods are closely spaced across the deck of the screen to provide the screening surface. Under these conditions, it is permissible to use a relatively hard and brittle material for the rods.

Table 7

Relative Wear Rates of Hardened Steels in Erosive Service
(Dry Screening of Crushed Siliceous Ore on Rod Deck Screens at Climax)

Item No.	Material	Hardness Rc	Relative Wear Rate
1	Type 420 stainless, oil quenched	55	66
2	C 1080 steel, austempered	57	76
3	C 1095 steel, oil quenched and tempered	52	77
4	C 1095 steel, oil quenched and tempered	44	82
5	C 1070 steel, austempered	54	87
6	C 1070 steel, oil quenched and tempered	53	91
7	C 1070 steel, oil quenched and tempered	44	100
8	C 1080 steel, cold drawn	37	109

To obtain the comparative data in table 7, the wear rate of all test rods was compared to the wear rate of the C1070 steel, oil quenched and tempered to 44 Rc. The test rods and standard rods were alternated in groups of five across the width of the screen. The relative wear rates were determined by comparing the weight loss of the test rods to that of the standard rods. Relative wear rates were then calculated by assigning the standard material a nominal rate of 100 on each test. Each test consisted of a comparison of 50 rods of the test material against 50 rods of the standard material.

The type 420 stainless steel listed in table 7 showed surprisingly good wear resistance, considering its relatively low carbon content. One possible explanation for this is that a hard, abrasion-resistant film of chromium oxide forms on the surface of this type of steel and this, in turn, supplies the hard surface necessary for good erosion resistance.

The remaining high carbon steels (items 2 to 8) in table 7 indicate the value of both high hardness and high carbon contents to resist erosive wear. A high carbon content appears to be somewhat more important than high hardness, as is indicated for the 1095 steel at 44 Rc, which was superior to the 1070 steel at 53 Rc.

Types and Composition of the Abrasion Resistant Ferrous Alloys

In the preceding sections of this paper, the abrasion resistant ferrous alloys have been listed and discussed according to type, with no detailed consideration of their compositon, heat treatment or procedures used in their production. While such detailed consideration of the metallurgical characteristics of these alloys is beyond the scope of this paper, some further information on their composition ranges, heat treating procedures, and certain other characteristics is probably necessary. It should be emphasized, however, that the various composition ranges which will be given in this section usually are of a general nature and are intended to cover a series of specific compositions from several sources or for several applications.

To provide an overall picture of the types of iron and steel used primarily for abrasion resistance, it is probably best to classify them according to their general metallurgical types or metallurgical structure, since this structure is the most important factor in determining their abrasion resistance and other mechanical properties. This classification, for the most generally used types of white iron, is given in table 8.

Table 8

Abrasion-Resistant Alloys - White Irons

1- High Chromium Irons
- (a) 27% Chromium type
- (b) 15% Chromium, 3% Molybdenum type
- (c) High Carbon, Cr-Mo-V "toolsteels"

2- Nickel-Chromium Martensitic White Irons
- (a) Ni-Hard
- (b) Climax 321 alloy

3- Pearlitic White and Chilled Irons
- (a) Low-alloy type (Mainly low Chromium)
- (b) Unalloyed

The high chromium irons in table 8 stand at the top of the list in so far as abrasion resistance and toughness are concerned. They have not, as yet, been made in large tonnages, but their excellent combination of properties should give these irons a very promising future.

Included in this high chromium iron classification are the high chromium, high carbon toolsteels which are well known for their excellent abrasion resistance. This type of "toolsteel" is really a white iron, with its carbon content held down to a range which allows it to be forged and hot rolled.

The best known material for the nickel-chromium type of martensitic white iron listed in table 8 is Ni-Hard, which is now made in large tonnages for applications where good abrasion resistance with little impact is involved. During the past several years, the author has been studying and testing modifications of this Ni-Hard composition, which has resulted in the development of Climax 321 alloy. This 321 alloy has a lower nickel content, along with a molybdenum addition and a generally higher carbon content. It is showing up well on various service tests (such as item 4 in table 5), and promises to be a worthy competitor to the conventional Ni-Hard composition.

The pearlitic white and chilled irons have been and are still being used in large tonnages for many applications. While they have a lower first cost than the other two types of white iron, they also are generally much inferior in wear resistance. It appears at this time that these pearlitic white irons will be displaced in most applications by the more wear-resistant, and on a service basis, more economical high chromium or nickel-chromium types of martensitic white irons.

Table 9

Abrasion-Resistant Alloys - Steels

(1) Martensitic High Carbon Steels

(a) Compositions for heavy sections - Medium alloy
(b) Compositions for light sections - Low alloy

(2) Martensitic Medium to Low Carbon Steels

(a) Compositions for both light and heavy sections

(3) Pearlitic Steels

(a) Compositions for both light and heavy sections

(4) Austenitic High Carbon Steels

(a) High manganese types. For both light and heavy sections
(b) "Lean alloy" types. (Experimental)

Table 9 lists the most generally used types of abrasion-resistant steels. They are normally used in those applications where the white irons are unsuitable because of insufficient toughness. It should be recognized, however, that the most abrasion-resistant steels may also have better wear resistance than the nickel-chromium, martensitic white irons in certain applications. This applies particularly to grinding mill liners and to some applications for grinding balls.

The various types of steel in table 9 are (with some exceptions) listed in their approximate order of decreasing abrasion resistance. An important exception to this statement occurs in type 4-b. This "lean alloy" austenitic type of steel, which uses combinations of chromium, molybdenum, manganese, nickel or copper, and a high carbon content, for austenite retention, has shown abrasion resistance in the author's tests which was equal to and in some cases, better than the martensitic high carbon steels. In toughness or ductility, the lean alloy austenitic type is inferior to the 4-a high manganese austenitic steels but it shows promise of being substantially tougher than the high carbon martensitic steels. If these indications are confirmed by further tests, the combination of high abrasion resistance and a moderate degree of toughness should give such a steel a promising future for many parts subject to abrasive wear.

Table 10

High Chromium White Irons

	Heavy Sections-General Purpose		Light Sections-Special Purpose	
	A	B	C	D
Carbon - %	2.25 - 2.85	3.00 - 3.50	3.00 - 4.00	1.40 - 2.60
Silicon	0.25 - 1.00	0.30 - 0.60	0.25 - 0.50	0.20 - 0.60
Manganese	0.50 - 1.25	0.50 - 0.90	0.60 - 0.90	0.25 - 0.60
Chromium	24.00 -30.00	15.00 -18.00	10.00 -15.00	11.00 -14.00
Molybdenum	0.00 - 1.00	2.00 - 4.00	0.50 - 1.50	0.80 - 1.20
Vanadium	0.00 - 1.00	0.00 - 0.50	---	0.30 - 5.00

Table 10 lists the composition ranges of representive types of the high chromium irons included in table 8. Type A represents a composition range which has been used for many years. Type B is a more recently developed composition with a lower chromium content and 2 to 4% molybdenum. It has shown better wear resistance than type A in the author's tests, so appears to be a preferable composition. It was developed as a result of tests at Climax and has been named Climax alloy 42. This better wear resistance is probably due largely to the fact that the alloy 42 can be

used successfully at higher carbon levels than the type A iron.

Type C iron is for those light section castings which can be given a hot shakeout and air quenched or which can be reheated and liquid quenched. Because of the quenching stresses which develop, such treatments are suitable only for simple shapes. This composition is still largely experimental, though it has been used commercially for wheelabrator blades. It is, however, an interesting composition because of its lower alloy cost than the other types of high chromium irons.

Type D iron includes the composition ranges of the high carbon high chromium, class 140 toolsteels, along with their high vanadium modifications. These compositions are produced mostly in wrought form, but because of their high carbon content and structure, it is permissible and probably more correct to classify them as white irons than as steels. They have shown outstanding abrasion resistance in brick mold liners and wearing parts for sand slingers and short blasting machines. Because of the difficulty involved and care required in producing wrought shapes from compositions of this type, they are relatively high in first cost and are consequently used only where a premium grade material can be justified by the excellent abrasion resistance and fairly good impact resistance which is characteristic of this type of material.

All of the high chromium iron castings are adaptable to use either in their as-cast or heat-treated condition. The choice of the most suitable treatment depends largely on such factors as section size, design, molybdenum content and to some extent, on end use.

Table 11

Nickel-Chromium Martensitic White Irons

	Heavy Sections-General Purpose		Light Sections-Special Purpose	
	A	B	C	D
Carbon - %	3.00 - 3.60	3.30 - 3.60	3.00 - 3.50	3.40 - 3.65
Silicon	0.40 - 0.70	0.25 - 0.60	0.40 - 0.60	0.25 - 0.50
Manganese	0.40 - 0.70	0.50 - 0.80	0.20 - 0.40	0.50 - 0.80
Nickel	4.00 - 4.75	2.75 - 3.25	2.50 - 4.00	1.50 - 2.25
Chromium	1.40 - 3.50	1.50 - 2.00	1.20 - 1.50	0.75 - 1.50
Molybdenum	0.00 - 0.70	0.70 - 1.10	---	0.50 - 1.00

Table 11 lists the composition ranges for the nickel-chromium types of martensitic white irons. One important characteristic of these is that they can be produced by cupola melting, which makes them available from almost any iron foundry. They are normally used in their as-cast and stress-relieved (400-550F) condition.

Ni-Hard, represented by types A and C, is the best known and most widely used material in abrasion-resistant white iron castings at the present time. The irons represented by types B and D are the Climax 321 alloy. The numbers 3, 2 and 1 in this designation represent the approximate proportions of nickel, chromium and molybdenum, respectively. On the basis of the author's tests to date, it appears that the 3:2:1 ratio is about the most favorable or efficient for production of the best structure and wear resistance.

The low alloy Ni-Hard and 321 compositions listed as types C and D in table 11 are suitable only for light section castings which can be cooled fairly rapidly, such as occurs when they are given a hot shakeout. The compositions are specifically designed for small grinding balls in low impact mills. Such balls are used in some ore grinding and rather extensively in cement plants.

Table 12

Martensitic High Carbon Abrasion-Resistant Steels

	Heavy Section		Light Section	
	A	B	C	D
Carbon - %	0.60 - 0.80	0.80 - 1.20	0.60 - 0.90	1.00 - 1.50
Manganese	0.60 - 1.25	0.60 - 0.90	0.50 - 0.90	0.25 - 0.70
Silicon	0.40 - 1.00	0.40 - 0.80	0.20 - 0.80	0.40 - 0.80
Chromium	1.25 - 7.00	5.00 - 7.00	0.00 - 1.00	0.40 - 2.00
Molybdenum	0.40 - 0.60	.70 - 1.00	0.00 - 0.30	0.15 - 0.70
Nickel	0.00 - 2.00	---	---	---

Table 12 gives typical composition ranges for the martensitic high carbon steels listed in table 9. To obtain optimum abrasion resistance from a cast or wrought steel composition, a high carbon content is essential. For a given carbon content, a fully hardened martensitic structure will normally give substantially better abrasion resistance than a pearlitic or bainitic structure. The production of a martensitic structure in a large heavy section casting, such as a grinding mill liner, requires a steel composition which will fully harden when given a rather mild quench, such as a quench in air or in a molten salt bath. This mild quench is necessary to avoid severe quenching stresses which might crack the casting. The type A composition range for heavy sections in table 12 represents one answer to the problem. Substantial tonnages of this type of steel are now being made. They are usually hardend by quenching in a molten salt bath. This type of quench allows the use of chromium contents near the lower end of the range. If the heat treatment involves an air quench, the chromium content must either be near the high

end of the range or intermediate chromium along with a nickel addition may be used.

Type B steel for heavy sections will normally be somewhat more wear resistant than type A. Due to the fact that it contains undissolved carbides and a fine grain size and is normally air-quenched, a relatively high alloy content is necessary. This type B composition is quite close to the air hardening, high carbon die steel compositions.

The types C and D steels for light sections are used principally in small wearing parts and in grinding balls at the present time. While the principal production of alloy steel grinding balls has been from the type C composition, the type D merits serious consideration, since it has shown an outstanding combination of abrasion resistance and toughness in the author's tests. The type D steel is also used for many wheelabrator blades. It may also have good possibilities for grinding rods, which are now being made from unalloyed high carbon steel.

Table 13

Martensitic Medium to Low Carbon A.R. Steels

Heavy and Light Sections

Carbon - %	0.15 - 0.50
Manganese	0.70 - 1.80
Silicon	0.15 - 1.00
Chromium	0.00 - 1.00
Molybdenum	0.15 - 0.70
Nickel	0.00 - 1.00
Vanadium	0.00 - 0.20
Boron	0.000- 0.003

The martensitic medium to low carbon abrasion-resistant steels are made by various producers from a fairly wide range and variety of compositions. Their hardening treatment involves a liquid quench and temper. Usually each producer has a preferred composition which is marketed under a specific trade name. The composition range shown in table 13 is intended to cover the entire range from the various producers of this type of steel and is obviously not a specific composition representative of one producer or one trade name.

These medium to low carbon martensitic steels probably should not be classed as having a true martensitic structure, since they are generally tempered at moderate to high temperatures to provide them with adequate toughness for specific applications. As castings they find their principal use in wearing parts for earthmoving equipment such as dipper teeth and bulldozer corner bits. They are showing better wear

resistance than austenitic manganese steel in many of these applications. Their high yield strength also gives them some advantage over manganese steel in certain wearing parts which are specifically designed to take advantage of this high yield strength. As wrought steels they are used principally in plate form for such applications as chute liners, mine car and dump truck body liners, or they may be used in bar form for such parts as the bit bodies for the carbide tipped bits used on coal cutting machines.

Table 14

Pearlitic Low-Alloy Abrasion-Resistant Steels
(For both Heavy and Light Sections)

Carbon - %	0.40 - 1.30
Manganese	0.25 - 0.90
Silicon	0.30 - 0.80
Chromium	1.00 - 3.00
Molybdenum	0.20 - 0.50
Nickel	0.00 - 1.50
Vanadium	0.00 - 0.20

The pearlitic low-alloy types of abrasion-resistant steel, whose composition range is given in table 14, cover a rather wide range of carbon and alloy contents, particularly when they are made as castings. Their heat treatment is relatively simple, consisting of a normalize and temper, or in some applications they are used to their as-rolled, as forged or as-cast condition. They are used in a wide variety of applications where combinations of abrasion resistance and structural strength are necessary. An advantage of these pearlitic steels is that they are easily produced either as castings or rolled products. They are much less likely to contain the high residual stresses which often give trouble in martensitic steels. This is a definite advantage in large parts, such as ball mill liners, and as a result the pearlitic types of steel have been and are being used quite extensively in applications such as this. The higher carbon grades of pearlitic steels are normally somewhat more wear resistant than austenitic manganese steel in both high and low stress abrasion. Their higher yield strength and freedom from flow in service also give them an advantage over austenitic manganese steel in certain applications. However, these pearlitic steels do not have the high toughness of austenitic manganese steel, which limits their field of use to applications where impact is not very severe. Also, they do not have the superior wear resistance of the martensitic steels. As a result, these martensitic steels are now displacing the pearlitic steels in various applications, though it should be recognized that for certain

applications, the inherent advantages of the pearlitic steels may keep them in the picture for many years to come.

Figure 6, which is a picture of a ball mill discharge grate assembly, shows a typical application for a low-alloy pearlitic type of steel. The castings in this assembly are made from a composition which contains approximately 0.60% carbon, 0.80% manganese, 2.0% chromium and 0.4% molybdenum

Table 15

"Conventional" Austenitic Manganese Steels

	Casting Grades		Welding Rod Grades		
	A	B	C	D	E
	Plain	Alloyed	Ni	Ni-Mo	Mo
Carbon - %	1.00 - 1.30	1.00 - 1.40	0.70 - 0.90	0.70 - 0.90	0.70 - 0.90
Manganese	11.50 -14.00	11.50 -14.00	12.00 -14.50	12.00 -14.50	12.00 -14.50
Silicon	0.40 - 1.00	0.40 - 1.00	0.50 - 1.00	0.50 - 1.00	0.50 - 1.00
Phosphorus	0.07 max	0.07 max	0.07 max	0.07 max	0.07 max
Chromium	---	0.00 - 2.50	---	---	---
Molybdenum	---	0.00 - 2.00	---	0.40 - 0.60	1.00 - 2.00
Nickel	---	---	3.0 - 5.0	1.75 - 2.25	---

Table 15 gives the composition ranges for the conventional types of austenitic manganese steels. Types A and B are normally heat treated by a water quench from 1900 - 2000 F. Types C, D and E are designed to retain a fully austenitic structure after air quenching. For the casting grades with a conventional heat treatment, chromium up to about 2.5% is frequently used to improve yield strength and resistance to flow in service. It is also supposed to improve wear resistance somewhat, though this has never really been proven, due probably to the fact that the difference obtained by adding chromium is small. Some producers replace a part of this chromium with about 0.50% molybdenum and claim to have found additional benefits.

Molybdenum in these conventionally treated manganese steels is very effective in reducing tendencies toward carbide embrittlement in heavy sections. It also is quite effective in raising the yield strength. Recent laboratory data have indicated that when about 2% molybdenum is present in these austenitic manganese steels, a higher carbon content can be safely tolerated, which in turn should provide improved abrasion resistance.

In the welding rod grades, which are used both for welding rod and many rolled shapes, the type C composition with 3 to 5% nickel was originally used for most applications. During World War II, the merit of molybdenum as a replacement for nickel in this steel was established. The type D nickel-moly composition is probably the one produced in greatest tonnage at the present time. Tests which have been run on the type E composition with 1 to 2% molybdenum have indicated it has a modest degree of superiority over the other types[15]. Consequently, this type E composition may eventually become the most popular grade for welding rods.

Table 16

"Dispersion Hardened" Mo-Mn Austenitic Steels

	A	B
	Regular	High Carbon
Carbon - %	1.10 - 1.20	1.25 - 1.40
Manganese	13.00 -14.00	13.00 -14.00
Silicon	0.40 - 1.00	0.40 - 1.00
Molybdenum	1.90 - 2.10	1.90 - 1.00
Phosphorus	0.06 max	0.06 max

Laboratory and field tests on the effects of molybdenum in austenitic manganese steel castings indicate that the molybdenum addition shows its greatest benefits when it is combined with a special "dispersion hardening" heat treatment. The "dispersion hardening" is obtained by first soaking the castings for about 8 to 12 hours at 1100 F to produce pearlite in their structure and following this by reaustenitization at about 1800 F, followed by a water quench. This treatment produces a fine dispersion of spheroidized carbides in the austenite, which materially strengthens and hardens the steel. These dispersion hardened compositions are listed in table 16. The type A regular carbon grade is giving an average of about 35% longer life than plain manganese steel in cone crusher liners at Climax. These results are based on two years of comparative testing. Tests are now in progress on the type B higher carbon grade, which are expected to provide an additional improvement.

Table 17

"Lean Alloy" Austenitic Steels
(Experimental)

	A	B
	Modified Hadfield Mn	Medium Mn Type
Carbon - %	1.25 - 1.45	1.20 - 1.70
Manganese	8.00 -11.50	3.70 - 6.00
Molybdenum	1.00 - 2.50	0.50 - 3.00
Chromium	---	0.00 - (?)*
Nickel	---	0.00 - 6.00 (or Cu)
Silicon	0.40 - 1.00	1.50 max
Phosphorus	0.06 max	0.10 max

* The maximum permissible limits for chromium are not yet defined.

Table 17 indicates two possible composition ranges which could be considered in the development of the lean-alloy austenitic steels. A review of the small-scale wear tests which the author has run to date, and other metallurgical data, have provided some clues which may lead to the development of a type of steel having a combination of toughness and wear resistance which could make it very suitable for many applications for steel castings and also for certain wrought products. Basically this new steel will be an austenitic type. It has been observed[13] that by the use of as much carbon as can be kept in solution, along with moderate amounts of molybdenum and certain austenite-retaining elements such as chromium, manganese, nickel and copper, it is possible to produce an austenitic steel which has equal and in some cases better abrasion resistance than the high carbon martensitic steels. This new type of steel might well be called a "lean alloy" austenite, since in its basic concept, it should use only the minimum amount needed of such austenite stabilizing elements as manganese, nickel and/or copper. The possible combination of reasonable toughness and high abrasion resistance, together with a moderate alloy cost, indicate that such a steel should have intersting possibilities. It may be significant that certain hard facing alloys are made from compositions similar to these lean alloy austenitic steels.

It will require a considerable amount of further research and field testing to determine the proper composition range and heat treatment for lean alloy austenites with the best combination of properties. Composition A in table 10 represents a fairly conservative approach to the problem. Basically, it involves a modest lowering of the manganese content of the 2% molybdenum, dispersion hardened, austenitic manganese

steel. The change in composition A from the regular austenitic moly-manganese steels is hardly sufficient to allow it to be classed as a true lean-alloy austenite.

Compositions from the range under B in table 17 are capable of producing true lean-alloy austenites. It should be explained that the wide range shown here is merely an indication of the ranges in various alloy contents which might be studied by preliminary laboratory and wear tests. One requirement of any specific composition selected from this range is that its content of austenite-retaining elements be sufficient to produce and retain a fully austenitic structure, free from any detectable amount of martensite or pearlite.

Comparative Mechanical Properties and Relative Toughness of Some Abrasion-Resistant Alloys

Many part subject to abrasive wear are required to have a certain degree of strength and toughness along with abrasion resistance, so that they will stand up in service without premature failure from breakage, spalling or excessive plastic deformation. While the toughness of a material is a rather indefinite term which cannot be expressed in any specific units, it is associated principally with the ability of a material to yield plastically when stressed beyond its elastic limit. The ability to yield plastically by even very small amounts may have a very significant influence on the relative toughness of some of the harder types of abrasion resistant alloys.

Elongation or reduction of area on a tensile test is commonly used as one measure of toughness in steel. For most abrasion resistant alloys, however, the difficulty involved in preparing and machining representative tensile specimens is usually so great that such specimens are seldom made. Consequently, there is relatively little comparative information on their tensile properties. Usually an evaluation of the relative toughness of these alloys is based largely on their past performance in actual applications. Obviously, information of this type is largely qualitative, and it would be most helpful, particularly in the development of new materials, to be able to apply laboratory tests which would rate the toughness of the material on some sort of quantitative basis. A rather similar situation has existed in connection with the use and development of toolsteels.

Because of certain requirements as to size, shape and composition, a large and probably a major proportion of abrasion resistant parts are produced as castings. The relative toughness, and sometimes the strength, of the ferrous alloys used for these castings is frequently an important consideration. To provide some idea of the mechanical properties of the more commonly used types of abrasion resistant alloys, the author has compiled the data in tables 18 and 19. While the properties which are given are believed to be reasonably typical, it should be appreciated that with the exception of the two austenitic manganese steel compositions in table 18,

the remainder of the data is based on the results of a relatively few tests. Some of these results are from published information and some are from unpublished laboratory test data.

Table 18

Typical Tensile Properties of Some Cast Abrasion Resistant Alloys

Item No.	Material	Hardness (BHN)	T.S. psi	Y.S. psi	Elong. %
1	Austenitic 12% Mn steel, Regular heat treatment	175	119,000	55,000	38
2	Austenitic 12% Mn, 2% Mo steel Dispersion hardened	212	130,000	70,000	31
3	Tempered martensitic, low alloy, 0.3% C steel	475	230,000	195,000	10
4	Pearlitic, low alloy, 0.8% C steel (Norm & temp)	395	203,000	122,000	3.5
5	Tempered martensitic, low alloy, 0.8% C steel	475	225,000	-	1.5
6	"Martensitic" Ni-Cr white iron (Temp 500 F)	652	50,000	-	0.0044
7	Pearlitic 1.5% chromium white iron	495	46,000	-	0.0000

Notes:

Items 1 and 2 were cut from 2" thick keel blocks. Item 1 was water quenched from 1900 F. Item 2 was partially pearlitized by soaking 12 hr. at 1100 F then re-austenitized at 1800 F and water quenched.

Data on items 6 and 7 are from Flinn and Chapin[16]. The "martensitic" white iron in item 6 had a matrix consisting of about 70% austenite plus 30% martensite.

The properties listed for austenitic manganese steel (item 1 in table 18) provide a good indication of why this material has become so popular for applications requiring a high degree of toughness. Under high impact or high stress, the material is capable of yielding plastically

to a very considerable degree before breakage occurs. The relatively low yield strength of the material is, however, a drawback in certain applications since it may allow an excessive amount of plastic flow to occur on the part while it is in service. The dispersion hardened 2% molybdenum austenitic manganese steel represented by item 2 may provide a more suitable material under such conditions because of its higher yield strength, which is obtainable with little sacrifice in ductility. In addition, it has already been observed that this dispersion hardened 2% molybdenum manganese steel provides additional wear resistance.

The tempered martensitic low alloy steel, represented by item 3 in table 18 and by the composition range in table 13, has a combination of high yield strength and tensile strength, combined with a reasonable degree of ductility and relatively high hardness. This combination of properties has made this type of steel very useful in certain parts of earthmoving equipment. Its field of application is being explored for a number of other wearing parts. In certain instances it has been found advantageous and worthwhile to redesign a wearing part, such as a dipper tooth, to take advantage of this high yield strength. It should be mentioned, however, that in other cases, this high yield strength may prove to be a liability, since it permits the retention of high residual stresses developed during liquid quenching of the casting, which might cause it to break in service. This applies particularly to large cylindrical type castings where the high residual stresses may be largely of a triaxial nature, which could cause sudden and apparently brittle failure from breakage even though the ductility of the steel on a conventional tensile test is relatively good.

The pearlitic, low alloy, high carbon steel (item 4) shows good strength values, but relatively low ductility on a tensile test. For this reason, it has not been able to compete with austenitic manganese steel in high impact service, but it is still much tougher than the white irons listed below it in table 18. Also, because of the fact that this pearlitic steel is normally hardened by a relatively mild air quench, it is not as likely to contain high residual stresses in heavy section castings as item 3 in this list. Consequently, even though this pearlitic, low alloy steel appears to have relatively low ductility, it may actually be less prone to breakage in certain heavy section castings than the more ductile material represented by item 3.

The tempered martensitic, low alloy, high carbon steel (item 5 in table 18) is similar to composition A in table 12. It is interesting to compare this material to item 3 in table 18, which has about the same strength and hardness but much better ductility. However, because of the higher carbon content of item 5, it will normally have better wear resistance, so would be a preferred material in applications where relatively little toughness or ductility is required.

While white irons have generally been considered as having practically no ductility and relatively low toughness, it is interesting

Table 19

Typical Transverse Strength and Toughness
of Some Cast Abrasion Resistant Alloys*

Item No.	Material	Hardness BHN	Transverse Strength Lb.	Deflection In.	Relative** Toughness
1	Tempered martensitic, low alloy, 0.8% C steel (air quenched and tempered)	363	9600	0.410	3940
2	Pearlitic, low alloy, 0.8% C steel (Norm & temp)	395	9000	0.350	3150
3	High chromium white iron	555	4800	0.200	960
4	"Martensitic" Ni-Cr white iron	578	2100	0.115	242
5	Pearlitic 1.5% chromium white iron	534	1600	0.085	136

* Transverse tests were run by loading 1.2" diameter sand cast bars midway between 18" centers.

** Relative toughness as listed here is the product of transverse breaking strength times deflection.

Notes:

The steels (items 1 and 2) were heat treated to the indicated hardnesses.

The white irons (items 3, 4 and 5) were shaken out of their sand molds at about 1800 F, air cooled to room temperature, then stress relieved at 450 F.

The "martensitic" white irons (items 3 and 4) contained a greater proportion of austenite than martensite in their matrix. The carbides in the white irons represented by items 4 and 5 were of the Fe_3C type.

to compare the properties listed for items 6 and 7 in table 18. Even the very low elongation value for the martensitic white iron (item 6) is sufficient to provide it with substantially greater toughness than the pearlitic white iron (item 7) in many wearing parts. This has been repeatedly observed in service tests and is also indicated in the comparison of transverse test properties, as listed in table 19. It is also interesting to note that even though the ductility and apparent toughness of this martensitic white iron is far below that of the materials above it in table 18, nevertheless this martensitic white iron is successfully competing with many of these materials listed above it in various applications where moderate degrees of impact are involved. Possibly a contributing factor to this apparent toughness of the martensitic white iron is the fact that precautions are taken to avoid high residual stresses in castings made of this material, by slow cooling them after casting. This treatment is usually supplemented with a stress relieving treatment at 500 F. It should also be appreciated that these castings are generally more austenitic than martensitic, which may be a factor contributing to their relative toughness.

Table 19 lists some typical transverse strength and relative toughness properties of two high carbn types of low alloy steel and three types of white iron. Normally this transverse test is used only for measuring the strength and toughness of gray and white irons. Here the values given for the two steels again confirm the fact that even the more brittle types of steel tend to be tougher than the toughest types of white iron. For example, the relative toughness value of 960 for the high chromium type of white iron (item 3) is outstanding for a white iron material. Nevertheless, it is still substantially lower than the values obtained for the two steel compositions.

In comparing items 4 and 5 in table 19, it is again apparent that the martensitic nickel-chromium white iron is substantially tougher than the pearlitic type of white iron. This martensitic nickel-chromium white iron is not, however, normally as tough as the high chromium white irons. This is confirmed by a comparison of items 3 and 4. The high toughness of these high chromium white irons is believed to be due to their more favorable distribution of primary carbides in their structure.

Summary

The three main types of abrasive wear, namely, goughing, high stress grinding and low stress erosion, are briefly described and discussed.

Typical rates of wear are given for a number of wearing parts used in the three types of abrasive service. These rates on some commonly used ferrous alloys range from a maximum of about 1000 mils (thousandths of an inch) per hour down to 0.005 mils per hour.

In the mining and concentration of low grade siliceous ores, a total of about 1 to 3 pounds of wearing parts is consumed per ton of ore handled. A typical distribution of this wear is given in table 2.

The influence of the hardness of the abrasive mineral on wear rates of various materials is illustrated and discussed.

Comparative wear rates of some commonly used materials in each type of abrasion are compiled and discussed.

The types and composition ranges of commonly used abrasion resistant ferrous alloys are given and discussed briefly.

Comparative mechanical properties and relative toughness of some abrasion resistant ferrous alloys are listed and discussed. Consideration is given to the influence of residual stresses in conjunction with these mechanical properties, particularly when large wearing parts are involved.

Acknowledgment

The author is grateful to the Management of Climax Molybdenum Company for permission to prepare and publish this paper. The cooperation and assistance of the Mine and Mill Departments at Climax, Colorado, and the Research Laboratory at Detroit is gratefully acknowledged.

REFERENCES

1. H. S. Avery: Surface Protection Against Wear and Corrosion. 1954. Chapter 3. American Society for Metals, Cleveland, Ohio.

2. T. E. Norman and C. M. Loeb, Jr.: Wear Tests on Grinding Balls. T. P. 2319, Metals Technology and Transactions AIME, Vol 176, 1948, p. 490-520.

3. A. L. Wesner, M. Pobereskin and J. E. Campbell: A Study of Grinding-Ball Wear Employing a Radioactive-Tracer Technique. Presented at the Annual Meeting of the AIME, February 1958.

4. O. W. Ellis: Wear Tests on Ferrous Alloys. Transactions, American Society for Metals, Vol 30, 1942, p. 249-286.

5. R. D. Haworth, Jr.: The Abrasion Resistance of Metals. Transactions American Society for Metals, Vol 41, 1949, p. 819-869.

6. W. A. Stauffer: Wear of Metals by Sand Erosion. Metal Progress, January 1956, p. 102-107.

7. M. M. Tenenbaum: Laboratory Evaluation of the Wear Resistance of Steels on Abrasion with Sand Paper. Vestnik Machinostroyeniya, Vol 36, 1956, no. 8, p. 24-30.

8. J. N. Carter and D. N. Rosenblatt: U. S. Patent 2,751, 291, June 19, 1956.

9. Alloy Steels Pay Off. December 1953, Case Histories No. 40 and 42. Climax Molybdenum Company, New York, N. Y.

10. O. W. Ellis: Wear Tests on Ferrous Alloys. Transactions, Institute of British Foundarymen, June 1937.

11. T. K. Prentice: Ball Wear in Cylindrical Mills. Journal, Chemical, Metallurgical and Mining Society of South Africa, Jan.-Feb. 1943.

12. D. E. Norquist and J. E. Moeller: Relative Wear Rates of Various Diameter Grinding Balls in Production Mills. Mining Engineering, 1950, Vol 187, p. 712-714.

13. T. E. Norman: Factors Influencing the Resistance of Steel Castings to High Stress Abrasion. Paper 58-9, Presented at the Annaul Meeting of the American Foundarymen's Society, May 1958.

14. T. E. Norman: How to Select Chrome-Moly Steels for Ball and Rod Mill Liners. Engineering and Mining Journal, July 1957, p. 102-106.

15. H. S. Avery and H. J. Chapin: Austenitic Manganese Steel Welding Electrodes. The Welding Journal, May 1954.

16. R. A. Flinn and H. J. Chapin: Ductility and Elasticity of White and Gray Irons. Transactions, American Foundarymen's Association, Vol 54, 1946, p. 141-153.

WEAR RESISTANCE

Howard S. Avery
Research Metallurgist
American Brake Shoe Company

WEAR RESISTANCE

by

Howard S. Avery

INTRODUCTION

Engineers are concerned with wear because of the economic loss that it causes. They encounter many practical problems where design and material selection must be concerned with wear resistance as well as the functional aspects of an engineering part. These may lead to difficult compromises.

The problems that are concerned with the effect of stress on metals that make intimate contact with each other or are subject to chemical attack from corrosive media are covered by other sessions of this symposium. The following discussion will emphasize the area where the stress is applied thru hard particles or by impact. Consideration will also be given to the effects of temperature.

Wear is defined as deterioration due to use. This could include such mechanisms as structural damage (fatigue) from repeated stressing, stretching out of shape from overloads, or intergranular corrosion. For simplification the present coverage will be limited to surface wear and will also omit corrosion except where it is a necessary complication.

Hardness and wear resistance are so frequently associated that the usual approach to metallic wear is to make the metal harder. This may involve selection of an alloy that contains hard constituents, such as white cast iron. It frequently involves heat treatment to confer hardness, as in tool steels. These parts are usually rolled shapes, forgings, or castings.

However, a treatment that changes the surface by adding elements such as carbon, nitrogen, chromium, etc. by diffusion, whether these are later hardened or not, is pertinent. Overlays of all kinds, where they can increase wear resistance, are of particular interest. These include the techniques of plating, metal spraying, and weld deposition.

Surface protection is not confined to metallic materials, either for base or for overlay. However, since the nonmetallic field is well covered by texts on paints and the like, or by "Engineering Laminates" (1)*, which deals with composite structures, this paper will be confined to metallurgical materials.

---

* The figures appearing in parentheses pertain to the references appended to this chapter.

(1) The author, Howard S. Avery, is research metallurgist, American Brake Shoe Co., Mahwah, N. J.

THE ENGINEERING APPROACH

The field of wear is so complex that it seldom yields a pattern than can be reduced to a simple formula. Nevertheless, it can be dealt with by engineering methods that are too frequently neglected. Important aspects are careful analysis of the conditions that cause wear, tests, and critical evaluation of test data together with the comparisons that are involved. Statistical mathematics can do much to remove the guess work from test data evaluation.

For surface protection the properties of the exposed face are of primary importance. These may be the same or they may contrast sharply with the base metal or body properties. It should be recognized that such engineering values as tensile strength, ductility and the like may have little or no value for predicting surface behavior, especially for thin hard layers.

In normal use most surface areas are subjected to compressive stress under wearing conditions. Thus, compressive strength is likely to be pertinent, and, since hardness tests are usually compressive, hardness is almost universally employed as a significant index of merit. However, hardness may tell a misleading story. Careful engineering, therefore, requires that hardness be considered an unvalidated wear test until it is proven otherwise.

Wear is not a simple phenomenon, which accounts for many unsatisfactory features of wear tests. It is generally accepted[2]* that a universal wear test is not feasible, which means that tests must be rather specific and simulate service conditions as nearly as possible. However, if the simulation is only superficial, the test may have little value. Conversely, if in the wear test the dominant factors in service are present in about the right proportions, the superficial mechanics of the test might differ much from the service picture and yet provide a good basis for predicting behavior.

Criteria of Good Wear Tests

These and other limitations establish the need for a careful procedure in using wear tests. Each test, as far as possible, should meet three requirements:

1. It should have proven reliability or reproducibility. This should be reported in quantitative terms, and be used in judging how far the test evidence should be trusted in making comparisons.
2. It should have a proven ability to rank various materials that are receiving engineering consideration. If the range of values obtained on a variety of materials is too small, even if reproducibility is good, it will be difficult to predict service behavior.

3. It should be validated by correlation with service tests. Only when all three of these conditions are met does a laboratory test become a valuable tool for selecting and judging materials with assurance.

Validation is the most difficult, and usually the most unsatisfactory of these three requirements, since to establish confidence the service test should satisfy the first two criteria. Unfortunately many service tests are unreliable because variations in the conditions destroy their reproducibility. Along with this, few service tests include enough replication to permit calculation of the reliability and the expected experimental error.

Statistical Evaluation

In handling the data for these three stages accepted statistical procedures should be used. Averages, ranges, standard deviations, sample sizes, reliability and correlation coefficients should be reported. Confidence limits or tests for the significance of the differences between averages should be included to permit judging the part that chance can play in the results.

It will be apparent that many engineering procedures other than wear tests will not completely pass the requirements above. To the extent that they do not, guess work is being substituted for engineering. The size of "safety factors" used in engineering design is frequently a measure of the discrepancy between these two extremes.

Wear resistance is represented by fewer standardized tests than other engineering properties, and it is not surprising that good data for comparisons are meager. This imposes a need for good judgment on the engineer, mechanic or technician who selects materials to withstand wear. Success may depend on how well shrewd deductions and close observation are substituted for guess work in bridging the gap between data available and life expectancy in service.

In general, great caution should be applied to conclusions based on one test, unless it is one of a series that already has a reliability pattern established. The average of two is better, but the 95% confidence interval ($\pm$ the mean) is 6.4 x the range between the two values, and this is subject to the vagaries of a single sample of two values. Three tests are a desirable minimum, since the 95% confidence interval is 1.3 x the range of the three. These convidence intervals (meaning that the probable true central value, would be within this range 95% of the time) apply to the average of many cases, and when applied to a single set of figures should be used more for proving uncertainty than for assurance. On the other hand, the average range of a number of replicated samples provides a good estimate of the appropriate standard deviation.[3,4]

Of course, more than three tests to represent a single material under one test condition would be desirable and would lend greater assurance to the results. However, even a group of three is such a rarity in field and service testing that discussion of greater numbers is likely to become academic.

When the range or confidence intervals representing two materials being compared overlap, it is obvious that the apparent superiority of one (assuming the average values differ) may be due to chance. Just how large the chance probability is can be computed. Details of this are out of place here, butthis should be examined where the penalties of mistakes are expensive. (Calculations of this type are not yet included in all engineering curricula, and the engineer may have to educate himself from the literature.)

Even with wide scatter band ranges, if the gulf between two averages is wide the apparent superiority is likely to be valid qualitatively. This pattern is subconsciously used in many judgments. It is in the area of modest superiority that good data are needed to provide valid conclusions. Since even a few percent average improvement may give attractive economic savings in some areas of severe wear, it may be worth while to make the effort needed to statistically prove the ranking of wear resistant materials.

It is noteworthy that estimates of experimental error are not necessarily based on replicate specimens tested under identical conditions. Statistically planned experiments may use the variance from the interaction of major factors, where this is not otherwise significant, as an estimate of error. A simple way of using this principle is the drafting of a scatter band about the central line correlating a series of points on a graph, even if no replicates are present. Plots of hardness or strength versus temperature, and stress versus creep rate or rupture time are examples where replication is unusual. However, the habit of the central tendency line must be known from experience or else be established by enough different test materials in a test program.

Economy of effort frequently dictates the use of this procedure, but the disadvantages of insufficient data are not thereby eliminated.

Properties Pertinent to Surface Protection

The properties that should be examined when selecting wear resistant metals include:

1. Hardness
   (a) Gross or macroscopic hardness.
   (b) Micro hardness -- or the hardness of individual constituents of a heterogeneous structure.
   (c) The influence of temperature on hardness.
   (d) The effect of time at temperature on apparent hardness (creep).

2. Abrasion Resistance
   (a) Under low stress conditions.
   (b) Under high stress conditions.
   (c) Under gouging conditions.
   (d) The effect of different abrasives.
3. Impact Resistance
   (a) Resistance to flow under repeated impact. (This is related to yield strength.)
   (b) Resistance to cracking under impact. (This is related to both strength and ductility.)
   (c) Compressive strength.
   (d) Compressive ductility.
4. Heat Resistance
   (a) Resistance to tempering.
   (b) Retention of strength when hot. (This includes hot hardness.)
   (c) Creep resistance (time factor added to (b)).
   (d) Oxidation or hot gas corrosion resistance.
   (e) Resistance to thermal fatigue.
5. Corrosion Resistance
   This is such a broad and specialized field that details will not be included here, and other references should be sought.
6. Frictional Properties and welding tendencies
   (a) Friction coefficients.
   (b) Galling tendency.
   (c) Surface films.
   (d) Lubricity.
   (e) Plasticity.

Data on some of these properties will be detailed herein. For others only qualitative information is available and for some the status is very unsatisfactory from an engineering viewpoint.

Some less defensible criteria have been used to judge wear resistance. An example is the pattern of hard facing alloys that appears in some Handbooks. A group is listed as high alloy types, with the implication that merit (in terms of wear resistance) increases with total alloy content. This concept has also been carried in manufacturers' sales literature. Experimental data disprove the validity of this generalization, Figure 1. Alloying elements, of course, do contribute to performance, but the effects are more specific and individual and require proper metallurgical formulation and control to exploit their usefulness. It is naive to expect that a simple total could provide a valid index of merit under the many different conditions that occur in service.

An example of the importance of service conditions can also be drawn from Figure 1. The cobalt-base alloy that is the worst of the group for the high stress abrasion is outstanding for hot wear. It is a premium material for surfacing exhaust valves in automotive and aircraft service, and moreover it is machinable despite its high hardness. The claims of excellent all around abrasion resistance sometimes made for it are obviously misleading, but they should not reflect on its performance under other conditions.

These comments should serve as a warning that efficient and economical protection against wear requires an adequate knowledge of materials that is based on acceptable data. This should be coupled with a careful and critical analysis of the conditions that are causing wear.

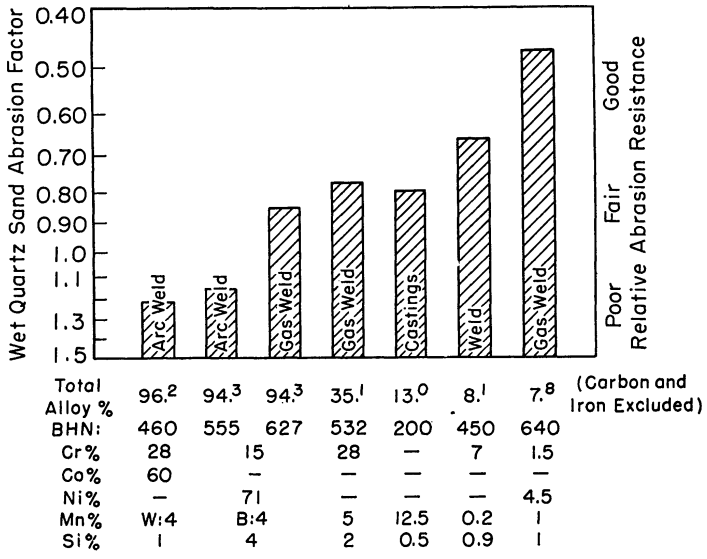

Figure 1. Relative abrasion resistance versus total alloy content. Illustrating the fallacy of assuming that alloy content regardless of structure is a reliable criterion for judging abrasion resistance.

SELECTION OF MATERIALS OR TECHNIQUES

Careful selection of special materials is likely to pay gratifying dividends if wear conditions are severe. The range of materials should include homogeneous alloys, "hard-case plus tough core" combinations and special treatments. The choices may include:

1. Depending upon complete replacement of worn out parts, with allowance for replacement time and cost.
2. Overall heat treatment to obtain higher hardness of a part made throughout of a hardenable steel.
3. Surface heat treatment to obtain higher surface hardness of a part made throughout of hardenable steel.
4. Making the wearing part of premium materials throughout. Tungsten carbide, high chromium irons, martensitic irons, tool steels, heat resistant alloys and austenitic steels are among the materials that are frequently selected if the usual engineering steels lack adequate wear resistance.
5. Case hardening by a treatment to introduce carbon or nitrogen or both into the surface to create a high surface hardness.
6. Hardening by diffusing into the surface an adequate quantity of silicon, chromium, molybdenum, or tungsten to create a hard surface layer.
7. Applying a relatively thin protective layer by electrodeposition of a hard metal or alloy.
8. Applying a relatively thin layer by hot dip treatment in a molten metal.
9. Developing of a relatively thin surface protective layer electrolytic or chemical treatment.
10. Developing a hard surface layer by cold working as by shot peening or hammering.
11. Applying a relatively thick layer of a wear resistant metal by metallizing (metal spraying).
12. Metallizing as above followed by fusion of the applied layer.
13. Welding on a relatively thick layer of a protective alloy. This can provide the properties of any of the alloys under item 4 above, with the advantage of a tough back-up material.

The depth of protection provided by these choices differs considerably, and may influence the choice. Table 1 will provide guidance.

TABLE 1

Depth of Surface Protection Provided by Various Techniques

Method and Material	Depth in Inches Min.	Average Inch	Max.	Surface Hardness Rockwell	BHN or VPN	Speed
Electroplating						
Chromium	0.0001	0.005	0.025		1000	
Nickel	0.001	0.005	0.100		140/425	
Rhodium	0.000001	0.0001	0.001		600	
Anodizing						
Aluminum	0.0001	0.002	0.005			
Magnesium	0.0004	0.0006	0.0015			
Zinc	0.0001		0.0002			
Chromizing						
Low-carbon Steel	0.0005	0.0015	0.0060			5 hrs. at 1750 °F to form 0.0015 in. chromized coating.
High-carbon Steel	0.0002	0.0008	0.0030			
Diffusion						
Carburizing	0.010	0.030	0.100	C55–65		4 hrs. at 1700 °F—0.050 in.
Carbonitriding	0.003	0.010	0.030	C50–65		2 hrs. at 1550 °F—0.015 in.
Cyanidizing	0.00025	0.005	0.010	C50–65		¾ hr. at 1500 °F—0.005 in.
Nitriding	0.0005	0.015	0.030	C70		30 hrs.—0.015 in., using two-stage process.
Chromium Silicon	0.005		0.100			4 hrs. at 1975 °F—0.002 in. 2 hrs. at 1850 °F—0.030 in.
Metal Spraying ("Metalizing") non-fused-coatings						
Carbon steels	Limited only by			C25–40		
Stainless and Cr steels	economic factors			C35–40		
Bronzes		0.050		B78–B30		
Babbitts	(0.0010)					20–30 lbs. per hour
Molybdenum		0.002	(0.075)	C40		
Misc. fused coatings		(0.045)				
Ni-Cr-B alloys			0.060	C60		
Hard Facing						
Tungsten Carbide	1/32	1/8	3/8	C50 to 2500		
Hi-Chromium Irons	1/32	1/8	3/8	C56		
Martensitic Irons	1/32	1/8	5/16	C50–68		From one lb. per hour to 40 lbs. per hour
Cobalt Base Alloys	1/32	1/8	1/2	C40–65		
Nickel Base Alloys	1/32	1/8	3/8	C17–65		
Copper Base Alloys	1/8	3/8	no limit		100–380	
Martensitic Steels	1/16	1/4	4	C40–65	500–700	
Pearlitic Steels	1/8	3/8	4		to 400	
Austenitic Steels	1/8	5/16	4		100–200	
Chill Casting						
White Cast Iron	1/8	1	2		450	
Flame Hardening	0.10	0.150	0.250		350–650	
Induction Hardening	0.010	0.10	thru out		350–650	

TABLE 2

Wear Classification

BASIC FACTORS	MECHANICAL				THERMAL	CHEMICAL
Nominal Cause of Wear	Impact	Friction	Abrasion	Vibration	Heat	Corrosion
Varieties of Wear Illustrating the Interaction of various basic factors	Battering Stress Deformation Rupture Stress Deformation Brittleness Cavitation Stress (corrosion)	Smoothing Stress Shear Seizing Stress Deformation Welding Galling Stress Deformation Welding Shear	Erosion Velocity Impact Stress Shear Scratching Low Stress Shear Grinding High Stress Shear Deformation Gouging High Stress Shear (Impact) Deformation	Fatigue Stress reversals Time (deformation) Cracking Reduced area Corrosion Fatigue Stress Time Corrosion Concentration Stress Cracking	Creep Stress Softening Time Deformation Reduced area Scaling Oxidation Corrosion Time Reduced area Crazing Expansion Stress Deformation Stress Reversal Reversed deformation Time Cracking Fatigue Growth Graphitization Phase changes Oxidation Transformations Expansion and Contraction induced Stresses Development of weak or brittle phases	Solution Heat Time Chemical action Erosion Solution Velocity Stress Intergranular Time Chemical action Electrolytic action (Heat) Dissimilar Phases Scaling Heat Time Chemical action Diffusion Galvanic Electrolytic action Dissimilar phases Pitting Electrolytic action Dissimilar media

Wear is defined as unintentional deterioration due to use or environment. It is usually a surface phenomenon.

Wear Analysis[5]*

At this point an analysis of the factors that cause wear is advisable. The basic causes are mechanical, thermal, or chemical, but they usually operate in combination. They take enough different forms to make wear analysis rather complex. Table 2 shows some of the relationships involved and how they may combine. Since we are concerned with surface protection those mechanisms like creep and internal oxidation (growth) that cause general deterioration in use will be neglected.

Of the many possible wear factors that may occur, certain ones are outstanding. These are impact, heat, corrosion, friction, abrasion and vibration. Four of these involve stress directly and the other two may modify the reactions to stress.

Impact As a Factor In Wear

Impact is merely one way to produce stress, but the mechanical advantage of an impact blow is so great that this frequently causes the most severe stress imposed on a part. Wear from impact, if cracking and major failure is avoided, will appear as battering out of shape or plastic flow that causes a loss of proper dimensions. The first consideration is to avoid cracking, either by good design or by choosing a sufficiently tough material.

Good design will help avoid impact failure by eliminating unnecessary stress concentration areas such as sharp notches, etc., and by providing adequate supporting strength under the hard surface layer if the hard case, tough core idea is adopted.[6] Thin hard surface layers are especially vulnerable to cracking under impact if their base is too soft in relation to the stresses from impact.

Impact blows will not cause cracking if they do not overstress some part of the structure that receives them. If the yield strength in compression at the surface is above the compressive stress produced by impact, and there is adequate support so that subsurface flow does not occur, a long useful life may be expected even if the surface material is brittle. Note, however, that velocity is so important that it alone can overstress the surface, even if the calculated impact energy is low.[6,7] The effect of velocity is shown in Figure 2.

There are many applications where the superior abrasion resistance of brittle alloys can be effectively exploited even when impact is prominent. Cast iron freight car wheels with chilled treads are an example. The tread for a depth of perhaps 2 inches is a brittle white iron that can stand only about 2% plastic deformation in compression

---

* Much of this material has been drawn from American Society for Metals Educational Lectures given by the author in October 1953.[5]

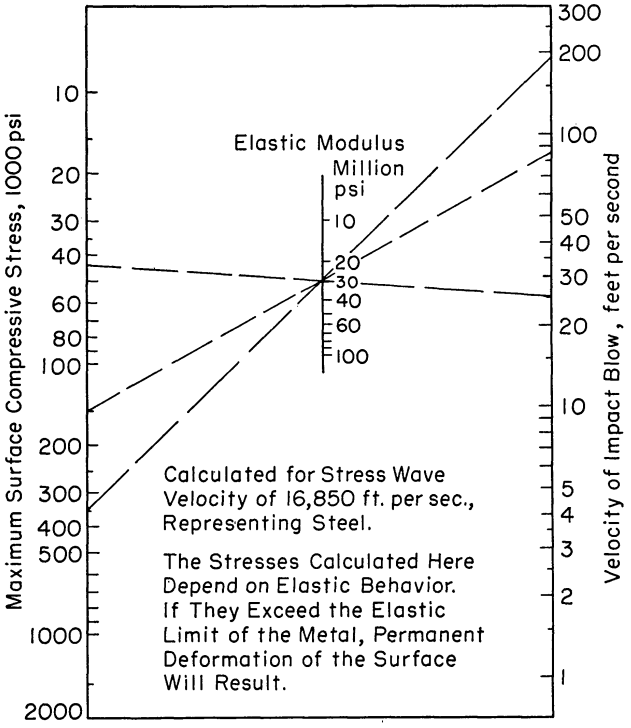

Figure 2. Nomograph relating impact velocity to maximum surface stress.

without failures. The impact blow at the tread surface when a loaded freight car goes over a bumpy railway crossing may range from 1115 to 33,300 ft-lb, yet thousands of such blows are absorbed elastically and returned as rebound month after month in normal freight car operation. Tread failures from impact are rare.(6)

Among the iron-base alloys, pearlitic white cast iron, martensitic medium alloy irons, high chromium irons, martensitic steels and austenitic steels should be considered in this order, selecting the one that seems tough enough for the purpose. If the hard irons are appropriate they are unlikely to benefit by special surface protection. The steels, however, have sacrificed abrasion resistance for toughness, and if conditions are severe they may benefit from hard surfacing.

Caution should be used when judging either brittleness or wear resistance from hardness. There are many cases where steels are tougher than cast irons at the same hardness level, and others where carbon content and structure are more important than hardness in controlling wear. Specific details will appear later.

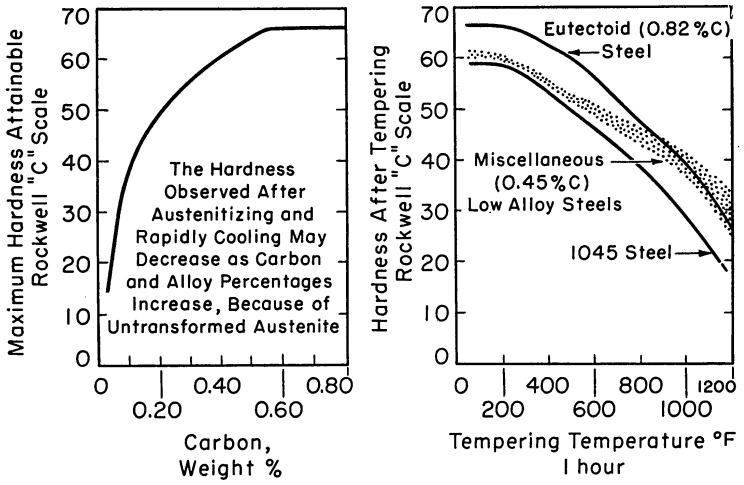

Figure 3. Effect of tempering as well as effect of carbon content in steels as factors in wear.

Heat As a Factor In Wear

Heat influences wear resistance in several ways. It may temper hardened structures, it may temporarily soften stable structures, it may cause phase changes that increase hardness and brittleness, and it accelerates chemical attack, such as oxidation and scaling. The heat may be an obvious part of the service environment or it may be an unnoticed effect of friction at the wearing face. The superficial temperatures produced by friction can be surprisingly high.

The effects of tempering as well as carbon content in steels are indicated in Figure 3. Handbooks will supply additional details if they are needed. The softening effect, independent of tempering, is portrayed by Figure 4, and the additional effect of time by Figure 5. Hardness versus temperature curves for various alloys are available.

Where protective coatings are not used, resistance against progressive oxidation and scaling is usually provided by chromium. Its potent effect appears in Figure 6, where 25% chromium is seen to provide effective resistance to progressive oxidation up to 1800 or 2000°F. Nickel has a similar effect up to a certain point if substituted for chromium in a 3:1 ratio.[8] It is only justified economically where carburizing resistance (to avoid embrittlement) or special high temperature properties are needed.

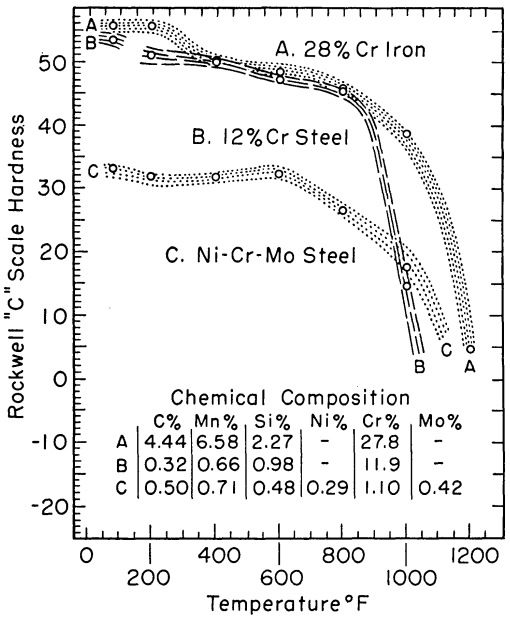

Figure 4. Effect of temperature on apparent hot hardness.

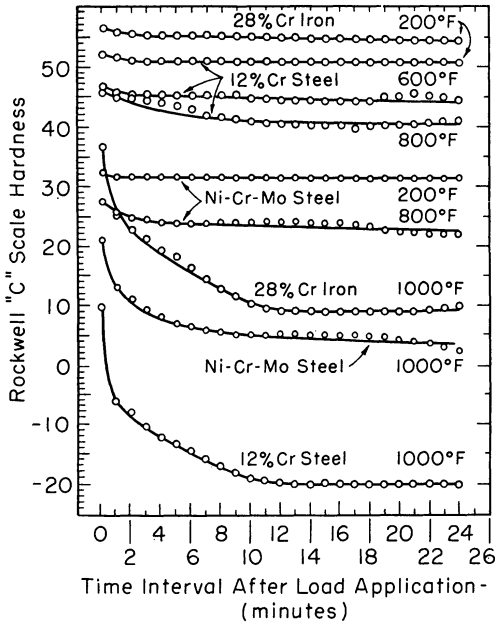

Figure 5. Effect of time on apparent hot hardness of three iron-base alloys, showing creep phenomena at the higher temperatures.

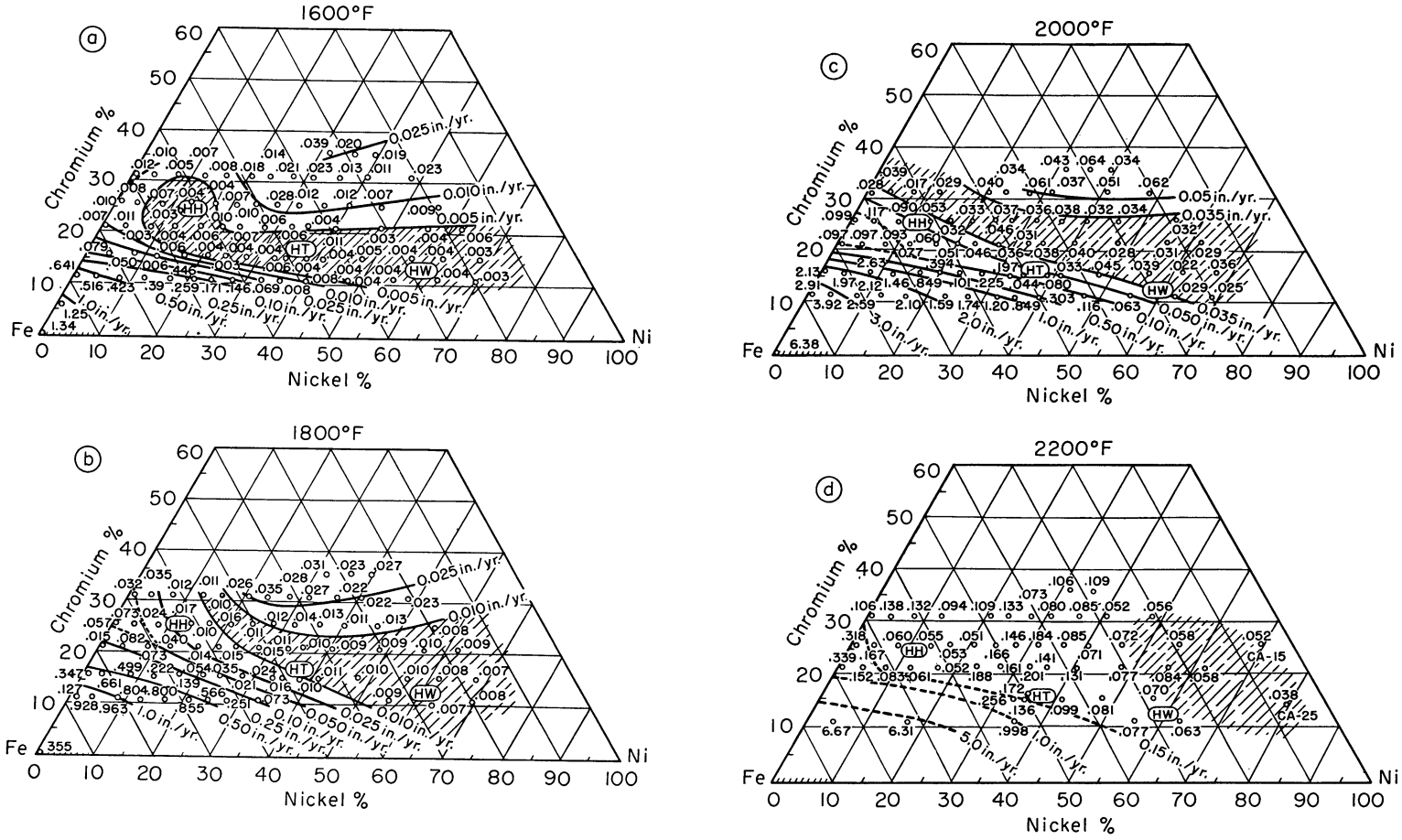

Figure 6. Effect of chromium and nickel on oxidation resistance from Alloy Casting Institute Research.(8) Metal loss in air atmosphere at temperatures shown with corrosion expressed in inches of penetration per year. Alloys contained 0.4% carbon, 1.25% silicon, 0.75% manganese, balance iron. Data based on 100-hour tests.

Corrosion As a Factor In Wear

Chemical corrosion can occur alone or it may complicate mechanical and abrasive wear. The same units can be used to measure each of these and also their total effect. Corrosion resistance is a complex matter, and since it is the subject of the second section of this book, will not be covered in detail here.

Friction As a Factor In Wear

Since much of this symposium is devoted to this area, the comments here are brief. They are based on the ideas that friction stems from the seizing or welding of mating surfaces and that preventive measures that depend on separation of the surfaces, like lubrication, have a least partially failed. A desirable property of a friction face is believed to be high elastic compressive strength. A soft, low yield strength metal is more easily pressed into the intimate contact that leads to welding.

Some advantage is obtained by using dissimilar metals for contact, but this is believed to be secondary to the important requirements of high strength and separation of the contact faces. Those metals that have relatively low yield strengths, such as the austenitic stainless steels or low carbon irons, are especially likely to gall when surfaces are forced into close contact by heavy pressure.

Where low or medium carbon steels have adequate overall strength for the service to which a part is to be put, but must have wear resistance at some surface areas, some form of surface hardening is desirable. The particular form of surface treatment to be adopted depends upon the nature of the part, the nature of the service, and the situation involved.

Lubrication is the most common means of keeping metal faces apart, but oxide or other films may be quite effective when lubrication is imperfect or impracticable. Graphite and molybdenum sulphide are solids that can replace or supplement liquid lubricants, while aluminum oxide can effectively prevent welding. Aluminum bronze, for example, is excellent for surfacing where metal to metal wear is a problem. It develops an aluminum oxide film readily. The potency of this film in preventing welding appears when joining by oxyacetylene welding is attempted. This operation is so difficult that most aluminum bronze welding is done with heavily flux coated electrodes. Aluminum bronze alloys that can be used for wear resistant parts and for welded overlays are covered by AWS-ASTM Specification Designation B-225-48T. It should be noted that the abrasion resistance of aluminum bronzes, when measured by the two devices described herein, is very poor. Their wear resistance probably depends on maintaining the surface oxide films intact, whereas abrasion removes them readily.

Vibration and Fatigue

Vibration or other conditions that cause cyclic stresses may lead to fatigue failure.[9,10] Because this is a form of deterioration due to use it may be included in a discussion of wear. Correct design is considered the most important preventive of fatigue damage, but benefit is also obtained from materials. Design seeks to eliminate stress concentrations such as appear at notches, sharp angles, and the like.[6] Raising the strength of a material can also increase life expectancy under fatigue stresses if other adverse factors are minimized. The fact that harder materials tend to contain higher residual stresses, operates to set a limit on the strength that can be used.[9,12]

Surface conditions are important where fatigue can occur. Processing should be controlled to leave a smooth, unnotched surface and also to avoid any weakening effect. If decarburization should occur in heat treatment, for example, the resulting softer, weaker layer is an invitation to fatigue. Conversely, carburizing can add fatigue resistance, and this may be an important consideration in selecting case hardening.

Other ways of surface hardening, within the limits suggested above, can minimize fatigue damage. Since fatigue is most evident as a tensile failure, residual compressive stress at the surface can effectively combine with the normal strength of the material to provide additional protection. Shot peening, which produces moderate surface hardness while it induces compressive stress, is thus a useful technique.

Abrasive Wear

Abrasive wear, like impact failure, is a result of stress, but the details are so different that separate classification and treatment are justified. Much remains to be clarified, but it is currently helpful to classify abrasion into three types: gouging, grinding, and scratching. These are not sharply defined areas, since they are expected to overlap, but they can be recognized as distinct types and the useful tests for them are significantly different.

Gouging abrasion implies high stresses on a gross scale and is usually associated with impact in service. It is also characterized by anchorage or good support of the cutting agent, much like that for a machine tool cutting bit. It seems closely related to machining with a tool or by an abrasive wheel.

Power shovel digging in rock fragments, Figure 8, and rock crusher operation are considered to involve gouging abrasion. Such service causes prominent grooves or gouges to be cut in the wearing surfaces, especially if these are soft.

Laboratory tests have been devised to evaluate wear from this mechanism. Perhaps the simplest is a grinding wheel test with a brake shoe type specimen. A few results from tests with an alundum

wheel appear in Figure 7. This shows excellent reproducibility and ranking ability. Satisfactory test data to validate this test properly are lacking. Qualitative confirmation of the ranking has appeared but has had small practical application because of the heavy impact that so frequently appears in service. Massive parts of the more wear resistant alloys like the special cast irons are likely to fracture under impact with the result that austenitic manganese steel is the usual choice because of its toughness.

Grinding abrasion is evidenced by the fragmentation of small hard particles between hard faces that are usually of metal. It may also be termed high stress abrasion because the crushing strength of the abrasive (which is about 30,000 psi for ordinary quartz) determines the stress that acts on a microscopic scale even when the nominal loads are low. The broken abrasive grains are sharp and can scratch effectively. Moreover, the concentrated stress on the metallic face can disrupt the metal or fragment some of its micro constituents. Deterioration then occurs from scratching, local plastic flow, and micro cracking.

The presence of high stress abrasion can be deduced from observation of a metal sandwich and the fact that an abrasive is crushed or ground between. Ball milling is an excellent example.[13,14] In machinery such abrasion may be observed where parts rub in a gritty environment.

The laboratory apparatus for producing this kind of abrasion is illustrated in Figure 9 and schematically diagrammed in Figure 10. The wet sand abrasion factors reported herein were obtained with this machine, which was first described by Blake[15] in 1928. A number of refinements and modifications have been made since then. The essential parts of the apparatus are a lap, a trough for abrasive, arms for holding the specimens and applying uniform and measured pressure, a hydraulic classification system for removing fines, and mechanism for dragging the test specimen over the lap, which is a flat circular copper track about 2 inches wide and 4 feet in diameter. The standard abrasive consists of 40 pounds of quartz sand with a grain fineness number near 50, mixed with 30 quarts of water. Test pieces with a wearing face 1-1/2 x 2-1/4 inch are held against the lap under a weight load of 54 psi while being moved at the rate of about 119 feet per minute for a total distance of 1.35 miles. Before each test, the specimen under investigation is worn in against the track until it has completely conformed to the minor irregularities in surface contour. It is then carefully cleaned, dried, and weighed after which the test is begun on two specimens, the second of which is of annealed SAE 1020 steel. Inclusion of this readily duplicated material provides a standard that will indicate any serious departure from the correct testing conditions. The final report of wear is given in terms of weight loss in comparison with the standard, thus reducing the data for many materials to a common denominator. The relative ranking of several interesting engineering alloys and metallographic structures appears in Table 3.

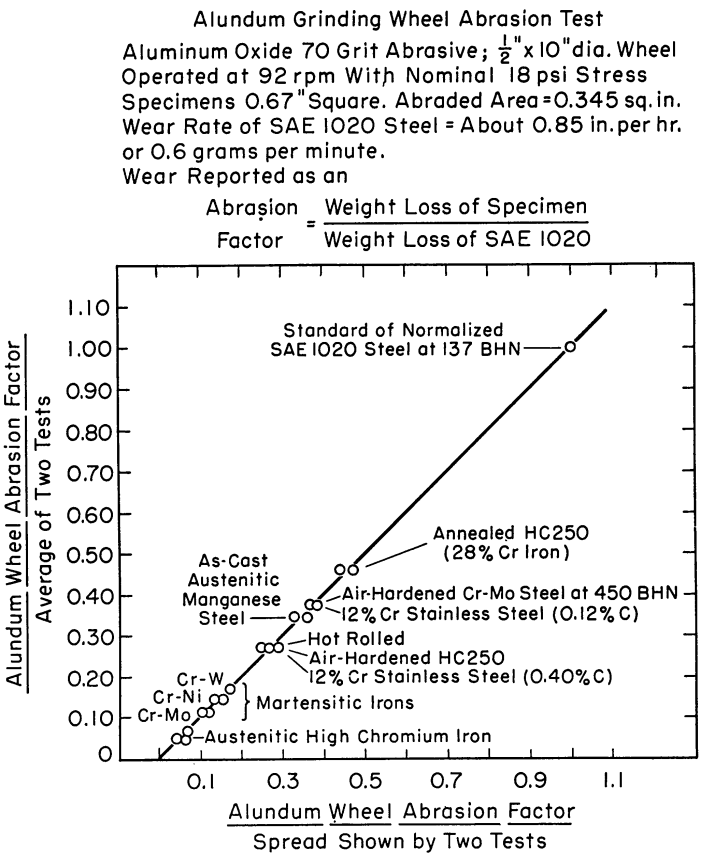

Figure 7. Alundum grinding wheel abrasion test. This test has good reproducibility and ranking ability but the service conditions with which it can be correlated have not been satisfactorily defined.

Figure 8. Power shovel bucket digging in rocks and boulders. The wear situation provides gouging abrasion and considerable impact. Both are associated with high stresses and require tough alloys to withstand them. Austenitic manganese steel is usually the preferred material.

Figure 9. Apparatus for abrasion testing in a gritty environment.

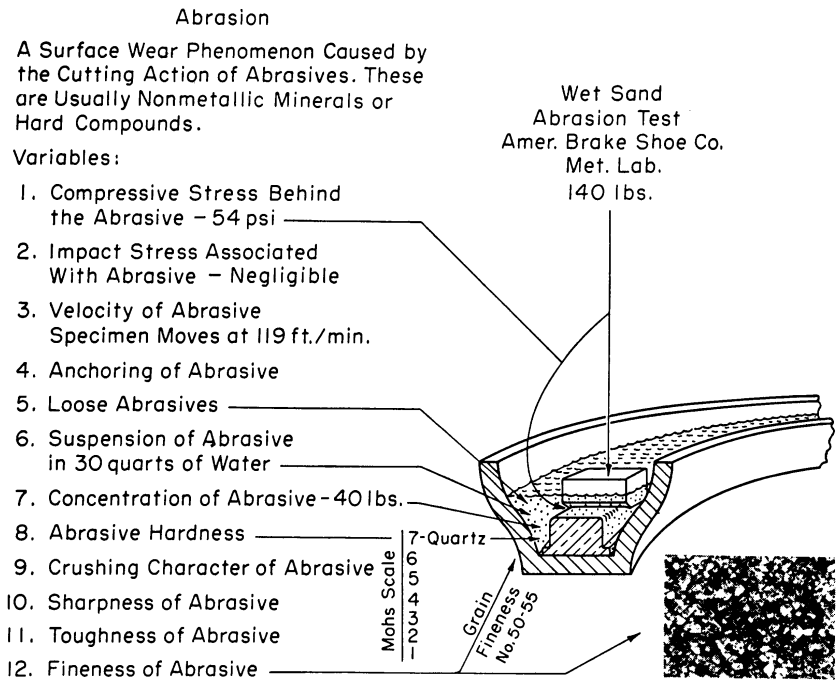

Figure 10. Schematic diagram of apparatus shown in Figure 9.

TABLE 3

Typical Wet Sand Abrasion Factors

Material	Hardness BHN	Abrasion Factor
Ferrite (Armco Ingot Iron)	90	1.40
Grey Cast Irons	200 ±	1.00–1.50
SAE 1020 Steel (standard)	107	1.00
White Cast Irons (pearlitic)	400 ±	0.90–1.00
Alloy White Cast Irons	400–600	0.70–1.00
Pearlite (0.85% C Steel)	220–350	0.75–0.85
Austenite (12% Mn Steel)	200	0.75–0.85
Bainite	512	0.75 ±
Martensite	715	0.60 ±
Martensitic Cast Iron (Ni-Hard)	550–750	0.25–0.60
Cemented Tungsten Carbide		0.17

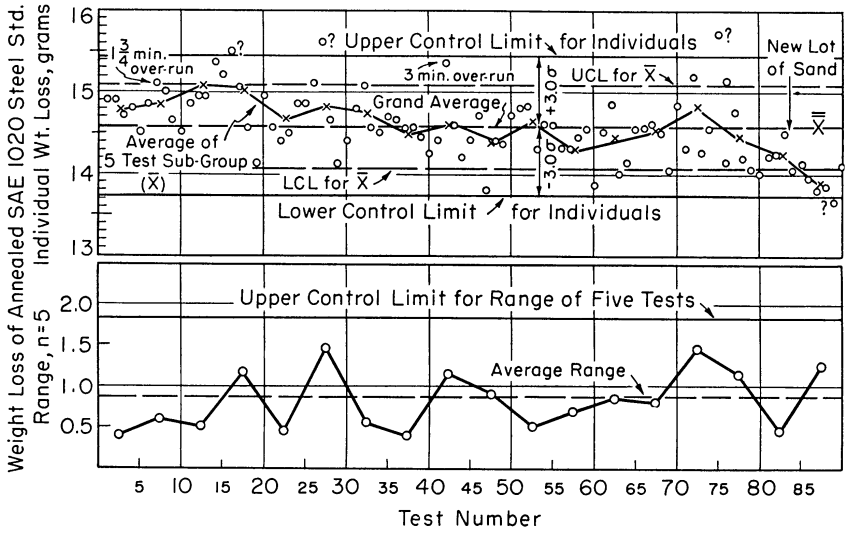

Figure 11. Quality control chart - wet quartz sand grinding abrasion.

With the present standardized procedure, excellent reproducibility is obtained as evidenced by duplicate tests. As calculated by statistical methods(16), the correlation coefficient (Pearson product moment) between duplicate tests is 0.97. The reliability of the average of two such tests would be 0.985; a correlation of unity (1.00), is said to indicate perfect reliability and one of zero (0.00) its complete absence. The standard error (S.E.) of a single determination is 0.028; of the average of two tests, 0.020. Theoretically this implies that a second determination will be within plus or minus this standard error approximately 2/3 of the time, or in other words, 2/3 of such test values should fall with ± 1 S.E., practically all (99 + %) within ± 3 S.E. For those more accustomed to dealing with probable error (P.E.), P.E. = 0.6745 x S.E. These correlations are based on uniform materials. The agreement between duplicate tests on weld deposits is usually poorer because of nonuniformity in the specimens.

A specimen quality control chart on the SAE 1020 standards that are an important part of the test appears in Figure 11. The weight losses are usually within a zone defined by a weight loss of 15 grams ± 1.2 grams (3 sigma limits) but changes of sand, wear of the copper track, and departures from standard specimen and holder geometry tend to throw the standard weight loss out of the 3 sigma control limits.

By reporting the data as an abrasion factor, the effect of such irregularities are minimized since within reasonable limits the abrasive and track variables affect both specimens similarly.

Note that while the test is usually run with water, it can be made dry. The liquid serves to keep temperature from rising and assists

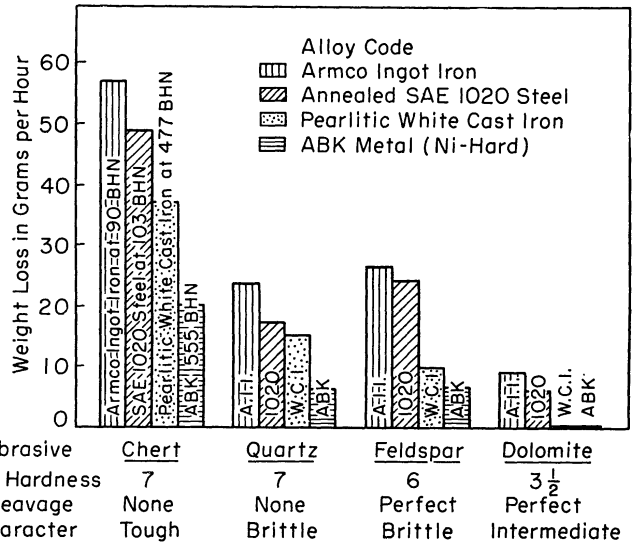

Figure 12. Relative abrasiveness of common mineral abrasives.

mechanically in carrying the abrasive to the wearing face, but it is not the salient feature of the test. The dominant factor is the grinding of the abrasive and the high stresses that result.

The kind and character of the abrasive is quite important. If initially round and smooth, it quickly becomes angular and sharp by fragmentation, so this factor is quickly modified after the test begins. The hardness and toughness of the abrasive are more stable properties and largely determine the weight loss values under standardized conditions. Figure 12 shows the effect of several common abrasives on some metallic materials. Note that quartz sand and chert are identical in composition and hardness, but differ markedly in toughness and abrasiveness.

Particle size of the abrasive affects the weight loss values, as does the nominal applied load. For this reason, they are standardized in routine testing. There is a tendency for weight loss (particularly for hard alloys), to decrease as particle size decreases. In

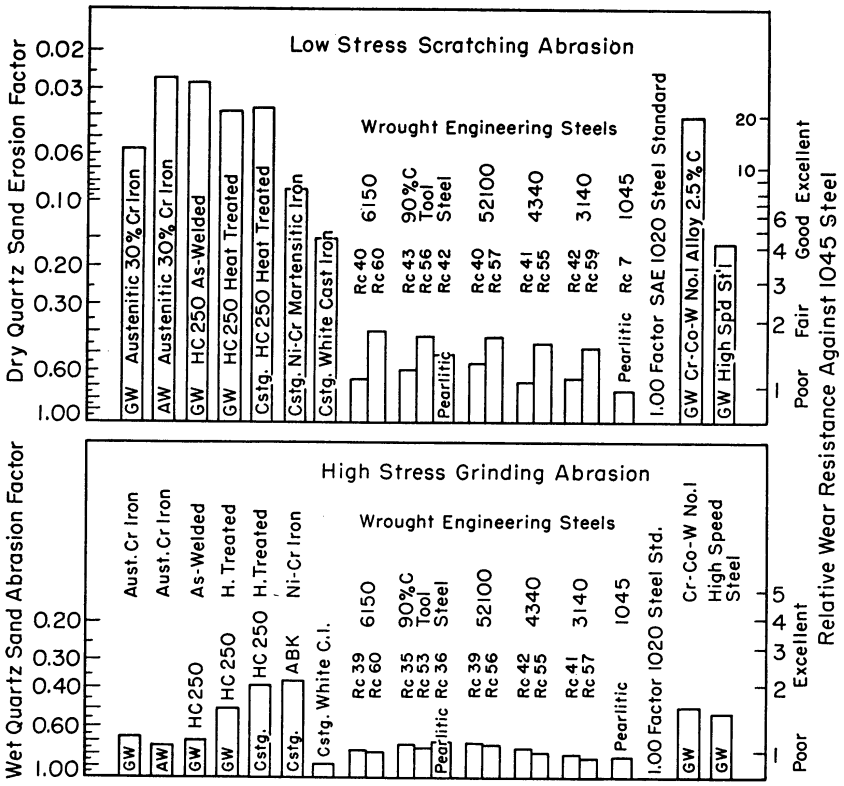

Figure 13. Comparative performance of various engineering alloys under abrasive conditions where the stress applied thru the abrasive differs considerably.

extreme cases, using silica flour for example, the wear behavior is not considered that of grinding abrasion and perhaps is more like the low stress abrasion described later.

The test has been validated by ball mill service, as shown in Figure 14. The materials tested were in the form of balls or specimens cut from balls. Both tests used alloys from the same heats of cast metal. Data from the laboratory test were obtained in a few weeks, while the service data required much longer. Very seldom is as much service data available as in this correlation. Subsequent field experience with ball mill liners established that a 25% improvement in material, as shown by the laboratory test, could be also confirmed in the field when performance records were carefully kept.

Since this discussion is concerned primarily with surface protection, the abrasion factor for a group of pertinent alloys is shown in Figure 13. Other data appear in later sections.

Low stress scratching abrasion, a third type, is usually less severe than the previous two. It will here be termed erosion for simplicity, and ordinarily depends on hard and usually sharp particles for effective wear. However, the chief source of stress is velocity.

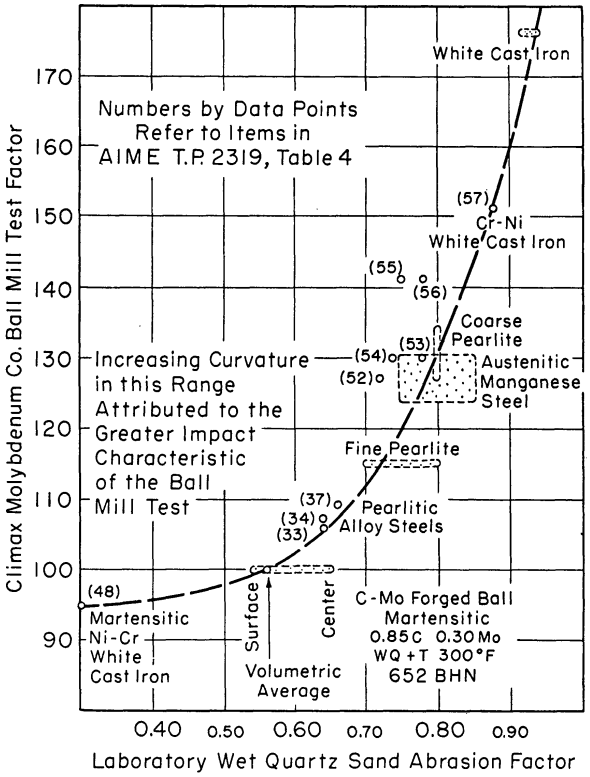

Figure 14. Correlation of ball wear tests and laboratory abrasion tests. The numbers adjacent to data points refer to items in AIME Technical Paper, Table 4.

The most severe form of erosion is generally associated with sharp abrasive particles. Greater abrasive hardness and sharper cutting edges increase its severity while the erosive power of rivers, wind and industrial imitations of these (such as slush or mud carried by a pipe, or a sand blast) increases rapidly with velocity.

The stresses involved with erosive wear are only occasionally great enough to break the abrasive grains. This means that the original smoothness or angularity is important since there is little change with use, particularly in a laboratory test. This contrasts with the fracturing that occurs in the high stress abrasion test described above.

Liquid abrasive slurries or airborne "dust cloud" streams have been used to simulate service erosion, but perhaps the best current test technique employs a rubber wheel to carry the abrasive against the wearing face.[17] The rubber performs the important function of yielding and cushioning the abrasive so the stress applied is held to a low level. One such device is illustrated in Figures 15 and 17. In practice, after dressing the wheel smooth, a conditioning run is followed by a multi-layer sandwich that brackets test runs on a specimen under investigation between runs on a standard material. Two wheels are used to speed operations, but they are used for independent tests.

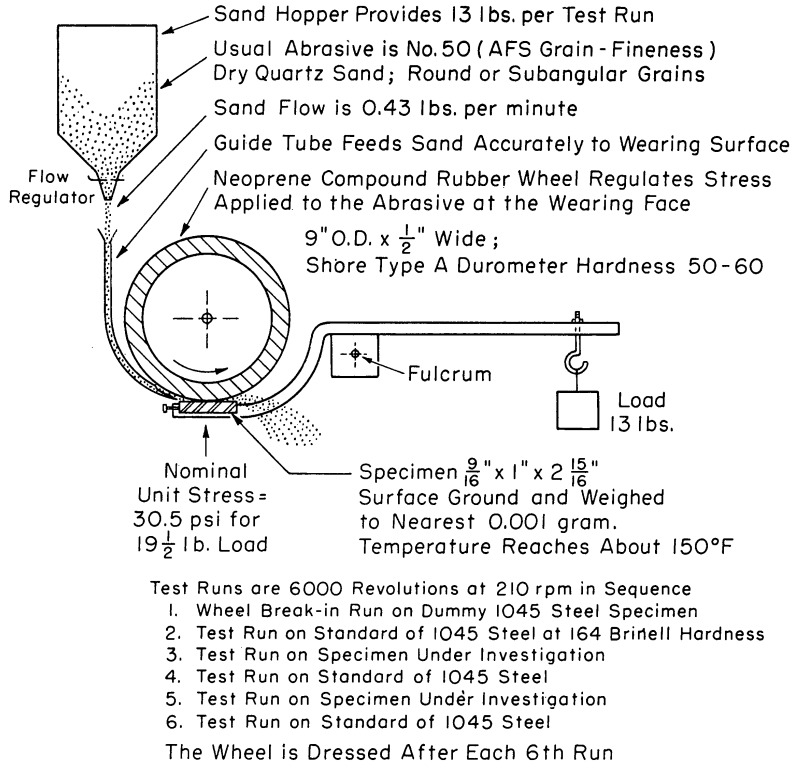

Figure 15. Schematic diagram of dry sand erosion machine.

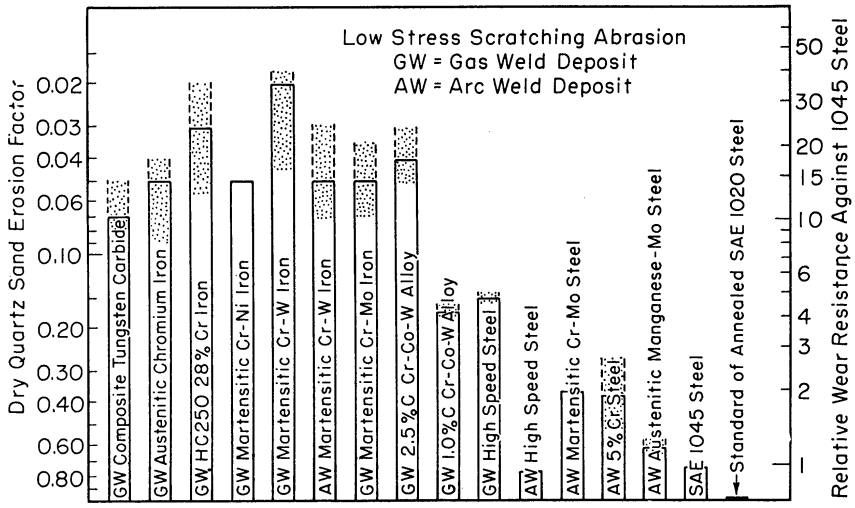

Figure 16. Comparative wear or erosion of hard facing alloys by dry quartz sand under low stress.

Results from wear tests can be reported in several ways. A fundamental approach provides data in terms of depth of metal removed per unit of time. This requires density and area measurements as well as time and weight loss values. However, perhaps the most serious objection to such a system is the difficulty in translating it into service performance unless comparative values are available.

Experience has tended to favor a comparison method of reporting, by means of a ratio against some standard material, although surface loss per unit of time is widely used for liquid and hot gas corrosion where areas are easily defined. The abrasion factor or ratio method can emphasize either wear or wear resistance, depending on the trend of an individual's thinking. One is the reciprocal of the other, and they can be readily converted. Herein, wear is emphasized so that small wear factors mean slight wear or weight loss. The reciprocal merit ratio evaluation is served by inverting the wear factor scale in graphic plots, so the height of a bar, as in Figure 13 indicates relative merit or wear resistance.

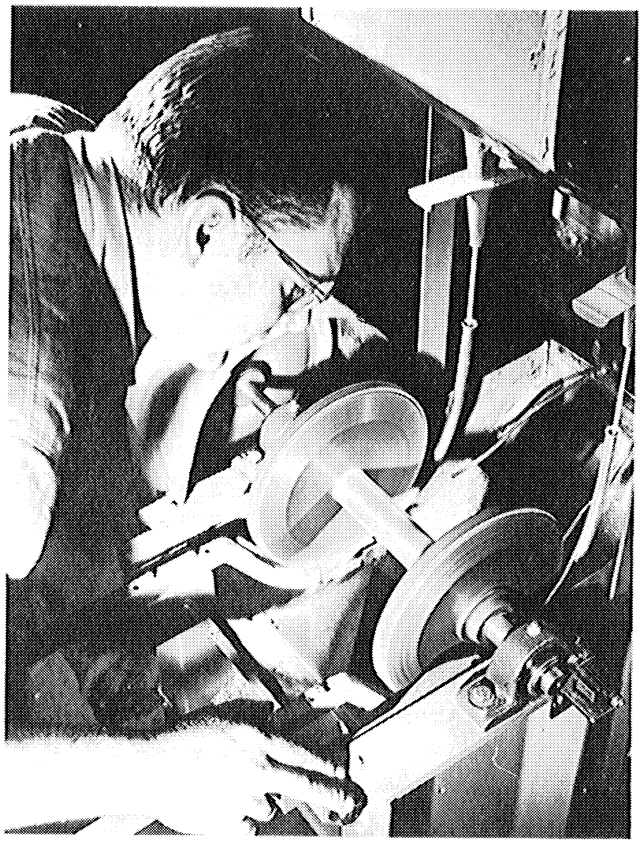

Figure 17. Photograph of dry sand erosion machine.

Comparative data from the dry rubber wheel erosion test are given for representative hard facing types in Figure 16. The ranking from such service conditions as plowing in sandy soil, foundry sand-slinger parts, and wheelabrator blades correlate with these data. However, the wear ratios may vary considerably. Experience suggests that mild conditions will create a much greater spread in apparent wear resistance than will severe service. Quartz sand was selected for the test because it is the commonest abrasive present in nature. It is undoubtedly the greatest cause of abrasive wear, even though its operation may not be obvious. Iron ore, for example, is likely to owe much of its abrasiveness to the siliceous matter present, since quartz in all of its manifold varieties is harder than the iron oxides.

If abrasives other than quartz are involved, it is reasonable to expect greater spreads in performance if they are softer, but associated with lower wear rates, while harder abrasives will abrade all of the materials more rapidly at rates that reduce the spread between alloys.

A number of engineering alloys are ranked by both high and low stress abrasion tests in Figure 13. Note that similarities occur but that complete reversals are also possible.

Hardness as such seems to make little difference in resistance to high stress abrasion. The group of engineering steels at about 340 and 550 Brinell hardnesses in Figure 13 do not differ enough to be significant in view of the experimental error. Under low stress abrasion the difference is marked, though steels, regardless of hardness, are generally inferior to cast iron types.

Erosion can be produced by clean fluids such as water or wet steam, as in hydraulic mining or steam turbine blade service. The sudden collapse of vapor bubbles in turbulent fluids is able to produce a type of wear termed cavitation erosion, which has been duplicated by supersonic vibration techniques in the laboratory.(19) High strength stainless alloys tend to minimize cavitation erosion.

The various tests described here may be used to rank and judge wrought metal products, cast alloys, welded overlays and other materials when homogeneous to perhaps a depth of 1/8 inch. Case hardened zones and other thin layers can be evaluated best by duplicating their average composition with homogeneous specimens. Thin cases, electroplates and like are worn through so rapidly that the test is not useful for rating them directly. None of these abrasion tests is considered applicable to abrasive free frictional metal to metal wear or to lubricated wear. Since temperature is held low they do not provide specific evidence for hot wear problems.

Hot Wear

An attempt has been made to develop a hot wear test by using a metal wheel heated with oxyacetylene flame jets. The apparatus produced wear on brake shoe type specimens, but the pattern was so obviously

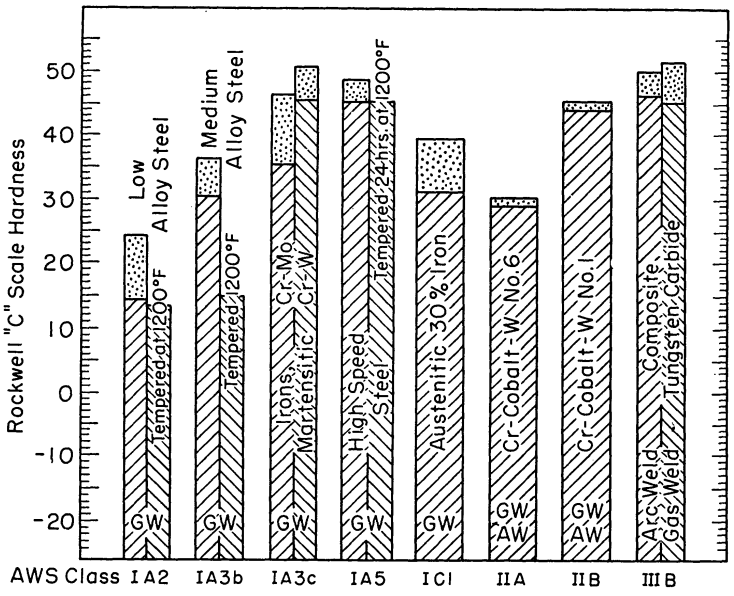

Figure 18. Apparent hot hardness of hard facing alloys at 1000°F. Stippled zones indicate loss of hardness during 2 minutes under load.

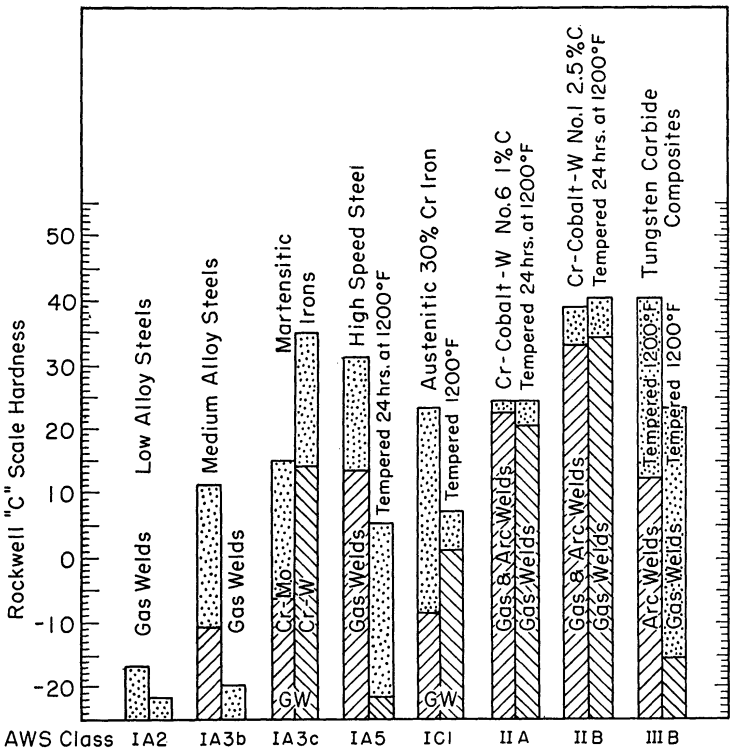

Figure 19. Apparent hot hardness of hard facing alloys at 1200°F. Stippled zones indicate loss of hardness during 2 minutes under load.

one of excessive plastic flow that conventional creep and stress-rupture laboratory techniques are considered superior. Present dependence for hot wear problems is chiefly on these and hot hardness that includes creep effects. The effect of thermal fatigue[20] is considered important for some surface problems. However, the data are confined chiefly to various grades of heat resistant alloys.

Hot hardness[21] is the only high temperature property that has been extensively studied for a variety of surfacing materials. A condensed summary of such data appears in Figures 18 and 19.

A network of cracks is frequently observed on the surface of metals that have been heated and cooled, Figure 1. They develop characteristically when one surface of an object is heated (and cooled) selectively, or faster than the bulk of the object. Either a rigid body or part of a structure may suffer. The cracks are evideace of thermal fatigue, which is a kind of deterioration that comes from changing temperatures.

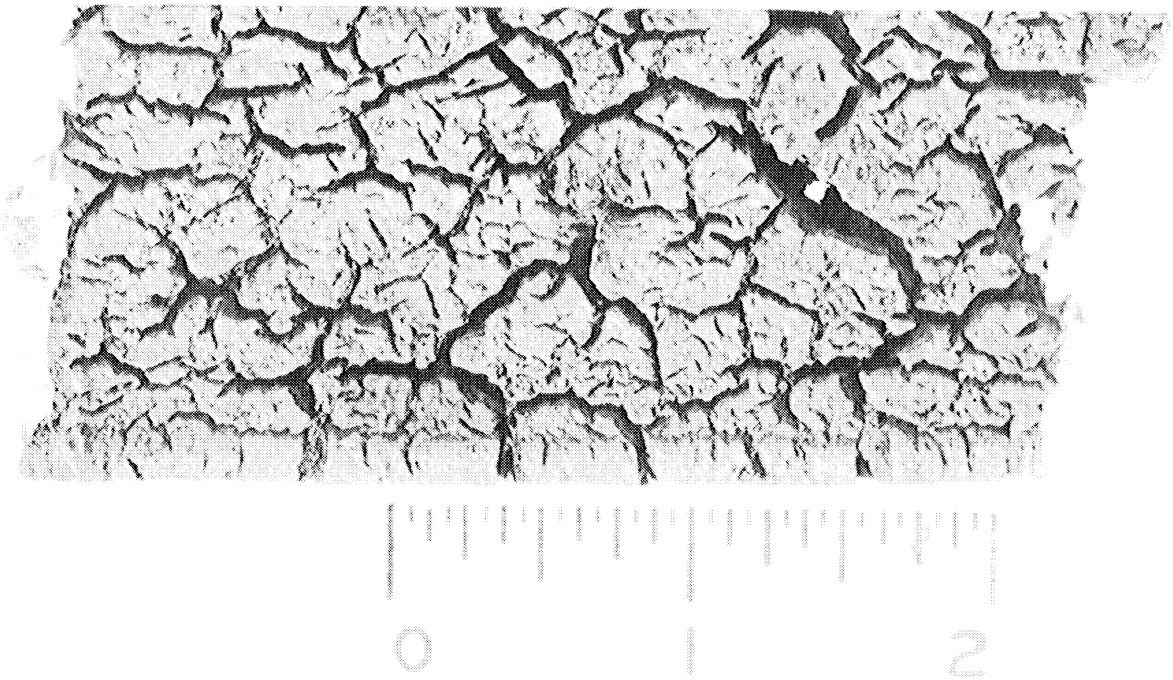

Figure 20. Pronounced thermal fatigue cracks in heat resistant alloy carburizing tray. This is the common failure mechanism of these parts.

Examples of this deterioration occur on the working faces of ingot molds and on the skin of fixtures and parts in heat treating and carburizing furnaces. It is sometimes called "fire cracking."

Thermal fatigue is considered by some as the principal mechanism by which heat resistant alloys deteriorate in use. It is the obvious failure mechanism of carburizing fixtures. It has become an important problem in the utilization of alloys in steam power plants, heat treating furnaces, nuclear power plants, and petroleum refining. Thus an understanding of how it develops is important to those concerned with these fields.

Thermal fatigue is a type of wear, if "deterioration due to use" is accepted as a definition of wear. Like other wear factors, the basic mechanism seldom operates entirely alone but may be modified or augmented by other phenomena such as oxidation, carburization, and changes in the internal structures of alloys. Defects, sharp angles, or changes in metal thickness may play a part, and conditions of service obviously have important effects.

Thermal shock is a related condition that should be distinguished from thermal fatigue. Both involve thermal stresses that can lead to failure. The terms are sometimes used interchangeably, but close consideration will clarify the difference. Thermal shock can be defined as the sudden application of heat (or cold). Ductile metals respond by deformation, but they seldom break. A brittle material is likely to fracture; this would be thermal shock failure. However, if the thermal shocks must be applied repeatedly, and there is some structural damage, the correct term is thermal fatigue. It is a progressive or cumulative mechanism and may be expected to cause failure.

Thermal fatigue should be recognized as a kind of damage. Thermal shock is part of service conditions. The repetition of thermal shocks can cause thermal fatigue, but shocks are not necessary. Repetition of slow heating and cooling can also produce the same kind of failure.

If an object breaks from one sudden temperature change the result should be called thermal shock failure. If more than one is required the thermal fatigue mechanism is at work.

Consider an example. If a piece of ordinary glass is heated red hot and then plunged into cold water, it will break up with many cracks. Here is obviously a case of thermal shock (as a cause) and thermal shock failure (as a result). But suppose a piece of fused silica or a piece of steel is substituted for the glass. With the same treatment no cracking results. The shock as a cause is present, but thermal shock failure is not. However, if the metal is heated and cooled this way often enough, it will eventually crack. This is thermal fatigue failure.

If the cycles of heating and cooling are stopped short of the point of cracking, thermal fatigue failure is not present. But minute internal changes have developed. When the cycling of temperature is resumed, the failure point is nearer than for the original specimen. Some sort of concealed structural damage has occurred. This is thermal fatigue, a kind of damage that can lead to failure.

The mechanism of thermal fatigue involves several properties of the material and a sequence of events. The pattern that causes surface cracks as in Figure 20 is somewhat as follows:

The surface is heated externally, producing thermal expansion as its temperature rises. This is resisted by the rigidity and strength of the colder portion of the section. This resistance builds up elastic stress until the yield strength of the material is exceeded, with consequent plastic flow (up setting) in compression of the hottest portion. The severity of the developed stress and its subsequent plastic flow depends on the magnitude of the temperature gradient and the maximum temperature reached. As the temperature equalizes from heat flow the gradient drops and the expansion stresses fall. However, when the heating part of the cycle is complete the upset portion will retain residual compressive stress. The amount of relaxation from this stress will depend on the time the temperature is constant.

When cooling occurs the residual compression stress declines by elastic recovery until zero stress is reached at some intermediate temperature. Further cooling develops tension. On the cooling side of the cycle the pattern reverses. The external chilling develops a temperature gradient, the contracting surface is resisted by the longer and hotter interior and plastic flow is again produced. Because the hot portion is usually weaker it may be upset by the strong, cooling surface, but usually its greater volume resists the stresses elastically. This resistance causes surface tension which may build up until the yield strength is again exceeded and the previously foreshortened zone is stretched plastically. If this tensile flow is not excessive the upset area will return apparently intact to its initial temperature, but with the important difference of containing high residual tensile stress.

The second and subsequent cycles differ in that heating and consequent expansion first relieves the tensile stress, passing zero at some moderately elevated temperature, and then builds up compressive stress. It is possible, because of the different zero stress location, that the maximum temperature can be attained without plastic flow on this cycle. If so, the return to room temperature may also take place without producing additional plastic flow in tension. Under these circumstances, a long life in cyclic service may be expected.

If the second cycle includes so much expansion that upsetting occurs again at the maximum temperature, tensile flow will be induced as the subsequent minimum temperature is approached. Each following similar cycle will also involve both compressive and tensile flow. It is postulated that the alteration of these will eventually exhaust the inherent ductility of the material and finally produce cracking. This result is termed "thermal fatigue". The failure will naturally occur on the tensile portion of a cycle. As precisely uniaxial stresses are rare, compressive flow portions of the cycles generally will be associated with warping and buckling, which usually accompany thermal fatigue cracks.

The number of cycles before failure, provided some flow takes place at each temperature extreme, will depend on the amount of such flow, which in turn depends on the part design and thermal gradient complex. The susceptibility of a given alloy to thermal fatigue will also depend on thermal expansion (a low coefficient will lessen the tendency for a given set of conditions to cause stresses reaching the plastic flow for a given set of conditions to cause stresses reaching the plastic flow points), on strength at both high and low temperatures (elastic limits must be exceeded before the damaging flow occurs), and on ductility near the temperature extremes. Values for the latter differ considerably for different alloys and at different temperatures, making prediction of behavior based on one set of conditions very uncertain of application to another case with a different temperature range. Ductility at the lowest temperature of a thermal cycle is probably critical.

The avoidance of thermal fatigue damage depends on design to minimize stress concentration, minimizing temperature gradients, and careful selection of materials. One set of experimental data for various heat resistant alloys appears in Figure 21.

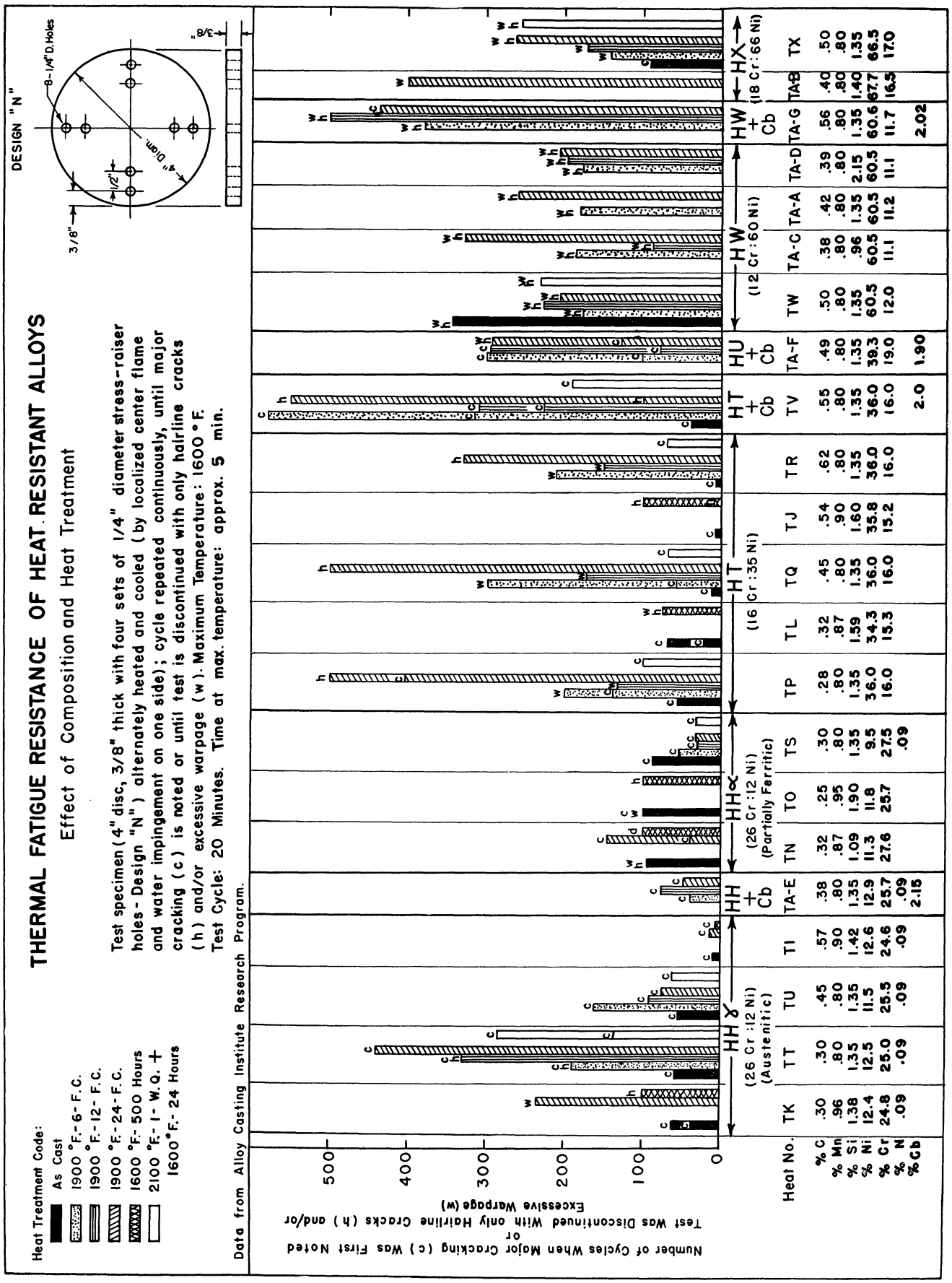

Figure 21. Relative performance of various alloys in thermal fatigue test.

ELASTIC MODULUS

The modulus of elasticity has an effect on wear resistance because it controls stress distribution at the wearing face. Deformation under load is readily spread over a large area to produce low unit elastic stress if the modulus is low. Oberle[22] has called attention to this and advocates using a combination of hardness and elasticity called Modell as an index of wear resistance. The Modell number is defined as one million times the ratio of Brinell hardness to elastic modulus.

Unfortunately, there is little that can be done to modify the elastic modulus of sound metallic materials. Aluminum bronze can be varied over a modest range by heat treatment. Some metals, like chromium electroplates, can be applied with a crystal orientation that presents a low modulus to the surface. The modulus of crystals may vary with crystal lographic directions; thus the usual figure of 29 to 30 million psi for steel is a statistical average of iron crystals that vary from about 19 million to 41 million psi, depending on the direction in which the crystal is stressed. However, no commercial process for controlling the surface modulus of iron and steel parts has been introduced.

Some latitude is provided by composite and porous structures. The graphite flakes in cast iron, the pores in powder metallurgy products, and the porosity in metal sprayed coatings are practical ways of attaining a low elastic modulus.

There are some applications where such porous materials exhibit an advantage, though it may stem considerably from the ability of the voids to function as oil resevoirs. However, the effects of high stress abrasion by coarse, hard particles result in high wear rates for porous alloys.

Alloys For Wear Resistance

With hundreds of compositions to choose from, it is not easy to simplify the selection problem. Nevertheless it is necessary to reduce the possible choices to a manageable group in order to facilitate the engineering approach. A combination of composition and structure is used in Table 4, since neither alone seems adequate. These nine groups will serve perhaps ninety percent of the engineering needs for protection in depth against wear. Castings as well as hard facing rods and electrodes are obtainable for each group and for some grades wrought products are also available. Some groups have many representatives, but usually a group has certain characteristics that permit generalizations about selection.

Space does not provide for detailed information here about each of the alloys, but they can be studied in other references. The ASM book on "Surface Protection Against Wear and Corrosion"[5]

contains chapters on several of them, some are featured in separate papers (23),(24),(25),(6),(18),(26) and ASTM specifications are available for a few.(27)(28)

The following discussion will aid in choosing between them, and is founded on preceeding ideas about wear.

Table 4

A Graded Series of
WEAR RESISTANT ALLOYS

Increasing Toughness — Increasing Abrasion Resistance

Properties Sensitive to Carbon Content and Structure

1.	Tungsten Carbide Composites	Maximum abrasion resistance Worn surfaces become rough
2.	High Chromium Irons	Excellent erosion resistance Oxidation resistance
3.	Martensitic Irons	Excellent abrasion resistance High compressive strength
4.	Cobalt Base Alloys	Oxidation resistance Corrosion resistance Hot strength and creep resistance.
5.	Austenitic Irons	Good erosion resistance
6.	Nickel Base Alloys	Corrosion resistance May have oxidation and creep resistance
7.	Martensitic Steels	Good combinations of abrasion and impact resistance Good compressive strength
8.	Pearlitic Steels	Inexpensive. Fair abrasion and impact resistance
9.	Austenitic Steels Stainless Steels Manganese Steel	Work hardening Corrosion Resistance Maximum toughness with fair abrasion resistance. Good Metal to metal wear resistance under impact

Selection Based On Wear Analysis

Though they are an incomplete assortment, the tests described here will provide a rational approach to the selection problem. In using this background it is suggested that the impact factor be evaluated first. If heat, corrosion and vibration are negligible the choice will probably be among the hard brittle carbides, nitriding, etc., and the martensitic irons on one extreme; martensitic or pearlitic steels in the mid-range area; and austenitic steels on the other extreme as the need for toughness increases. If protection in depth is required, the relative resistance to grinding abrasion of the pertinent hard facing alloys appears in Figure 22. If only shallow protection is needed, the electroplates, oxide layers (anodizing) and diffusion coatings are likely to be more economical.

For lubricated machine parts where boundary lubrication and vibration are involved the case hardening and selective hardening techniques are popular manufacturing procedures. Metal spraying, which produces a porous surface that helps to hold oil under adverse circumstances, is excellent where frictional conditions are not complicated with abrasion.

If heat is suspected as an important wear factor, the hot hardness of the otherwise appropriate alloys should be examined. Figure 18 and 19 will provide a convenient guide for hard facing alloys and the similar materials available in cast and wrought form. In general simple alloy steels and irons are not suitable above perhaps 800°F if hot hardness is needed. In the range from 800 to 1200°F there is considerable latitude in selection, which should be guided by the available data on hot hardness and strength. Above 1200°F the choice narrows to the austenitic stainless alloys, certain nickel-base alloys and the chromium-cobalt-tungsten (and molybdenum) types. At 1800°F and above the Cr-Co-W types appear to provide the highest hot strength.(21)

If abrasion is involved, the type should be identified if possible. If impact is negligible the choice is usually between high stress grinding and low stress scratching abrasion. Tungsten carbide excels for the first while the chromium carbide alloys are usually the economical selection for the latter. Martensitic irons are good for both types and where a smooth wearing surface is wanted, they may be preferred to tungsten carbide. The martensitic irons also provide high compressive strength for resistance to metal to metal wear and light impact.

Martensitic steels as heat treated parts, as the case produced by a diffusion process or as a welded overlay, come next in the abrasion versus impact compromise.

The high carbon Cr-Co-W alloy can give good resistance to grinding abrasion and the Ni-Cr-B alloys may be excellent for scratching abrasion, but these represent unnecessarily expensive choices unless corrosion or heat are significant factors. Even in the latter case the

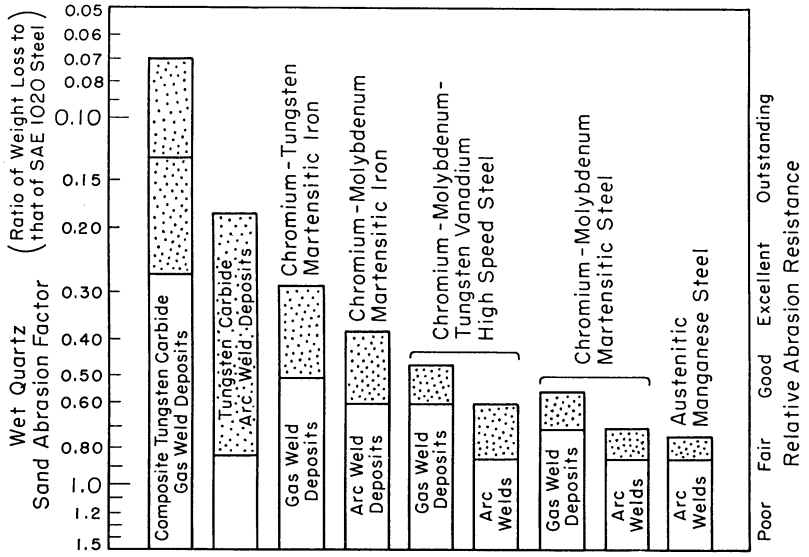

Figure 22. Abrasion Resistance of Some Martensitic Alloys. Stippled areas indicate observed scatter bands.

the suitability of the stainless steels should be examined because of their lower cost. Corrosive conditions may narrow consideration to the three general types noted in this paragraph in which case data from other sources should be consulted.

Finally, where heavy impact is prominent, austenitic manganese steel may be required because of its extreme toughness. Its remarkable capacity to work harden from impact deformation permits it to case harden in metal to metal service. It can develop a deep case with a smooth transition in hardness from case to core. When worn away, its surface can be replaced by welding. However, it is not corrosion resistant, and it is not suitable for use above 500°F.

Some of the austenitic stainless steels are also very tough. While they are more expensive than austenitic manganese steel, they have heat and corrosion resistance. As homogeneous parts or welded overlays, they are appropriate where heavy impact and heat or corrosion combine.

Mechanical wear that is primarily of the frictional or metal-to-metal type is likely to involve machinability considerations that rule out the carbides, the hard irons and similar alloys. Aluminum bronzes, engineering steels that are hardened after machining, and the case hardening techniques and plating that causes little dimensional change should then receive consideration.

This discussion has assumed that most of the problems will involve iron or steel structures. Where other alloys are concerned the plating, metal spraying and anodizing techniques are of particular interest. Low melting alloys like aluminum are not adapted to hard facing with high melting alloys. Thus a metallurgical bond is not feasible, but mechanical attachment of wear resistant materials may be possible. Copper-base alloys and somewhat higher melting base metals can be welded in some cases, but they require quite careful handling. Brazing overlays on them is practicable.

In each case where a tentative selection is made against the background above it is suggested that more details be sought in the references.

REFERENCE

1. Dietz, A.G.H., Engineering Laminates, John Wiley & Sons, New York, 1949.

2. Gillett, H.W., "Considerations Involved in the Wear Testing of Metals," Symposium on Wear of Metals, ASTM-1937 (out of print).

3. Dean and Dixon, "Simplified Statistics for Small Numbers of Observations," Analytical Chemistry, 1951, Vol. 23, (4), p. 636-638.

4. Simon, Leslie E., An Engineer's Manual of Statistical Methods, John Wiley & Sons, New York, 1941, p. 138.

5. "Surface Protection Against Wear and Corrosion," American Society for Metals, 1954, Cleveland, Ohio.

6. Avery, H.S., "Hard Facing for Impact," The Welding Journal, Vol. 31, (2) 1952, p. 116-143.

7. Timoschenko, S., Theory of Elasticity, McGraw-Hill Book Co., Inc., New York, 1934, p. 383-385.

8. Brasunas, Anton deS., Gow, James T., and Harder, Oscar E., "Resistance of Iron-Nickel-Chromium Alloys to Corrosion in Air at 1600 to 2200°F," Proceedings, American Society for Testing Materials, Vol. 46, 1946, p. 129-160.

9. "The Failure of Metals by Fatigue," A Symposium, Melbourne University Press, Melbourne, Australia, 1947.

10. Murray, Wm. M., Fatigue and Fracture of Metals, Technology Press, M.I.T. and John Wiley & Sons, New York, 1952.

11. Battelle Memorial Institute Staff, Failure of Metals Under Repeated Stress, John Wiley & Sons, New York, 1941.

12. Garwood et al, Interpretation of Tests and Correlation With Service, published by American Society for Metals, 1951.

13. Norman, T.E., and Loeb, C.M, "Wear Tests on Grinding Balls," AIME TP 2319 and Transactions, American Institute of Mining and Metallurgical Engineers, Vol. 176, Metals Technology, 1948, p. 490-520.

14. Avery, Howard S., "Discussion of 'Wear Tests on Grinding Balls'," AIME Tech. Pub. No. 2448 and Transactions, American Institute of Mining and Metallurgical Engineers, Vol. 176, 1948, p. 521-523.

REFERENCES (CONT'D)

15. Blake, J.M., "Wear Testing of Various Types of Steel," Proceedings, American Society for Testing Materials, No. 28, Part II, 1928, p. 341-355.

16. Peters and Van Voorhis, Statistical Procedures and Their Mathematical Bases, Rev. Ed. McGraw-Hill, 1940.

17. Haworth, R.D., Jr., "The Abrasion Resistance of Metals," Transactions, American Society for Metals, Vol. 41, 1949, p. 819.

18. Avery, H.S., and Chapin, H.J., "Hard Facing Alloys of the Chromium Carbide Type," The Welding Journal, Vol. 31, (10), Oct. 1952, p. 917-930.

19. Hunsaker, J.C., "Progress Report on Cavitation Research at Mass. Inst. of Technology," Transactions, American Society of Mechanical Engineers, Vol. 57, 1935, Paper HYD-57-11.

20. Avery, H.S., and Wilks, C.R., "Alloy Casting Institute Thermal Fatigue Testing," Alloy Casting Bulletin, No. 14, May, 1950.

21. Avery, Howard S., "Hot Hardness of Hard Facing Alloys," The Welding Journal, Vol. 29 (7) 1950, p. 552-578.

22. Oberle, T.L., "Properties Which Influence Wear of Metals," unpublished manuscript, 1950.

23. Avery, Howard S., "Composite Tungsten Carbide Weld Deposits," The Welding Journal, Vol. 30 (2) February 1951, p. 144-160.

24. Avery, Howard S., "Hard Facing by Fusion Welding," American Brake Shoe Company, New York, 1947.

25. Avery, Howard S., "Hard Facing Alloys for Steel Mill Use," Iron and Steel Engineer, Vol. 28 (9) September 1951, p. 81-106.

26. Avery, Howard S., "Austenitic Manganese Steel," American Brake Shoe Company, New York, 1949.

27. AWS A 5.13-56C, ASTM A 399-56T, "Tentative Specifications for Surfacing Welding Rods and Electrodes," American Welding Society, New York, 1956.

28. ASTM A128-33, "Standard Specifications for Austenitic Manganese Steel Castings," American Society for Testing Materials, Philadelphia, Pa.

WEAR RESISTANCE OF CAST IRON COMPONENTS

J. E. LaBelle
Chief Metallurgist, Detroit Diesel Engine Division
General Motors Corporation

WEAR RESISTANCE OF CAST IRON COMPONENTS

by

J. E. LaBelle

TYPES OF WEAR

One of the principal topics of wear concerns sliding contact between mating metal parts in machinery where the load and velocity are high enough to require forced lubrication. Typical of this type of mechanism are engine cylinders and pistons, valve stems and guides, and sleeve bearings and bearing journals.

Wear can occur in such mechanisms in several ways. Abrasion can occur because of foreign particles in the lubricating oil or because the mating surfaces are too rough. Corrosion can become a significant factor if acidic compounds contaminate the lubricating oil. The principle cause of wear, however, is best described as frictional wear.[1,2,3]*

Characteristics of Frictional Wear

Bowden and Tabor[4] describe frictional wear in detail. It is assumed in high-speed machinery that an oil film will continuously separate the mating pieces where sliding contact occurs. For the most part, this is true in good designs, however, there are conditions during the operation which will momentarily cause the film to partially or completely break down. When this occurs, some metal-to-metal contact occurs producing frictional wear. The actual mechanism whereby metal is removed when this contact occurs is debatable, but it is known that the temperatures, at the points of contact on the interface, approach the melting point of the lowest melting of the two mating metals and in all likelihood welds occur, and are immediately ruptured, pulling particles from the surfaces. This process of welding, and weld breaking occurs on a microscopic scale under normal conditions, and the rate of metal removal is slow.

In Figure 1 is a plot of electrical resistance between a piston ring and a cylinder wall in an operating engine. The plot is of one engine revolution. The test was made by impressing a voltage between the ring and cylinder wall, and measuring resistance to current flow. If metal-to-metal contact occurs, current flows showing oil film breakdown and vice versa. As can be seen at slow speeds some contact occurred, but at the higher speed the oil film was almost 100% effective. It should be recognized that any contact at any point will cause current to flow so that even at slow speeds, the amount of contact is not necessarily very much. In fact, it could not be very much, and still have a successful mechanism.

---

* Refers to references listed at the end of this paper.

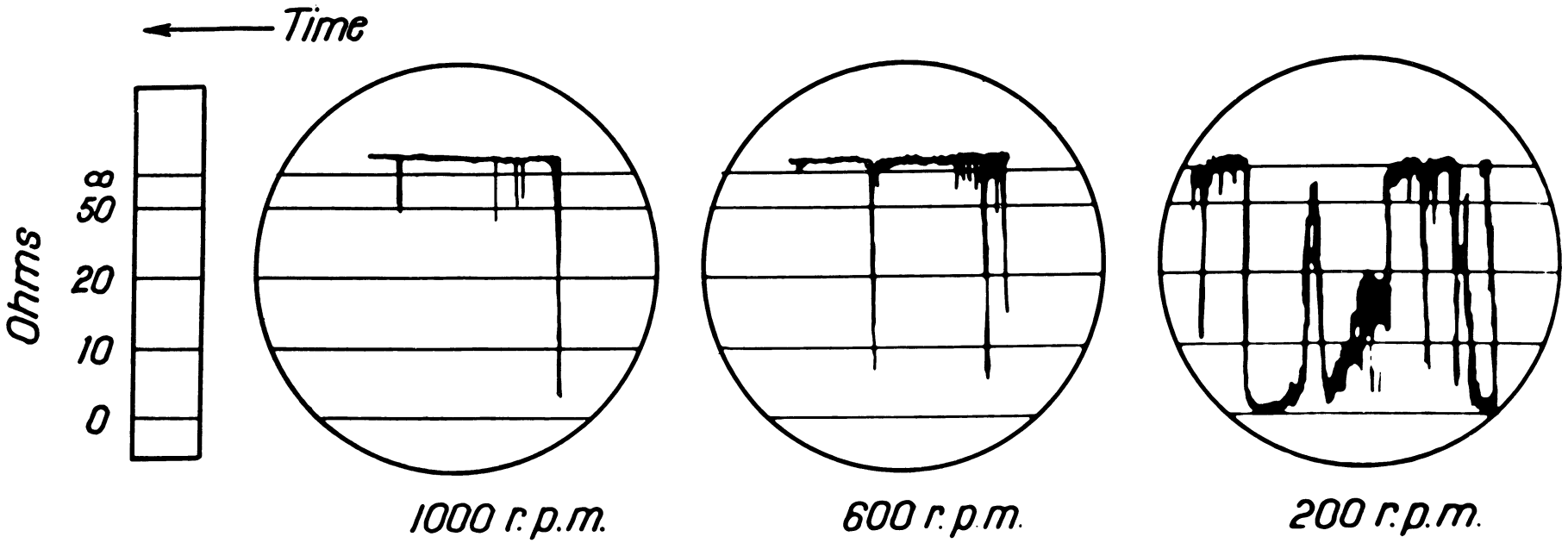

Figure 60. Cathode ray traces showing electrical resistance from piston ring to cylinder wall of a running engine. (Courtney-Pratt and Tudor.[60]) A high resistance indicates predominantly hydrodynamic conditions; a low resistance means metallic contact or at least a regime of boundary lubrication. Although the amount of hydrodynamic lubrication increases with the speed of rotation, there is a definite amount of breakdown of the hydrodynamic film even at the highest speeds recorded.

It can be postulated that if a clean oil film can be continuously maintained, wear will be negligible. One of the characteristics of well-designed and properly operated machinery is that, of necessity, it must closely approach perfection. This is due to its inability to function if appreciable wear occurs. In diesel engine cylinders, for example, 240,000,000 strokes of the piston will produce, as a typical value, only .001" of wear. When wear occurs at a slow rate, with no complications such as scoring or rapid metal removal by abrasives in the lubricant, we call the wear which does occur, normal wear.

Scuffing, Scoring, and Galling

All too often the achievement of a good normal wearing condition is prevented by a destructive wear condition called scuffing, scoring, or galling depending upon its severity. This damaging effect can lead to destruction of the mating surfaces and seizure. It would appear that mechanisms have a tolerance for a certain frequency and duration of oil film interruptions, which, if exceeded, leads to enough metal-to-metal contact to overheat large areas, and cause a smearing action. In this process, comparatively large amounts of material are picked up and moved to adjacent surfaces, and rewelded. In Figure 2 is the scuffed area of an engine cylinder produced by this process. Figure 3 shows a 100 X magnification of the cylinder before running, the normal wear pattern, and an area where scuffing has just started. It shows that metal has been welded over the top of an existing surface, covering the hone lines. If the oil film is reestablished before much damage is done, scuffing is usually healed without permanent injury. If the condition progresses too far, a snowballing effect develops leading to rapid failure by galling.

In designing machinery, the wear problem should be regarded as having two aspects. It is first necessary to establish conditions which overcome any tendency to scuff or gall in order that only normal wear takes place. Second, it is necessary to bring normal wear into acceptable limits.(2)

General Characteristics of Bearing Metals

Before proceeding with the subject of gray cast iron, it is probably desirable to also review some aspects of sleeve-bearing metals. These metals, in general, depend on having a soft low-melting point metal such as tin, lead, cadmium, or an alloy of these in their make-up. In some cases, the entire bearing surface has a low melting point as in the case of the babbits. Copper lead, aluminum cadmium, and aluminum tin have the low melting point material distributed throughout a harder and higher melting point matrix. The heat generated, during moments of oil film interruption with such bearings, is limited by the melting point of the material, since at that point a microscopic film of molten-bearing

Figure 2.

Comparison of Normal Wear and Scuffing
on Cylinder Liner Surface

x 90 Unetched

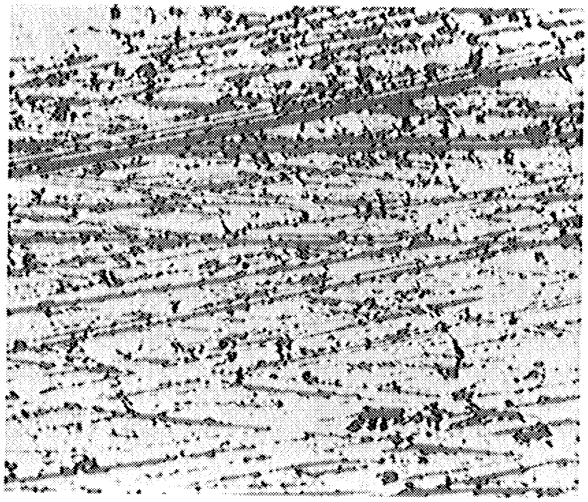

As Honed
Before Running

x 90 Unetched

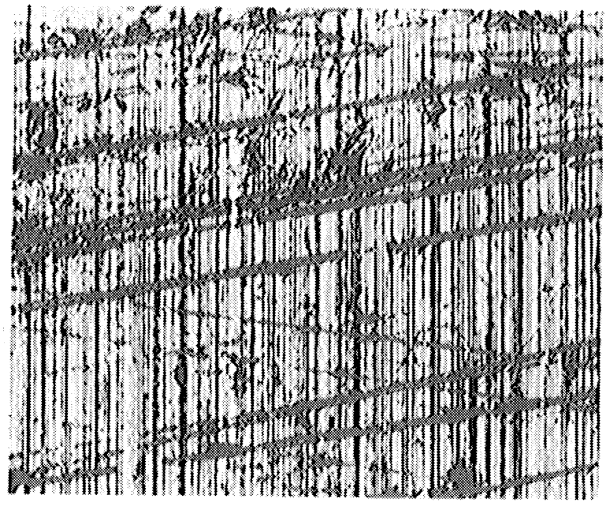

After 1 1/2 hours in Engine
Normal Wear

x 90 Unetched

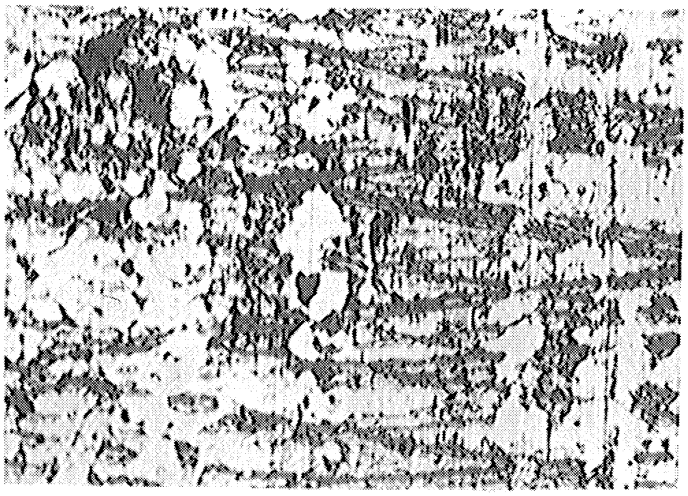

Slightly Scuffed Area
(Same Liner as Right Top)

Figure 3.

metal takes over as a lubricant and temporarily prevents extensive damage. Of course the oil film must be reestablished rapidly or the bearing will burn out regardless. The principle feature, however, is that this low temperature melting action in bearings greatly increases the tolerance for temporary oil film breakdown by comparison with other metal pairs in sliding contact such as steel on steel.

Gray Cast Iron

Gray cast iron is an amazing metal because the features that make it inexpensive and versatile as a casting material also make it exceptional from a wearing standpoint. Actually gray iron can best be defined as steel with flake graphite in it. In Figure 4 is a typical microstructure of as cast gray iron. As noted three constituents predominate. Ferrite, which is nearly pure iron, is very soft with a hardness of Brinell 100-150, and has poor wear resistance. Iron carbide is

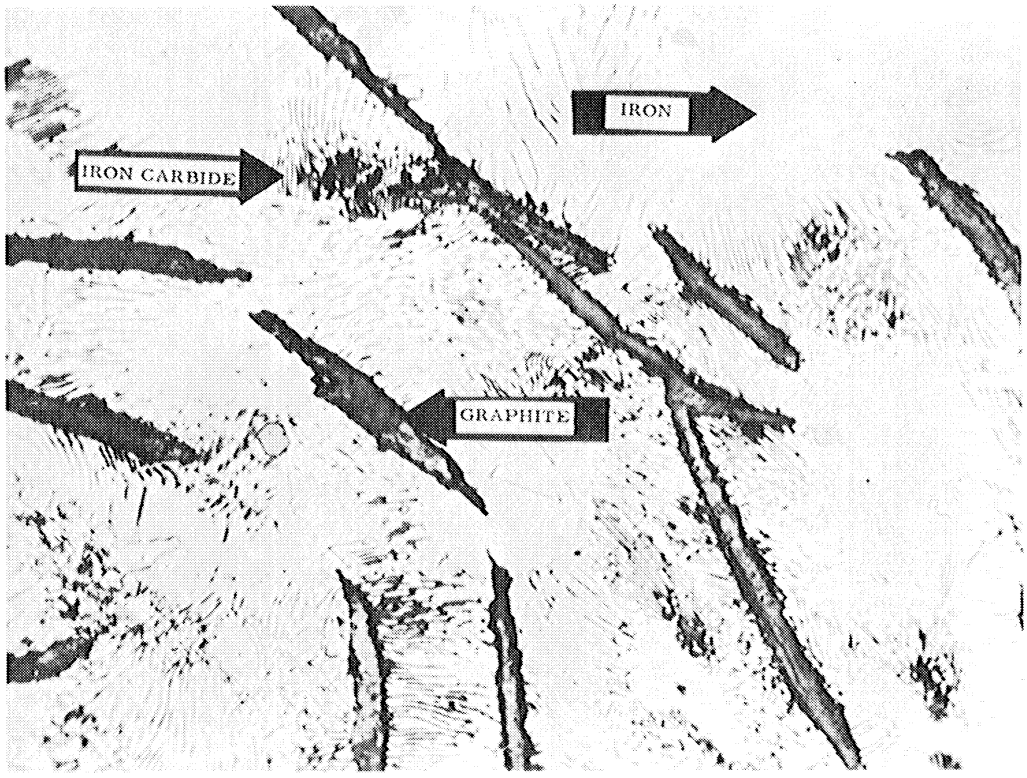

Figure 4.

is a compound of iron and carbon with the chemical formula Fe_3C. It is very hard and occurs in alternate plates with Ferrite in one form which is called pearlite. The hardness of the pearlite is dependent on the fineness of the alternate plates, and can range from about 190 to 300 Brinell. In hardened steel, and gray iron, the Fe_3C occurs as submicroscopic particles distributed throughout ferrite. The graphite in gray iron occurs in the form of flakes of the general shape of corn flakes only on a micro scale and is a soft, non-abrasive, almost greasy form of carbon. It is the graphite which makes cast iron very castable and machinable, and in addition is the main factor in its unusual wearing properties.

It is felt that the graphite smears over the surface in wearing applications acting as a dry lubricant and as an anti-welding medium since metal to metal contact cannot take place through a film of graphite. In addition the pockets of graphite create a surface filled with tiny reservoirs capable of holding oil and therefore help to maintain the oil film in reciprocating sliding contact where a dynamic oil film is especially hard to achieve.

As previously stated gray cast iron can be defined as steel containing graphite flakes which are scattered throughout. There are as a result two principle variables, the metal matrix and the graphite. Basically, as in steel, cast iron is an alloy of iron and carbon. Instead of a carbon content ranging from .05% to about 1.00% which is typical of steel, the carbon content of cast iron is generally in the range of 3.00 to 3.50%. As in the case of steel however, usually less than 1.00% of the carbon is contained in the metal matrix as iron carbide. The balance of the carbon forms graphite.

The graphitic microstructure can be varied considerably with respect to size, amount, and distribution of flakes. Figure 5 is a chart showing the ASTM classifications of graphite type and flake size.

Type A is universally preferred in wear applications. The high carbon version type C is used for special jobs such as break drums, clutch faces, and the like where no lubricant is used and high resistance to heat checking is desired. Type B is not as desirable as type A, but occurs with it in some cases. Type D and E are produced by rapid solidification such as occurs in permanent mold castings, and are generally regarded as poor from a wear standpoint. In general the graphitic microstructure is finalized when the metal first solidifies, and cannot be altered thereafter except in quantity unless the metal is remelted.

The metal matrix in gray iron contains the same principle constituents as steel, namely iron and iron carbide, however, one distinct difference exists. The quantity of iron carbide in steel is fixed by the amount of carbon present in the steel whereas the quantity of iron carbide in gray iron is not precisely controlled by the total carbon content, and if anything varies inversely to it. This is due to the fact that an increase in carbon tends to throw even more carbon into the graphitic state than the addition leaving less to occur as iron carbide.

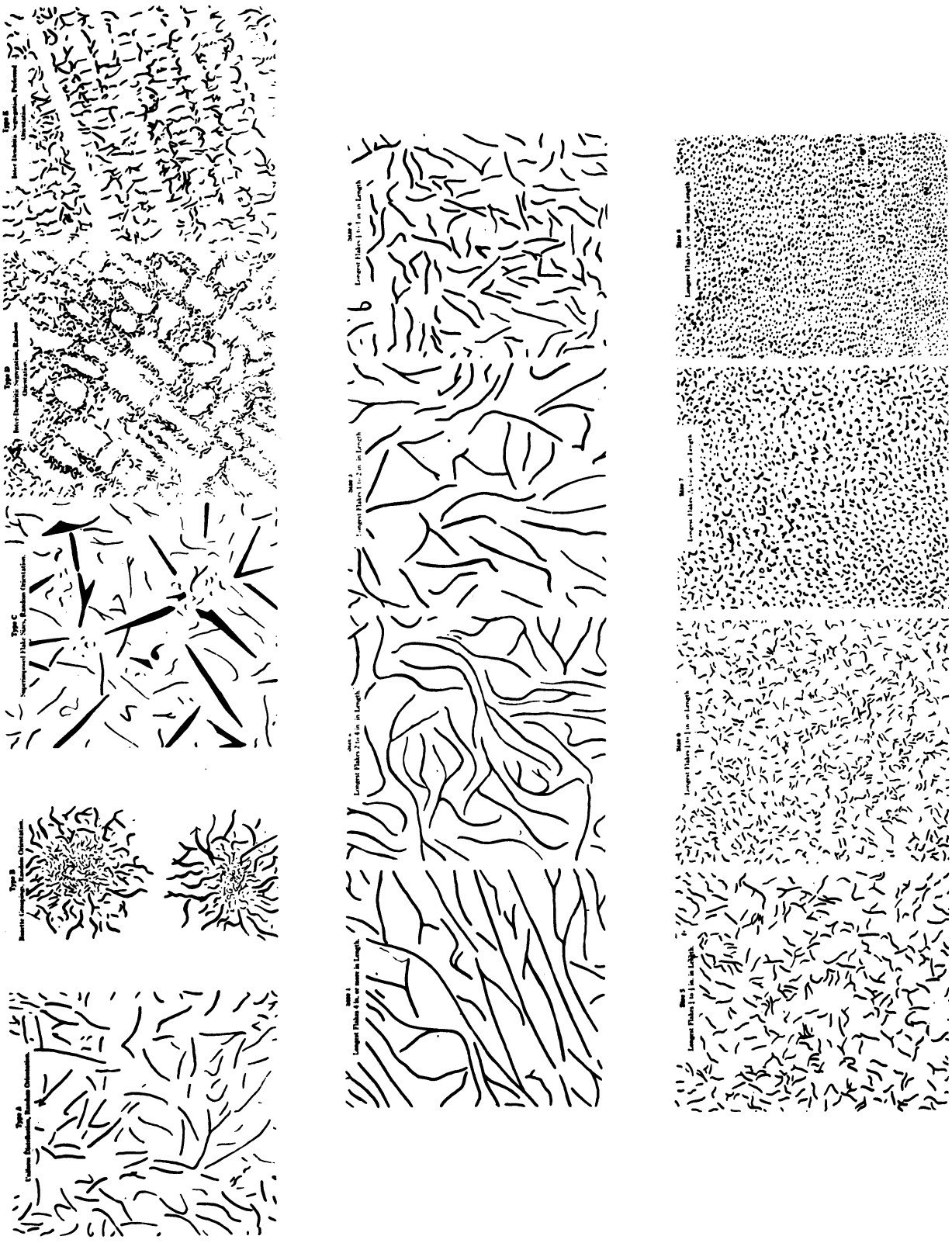

Figure 5.

It is not the purpose of this paper to dwell extensively on the metallurgy of cast iron, however, so the factors governing the control of iron carbide quantity in as cast gray iron will be dispensed with.

It is possible, however, to change the metal matrix from high carbon to low carbon and vice versa by heat treatment. Figure 6 shows a graph of hardness versus quenching temperature for a gray iron. As can be observed increasing temperature up to 1300°F causes the material to soften. Above this temperature hardening takes place as in steel.

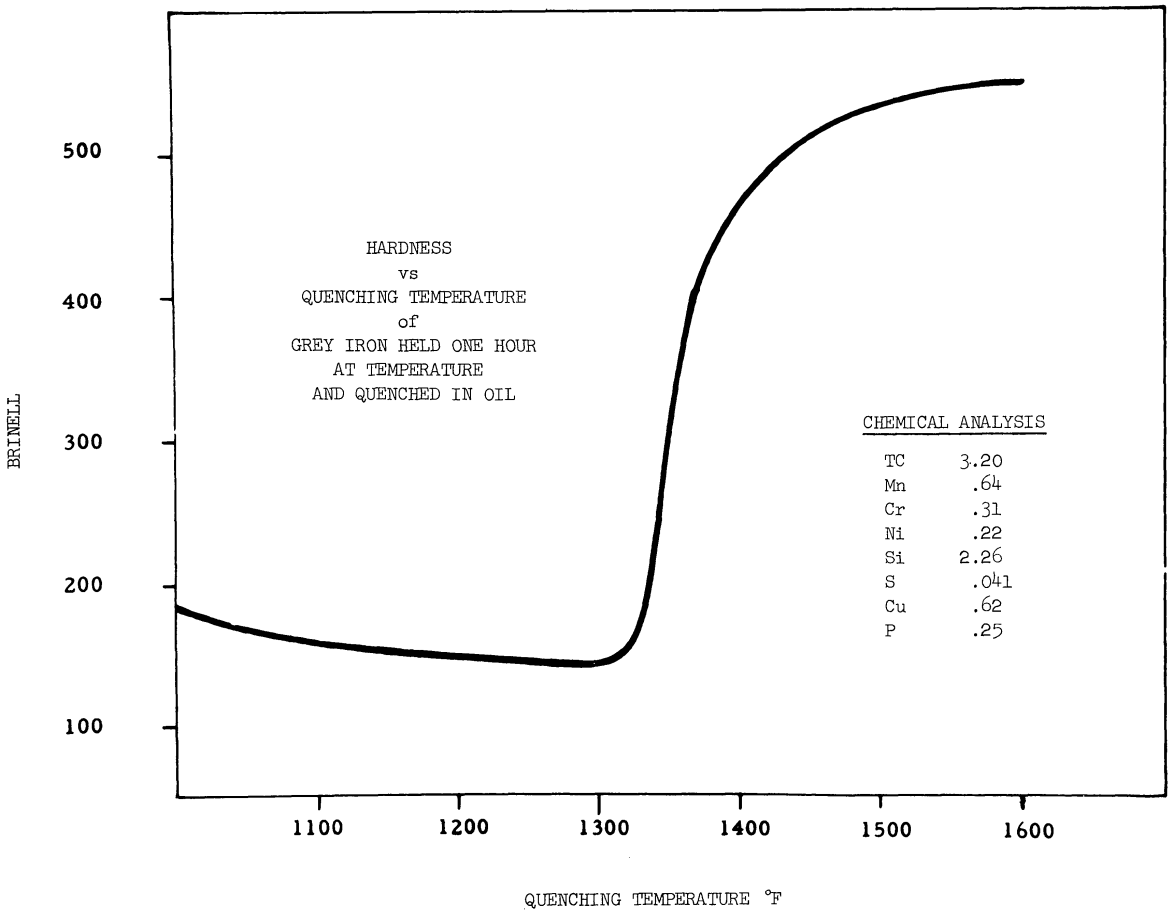

Figure 6.

In Figure 7 are microstructures showing what happens. At 1300°F the carbide in the pearlite of the as cast structure has broken down considerably into more graphite and Ferrite. At 1600°F the structure which is hardened martensite shows that considerable graphitic carbon has re-dissolved to form Fe_3C and caused hardening similar to any high carbon steel. It is thus possible by controlled heating and cooling to obtain just about any kind of a matrix microstructure found in steel, and with even greater versatility, because the combined carbon content can be altered so easily.

Etched X 500
As Cast

Etched X 500
Quenched in Oil
from 1300°F

Etched X 500
Quenched in Oil
from 1600°F

Figure 7. Affect of Quenching Temperature on the Micro Structure of Gray Cast Iron

Up until a few years ago a common belief prevailed and is probably still carried over in many quarters that the chemical composition of gray iron exerts a major influence on its wear resistance. This probably originated from the fact that poor results were usually corrected by composition changes. Apparently the microstructure changes were noted but regarded as secondary. Unfortunately the composition changes which corrected one wear problem might not correct another, and great confusion resulted. It is now believed that with only one or two minor exceptions chemical analysis is important only as it effects graphitic and matrix microstructure.

Accelerated Wear Tests

Over the years there have been a great many wear tests made to evaluate the wearing qualities of cast iron. Unfortunately practically all of these were conducted in a manner so as to create considerable wear in a short period of time. It is likely that in most of these accelerated tests the type of wear evaluated was similar to scuffing. A.B. Shuck, for example in the transactions of The American Foundrymen's Society for 1948, reported tests using a brake shoe specimen against a dry rotating drum.(5) This investigation was extensive and produced the following conclusions which agree with those of practically all other investigations of this nature.

1. Microstructure, not chemical analysis, determines the wearing characteristics.
2. As the graphitic microstructure becomes coarser and tends toward type A, wear is decreased.
3. Interdendritic type D graphite and its associated ferrite gives very poor results.
4. Secondary ferrite associated with random type A graphite is less damaging than that associated with type D.
5. Pearlitic, acicular, or tempered martensite structures in the same hardness range are equal in wear resistance.
6. For a given type of graphite, as the matrix becomes more pearlitic, and harder, wear resistance increases.

The Detroit Diesel Cylinder Wear Program

These results, when compared with data of some extensive cylinder wear tests run at Detroit Diesel indicate that they apply specifically to scuff resistance. The Detroit Diesel tests involved 108 different combinations of material, and design, and utilized about 550 cylinder sleeves, 360 pistons, and over 2,150 compression piston rings. Part of the tests were designed to evaluate basic material factors in an extensive systematic study. Some of these were reported in the 1955 supplement of the metals handbook published by the American Society for Metals.(2)

Since then some new tests have been run which have provided additional data, and these will also be included in todays discussion. The Detroit Diesel tests were of two types, one to evaluate scuff resistance based on severity of operation to produce scuffing, and the other evaluated normal wear resistance in about 1,000 hrs. of engine operation on a controlled cycle. The results were the averages of from six to thirty tests for each value reported.

Scuff Resistance

The scuff test was conducted in a three cylinder engine normally rated at 90 horsepower at 2,000 R.P.M. By increasing fuel injection per stroke it was possible to produce 115 horsepower at 2,000 R.P.M., and by then changing speed to 2,200 R.P.M. it was possible to go to 135 horsepower. The engine was equipped with three test liners, new pistons and rings, and after a standard break in cycle was run at 90 horsepower for thirty minutes. The engine was then removed from test, and the cylinders examined for scuffing. It was then reassembled and again run for thirty minutes after increasing the horsepower by 5 to 95. After each run it was examined for scuffing, reassembled, run for another thirty minutes at an increase by 5 in horsepower until the horsepower which first produced scuffing, in each cylinder, had been determined. By increasing horsepower at the same engine speed, ring pressure was increased in an almost straight proportion to horsepower, and the scuff resistance was therefore judged as the ability of the cylinder wall to withstand increases in ring pressure without scuffing. The figures in the scuff charts are a comparison of horsepower to produce scuffing using 90 horsepower as a base line of 1.00.

Effect of Graphite on Scuff Resistance

Our first tests were run to compare type A and type D graphite. Later these were amplified to include other graphite variables. We were able to standardize the effect of metal matrix variables by the expedient of hardening the test sleeves so that the metal matrix was tempered martensite in all tests. Figure 8 shows a comparison of microstructures of the types of gray iron tested. Table 1 shows the test results. The results indicate first the superiority of gray iron over steel, then the superiority of type A graphite over type D, and finally the superiority of larger graphite flakes and greater quantities over the smaller size and lesser quantities. We would like to have determined the precise value for the coarse graphite 4% carbon material, however, the maximum power achievable at that time was 135 horsepower which limited the severity of the test.

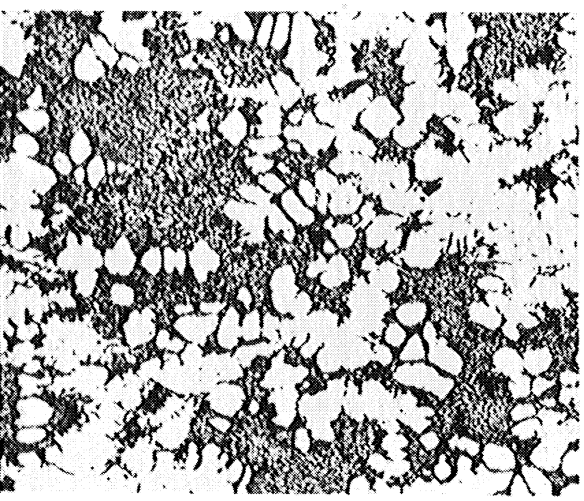

Type D X 100
Unetched

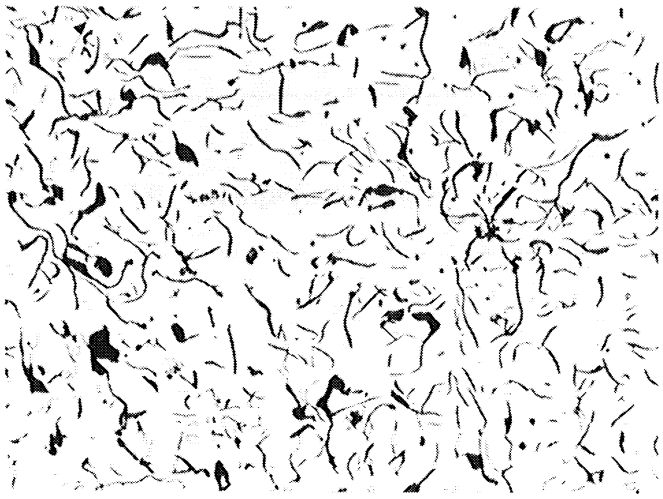

Type A X 100
Unetched

Cause Type A X 100
Unetched 4.00 Carbon

Typical Martensitic
Matrix of Hardened Material
Etched X 500

Figure 8.

TABLE 1

Effect of Graphitic Microstructure on Resistance to Scuffing

Test No.	Type of Graphite[a]	Total Carbon, %	Resistance to Scuffing[b]
1	None	(5150 steel)	< 1[c]
2	100% Type D centrifugally cast	3.25 (avg)	1.11
3	Type A, size 4 to 6, some Type B, centrifugally cast	3.28	1.33
4	Same as 3 except cast in sand mold	3.35 (avg)	1.30
5	Type A, size 3 to 4, some Type C, sand cast	4.00	> 1.45[d]

(a) Different chemical compositions were tested in two of the four types of iron. See Table 3 for compositions. Matrix of all specimens was tempered martensite. (b) Expressed as the ratio of horsepower to produce scuffing divided by normal horsepower. (c) All the steel sleeves scuffed below normal horsepower. (d) Maximum available engine horsepower produced no scuffing.

Effect of Metal Matrix on Scuff Resistance

A second test series evaluated the effect of variables in metal matrix on scuff resistance. To maintain a graphite type which was constant and capable of causing scuffing, type D graphite material was used. The material of the first test is shown in Figure 9. This unhardened type D structure is the same as that described by Shuck in his tests and by many others as especially poor. Some years ago Detroit Diesel employed a permanent mold cast valve guide which likewise exhibited this type D graphite, and its associated ferrite. Considerable trouble was experienced with stuck valves, apparently because of the poor scuff resistance of the material. The other tests of type D graphite were made on hardened pieces tempered to different hardness values.

Table 2 shows the results of the engine scuff tests where the metal matrix was varied. It is interesting to note that the poorest structure was the softest, but the next poorest was the hardest. As the

Unhardened Type D Graphite Iron
Showing Ferrite Surrounding Graphite Clusters

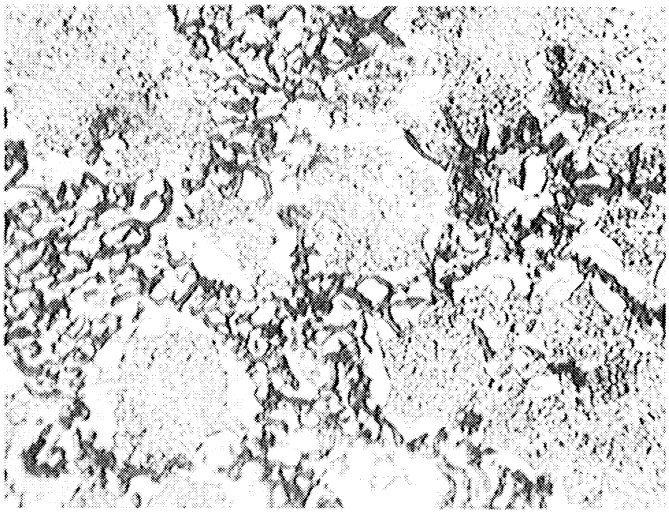

Etched X 500

Figure 9.

hardened structure was tempered, scuff resistance picked up by a surprising amount. This effect of tempering was run on type D graphite liners from two foundries with almost identical results.

TABLE 2

Effect of Matrix Microstructure on Resistance to Scuffing

Test No.	Microstructure of Matrix	Hardness	Resistance to Scuffing
1	Pearlite with ferrite occurring in areas of Type D graphite	196 to 227 Brinell	< 1[a]
2	Martensite tempered at 400 F	Rockwell C 53 to 56	1.06
3	Martensite tempered at 800 F	Rockwell C 44 to 47	1.22
4	Martensite tempered at 950 F	Rockwell C 39 to 41	1.39

(a) All sleeves scuffed below normal operating range.

Lane,(6) expressed this same effect as follows, "Going from 160 to 260 Brinell in hardness results in decreasing scuffing tendencies, however, going from 260 Brinell upward, including the heat treated

structures, increases the tendency to scuff." While we did not test the same conditions that Lane referred to, we were able to draw a similar conclusion. It is apparent that if the graphite is held constant and scuffing tendencies can be changed by softening a hardened matrix then some explanation should be found in current theories. It would appear that the tempered intermediate hardness structures either are not readily welded by metal to metal contact, which seems unlikely, or when the welds are fractured less material is broken away. This latter theory seems plausible because the resistance to scuffing, as influenced by matrix microstructure, seems to correlate with strength and toughness. Bowden has stated that if the base metal strength is weaker than the weld, large particles will be broken away and damage by scuffing will be extensive. If the weld is the weakest link then only small particles are broken away.(4) Therefore as strength and toughness are increased, wear should decrease. More will be said about this point later.

Effect of Chemical Composition on Scuff Resistance

The Detroit Diesel work on scuffing would not have been complete, from a material standpoint, if it did not include variations in the composition of the test materials. Different foundries submitted different materials for test giving a fair check on material variations. No effect of chemical composition was noted on scuff resistance, except as it effected microstructure. The various compositions are shown in Table 3.

Other investigators have observed that a fine network of steadite (iron phosphide - iron carbide eutectic) increases scuff resistance while massive carbides, associated with chilled iron, promote scuffing.(7) We will have more to say on the steadite later.

Surface Finish Effects

During the early part of our investigation, experiments were conducted on surface finish on the premise that a good finish for break in might condition the surface during break in and minimize the scuffing tendencies of the material. The type D graphite iron, hardened and tempered with a 30 R.M.S. finish, had given us a scuff resistance value of 1.11. By increasing this to 90 R.M.S., we succeeded in increasing the scuff resistance to 1.33. After operating a 90 R.M.S. finish for approximately fifty hours at normal out-put, however, the R.M.S. finish was reduced to 20, and when this was again given the scuff test the value was back to 1.11. It might also be mentioned that the piston rings were worn badly with the 90 R.M.S. finish apparently from cutting wear. This brings up the point that if such rough finishes can be incorporated, without the sharp edges, scuff resistance might be improved without increasing wear of the mating part. Previously it was mentioned that

TABLE 3

Compositions of Irons Reported in Table 1

No.	TC	Si	P	S	Mn	Cr	Ni	Cu	Mo
				Type D Graphite (a)					
1(c)	3.20	2.20	0.15	0.04	0.65	0.25	0.30	0.30	0.15
2	3.08	2.34	0.110	0.033	0.68	0.45	0.56	--	0.22
3	3.43	2.28	0.143	0.068	0.73	0.44	0.09	1.29	--
				Type A Fine Graphite(b)					
1	3.38	1.99	--	--	0.61	0.45	0.59	1.63	--
2	3.28	2.46	0.23	0.068	0.70	0.24	0.27	0.94	--
3(c)	3.35	2.20	0.12	0.09	0.70	0.35	0.12	1.15	--
4	3.28	2.08	0.125	0.067	0.67	--	--	0.40	--
5	3.12	2.67	0.176	0.047	0.35	0.38	0.27	1.23	0.11
				Type A Coarse Graphite					
1	4.00	1.54	0.056	0.023	0.77	--	1.39	--	0.42

(a) Corresponds to test 2 in Table 1. (b) Corresponds to tests 3 and 4 in Table 1. (c) Typical composition.

valve guides made of type D graphite iron resulted in sticking from galling. One of the corrective measures taken amounted to a type of tapped hole followed by a ream. The actual surface is shown in Figure 10. Since going to this finish, and incidentally type A graphite, and a pearlitic microstructure, no trouble with valve sticking or excessive guide wear has occurred. A similar type of surface, namely knurling followed by honing has been used on cylinder liners by one manufacturer. These surfaces obviously increase the lubrication, and it is probable that this is the principle reason they increase scuff resistance.

It has been realized for many years that the initial surface finish has a great deal to do with successful break in. Surfaces rougher than those ultimately achieved with running assist break in. Apparently the rougher surfaces cause faster wear, and accelerate mating during the break in period. At the same time they give improved lubrication, and prevent scuffing. In the case of diesel cylinders, as the severity of operation is increased, it becomes necessary to exercise more control over surface finish as well as material. Typical, for example, is a 20-40 R.M.S. finish. All liners used in Detroit Diesel tests were held as close to this range as possible, except where the finish itself was studied. It appears that the coarse type A graphite material, which showed up so well in these scuff tests, might owe part of its success

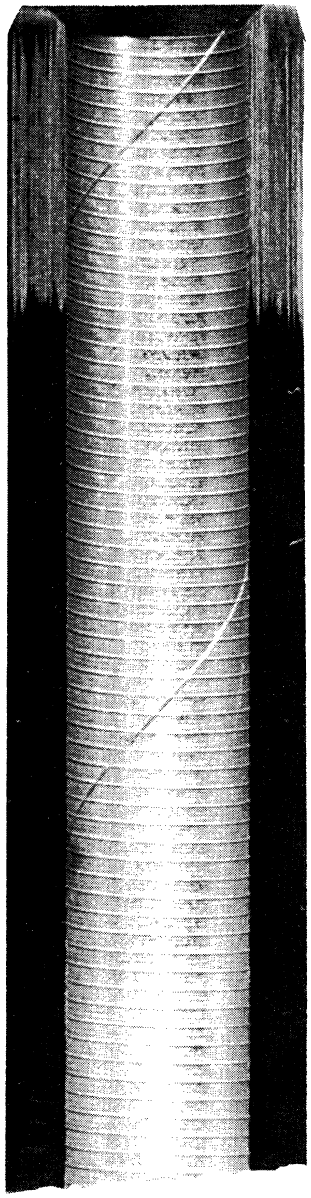

Figure 10. Longitudinal Section of Detroit Diesel Valve Guide Showing Special "tap" plus Ream Finish

to a naturally built-in service roughness, which would exist regardless of the smoothing effect of normal wear. As a check on this probability, the four graphite types tested for wear resistance were mounted in a metallographic mount, and then metallographically polished. A surface finish check was then run on the polished specimens with results as follows:

Steel	1.5 R.M.S.
Type D	4.5 R.M.S.
Medium Type A	9-11 R.M.S.
Coarse Type A	28-30 R.M.S.

Graphite Flake Size Versus Amount

More recently we have seen evidence that would indicate that the quantity of graphite is a more important factor than particle size. That is a 3.00% carbon iron with coarse size 3 flakes is not as good as a 3.50% carbon iron with fine size 6 flakes. We have no controlled test figures to show this effect as yet, however, we are regarding it as fact as a result of much experience and are using it in making current decisions. It could have the advantage of improving scuff resistance without effecting normal wear resistance, which normal wear tests show to be a problem with the coarse type A graphite iron.

Normal Wear Tests

Normal wear tests have always been difficult to run and interpret because both mating pieces have to be evaluated and in addition all factors except the one being evaluated must be held constant. Despite the best efforts to control all factors, the results are usually characterized by considerable scatter. The normal wear tests at Detroit Diesel were conducted by installing test cylinders, and new pistons, and rings in a six cylinder engine, and operating on a prescribed cycle for about 1,000 hours. For the purpose of testing cylinder materials, four chromium plated steel compression rings were used with standard pistons, and plain iron oil control rings. The engine cycle and lube oil type were held constant throughout all tests. Because of the known scatter, which occurs in this type of testing, no less than six pieces were tested of each type, and in most cases from eight to thirty. It is necessary in such testing to run for 1,000 hours to minimize the effect of fairly rapid break in wear on the results.

Effect of Graphitic Microstructure on Normal Wear

Table 4 shows the effect of graphitic microstructure on normal wear resistance. The sleeves were hardened and tempered to keep the metal matrix constant, and were made of the same types of iron as those shown in Figure 8.

TABLE 4

Effect of Type of Graphite on Wear Resistance

Test No.	Type of Graphite	Total Carbon, %	Resistance to Scuffing (a)	Sleeve Wear (b)	Ring Wear (c)
1	100% type D	3.10 to 3.40	1.11	0.003	<u>0.020</u>
2	Type A, size 4 to 6, some type B	3.25 to 3.50	1.30	<u>0.002</u>	0.027
3	Type A, size 3 to 4, some type C	4.00	<u>1.45</u>	0.0035	0.085

(a) See Table 1. (b) Inches per 1,000 hr. (c) Gap-increase, in. per 1,000 hr.

The complexity of the wear problem is demonstrated by the fact that each type was superior in one of the three categories of wear as shown by the underlined figures.

Our analysis of the results is only partially enlightening. First the ring wear appears to be proportional to the carbon content and the coarseness of the graphite. This is directly opposite to the effect of these factors on scuff resistance. It could be that a cutting action is introduced because of the inherent surface roughening effect when going to coarser graphite. High ring wear also characterized some coarse finish tests of type D which also showed better scuff resistance.

A second and less definite conclusion is the significantly higher wear of the liner of type D graphite compared to regular type A, and the greater wear of coarse type A. We were prepared for the first result on the basis that if a material tends to scuff, any disruption of the oil film should produce wear to a greater extent then on a material with less tendency to scuff. This does not however, explain the lesser amount of wear on the rings unless the low cutting wear previously referred to overshadows this scuffing effect. The still greater wear of the coarse type A graphite material is believed due to the reduction in load carrying surface as graphite is increased. Obviously a sleeve made of 100% graphite could not handle the load and would wear out very rapidly.

Similarly as the graphite is increased beyond that required to prevent scuffing, load carrying ability is reduced, and greater wear should occur. This leads to the conclusion that normal wear resistance will be sacrificed if more and coarser graphite is present than is required to eliminate scuffing.

Effect of Composition and Matrix on Normal Wear

Matrix microstructure effects on normal wear resistance were not approached with the systematic study that was used in evaluating graphite effects. Part of this was due to the reluctance to evaluate microstructures known to be inferior. In previous years many tests had been run on unhardened pearlitic cast iron in hardness ranges from about 190 to 250 Brinell. The best of these tests showed wear on the order of twice that obtained with hardened material. These results are confirmed by other investigations.[8,9] In addition, the Diesel results exhibited considerable scatter with the poorest showing very accelerated wear rates. These results merely indicated that unhardened pearlitic microstructures were unacceptable for our specific cylinder application. The largest usage of cast iron in wear resistant applications, however, has been with unhardened pearlitic microstructures containing small amounts or even large amounts of ferrite. Automotive gasoline engines utilize 30,000 PSI iron cylinder blocks with integral cylinder bores. Our 30,000 PSI iron cylinder heads have three 1-1/16" bored holes per cylinder in which slides a steel cam follower body. Our valve guides, and those of most automotive engines are made of as cast gray iron. Experience has shown that pearlitic type A gray iron of about 200 to 250 Brinell in hardness gives optimum performance in unhardened microstructures. The amount of ferrite and the degree of departure from type A graphite which can be tolerated is a function of the severity of application. The section sizes of the design, and the design complexity must be matched with composition in order to achieve the desired microstructure in such applications. The ferritic type D graphite structure is undoubtedly the poorest of all gray iron microstructures for wear resistance.

Some of the effects of metal matrix, hardness, and composition in the cylinder tests run at Detroit Diesel are shown in Table 5.

The first 5 columns represent materials hardened and tempered to produce the same martensitic metal matrix structure. The actual matrix hardness in each material was about 60 Rockwell "C" as determined by micro hardness measurements. The lower hardness values shown are due to the effect of the soft graphite on conventional hardness measurements.

The variations in chemical analysis of the first four materials were not sufficient to cause perceptible changes in microstructure when hardened. The results show that the wearing characteristics were not significantly effected by these changes in composition.

The fifth material however, with the high carbon content and coarse graphite significantly effected wear resistance as previously

Table 5

Affect of Some Variables on Normal
Wear Resistance of Type A Graphite Materials

Type	Hardened and Tempered at 400°F					Tempered at 950°F Chrome Copper	Not Hardened Manganese Phosphorus
	Plain	Chrome	Chrome Copper	Chrome Copper Moly.	High Carbon Nickel Moly.		
Chemistry							
TC	3.28	3.41	3.35	3.12	4.00		3.35
Si	2.08	1.93	2.20	2.67	1.54		2.33
Mn	.67	.71	.70	.35	.77	Analysis	1.75
P	.125	.148	.12	.176	.056	Not	1.24
S	.067	.055	.09	.047	.023	Recorded	.030
Ni	-	.20	.12	.27	1.39		.25
Cr	-	.34	.35	.38	-		.66
Mo	-	-	-	.11	.42		.28
Cu	.40	.38	1.15	1.23	-		.95
Hardness after Hardening Rockwell "C"	52	45-46	45	46-47	32	38	302 Brinell
Quantity Tested	11	13	23	16	6	6	8
Liner Wear I.P.T.H.	.0024	.0021	.0020	.0021	.0035	.0015	.0012
Compression Ring Wear I.P.T.H.	Not Record-ed	Reported Normal	.027	.036	.085	.019	.006

noted. The effect on the hardness of this appreciable quantity of graphite is clearly indicated by the low Rockwell "C" hardness of 32. As previously stated micro hardness readings of the metal matrix showed it to be approximately 60 Rockwell "C".

The sixth column shows the result of a test of the material composition in column three, except the tempering temperature was increased from 400°F to 950°F, thereby softening the material. The purpose of this test was to evaluate maximum strength instead of maximum hardness. It was reasoned, as previously stated, that less material would be worn away if the base metal was stronger and the fracturing of the micro welds, during wear, occurred in the weld itself without pulling particles from the underlying base metal.

It would appear from these results that the theory is correct. A great deal more work is required, however, to determine whether these results will repeat in operating field engines where the possibility of entrained abrasives in the lubricant is greater than in test engines. Certainly these results are a distinct departure from the widespread belief that the greater the hardness the less will be the wear.

The last column is even more surprising. Here an as cast material containing an exceptionally large amount of phosphorus and manganese with a hardness of only about 30 Rockwell "C" showed about half the cylinder wear and 1/5 the piston ring wear of the standard hardened cylinders. Again the change in composition produced a significant change in microstructure. Figure 11 shows the large amount of phosphorus eutectic (steadite) scattered through the microstructure. It has long been recognized that phosphorus has a beneficial effect on wear resistance, however, it has had a reputation for unreliability. It is believed that if the eutectic forms a continuous network in the microstructure the wear results will be poor. To minimize this possibility the quantity is usually held to about .5%. In this case the quantity is 1.24% and it is scattered throughout so that no continuous network has formed. The eutectic is over 50 Rockwell "C" in hardness, and has a relatively low melting point of about 1750°F. Any welds formed with steadite would undoubtedly be weak. These properties would be expected to give good wear results, and in this case they were exceptional. Unfortunately the material is more expensive to produce, and is difficult to machine. There is also a possibility that under abrasive conditions its performance would not be as good. The results, however, clearly point out some exceptional characteristics of phosphorus on the wear resistance of cast iron.

The conclusions from the Detroit Diesel tests agree with those of other investigators in a general way, however, there are some exceptions. The principle points are as follows:

As the microstructure is pushed toward coarse type A graphite and larger quantities and the surface finish is made rougher, scuff resistance increases, but normal wear especially for the mating part becomes greater. A compromise is therefore necessary.

High Phosphorus, High Manganese, Cylinder Iron

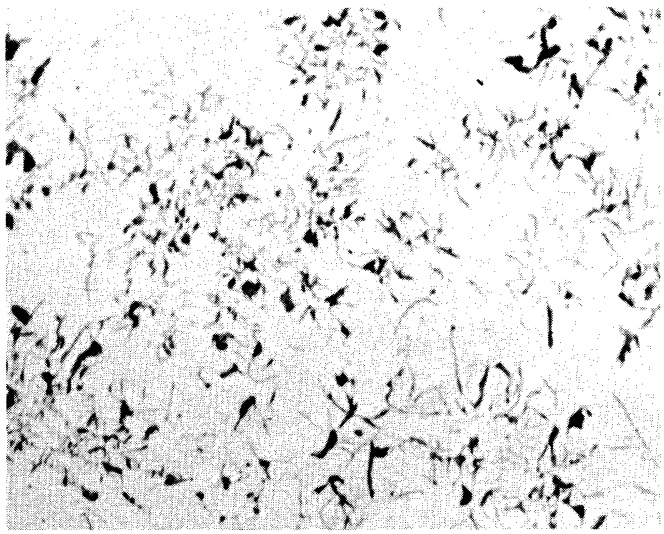

Unetched X 100

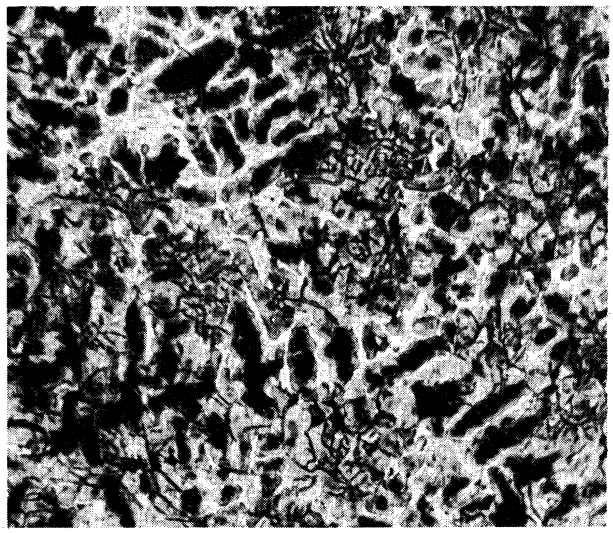

Etched X 100

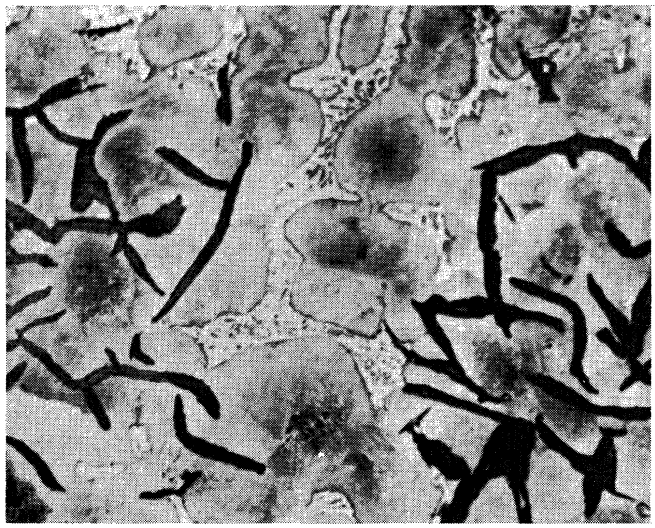

Etched X 500

Composition

Total Carbon	3.35
Silicon	2.33
Sulfur	.030
Phosphorus	1.24
Manganese	1.75
Chromium	.66
Nickel	.25
Copper	.95
Molybdenum	.28
Hardness	302 Brinnell
Tensile Strength	29,500 -31,100

Scuff resistance is related to metal matrix microstructure in that an intermediate hardness range of about 250 to 300 Brinell gives best results. There is also evidence that normal wear resistance might be better in some instances at hardness levels corresponding to maximum strength instead of at the maximum hardness achievable by heat treatment.

Chemical composition as such does not effect wear resistance unless it produces changes in either the graphitic or metal matrix microstructure.

A general recommendation is that in sliding parts where wear resistance is a critical factor, such as engine cylinders, valve guides, and latheways, the iron should be specified by microstructure with the composition a secondary consideration. A good starting point is a pearlitic matrix, type A, medium graphite size 4 to 6, and a hardness of 200 to 250 Brinell to allow reasonably good machining characteristics. The carbon content should be in the range of 3.00 to 3.50%.

The employment of heat treatment and changes in graphite size, type, and amount, as well as alterations in surface finish can be made to accomodate problems which arise, if any.

To make this paper complete it should be emphasized that the data given shows specific results for one application. It would be erroneous to assume that the optimum materials indicated would be optimum for all applications. The results are useful in pointing out steps which might be taken to solve problems in other applications.

REFERENCES

1. Burwell, J.T., Wear Tests and Service Performance Interpretations of Tests and Correlation with Service, American Society for Metals, 1951.

2. Metals Handbook, 1955 Supplement, American Society for Metals.

3. Gray Iron Castings Handbook, 1958 Edition, Gray Iron Founders Society.

4. Bowden, F.P. and Tabor, D., Mechanical Wear, American Society for Metals, 1950.

5. Shuck, A.B., A Laboratory Evaluation of Some Automotive Cast Irons, Transactions American Foundrymen's Society, 1948.

6. Lane, P., Bore Wear from the Viewpoint of Materials, SAE Journal, Vol. 45, No. 4, 1939.

7. Sefing, F.G., On Wear Resistance of Gray Iron, ASME Petroleum Engineering Conference, Tulsa, Oklahoma, October, 1946.

8. Eagan, T.E., Wear as Applied Particularly to Cylinders and Piston Rings, Cooper Bessemer, 1948.

9. Phillips, G.P., Hardened Gray Iron, Foundry, January, 1952.

RESIDUAL STRESSES IN METAL CUTTING

L. V. Colwell
Professor of Mechanical Engineering
University of Michigan

RESIDUAL STRESSES IN METAL CUTTING

By

L. V. Colwell

SURFACES PRODUCED BY MANUFACTURING PROCESSES

As we have seen, many things can happen to surfaces to either impair or improve their usefulness in engineering structures. The purpose of this paper is to explore the role of manufacturing processes in this problem. Casting and plastic working operations are relatively better understood so the majority of this discussion will be devoted to machining and grinding.

The nature, mechanisms and extent of surface damage from metal cutting operations are far from being completely understood, although some positive evidence is available and this will be discussed in the latter part of the paper. Prior to this it appears desirable to review the nature of metal cutting as a background against which surface damage evidence can be evaluated.

Metal cutting behavior will be presented in the form of a few examples of experimental data plus a discussion of basic mechanics as they are now understood. Surface damage will be discussed under three headings as surface finish, subsurface strain, and residual stresses.

Part I: The Nature of Metal Cutting

Figure 1 is a simple schematic of an idealized cross section of a cut. Three zones of significance are identified by the letters A, B and C. Zone A is the chip-tool interface which is characterized by high temperature, pressure and rubbing velocity. This region is known to be highly sensitive to friction which in turn exerts considerable influence on stress distribution and resultant strains as will be shown a little later.

Zone B represents the flank of the tool where the relief angle determines the clearance space between the tool and the cut surface. Elastic relaxation of the work material can cause substantial rubbing of the cut surface against the tool. This in turn produces varied results in the work ranging from high residual tensile stresses and surface tears to a highly burnished surface with at least moderate compressive residual stresses.

Zone C is known as the shear zone since the work material is caused to flow in shear in forming the chip. It is a region of high energy release where behavior is sensitive both to physical properties of the work material and to friction conditions in Zone A at the chip-tool interface. An analysis of these relationships will be developed after taking a look at a few practical examples of the significance of these three zones.

Examples of Chip Formation

Figure 2 shows a common type of chip formation which causes extensive surface damage. The built-up-edge or "tool loading" dominates cutting behavior when it is present. It is the result of very high friction between the chip and the cutting tool. The high friction can appropriately be characterized as a property of the material being cut in this instance.

It can be seen that the built-up-edge takes over the "stress-raiser" function of the cutting edge with the result that permanent strain extends below the cut surface. Note the presence of flow-lines in individual grains remote from the cutting zone and the already cut and smeared work surface. The built-up-edge probably is the most important single factor of metal cutting from the viewpoint of surface damage. It is very common in cutting all face-centered-cubic metals as well as in cutting all ferrous alloys except cast iron. Whenever a built-up-edge is present, poor surface finish and tears can be expected.

Figure 3 shows the results of a micro-hardness survey[1]* of the same stainless steel chip shown in Figure 2. Note the sharp increase in hardness within an interval of 0.001 inches in crossing the shear zone. The smear-metal on the cut surface can be expected to be equally hard although readings could not be made close enough to the surface to confirm this. Note also the very high hardness of the built-up-edge. This is a good example of the interdependent relationships between Zones A and C, and the surface damage that can result both directly and indirectly from high friction in the chip-tool interface.

Figure 4 on the other hand is a good example of the results of rubbing in Zone B[2]. These are photos of internal broaches used to broach holes in titanium. Despite the relative slipperiness of titanium, the one-half degree relief angle of the broach in the upper photo combined with the lower modulus of titanium to produce smearing which was reflected in damage to the work surface. This condition was reduced considerably by increasing the relief angle to 5° as shown in the lower photos of Figure 4.

Figure 5 shows three more examples of chip formation where a built-up-edge is not involved. The condition shown at the right is described as a continuous chip wherein cutting is quite smooth and there will be little surface damage beyond superficial hardening which could actually prove to be advantageous if the residual stresses are compressive. Most of the surface damage created by cutting in the absence of a built-up-edge will be either roughness associated with chip segmentation as shown in the middle of Figure 5 or with warpage resulting from either tensile or compressive residual stresses.

---

* Numbers in parentheses indicate references cited in the Bibliography.

Mechanics of Metal Cutting

Figure 6 shows examples of actual chips obtained in cutting titanium. These were selected as illustrations for two reasons. First, because the friction between the chip and the tool was low enough so that a built-up-edge was not formed, yet it appeared to be on the verge of forming as indicated by the "secondary shear" cracks appearing on the underside of the chips. The other reason was the similarity between location of the cracks and the position of planes of principal shear stress as proposed by M. C. Shaw et al[3], as shown at the bottom of Figure 6. Attention is called to this apparent correlation because competent investigators have not yet been able to agree upon the fundamental mechanics of metal cutting in relating causes and effects.

Force relationships in metal cutting are illustrated for simple orthogonal cuts in Figure 7. This figure is representative of most metal cutting conditions except for the use of a secondary rake angle, α' which can limit the contact area represented by the width "w."

Let us consider first the case where the secondary rake is equal to the primary rake and "w" will not be limited by availability of tool surface. In this case the shear stress on the shear plane can be written as a function of applied forces, shear angle, rake angle and coefficient of friction. If this equation is differentiated with respect to the shear angle as was done by Merchant[4,5], it leads to the simple conclusion that

$$2\varphi = 90 - \beta + \alpha \qquad (1)$$

where the tangent of β is the coefficient of friction between the chip and the cutting tool.

Recent work with limited contact tools[6,7] appears to indicate that the relationship of Equation (1) tends to exaggerate the influence of the rake angle. If this be true, its fundamental significance arises from an inaccurate description of the frictional forces. Still more recent work by the author[1] tends to support the contention by Takeyama[7] that the frictional component of force in metal cutting is:

$$T = w\tau \qquad (2)$$

where "w" represents the actual contact area between the chip and the cutting tool and "τ" is the shear-flow stress of the work material.

The author has analyzed the mechanics of limited contact tools and has arrived at the rather complex relationship:

$$\tan \varphi = \frac{t \sin \alpha + \sqrt{t^2 + wt \cos \alpha}}{w + t \cos \alpha} \qquad (3)$$

This equation comes closer to predicting the measured shear angles plotted in Figure 8, but the relationship is still somewhat misleading since further analysis of experimental results indicate that the shear stress in the chip-tool interface approaches the flow stress but equals it only at rather special conditions.

Measured values of cutting forces indicate they can change appreciably with tool wear as illustrated in Figure 9.[8] Consequently, analyses of the mechanics of metal cutting must progress to a higher degree of refinement and dependability before they can be relied upon as a basis for interpreting such changes as those plotted in Figure 9.

Cutting Temperature

Figures 10, 11, 12, and 13 are examples of several types of information concerning temperatures in metal cutting. Figure 10 shows the temperature distribution calculated by Chao and Trigger[9] for the chip-tool interface. The results bear a striking similarity to observed behavior in cratering of the rake face and lead to the interesting observation that tool wear may be influenced strongly by temperature dependent diffusion.

Figure 11 shows a correlation between temperature measurements and actual tool life data.[2] This further supports the concept of temperature dependent tool wear and is not inconsistent with the results displayed in Figure 9 since increased rate of wear as the result of higher temperature simply hastens the approach to the same type of structural failure. The point in Figure 11 for the 130-B titanium points up this material as a non-conformist. This is associated with the fact that this alloy cut with a stick-slip motion as indicated at the center in Figure 5. Consequently, the measured temperature also fluctuated and the ballistic average produced a reading significantly lower than the dominant peaks.

Figure 12 shows an interesting analysis by Chao and Trigger[10] for tools with limited contact area. Practical interpretation of these results concludes that cutting temperature can be influenced significantly by both Zone A and Zone C as indicated by Curves 2 and 3. Up to this point in the discussion, cutting temperature has derived its significance from the fact that higher temperatures accelerate tool wear which in turn influences cutting forces and stresses which directly influence residual stresses and other forms of surface damage by mechanical means.

Temperature can cause damage directly if it is high enough as in grinding. Typical grinding temperatures are illustrated in Figure 13[11] where oscilloscope traces of thermocouple outputs are reproduced for two grinding conditions. Curve 2 is for conventional grinding while Curve 1 represents the effects of superimposing high frequency vibrations on the operation. The reduction in temperature was attributed to:

1. High radiation losses,
2. Higher average sharpness of the abrasive grains, and
3. Smaller built-up-edges and lower wheel loading.

Cutting Forces

Figures 14, 15 and 16 contain representative cutting force information relevant to metal cutting behavior and surface damage. Figures 14 and 15 show typical feeding force results for bandsawing[12] and for form-turning in automatic screw machines. Two conclusions can be drawn from these illustrations:

1. Feeding forces can increase many times during the useful life of a cutting edge, and
2. Residual stresses will change considerably as a result of change in feeding force.

The second conclusion is borne out by experiment and can be predicted by application of Hertzian equations.

Figure 16 is a slightly idealized version of experimental cutting force data obtained with cutting tools having limited contact area. These results indicate that the friction component of cutting force is a function of the shear-flow stress of the metal being cut. The actual, unmodified or unsimplified data also indicate that there is a pronounced strain-rate or velocity effect which can be interpreted in various ways.

Tool Life

Tool life can have many different bases and meanings depending upon the conditions to be controlled. Several examples are discussed in the literature[13,14], and time will not be taken to elaborate on them here. It will be sufficient to point out that some of the bases are in themselves measures of surface or product damage; these are represented in part by the laboratory data shown in Figures 17 to 20 inclusive.

Part II: Surface Damage

Several examples of metal cutting behavior have been cited for the purpose of providing some understanding of the nature of the process and its dependency upon materials properties and cutting conditions. There has been no particular emphasis placed on differences between machining and grinding since it is believed that both processes are influenced by essentially the same factors. Grinding differs only in that high temperature can damage surfaces directly in what might be called thermal-damage. However, the author has chosen to classify all damage resulting from machining operations as:

1. Surface defects,
2. Sub-surface strains, or
3. Residual stresses.

Surface Defects

Both roughness and tears or cracks may be classified as surface defects although the former lends itself reasonably well to measurement and can be demonstrated as an asset in some functional applications. Any tears or cracks, however, can be expected to diminish the quality of a product.

Figure 21 is an example of good and bad surface finish wherein the difference is primarily in the size of the tears produced during a typical finish turning cut on a medium carbon steel forging. The surface shown at the right involves tears large enough to reduce the fatigue life of the product despite subsequent roll-burnishing; this is surface damage.

Figure 22 shows another finish-turned surface on which the application of ultrasonic vibration reduced friction to the point where tears appear to be eliminated. That high friction is the cause of surface-tears appears to be substantiated both by experiment and analysis. A further example of the improvement resulting from reduced friction is shown in Figure 23 for surfaces ground with and without high frequency vibration.

High frequency vibrations also influence the incidence of thermal damage as indicated by the cracks appearing in ground surfaces of the AISI 52100 steel specimens in Figure 24. Here the improvement results from a reduction in the time during which the surface is subjected to elevated temperature; a similar effect is illustrated later in Figure 31.

Subsurface Strains

Subsurface strains are important only to the extent that they impose limits on the load carrying capacity of a structure. From this viewpoint such strains may be either good or bad. depending upon whether the loading of the structure is either static or alternating. Examples of subsurface strains in metal cutting are illustrated in Figures 25 and 26.

The scribed grid of Figure 25 shows that visible strain of the work piece extends at least as deep as the cut below the machined surface in such ductile materials as 18-8 stainless steel. The other extreme is demonstrated in Figure 26 where permanent strain still is in evidence for such slippery materials as titanium.

Residual Stresses in Metal Cutting

The purpose of this section of Part II of the paper is to make a critical review of the work that has been done on the relation of residual stresses to metal cutting processes with the further objective of evaluating progress toward the ultimate understanding and solutions to this intriguing problem. Awareness of the existence of the problem appears to have developed almost concurrently with the development of machining processes;

this is indicated in early references to the warpage of castings after machining. Former practice in the automotive industry of the USA found huge inventories of motor blocks in storage yards between machining operations. A few months of aging was needed to relax both machining and casting stresses.

The advent of interchangeable manufacture with ever smaller tolerances, and higher load-carrying capacities or smaller safety factors changed the phenomena of residual stresses from a curiosity to an engineering problem thus stimulating investigation into their nature, causes, and effects. Until quite recently, however, most research in this area has been directed at the effects of residual stresses on the functional qualities of manufactured products with little attention being given to metal cutting processes as causes. The majority of publications treating residual stresses in metal cutting are concerned with grinding; there are very vew devoted to what might be called "thick-chip operations."

Two major topics will be discussed in this review; experimental evidence and theory or mechanisms of creating residual stresses in metal cutting. Reference is limited to publications within the last forty years. Space and time limitations prevent discussion of all significant contributions during this time interval. Mention is made of only a few typical disclosures which characterize the development and state of knowledge of the problem.

Experimental Evidence

Although they overlap considerably, one can recognize four distinct historical periods in the accumulation of experimental evidence. Each of these periods is dominated by a different experimental technique, all of which are still useful. In sequence of appearance they are:

1. Work-hardening by hardness determinations
2. Work hardening by X-Ray
3. Dominant stress by warpage or specimen distortion
4. Stress distribution by differential metal removal.

Early investigators were aware of the severe distortion which metal cutting causes at the machined surface. However, they were inclined to characterize the result simply as work-hardening. If they appreciated the complex stress distribution associated with this hardening it does not appear in their writings. Thus, it appears that progress in residual stress can be characterized as a gradual increase in awareness of the complexity of actual stress distribution.

Work-Hardening by Hardness Measurements

Hardness measurements constitute the earliest quantitative evidence of residual stress caused by machining. E. G. Herbert[16] reported in 1926 that "metals are hardened by any process which deforms them so as to cause a permanent change of shape while they are at low or moderate

temperature." He identified this effect with his Pendulum hardness tests on both the chips and the cut surface. His primary concern, however, was with the correlation of tool life to work-hardening capacity. His most significant conclusion with reference to cutting practice was "an obtuse-angle tool would harden the chip more"; thus, indicating greater work-hardening of the work surface as well.

In 1932, T. G. Digges[17] reported on "work-hardening near the machined surface of steel forgings." Like Herbert's work, this study involved lathe turning and hardness surveys. Digges concluded:

1. "The amount of work-hardening was not influenced by changes in cutting speed."
2. "With a given area of cut, the amount of work hardening was affected equally by changes in the feed or depth of cut."
3. "The maximum hardness developed at the surface by machining decreased rapidly with increasing carbon contents of the steels up to 0.4 percent carbon and thereafter less rapidly--."

Hardness measurements continue to be a convenient though oversimplified indication of the presence of residual stresses in machined surfaces. The recent development of the micro-hardness tester has augmented the usefulness of this technique as a means of identifying significant trends arising from changes in cutting practice. Figure 27 shows the results of a study made by Dr. W. W. Gilbert in the Production Engineering Laboratories at the University of Michigan. Micro-hardness tests were made on planes perpendicular to the axis of drilled holes. Increased hardness is seen to result from the cutting action by both sharp and dull drills with greater increases and greater penetration being associated with dull drills. The same type of result was observed for a range of titanium alloys and carbon steel as well as for the 18-8 stainless steel as portrayed in Figure 27.

Many other investigators have contributed hardness data on this subject and most are in agreement that metal cutting does indeed harden the cut surface except in grinding where the hardness has been observed either to increase or to decrease depending upon grinding conditions. The increasing mass of work-hardening evidence has produced certain anomalies which have prompted some investigators to question interpretation of hardness measurements in such cases. This situation has stimulated recent investigations in this area.[18-20] In uniform stress situations it can be expected that residual tension parallel to a surface will decrease hardness while residual compression would increase it. On this basis one would conclude that all work-hardened surfaces represented residual compression. Such a conclusion is fundamentally unsound since a work-hardened surface in which the residual stress is dominantly tension can exhibit either an increase or a decrease in measured hardness depending upon the amount of shear strain, the rate of strain-strengthening,

the depth affected and the amount of relaxation after cutting. This problem is not yet solved and merits considerable attention because of the large volume of hardness data available and the convenience of the hardness test for future studies.

Work-Hardening by X-Ray

X-ray techniques have also been used to study the effects of metal cutting on the resulting surfaces. Here again the earlier references mention work-hardening or cold work in characterizing these effects. Thomassen and McCutcheon[21] used X-ray on turned and milled specimens of leaded, free-machining brass and 70-30 brass respectively. They noted marked sensitivity to feed rate or thickness of chip but failed to confirm Digges'[17] observation of equal sensitivity to depth of cut. One of the more important findings of this study was that a "dull" milling cutter increased the depth of cold work by 300 percent over that created by a sharp cutter.

Dr. A. O. Schmidt and his associates[22,23], have also made extensive use of X-ray for studying the effects of a wide range of materials and cutting conditions. These results indicate increasing amounts of work-hardening with larger cuts and decreases when either the rake angles or the cutting speeds are increased. The total results indicate sensitivity to total strain and strain rate respectively.

Only recently have X-ray techniques developed to the point where this method is dependable for resolving the distribution of residual stresses in machined surfaces. Some investigators have expressed doubts to the author as to the ability of X-ray to follow the rapidly varying stresses in ground surfaces. This fact, if it be a fact, coupled with the time required for X-ray evaluations tends to limit the usefulness of this method for all but the most exacting studies.

The Warpage Era

Dr. George Sachs[36] has done much to promote the use of warpage or curvature change techniques in investigating residual stresses. When coupled with etching or similar differential processes of metal removal, this approach can resolve the stress distribution quite satisfactorily. However, etching is slow, expensive and difficult to control. For this reason, the total warpage of a part or test specimen is used as a quick indication of trends in residual stress distribution resulting from changes in cutting practice.

Professor Henriksen[24] used this technique in the studies which he reported in 1934. This was an extensive investigation with single-point tools in planing cuts on low carbon steels. It was concluded that the dominant stress was tension and Henriksen suggested a plausible mechanism

for this type of result. Disregarding the type of stress and considering it only as cold work, his results agree with other investigators; notably Digges.[17] Henriksen was puzzled, however, by the existence of an optimum normal rake angle for side cutting tools whereas the stress continued to decrease with increasing normal rake with square ended tools. This difference could be attributed to changes in lateral direction of the resultant cutting force with the side cutting tool. However, this is pure speculation until more is known about the actual distribution of stresses and the mechanism of their formation.

The author has made several exploratory studies of residual stresses as secondary activities in connection with other investigations in the Production Engineering Laboratories at the University of Michigan. Since they were secondary objectives, total curvature changes were used as gross indications of the predominant stress. Mention of a couple of these will serve to emphasize the broad scope of results which can be obtained.

Figure 28 shows a representative torque-time chart obtained for reaming steel at different lubricating conditions. Upon initiating cutting, the torque increased rapidly to a value determined by the size of cut. When cutting dry and in the presence of a built-up-edge, the torque did not increase beyond this point. Curvature changes resulting from longitudinal saw cuts on the reamed bushing indicated a dominance of residual tensile stress at the reamed surface.

On the other hand, the use of carbon tetrachloride as a cutting fluid eliminated the built-up-edge and caused considerable rubbing on the margin of the reamer resulting in a smaller, more accurate hole, a smoothed burnished surface and dominant residual compressive stress. Thus despite an increase in tangential rubbing which was expected to increase tension, just the opposite occurred. It is possible that the considerable normal pressure between the reamer margin and the wall of the hole brought about this stress reversal.

Following the above result another series of tests were made on the same low carbon steel while using a chemical emulsion as a cutting fluid. The torque measurements are plotted in Figure 29. In this series the effectiveness of the fluid in reducing the built-up-edge decreased at higher feeds. Residual stress analysis showed a gradual change from dominant compression at the lowest feed to dominant tension at the highest feed. Further, the rate of change in the tensile direction was faster than was observed for increased feeds while reaming dry.

Similar studies by the author with single point tool operations on magnesium and aluminum reveal that either dominant compressive stress or dominant tensile stress will be caused by cutting. The type and magnitude of stress appears to depend primarily on tool shape and condition coupled with cutting speed, size of cut, and the degree of lubrication in effect between the flank of the tool and the cut surface. It was tentatively concluded that:

1. Negative rake, sharp tools produce compressive stress.
2. Large-positive-rake tools produce tensile stress.
3. Sharp-nosed tools produce strong compressive stress lateral to the cutting direction.
4. Light feed and well-lubricated tool flank produces compressive stress.
5. "Smear-metal" on tool flanks produces very high tensile stresses.
6. Worn or dulled tool flanks produce either compression or tension depending on the degree of lubrication, type of tool wear (polished or abraded) and the ratio of the modulus of elasticity of the tool material to that of the metal being cut.

Complete interpretation of residual stress behavior from gross curvature changes is hazardous and may lead to incorrect conclusions since differences in curvature change may be accompanied by radical changes in the type of stress distribution.

Actual Stress Distribution

Some of the most careful work on residual stresses produced by metal cutting has been in the area of precision grinding. Dr. H. R. Letner[28] has contributed several notable publications on this subject from the results obtained at the Mellon Institute in Pittsburgh, Penn. The principal objective of his work was to assess the effects of practical variables but the thoroughness of his techniques has thrown considerable light on the probable mechanisms of producing residual stresses by all types of metal cutting operations.

Figure 30 is a generalized curve of residual stress distribution in grinding as obtained by Dr. Letner and by Colwell, Sinnot and Tobin[29]. This qualitative curve represents all of the different effects which have been observed in surface grinding wherein the wheel traverses the work surface and portions of the wheel travel over the same area several times resulting in rubbing. Tensile stresses are plotted above the horizontal line and compressive stresses below the same line.

Four distinct causes of stress are identified. Proceeding from the right within the metal to the left toward the surface the first zone encountered is labeled TC to designate a thermal effect resulting from the cutting pass during grinding. The next section which turns abruptly toward the compressive direction is labeled MC designating mechanical effect from the cutting pass. This is followed by a steep trend toward the tensile direction which is labeled TR designating a thermal reaction to rubbing near the surface. The final source is a mechanical or compressive trend labeled MR designating a mechanical or compressive reaction to the same rubbing. This is the author's interpretation and it does not agree in every respect with Dr. Letner's interpretation of the corresponding sections.

Dr Letner has indicated that he believes the section labeled TR is thermal but that it is the result of the original grinding or cutting pass while both of the sections labeled MC and TC, respectively, are the result of the mechanical reaction to the external forces applied to the surface. This, too, is a rational and theoretically sound interpretation; more investigation and analysis is required before this question can be resolved.

Both Dr. Letner and the author have obtained many distribution curves including only the TC and MC sections. The addition of the third section designated as TR is representative of more severe grinding conditions bordering on the condition commonly known as "burning." Halverstadt[30] and Clorite and Reed[31] have reported similar distributions for the grinding of high temperature alloys and titanium, respectively.

The warpage approach is relatively simple and has been used by several investigators to reveal the more fruitful areas for more rigorous analysis. One such result is shown plotted qualitatively in Figure 31. Here the dominant stress from grinding varies with the work speed; other factors were held constant in surface grinding full hard AISI 4340 steel. At slow speeds the theoretical chip thickness is very small so that rubbing increases power requirements and excess heat coupled with slow movement of the heat source creates very high tensile stresses. This effect drops off rapidly as increasing work speed increases the chip thickness and the speed of the heat source across the ground surface.

The above trend may cause the dominant stress to drop into the compressive range before more rapid dulling of the abrasive grains halts and reverses it. The reverse trend toward the tensile stress region will continue with further increases in work speed until the larger chips create forces large enough to overcome the bond posts and expose sharp abrasive grains. At higher work speeds the abrasive wheel becomes increasingly "self-dressing" and the dominant residual stress will remain in or near the compressive region.

Possible Mechanisms

The mechanisms which create residual stresses in machined and ground surfaces are not at all well understood. However, tentative conclusions can be drawn from the experimental evidence available in the literature. It will be well to supplement these with some speculation as to the possible but not necessarily probable mechanisms in the hope that this will stimulate some critical thought on the subject. It is suggested that the sources or causes of residual stresses be separated into two groups identified as thermal and mechanical. It will be proposed that the thermal source always creates residual tensile stresses and that mechanical sources can create either tension or compression depending upon the conditions prevailing.

The Thermal Mechanism

The author has carried on a number of investigations which indicate a dependency of residual stresses to the shape of the heat source in grinding. This same characteristic has been noticed in the production shop.

The basic mechanism is the same as that which occurs in the quenching of a part which is being hardened by heat treating; differential rates of cooling create residual stresses resulting in warpage of the part. Those areas which cool faster wind up with residual tensile stresses; essentially, the same thing happens in grinding. If a point source of heat is applied alternately to all portions of a surface even though at different times, it will create tensile stresses parallel to the surface and equal in all directions and this will cause a thin part of uniform section to warp into a spherical surface with the same curvature in all directions.

On the other hand, if the surface is heated up in a narrow band across the entire surface, then subsequent quenching will result in warpage or curvature in only one direction; this will be perpendicular to the band or line.

In traverse grinding the hot zone is relatively small and substantially circular in shape so that it might be characterized as a point source. In plunge grinding, on the other hand, metal is being cut all the way across the tool face resulting in substantially a line source of heat. This condition would prevail in cylindrical grinding wherein the abrasive wheel was fed in radially to the work. In this case, if the thermal conditions were sufficiently severe, the resulting cracks would be parallel to the axis of the workpiece.

Figure 32 shows the results of a recent laboratory investigation carried out by the author wherein relatively thin specimens capable of warping were surface ground in a traverse type of grinding action. The resulting curvatures in both the grinding and traverse directions are shown plotted for a range of down feeds or thicknesses of metal removal. The two curves at the left in Figure 32 were obtained for conventional grinding practices on a high temperature alloy. The two lines shown at the right in the figure are for similar practice except for the superposition of ultrasonic vibration on the specimen being ground. The solid lines represent average curvatures in the direction of table traverse which was the same as the direction of rotation of the grinding wheel. The dashed lines represent average curvature in a perpendicular direction.

At a down feed of 0.001 inch both sets of curvature curves or lines result in a behavior approximating that to be expected from a point source of heat. As the down feed or thickness of metal removal is increased, in conventional grinding the curvature in the grinding direction increases while that across the grinding direction decreases which could be the result of a gradual change in the shape in the heat source from substantially

a point source to a line source at the heavier down feeds where it would appear that considerable energy is being released as heat due to rubbing across the entire face of the grinding wheel. In contrast to this the ultrasonic vibration appeared to inhibit the rubbing action resulting in little change in what might be characterized as an eliptical heat source over a broad range of down feed.

It is the author's opinion that any thermally induced residual stresses in metal cutting will be tensile. There may be exceptions to this generalization where structural or phase changes take place at exceptionally high temperatures. Another exception may be cited in the case of electro-spark machining wherein a combination of very high temperatures, shallow heated regions and high radiation losses have been observed to create residual compressive stresses in a very superficial zone.

Mechanical Mechanisms

The mechanical sources of residual stresses would appear to be much more complex than thermal sources. The technical literature reports both tensile and compressive stresses resulting from ordinary metal cutting operations and there can be no doubt that both have been observed at relatively low temperatures which could not have been the source of tensile stresses of the magnitude which are reported. Therefore, it is necessary that we search for mechanical mechanisms which could result in either tensile or compressive residual stresses.

A rather interesting solution to this problem can be obtained by combining recent findings in the cold rolling of steel with published observations in metal cutting more than thirty-five years ago. This author has contended that all of the theory applicable to plastic working operations like rolling, wire drawing, tube sinking and extrusion are likewise applicable to cutting ductile metals since metal cutting is also a plastic working operation and extrusion and wire drawing dies are analogous to cutting tools with very large negative rake angles. The literature references cited in this instance are by W. M. Baldwin, Jr.[32], Professor Dempster Smith[33], Professor E. G. Coker[34], and Professor S. Fukui[35].

It has been demonstrated in connection with the cold rolling of strip steel that the residual surface stresses can be either compression or tension depending upon rolling conditions. Residual compression at the surface is created by what is called non-penetrating rolling as illustrated at the top in Figure 33. There will be a shallow region of residual compressive stress on both sides of the strip with moderate tensile stress more or less uniformly distributed in between. This rolling condition has been referred to as "skin-pass," "temper-pass" and "stress-relief-pass." In any case it is accomplished with relatively small diameter rolls for any given reduction in strip thickness. Larger diameter rolls or greater reductions for a given roll diameter can result in residual surface tension with a distribution substantially as illustrated at the bottom of Figure 33.

Professor Baldwin has suggested that the differences in rolling conditions represented by these different results are analogous to the known solutions for the behavior of metal between flat dies. This behavior is illustrated in Figure 34 with a flat end tool applied to the flat surface of relatively thick strip at a, b, and c and relatively thin strip at d, e, and f. The force applied to the tool is assumed to be increased from a to b to c in the first group and from d to e to f in the second group. The progress of development of plastic zones is illustrated by the spread of cross-hatched areas.

The plastic zone with the thick strip is shallow and the operation could be characterized as non-penetrating while in the case of the thin strip the plastic zone quickly spreads clear across the sheet with increasing load on the tool. The same type of differences would be observed qualitatively if the strips were both of the same thickness but the tools were rounded on the end. A small radius would produce a shallow or non-penetrating distribution of the plastic zone, whereas a large radius approaching a flat end tool as a limit can penetrate to the center. It is quite possible that these same mechanisms with some modifications will be found to be operating in metal cutting.

There is considerable experimental evidence indicating that the non-penetrating mechanism is a major contributor in causing residual compressive stresses in metal cutting. It is reasonable to assume that the somewhat rounded corners of abrasive grains would create the same type of stress distribution superficially in the surface of the metal. Thus, we would expect residual compressive stresses to be created by such abrasive operations as lapping, honing, and even grinding except where local temperatures and heat energy are great enough to completely overcome and mask this effect.

There is increasing evidence that substantially the same condition can occur with ordinary cutting tools where a built-up-edge does not exist and elastic relaxation permits rubbing between the flank of the tool and the cut surface. As long ago as 1922 Dempster Smith[33] called attention to forces acting between the work surface and the flank of the tool. Since then, there has been a strong tendency to ignore such forces in theoretical analyses of the mechanics of metal cutting. Recent studies at the University of Michigan have demonstrated that the feeding force in a form-turning cut, see Figure 15, can increase as much as twenty times or more during the useful life of the cutting tool. This increase must be attributed almost entirely to increased contact between the flank of the tool and the workpiece.

When the cutting tool is well-lubricated in a form-turning cut as in an automatic screw machine, wear on the flank of the tool is accompanied by some plastic flow and polishing with an appreciable radius; thus, non-penetrating rolling of strip. Preliminary analysis of parts machined by form-turning indicates that increased feeding force is indeed accompanied by substantial compressive stress at the cut surface.

The mechanism for the formation of residual tensile stresses in a machined surface cannot be as simple as that set forth for penetrating rolling of strip steel. Also in 1922, Professor E. G. Coker[34] published a very interesting analysis of metal cutting behavior. He used photo-elastic techniques which indicated the presence of tensile stresses in the cut surface in back of the cutting tool during the cutting process. Similarly, Professor Fukui reported on a very thorough photo-elastic analysis in 1933, excerpts from his results are illustrated in Figure 35.

The curves in Figure 35 represent the stresses acting on the plane of the cut surface ahead of the cutting tool. It will be noted that a positive-rake tool with large contact area as shown at the left in the figure produces a tensile stress parallel to this plane and for some appreciable distance in ahead of the cutting tool. On the other hand, a zero-rake angle tool ground so as to concentrate the applied forces near the cutting edge results in high compressive stress parallel to the cut surface. These tests were made at static loading conditions and it can be expected that the friction component of cutting force would alter this distribution.

The final solution as to the mechanism of forming residual tensile stresses in the machined surface probably will require rigorous mathematical treatment of the mechanics of metal cutting as an elasto-plastic problem. This could come from an extension of the solutions obtained by theory of elasticity for a semi-infinite plate as discussed by Professor S. Timoshenko[37].

Conclusions

1. Metal cutting operations encompass broad ranges of temperature, pressure, strains, strain rate, friction and other environmental conditions which can influence the condition and quality of machined surfaces. Consequently, the results can be expected to be equally variable.
2. Significant extremes of stress, pressure, strain rate and temperature can combine in many different ways to create serious damage to surfaces during machining.
3. The most severe combinations produce tears in thick-chip cutting and cracks in grinding. The former occurs in cutting ductile metals like copper, aluminum, stainless steel and other face-centered-cubic metals. Grinding cracks are most likely to occur with brittle, hard metals at a combination of high cutting speed, low work speed and poor heat transfer conditions. The presence of residual stresses is almost incidental in either case.
4. The most significant conclusion with reference to induced residual stresses is that they can be either tension or compression.

5. Metal removal with both bonded and unbonded abrasives shows a strong tendency to produce residual compressive stresses at the surface This effect is always present. When the surface temperature and rate of release of heat energy reach high enough values, tensile stresses will be superimposed on the ever present compressive stresses. In cases of severe grinding the tensile stresses will dominate.
6. Cutting temperature does not appear to be a major factor in the creation of residual stresses by ordinary cutting tools.
7. Compressive residual stress has been observed to occur frequently in ordinary metal cutting particularly where some combination of "slippery" metals, good lubrication and low modulus of elasticity is involved.
8. "Smear" of the tool flank or work surface is invariably accompanied by high residual tension.
9. It appears that larger built-up-edges are accompanied by higher tensile stresses.
10. The relationship of residual stress to size of cut, cutting speed and tool shape is not yet clear and requires considerable investigation.

Summary

This paper has attempted to explain and in part to sell the idea that manufacturing processes are important sources of damage to their products. To this end, a partial description of metal cutting is intended to emphasize the broad latitude of machining conditions. A further objective has been to provide a critical review of information regarding machining and grinding as causes of surface damage. The subject material is derived from publications of the past forty years and from the opinions of people engaged in research on this subject in the United States. It is almost certain that either tensile stresses or compressive stresses will be created at the surface depending upon how the metal is cut. This appears to be true for both machining and grinding.

The mechanisms which produce residual stresses have not been described rigorously. High temperature can cause tensile stresses but this appears to be an important factor only in grinding. It has been demonstrated that "sharp" tools can produce compressive stress whereas "dull" or "smeared" tools result in dominant tension. Considerable research is needed before the mechanisms can be completely understood and their relation to metal cutting practices reduced to routine knowledge.

Surface tears, cracks and similar defects other than roughness cannot be evaluated numerically as readily as residual stresses. However,

they depend upon the same causes and represent more serious combinations of these causes. Consequently, most damage of this type will be brought under control when it is learned how to control the residual stresses arising from machining.

The fact that much more research is needed in this area stems from the naive attitude of the engineering profession toward the production shop; an attitude of indifference or denial of the existence of problems worthy of engineering talent. Vigorous efforts are needed and they can be expected to benefit design engineering as much as the production shop.

REFERENCES

1. Colwell, L.V., and Truckenmiller, W.E., "Cutting Characteristics of Titanium and Its Alloys," Mechanical Engineering, Vol. 75, No. 6, June, 1953, p. 461.

2. Boston, O.W., Caddell, R.M., Colwell, L.V., McKee, R.E., Packer, K.F., and Visser, P.R., "Machining Titanium," Technical Report No. 1993-16F, Detroit Ordnance District Contract No. 20-018-ORD-11918, June, 1955.

3. Shaw, M.C., Cook, N.H., and Finnie, I., "The Shear-Angle Relationship in Metal Cutting," Trans. ASME, Vol. 75, February 1953, pp. 273-288.

4. Ernst, H. and Merchant, M.E., "Chip Formation, Friction and High Quality Machined Surfaces," Surface Treatment of Metals, American Society for Metals, 1941, p. 299.

5. Merchant, M.E., "Mechanics of the Metal Cutting Process," Journal of Applied Physics, Vol. 16, 1945, pp. 267, 318.

6. Stabler, G.V., "The Fundamental Geometry of Cutting, Tools," Proceedings of the Institution of Mechanical Engineers, London, England, Vol. 165, 1951, p. 14.

7. Takeyama, H. and Usui, E., "The Effect of Tool-Chip Contact Area in Metal Machining," ASME Preprint No. 57-A-45.

8. Boston, O.W., "Machinability of Steel," ASME Metals Handbook, 1948, p. 360.

9. Chao, B.T. and Trigger, K.J., "Temperature Distribution at the Tool-Chip Interface in Metal Cutting," Trans. ASME, Vol. 77, 1955, pp. 1107-1121.

10. Chao, B.T. and Trigger, K.J., "Controlled Contact Cutting Tools," ASME Preprint No. 58-SA-42.

11. Colwell, L.V., "The Effects of High-Frequency Vibrations in Grinding," ASME Transactions, Vol. 78, No. 4, May 1956, p. 837.

12. Colwell, L.V. and McKee, R.E., "Evaluation of Bandsaw Performance," Transactions of the ASME, Vol. 76, pp. 951-960, (1954) August.

REFERENCES (CONT'D)

13. Takeyama, H., Murai, T., and Usui, E., "Study on Wear Process of Carbide Tools," Journal of Mechanical Laboratory of Japan, 2 (1956) No. 2.

14. Colwell, L.V., "Tool Life," ASTE Technical Paper No. 53, Vol. 58, 1958.

15. Colwell, L.V., "Residual Stresses in Metal Cutting," The Institution of Mechanical Engineers, Conference on Technology of Engineering Manufacture, Paper No. 56, London, England, 1958.

16. Herbert, Edward G., "Work-Hardening Properties of Metals," Transactions, The American Society of Mechanical Engineers, Vol. 48, 1926.

17. Digges, T.G., "Effect of Lathe Cutting Conditions on the Hardness of Carbon and Alloy Steels," Transactions, The American Society of Mechnical Engineers, Vol. 54, 1932.

18. Blain, P.A., "Influence of Residual Stresses on Hardness," Metal Progress, Vol. 71, January 1957, pp. 99-100.

19. Setty, S.K., Lapsley, Jr., J.T., and Thomsen, E.G., "An Investigation of the Effect of Various Stresses on Hardness," Preprint No. 57-A-77, presented at the Annual Meeting of the American Society of Mechanical Engineers, December 1957.

20. Zlatin, Norman and Merchant, M. Eugene, "The Distribution of Hardness in Chips and Machined Surfaces," Transactions, The American Society of Mechanical Engineers, Vol. 69, 1947.

21. Thomassen, L. and McCutcheon, D.M., "Use of X-Ray on Depth of Cold Work by Machining," Mechanical Engineering, Vol. 56, 1934, pp. 155-157.

22. Zankl, F., Barkow, A.G., and Schmidt, A.O., "X-Ray Diffraction as a Gage for Measuring Cold Work Produced in Milling," Transactions, The American Society of Mechanical Engineers, Vol. 69, 1947.

23. Found, G.H., "Strains Introduced by Sawing the Magnesium," Discussion: "Experimental Stress Analysis," Vol. 2, 1944.

24. Henriksen, E.K., "Residual Stresses in Machined Surfaces," Transactions of the Danish Academy of Technical Sciences, No. 7, 1948 (Copenhagen).

REFERENCES (CONT'D)

25. Branders, Henrik and Colwell, L.V., "Behavior of Cutting Fluids in Reaming Steels," Transactions, The American Society of Mechanical Engineers, Preprint No. 57-A-168, December 1957.

26. Thomsen, E.G., Lapsley, Jr., J.T., and Grassi, R.C., "Deformation Work Absorbed by the Work Piece During Metal Cutting," Transactions, The American Societyof Mechanical Engineers, Vol. 75, 1953.

27. Leyensetter, Walter, "Verformung von Span und Randzone beim Drehen," (Deformation of Chip and Work Surface in Turning), Stahl und Eisen, Vol. 72, (1952), No. 19, pp. 1139-1144.

28. Letner, H.R., "Grinding and Lapping Stresses in Manganese Oil-Hardening Tool Steel," Transactions, The American Society of Mechanical Engineers, Vol. 75, 1953.

29. Colwell, L.V., Sinnott, M.J., and Tobin, J.C., "The Determination of Residual Stresses in Hardened, Ground Steel," Transactions, The American Society of Mechanical Engineers, Vol. 77, 1955.

30. Halverstadt, R.D., "Analysis of Residual Stress in Ground Surfaces of High-Temperature Alloys," Preprint No. 57-SA-62, The American Society of Mechanical Engineers, presented at San Francisco, June, 1957.

31. Clorite, P.A. and Reed, E.C., "Influence of Various Grinding Conditions Upon Residual Stresses in Titanium," Preprint No. 56-A-44, The American Society of Mechanical Engineers, presented at New York in December 1956.

32. Baldwin, Jr., W.M., "Macro-Residual Stresses in Metals Resulting From Plastic Deformation," Paper presented at a seminar on Cold Working of Metals, published by The American Society for Metals, 1949, pp. 31-56.

33. Smith, Dempster and Leigh, Arthur, "Experiments with Lathe Tools on Fine Cuts, and some Physical Properties of the Tool Steels and Metals Operated On," Transactions, The Institution of Mechanical Engineers, presented March 13, 1925.

34. Coker, E.G. and Chakko, K.C., "The Action of Cutting Tools," Transactions, The Institute of Mechanical Engineers, London, 1922.

REFERENCES (CONT'D)

35. Fukui, S. and Okoshi, M., "Researches on the Cutting Action of Planing Tool," The Institute of Physical & Chemical Research, Tokyo, Japan, Vol. 22, pp. 97-166, October 1933.

36. Sachs, George, "Control of Residual Stresses in Practice," Paper No. 448, presented at the meeting of The Society of Automotive Engineers, Detroit, Michigan, January 1955.

37. Timoshenko, S., Theory of Elasticity, McGraw-Hill Book Company, New York, New York, 1934.

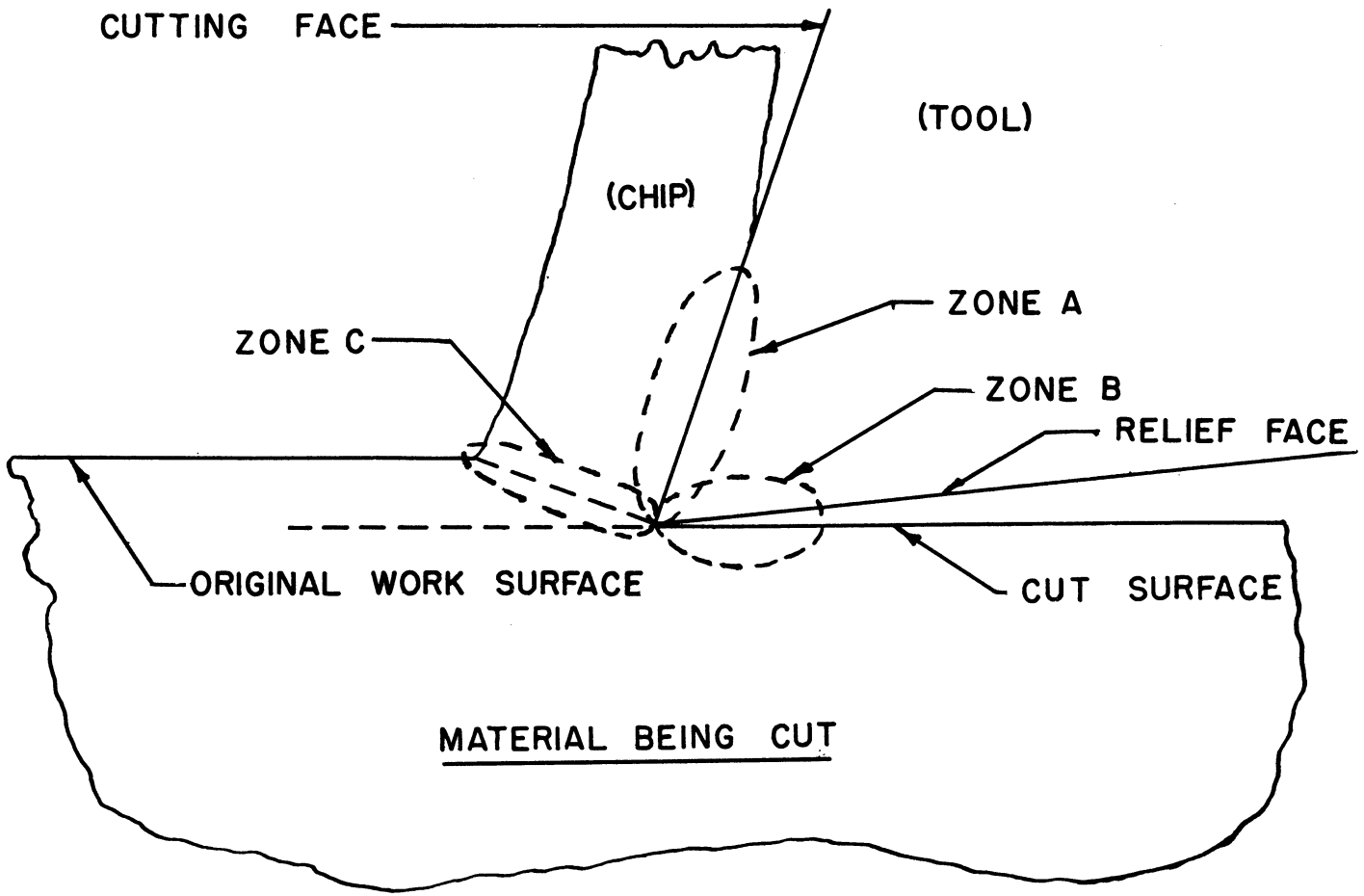

Figure 1. A schematic of idealized chip formation identifying three zones of prime significance. Zones A and B involve rubbing contact between the cutting tool and work material; both may be regions of high temperature and represent the areas where significant wear takes place. Zone C, the shear surface, is a major source of heat.

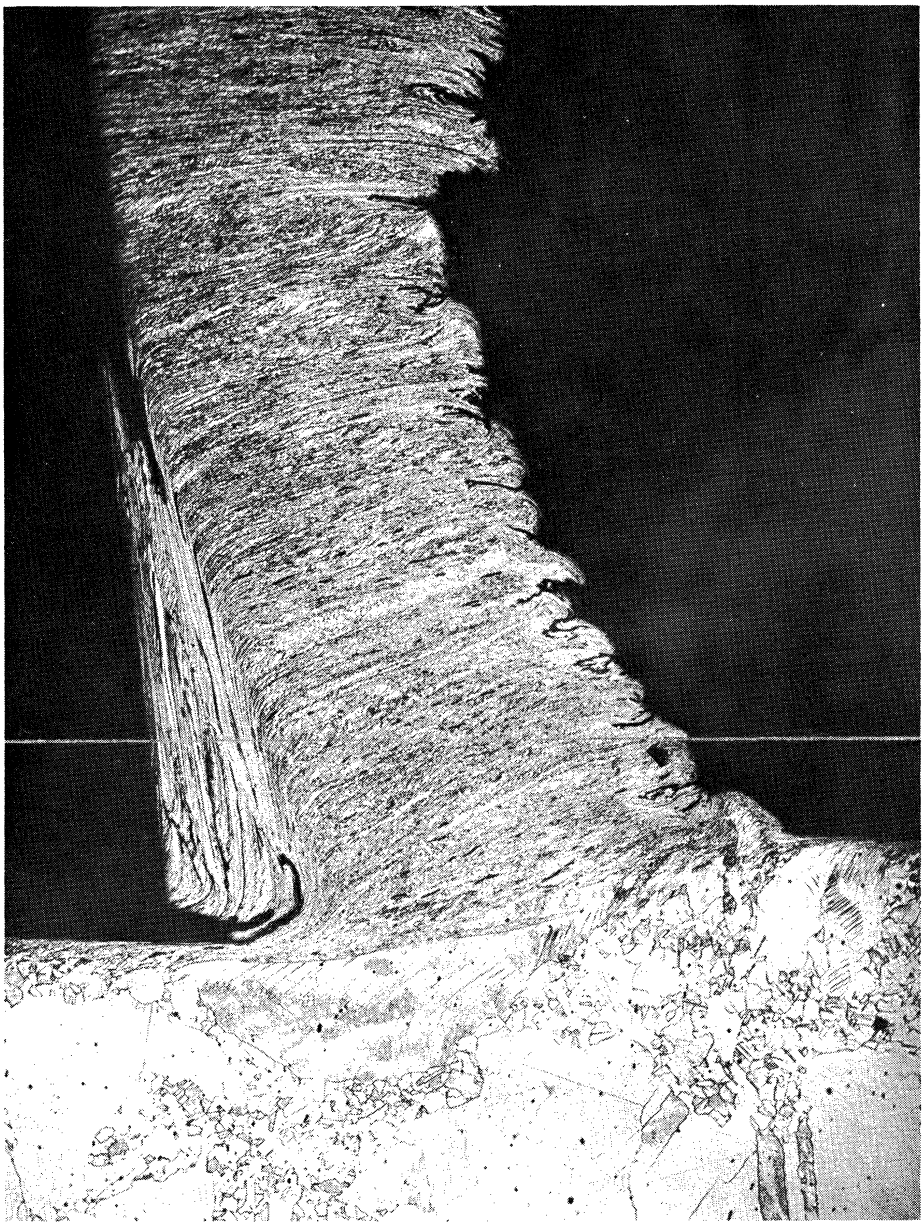

Figure 2. An example of a common type of chip formation which causes exyensive surface damage. Stress distribution and the resultant strains are dominated by the presence of the built-up-edge or "tool loading". Chip was formed from Type 304 stainless steel (18-8) at low cutting speed with a high speed steel tool. Magnification 50X.

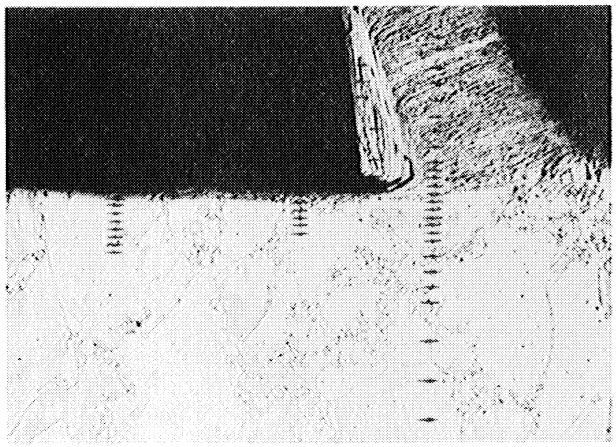

0.002" INTERVALS: 520, 443, 526, 510, ( ), 470

0.002" INTERVALS: 380, 393, 454, 403, 380, 374, 432, 389

0.001" INTERVALS: 399, 389, 420, 393, 399, 282, 275, 269, 294, 293, 271

0.001" INTERVALS: 287, 287, 293, 284, 287, 258, 261, 267

0.001" INTERVALS: 350, 301, 316, 254, 254, 250

0.002" INTERVALS: 246, 269, 275, 261

0.005" INTERVALS: 246, 271, 261

Figure 3. A micro-hardness survey of the chip-work specimen of Figure 2. Note sharp demarcation in shear zone and high level of hardness in built-up-edge. Tukon operation: 100 gram load; Knoop penetrator.

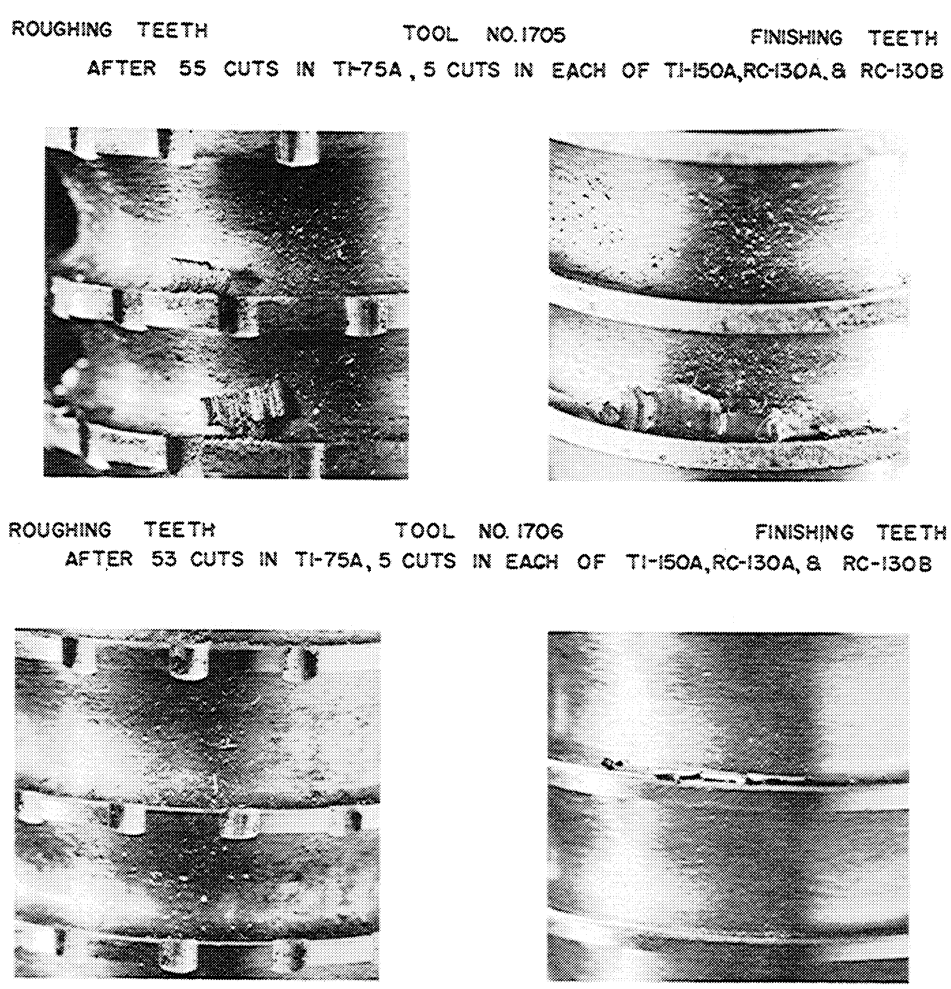

Figure 4. Surface damage can be caused by rubbing and seizure in Zone B of Figure 1. Note "smear" on lands of broaches in upper photos. This was caused by elastic relaxation and only one-half degree relief angle. Five degrees relief on broaches in lower photos reduced smear but did not eliminate it.

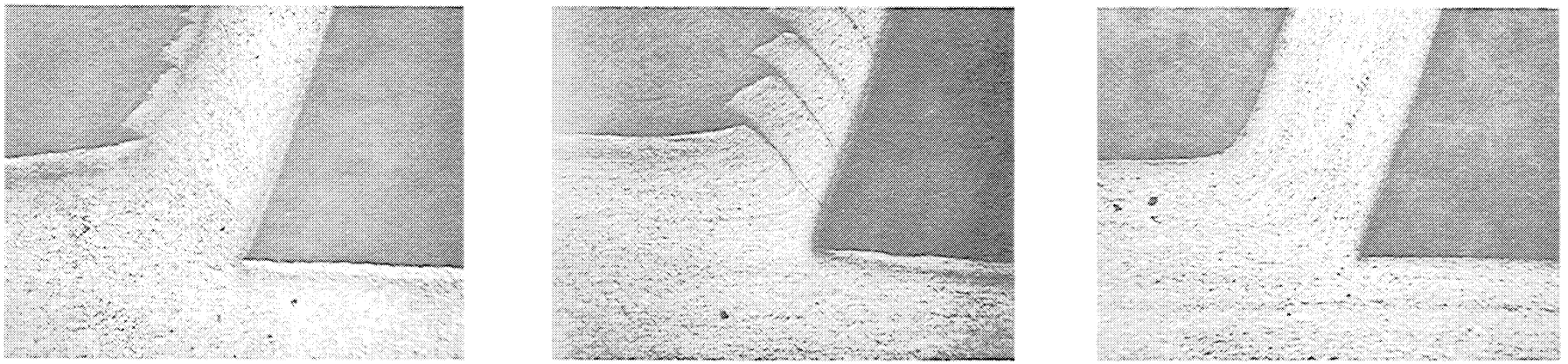

Figure 5. Examples of three common types of chip formation involving no built-up-edge. Surface damage varies with degree of segmentation of the chip. Specimens are titanium cut at low speed on a shaper. Magnification

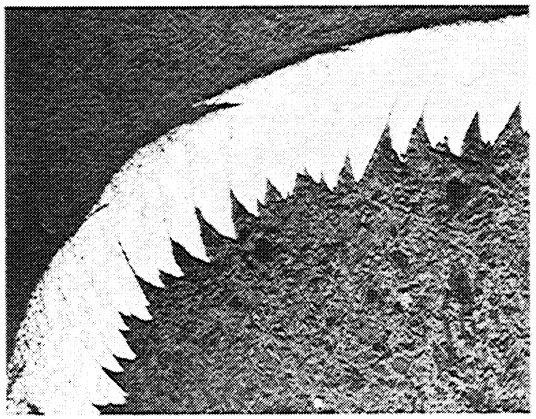

-15° RAKE

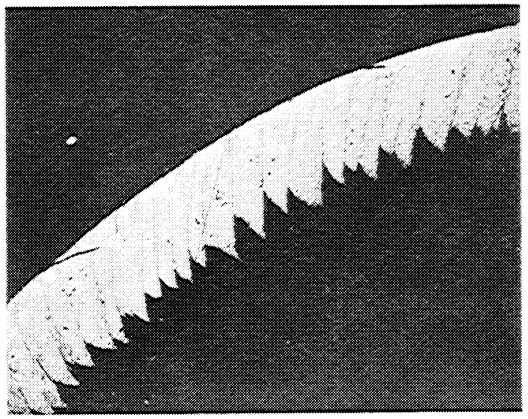

0° RAKE

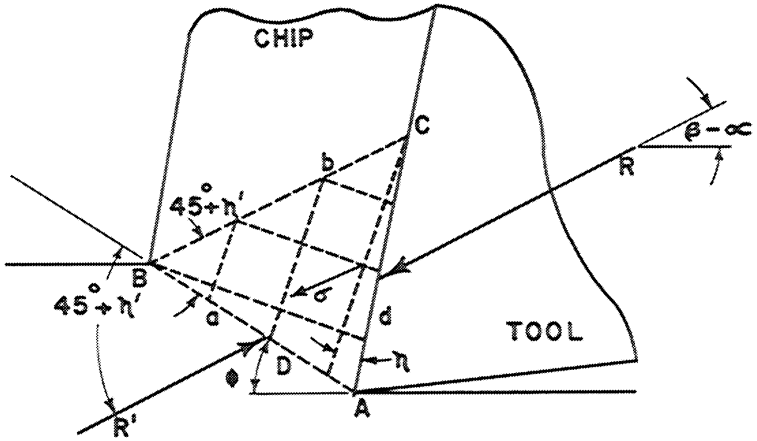

STRESS FIELD AT TOOL POINT

Figure 6. Chips showing two surfaces of shear obtained with tools having different rake angles. Note similarity to stress field proposed in Reference 3. Maximum shear stress at chip tool interface approaches that within the chip. Material: Type 130 B titanium alloy; magnification

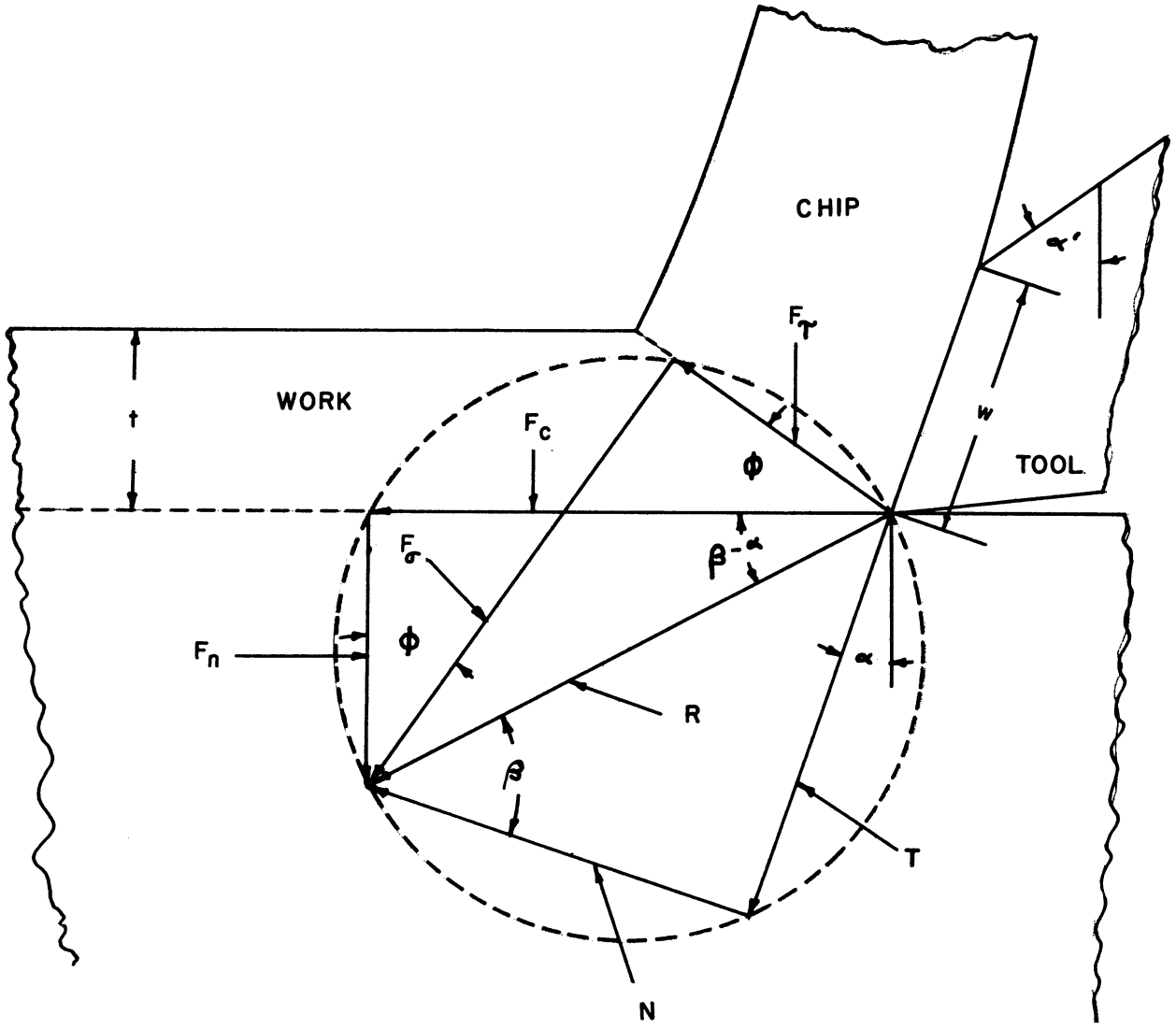

Figure 7. Mechanics of metal cutting are illustrated by three pairs of inter-dependent force components. F_σ and F_τ are dependent upon the normal and shear stresses respectively in the shear zone. "N" and "T" are the normal and tangential forces in the chip-tool interface. F_c is the external reaction force in the direction of cutting motion while F_n is the normal or thrust force perpendicular to the cutting direction. "Φ" is the shear angle, "α" is the primary rake angle, α' is the secondary rake angle when applied, "w" is the width of the limited contact area created by secondary rake and "t" is the thickness of the cut.

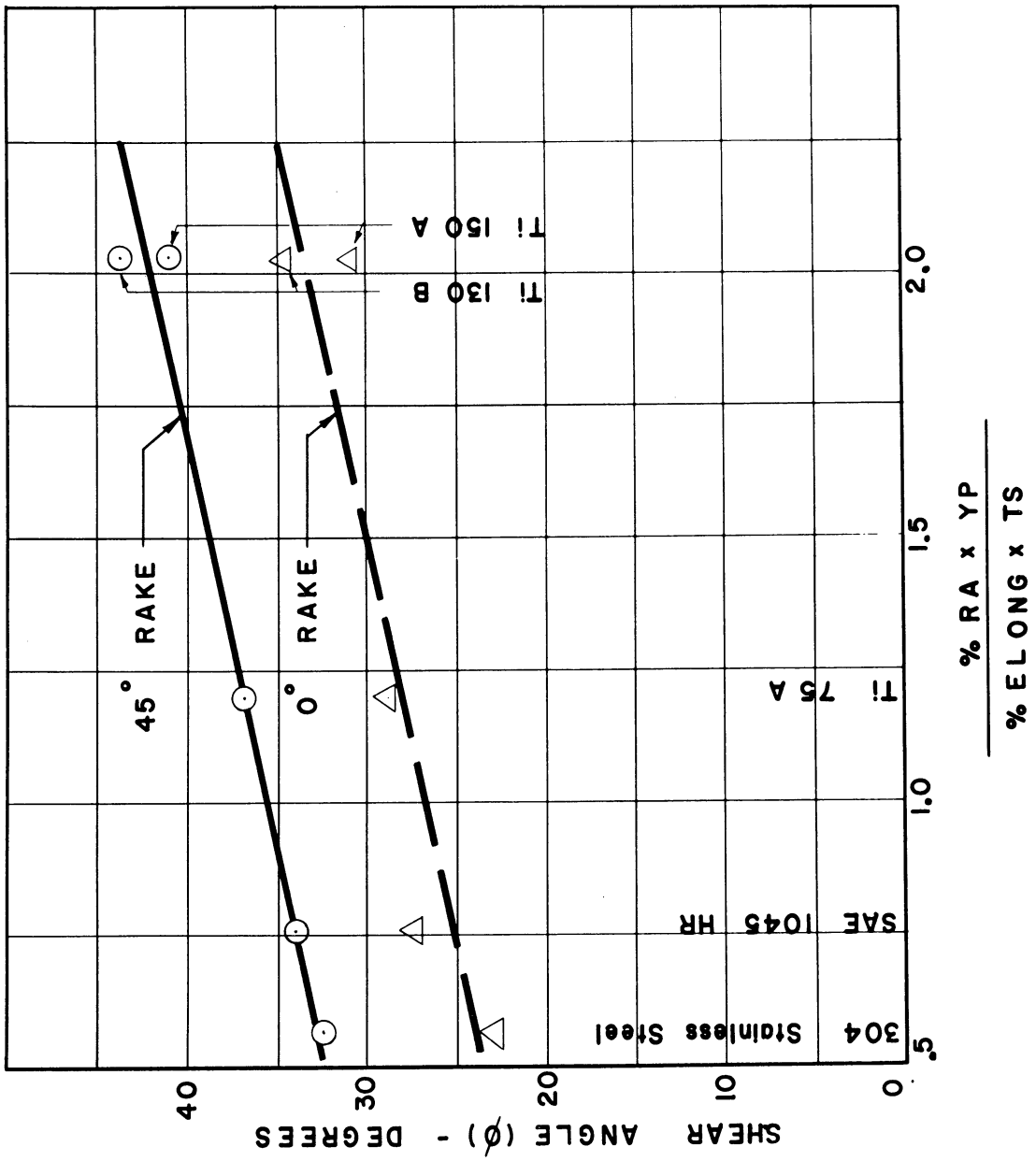

Figure 8. Average shear angle as a function of tensile properties for five materials, several depths and widths of cut, using carbon tetrachloride, white mineral oil, sulphurized oil, and dry cutting.

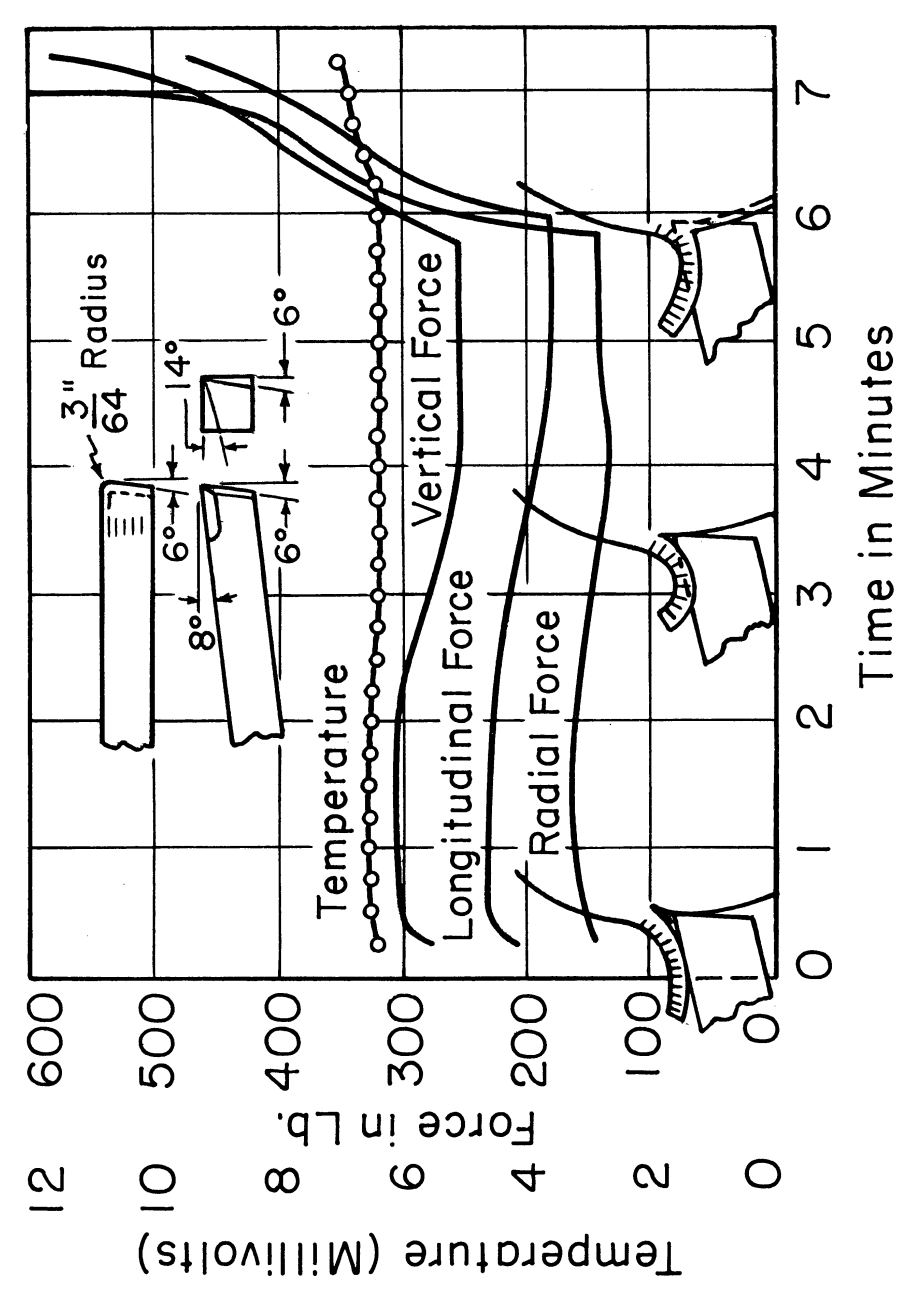

Figure 9. An example of typical ractions to wear of high speed steel tools. Cratering of the rake face reduces forces and built-up-edge until structural failure sets in; final failure is not due to a critical or threshold temperature although the rate of wear may be strongly temperative dependent. (from O.W. Boston, Reference No. 8)

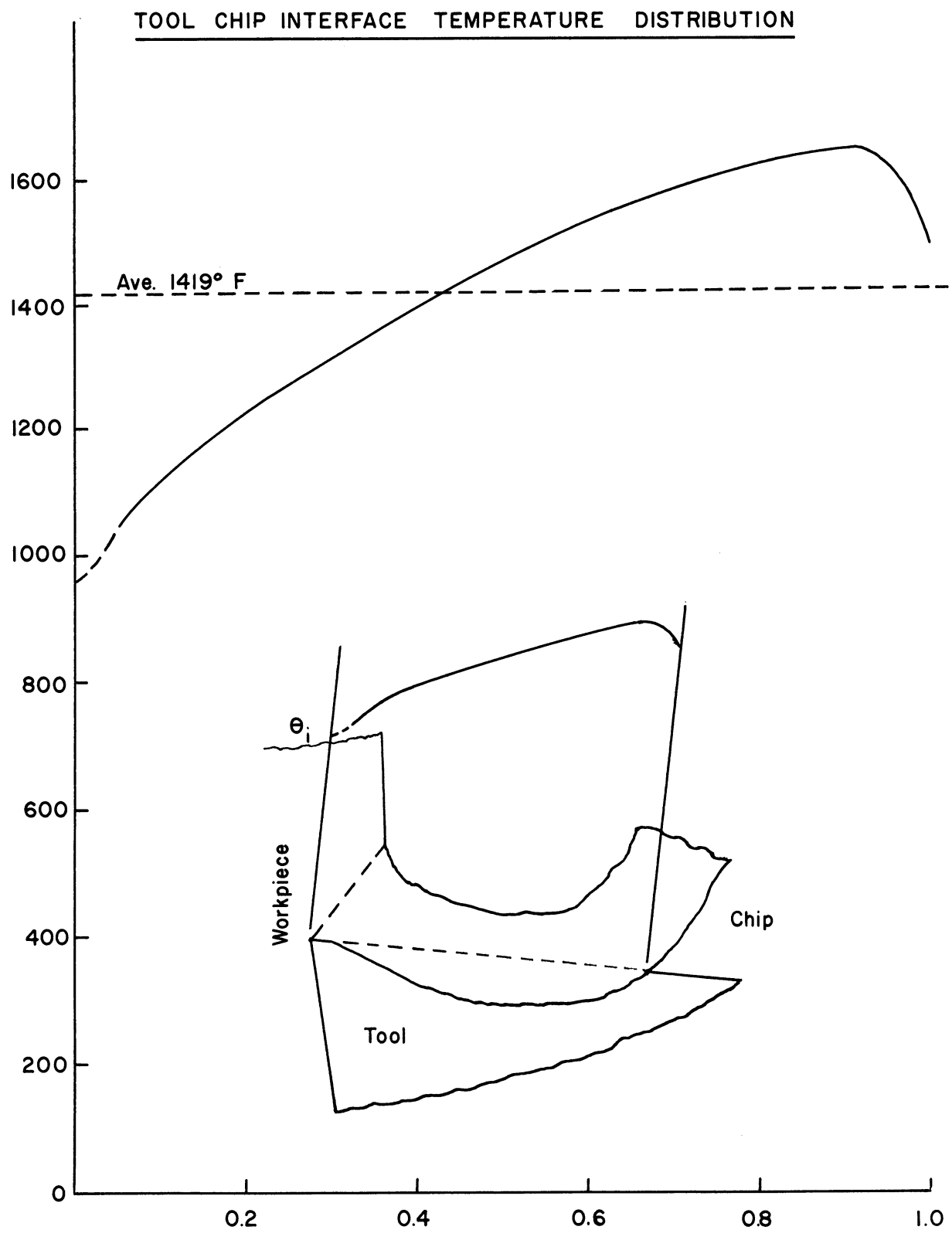

Figure 10. Temperature distribution between chip and tool as calculated by relaxation method; corresponding heat flux is not uniformly distributed. Results suggest temperature-dependent diffusion as significant mechanism of tool wear. (from Chao and Trigger, Reference No. 9)

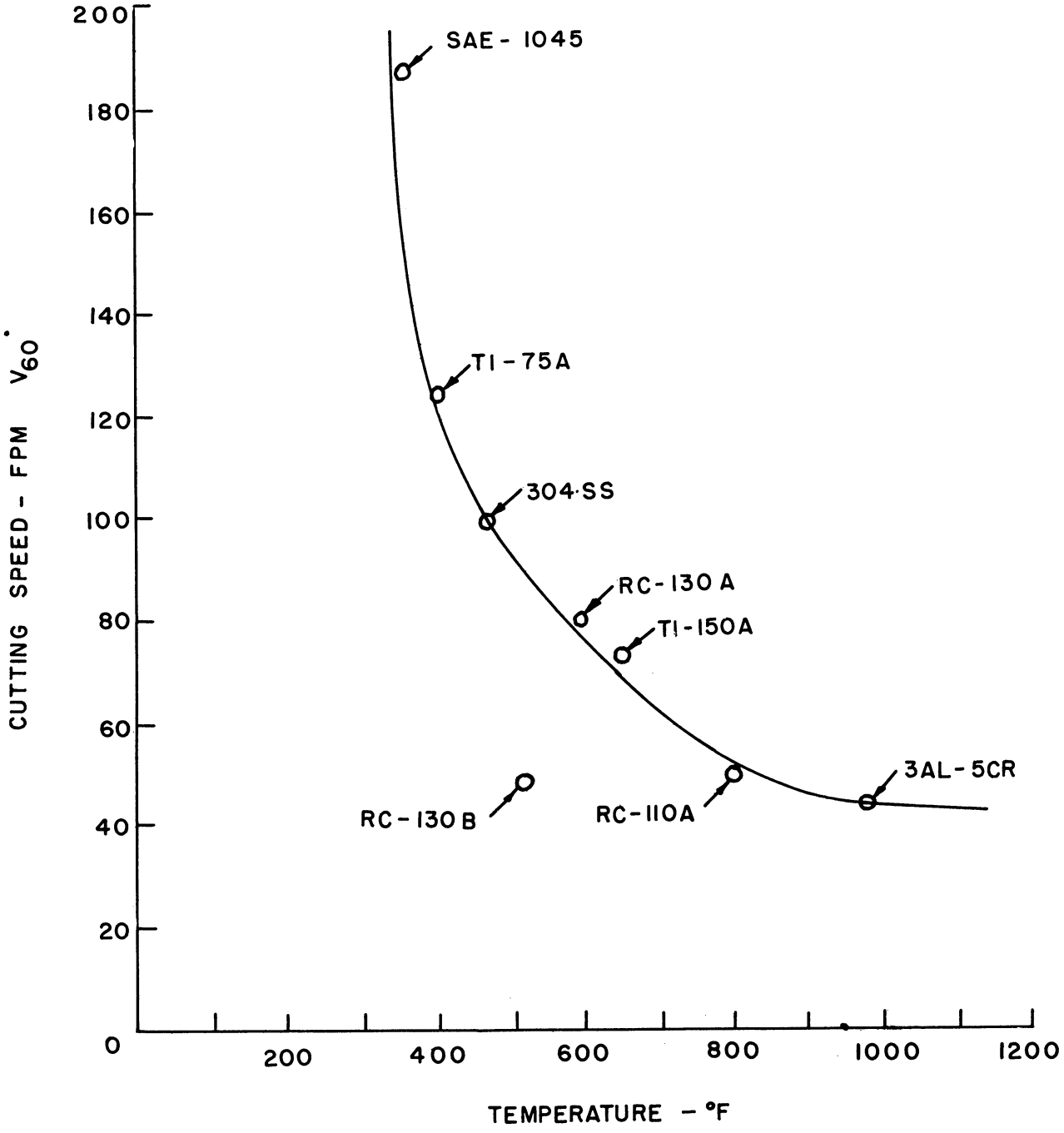

Figure 11. Measurements of cutting temperature reveal a consistent correlation with tool life for a broad range of materials properties. V_{60} is cutting speed for a one-hour tool life. Abcissa shows temperature for constant cutting speed of 25 fpm for same size of cut. Cutting tools were high speed steel.

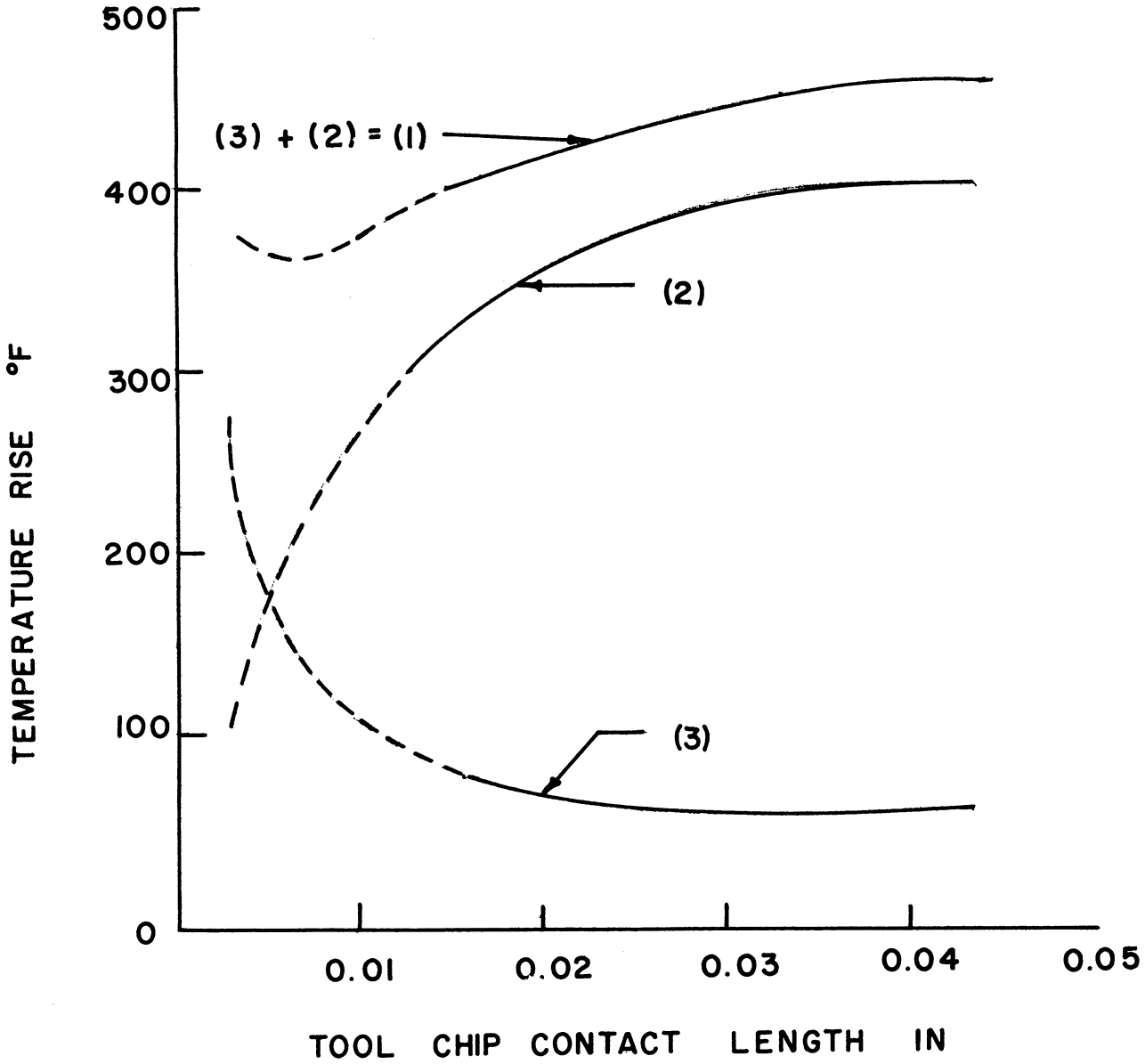

Figure 12. Variation of cutting temperature with controlled contact area between chip and cutting tool. Curve (1) represents measured temperature, Curve (2) represents average temperature rise of chip body due to main chip shear and Curve (3) represents temperature rise due to tool-chip sliding. The two components, Curves 2 and 3, were calculated from the cutting conditions and the measured temperature. (from Chao and Trigger, Reference No. 10.)

Work Material:	Electrolitic Copper
Tool Material:	18-4-1 HSS
Tool Geometry:	0,6,7,7,10,0,0.025
Feed:	0.0039 ipr
Depth of Cut:	0.101 in.
Cutting Environment:	Air (Dry cutting)
Cutting Speed:	500 fpm

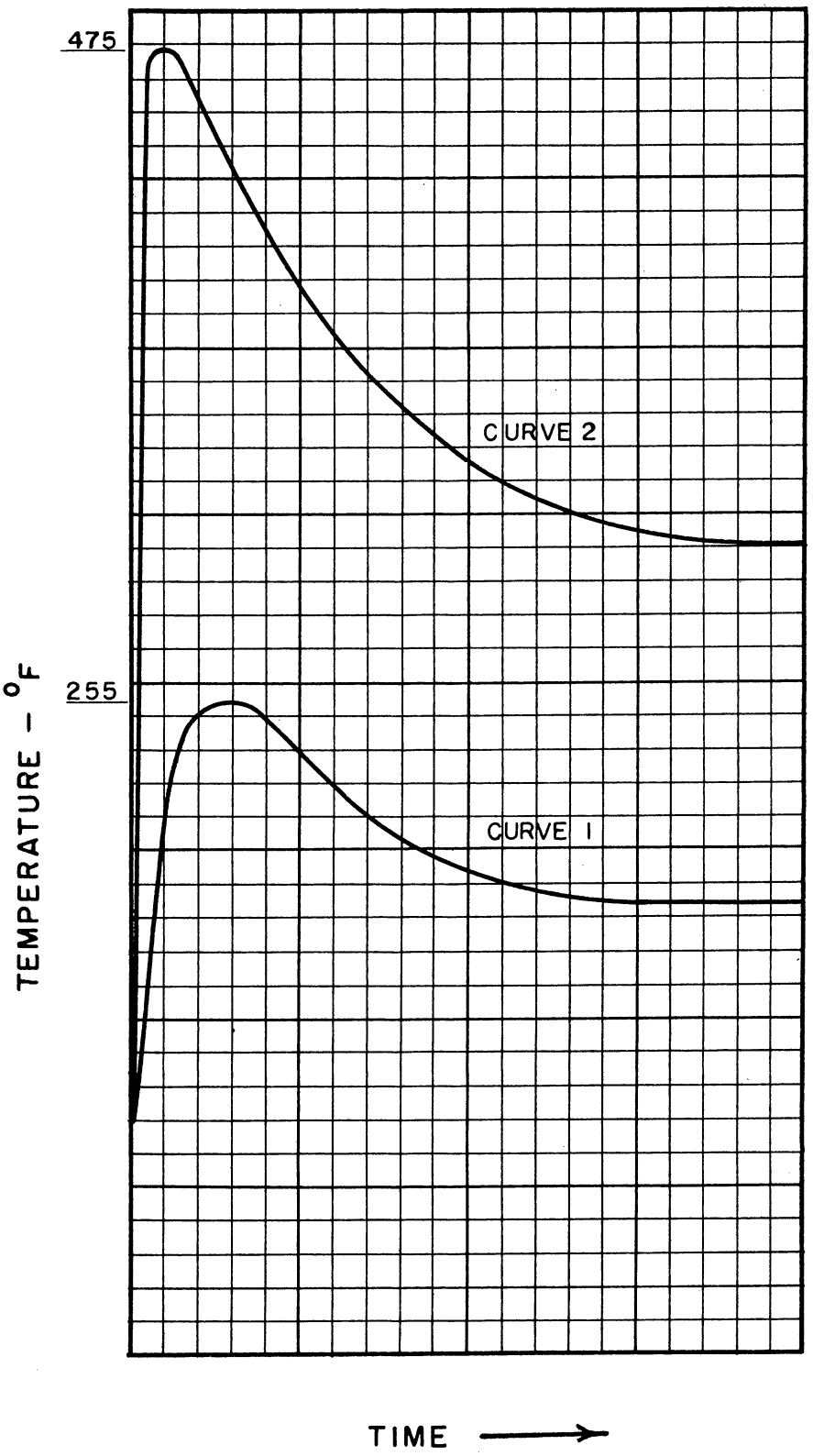

Figure 13. Oscilloscope traces of temperature rise in ground specimen of full-hard AISI 52100 steel, 0.014 inches below ground face. Curve (1); vibrated at 11 Kcps with an amplitude less than 0.001 inches. Curve (2); conventional or not vibrated. Depth of cut is 0.002 inches; work speed is 22 fpm.

BANDSAWING

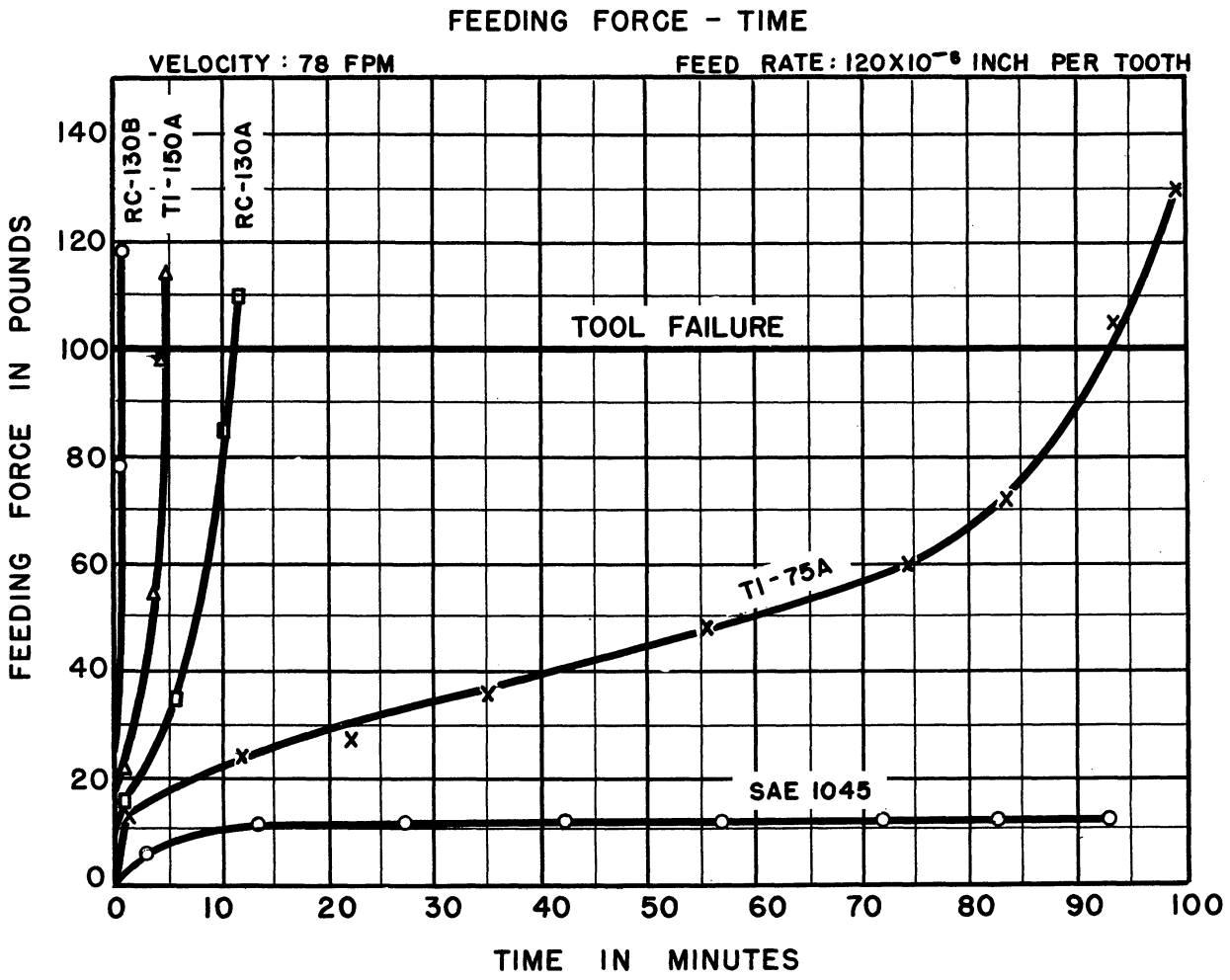

Figure 14. The feeding thrust force in bandsawing is very sensitive to properties of the work material and can increase several times during the useful life of the tool. Such increases bring about considerable change in surface finishe and can be expected to be important sources of surface damage.

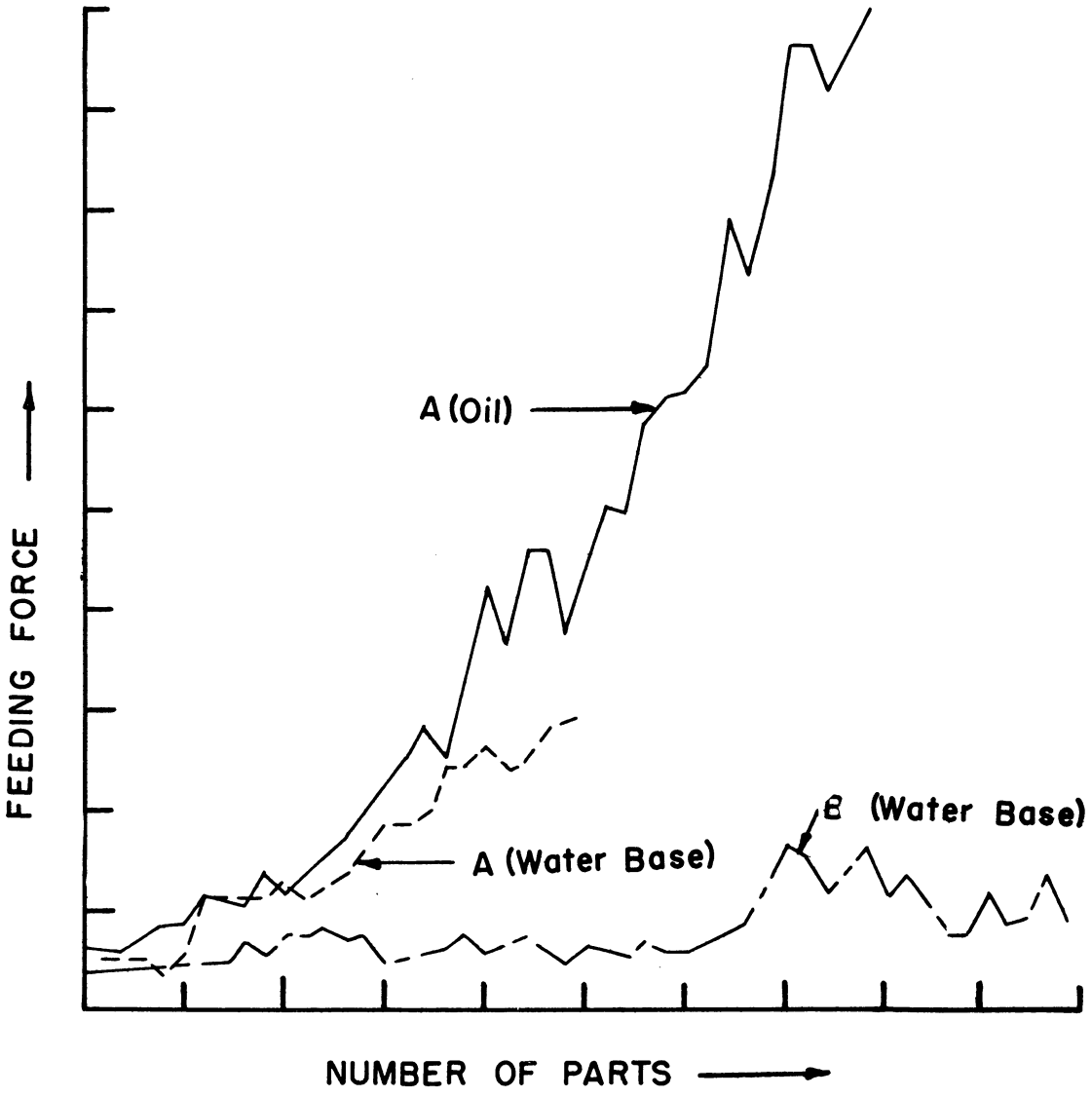

Figure 15. The feeding component of cutting force may increase many times in automatic screw machine operations. Materials A and B were different heats of the same aluminum alloy; both had compositions within industry specifications. Surface finish, size, and residual stresses varied significantly with increases in feeding force. Material A with a water base cutting fluid caused the machine to stall for a lack of power at only half the number of parts produced from Material B without any indication of similar effects.

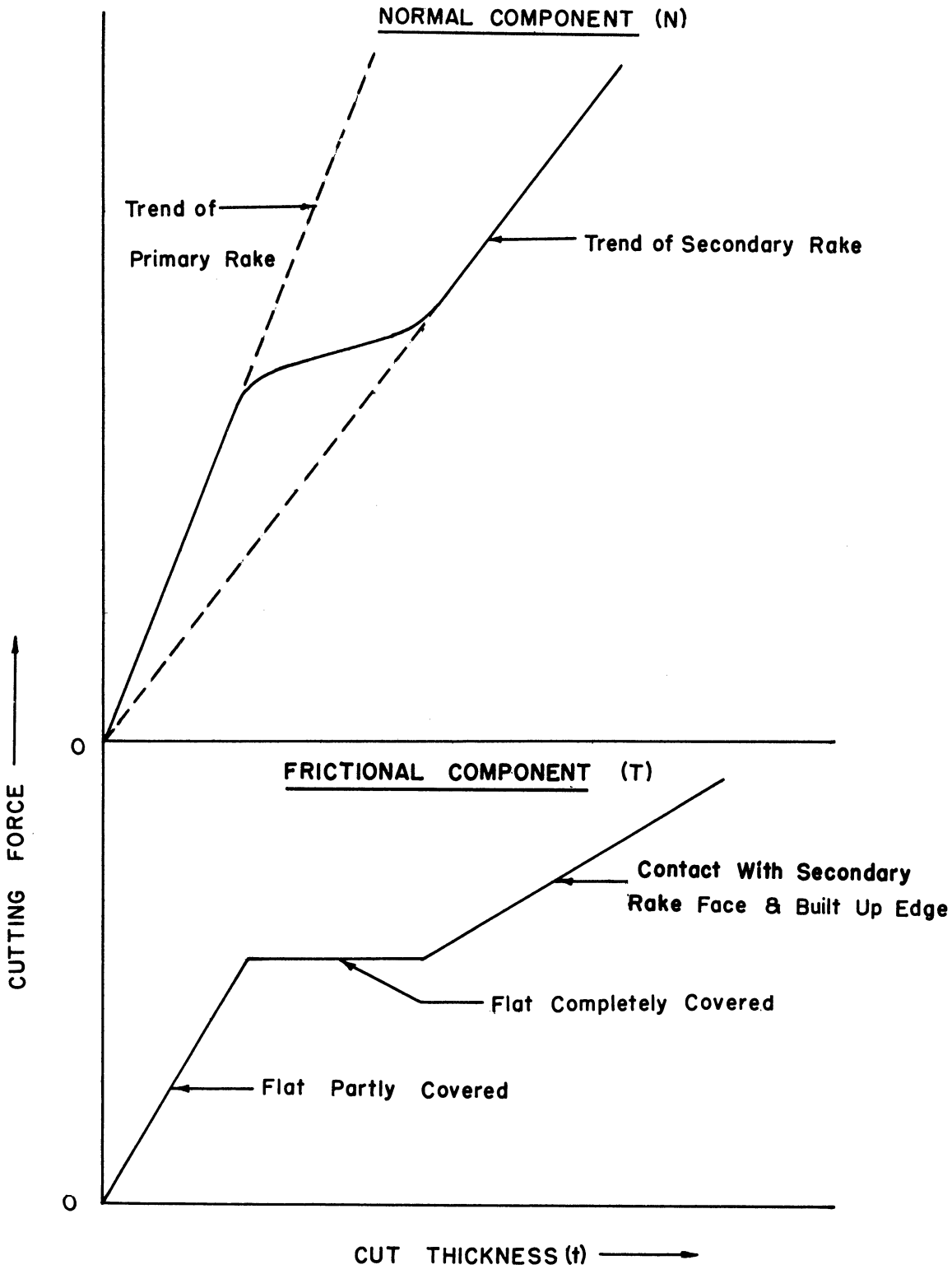

Figure 16. The friction forces which dominate metal processing operations are strong functions of contact area as well as material properties. The above curves show qualitatively how both components at the chip-tool interface vary with the available contact area. In this instance the available contact area is held constant as the size of cut is increased.

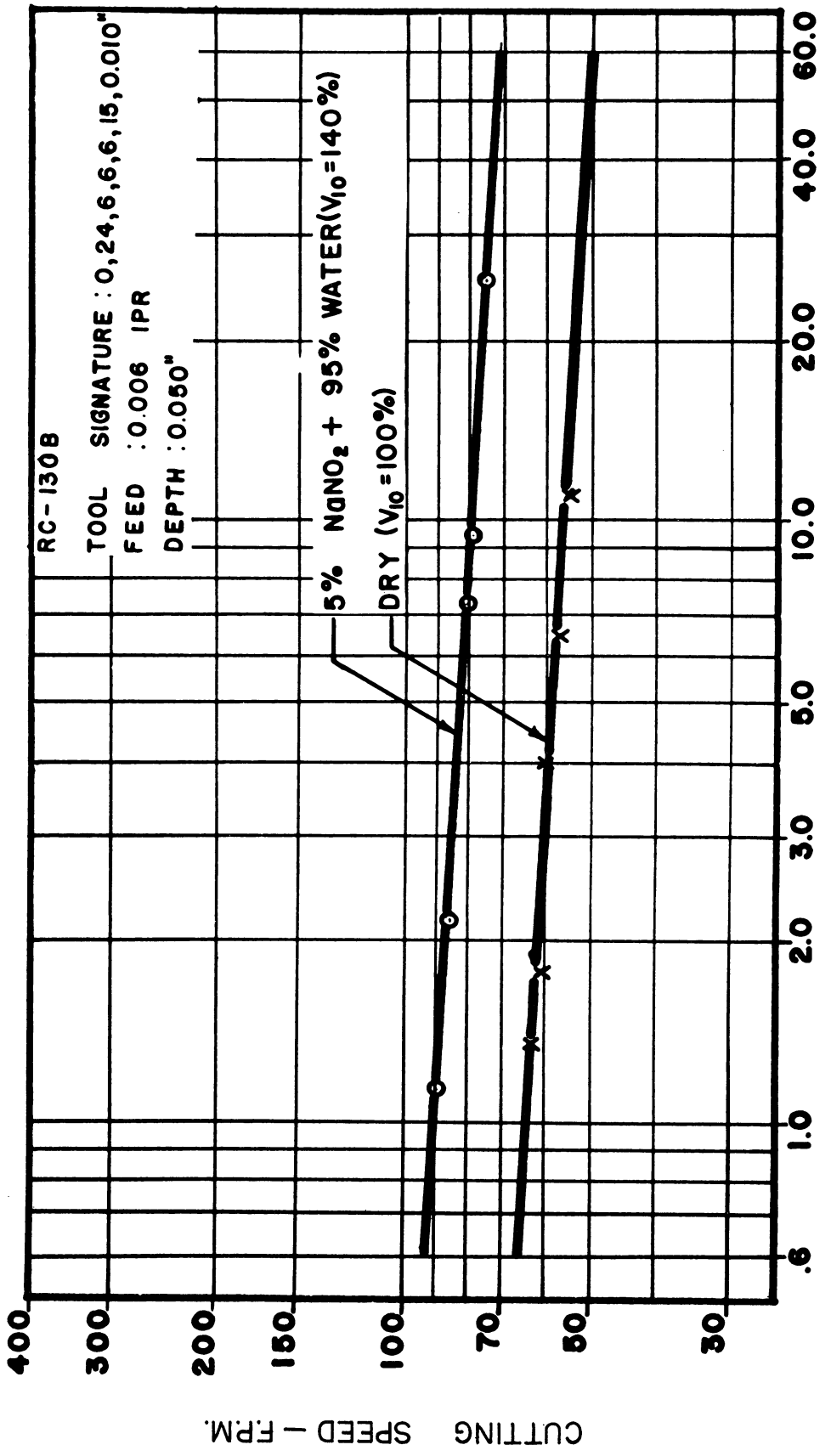

Figure 17. Tool life can be very sensitive to temperature as illustrated by the relatively flat slopes of the above curves. This conclusion is further substantiated by the addition of a good coolant. The fact that tool life is an orderly function of cutting conditions indicates feasibility of control of surface damage arising from such operations. These results are typical of the behavior of high speed tools.

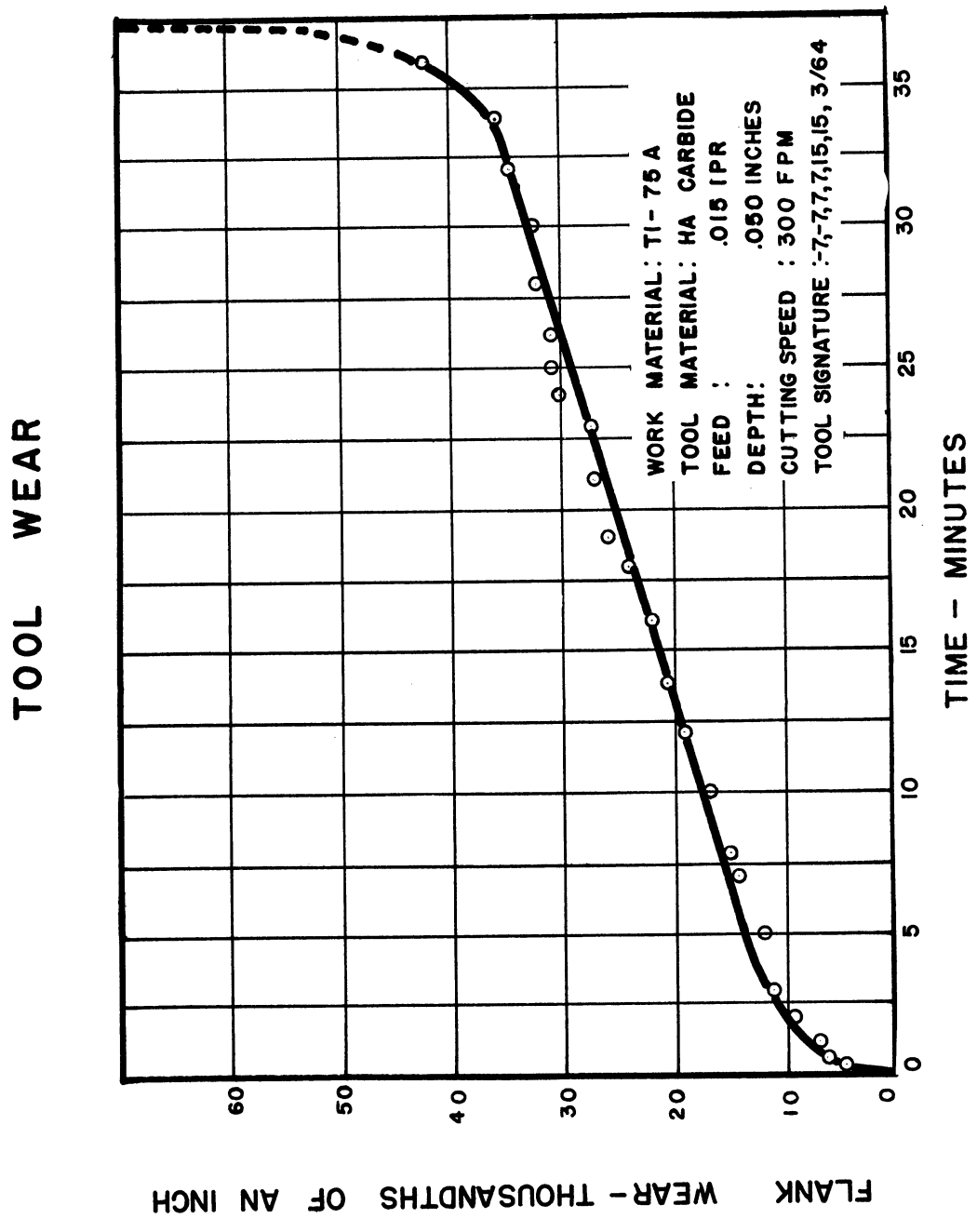

Figure 18. Sintered carbide tools wear gradually and seldom exhibit the sudden breakdown characteristics of carbon and high speed steel tools. Wear of the tool flank or relief face increases almost linearly with cutting time until a product of temperature and pressure (feeding force) reaches acritical level as indicated by the rapid rise in wear at the right.

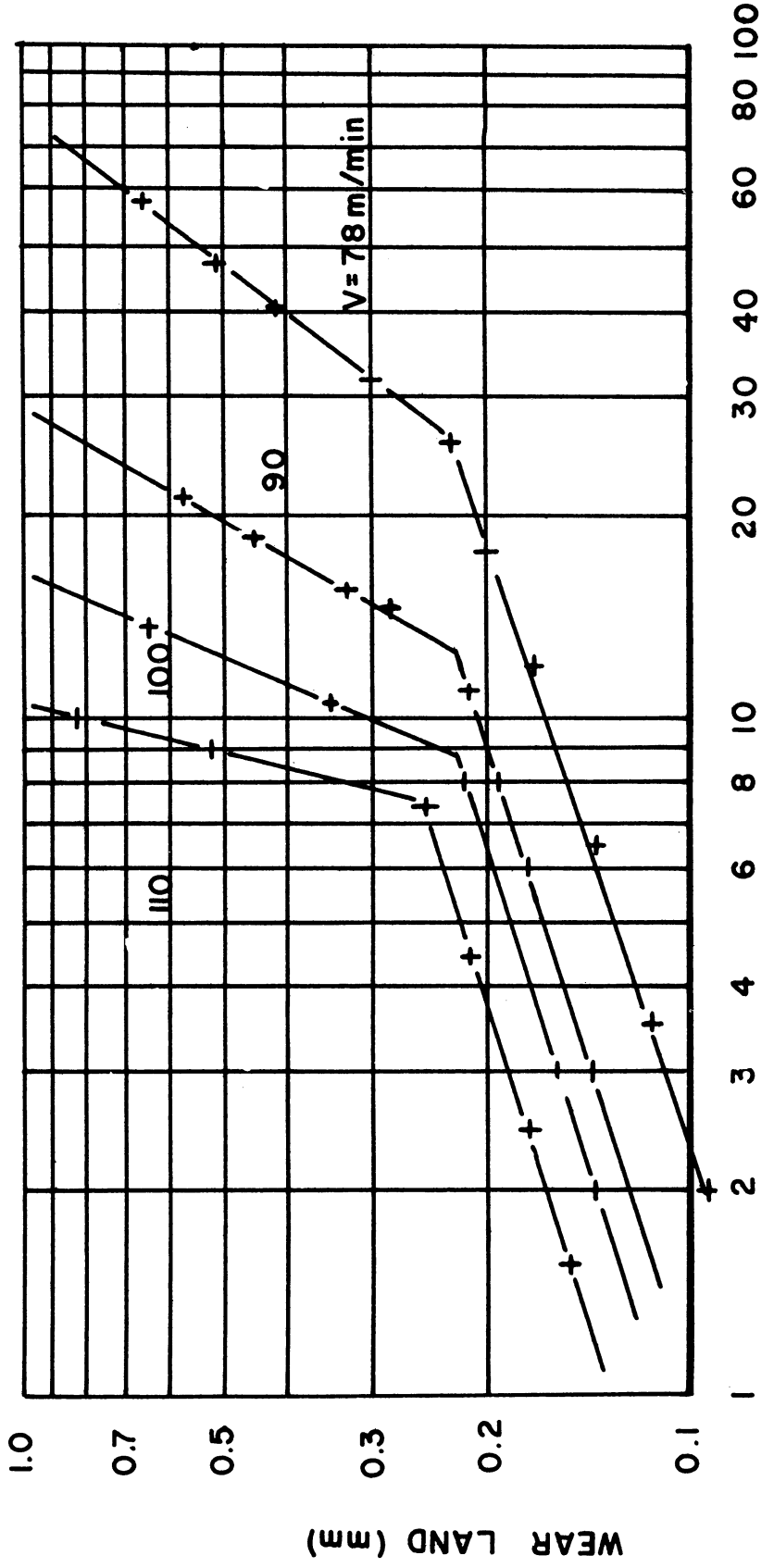

Figure 19. Wear data of the type shown in Figure 18 exhi it a sharp transition when plotted on logarthmic coordinated as above. Such behavior can be expected to influence surface damage. This data was observed for cutting cast iron with carbide tools. Similar behavior has been demonstrated for cutting steel. (from Takeyama et al. Reference 13.)

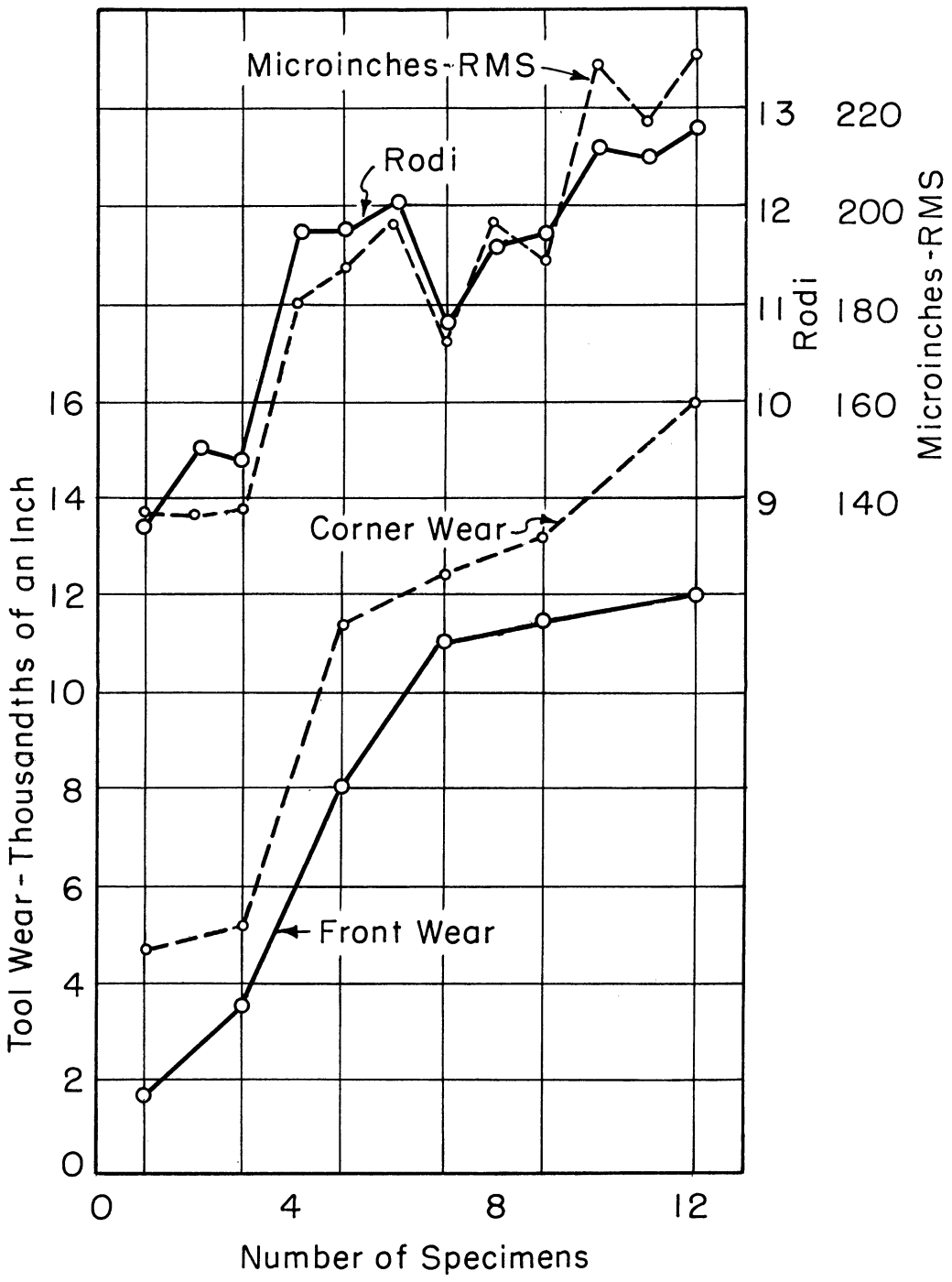

Figure 20. Surface finish changes with tool wear as indicated in the form-turning of free cutting steel. Drop in surface roughness near mid-point of test indicates appearance of shiny, burnished rings created by disappearance of built-up-edge.

FINISH TURNING

With

High Speed Steel Tools

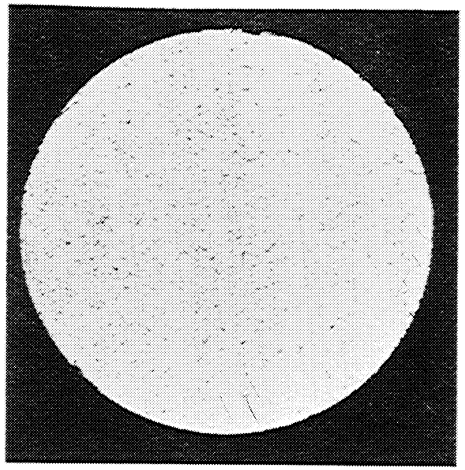

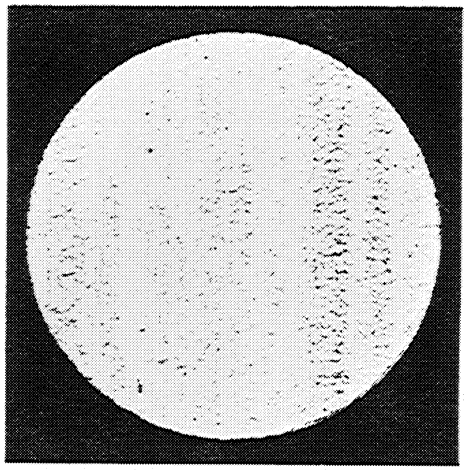

GOOD

POOR (Tool Failed)

Figure 21. The appearance of small "tears" signifies the end of useful tool life where fatigue life is critical. "Tears" shown at right were caused by almost imperceptible tool wear in finish turning medium carbon steel forgings.

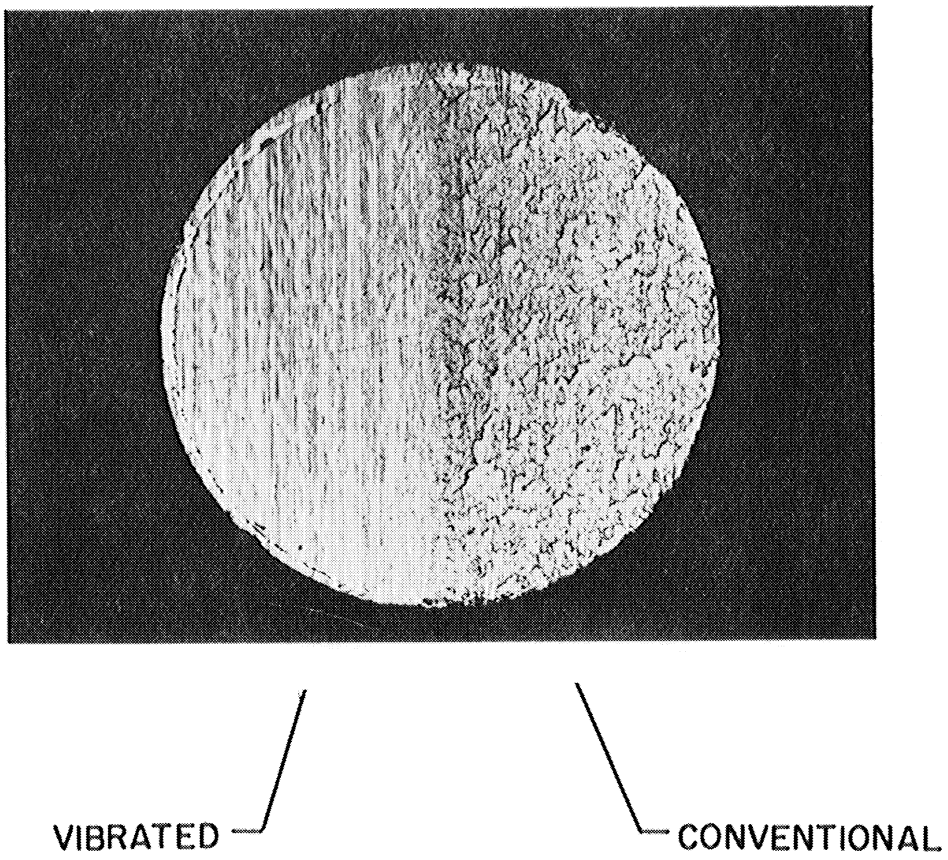

Figure 22. Ultrasonic vibration (13Kcps) of a single-point, turning tool reduced friction at the chip-tool interface and greatly reduced the "tears" caused by high friction. The work material was C 1018, cold drawn steel. It was being turned with a high speed steel tool at 30 fpm.

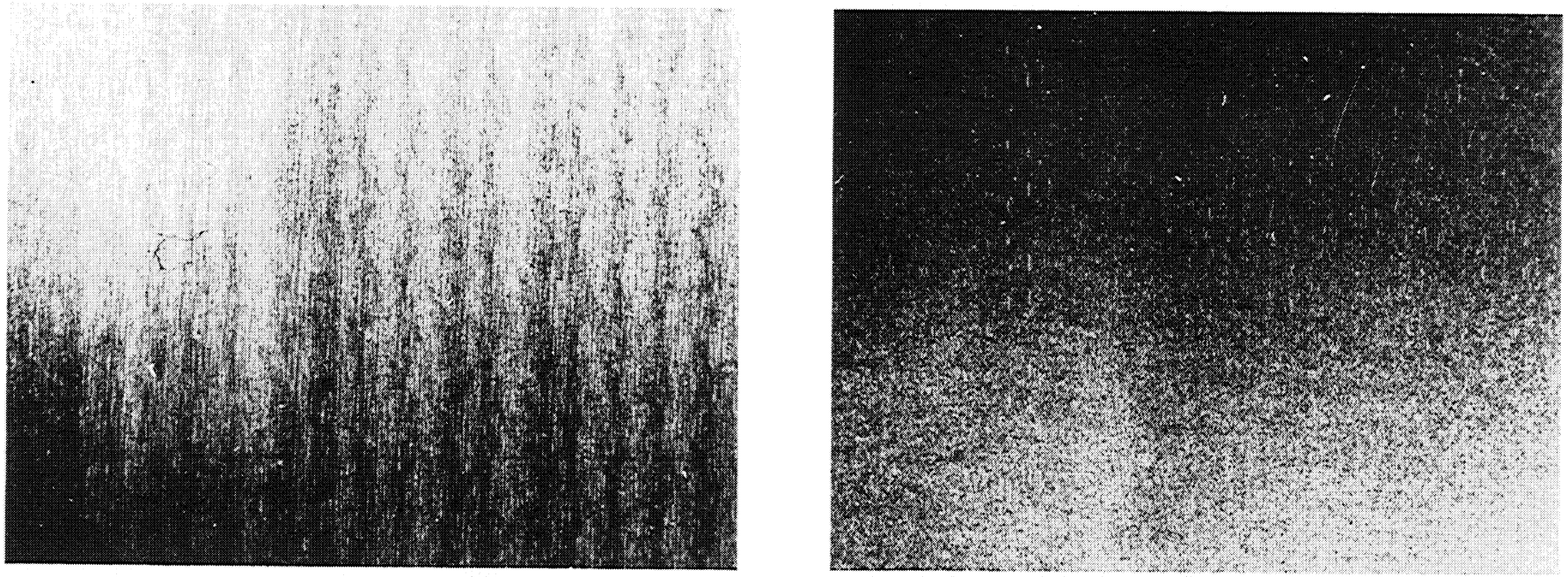

CONVENTIONAL

VIBRATED

Figure 23. Ultrasonic vibration (25Kcps: amplitude, 700 micro-inches) of a high temperature alloy reduces friction and built-up-edge and results in improved finish in grinding.

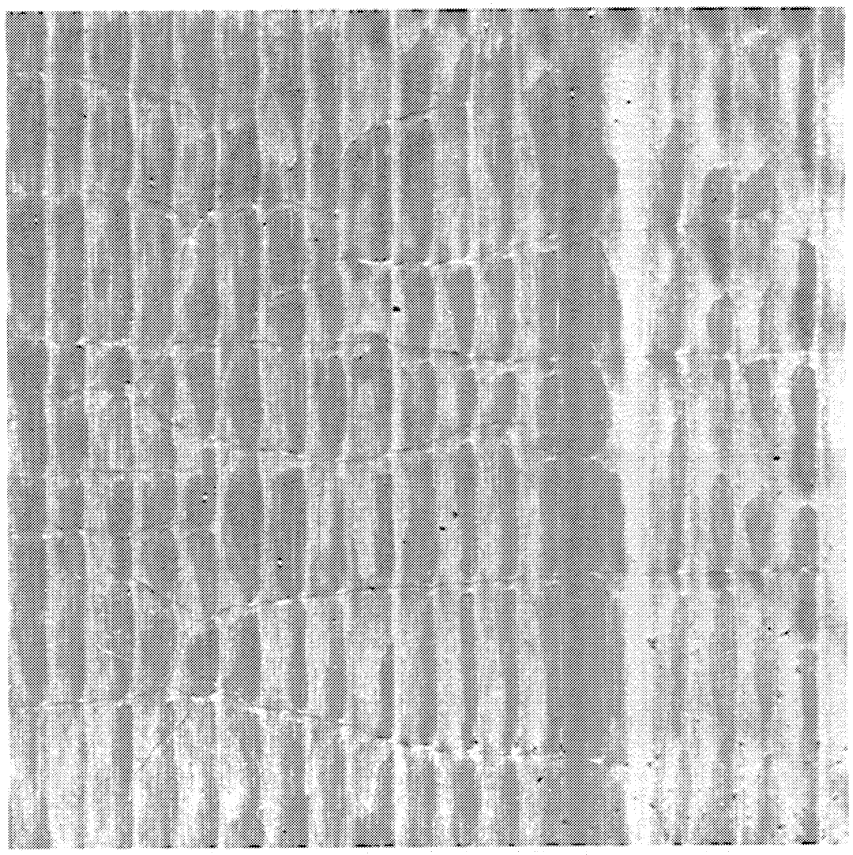

CONVENTIONAL

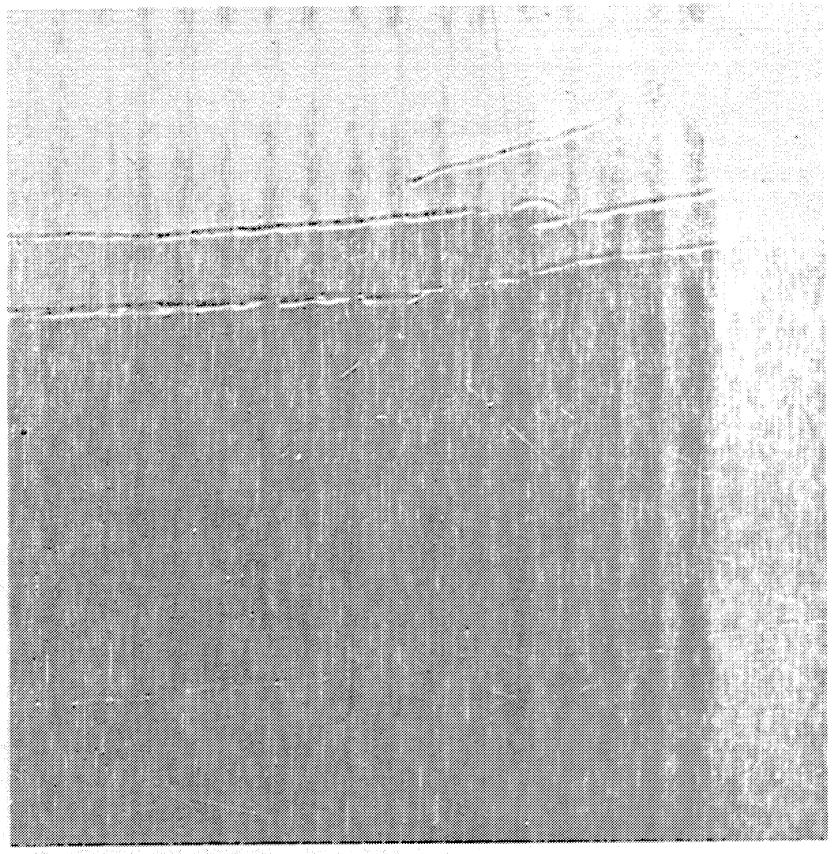

VIBRATED

Figure 24. Thermal cracks from surface grinding are reduced by high frequency vibration of full-hard AISI 52100 steel. Frequency: 11Kcps; amplitude less than 0.001 inches. Note that residual stress in vibrated specimen was low enough to permit local necking adjacent to the cracks.

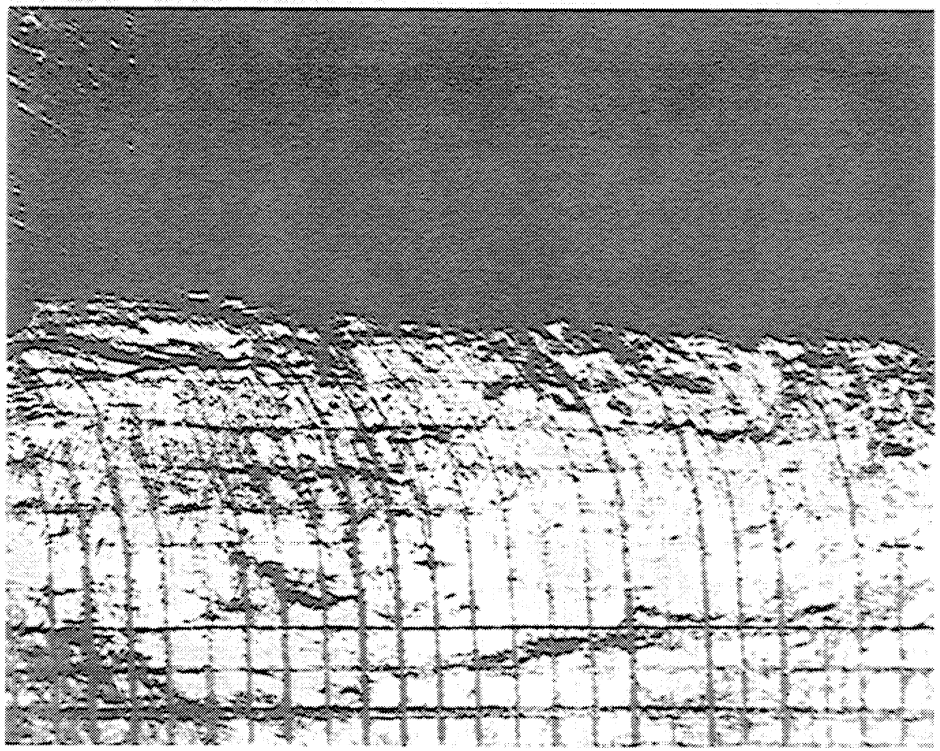

18-8 STAINLESS STEEL
YIELD STRENGTH = 39,250 PSI.
TENSILE STRENGTH = 85,600 PSI.
GRID = 0.003 INCHES SQUARE
0° RAKE, 0.015" DEPTH, 0.218" WIDTH

Figure 25. Strain damage extends beneath the surface in all metals but more in some than in others. The built-up-edge and high friction forces peculiar to low-speed cutting of face-centered-cubic metals is responsible for strain to considerable depth as illustrated in this specimen.

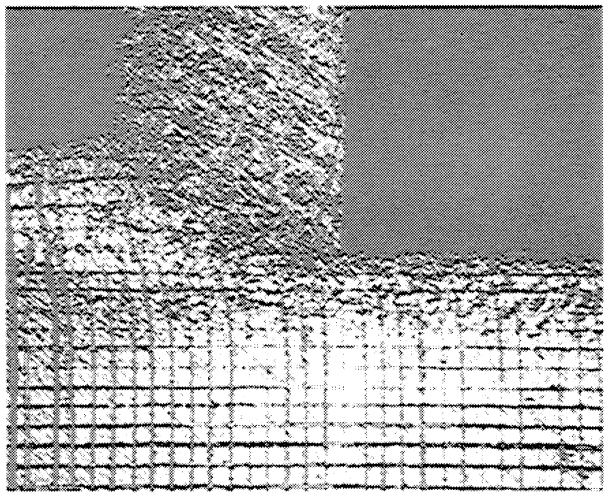

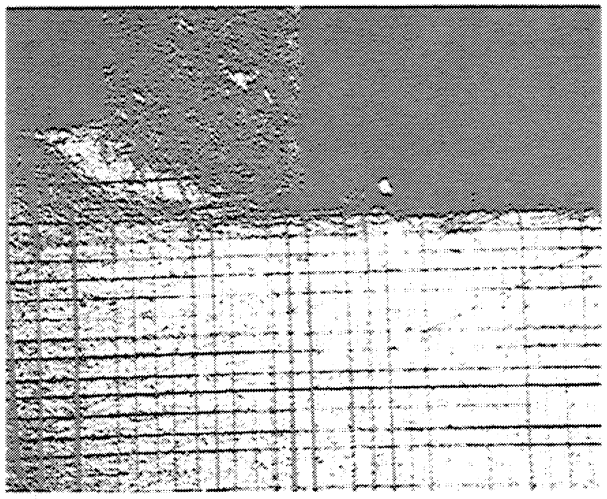

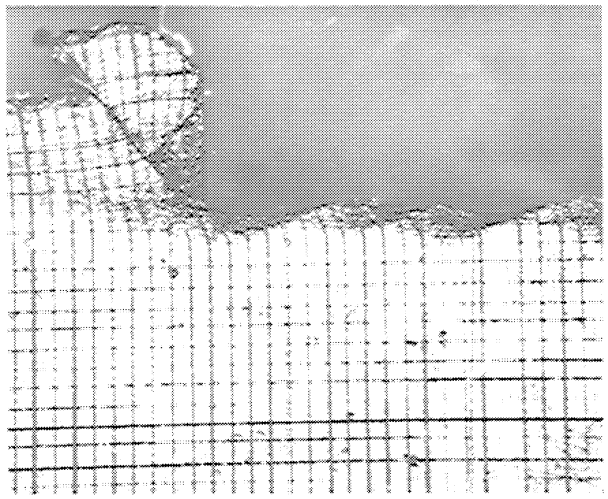

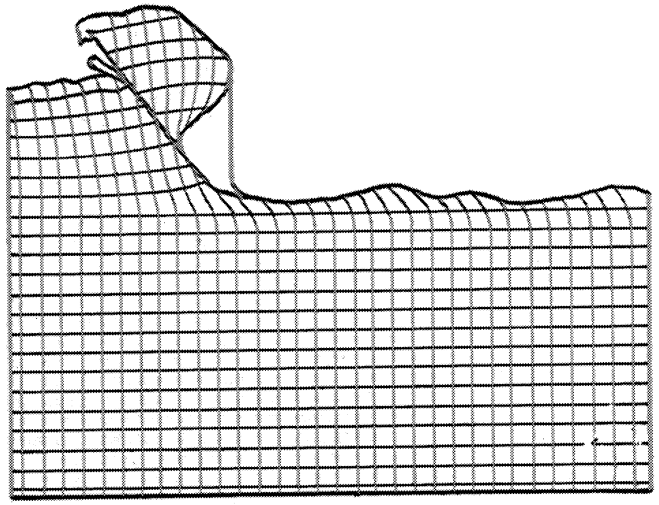

TI. 130B

TI. 130B

Figure 26. Even "slippery" metals like titanium, magnesium and yellow brass exhibit measurable sub-surface strain from cutting despite lower friction forces

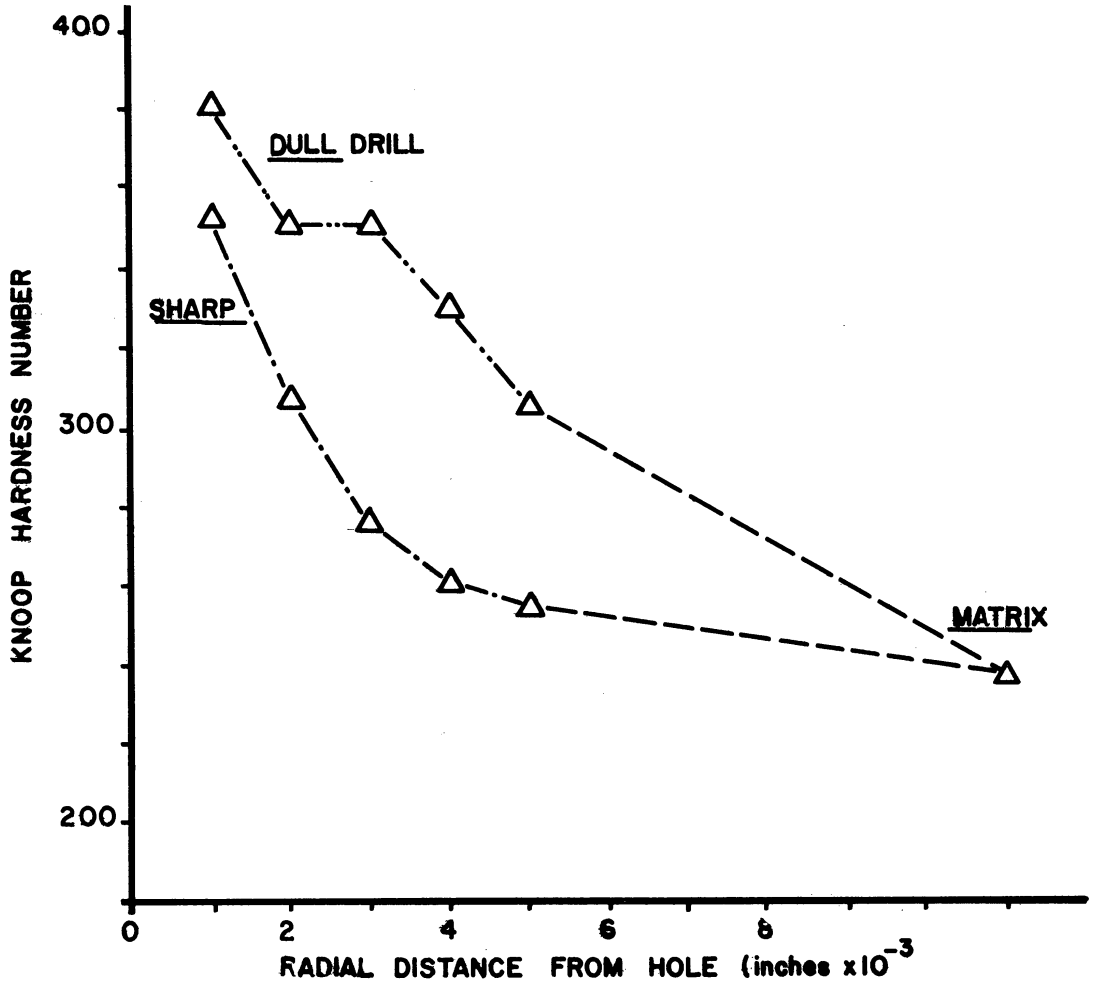

Figure 27. Micro-hardness tests were made at intervals of 0.001 inch radially outward from the wall of 3/8 inch diameter drilled holes in 1808 stainless steel. Both "sharp" and "dulled" drills were used at a feed of 0.009 ipr. and a speed of 557 rpm. All hardness values shown are averages of at least four separate tests at intervals of 90 degrees around the hole.

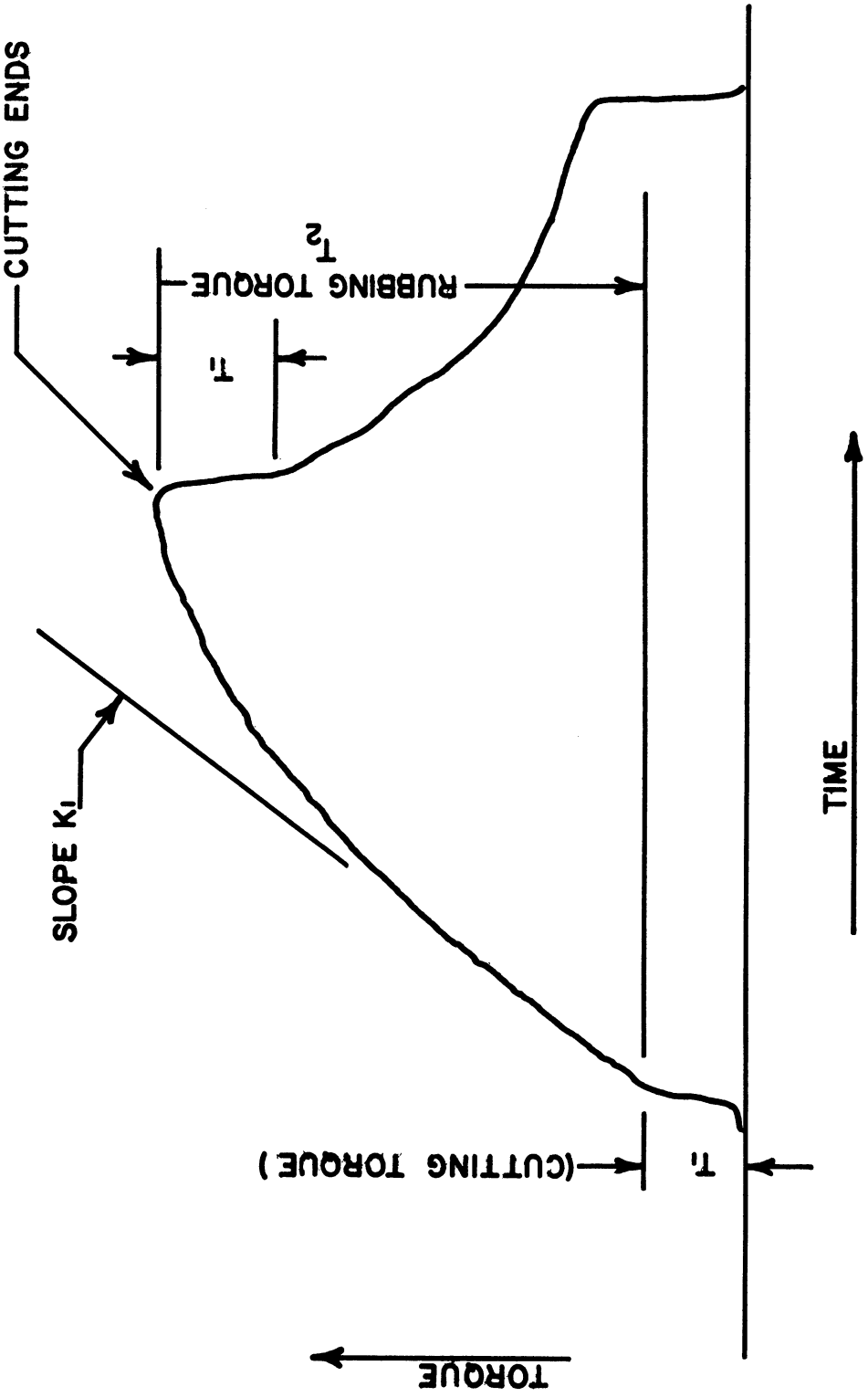

Figure 28. Typical-time chart for reaming when rubbing occurs. Deviation from linear trend is due to plastic flow or burnishing in the presence of an effective lubricant. Torque for dry cutting remains constant at T_1 level. Dry reaming creates residual tension in peripheral direction. Dominant compression accompanies the high rubbing torques observed with some lubricants.

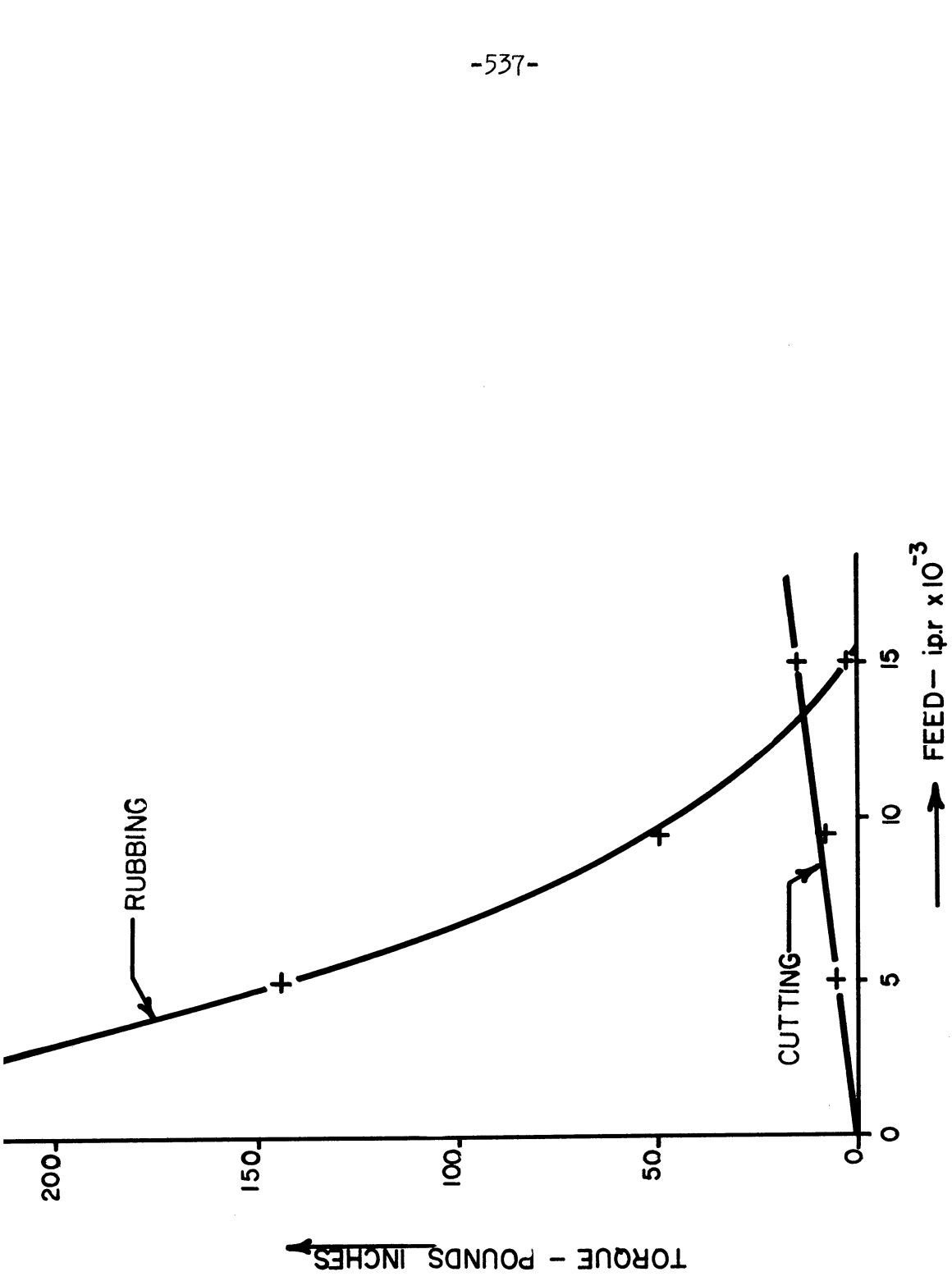

Figure 29. Increased feed with sharp reamer on C-1045 steel resulted in considerable reduction of rubbing torque as size of built-up-edge increased. Finish deteriorated with increased feed and residual peripherial stresses changed from dominant compression to dominant tension. Initial hole diameter was 0.745 inches; reamer diameter was 0.7504 inches.

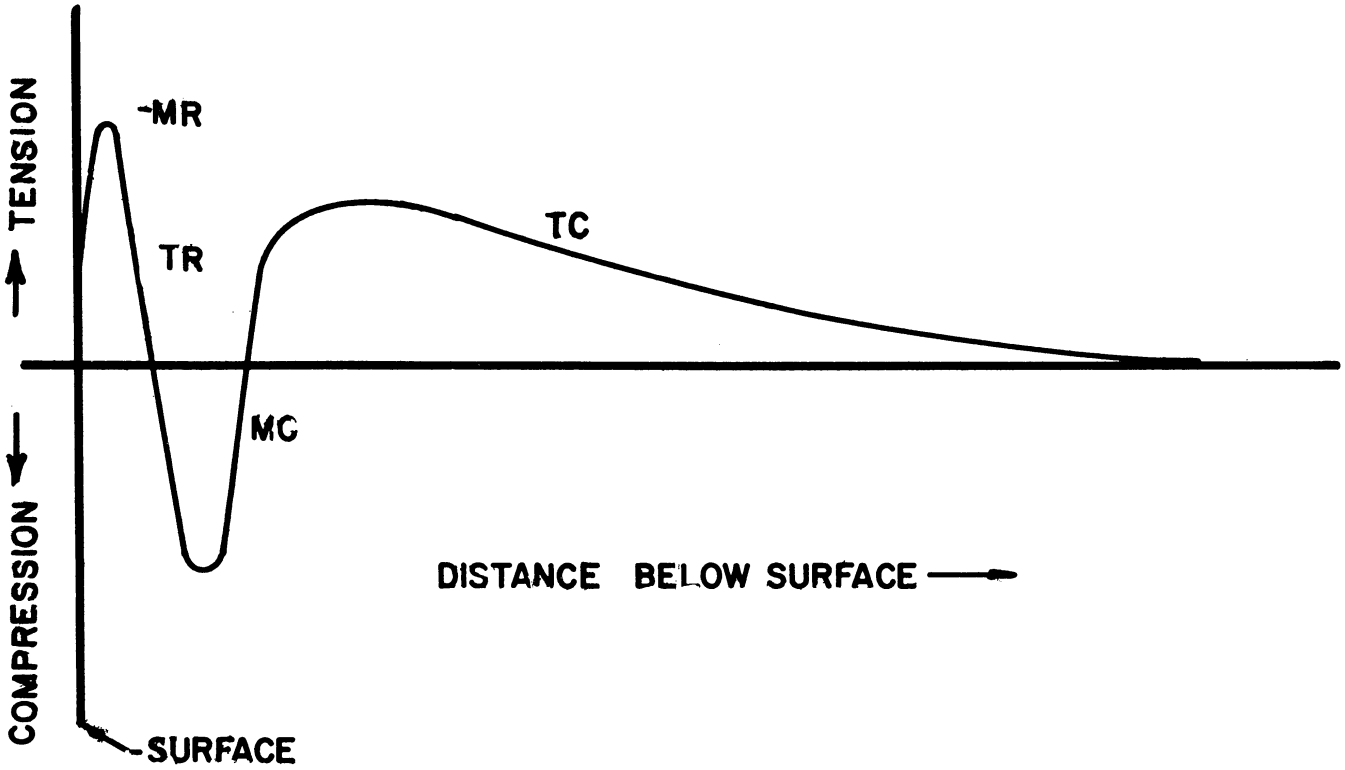

Figure 30. A generalized stress distribution curve typical of surface grinding. Stress arising from four distinct sources are identified at TC (Thermal from cutting), MC (Mechanical from cutting), TR (Thermal from rubbing) and MR (Mechanical from rubbing). The section designated as TR usually is absent in carefully ground surfaces. Sections TC and MC may be related and both arise from mechanical sources.

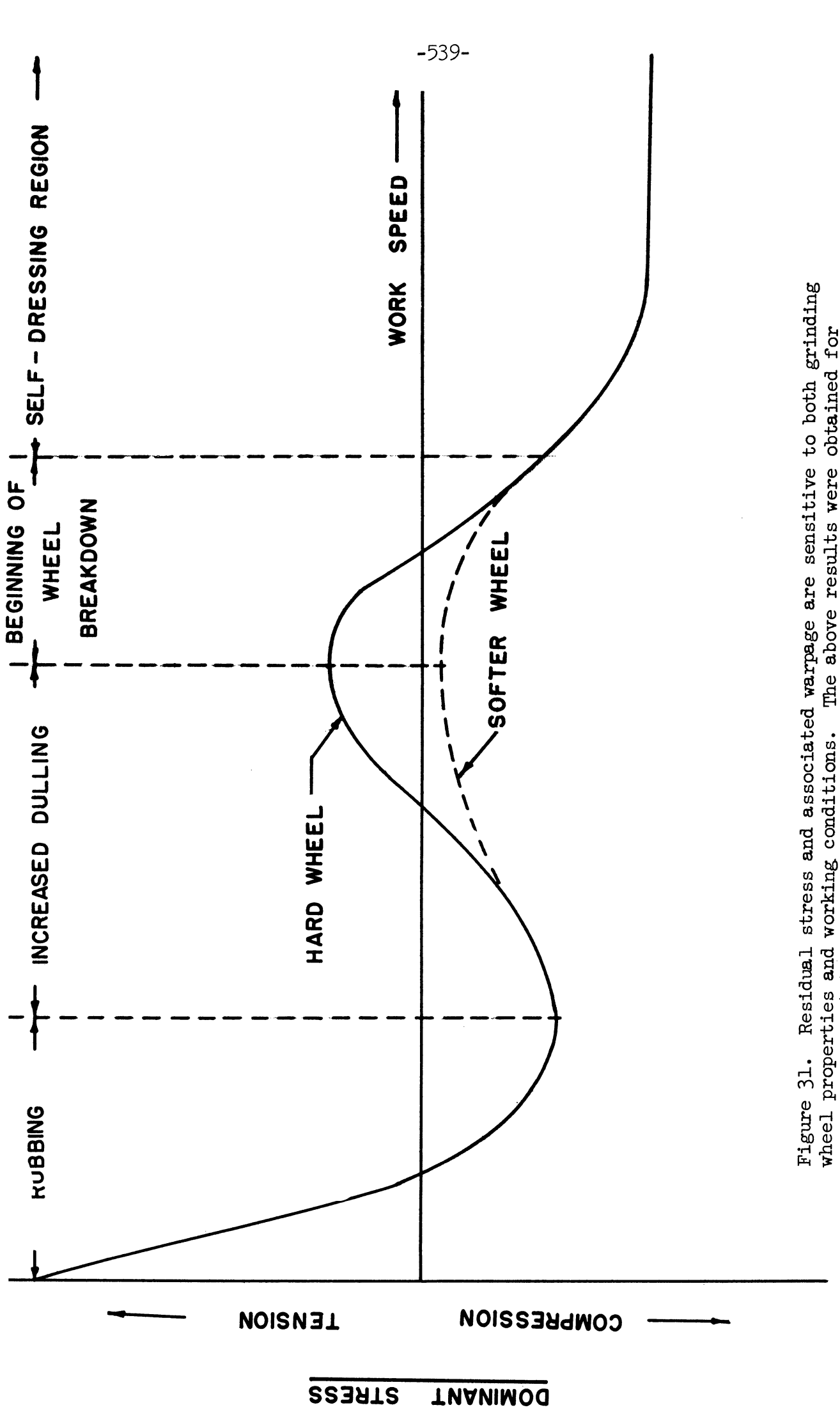

Figure 31. Residual stress and associated warpage are sensitive to both grinding wheel properties and working conditions. The above results were obtained for full-hard AISI 4340 steel but are typical of grinding operations where thermally-induced tensile stresses are possible.

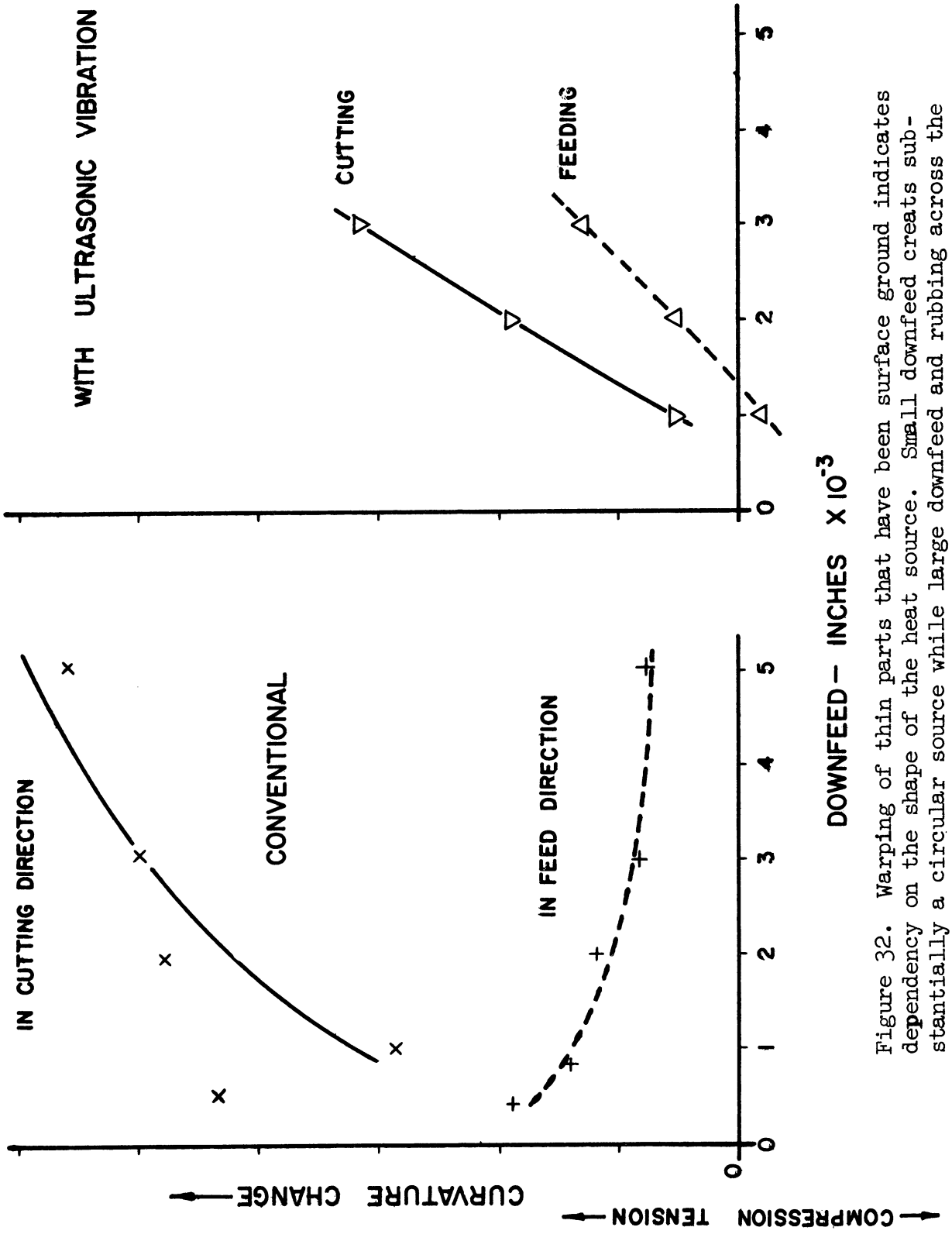

Figure 32. Warping of thin parts that have been surface ground indicates dependency on the shape of the heat source. Small downfeed creats substantially a circular source while large downfeed and rubbing across the wheel face cuases shape of the source to approach a line. This property is demonstrated for conventional grinding by curves at left. Superimposing ultrasonic vibration prevents formation of line sources.

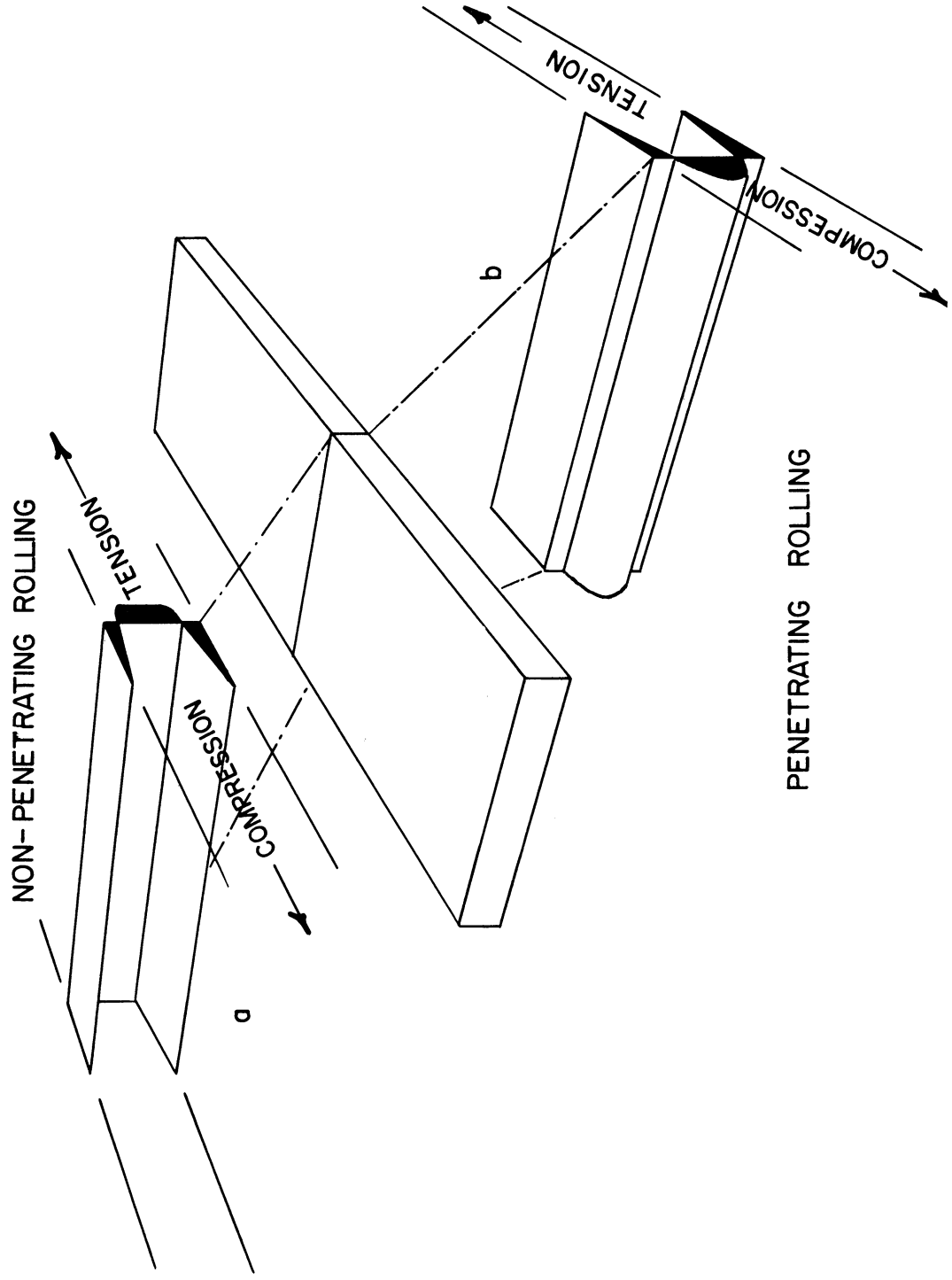

Figure 33. Residual stress distribution produced in rolled strip. (a) For non-penetrating rolling. (b) For penetrating rolling. (From "Cold Working of Metals", pg. 41, The American Society foe Metals, Cleveland, Ohio, 1949).

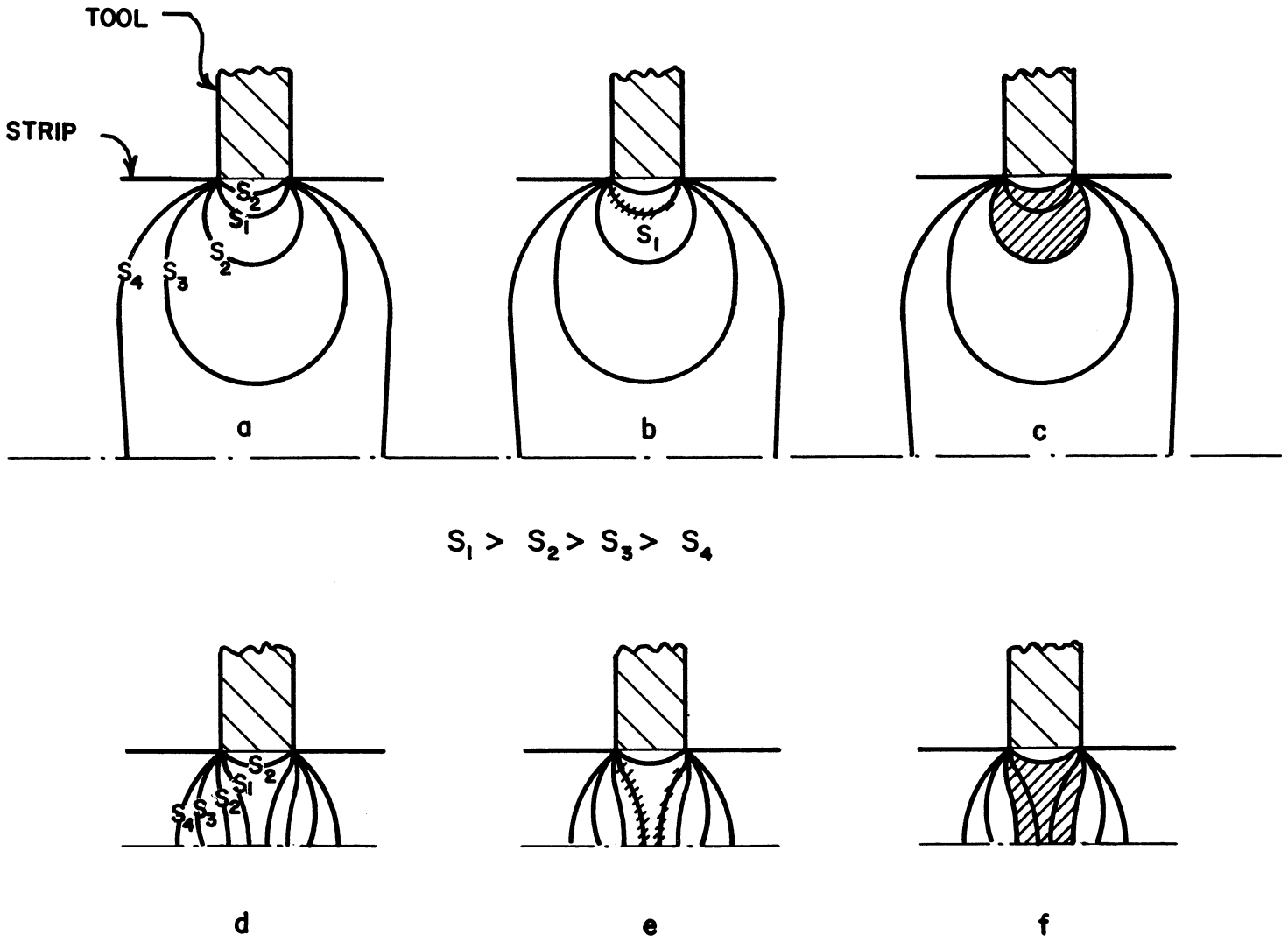

Figure 34. Manner in which plasticity is developed in strip compressed between flat-faced tools. Only upper half of full arrangement is shown. Upper set of conditions produces residual compression in surface; lower produces tension. Upper set could be analogous to contact between flank for cutting tool and machined surface. (From "Cold Working Metals", pg. 43, The American Society for Metals, Cleveland, Ohio, 1949).

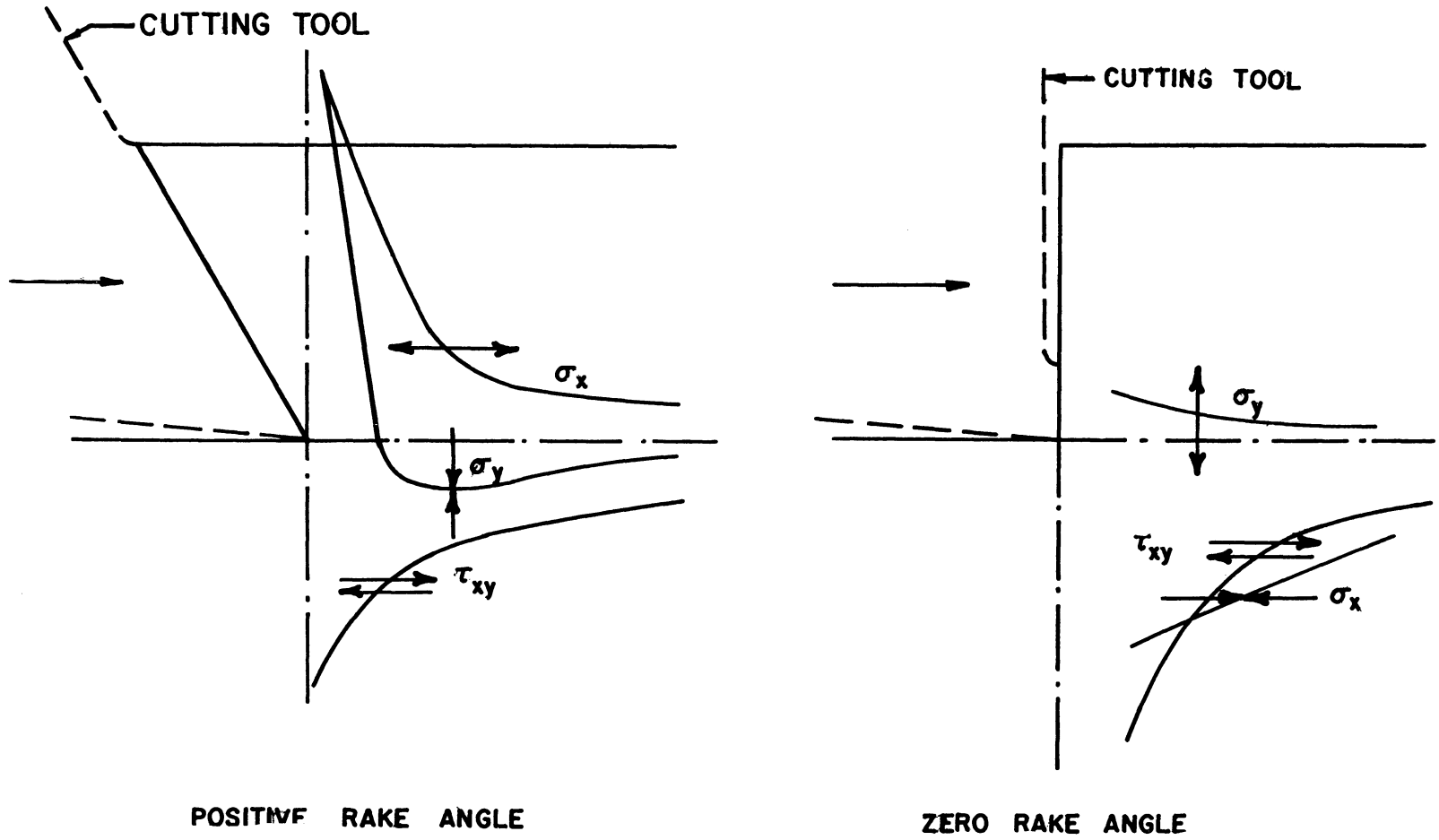

Figure 35. Stresses acting on plane of cut surface in ahead of cutting tools; determined by static photo-elastic analysis. Note change of normal stress in cutting direction from tension at left to compression at right in figure. (From "Scientific Papers of The Institute of Physical and Chemical Research," Vol. 22, pp. 139 and 147, Tokyo, Japan, October, 1953).

SUMMARY

Charles Lipson
Professor of Mechanical Engineering
University of Michigan

SUMMARY

By

Charles Lipson

The papers presented in this volume cover many phases of surface damage, ranging from the fundamental aspects of wear to the actual application of materials and techniques. It is the purpose of this summary to bring forth and analyse some of the significant information contained in these papers.

Fundamental Aspects of Wear

The mechanism of surface damage under boundary type of lubrication is taken up by Bisson. Film thickness in boundary lubrication is small and surface asperities, therefore, can and do contact through the oil film. The properties of metal are of primary importance since there is a true metal-to-metal contact at the asperities. While the properties of the lubricant under these conditions are of secondary importance, they are not to be neglected since they can strongly influence the type of damage which will occur. The lubricant in this case is serving as a contaminant.

The presence of a contaminating film between sliding surfaces can have a marked effect on friction, wear, and surface damage. Some contaminants are beneficial (lubricants) while others are detrimental (abrasives).

The study indicates that under extreme boundary lubrication conditions, where metal-to-metal contact takes place, friction and tendency to surface failure (by welding) of rubbing metals can be reduced by the use of thin low shear strength films on hard base materials. Thus, any low shear strength material (certain oxides, sulfides, plated films, liquid lubricants, etc.) that acts as a contaminant between sliding surfaces, should be effective in reducing friction and surface failure.

Wear studies also show that prevention of surface damage and maintenance of low wear can be associated with the formation of naturally occurring surface films on one or both of the sliding specimens. Data are given in Bisson's paper for some specific materials and applications.

Davies points out that even with boundary lubrication two metals may seize, score and gall when they slide over each other. Thus, it is desirable to know which metal pairs score the least. He suggests the following criterion. Two metals can slide on each other with relatively little scoring if both of the following conditions are met:

1. The metals are insoluble in each other, that is, neither metal dissolves in the other or forms an alloy with it.

2. At least one of the metals is from the B - subgroup of the periodic table - the elements to the right of the Ni-Pd-Pt column in the periodic table.

These criteria were tested by holding small square sliders of one metal against a rotating disk of the other metal. Score resistance of the sliders are given and the results that agree and do not agree with the criteria are indicated.

Surface damage is admittedly a complex form of failure as it is affected by many variables. The effect of one of these variables, that of surface temperature caused by friction heating, is taken up by Kelly.

His paper deals principally with two forms of failure: scoring and pitting. Scoring is gradually being recognized as a direct function of surface temperature. In the case of unlubricated surfaces, this temperature is associated with the melting point of the materials. In the case of solid lubricant films, it is directly related to the softening point of these films. More recently it has been found that surface temperatures far lower than melting points bring about the onset of scoring of liquid lubricated surfaces. Non-reactive mineral oils and very likely most other commercial oils have a critical temperature beyond which they are no longer capable of satisfactory lubrication.

As to pitting, three forms are recognized: 1) Pitting that occurs on machinable hardness members. These pits are generally not deep and are due to the maximum subsurface shear; 2) "case crushing," which originates at the junction of the case and the core and is due principally to the deeper shears below the maximum; 3) Pitting which occurs at the surface of very hard members, and has the appearance of spalling in a fan-shape pattern. This is the most common type of pitting.

Kelly examines pitting by combining stress distribution in and below the surface with thermal stress effects. He feels that thermal stresses can play an important role in surface damage.

Abrasion

Abrasive wear is taken up in some detail by Norman and Avery. This type of wear occurs in a wide variety of industries and operations, and the annual cost of replacing worn parts is a major expense in many of these industries. Consequently, increasing attention is being devoted to ways and means of reducing abrasion by the development of better abrasion resistant materials and by better choice of the materials now available.

Three main types of abrasive wear, namely: gouging, high stress grinding and low stress erosion are described and discussed by Norman. Typical rates of wear are given. These rates on some commonly used ferrous alloys range from a maximum of about 1000 mils per hour down to .005 mils per hour. The following factors are listed and discussed:

1. The influence of the hardness of the abrasive mineral on wear rates of various materials.
2. Comparative wear rates of some commonly used materials in each type of abrasion.
3. The types and composition ranges of commonly used abrasion resistant ferrous alloys.
4. Comparative mechanical properties and relative toughness of some abrasion resistant ferrous alloys.
5. The influence of residual stresses in conjunction with these mechanical properties.

Avery discusses various aspects of wear, such as properties pertinent to surface protection and the influence of impact, heat, corrosion and friction. He points out that such characteristics as tensile strength and ductility may have little or no value for predicting surface behavior. Compressive strength, on the other hand, is likely to be pertinent and hardness is almost universally employed as a significant index of merit. Considerable information is given by Avery on wear testing technique and test data, such as the comparative merits of various materials. He points out that a universal wear test is not feasible, which means that tests must be specific and should simulate service conditions as nearly as possible.

Scuffing, Galling and Normal Wear

In high speed machinery, sliding contact between mating surfaces involves two types of wear. The first is destructive and is commonly called scuffing, galling, or scoring, depending on its severity. The second is normal wear and it may or may not be greater than desirable depending on the frequency of parts replacement. Selection of materials and properties for scuff resistance is distinctly different from selection for normal wear, and care must be exercised to arrive at a good compromise. Surface finish, the mating material and lubrication are inseparable parts of the same problem.

LaBelle applies these considerations to the study of cast iron. Engine test data are given, some pertaining to the scuff resistance, based on severity of operation to produce scuffing, and the other to normal wear resistance in about 1,000 hours of engine operation on a controlled cycle. The effect of graphite, metal matrix, chemical composition and surface finish is indicated. LaBelle points out that the data given in his paper show specific results for a specific application. It would be erroneous to assume that the optimum materials indicated here would be optimum for all applications. The results, however, should be useful in pointing out steps which might be taken to solve problems in other applications.

Pitting and Rolling Fatigue

Metal failures by rolling fatigue are common in many machine components, such as bearings, gears, cams, etc. The major characteristic of rolling fatigue is that the load is concentrated on a small area of contact between the two bodies. Graham brings out that rolling fatigue, and pitting associated with it, involves the following: Hertzian stresses, sliding action accompanying rolling action, the elastic wave, subsurface fatigue, surface flow, incipient pitting and destructive pitting. Grover emphasizes the deleterious effect of subsurface faults, such as inclusions, seams and cracks, when they occur in regions of otherwise high stresses. He also considers the effect of residual stresses, particularly in surface hardened parts.

Cram points out that in the design of machine elements subjected to rolling or combined rolling and sliding action, knowledge of the surface endurance limits of mating materials is of primary importance. Surface wear tests were conducted in author's company laboratories and a great deal of data are presented on cast iron, steel, bronze, aluminum and non-metallic materials. He establishes experimental load-stress factors and points out how to use these factors for determining safe measuring loads on cam and roll surfaces and involute spur, helical and bevel gears.

Rowland ran numerous life tests on actual anti-friction bearings to determine the constants used to establish bearing ratings and to measure the effect of composition, heat treatment and other variables. The statistical nature of fatigue is evident in the broad scatter of life obtained for identical bearings tested under identical conditions. Engineering requisites for steels used for rolling contact application are pointed out.

Pitting of gears and the factors to reduce pitting are considered in Graham's paper. He discusses accuracy of gear teeth, surface finish, gear design changes such as an increase in pressure angle and profile modifications, coatings, lubrication and metallurgical changes. These various controls have proved themselves reasonably effective, even though in many cases we do not know the precise mechanism by which pitting has occurred.

Frettage

Frettage or fretting corrosion can be considered as a special type of wear leading generally to corrosion products. It is always characterized by minute reciprocating motion between the wearing materials which are held together by a normal force. The damage may vary from only a discoloration of the mating surfaces to the wearing away of a sixteenth inch of material. The surface may show the formation of an abundance of corroded materials or merely a heavily galled appearance with little oxide debris.

McDowell, in his paper, outlines the most significant contributions to our understanding of the causes of fretting corrosion and the theories of the mechanism by which it takes place. The effect of motion, pressure, number of cycles, frequency, hardness, temperature, coefficient of friction, humidity, lubrication, vacuum and inert atmospheres are discussed in some detail. Suggestions for identifying fretting corrosion are listed.

As to the preventive measures, the following are offered:

1. The most obvious solution is to prevent relative motion or, at least, to reduce it. This can be done by designing a more rigid mount or by making clamps extremely tight. The insertion of a rubber gasket between the surfaces to take up the motion elastically can be effective.
2. Flooding the area with a lubricant or the sealing of the area with rubber cement or other sealing material to exclude the atmosphere will reduce fretting corrosion.
3. Increasing the abrasion resistance by nitriding, chrome plating, shot peening, flame plating or spray metal coating will have beneficial results.

Galvanic Corrosion

Ordinarily, galvanic corrosion is the accelerated attack which results from the flow of current between dissimilar metals in electrical contact in a liquid capable of conducting current. LaQue, in his paper, discusses galvanic corrosion --- in a broader sense, and he includes galvanic action as it is related to corrosion in and around crevices and pitting. From a practical point of view, inclusion of these forms of corrosive attack serves to cover a large portion of difficulties likely to be encountered as a result of corrosion.

Three conditions necessary for galvanic action are listed and discussed in some detail. These are:

1. A combination of dissimilar metals having a difference in potential in the corrosive environment.
2. A metallic connection between the dissimilar metals capable of permitting a flow of electrons from one metal to another.
3. An ionized liquid capable of conducting electric current between the dissimilar metals.

Various factors used for inhibiting galvanic corrosion are listed. Chart is appended, based on experiences with galvanic couples in sea water which may be used as a practical guide for estimating the probable direction and extent of galvanic corrosion in couples of several common metals and alloys.

Crevice corrosion exists between overlapping metal surfaces or between a metal and some substance resting on it. Causes and conditions conducive to crevice corrosion are listed. The best way to avoid crevice corrosion is to avoid crevices in the first place and several suggestions are offered in this respect. If this is not possible, use alloys showing minimum susceptibility to metallic iron concentration cell effects.

High Temperature Corrosion

The problem of corrosion at high temperatures usually resolves itself into gross oxidation of the alloy. This type of corrosion is most often encountered in internal combustion engines. Here oxygen resulting from excess air charging or from incomplete combustion of the air is the principal corrodant on the hot gas side of the engine.

Tauschek states in his paper that the theory underlying high temperature oxidation of metals is well developed and the processes controlling such oxidation reasonably well understood. However, actual corrosion problems are invariably so complex that they cannot be adequately handled from a purely analytical standpoint. Tauschek offers a number of examples of corrosion on gasoline engine exhaust valves, including comments on the metallurgy of alloys used for corrosion resistance.

Cavitation Erosion

Rheingans' paper deals with accelerated cavitation machine and the test data derived from it. The tests on variation in amplitude of vibration, depth of submergence and various liquids answer some of the questions regarding the phenomenon of cavitation. More specifically, the following was found:

1. Materials such as Ampco bronze, Colmonoy and Thiokol rubber might be better for the resistance to cavitation than the materials now in use.
2. Number of layers to be used when making repairs by welding influences the resistance to pitting, while preheating the base metal has very little effect.
3. Hardness has a definite effect on resistance to pitting, regardless of the material being used.

Surface Damage in Metal Cutting

Metal cutting operations encompass broad ranges of temperature, pressure, stresses, friction and other environmental conditions and these can influence, in a marked degree, the quality of the machined surface.

Colwell points out that the most severe combinations produce tears in thick-chip cutting and cracks in grinding. The former occurs

in cutting ductile metals; the latter takes place with brittle, hard metals at a combination of a high cutting speed, low work speed and poor transfer conditions.

Residual stresses can be either tensile or compressive. Tensile stresses are produced by severe grinding or by a "smear" of the tool flank or work surface. Compressive stresses occur in ordinary metal cutting or when metal is removed with abrasives. The relationship of residual stresses to the size of cut, cutting speed and tool shape is not clear. In general, "sharp" tools produce compressive stresses, whereas "dull" or "smeared" tools result in dominant tension.